New Methods in ^{18}F-Fluorination and Fluoroalkylation



A thesis submitted to the Board of the Faculty of Physical Sciences, in partial fulfilment of the requirements for the degree of Doctor of Philosophy at the University of Oxford.

Joseph Ford

Lady Margaret Hall

University of Oxford

Trinity Term 2024

Author's Declaration

The work presented in this thesis was conducted under the supervision of Prof. Véronique Gouverneur at the Department of Chemistry, University of Oxford. All of the work is my own, unless otherwise stated, and has not been submitted for any other degree at this or any other university.

Joseph Ford

July 2024

Table of Contents

Abstract v
Acknowledgements vi
Abbreviations and Acronyms viii

Chapter 1: Introduction **1**

1.1. Positron Emission Tomography 1

1.1.1. The Principles of PET Imaging 1

1.1.2. The Applications of PET Imaging 2

1.2. Fluorine-18 in PET imaging 3

1.2.1. PET Radionuclides 3

1.2.2. Production of Fluorine-18 5

1.2.3. Fluorine-18 Radiotracers 5

1.2.4. The Properties of Fluorinated Molecules 6

1.3. Fluorine-18 Radiochemistry 8

1.3.1. Key Considerations and Concepts in PET Radiochemistry 8

1.3.2. Preparation of [^{18}F]Fluoride 13

1.3.3. Nucleophilic Aliphatic Radiofluorination 15

1.3.4. Nucleophilic Aromatic Radiofluorination 17

1.3.5. ^{18}F-Fluoroalkylation 21

1.4. Thesis Outline 26

1.5. References 27

Chapter 2: ^{18}F-Difluoromethylation with [^{18}F]Difluorocarbene **35**

2.1. Introduction 36

2.1.1. The Difluoromethyl Group 36

2.1.2. Difluoromethylation 41

2.1.2.1. Nucleophilic Difluoromethylation 42

2.1.2.2. Radical Difluoromethylation 43

2.1.2.3. Electrophilic Difluoromethylation 46
2.1.2.4. Difluoromethylation with Difluorocarbene 46
2.1.3. Radiosynthetic Approaches to the ^{18}F-Difluoromethyl Group 56
2.1.3.1. Radiosynthesis *via* ^{18}F-Fluorination 57
2.1.3.2. Radiosynthesis *via* ^{18}F-Difluoromethylation 67
2.1.4. [^{18}F]Difluorocarbene Radiochemistry 70
2.1.5. Project Outline 74
2.2. Results and Discussion 75
2.2.1. Radiosynthetic Studies towards an Improved [^{18}F]DFC Reagent 75
2.2.1.1. Preparation of ^{18}F-Difluoromethyl Aryl Sulfones and Evaluation of their A_m 76
2.2.1.2. Substituent Effects on the Reactivity of ^{18}F-Difluoromethyl Aryl Sulfones ... 83
2.2.1.3. Radiosynthesis of ^{18}F-Difluoromethyl Aryl Sulfones in Improved AY 85
2.2.2. Application of [^{18}F]DFC Radiochemistry to PET Radiotracer Production 87
2.2.2.1. Target Identification 87
2.2.2.2. Radiosynthesis of [^{18}F]DPA-714 and [^{18}F]DPA-OCF_2H 89
2.2.2.3. Comparative Imaging and In Vivo Experiments 92
2.2.3. ^{18}F-Difluoromethylation of Aryl Boronic Acids 99
2.2.3.1. Preliminary Experiments on Non-Radioactive Material 100
2.2.3.2. Optimisation of the Pd-Mediated ^{18}F-Difluoromethylation 103
2.2.3.3. Scope of the Pd-Mediated ^{18}F-Difluoromethylation 112
2.2.3.4. Two-step, One-pot ^{18}F-Difluoromethoxylation of Aryl Boronic Acids 118
2.3. Conclusion and Outlook 120
2.4. References 123
Chapter 3: Deaminative ^{18}F-Fluorination of Heteroaryl Pyridinium Salts 131
3.1. Introduction 132
3.1.1. Nucleophilic Aromatic Substitution with Fluoride 132
3.1.2. Nucleophilic Aromatic Substitution with [^{18}F]Fluoride 137
3.1.2.1. ^{18}F-S_NAr from Halide Precursors 138
3.1.2.2. ^{18}F-S_NAr from Nitro Precursors 142
3.1.2.3. ^{18}F-S_NAr from Ammonium Precursors 143
3.1.2.4. ^{18}F-S_NAr from Other Precursors 147
3.1.3. The Synthesis and Reactivity of Pyridinium Salts 150
3.1.3.1. Synthetic Approaches towards Pyridinium Salts 150

3.1.3.2. The Reactivity of Pyridinium Salts 153
3.1.4. Project Outline 156
3.2. Results and Discussion 158
3.2.1. Reaction Design 158
3.2.1.1. Initial Considerations 158
3.2.1.2. Synthesis of Pyridinium Tetrafluoroborate Substrates 159
3.2.2. Reaction Discovery and Optimisation 161
3.2.2.1. Initial Experiments 161
3.2.2.2. Effect of Reaction Parameters 164
3.2.3. Robustness Screening 169
3.2.4. Reaction Scope 172
3.2.5. Studies towards the Development of a One-pot ^{18}F-Fluorodeamination of Crude Pyridinium Salts 177
3.2.6. Elution of [^{18}F]Fluoride with Pyridinium Tetrafluoroborates 180
3.2.7. Reaction Automation, Product Isolation and A_m Measurement 184
3.2.7.1. Undesired ^{19}F-Fluorination of Heteroaryl Pyridinium Tetrafluoroborates 185
3.2.7.2. Automation of the ^{18}F-Fluorination of Heteroaryl Pyridinium Tetrafluoroborates 187
3.2.8. Comparison with Other Methods 191
3.3. Conclusion and Outlook 194
3.4. References 196
Chapter 4: Experimental **203**
4.1. General Information (Chemistry) 203
4.2. General Information (Radiochemistry) 204
4.2.1. HPLC Conditions 205
4.3. Experimental Details for Chapter 2 207
4.3.1. Preparation of Radiolabelling Substrates, Intermediates and Reference Compounds 207
4.3.1.1. Preparation of Bromofluoromethyl Sulfide Radiolabelling Precursors 207
4.3.1.2. Preparation of Difluoromethyl Aryl Sulfone Authentic References 211
4.3.1.3. Preparation of Radiolabelling Substrates and Related Synthetic Intermediates 214

4.3.1.4. Preparation of Authentic References and Related Synthetic Intermediates 224
4.3.2. Experiments on Non-Radioactive Material 239
4.3.2.1. ^{19}F-Fluoride Leaching Experiments with Bromofluoromethyl Aryl Sulfides 239
4.3.2.2. Comparison of ^{19}F-Difluoromethylation Reactivity of Difluoromethyl Aryl Sulfones 240
4.3.2.3. ^{19}F-Difluoromethylation of Aryl Boronic Acids 241
4.3.3. Radiochemistry 241
4.3.3.1. Manual Radiochemistry Experiments 241
4.3.3.2. Automated Radiochemistry Experiments 245
4.3.3.3. ICP-MS Analysis 258
4.3.3.4. Radio and UV HPLC Overlays and Radiochemical Yield Calculations 259
4.3.4. PET Imaging and In Vivo Studies 279
4.4. Experimental Details for Chapter 3 282
4.4.1. Preparation of Radiolabelling Substrates, Intermediates and Reference Compounds 282
4.4.1.1. Preparation of Starting Materials and Synthetic Intermediates 282
4.4.1.2. Preparation of Pyridinium Tetrafluoroborate Substrates 287
4.4.1.3. Preparation of Authentic References 309
4.4.2. Radiochemistry 325
4.4.2.1. Manual Radiochemistry Experiments 325
4.4.2.2. Automated Radiochemistry Experiments 332
4.4.2.3. Radio and UV HPLC Overlays and Radiochemical Yield Calculations 343
4.5. References 375

Abstract

Chapter 1 (*Introduction*) summarises the key concepts surrounding Positron Emission Tomography (PET) imaging, including the underlying physical principles and its applications and the use of fluorine-18 as a PET radioisotope. A brief account of fluorine-18 radiochemistry, including the ^{18}F-fluorination of aliphatic and aromatic scaffolds, as well as ^{18}F-fluoroalkylation chemistry is also provided. The chapter concludes with an outline of the work disclosed in this thesis.

Chapter 2 (*^{18}F-Difluoromethylation with [^{18}F]Difluorocarbene*) begins with an account of the properties of difluoromethylated molecules and the methods employed to access them in non-radiolabelled and radiolabelled form. [^{18}F]Difluorocarbene is next introduced as a new reactive intermediate for ^{18}F-radiochemistry. Three key advances in this area are disclosed. Firstly, the development of a new-generation [^{18}F]difluorocarbene reagent with improved properties is described, followed by the first application of this chemistry to PET imaging. Finally, a novel Pd-mediated ^{18}F-difluoromethylation of aryl boronic acids is disclosed.

Chapter 3 (*Deaminative ^{18}F-Fluorination of Heteroaryl Pyridinium Salts*) first provides an overview of S_NAr reactivity with both ^{19}F-fluoride and [^{18}F]fluoride, followed by a summary of the synthesis of pyridinium salts, as well as their reactivity. The development of a pyridinium-based ^{18}F-fluorodeamination of heteroaryl amines is then disclosed. Attention is then given to the automation and scale-up of the reaction, the use of pyridinium salts as elution reagents, the evaluation of crude pyridinium salts in ^{18}F-fluorination and comparison to other substrates.

Chapter 4 (*Experimental*) contains experimental details for the work disclosed in Chapters 2 and 3, including procedures and characterisation for synthesised compounds, as well as radiosynthesis procedures and data.

Acknowledgements

First and foremost, I would like to thank my supervisor Véronique for her support and guidance throughout my DPhil. I feel very grateful to have had had the opportunity to work in her research group and especially to have been given the opportunity to start working on radiochemistry. She has been a truly inspirational supervisor and I have greatly benefitted from her wisdom and her willingness to share it.

I would also like to extend my special thanks to Matthew Tredwell for all of his help and guidance during the completion of this thesis. In particular, I am very grateful for him accommodating our radiochemistry work after SOMIL closed in 2023, without which much of the work in Chapter 3 would have been impossible. I would also like to thank Stephen Paisey for his help with the PET imaging experiments and for preparing the images featured in Chapter 2. Thanks to Mariah for her help with the imaging and *in vivo* experiments. I would also like to thank the entire team in PETIC for accommodating us; I have really enjoyed my time working there.

Very special thanks go to Jeroen for introducing me to radiochemistry, which became a real passion for me, and for teaching me everything I know. I feel very fortunate to have worked together on both of the projects in this thesis and I am very glad that we became close friends. I would also like to thank Claudio for teaching me a lot during those first days in SOMIL; I really enjoyed our time working together on the project. I was very grateful to have two excellent chemists as role models at the start of my DPhil.

A special thanks must go to Seb for his immense support throughout my DPhil, I am incredibly grateful to have such a kind and talented colleague and friend. It has been an absolute joy to work with you on various projects. Thank you for always looking out for me and making sure I didn't have to face anything alone. Thank you to Claire for being a great friend right from the start, it was a privilege to go through this process together and you certainly helped me

a lot. Thank you to Calum for being an excellent colleague and friend. I feel very fortunate for the good memories the four of us have together.

I would also like to thank Adeline, Ella, Dimitris and Artemis for being such brilliant radiochemistry colleagues and for letting me help out with their challenging yet fun projects. Thanks to Zijun for her help with some of the radiochemistry and for always making me smile.

Warm thanks are extended to the former members of the VG group, who all welcomed me so warmly and taught me a lot. Rob and Gianluca as SOMIL co-workers, Konstantinos, Giulia, Jimmy, Natan, Sandrine in the CRL, it was great to work with you all. Special thanks to Gabri, Francesco and Anna for teaching me a lot when I first started in the group. Also, thank you to Alex for being a good friend-it was great to work with you (although briefly!) before I started with radiochemistry. Thanks to the rest of the VG group for being excellent co-workers; I have really enjoyed my time here with you.

I would like to thank the SBM CDT (supported by GSK, MSD, Vertex and Syngenta) for the studentship and financial support that allowed me to complete this work. I would also like to thank my industrial mentor David from Vertex Pharmaceuticals for his useful insights, support and the invitations to several enjoyable PhD events at Vertex during my time.

Finally, I would like to thank my parents and my sister for their love and support during the completion of this thesis. It would not have been possible without them.

Abbreviations and Acronyms

15-crown-5	1,4,7,10,13-Pentaoxacyclopentadecane	**Cl_i**	intrinsic clearance
18-crown-6	1,4,7,10,13,16-Hexaoxacyclooctadecane	**CT**	computed tomography
α	alpha	**CyJohnPhos**	2-(Dicyclohexylphosphino) biphenyl
$[\alpha]_D$	specific rotation (λ=589 nm)	**D**	distribution coefficient
Å	angstrom, 10^{-10} m	**d**	doublet
Ac	acetyl	**d.c.**	decay-corrected
A_m	molar activity	**d1**	relaxation delay
API	active pharmaceutical agent	**Da**	Dalton
A_s	specific activity	**DABCO**	1,4-diazabicyclo[2.2.2]octane
Au	absorbance unit	**DAST**	diethylaminosulfur trioxide
AY	activity yield	**dba**	dibenzylideneacetone
β	beta	**DeoxoFluor**	bis(2-methoxyethyl) aminosulfur trifluoride
β^+	beta-plus decay	**δ**	chemical shift (ppm)
BINAP	[1,1'-Binaphthalene]-2,2'-diyl)bis(diphenylphosphane)	**Δ**	heat
Bn	benzyl	**DFC**	difluorocarbene
Boc	*tert*-Butyloxycarbonyl	**DIPEA**	diisopropylethylamine
Bq	Becquerel	**Dipp**	2,6-diisopropylphenyl
BQ	benzoquinone	**DMA**	Dimethylacetamide
br	broad	**DMAP**	4-dimethylaminopyridine
° C	degrees Celcius	**DMF**	Dimethylformamide
cal	calorie	**DMI**	1,3-Dimethyl-2-imidazolidinone
cGMP	current Good Manufacturing Practice	**DMPU**	1,3-Dimethyl-1,3-diazinan-2-one

DMSO	Dimethylsulfoxide	**FMPEP**	(3*R*,5*R*)-5-(3-(fluoromethoxy)phenyl)-3-(((*R*)-1-phenylethyl)amino)-1-(4-(trifluoromethyl) phenyl)pyrrolidin-2-one
dppb	1,3-Bis(diphenylphosphino) butane	**FMTEB**	fluoro-5-[(2-methyl-1,3-thiazol-4-yl)ethynyl] benzonitrile
dppe	1,3-Bis(diphenylphosphino) ethane	**FT**	Fourier transform
dppf	1,1′-Bis(diphenylphosphino) ferrocene	**γ**	gamma, gamma ray
dppm	1,3-Bis(diphenylphosphino) methane	**G**	giga
dppp	1,3-Bis(diphenylphosphino) propane	**g**	gram
e^-	electron	**GC**	gas chromatography
e^+	positron	**h**	hour
EE	elution efficiency	**HBV**	hepatitis B virus
ee	enantiomeric excess	**hept**	heptet
EI	electron impact ionisation	**HPLC**	high performance liquid chromatography
EOB	end-of-bombardment	**HQ**	hydroquinone
EOS	end-of-synthesis	**HRMS**	high resolution mass spectrometry
equiv	equivalents	**Hz**	hertz
ESI	electrospray ionisation	**ICP-MS**	inductively coupled plasma mass spectrometry
Et	ethyl	***i*Pr**	iso-propyl
eV	electronvolt	**IR**	infrared spectroscopy
FDG	2-fluoro-2-deoxy-D-glucose	**J**	scalar coupling constant
FDOPA	6-fluoro-L-DOPA	**k**	kilo
FET	fluoroethyl-L-tyrosine	**K**	Kelvin
FMISO	fluoromisonidazole	**K_{222}**	Kryptofix 222; (4,7,13,16,21, 24-Hexaoxa-1,10-diaza bicyclo[8.8.8]hexacosane)

L	litre	**NBS**	*N*-bromosuccinimide
LC	liquid chromatography	**NMM**	*N*-methylmorpholine
LED	light-emitting diode	**NMR**	nuclear magnetic resonance spectroscopy
LG	leaving group	**O1p**	transmitter excitation frequency
LiHMDS	lithium hexamethyldisilazide	**p**	proton
M	mega	**P**	partition coefficient
M	molar	**PDFA**	(triphenylphosphonio) difluoroacetate
m	milli	**pent**	pentet
m	metre	**PET**	positron emission tomography
mCPBA	*meta*-Chloroperoxybenzoic acid	**Ph**	phenyl
Me	methyl	**Phe**	phenylalanine
MeCN	acetonitrile	**PhenoFluor**	1,3-Bis(2,6-diisopropylphenyl) -2,2-difluoro-4-imidazoline
min	minute	**pin**	pinacol
mol	mole	**pK_a**	-$\log_{10}$(acid dissociation constant)
MP	meting point	**P(*o*-Tol)$_3$**	Tri(*o*-tolyl)phosphine
MS	mass spectrometry	**ppy**	2-phenylpyridine
Ms	methanesulfonyl	**PSMA**	prostate specific membrane antigen
µ	micro	**q**	quartet
n	neutron	**QMA**	quaternary methyl ammonium
n	number of experiments	**qNMR**	quantitative nuclear magnetic resonance
N	number of scans	***R***	positron range
n.d.c.	non-decay-corrected	**RCP**	radiochemical purity
LC	liquid chromatography	**RCY**	radiochemical yield

rt	room temperature	**TLC**	thin layer chromatography
s	second	**TMAF**	tetramethylammonium fluoride
s	singlet	**tmp**	tetramesitylporphyrin
Selectfluor	*N*-Chloromethyl-*N*'-fluoro-triethylenediammonium bis(tetrafluoroborate)	**TMS**	trimethylsilane
SET	single electron transfer	**TOF**	time-of-flight
SIPrAgCl	1,3-Bis-(2,6-diisopropyl phenyl)imidazolinium silver(I) chloride	**TPPy**	2,4,6-triphenylpyridine
S_NAr	nucleophilic aromatic substitution	**Ts**	toluenesulfonyl
SUV	standard uptake value	**TSPO**	translocator protein
T	tera	**UV**	ultraviolet
T	temperature	**V**	volt
t	time	**v/v**	volume to volume
t	triplet	**λ**	wavelength
$t_{1/2}$	half life	**ν**	wavenumber (cm^{-1})
TBAF	tetrabutylammonium fluoride	**w/w**	weight per weight
***t*Bu**	*tert*-butyl	**Xantphos**	(9,9-Dimethyl-9*H*-xanthene-4,5-diyl)bis(diphenylphosphane)
TEAF	tetraethylammonium fluoride	**XPhos**	Dicyclohexyl[2',4',6'-tris(propan-2-yl)[1,1'-biphenyl]-2-yl]phosphane
TEMPO	(2,2,6,6-Tetramethyl piperidin-1-yl)oxyl		
TFA	trifluoroacetic acid		
Tf	trifluoromethanesulfonyl		
TFAA	trifluoroacetic anhydride		
THF	tetrahydrofuran		

Chapter 1: Introduction

1.1. Positron Emission Tomography

Medical imaging is a vital tool in modern medicine and numerous medical imaging techniques have emerged that have had a major impact on clinical outcomes worldwide. Various modalities can be used to obtain both structural and functional information. Structural imaging techniques, such as radiography (or X-ray) or computed tomography (CT) enable the visualisation of internal tissues and anatomical structures. In contrast, functional imaging allows for the tracking of physiological processes or biological activity, which is often achieved with a molecular imaging probe or tracer.[1,2]

Positron Emission Tomography (PET) imaging is a functional, diagnostic nuclear medicine technique, which uses tracer molecules labelled with a positron-emitting radionuclide.[3] PET imaging is non-invasive, highly sensitive and quantitative, requiring miniscule amounts of radiotracer, often falling well below doses that elicit a pharmacological response.[4]

1.1.1. The Principles of PET Imaging

During PET imaging, the synthetic positron-emitting radioisotope must first be produced, e.g. using a cyclotron or generator, and then incorporated into the tracer using radiochemical synthesis, which is followed by purification and formulation processes to prepare a radiotracer in injectable form.[3-5] Before it can be administered, rigorous quality control protocols ensure the product is of sufficient purity, in line with legal guidelines. A solution of the radiotracer is then injected into a peripheral vein. The tracer is allowed to distribute around the body, accumulating in various organs depending on its properties. After a delay, PET scanning can begin and the patient is moved to the scanner. The emission of positrons occurs during β^+ decay of the proton-rich radionuclide. In this process, a proton is converted into a neutron, with the production of a positron and an electron neutrino (Figure 1.1). As an

antiparticle, the eventual fate of the positron is annihilation with an electron, and the mean distance that the positron travels in tissue (over which it loses its kinetic energy in collisions) before annihilation is referred to as the positron range (*R*). During annihilation, the mass-energy of the colliding positron and electron is converted into a pair of γ-photons, at an angle of near 180° to each other. The gamma rays travel in a straight line and they are detected by the scintillation detectors of the PET scanner. These are conventionally arranged in a ring-shaped array, usually with a diameter of 60–90 cm. The detectors record the coincident arrival of the pair of γ-photons, and the line between them ('line of response') can be constructed. This allows for the localisation of the event in image reconstruction. Applying this principle across the millions of events acquired during a PET scan in image reconstruction, a 3D image is obtained, which can be viewed in layers and in various projections. In modern scanners, it is possible and common practice to also acquire a CT scan concomitantly (PET-CT), such that the anatomical and structural data from CT can assist practitioners in analysing the physiological imaging data from PET.[6]

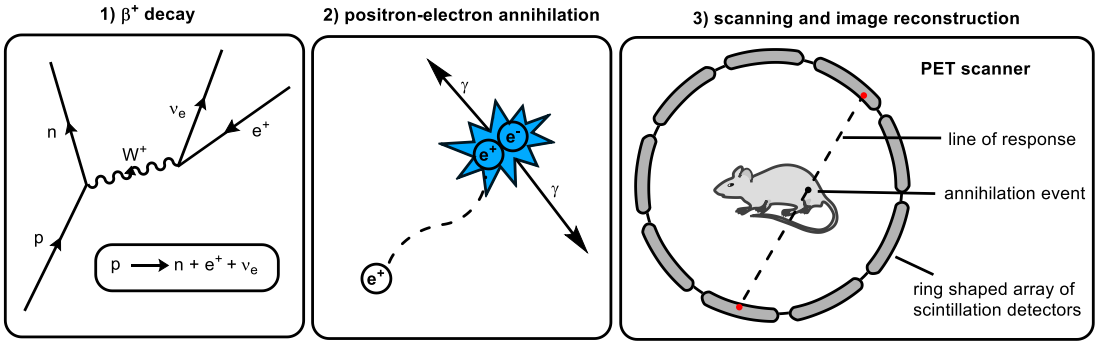


Figure 1.1. *The physical principles of PET imaging: 1) β⁺ decay, 2) positron-electron annihilation, 3) PET imaging.*

1.1.2. The Applications of PET Imaging

PET imaging finds significant application in clinical medicine, where it can be used for diagnosis of disease, clinical staging, or therapy assessment.[7,8] Several medical disciplines apply PET imaging routinely for any or all of these purposes, most notably oncology,

cardiology and neuroscience. For example, the use of PET-CT imaging with the radiotracer [^{18}F]2-fluoro-2-deoxy-D-glucose is widespread and can be used for the imaging of numerous disease states, despite its initial design as an oncology tracer for the metabolic imaging of glycolysis in tumours.[6]

Beyond clinical medicine, PET can be used for research and in the development of novel active pharmaceutical agents (APIs).[9-11] Small animal PET imaging is most commonly applied in preclinical studies and dedicated scanners for imaging of mice and rats are commercially available. PET imaging can provide answers to key questions arising during the various stages of the discovery and development of novel APIs.[12,13] For example, PET can be used to obtain biodistribution data, which confirms the molecule's accumulation in the tissue of interest and can be used to rule out non-specific binding, or accumulation in off-target sites. PET studies are also used to probe receptor binding in blocking studies, by comparing the uptake response in the presence of a drug molecule under consideration. Such studies can provide early insight into efficacy and target occupancy for drug candidates.[14] Furthermore, this strategy can also be used for dose selection, as the administered picomolar quantities of radiotracer do often not elicit a pharmacological dose response.[10-14]

1.2. Fluorine-18 in PET Imaging

1.2.1. PET Radionuclides

There are numerous positron-emitting radionuclides that can be applied in PET imaging, and these differ in both their chemistry and their decay properties.[5] The decay properties of various PET radionuclides are summarised in Table 1.1.

Half-life ($t_{1/2}$) is a key parameter and is defined as the characteristic length of time over which the activity of a radioactive sample decays by half. Ideally, a radionuclide to be used in PET imaging would have an intermediate half-life. This allows sufficient time for radiotracer production, quality control, tracer injection and imaging, but ensures that the radiotracer is

cleared quickly after imaging, minimising patient radiation dose. Very short half-life radionuclides, such as oxygen-15 and nitrogen-13, do not permit time-consuming radiochemical transformations, rendering their incorporation into radiotracers more challenging.[15] For preclinical or research applications, longer half-life radioisotopes that are less appropriate for clinical PET imaging can be used to image slower biological processes, such as the use of zirconium-89 in immuno-PET for studying the distribution of monoclonal antibodies.[16]

Furthermore, the proportion of decay events proceeding *via* β^+ decay should be as high as possible for radionuclides used for PET imaging, to reduce losses to other decay modes, such as electron capture, and reduce patient radiation doses. The maximum positron energy and positron range (*R*) should also be as low as possible; high energy positrons travel further in tissue before annihilation, which results in images with lower spatial resolution.[17,18]

Radionuclide	$t_{1/2}$	**β^+ decay**	R_{mean} **/mm**	**Daughter nuclide**
^{15}O	2.04 min	100%	2.97	^{15}N
^{13}N	10.0 min	100%	1.73	^{13}C
^{11}C	20.3 min	>99%	1.27	^{11}B
^{68}Ga	67.7 min	89%	3.56	^{68}Zn
^{18}F	110 min	97%	0.660	^{18}O
^{64}Cu	12.7 h	17%	0.560	^{64}Ni
^{89}Zr	78.4 h	23%	1.27	^{89}Y

Table 1.1. *Nuclear decay properties of common positron-emitting radionuclides used for PET imaging, arranged by ascending half-life.* R_{mean} *= mean positron range in water.*

1.2.2. Production of Fluorine-18

Fluorine-18 is produced using a cyclotron, which is a type of particle accelerator that can accelerate charged particles in a circular path. Once these particles have been accelerated to the required energy, the beam of particles is then directed towards a target. The bombardment of the target material with the accelerated particles causes the production of synthetic radioisotopes, such as those used in PET imaging.[19]

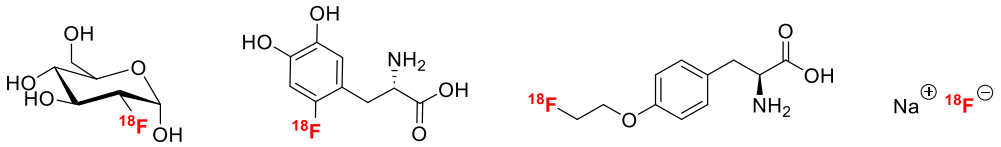
Fluorine-18 is produced primarily in the high yielding $^{18}O(p,n)^{18}F$ nuclear reaction, in which an [^{18}O]water target is bombarded with high energy protons to produce a neutron and fluorine-18 as a solution of [^{18}F]fluoride in water.[19,20] The exact identity of the countercation is not known and depends on the material the target is made from.[21] [^{18}O]O_2 or Ne gas targets can also be used to produce [^{18}F]F_2 gas, however the route *via* an [^{18}O]water target is preferred, as handling in solution phase is easier and the molar activity of the produced [^{18}F]F_2 gas is lower than that of [^{18}F]fluoride.[20] The radiochemistry described in this thesis exclusively uses [^{18}F]fluoride produced in the $^{18}O(p,n)^{18}F$ nuclear reaction.

1.2.3. Fluorine-18 Radiotracers

Based on the set of decay properties described in section 1.2.1, fluorine-18 has emerged as the most used PET radionuclide, and the majority of PET scans are conducted using ^{18}F-radiotracers. Conveniently, its intermediate half-life (109.8 min) also allows for transportation of radiotracers from a 'hub' radiopharmacy to 'spoke' scanning units for patient imaging.[5]

Several fluorine-18-containing radiotracers are used in clinical PET imaging (Figure 1.2). The most widely used PET radiotracer is [^{18}F]2-fluoro-2-deoxy-D-glucose ([^{18}F]**1.1**), which has a wide variety of applications as described in section 1.1.2.[6] Other ^{18}F-radiotracers include [^{18}F]FDOPA ([^{18}F]**1.2**), a fluorinated analogue of L-DOPA, which can be used for imaging of Parkinson's disease and related neurodegenerative disorders.[22] [^{18}F]Fluoroethyltyrosine ([^{18}F]FET, [^{18}F]**1.3**) is derived from the amino acid tyrosine and can be used for assessing brain

cancers.[23] Finally, sodium [^{18}F]fluoride ([^{18}F]**1.4**) can be used for skeletal imaging, with applications in benign conditions and also bone cancers.[24]



[^{18}F]FDG
[^{18}F]**1.1**

[^{18}F]FDOPA
[^{18}F]**1.2**

[^{18}F]FET
[^{18}F]**1.3**

[^{18}F]NaF
[^{18}F]**1.4**

Figure 1.2. *Examples of fluorine-18 containing radiotracers.*

Beyond clinical applications, ^{18}F-radiotracers are also widely used in preclinical work and research and development.[8-14] Furthermore, the frequent inclusion of one or more fluorine atoms in small molecule pharmaceuticals (section 1.2.4) provides further relevance to ^{18}F-fluorinated molecules in the development of novel fluorine-containing APIs, as their *in vivo* behaviour can be directly observed with PET imaging.[25]

1.2.4. The Properties of Fluorinated Molecules

Fluorine is the most electronegative element, with a Pauling electronegativity (χ) of 4. The atomic radius of the fluorine atom (van der Waals radius = 1.47 Å) is most similar to that of the oxygen atom (van der Waals radius = 1.52 Å) and slightly larger than the hydrogen atom (van der Waals radius = 1.20 Å). The C–F bond is the strongest bond in organic chemistry (bond dissociation energy = 105.4 kcal/mol), and it is highly polarised towards the electronegative fluorine atom.[26]

Fluorinated molecules find significant applications as pharmaceuticals and agrochemicals, and a recent estimate suggests 20% of market pharmaceuticals contain one or more fluorine atom.[27,28] This is likely caused by the well-documented effect fluorine atom or fluorine-containing group substitution can exert on the pharmacological and physicochemical properties of drug molecules.[26]

Firstly, the presence of electronegative fluorine atoms can modulate the pK_a of nearby protons and thus affect the extent to which a functional group is basic or acidic. For example, the pK_a of acetic acid is 4.8, compared to 0.5 for trifluoroacetic acid. Furthermore, ethylamine has a pK_a of 10.7, but 1,1,1-trifluoroethylamine is substantially less basic with a pK_a of 5.7.[29] This can affect protonation state and speciation in biological media, resulting in changes in pharmacokinetic profile. In addition, fluorine atom substitution modulates lipophilicity, an important factor in the design of novel APIs, as it affects membrane permeability and solubility, both of which impact the availability of the drug molecule at its intended target.[30] Fluorine can also exert conformational effects, which can be driven by stereoelectronic effects, such as the gauche effect observed in 1,2-difluoroethane, due to σ_{C-H} to σ^*_{C-F} orbital overlap.[31]

A key application of fluorine in drug discovery and development is its use in improving the metabolic stability of drug candidates.[29] One strategy uses fluorine as a blocking group for sites that are vulnerable to metabolism, for example in electron rich arenes that are susceptible to C–H oxidation.[25,32] Methyl groups that are vulnerable to demethylation can be replaced with trifluoromethyl or difluoromethyl groups, which offer improved stability to oxidative metabolic processes.[29]

Various fluorinated functional groups have also been applied as bioisosteres of common functional groups, including alcohols, thiols and carbonyls, so where a functional group is found to be vulnerable to metabolism or have other detrimental effects, such as toxicity, its fluorinated bioisostere may be employed instead.[33] This is particularly pertinent to the work described in Chapter 2, as many difluoromethyl moieties have been identified as bioisosteric with common functional groups.

Although fluorinated molecules have made a largely positive contribution to the development of novel APIs and healthcare, there are some cases where fluorine

incorporation into drugs or drug candidates has led to detrimental effects.[34,35] The propensity of primary alkyl fluorides to metabolically convert to toxic fluoroacetate is well known and must be considered in the design of new drug molecules. Fluorine can also be displaced by nucleophilic functionality, or eliminated either directly or after oxidation, ultimately releasing fluoride. In the light of this, in addition to the recent concerns regarding the accumulation of perfluorinated molecules, such as trifluoroacetic acid or perfluoroalkyl sulfonates, in the environment, it is the responsibility of chemists to ensure prudent use of fluorine in the design of novel APIs in the future.[36]

1.3. Fluorine-18 Radiochemistry

This section will provide an overview of fluorine-18 radiochemistry. For brevity, the discussion in this section is limited to the solution-phase chemistry using cyclotron-produced [^{18}F]fluoride (specifically nucleophilic radiofluorination), as well as the radiochemistry of labelled reagents obtained from [^{18}F]fluoride. Separate, detailed accounts of the fluorine-18 radiochemistry directly relevant to work presented in this thesis will be provided in Chapters 2 and 3.

1.3.1. Key Considerations and Concepts in PET Radiochemistry

PET radiochemistry demands additional considerations beyond the scope of conventional organic synthesis.[20,21] The most apparent constraint on fluorine-18 radiochemistry is the short half-life of fluorine-18. This demands rapid synthesis and purification procedures, to minimise losses to decay. This also has implications for the radiosynthetic strategies that are suitable; ideally, the radiofluorination step should be the last synthetic step. Routes requiring many post-labelling transformations are unlikely to be viable, especially if the yield of any of these steps is low. These constraints place an emphasis on late-stage functionalisation.

A second challenge is that [^{18}F]fluoride is produced in very low concentrations; it is estimated the concentration of [^{18}F]fluoride under radiolabelling conditions is in the nano- to picomolar

range.[21] In radiochemical reactions, this means the radiofluorinated component is almost always the limiting reagent and all other reagents will be present in vast excess. In ^{19}F-chemistry, the fluorination/fluoroalkylation reagent is usually used in excess and this inverted stoichiometry causes substantial kinetic changes compared to reactions on non-radioactive material, such that the majority of radiolabelling reactions can be considered to proceed under pseudo-first order kinetics.[37]

Beyond stoichiometry differences, there are several other factors which present challenges in the translation of ^{19}F-chemistry to ^{18}F-radiochemistry. For example, it is standard practice to exclude moisture and air from chemical reactions using Schlenk techniques or gloveboxes. This can be essential for fluorination chemistry proceeding *via* high-valent metal complexes, hygroscopic fluoride salts or air-sensitive reagents.[38] Meanwhile the exclusion of moisture and air is much more challenging and may not be possible at all for automated platforms. Water remaining from the preparation of reactive [^{18}F]fluoride as well as the presence of elution additives, such as inorganic bases, may also present reactivity challenges (see section 1.3.2).[21] Furthermore, quality control legislation for the production of radiotracers under current Good Manufacturing Practices (cGMP) can rule out the use of metal additives that promote reactivity, as the allowed residual concentration of transition metals in the final product is controlled by pharmacopeia guidelines.[39] Despite this, the use of transition metal catalysts can enable modes of reactivity not yet possible under metal-free conditions, which can overcome any drawbacks associated with their use in radiosynthesis.[40]

As it involves work with the positron-emitting radioisotope of fluorine, fluorine-18 radiochemistry requires that suitable radiation protection measures are in place to protect the operator from γ-radiation.[41] All radiosynthetic work must be carried out in a shielded, lead-walled hot cell, which minimises operator exposure and contains the radioactivity. Manual radiochemistry procedures are challenging and must be carried out using

telemanipulators or telepliers mounted to the hot cells, which limits the scope of possible manipulations compared to manual organic synthesis. Trivial operations in a synthesis laboratory may not be possible in a radiochemistry laboratory. Where the activity of the sample is low enough, manual handling may be executed in a glovebox or dispensing unit, using long handled forceps for manipulations.

For the routine preparation of clinical PET radiotracers under cGMP, operator intervention is removed and automated radiosynthesis is standard practice in radiopharmacies worldwide.[41] This requires a commercial radiosynthesiser. These are often 'cassette-based', making use of a single-use plastic consumable (cassette), made up of an array of valves, which can be used to direct a flow path, and fittings, to which tubing, syringes and vials can be connected.[42] This interfaces with the synthesiser's actuators, syringe drivers and pumps/gas pressures to transfer reagents and liquids during the radiosynthesis. In addition, the automated synthesiser will often have built-in equipment, such as heating mantles and HPLC systems. During an automated radiosynthesis, the operator first installs the relevant cassette, including any reagents needed for the synthesis, before the synthesiser runs the programme, which encodes all steps required for the preparation of the desired tracer. The duration of such programmes depends on the complexity of the radiosynthesis, for example, [^{18}F]NaF ([^{18}F]**1.4**) is prepared in 4 min,[43] while the multi-step route to [^{18}F]FDOPA ([^{18}F]**1.2**) takes 70 min from the end of bombardment (EOB) using the same radiosynthesis platform (TRASIS AllinOne).[44] The use of automated synthesisers, while safer for the operator and more reproducible for routine production, can rule out certain operations that are easily carried out manually, resulting in less flexibility.[42] Their implementation also requires more careful design, which can be a limitation for early-stage or investigational work. Despite these challenges, the translation of new radiosynthetic methodologies to automated radiosynthesis adds value for radiochemistry practitioners and thus encourages uptake by the community.

Due to the very low concentrations of radioactive components under radiochemical conditions, low sensitivity analytical methods, such as nuclear magnetic resonance (NMR) spectroscopy or those depending on UV absorbance, cannot be applied to analyse radioproducts. The analytical methods most often used in fluorine-18 radiochemistry for the characterisation and quality control of radiolabelled products rely on the detection of radioactivity using scintillation counters, primarily radio high performance liquid chromatography (HPLC) and radio thin layer chromatography (TLC). Radio-HPLC analysis can be used for the characterisation of radioproducts (by referencing retention time externally to an authentic standard) and as well as quantification (including measurement of process efficiency and molar activity). Radio-TLC methods can also be used to quantify the efficiency of radiochemical processes, and this is particularly effective for radiofluorination with [^{18}F]fluoride, as this is retained on the baseline of the silica or alumina plate. Mass spectrometry (MS) methods can also be used, however, were not implemented for any of the work described herein.[45]

The community has established a set of guidelines establishing consensus nomenclature rules for radiochemistry, to which this thesis will be faithful.[46,47] For completeness and clarity, the definitions of key concepts and terms are described in this section.

Radiochemical yield (RCY) is defined as the percentage of starting radioactivity converted to product in a process, expressed as a percentage (%)[46,47] By definition, it is decay-corrected and the activities used in its calculation must be corrected to the same point in time and relate to the same radionuclide (e.g., fluorine-18). It should be stated whether the RCY reported refers to an isolated product or not, and how it was measured. In this thesis, where non-isolated radiochemical yields of radiolabelling reactions are estimated by radio-HPLC analysis, such will be described as RCY_{HPLC}. This shorthand has not been adopted by the community at large and is used here for brevity.

Activity yield (AY) is defined as the radioactivity of a collected product obtained in a process from a starting amount of radioactivity and is not decay-corrected. [46,47] The unit of AY is Bq, which is defined as the activity of a sample undergoing decay at a rate of one disintegration per second. Here, MBq or GBq are used, due to the higher activities of product isolated.

Molar activity (A_m) is defined as the radioactivity per mole of a compound, with units most typically given as GBq/μmol. [46-48] It can be considered an expression of the ratio of radioactive material (given in terms of activity in Bq) to non-radioactive material (carrier) (given in terms of amount of material in mol), assuming that the quantity of radiolabelled compound is negligible.

$$A_m(GBq/\mu mol) = \frac{radioactivity\ of\ sample\ (GBq)}{amount\ of\ sample\ (\mu mol)}$$

A_m is not to be confused with specific activity (A_s), which uses mass of sample (in g) rather than the amount of sample (in mol). The time at which A_m is measured must also be given, as it is affected by radioactive decay, so it is often decay-corrected to a relevant point. Most commonly, the reference times used to decay-correct A_m will be end-of-synthesis (EOS) or end-of-bombardment (EOB). The method used to measure A_m in this thesis will be described in detail in Chapter 4; briefly, using radio-HPLC analysis on purified material, the activity of the sample injected was decay-corrected to EOS and the UV response associated with the desired product allowed for the calculation of the molar amount of carrier in the sample, using a calibration curve.

A_m is an important radiosynthetic parameter, as it can affect how a radiotracer can be used, e.g., for a specific PET imaging application. Where A_m is too low, carrier may saturate the target of interest, leading to poor image quality.[48] This is especially relevant for diffuse targets, such as those associated with the central nervous system.[49] Low A_m radiotracers may also elicit a pharmacological response, as the amount of carrier approaches the lower end of the

therapeutic window, which can cause undesired effects, such as toxicity.[48] Equally for some imaging applications, A_m is less significant, such as in the case of [^{18}F]FDG ([^{18}F]**1.1**) where competition from glucose is not detrimental.[48] Obtaining poly-fluorinated molecules in high A_m presents further radiosynthetic challenges, which will be discussed in detail in Chapter 2.

Finally, radiochemical purity (RCP) expresses the degree to which a sample is free of other radioactive species. Herein, it is given as a percentage of the desired radioactive product relative to all radioactive species, as determined by radio-HPLC analysis.

1.3.2. Preparation of [^{18}F]Fluoride

[^{18}F]Fluoride has emerged as the most prevalent starting material for radiofluorination processes. As described in section 1.2.2, the cyclotron product of the proton bombardment of [^{18}O]water is an aqueous solution of [^{18}F]fluoride.[21] In this state, as an excellent hydrogen bond acceptor, [^{18}F]fluoride is extensively hydrated, which renders it poorly nucleophilic and therefore largely unreactive for ^{18}F-fluorination.[21] It is noteworthy that some ^{18}F-fluorination processes remain viable in water, e.g. forming P–^{18}F, Si–^{18}F or Al–^{18}F bonds,[50-52] but the overwhelming majority of C–^{18}F bond forming processes, which are the object of this thesis, are not possible in water. A notable exception is O'Hagan and co-workers' reports of enzymatic ^{18}F-fluorination with the fluorinase enzyme.[53]

The bulk [^{18}O]water is most conventionally removed using an anion exchange cartridge, which contain resins with positively charged groups and associated counteranions, such as chloride, carbonate, bicarbonate and triflate. [^{18}F]Fluoride can then exchange with the counteranions, being retained on the cartridge, while the water is flushed through (Figure 1.3).[21] The most common type of anion exchange resin is the QMA (quaternary methyl ammonium) type, which is made up of trimethylammonium groups grafted onto a silica support. Other types of ion exchange cartridge can also be used and other variables include the mass of sorbent used,

as well as the counteranion, which can be exchanged by preconditioning with a solution containing the desired counterion.[54]

Once the cartridge has been loaded, [^{18}F]fluoride can then be eluted from the cartridge, typically using a solution of inorganic base, such as K_2CO_3 or NEt_4HCO_3, in a mixture of water and organic solvent, such as MeCN.[54] Organic bases can also be employed in place of an inorganic base. A phase transfer additive, such as Kryptofix 222 (K_{222}) or 18-crown-6 can also be used to improve the solubility of the [^{18}F]fluoride in organic solvents, but these are often not required if the elution base has a weakly coordinating cation, such as a tetraalkylammonium ion.[21,54] The efficiency of this process is referred to as elution efficiency (EE), which is the percentage of activity loaded onto the anion exchange cartridge that elutes with a given eluent preparation.

The eluate is then dried by heating to elevated temperatures and often under a flow of inert gas and/or under reduced pressure. Any water used in the eluent is removed over several cycles of azeotropic drying with additional MeCN or other volatile organic solvent. Once this drying process is complete (typical duration = 5–20 min), the [^{18}F]fluoride displays significantly improved nucleophilicity and can thus be used in C–^{18}F bond forming chemistries. It is unknown to what extent azeotropically dried [^{18}F]fluoride is hydrated, but it is very likely that some water of hydration remains.[21]

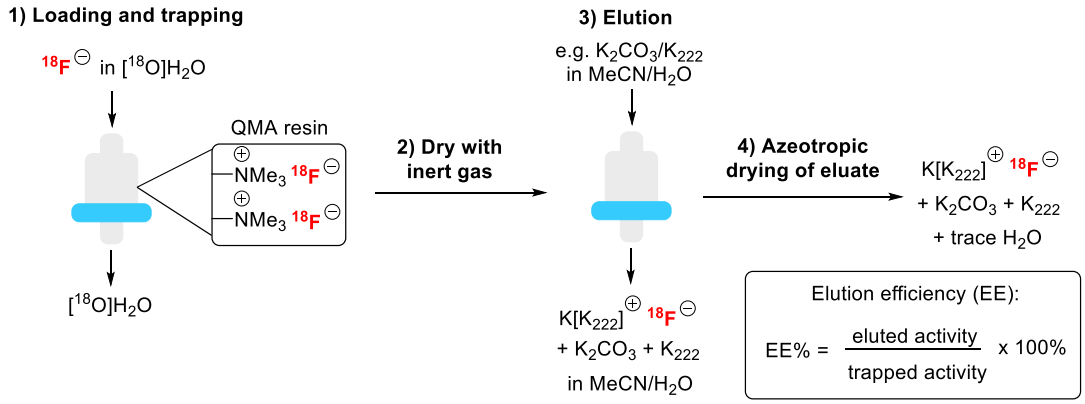
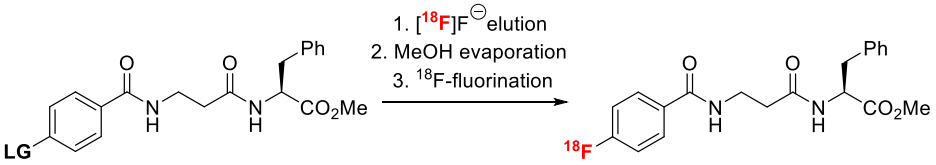


Figure 1.3. *The preparation of [^{18}F]fluoride for nucleophilic radiofluorination using a QMA cartridge.*

Classically, the eluent used in this process uses K_2CO_3 and K_{222} in an MeCN and water mixture, however the presence of these additives may hinder certain radiofluorination reactions that display sensitivity to bases. Therefore, several groups have investigated the effect on EE and reactivity of using non-basic anions for the elution of [^{18}F]fluoride.[55,56] Promisingly the use of bespoke elution conditions with non-basic elution salts, such as NBu_4OMs or NBu_4OTf, has been demonstrated to be effective in improving the S_N2 reactivity of base sensitive substrates.[57] Another approach allows for the direct use of charged onium salts for the elution of [^{18}F]fluoride. Pioneered by Neumeier and co-workers, this 'minimalist' approach allows for efficient elution of [^{18}F]fluoride in methanol and its reaction with charged iodonium, ammonium and sulfonium-derived substrates, with improved radiofluorination of base-sensitive substrates (e.g. [^{18}F]**1.5**) (Scheme 1.1).[58] In Chapter 3, the application of pyridinium salts for the elution of [^{18}F]fluoride from anion exchange cartridges is described.



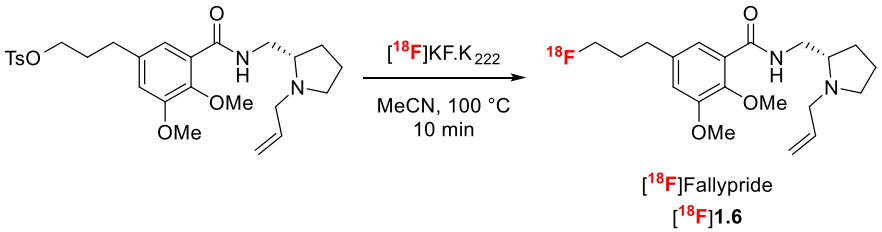
Scheme 1.1. *Minimalist radiofluorination of onium salt precursors reported by Neumaier and co-workers. LG (onium leaving group) = 4-MeOPhI$^+$I$^-$, NMe$_3^+$X$^-$ (X = OTf, HCO$_3$, I).*

A third approach uses the aqueous [^{18}F]fluoride cyclotron product to produce an auxiliary reagent, which can then be transferred in gaseous form to a reactor, where it can release [^{18}F]fluoride for a radiofluorination step under low-base conditions. While various reagents have been suggested, [^{18}F]ethenesulfonyl fluoride and [^{18}F]trifyl fluoride have emerged as the most promising candidates.[59,60]

1.3.3. Nucleophilic Aliphatic Radiofluorination

The classical method for the installation of F-18 onto aliphatic scaffolds is nucleophilic substitution.[61] This disconnection requires that the substrate is loaded with a labile functional

group or leaving group, which can be substituted by [^{18}F]fluoride. Examples of common leaving groups for nucleophilic aliphatic radiofluorination are sulfonates (e.g. tosylate, mesylate, triflate) and halide (chloride, bromide, iodide). In general, sulfonate leaving groups are preferred over halides, as these are easier to separate from the alkyl ^{18}F-fluoride product than the halide substrate with similar polarity. This approach is well exploited for the preparation of PET radiotracers, such as [^{18}F]FDG ([^{18}F]**1.1**), [^{18}F]FET ([^{18}F]**1.3**) and [^{18}F]fallypride ([^{18}F]**1.6**) (Scheme 1.2).[62] This radiochemistry is also used to prepare the ^{18}F-labelled reagents used in Chapter 2 of this thesis.

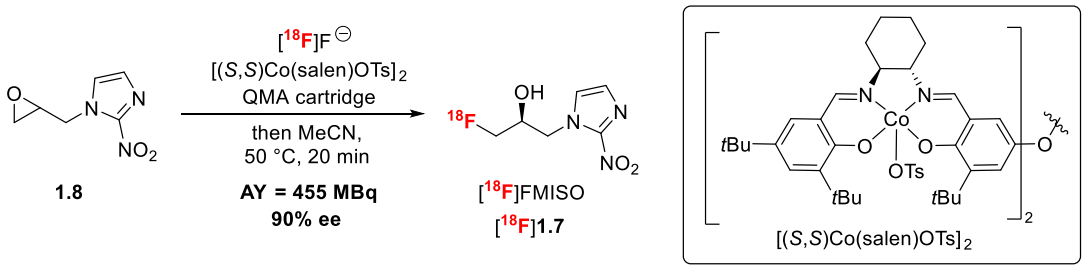


Scheme 1.2. *Radiosynthesis of [^{18}F]fallypride ([^{18}F]**1.6**) by nucleophilic substitution of an alkyl tosylate precursor.*

While appealing as a simple disconnection, certain precursors may suffer from low reactivity and/or side reactivity, such as E2-type elimination or hydrolysis, particularly when basic elution additives are present.[61] For this reason, it can be prudent to apply a prosthetic group approach in place of a potentially challenging direct substitution with [^{18}F]fluoride. These chemistries will be discussed in more detail in section 1.3.5.

Metal-mediated approaches to nucleophilic aliphatic radiofluorination have also been reported, which has expanded the scope of accessible alkyl ^{18}F-fluorides. For example, several groups including those of Gouverneur and Nguyen have reported allylic ^{18}F-fluorination protocols mediated by Pd and Ir, respectively.[63,64] Meanwhile, the Groves lab has conducted pioneering work in the field of C–H radiofluorination, functionalising benzylic positions using a Mn-salen complex and unactivated C–H bonds with a Mn-porphyrin complex.[65,66] Groves and co-workers showed that this concept could be extended to decarboxylative radiofluorination using the same catalyst.[67] Applying a similar concept, Sanford and co-

workers disclosed a benzylic C–H radiofluorination proposed to proceed *via* a Pd(IV) intermediate.[68] Doyle and co-workers have also reported several transition metal-mediated ^{18}F-fluorination protocols. Using a Co-salen catalyst, the enantioselective preparation of high value ^{18}F-fluorohydrins, such as the radiotracer [^{18}F]FMISO ([^{18}F]**1.7**), was possible in a kinetic resolution of epoxide **1.8** (Scheme 1.3).[69] Her group also reported a Cu-mediated radiofluorination of α-diazocarbonyls.[70] In addition, the Doyle group have also demonstrated the proof-of-concept for [^{18}F]PyFluor as a reagent for nucleophilic aliphatic radiofluorination as well as a photoredox-catalysed nucleophilic radiofluorination of alkyl *N*-hydroxyphthalimide esters.[71,72]



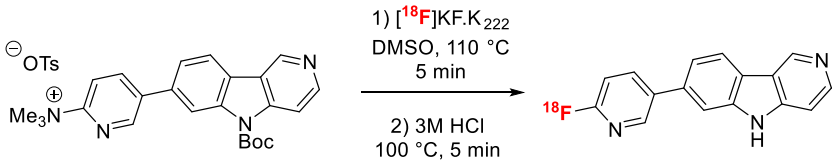
Scheme 1.3. *Enantioselective Co-mediated radiosynthesis of [^{18}F]FMISO ([^{18}F]**1.7**) by nucleophilic ^{18}F-fluorination of epoxide **1.8**.*

1.3.4. Nucleophilic Aromatic Radiofluorination

Analogous to aliphatic radiofluorination, the classical approach to the ^{18}F-fluorination of aromatic scaffolds is direct nucleophilic aromatic substitution (S_NAr) of a labile group with [^{18}F]fluoride.[73] This section aims to provide an overview of this concept and summarise other key routes to ^{18}F-fluoro(hetero)arenes, but the topic will be revisted in greater detail in the introduction of Chapter 3, where the development of a novel ^{18}F-S_NAr reaction using heteroaryl pyridinium salts is described.

S_NAr reactions with [^{18}F]fluoride rely on the presence of a suitable leaving group, most commonly halides (chloride, bromide, iodide), nitro groups or trialkylammonium salts (trimethylammonium, also those derived from DABCO). It is applied routinely in the synthesis of PET radiotracers, such as in the radiosynthesis of [^{18}F]Flortaucipir ([^{18}F]**1.9**) from trimethylammonium tosylate precursor **1.10**, and is well established in the field (Scheme

1.4).[74] Despite the simplicity of this disconnection, its application can be limited by reactivity challenges, as substitution is most efficient at specific positions in the case of heteroarenes and/or in the presence of electron-withdrawing functionality, such as nitro, cyano and carbonyl groups.[40] This has prompted radiochemists to devise new methods to access ^{18}F-fluoro(hetero)arenes.



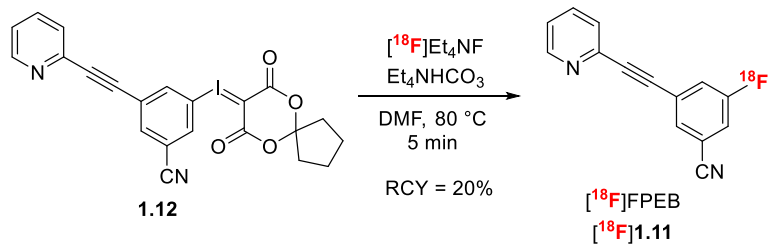
1.10 [^{18}F]Flortaucipir [^{18}F]**1.9**

Scheme 1.4. *Radiosynthesis of [^{18}F]Flortaucipir ([^{18}F]**1.9**) by nucleophilic aromatic substitution of a heteroaryl trimethylammonium tosylate precursor (**1.10**).*

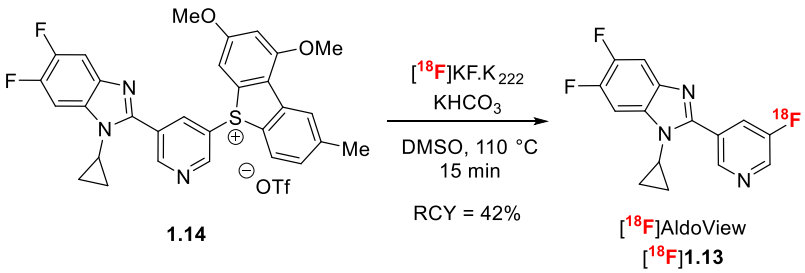
The first strategy involves the design of leaving groups with improved reactivity towards [^{18}F]fluoride. Aryl iodonium salts display excellent substitution reactivity for the preparation of aryl ^{18}F-fluorides. An early report from Pike and Aigbirhio demonstrated that diaryliodonium salts were suitable substrates for ^{18}F-fluorination.[75] They also observed that unsymmetrical diaryliodoniums could give rise to product mixtures. Over the next two decades, radiochemists continued to investigate this reactivity. Coenen and co-workers found that a 2-thienyl substituent was largely unreactive to substitution, which improved the selectivity of the reaction,[76] while Sanford, Scott and co-workers disclosed that the use of a Cu(I) catalyst in the radiofluorination of (mesityl)(aryl)iodonium tetrafluoroborates allowed the reaction to proceed in higher radiochemical yields and operate at lower temperatures.[77] Vasdev, Liang and co-workers proposed a spirocyclic class of iodine(III) precursors, which proved to be effective for the radiosynthesis of ^{18}F-fluoroarenes, including the radiotracer [^{18}F]FPEB ([^{18}F]**1.11**) (Scheme 1.5).[78,79]

In addition to iodonium precursors, sulfonium salts have also emerged as useful substrates for ^{18}F-fluorination. An early proof-of-concept from the 1980s from Maeda and co-workers demonstrated the feasibility of using dimethylsulfonium salts as radiofluorination

substrates.[80] Over 20 years later, Ametamey and co-workers presented the improved reactivity of diphenyl(aryl)sulfonium salts towards [^{18}F]fluoride with an expanded scope of products, however as with the iodonium salts, these could react with low selectivity, giving [^{18}F]fluorobenzene as a by-product.[81] Årstad and co-workers next discovered that 4-methoxyphenyl groups delivered improved regioselectivity, [82] which was followed by a ring-closing synthesis of a novel class of dibenzothiophene derived sulfonium salts and their application in aromatic ^{18}F-fluorination.[83] Since then, sulfonium precursors have found ample use in the synthesis of PET radiotracers, e.g. [^{18}F]AldoView ([^{18}F]**1.13**) from sulfonium salt **1.14**.[84] Ritter and co-workers also showed that these substrates could be conveniently formed by aromatic C–H functionalisation using dibenzothiophene *S*-oxide.[85]



Scheme 1.5. *Radiosynthesis of [^{18}F]FPEB ([^{18}F]**1.11**) by nucleophilic aromatic substitution of a spirocyclic iodine(III) precursor (**1.12**).*



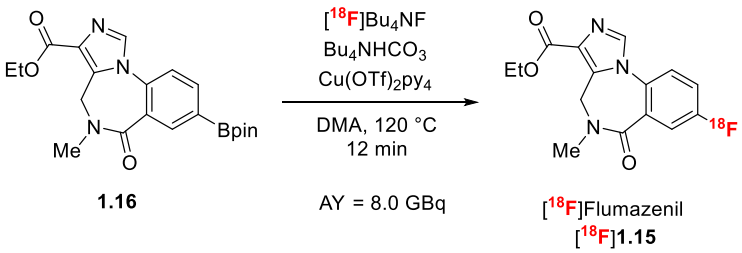
Scheme 1.6. *Radiosynthesis of [^{18}F]AldoView ([^{18}F]**1.13**) by nucleophilic aromatic substitution of a sulfonium triflate precursor (**1.14**).*

Other activated precursors have been disclosed, including Ritter and co-workers' ^{18}F-deoxyfluorination platform using imidazolium intermediates derived from phenols.[86] Specific attention to deaminative approaches to ^{18}F-fluoroarenes will be given later in Chapter 3.

The second strategy to access ^{18}F-fluoroarenes has been to embrace the chemistry of transition metals to overcome challenges with direct *ipso*-substitution of leaving groups with [^{18}F]fluoride.

Ritter, Hooker and co-workers disclosed early studies into the use of high-valent Pd and Ni aryl complexes with [^{18}F]fluoride to achieve aromatic ^{18}F-fluorination *via* reductive elimination.[87,88] Ritter and co-workers also later investigated the use of Ru-complexes in their ^{18}F-deoxyfluorination system, which were suggested to improve reactivity and scope of accessible arenes.[89]

The advent of Cu-mediated radiofluorination has had an appreciable impact on the field since it was first disclosed by Gouverneur and co-workers in 2014. In this report, they describe that the use of a Cu(II) triflate complex enabled access to ^{18}F-fluoroarenes from convenient aryl boronic pinacol ester precursors and [^{18}F]fluoride.[90] A separate report from Sanford, Scott and co-workers achieved the same transformation from aryl boronic acids with a Cu(II) additive and they later demonstrated the applicability of aryl stannanes to Cu mediated radiofluorination.[91,92] Cu-mediated radiofluorination has also been extended to C–H ^{18}F-fluorination of electron-rich (hetero)arenes and directed halogen exchange (halex) processes.[93,94] These reactions have been extensively studied for the preparation of PET radiotracers,[95,96] including their automation and cGMP-compliant production,[97,98] such as in the recent synthesis of the PET radiotracer [^{18}F]flumazenil ([^{18}F]**1.15**) from the aryl pinacol boronate **1.16** by Tredwell, Gouverneur and co-workers (Scheme 1.7).[99]



1.16

[^{18}F]Flumazenil
[^{18}F]**1.15**

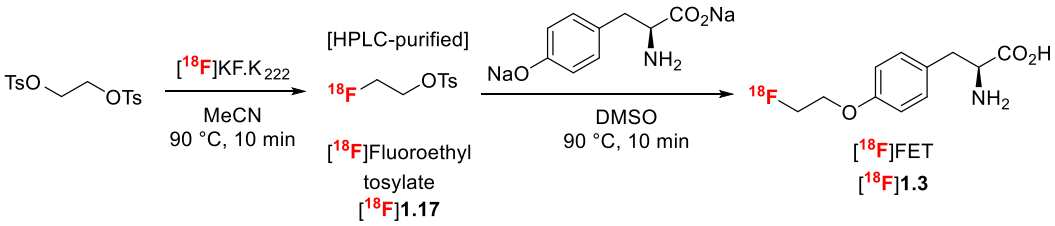
Scheme 1.7. *Automated radiosynthesis (Trasis AllinOne) of [^{18}F]Flumazenil ([^{18}F]**1.15**) by copper-mediated radiofluorination of aryl pinacol boronate precursor **1.16**.*

Emerging technologies, such as photochemistry, have made an important contribution to the preparation of ^{18}F-fluoroarenes. The groups of Nicewicz and Li have reported several methods allowing access to such products. In 2019, they reported an organophotoredox-mediated oxidative C–H ^{18}F-fluorination of arenes and in a follow-up study from 2020, they report modified conditions allowing the reaction to take place under LED rather than laser irradiation and without the need for an O_2 atmosphere.[100,101] Further applications of their oxidative photoredox ^{18}F-fluorination platform include a halex radiofluorination of aryl halides and a deoxygenative radiofluorination of aromatic ethers.[102,103]

1.3.5. ^{18}F-Fluoroalkylation

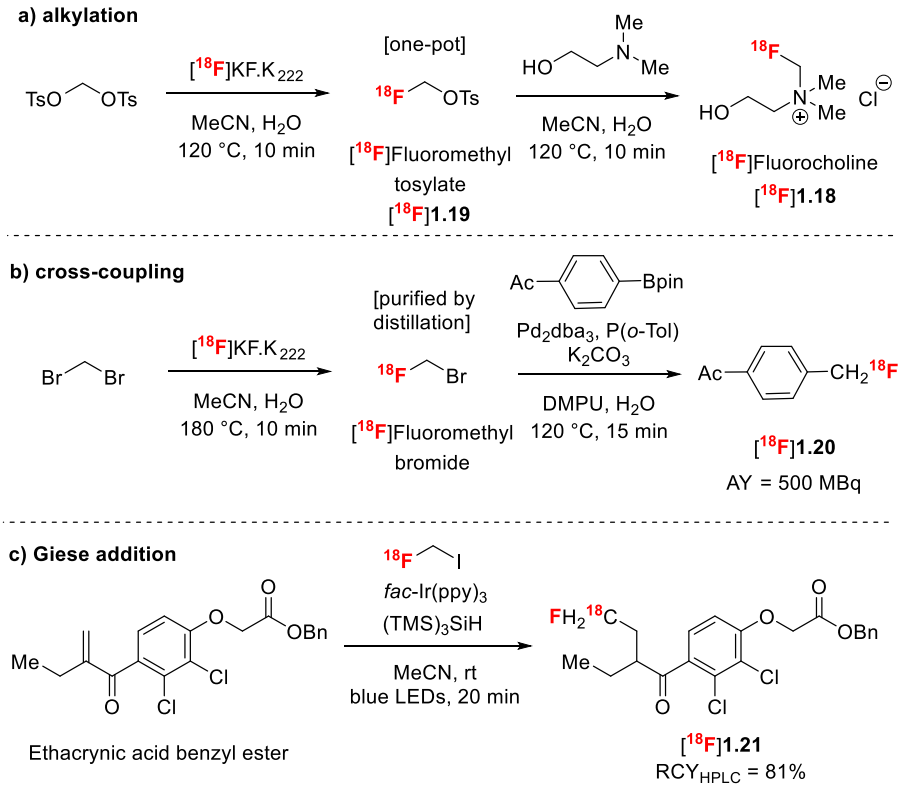
In contrast to sections 1.3.3 and 1.3.4, which concern direct ^{18}F-fluorination with [^{18}F]fluoride, this section will summarise some key reports to date on the use of radiolabelled reagents prepared from [^{18}F]fluoride for ^{18}F-fluoroalkylation. For an exhaustive account of this radiochemistry, a recent review on the topic by Vugts and co-workers is recommended.[104] Chapter 2 of this thesis describes the use of an ^{18}F-labelled reagent for ^{18}F-difluoromethylation.

The most widely used reagent for ^{18}F-fluoroalkylation chemistry is [^{18}F]fluoroethyl tosylate ([^{18}F]**1.17**), as it is easily prepared (under manual or automated radiosynthesis) and conveniently purified by HPLC due to its UV absorbance, but other halide or sulfonate derivatives are also used.[104,105] The ^{18}F-fluoroethyl group is often chosen as a prosthetic group, as it can be easily installed and has a good stability profile relative to the ^{18}F-fluoromethyl group.[105] Conventionally, [^{18}F]**1.17** is used in *O*- or *N*-alkylations, such as in an early radiosynthesis of [^{18}F]FET ([^{18}F]**1.3**) that proceeded *via O*-alkylation of the disodium salt of tyrosine with [^{18}F]**1.17** (Scheme 1.8).[23] This has now been superseded by a direct single step radiosynthesis.[106]



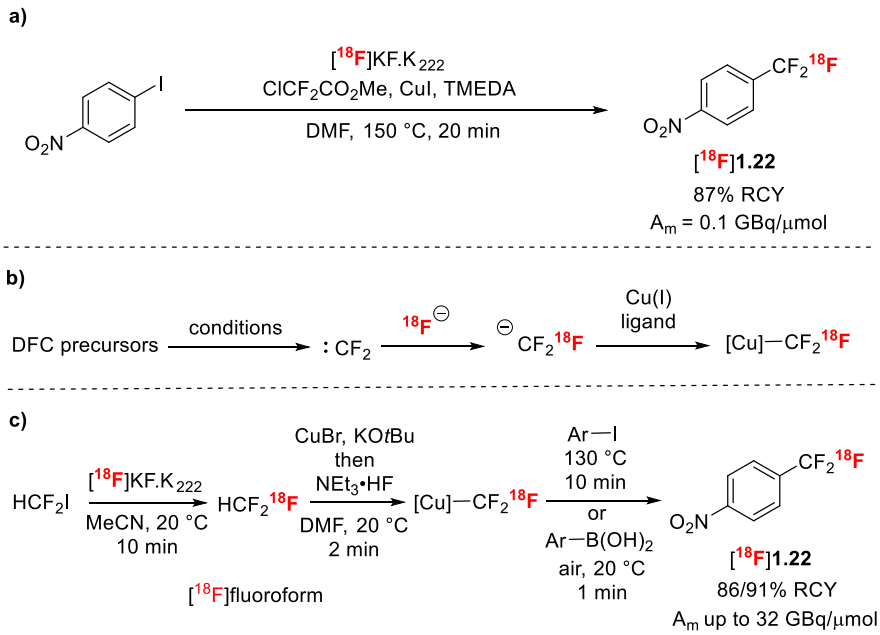
Scheme 1.8. *^{18}F-fluoroethylation of tyrosine with [^{18}F]fluoroethyl tosylate ([^{18}F]**1.17**) for the radiosynthesis of [^{18}F]FET ([^{18}F]**1.3**)*

^{18}F-Fluoromethylation can also be achieved using [^{18}F]fluoromethyl halides or sulfonates as reagents (Scheme 1.9). Alkylation of heteroatoms is possible with these reagents, such as in the preparation of [^{18}F]fluorocholine ([^{18}F]**1.18**) from [^{18}F]fluoromethyl tosylate ([^{18}F]**1.19**) (Scheme 1.9 a).[107] A Pd-mediated cross-coupling of [^{18}F]fluoromethyl bromide or iodide with aryl boronates analogous to prior work on ^{11}C-methylation has also been reported, e.g. [^{18}F]**1.20** could be prepared in AY of 500 MBq (Scheme 1.9 b).[108] Gouverneur and co-workers also disclosed the application of [^{18}F]fluoromethyl iodide in Giese-type addition to alkenes in 2021 (Scheme 1.9 c).[109] This included [^{18}F]**1.21** (a ^{18}F-fluoromethylated derivative of ethacrynic acid).



Scheme 1.9. *^{18}F-fluoromethylation via a) heteroatom alkylation, b) Pd-mediated cross-coupling of aryl boronic esters c) Giese-type addition to alkenes.*

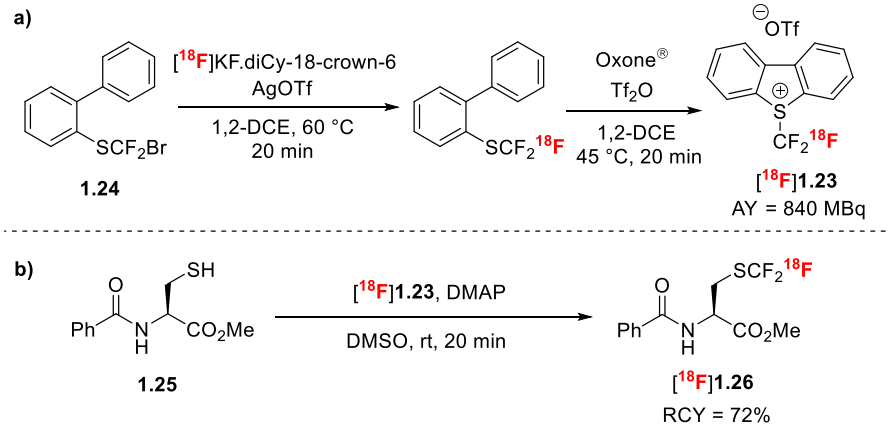
Several groups have also reported ^{18}F-trifluoromethylation using labelled reagents. The first report of ^{18}F-trifluoromethylation of arenes was disclosed by Gouverneur, Passchier and co-workers in 2013 (Scheme 1.10 a).[110] Using aryl iodide substrates, they demonstrated that a [^{18}F]$CuCF_3$ complex that was formed *in situ* from the difluorocarbene (DFC)-releasing reagent methyl chlorodifluoroacetate, [^{18}F]fluoride and CuI was effective for aromatic ^{18}F-trifluoromethylation. Other groups investigated alternative routes to this key [^{18}F]$CuCF_3$ complex, finding that it could be prepared from other DFC reagents, such as difluoromethyl diaryl sulfonium salts or difluoroiodomethane, which can be activated under various conditions (Scheme 1.10 b).[111,112] Vugts and co-workers also proposed the preparation of [^{18}F]fluoroform gas, which was accessible in higher A_m, for the preparation of the [^{18}F]$CuCF_3$ complex.[113] The A_m of [^{18}F]**1.22** as prepared by Gouverneur and co-workers was 0.1 GBq/µmol, while Vugts and co-workers reported a value in the range of 22–32 GBq/µmol (Scheme 1.10 c), achieved by optimisation of reaction temperature and reducing the loading of difluoroiodomethane by 40-fold. They also report conditions for the ^{18}F-trifluoromethylation of aryl boronic acids, which could provide the radiolabelled product in improved yield over the aryl iodide.



Scheme 1.10. *^{18}F-trifluoromethylation of arenes. a) Gouverneur's first report, b) proposed mechanism of the formation of the [^{18}F]$CuCF_3$ complex c) Vugts and co-workers' route via [^{18}F]fluoroform and cross-coupling of aryl boronic acids.*

Vugts and co-workers later reported the synthesis of the Ruppert-Prakash reagent ($TMSCF_3$) in radiolabelled form and its application in radiosynthesis.[114] This reagent has found extensive use in organic synthesis for fluoroalkylation.[115] [^{18}F]$TMSCF_3$ was prepared *via* the deprotonation of [^{18}F]fluoroform with KHMDS, addition to TMSCl and distillation. They demonstrated its radiosynthetic utility with its addition to aromatic ketones.

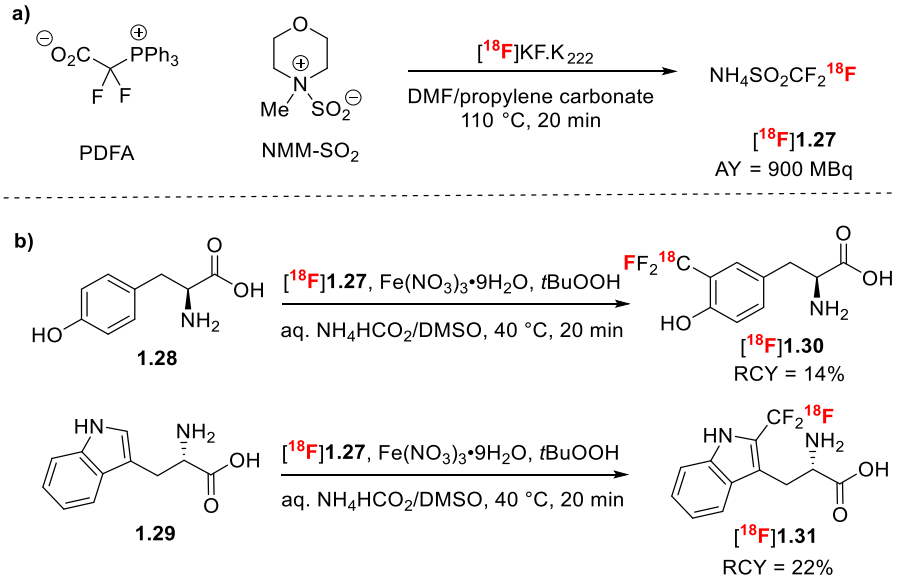
Gouverneur and co-workers have investigated the radiosyntheses of multiple reagents for ^{18}F-trifluoromethylation. Their first report described the preparation of 5-^{18}F-(trifluoromethyl)dibenzothiophenium trifluoromethanesulfonate ([^{18}F]**1.23**, commonly referred to as Umemoto's reagent) (Scheme 1.11).[116] This was achieved in a two-step radiosynthesis, where Gouverneur and co-workers utilised their Ag-promoted halex ^{18}F-fluorination to convert bromodifluoromethyl sulfide **1.24** to the ^{18}F-trifluoromethyl sulfide, which could then undergo an oxidative cyclisation with Oxone® and triflic anhydride to yield [^{18}F]**1.23**. The use of this reagent to radiolabel peptides *via* *S*-^{18}F-trifluoromethylation was disclosed, and it was shown to be effective in transferring the [^{18}F]CF_3 group to cysteine residues. For example, methyl ester and benzamide-protected **1.25** was converted to the *S*-^{18}F-trifluoromethylated compound [^{18}F]**1.26** in 72% RCY.



Scheme 1.11. *^{18}F-trifluoromethylation of amino acids and peptides with [^{18}F]**1.23**.*

Gouverneur and co-workers further expanded on their previous work on the ^{18}F-trifluoromethylation of peptides with the radiosynthesis of ammonium [^{18}F]trifluoromethanesulfinate ([^{18}F]**1.27**, commonly referred to as the Langlois reagent)

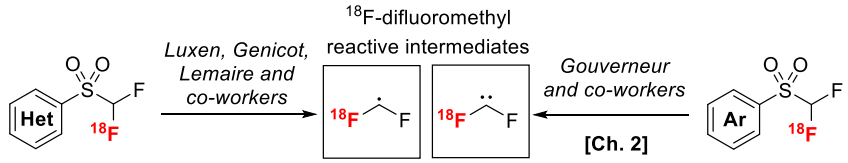
(Scheme 1.12).[117] This reagent can act as a source of the trifluoromethyl radical, which can react with electron-rich amino acid residues, such as tyrosine and tryptophan. [^{18}F]**1.27** was prepared applying a multi-component strategy similar to the radiosynthesis of the [^{18}F]$CuCF_3$ complex used for the ^{18}F-trifluoromethylation of aryl iodides. A DFC precursor (2,2-difluoro-2-(triphenylphosphonio)acetate, PDFA) was reacted with [^{18}F]fluoride and an SO_2-surrogate; the optimal source being *N*-methylmorpholine·SO_2 (NMM·SO_2). This allowed for the preparation of [^{18}F]**1.27** in an AY of 900 MBq. This process was automated using an Advion NanoTek microfluidic synthesiser. They next demonstrated that [^{18}F]**1.27** could release [^{18}F]CF_3 radicals under oxidising conditions for conjugation to peptides. For example, unprotected tyrosine (**1.28**) and tryptophan (**1.29**) could be ^{18}F-trifluoromethylated in up to 14% ([^{18}F]**1.30**) and 22% RCY ([^{18}F]**1.31**), respectively.



Scheme 1.12. *^{18}F-trifluoromethylation of amino acids and peptides with [^{18}F]**1.27**.*

Beyond ^{18}F-trifluoromethylation and ^{18}F-fluoromethylation, progress has also been made in the realm of ^{18}F-difluoromethylation (Scheme 1.13). This topic will be the subject of the work described in Chapter 2 and a detailed account is provided in section 2.1.3. The work to date in this area has centred around the radiosynthesis of labelled reagents that release ^{18}F-difluoromethyl reactive intermediates. Luxen, Genicot, Lemaire and co-workers have developed a [^{18}F]CF_2H radical-releasing reagent and described its application in Minisci-type

addition to heterocycles.[118] Gouverneur and co-workers have developed a class of [^{18}F]difluorocarbene (DFC)-releasing reagents and described their reactivity towards various reaction partners (Chapter 2).



Scheme 1.13. *^{18}F-difluoromethylation.*

1.4. Thesis Outline

As demonstrated by the account in section 1.3, radiochemists have made significant advances in the preparation of radiofluorinated compounds. Despite the huge progress that has been made to date, the preparation of many fluorine-18-containing molecules still presents substantial challenges. Expansion of the radiochemical space beyond what is currently accessible is crucial in providing new avenues for the discovery of new-generation PET radioligands. This will ultimately be driven by the development of novel reactivity, which facilitates access to compounds that were otherwise impossible or challenging to prepare with existing methods. Central to this challenge is the development of methods that can exploit ubiquitous precursor types as substrates. The bottleneck introduced into the PET ligand discovery process is substantial, especially if several structurally related analogues are to be assessed. Readily accessible substrate classes than can be subjected to late-stage ^{18}F-fluorination or fluoroalkylation should therefore be prioritised.

This first chapter has provided an overview of the principles of PET imaging, the key concepts relating to PET radiochemistry, as well as a brief account of progress in fluorine-18 radiochemistry to date, with a focus on the organic chemistry of [^{18}F]fluoride and synthons prepared from it.

Chapter 2 will describe the development of an ^{18}F-difluoromethylation platform centred around the reactive intermediate [^{18}F]difluorocarbene ([^{18}F]DFC). Starting from a first

generation ^{18}F-reagent, which had been applied previously to *O*,*S*,*N*-^{18}F-difluoromethylation, this chapter first describes the design of a second-generation reagent with improved properties including higher reactivity and A_m. The optimisation of an automated protocol to prepare these reagents and their application to radiotracer synthesis and preclinical PET imaging is next disclosed. This chapter also discusses the development and optimisation of a novel Pd-mediated cross-coupling with [^{18}F]DFC and its application to the radiosynthesis of ^{18}F-difluoromethylarenes from aryl boronic acids. A chemodivergent ^{18}F-difluoromethoxylation of complex aryl boronic acid substrates is also described.

Chapter 3 will focus on the development of a novel ^{18}F-fluorodeamination of aminoheterocycles, proceeding *via* pyridinium tetrafluoroborate intermediates. The optimisation and the discovery of the reaction is first described, followed by its application to the radiosynthesis of a scope of over 30 ^{18}F-fluoroheteroarenes. The development of a one-pot protocol exploiting crude pyridinium salts obtained from heteroanilines, as well as the propensity of pyridinium salts to act as elution reagents for [^{18}F]fluoride is also investigated. Finally, the automation of the reaction and isolation of three bioactive heteroaromatic ^{18}F-fluorides is discussed and comparison to existing literature methods is provided.

Detailed experimental procedures for the work described herein, including chemical and radiochemical synthesis and the full characterisation of novel compounds is given in Chapter 4.

1.5. References

1 Waterton, J. C. Medical Imaging: Overview and the Importance of Contrast. In Biomedical Imaging: The Chemistry of Labels, Probes and Contrast Agents, 1st ed.; M. Braddock, Ed.; The Royal Society of Chemistry, 2011, pp. 1–20.

2 Law, G.-L.; Wong, W.-T. An Introduction to Molecular Imaging. In The Chemistry of Molecular Imaging, 1st ed.; Wong, W-T.; Long, N., Eds.; John Wiley & Sons, 2015; pp 1–24.

3 Phelps, M. E. Positron emission tomography provides molecular imaging of biological processes. *Proc*. *Natl*. *Acad*. *Sci*. **2000**, *97* (16), 9226–9233.120

4 Ametamey, S. M.; Honer, M.; Schubiger, P. A. Molecular Imaging with PET. *Chem*. *Rev*. **2008**, *108* (5), 1501–1516.

5 Rong, J.; Haider, A.; Jeppesen, T. E.; Josephson, L.; Liang, S. H. Radiochemistry for positron emission tomography. *Nat*. *Commun*. **2023**, *14*, 3257.
6 Basu, S.; Hess, S; Nielsen Braad, P. E.; Brinkmann Olsen, B.; Inglev, S.; Høilund-Carlsen, P. F. The Basic Principles of FDG-PET/CT Imaging. *PET Clin.* **2014**, *9* (4), 355–370.
7 Gambhir, S. S. Molecular imaging of cancer with positron emission tomography. *Nat*. *Rev*. *Cancer* **2002**, *2* (9), 683–693.
8 Nordberg, A.; Rinne, J. O.; Kadir, A.; Långström, B. The use of PET in Alzheimer disease. *Nat*. *Rev*. *Neurol.* **2010**, *6* (2), 78–87.
9 Rudin, M.; Weissleder, R. Molecular imaging in drug discovery and development. *Nat. Rev. Drug Discov.* **2003**, *2*, 123–131.
10 Willmann, J.; van Bruggen, N.; Dinkelborg, L.; Gambhir, S. S. Molecular imaging in drug development. *Nat. Rev. Drug Discov.* **2008**, *7* (7), 591–607.
11 Nerella, S. G.; Singh, P.; Sanam, T.; Digwal, C. S. PET Molecular Imaging in Drug Development: The Imaging and Chemistry Perspective. *Front*. *Med*. **2022**, *9*, 812270.
12 Varrone, A.; Bundgaard, C.; Bang-Andersen, B. PET as a Translational Tool in Drug Development for Neuroscience Compounds. *Clin*. *Pharmacol*. *Ther*. **2022**, *111* (4), 774–785.
13 Luo, X.; Tan, B.; Zhao, X.; Zhang, Z.; Wang, G.; Wang, T.; Xing, B.; Song, A. Harnessing the power of molecular imaging for drug discovery and development. *iRADIOLOGY* **2023**, *1* (4), 362–377.
14 Patel, S.; Schmidt, K.; Hesterman, J.; Hoppin, J. Advancing Drug Discovery and Development Using Molecular Imaging (ADDMI): an Interest Group of the World Molecular Imaging Society and an Inaugural Session on Positron Emission Tomography (PET). *Mol. Imaging Biol*. **2017**, *19* (3), 348–356.
15 Miller, P.; Long, N.; Vilar, R.; Gee, A. Synthesis of ^{11}C, ^{18}F, ^{15}O, and ^{13}N Radiolabels for Positron Emission Tomography. *Angew*. *Chem*. *Int*. *Ed*. **2008**, *47* (47), 8998–9033.
16 Yoon, J.-K.; Park, B.-N.; Ryu, E.-K.; An, Y.-S.; Lee, S.-J. Current Perspectives on ^{89}Zr-PET Imaging. *Int*. *J*. *Mol*. *Sci*. **2020**, *21* (12), 4309.
17 Jødal, L.; Le Loirec, C.; Champion, C. Positron range in PET imaging: an alternative approach for assessing and correcting the blurring. *Phys*. *Med*. *Biol*. **2012**, *57* (12), 3931–3943.
18 Jødal, L.; Le Loirec, C.; Champion, C. Positron range in PET imaging: non-conventional isotopes. *Phys*. *Med*. *Biol*. **2014**, *59* (23), 7419–7434.
19 Guillaume, M.; Luxen, A.; Nebeling, B.; Argentini, M.; Clark, J. C.; Pike, V. W. Recommendations for fluorine-18 production. *Appl. Radiat. Isot.* **1991**, *42* (8), 749–762.
20 Jacobson, O.; Kiesewetter, D. O.; Chen, X. Fluorine-18 Radiochemistry, Labeling Strategies and Synthetic Routes. *Bioconjugate Chem*. **2015**, *26* (1), 1–18.
21 Cai, L.; Lu, S.; Pike, V. W. Chemistry with [^{18}F]Fluoride Ion. *Eur*. *J*. *Org*. *Chem*. **2008**, *2008* (17), 2853–2873.
22 Minn, H.; Kauhanen, S.; Seppänen, M.; Nuutila, P. ^{18}F-FDOPA: A Multiple-Target Molecule. *J*. *Nucl*. *Med*. **2009**, *50* (12) 1915–1918.
23 Wester, H. J.; Herz, M.; Weber, W.; Heiss, P.; Senekowitsch-Schmidtke, R.; Schwaiger, M.; Stöcklin, G. Synthesis and Radiopharmacology of *O*-(2-[^{18}F]fluoroethyl)-L-Tyrosine for Tumor Imaging. *J*. *Nucl*. *Med*. **1999**, *40* (1) 205–212.
24 Grant, F. D.; Fahey, F. H.; Packard, A. B.; Davis, R. T.; Alavi, A.; Treves, S. T. Skeletal PET with ^{18}F-Fluoride: Applying New Technology to an Old Tracer. *J*. *Nucl*. *Med*. **2008**, *49* (1) 68–78.
25 Purser, S.; Moore, P. R.; Swallow, S. Gouverneur, V. Fluorine in medicinal chemistry. *Chem*. *Soc*. *Rev*. **2008**, *37* (2), 320–330

26 O'Hagan, D. Understanding organofluorine chemistry. An introduction to the C–F bond. *Chem. Soc. Rev.* **2008**, *37* (2), 308–319.

27 Inoue, M.; Sumii, Y.; Shibata, N. Contribution of Organofluorine Compounds to Pharmaceuticals. *ACS Omega* **2020**, *5* (19), 10633–10640.

28 Ogawa, Y.; Tokunaga, E.; Kobayashi, O.; Hirai, K.; Shibata, N. Current Contributions of Organofluorine Compounds to the Agrochemical Industry. *iScience* **2020**, *23* (9), 101467.

29 Gillis, E. P.; Eastman, K. J.; Hill, M. D.; Donnelly, D. J.; Meanwell, N. A. Applications of Fluorine in Medicinal Chemistry. *J*. *Med*. *Chem*. **2015**, *58* (21), 8315–8359.

30 Jeffries, B.; Wang, Z.; Felstead, H. R.; Le Questel, J.-Y.; Scott, J. S.; Chiarparin, E.; Graton, J.; Linclau, B. Systematic Investigation of Lipophilicity Modulation by Aliphatic Fluorination Motifs. *J*. *Med*. *Chem*. **2020**, *63* (3), 1002–1031.

31 Thiehoff, C.; Rey, Y. P.; Gilmour, R. The Fluorine Gauche Effect: A Brief History. *Isr*. *J*. *Chem*. **2017**, *57* (1-2), 92–100.

32 Rosenblum, S. B.; Huynh, T.; Afonso, A.; Davis, H. R.; Yumibe, N.; Clader, J. W.; Burnett, D. A. Discovery of 1-(4-Fluorophenyl)-(3*R*)-[3-(4-fluorophenyl)-(3*S*)- hydroxypropyl]-(4*S*)-(4-hydroxyphenyl)-2-azetidinone (SCH 58235): A Designed, Potent, Orally Active Inhibitor of Cholesterol Absorption. *J*. *Med*. *Chem*. **1998**, *41* (6), 973–980.

33 Meanwell, N. A. Fluorine and Fluorinated Motifs in the Design and Application of Bioisosteres for Drug Design. *J*. *Med*. *Chem*. **2018**, *61* (14), 5822–5880.

34 Pan, Y. The Dark Side of Fluorine. *ACS Med*. *Chem*. *Lett*. **2019**, *10* (7), 1016–1019.

35 Young, R. J.; O'Hagan, D. Future challenges and opportunities with fluorine in drugs? *Med*. *Chem*. *Res*. **2023**, *32*, 1231–1234.

36 Hammel, E.; Webster, T. F.; Gurney, R.; Heiger-Bernays, W. Implications of PFAS definitions using fluorinated pharmaceuticals. *iScience* **2022**, *25* (4), 104020.

37 Holland, J. P. Chemical Kinetics of Radiolabelling Reactions. *Chem*. *Eur*. *J*. **2018**, *24* (62), 16472–16483.

38 Liang, T.; Neumann, C.N.; Ritter, T. Introduction of Fluorine and Fluorine-Containing Functional Groups. *Angew*. *Chem*. *Int*. *Ed*. **2013**, *52* (32), 8214–8264.

39 Chi, Y.-T.; Chu, P.-C.; Chao, H.-Y.; Shieh, W.-C.; Chen, C. C. Design of cGMP Production of ^{18}F- and ^{68}Ga-Radiopharmaceuticals, *BioMed Res*. *Int*. **2014**, *2014*, 680195.

40 Halder; R.; Ritter, T. ^{18}F-Fluorination: Challenge and Opportunity for Organic Chemists. *J*. *Org*. *Chem*. **2021**, *86* (20), 13873–13884.

41 Zanzonico, P.; Dauer, L.; St Germain, J. Operational radiation safety for PET-CT, SPECT-CT, and cyclotron facilities. *Health Phys*. **2008**, *95*(5), 554–570.

42 Barnes, C.; Nair, M.; Aboagye, E. O.; Archibald, S. J.; Allott, L. A practical guide to automating fluorine-18 PET radiochemistry using commercially available cassette-based platforms. *React*. *Chem*. *Eng*. **2022**, *7* (11), 2265–2279.

43 Collet, C.; Otabashi, M.; Giacomelli, F.; Veran, N.; Karcher, G.; Chapleur, Y.; Lamandé-Langle, S. Fully automated production of sodium [^{18}F]fluoride on AllInOne and miniAllInOne synthesizers. *Appl*. *Radiat*. *Isot*. **2015**, *102*, 87–92.

44 Andersen, V. L.; Soerensen, M. A.; Dam, J. H.; Langkjaer, N.; Petersen, H.; Bender, D. A.; Fugloe, D.; Huynh, T. H. V. GMP production of 6-[^{18}F]Fluoro-L-DOPA for PET/CT imaging by different synthetic routes: a three center experience. *EJNMMI Radiopharm*. *Chem*. **2021**, *6*, 21.

45 Shetty, H. U.; Morse, C. L.; Pike, V. W. Tandem Mass Spectrometry as an Independent Method for Corroborating Fluorine-18 Radioactivity Measurements in Positron Emission Tomography. *ACS Measurement Science Au* **2022**, *2* (4), 370–376.

46 Coenen, H. H.; Gee, A. D.; Adam, M.; Antoni, G.; Cutler, C. S.; Fujibayashi, Y.; Jeong, Y. M.; Mach, R. H.; Mindt, T. L.; Pike, V. W.; Windhorst, A. D. Consensus nomenclature rules for radiopharmaceutical chemistry — Setting the record straight. *Nucl*. *Med*. *Biol*. **2017**, *55*, v–xi.

47 Coenen, H. H.; Gee, A. D.; Adam, M.; Antoni, G.; Cutler, C. S.; Fujibayashi, Y.; Jeong, Y. M.; Mach, R. H.; Mindt, T. L.; Pike, V. W.; Windhorst, A. D. Status of the 'consensus nomenclature rules in radiopharmaceutical sciences' initiative. *Nucl*. *Med*. *Biol*. **2019**, 71, 19–22.

48 Luurtsema, G.; Pichler, V.; Bongarzone, S.; Seimbille, Y.; Elsinga, P.; Gee, A.; Vercouillie, J. EANM guideline for harmonisation on molar activity or specific activity of radiopharmaceuticals: impact on safety and imaging quality. *EJNMMI Radiopharm*. *Chem*. **2021**, *6*, 34.

49 McCluskey, S. P.; Plisson, C.; Rabiner, E. A.; Howes, O. Advances in CNS PET: the state-of-the-art for new imaging targets for pathophysiology and drug development. *Eur*. *J*. *Nucl*. *Med*. *Mol*. *Imaging* **2020**, *47* (2), 451–489.

50 Mou, Z.; Zhu, Y.; Zhang, L.; Ma, M.; Li, Z.; Guo, Y.; Zheng, J.; Zhao, Z.; Zhang, K.; Chen, X.; Li, Z. "AquaF" Building Blocks for Water-Compatible S_N2 ^{18}F-Fluorination of Small-Molecule Radiotracers. *J*. *Am*. *Chem*. *Soc*. **2024**, *146* (25), 17517–17529.

51 Bernard-Gauthier, V.; Wängler, C.; Schirrmacher, E.; Kostikov, A.; Jurkschat, K.; Wängler, B.; Schirrmacher, R. ^{18}F-Labeled Silicon-Based Fluoride Acceptors: Potential Opportunities for Novel Positron Emitting Radiopharmaceuticals. *Biomed*. *Res*. *Int*. **2014**, *2014*, 454503.

52 Archibald, S. J.; Allott, L. The aluminium-[^{18}F]fluoride revolution: simple radiochemistry with a big impact for radiolabelled biomolecules. *EJNMMI Radiopharm*. *Chem*. **2021**, *6*, 30.

53 Deng, H.; Cobb, S. L.; Gee, A. D.; Lockhart, A.; Martarello, L.; McGlinchey, R. P.; O'Hagan, D.; Onega, M. Fluorinase mediated C–^{18}F bond formation, an enzymatic tool for PET labelling. *Chem*. *Commun*. **2006**, *2006* (6), 652–654.

54 Haveman, L. Y. F.; Vugts, D. J.; Windhorst, A. D. State of the art procedures towards reactive [^{18}F]fluoride in PET tracer synthesis. *EJNMMI Radiopharm*. *Chem*. **2023**, *8*, 28.

55 Mossine, A. V.; Brooks, A. F.; Ichiishi, N.; Makaravage, K. J.; Sanford, M. S.; Scott, P. J. H. Development of Customized [^{18}F]Fluoride Elution Techniques for the Enhancement of Copper-Mediated Late-Stage Radiofluorination. *Sci*. *Rep*. **2017**, *7*, 233.

56 Inkster, J. A. H.; Akurathi, V.; Sromek, A. W.; Chen, Y.; Neumeyer, J. L.; Packard, A. B. A non-anhydrous, minimally basic protocol for the simplification of nucleophilic ^{18}F-fluorination chemistry. *Sci*. *Rep*. **2020**, *10*, 6818.

57 Bratteby, K.; Shalgunov, V.; Battisti, U. M.; Petersen, I. N.; van den Broek, S. L.; Ohlsson, T.; Gillings, N.; Erlandsson, M.; Herth, M. M. Insights into Elution of Anion Exchange Cartridges: Opening the Path toward Aliphatic ^{18}F-Radiolabeling of Base-Sensitive Tracers. *ACS Pharmacol*. *Transl*. *Sci*. **2021**, *4* (5), 1556–1566.

58 Richarz, R.; Krapf, P.; Zarrad, F.; Urusova, E. A.; Neumaier, B.; Zlatopolskiy, B. D. Neither azeotropic drying, nor base nor other additives: a minimalist approach to ^{18}F-labeling. *Org*. *Biomol*. *Chem*. **2014**, *12* (40), 8094–8099.

59 Zhang, B.; Fraser, B. H.; Klenner, M. A.; Chen, Z.; Liang, S. H.; Massi, M.; Robinson, A. J.; Pascali, G. [^{18}F]Ethenesulfonyl Fluoride as a Practical Radiofluoride Relay Reagent. *Chem*. *Eur*. *J*. **2019**, *25* (32), 7613–7617.

60 Pees, A.; Sewing, C.; Vosjan, M. J. W. D.; Tadino, V.; Herscheid, J. D. M.; Windhorst, A. D.; Vugts, D. J. Fast and reliable generation of [^{18}F]triflyl fluoride, a gaseous [^{18}F]fluoride source. *Chem*. *Commun*. **2018**, *54* (72), 10179–10182.

61 Bratteby, K.; Shalgunov, V.; Herth, M. M. Aliphatic ^{18}F-Radiofluorination: Recent Advances in the Labeling of Base-Sensitive Substrates. *ChemMedChem*, **2021**, *16* (17), 2612–2622.
62 Huhtala, T.; Poutiainen, P.; Rytkönen, J.; Lehtimäki, K.; Parkkari, T.; Kasanen, I.; Airaksinen, A. J.; Koivula, T.; Sweeney, P.; Kontkanen, O.; Wityak, J.; Dominiquez, C.; Park, L. C. Improved synthesis of [^{18}F]fallypride and characterization of a Huntington's disease mouse model, zQ175DN KI, using longitudinal PET imaging of D2/D3 receptors. *EJNMMI Radiopharm*. *Chem*. **2019**, *4*, 20.
63 Hollingworth, C.; Hazari, A.; Hopkinson, M. N.; Tredwell, M.; Benedetto, E.; Huiban, M.; Gee, A. D.; Brown, J. M.; Gouverneur, V. Palladium-Catalyzed Allylic Fluorination. *Angew*. *Chem*. *Int*. *Ed*. **2011**, *50* (11), 2613–2617.
64 Mixdorf, J. C.; Sorlin, A. M.; Dick, D. W.; Nguyen, H. M. Iridium-Catalyzed Radiosynthesis of Branched Allylic [^{18}F]Fluorides. *Org*. *Lett*. **2019**, *21* (1), 60–64.
65 Huang, X.; Liu, W.; Ren, H.; Neelamegam, R.; Hooker, J. M.; Groves, J. T. Late Stage Benzylic C–H Fluorination with [^{18}F]Fluoride for PET Imaging. *J*. *Am*. *Chem*. *Soc*. **2014**, *136* (19), 6842–6845.
66 Liu, W.; Huang, X.; Placzek, M. S.; Krska, S. W.; McQuade, P.; Hooker, J. M.; Groves, J. T. Site-selective ^{18}F fluorination of unactivated C–H bonds mediated by a manganese porphyrin. *Chem*. *Sci*. **2018**, *9* (5), 1168–1172.
67 Huang, X.; Liu, W.; Hooker, J.M.; Groves, J.T. Targeted Fluorination with the Fluoride Ion by Manganese-Catalyzed Decarboxylation. *Angew*. *Chem*. *Int*. *Ed*. **2015**, *54* (17), 5241–5245.
68 Lee, S. J.; Brooks, A. F.; Ichiishi, N.; Makaravage, K. J.; Mossine, A. V.; Sanford, M. S.; Scott, P. J. H. C–H ^{18}F-fluorination of 8-methylquinolines with Ag[^{18}F]F. *Chem. Commun.* **2019**, *55* (20), 2976–2979.
69 Graham, T. J. A.; Lambert, R. F.; Ploessl, K.; Kung; H. F.; Doyle, A. G. Enantioselective Radiosynthesis of Positron Emission Tomography (PET) Tracers Containing [^{18}F]Fluorohydrins. *J*. *Am*. *Chem*. *Soc*. **2014**, *136* (14), 5291–5294.
70 Gray, E. E.; Nielsen, M. K.; Choquette, K. A.; Kalow, J. A.; Graham, T. J. A.; Doyle, A. G. Nucleophilic (Radio)Fluorination of α-Diazocarbonyl Compounds Enabled by Copper-Catalyzed H–F Insertion. *J*. *Am*. *Chem*. *Soc*. **2016**, *138* (34), 10802–10805.
71 Nielsen, M. K.; Ugaz, C. R.; Li, W.; Doyle, A. G. PyFluor: A Low-Cost, Stable, and Selective Deoxyfluorination Reagent. *J*. *Am*. *Chem*. *Soc*. **2015**, *137* (30), 9571–9574.
72 Webb, E. W.; Park, J. B.; Cole, E. L.; Donnelly, D. J.; Bonacorsi, S. J.; Ewing, W. R.; Doyle, A. G. Nucleophilic (Radio)Fluorination of Redox-Active Esters *via* Radical-Polar Crossover Enabled by Photoredox Catalysis. *J*. *Am*. *Chem*. *Soc*. **2020**, *142* (20), 9493–9500.
73 Preshlock, S.; Tredwell, M.; Gouverneur, V. ^{18}F-Labeling of Arenes and Heteroarenes for Applications in Positron Emission Tomography. *Chem*. *Rev*. **2016**, *116* (2), 719–766.
74 Golla, S. S. V.; Timmers, T.; Ossenkoppele, R.; Groot, C.; Verfaillie, S.; Scheltens, P.; van der Flier, W. M.; Schwarte, L.; Mintun, M. A.; Devous, M.; Schuit, R. C.; Windhorst, A. D.; Lammertsma, A. A.; Boellaard, R.; van Berckel, B. N. M.; Yaqub, M. Quantification of Tau Load Using [^{18}F]AV1451 PET. *Mol. Imaging Biol*. **2017**, *19*, 963–971.
75 Pike, V. W.; Aigbirhio, F. I. Reactions of cyclotron-produced [^{18}F]fluoride with diaryliodonium salts—a novel single-step route to no-carrier-added [^{18}F]fluoroarenes. *J*. *Chem*. *Soc*. *Chem*. *Commun*. **1995**, *1995* (21), 2215–2216.
76 Ross, T. L.; Ermert, J.; Hocke, C.; Coenen, H. H. Nucleophilic ^{18}F-Fluorination of Heteroaromatic Iodonium Salts with No-Carrier-Added [^{18}F]Fluoride. *J*. *Am*. *Chem*. *Soc*. **2007**, *129* (25), 8018–8025.

77 Ichiishi, N.; Brooks, A. F.; Topczewski, J. J.; Rodnick, M. E.; Sanford, M. S.; Scott, P. J. H. Copper-Catalyzed [^{18}F]Fluorination of (Mesityl)(aryl)iodonium Salts. *Org*. *Lett*. **2014**, *16* (12), 3224–3227.

78 Rotstein, B.; Stephenson, N.; Vasdev, N.; Liang, S. H. Spirocyclic hypervalent iodine(III)-mediated radiofluorination of non-activated and hindered aromatics. *Nat. Commun*. **2014**, *5*, 4365.

79 Liang, S. H.; Wang, L.; Stephenson, N. A.; Rotstein, B. H. Facile ^{18}F labeling of non-activated arenes *via* a spirocyclic iodonium(III) ylide method and its application in the synthesis of the mGluR5 PET radiopharmaceutical [^{18}F]FPEB. *Nat. Protoc.* **2019***, 14* (5), 1530–1545.

80 Maeda, M.; Fukumura, T.; Kojima, M. The dimethylsulfonium moiety as a leaving group in aromatic radiofluorination using tetra-*n*-butylammonium [^{18}F]fluoride. *Appl*. *Radiat*. *Isot*. **1987**, *38* (4), 307–310.

81 Mu, L.; Fischer, C. R.; Holland, J. P.; Becaud, J.; Schubiger, P. A.; Schibli, R.; Ametamey, S. M.; Graham, K.; Stellfeld, T.; Dinkelborg, L. M.; Lehmann, L. ^{18}F-Radiolabeling of Aromatic Compounds Using Triarylsulfonium Salts. *Eur*. *J*. *Org*. *Chem*. **2012**, *2012* (5), 889–892.

82 Sander, K.; Gendron, T.; Yiannaki, E.; Cybulska, K.; Kalber, T. L.; Lythgoe, M. F.; Årstad, E. Sulfonium Salts as Leaving Groups for Aromatic Labelling of Drug-like Small Molecules with Fluorine-18. *Sci*. *Rep*. **2015**, *5*, 9941.

83 Gendron, T.; Sander, K.; Cybulska, K.; Benhamou, L.; Sin, P. K. B.; Khan, A.; Wood, M.; Porter, M. J.; Årstad, E. Ring-Closing Synthesis of Dibenzothiophene Sulfonium Salts and Their Use as Leaving Groups for Aromatic ^{18}F-Fluorination. *J*. *Am*. *Chem*. *Soc*. **2018**, *140* (35), 11125–11132.

84 Sander, K.; Gendron, T.; Cybulska, K.; Sirindil, F.; Zhou, J.; Kalber, T. L.; Lythgoe, M. F.; Kurzawinski, T. R.; Brown, M. J.; Williams, B.; Årstad, E. Development of [^{18}F]AldoView as the First Highly Selective Aldosterone Synthase PET Tracer for Imaging of Primary Hyperaldosteronism. *J*. *Med*. *Chem*. **2021**, *64* (13), 9321–9329.

85 Xu, P.; Zhao, D.; Berger, F.; Hamad, A.; Rickmeier, J.; Petzold, R.; Kondratiuk, M.; Bohdan, K.; Ritter, T. Site-Selective Late-Stage Aromatic [^{18}F]Fluorination *via* Aryl Sulfonium Salts. *Angew*. *Chem*. *Int*. *Ed*. **2020**, *59* (5), 1956–1960.

86 Neumann, C.; Hooker, J.; Ritter, T. Concerted nucleophilic aromatic substitution with $^{19}F^-$ and $^{18}F^-$. *Nature* **2016**, *534* (7607), 369–373.

87 Lee, E.; Kamlet, A. M.; Powers, D. C.; Neumann, C. N.; Boursalian, G. B.; Furuya, T.; Choi, D. C.; Hooker, J. M.; Ritter, T. A Fluoride-Derived Electrophilic Late-Stage Fluorination Reagent for PET Imaging. *Science* **2011**, *334* (6056), 639–642.

88 Lee, E.; Hooker, J. M.; Ritter, T. Nickel-Mediated Oxidative Fluorination for PET with Aqueous [^{18}F]Fluoride. *J*. *Am*. *Chem*. *Soc*. **2012**, *134* (42), 17456–17458.

89 Beyzavi, H.; Mandal, D.; Strebl, M. G.; Neumann, C. N.; D'Amato, E. M.; Chen, J.; Hooker, J. M.; Ritter, T. ^{18}F-Deoxyfluorination of Phenols *via* Ru π-Complexes. *ACS Cent. Sci.* **2017**, *3* (9), 944–948.

90 Tredwell, M.; Preshlock, S. M.; Taylor, N. J.; Gruber, S.; Huiban, M.; Passchier, J.; Mercier, J.; Genicot, C.; Gouverneur, V. A General Copper-Mediated Nucleophilic ^{18}F-Fluorination of Arenes. *Angew*. *Chem*. *Int*. *Ed*. **2014**, *53* (30), 7751–7755.

91 Mossine, A. V.; Brooks, A. F.; Makaravage, K. J.; Miller, J. M.; Ichiishi, N.; Sanford, M. S.; Scott, P. J. H. Synthesis of [^{18}F]Arenes *via* the Copper-Mediated [^{18}F]Fluorination of Boronic Acids. *Org*. *Lett*. **2015**, *17* (23), 5780–5783.

92 Makaravage, K. J.; Brooks, A. F.; Mossine, A. V.; Sanford, M. S.; Scott, P. J. H. Copper-Mediated Radiofluorination of Arylstannanes with [^{18}F]KF. *Org*. *Lett*. **2016**, *18* (20), 5440–5443.

93 McCammant, M. S.; Thompson, S.; Brooks, A. F.; Krska, S. W.; Scott, P. J. H.; Sanford, M. S. Cu-Mediated C-H ^{18}F-Fluorination of Electron-Rich (Hetero)arenes. *Org*. *Lett*. **2017**, *19* (14), 3939–3942.

94 Sharninghausen L. S.; Brooks A. F.; Winton W. P.; Makaravage K. J.; Scott P. J. H.; Sanford M. S. NHC-Copper Mediated Ligand-Directed Radiofluorination of Aryl Halides. *J*. *Am*. *Chem*. *Soc*. **2020**, *142* (16), 7362–7367.

95 Preshlock S.; Calderwood S.; Verhoog S.; Tredwell, M.; Huiban, M.; Hienzsch, A.; Gruber, S.; Wilson, T. C.; Taylor, N. J.; Cailly, T.; Schedler, M.; Collier, T. L.; Passchier, J.; Smits, R.; Mollitor, J.; Hoepping, A.; Mueller, M.; Genicot, C.; Mercier, J.; Gouverneur, V. Enhanced copper-mediated ^{18}F-fluorination of aryl boronic esters provides eight radiotracers for PET applications. *Chem Commun*. **2016**, *52* (54), 8361–8364.

96 Wright, J. S.; Kaur, T.; Preshlock, S.; Tanzey, S. S.; Winton, W. P.; Sharninghausen, L. S.; Wiesner, N.; Brooks, A. F.; Sanford, M. S.; Scott, P. J. H. Copper-mediated late-stage radiofluorination: five years of impact on preclinical and clinical PET imaging. *Clin. Transl. Imaging*. **2020**, *8* (3), 167–206

97 Guibbal, F.; Isenegger, P. G.; Wilson, T. C.; Pacelli, A.; Mahaut, D.; Sap, J. B. I.; Taylor, N. J.; Verhoog, S.; Preshlock, S.; Hueting, R.; Cornelissen, B.; Gouverneur, V. Manual and Automated Cu-Mediated Radiosynthesis of the PARP Inhibitor [^{18}F]olaparib. *Nat*. *Protoc*. **2020**, *15* (4), 1525–1541.

98 Mossine, A. V.; Tanzey, S. S.; Brooks, A. F.; Makaravage, K. J.; Ichiishi, N.; Miller, J. M.; Henderson, B. D.; Erhard, T.; Bruetting, C.; Skaddan, M. B.; Sanford, M. S.; Scott, P. J. H. Synthesis of High-Molar-Activity [^{18}F]6-Fluoro-L-DOPA Suitable for Human Use *via* Cu-Mediated Fluorination of a BPin Precursor. *Nat*. *Protoc*. **2020**, *15* (5), 1742–1759.

99 Gendron, T.; Destro, G.; Straathof, N. J. W.; Sap, J. B. I.; Guibbal, F.; Vriamont, C.; Caygill, C.; Atack, J. R.; Watkins, A. J.; Marshall, C.; Hueting, R.; Warnier, C.; Gouverneur, V.; Tredwell, M. Multi-patient dose synthesis of [^{18}F]Flumazenil *via* a copper-mediated ^{18}F-fluorination. *EJNMMI Radiopharm*. *Chem*. **2022**, *7*, 5.

100 Chen, W.; Huang, Z.; Tay, N. E. S.; Giglio, B.; Wang, M.; Wang, H.; Wu, Z.; Nicewicz, D. A.; Li, Z. Direct arene C–H fluorination with ^{18}F− *via* organic photoredox catalysis. *Science* **2019**, *364* (6446), 1170–1174.

101 Wang, L.; White, A. R.; Chen, W.; Wu, Z.; Nicewicz, D. A.; Li, Z. Direct Radiofluorination of Arene C–H Bonds *via* Photoredox Catalysis Using a Peroxide as the Terminal Oxidant. *Org*. *Lett*. **2020**, *22* (20), 7971–7975.

102 Chen, W.; Wang, H.; Tay, N. E. S.; Pistritto, V. A.; Li, K.-P.; Zhang, T.; Wu, Z.; Nicewicz, D. A.; Li, Z. Arene radiofluorination enabled by photoredox-mediated halide interconversion. *Nat*. *Chem*. **2022**, *14* (2), 216–223.

103 Tay, N. E. S.; Chen, W.; Levens, A.; Pistritto, V. A.; Huang, Z.; Wu, Z.; Li, Z.; Nicewicz, D. A. ^{19}F- and ^{18}F-arene deoxyfluorination *via* organic photoredox-catalysed polarity-reversed nucleophilic aromatic substitution. *Nat. Catal*. **2020**, *3* (9), 734–742.

104 van der Born, D.; Pees, A.; Poot, A. J.; Orru, R. V. A.; Windhorst, A. D.; Vugts, D. J. Fluorine-18 labelled building blocks for PET tracer synthesis. *Chem Soc*. *Rev*. **2017**, *46* (15), 4709–4773.

105 Kniess, T.; Laube, M.; Brust, P.; Steinbach, J. 2-[^{18}F]Fluoroethyl tosylate – a versatile tool for building ^{18}F-based radiotracers for positron emission tomography. *Med*. *Chem*. *Commun*. **2015**, *6* (10), 1714–1754.

106 Hamacher, K.; Coenen, H. H. Efficient routine production of the ^{18}F-labelled amino acid *O*-(2-[^{18}F]fluoroethyl)-l-tyrosine. *Appl*. *Radiat*. *Isot*. **2002**, *57* (6), 853–856.

107 Rodnick, M. E.; Brooks, A. F.; Hockley, B. G.; Henderson, B. D.; Scott, P. J. H. A fully-automated one-pot synthesis of [^{18}F]fluoromethylcholine with reduced dimethylaminoethanol contamination *via* [^{18}F]fluoromethyl tosylate. *Appl*. *Radiat*. *Isot*. **2013**, *78*, 26–32.

108 Doi, H.; Goto, M.; Suzuki, M. Pd^{0}-Mediated Rapid *C*-[^{18}F]Fluoromethylation by the Cross-Coupling Reaction of a [^{18}F]Fluoromethyl Halide with an Arylboronic Acid Ester: Novel Method for the Synthesis of a ^{18}F-Labeled Molecular Probe for Positron Emission Tomography. *Bull*. *Chem*. *Soc*. *Jpn*. **2012**, *85* (11), 1233–1238.

109 Hell, S. M.; Meyer, C. F.; Ortalli, S.; Sap, J. B. I.; Chen, X.; Gouverneur, V. Hydrofluoromethylation of alkenes with fluoroiodomethane and beyond. *Chem*. *Sci*. **2021**, *12* (36), 12149-12155

110 Huiban, M.; Tredwell, M.; Mizuta, S.; Wan, Z.; Zhang, X.; Collier, T. L.; Gouverneur, V.; Passchier, J. A broadly applicable [^{18}F]trifluoromethylation of aryl and heteroaryl iodides for PET imaging. *Nat*. *Chem*. **2013**, *5* (11), 941–944.

111 Ivashkin, P.; Lemonnier, G.; Cousin, J.; Grégoire, V.; Labar, D.; Jubault, P.; Pannecoucke, X. [^{18}F]$CuCF_3$: A [^{18}F]Trifluoromethylating Agent for Arylboronic Acids and Aryl Iodides. *Chem*. *Eur*. *J*. **2014**, *20* (31), 9514–9518.

112 Rühl, T.; Rafique, W.; Lien, V. T.; Riss, P. J. Cu(i)-mediated ^{18}F-trifluoromethylation of arenes: Rapid synthesis of ^{18}F-labeled trifluoromethyl arenes. *Chem. Commun*. **2014**, *50* (45), 6056–6059.

113 van der Born, D.; Sewing, C.; Herscheid, J. D. M.; Windhorst, A. D.; Orru, R. V. A.; Vugts, D. J. A Universal Procedure for the [^{18}F]Trifluoromethylation of Aryl Iodides and Aryl Boronic Acids with Highly Improved Specific Activity. *Angew*. *Chem*. *Int*. *Ed*. **2014**, *53* (41), 11046–11050.

114 Pees, A.; Vosjan, M. J. W. D.; Vasdev, N.; Windhorst, A. D.; Vugts, D. J. Fluorine-18 labelled Ruppert–Prakash reagent ([^{18}F]Me_3SiCF_3) for the synthesis of ^{18}F-trifluoromethylated compounds. *Chem. Commun*. **2021**, *57* (43), 5286–5289.

115 Liu, X.; Xu, C; Wang, M.; Liu, Q. Trifluoromethyltrimethylsilane: Nucleophilic Trifluoromethylation and Beyond. *Chem*. *Rev*. **2015**, *115* (2), 683–730.

116 Verhoog, S.; Kee, C. W.; Wang, Y.; Khotavivattana, T.; Wilson, T. C.; Kersemans, K.; Smart, S.; Tredwell, M.; Davis, B. G.; Gouverneur, V. ^{18}F-Trifluoromethylation of Unmodified Peptides with 5-^{18}F-(Trifluoromethyl)dibenzothiophenium Trifluoromethanesulfonate. *J*. *Am*. *Chem*. *Soc*. **2018**, *140* (5), 1572–1575.

117 Kee, C. W.; Tack, O.; Guibbal, F.; Wilson, T. C.; Isenegger, P. G.; Imiołek, M.; Verhoog, S.; Tilby, M.; Boscutti, G.; Ashworth, S.; Chupin, J.; Kashani, R.; Poh, A. W. J.; Sosabowski, J. K.; Macholl, S.; Plisson, C.; Cornelissen, B.; Willis, M. C.; Passchier, J.; Davis, B. G.; Gouverneur, V. ^{18}F-Trifluoromethanesulfinate Enables Direct C–H ^{18}F-Trifluoromethylation of Native Aromatic Residues in Peptides *J*. *Am*. *Chem*. *Soc*. **2020**, *142* (3), 1180–1185.

118 Trump, L.; Lemos, A.; Lallemand, B.; Pasau, P.; Mercier, J.; Lemaire, C.; Luxen, A.; Genicot, C. Late-Stage ^{18}F-Difluoromethyl Labeling of *N*-Heteroaromatics with High Molar Activity for PET Imaging. *Angew*. *Chem*. *Int*. *Ed*. **2019**, *58* (37), 13149–13154.

Chapter 2: ^{18}F-Difluoromethylation with [^{18}F]Difluorocarbene

This chapter first describes the properties of difluoromethylated compounds, followed by a short summary of key advances in difluoromethylation, with a focus on reactions proceeding *via* difluorocarbene (DFC). Next, an account of approaches towards the radiosynthesis of ^{18}F-difluoromethylated compounds is given. [^{18}F]DFC is next introduced as a radiosynthetic intermediate for ^{18}F-difluoromethylation. Progress made prior to the work presented in this thesis, including the discovery of a [^{18}F]DFC-releasing reagent and its first application, is outlined. This chapter then discloses advances to [^{18}F]DFC radiochemistry in three key areas. Firstly, a radiosynthetic study that led to the development of a second-generation [^{18}F]DFC-releasing reagent with improved properties is described. Next, the application of [^{18}F]DFC radiochemistry to the radiosynthesis of a ^{18}F-difluoromethylated PET radiotracer is reported. Finally, the development of a novel ^{18}F-difluoromethylation reaction is disclosed.

The work presented in this chapter has been published (J. B. I. Sap, C. F. Meyer, J. Ford, N. J. W. Straathof, A. B. Dürr, M. J. Lelos, S. J. Paisey, T. A. Mollner, S. M. Hell, A. A. Trabanco, C. Genicot, C. W. am Ende, R. S. Paton, M. Tredwell, V. Gouverneur. [^{18}F]Difluorocarbene for positron emission tomography. *Nature* **2022**, *606*, 102–108). A review on the topic covered in this chapter has also been published (J. Ford, S. Ortalli, V. Gouverneur. The ^{18}F-Difluoromethyl Group: Challenges, Impact and Outlook. *Angew. Chem. Int. Ed.* **2024**, *63* (26), e202404957).

All ^{18}F-radiolabelling experiments described in section 2.2 were conducted by J. Ford and Dr. J. Sap. Synthesis and non-radioactive experimentation described in section 2.2 were conducted by J. Ford and Dr. J. Sap. Dr. C. Meyer assisted with initial experiments for the ^{18}F-difluoromethylation of aryl boronic acids and synthesised selected compounds. PET imaging and *in vivo* experiments were conducted by Dr. S. Paisey and Dr. M. Lelos (Cardiff University). Further details are available in the Experimental section (Chapter 4).

2.1. Introduction

2.1.1. The Difluoromethyl Group

The difluoromethyl (CF_2H) group is a carbon-based functional group, in which two of the three protons of a methyl group are replaced with fluorine atoms. As well as the simple CF_2H unit, a series of analogues with heteroatom–CF_2H connectivity exist, such as with oxygen (-OCF_2H or difluoromethoxy group), sulfur (-SCF_2H or difluoromethylthio group), selenium (-$SeCF_2H$) or nitrogen (-NCF_2H). Other difluorinated functionalities contain moieties such as the difluoromethylene group (-CF_2-), where the two protons of a methylene group are substituted with fluorine. The effect of the substitution with two electronegative and polarising fluorine atoms manifests itself in the altered physicochemical properties of molecules bearing difluoromethyl functionality, compared to those with methyl, trifluoromethyl and other fluoroalkyl groups.[1,2] For this reason, the difluoromethyl group and other related groups have attracted the attention of industrial chemists, who have exploited these properties in the design of novel APIs in medicinal chemistry, as well as agrochemicals in crop science.[3-5] To date, numerous examples of difluoromethyl-containing bioactive molecules have been disclosed (Figure 2.1).

As discussed in Chapter 1, the presence of fluorine atoms can affect the pK_a of nearby protons.[1] This effect has also been noted in difluoromethylated compounds compared to their methylated analogues. For example, the pK_{a2} of the proton pump inhibitor pantoprazole is lower than the closely related omeprazole, which bears a methoxy group rather than a difluoromethoxy group (Figure 2.1).[6]

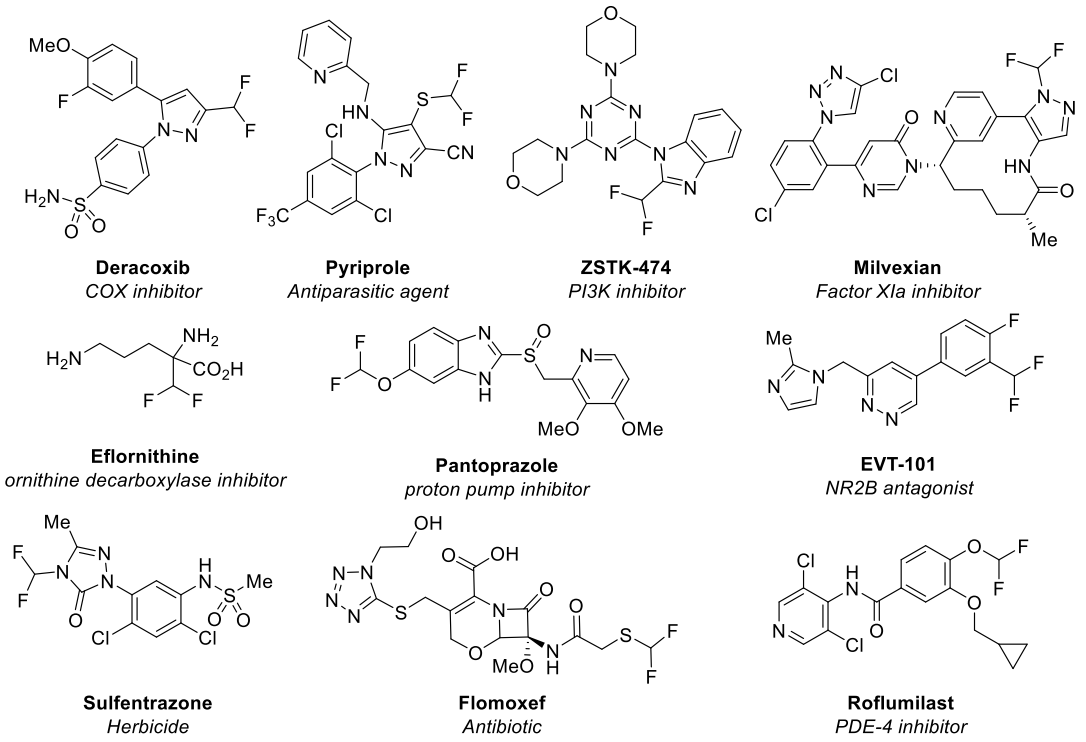


Figure 2.1. *Examples of difluoromethyl-containing bioactive molecules.*

Due to the strongly electron-withdrawing fluorine atoms, the C–H bond of the CF_2H group is sufficiently polarised to behave as a moderate hydrogen bond donor.[2] Erickson and McLoughlin first noted an intramolecular hydrogen bonding interaction in fungicidal compound **2.1** and suggested this effect contributed to its enhanced biological activity compared to the CF_3 analogue (Figure 2.2 a).[7] Lippard and co-workers also investigated the structural effects of hydrogen bonding in 2-difluoromethyl-1-nitrobenzene and found that this was able to form dimers (**2.2**) in the solid state analogous to those of 2-nitrophenol (Figure 2.2 b).[8] Brigaud and co-workers also demonstrated that the effect of intramolecular hydrogen bonding in CF_2H-substituted pseudoprolines (e.g. **2.3**) could affect their conformation and this favourable interaction reduced the energy barrier to *cis-trans* isomerisation (Figure 2.2 c).[9] These observations suggest that the CF_2H group is able to act as a hydrogen bond donor in such a way that may affect the conformation of molecules and their overall topology. Furthermore, the propensity of these groups to participate in hydrogen bonding interactions may affect how they interact with pharmaceutical targets such as proteins.

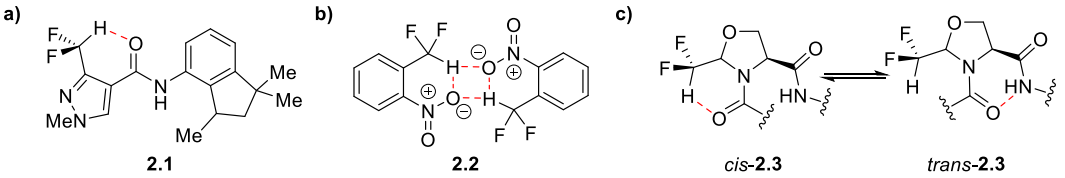


Figure 2.2. *Hydrogen bonding interactions in difluoromethyl-containing molecules. a) intramolecular hydrogen bonding observed in* ***2.1****; b) hydrogen-bonded dimer structure of* ***2.2*** *in the solid state; c) cis-trans isomerisation of* ***2.3****.*

The presence of difluoromethyl-containing functionality has also been suggested to modulate the lipophilicity of a compound. Lipophilicity is a measure of the extent to which a compound will mix with or dissolve in oils, or non-polar solvents. It can be quantified using log *P*, the logarithm of the partition coefficient *P*, which is the ratio of the concentration of a compound of interest in a 1-octanol phase compared to water in a biphasic water-octanol system.[10] More lipophilic compounds therefore have a higher value of log *P* compared to hydrophilic compounds. Another parameter, log *D,* is sometimes favoured to log *P*, as it more accurately describes the distribution of ionisable compounds as it accounts for differences in p*H*.[10] Various groups have investigated the effect of introducing difluorinated functionality on the lipophilicity of a given compound and a summary of the measured log *P* values for a set of model compounds is given below (Figure 2.3 a).[11] One example, disclosed by Bunnage and co-workers, analysed the differences in lipophilicity across a series of matched molecular pairs of anisoles, difluoroanisoles and trifluoroanisoles.[12] They noted that log *D* generally increased in the order: $ArOCH_3$ < $ArOCF_2H$ < $ArOCF_3$. They proposed that difluoromethoxy groups could be a useful alternative to methoxy groups in drug design, as they delivered a small increase in log *D* for a smaller increase in molecular weight, rather than the more significant increase observed for trifluoromethoxy groups. [12] A second example, by Müller and co-workers, found that for a series of aliphatic compounds the CF_2H-compound had reduced lipophilicity compared to the CH_3 or CF_3 analogue (Figure 2.3 b).[13] For this reason, as well as their similar sizes, the replacement of methyl or trifluoromethyl groups with difluoromethyl groups may be a useful strategy for the fine-tuning of lipophilicity in drug design.

As a result of their ability to participate in hydrogen bonding and their lipophilic nature, various difluoromethyl moieties have been suggested to be lipophilic bioisosteres of common functional groups, such as alcohols, thiols and amines.[11,14,15] In their study of this concept, Zafrani and co-workers also determined the '*A* value' (a parameter proposed by Abraham for hydrogen bond acidity determined by ^{1}H NMR analysis in $CDCl_3$ and DMSO-d_6) for various difluoromethylated compounds and other compounds with which they were hypothesised to be bioisosteric. (Figure 2.4).[11] Zafrani and co-workers' analysis suggested that the hydrogen bond acidity of difluoromethyl compounds is of a similar order to that of thiophenols and anilines, but much lower than alcohols, such as phenol.

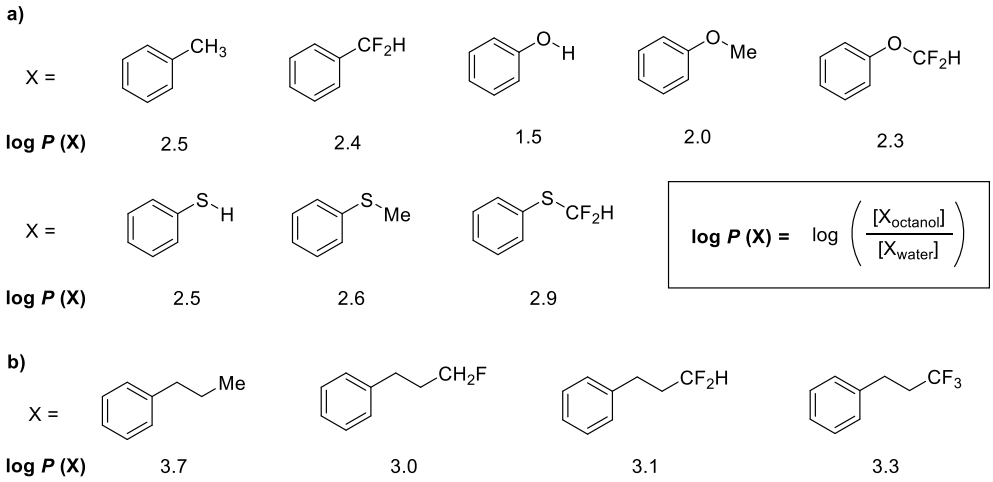


Figure 2.3. *The lipophilicities of difluoromethylated compounds. a) The lipophilicity (log P) for toluenes, phenols, thiophenols and their methylated and difluoromethylated derivatives. b) The lipophilicity (log P) of a model alkyl compound with increasing fluorine content.*

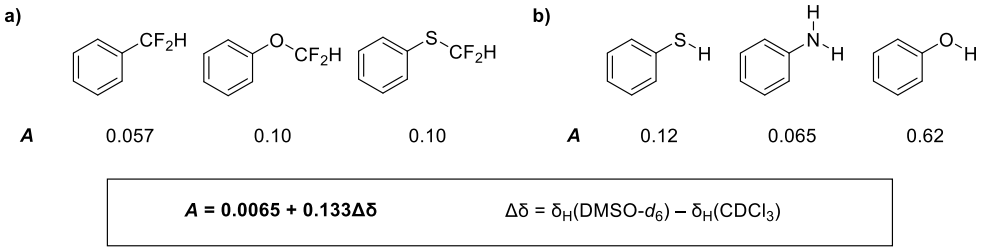


Figure 2.4. *The calculated hydrogen bond acidity, A, for a) difluoromethylated compounds b) model hydrogen bond donor compounds. δ_H = ^{1}H NMR chemical shift of the hydrogen bonded proton.*

Metabolic stability can also be modulated by the introduction of difluoromethyl functionalities. In their study of anisoles (*vide supra*), Bunnage and co-workers described that difluoromethoxy compounds exhibited a statistically significant improvement in metabolic

stability over the analogous methoxy compounds considered in a human liver microsome assay.[12] These compounds, as well as other difluoromethyl-derived functional groups, also exhibited good stability towards hydrolysis in solution phase under acidic and basic conditions, superior to fluoromethylated compounds, with their stability only surpassed by trifluoromethylated compounds.[16] Bunnage and co-workers also note in the case of fluoroalkyl ethers that the increased hydrolytic stability of trifluoromethoxyarenes can be offset by their higher lipophilicity.[12] The introduction of a difluoromethyl group can also assist in improving stability towards enzymatic demethylation that methyl groups may be susceptible to, as illustrated for **2.4** compared to **2.5**, which are experimental compounds proposed as candidates against African Trypanosomiasis (Figure 2.5).[17]

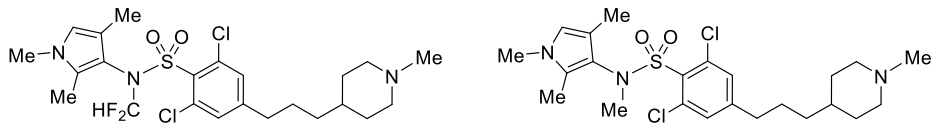


Figure 2.5. *The effect of difluoromethylation on intrinsic clearance (Cl_i) of two experimental inhibitors of N-myristoyltransferase.*

This is particularly interesting in the context of PET ligand discovery, as instability to ^{11}C-demethylation or ^{18}F-defluorination has been noted in the case of some ^{11}C-methylated and ^{18}F-fluoromethylated PET tracers, respectively (Figure 2.6).[18] For example, for the radiotracer [^{18}F]SP-203 ([^{18}F]**2.6**) ^{18}F-defluorination has been attributed to glutathionylation of the reactive ^{18}F-fluoromethyl group.[19] Practitioners have often leveraged deuterium substitution in the latter case to impart higher stability to ^{18}F-monofluoroalkyl compounds, such as in the case of the PET radiotracer [^{18}F]FMPEP ([^{18}F]**2.7**), where [^{18}F]FMPEP-d_2 ([^{2}H,^{18}F]**2.7**) has been shown to reduce uptake of radioactivity in the skull.[20] Alternative strategies involve installing the radiolabel at a different position or as a different functional group, as demonstrated for [^{11}C]WAY-100635 ([^{11}C]**2.8**) where improved signal quality was observed when the radiolabel was installed at the carbonyl carbon rather than at an *O*-methyl group.[21] Therefore, ^{18}F-

difluoromethyl groups may pose an interesting solution for PET ligand design, as they could impart a more favourable stability profile to a PET ligand of interest.

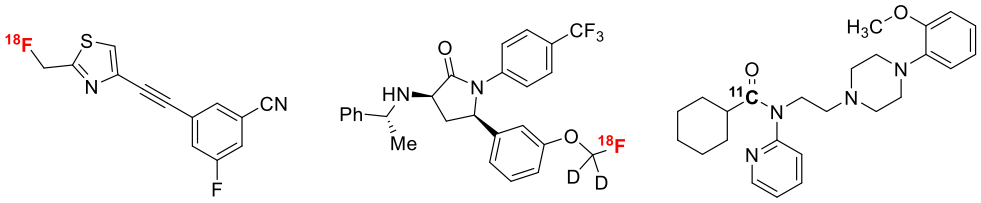


Figure 2.6. *PET radiotracers which have exhibited undesired metabolism (and where applicable, improvements made to address this).*

2.1.2. Difluoromethylation

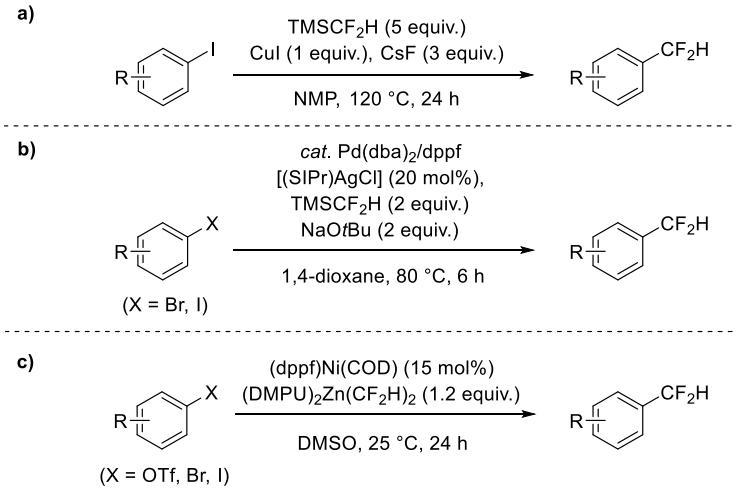
One of the most powerful modern synthetic routes to difluoromethylated compounds is difluoromethylation, which involves the transfer of a CF_2H unit to a substrate of interest.[2] This approach offers key advantages, such as facilitating the late-stage incorporation of the difluoromethyl group into complex molecules. This will be the focus of the discussion in this section, however it should be noted that alternative routes involving two discrete fluorination events are also commonly applied for the preparation of difluoromethylated compounds. Briefly, the most prevalent synthesis of difluoromethylated compounds has been the deoxyfluorination of aldehydes. This is most often achieved with SF_4 and its derivatives, e.g. *N*,*N*-diethylaminosulfur trifluoride (DAST).[22] While this has proven very effective for the preparation of difluoromethylated compounds, it has presented challenges including incompatibility with common functional groups, as well as the use of toxic and explosive reagents. Furthermore, its translation to radiochemistry is limited by the need for two sequential fluorination steps, which would be prohibited by the nano-to-picomolar concentrations of [^{18}F]fluoride present under radiolabelling conditions, or require the addition of carrier, which would afford products with low A_m. Radiochemical approaches to [^{18}F]CF_2H-compounds relying on a key ^{18}F-fluorination step will be summarised later in this chapter in section 2.1.3. Finally, while strategies involving the selective hydrodefluorination

of CF_3 compounds to CF_2H compounds *via* a key defluorination step have also been demonstrated, they are less promising for radiochemistry and thus such approaches will not be discussed in this account.[23]

Difluoromethylation reactions most often require a reagent that releases a specific CF_2H or CF_2 reactive intermediate or equivalent under the reaction conditions.[2] The account in this section will categorise difluoromethylation reactivity by CF_2-synthon.

2.1.2.1. Nucleophilic Difluoromethylation

Various reagents have emerged that react as nucleophilic difluoromethyl anion equivalents.[2] The most prominent is $TMSCF_2H$, which can either be used as the sole difluoromethylation reagent or in combination with a secondary shuttle for transmetallation. One application of this synthon is in transition metal-catalysed cross-coupling, where several groups have reported the difluoromethylation of aryl halides under copper, palladium, nickel and gold catalysis. Some key examples of this mode of reactivity are summarised herein (Scheme 2.1).



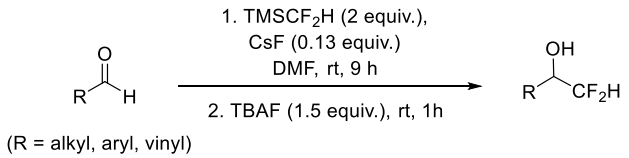
Scheme 2.1. *Examples of metal-catalysed difluoromethylation with anionic synthons with a) copper, b) palladium and c) nickel complexes.*

Hartwig and co-workers first reported a difluoromethylation of aryl iodides using stoichiometric CuI and $TMSCF_2H$,[24] while Prakash and co-workers reported a similar system using nBu$_3$SnCF_2H as a difluoromethylating reagent (Scheme 2.1 a).[25]

Palladium catalysis proved effective for difluoromethylation with CF_2H anion equivalents. For example, Shen and co-workers developed a Pd-catalysed difluoromethylation plaform, whereby $TMSCF_2H$ was used in combination with a silver complex bearing an NHC ligand ([(SIPr)AgCl]), which the authors suggested could facilitate the challenging transmetallation of CF_2H to Pd, by formation of a [(SIPr)AgCF_2H] complex (Scheme 2.1 b).[26] Sanford and co-workers reported that $TMSCF_2H$ could also be used directly for the difluoromethylation of aryl bromides and chlorides with an improved $Pd(dba)_2$-BrettPhos catalyst system.[27]

Using nickel catalysis, Vicic and co-workers described the preparation of a *bis*-difluoromethyl zinc reagent [$(DMPU)_2Zn(CF_2H)_2$] from $ZnEt_2$ and HCF_2I that could be applied in the difluoromethylation of aryl (pseudo)halides, [28] analogous to the Pd-catalysed cross-couplings disclosed by Shen and co-workers (Scheme 2.1 c).[26] Ritter and co-workers used the same reagent in combination with acyl chloride substrates and a $Pd(dba)_2$-RuPhos catalyst system to affect a decarbonylative difluoromethylation.[29]

Direct addition of nucleophilic CF_2H anion synthons to electrophiles is also possible. For example, the difluoromethylation of aldehydes and ketones with $TMSCF_2H$ has been reported with fluoride anion activation used to activate $TMSCF_2H$ to release a CF_2H anion, which can undergo nucleophilic addition to the carbonyl compound (Scheme 2.2).[30]

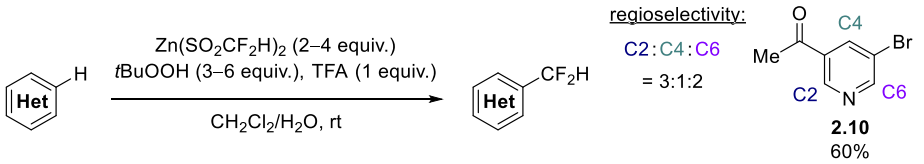


Scheme 2.2. *Difluoromethylation of aldehydes with the difluoromethyl anion equivalent, $TMSCF_2H$.*

2.1.2.2. Radical Difluoromethylation

The difluoromethyl radical is a powerful and versatile synthetic intermediate for difluoromethylation.[2] Direct difluoromethylation with the CF_2H radical is possible, however, the effectiveness of this approach depends on the philicity match between the radical and a given substrate. The CF_2H radical is considered to be nucleophilic, with intermediate philicity

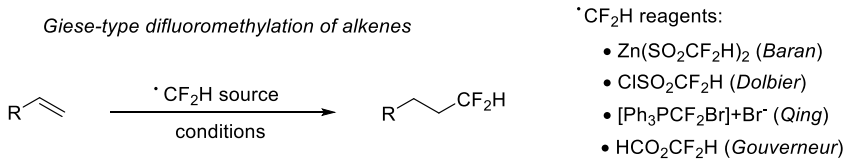
relative to the more electrophilic trifluoromethyl radical and the more nucleophilic monofluoromethyl radical.[31] For example, the Minisci-type addition to *N*-heterocycles has proven effective for accessing difluoromethylated compounds. In an early example, Baran and co-workers disclosed zinc difluoromethylsulfinate, which could release the CF_2H radical upon oxidation and loss of sulfur dioxide (Scheme 2.3).[32] They demonstrated that this radical could add directly to heteroarenes, however where multiple reactive sites were present, mixtures of regioisomers were obtained, as illustrated for substrate **2.10** (Scheme 2.3). The major regioisomer often corresponded to addition product at the most electron-poor carbon. This can be a limitation of the direct use of the CF_2H radical in C–H functionalisation, unless other reactive sites are blocked. Other groups have also shown that alternative reagents are equally effective as sources of the CF_2H radical in Minisci reactions, including difluoroacetic acid, which could be activated under various conditions,[33,34] and a combination of pyridine *N*-oxides and difluoromethylacetic anhydride under photoredox catalysis.[35]



Scheme 2.3. *Minisci-type difluoromethylation of heteroarenes with $Zn(SO_2CF_2H)_2$.*

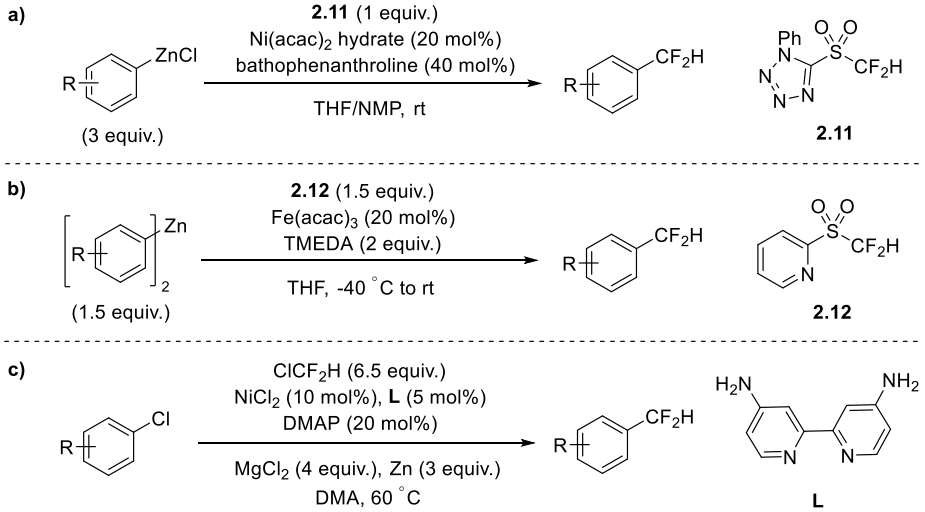
The Giese-type addition of the CF_2H radical to alkenes and unsaturated functionality has also proven effective to access alkyl-CF_2H compounds (Scheme 2.4).[2] Baran and co-workers demonstrated that the nucleophilic CF_2H radical generated from their zinc difluoromethylsulfinate reagent could add to enones,[32] while Dolbier and co-workers showed that difluoromethanesulfonyl chloride could effectively difluoromethylate electron-deficient alkenes, under blue light irradiation in the presence of an Ir-photocatalyst and $(TMS)_3SiH$ as a H-atom transfer reagent.[36] Other groups developed further photochemical protocols, including Qing and co-workers, who used the reagent bromodifluoromethylphosphonium bromide and *fac*-[Ir(ppy)$_3$] to access the CF_2H radical,[37] as well as Gouverneur and co-workers who applied difluoroacetic acid in combination with phenyliodine(III) diacetate under visible

light irradiation.[38] These reports suggested that Giese-type reactions could also be extended to unactivated alkenes, with an expanded scope of alkene partners shown to be amenable to this chemistry.



Scheme 2.4. *Giese-type difluoromethylation of alkenes.*

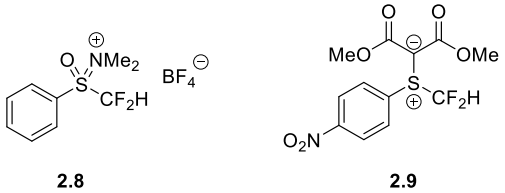
The difluoromethyl radical has also proven to be useful in transition metal-catalysed cross-coupling reactions. While these reactions require the use of a metal catalyst, such approaches can address challenges associated with the direct use of the difluoromethyl radical, such as limited substrate scope and regioselectivity challenges. Baran and co-workers described that a difluoromethyl sulfone derived from 1-phenyl-1*H*-tetrazole (**2.11**) could be engaged in a Ni-catalysed cross-coupling with aryl zinc reagents (Scheme 2.5 a).[39] They proposed that under the reaction conditions, the sulfone could release a difluoromethyl radical, which could add to a Ni-complex. Using a similar 2-pyridyl difluoromethyl sulfone reagent (**2.12**), Hu and co-workers disclosed an iron-catalysed difluoromethylation of aryl zinc reagents (Scheme 2.5 b).[40] Macmillan and co-workers also developed a Ni-catalysed difluoromethylation under metallaphotoredox catalysis, using silyl radical activation of bromodifluoromethane and aryl bromide substrates.[41] Zhang and co-workers reported a similar protocol, albeit using a stoichiometric Zn metal reductant, rather than photoredox catalysis, that enabled the conversion of (hetero)aryl chlorides to the difluoromethyl-(hetero)arene using a $NiCl_2$-diaminobipyridine (**L**) catalyst system and ozone-depleting chlorodifluoromethane ($ClCF_2H$) as a source of the CF_2H radical (Scheme 2.5 c).[42] More recently, Hu and co-workers also applied a similar approach to the Ni-catalysed difluoromethylation of aryl iodides using their sulfone reagent **2.12** and a stoichiometric Zn reductant.[43]



Scheme 2.5. *Difluoromethylation of arenes via radical cross-coupling. a) Baran and co-workers' report with* ***2.11****, b) Hu and co-workers' report with* ***2.12****, c) Zhang and co-workers' report with* $ClCF_2H$.

2.1.2.3. Electrophilic Difluoromethylation

Difluoromethylation *via* an electrophilic CF_2H cation equivalent is the least common mode of difluoromethylation reactivity, with only a handful of reports in the literature. Most electrophilic difluoromethylation reactions are suggested to proceed *via* a difluorocarbene pathway (*vide infra*), which will be treated separately in this account. Prakash and co-workers reported an electrophilic reagent equivalent to a CF_2H cation, *N,N*-dimethyl-*S*-difluoromethyl-*S*-phenylsulfoximinium tetrafluoroborate (**2.8**), which they demonstrated to be able to difluoromethylate various *O*, *S*, *N* and *P*-nucleophiles.[44] Using a sulfonium reagent that also acted as an electrophilic difluoromethylating reagent (**2.9**), Shen and co-workers described the *O*-difluoromethylation of alcohols (Figure 2.7).[45]



2.8 **2.9**

Figure 2.7. *Electrophilic difluoromethylating reagents.*

2.1.2.4. Difluoromethylation with Difluorocarbene

Difluorocarbene (DFC) is a versatile intermediate for difluoromethylation.[46] It has a singlet ground state, as a result of the stabilising π-donation from fluorine lone pairs into the carbon-

centred vacant molecular orbital.[47] DFC is electrophilic and therefore reactive towards nucleophiles; after nucleophilic addition, a formal negative charge develops at carbon, which renders it nucleophilic.[46] Most often, this results in protonation of the carbon atom, however trapping with other electrophiles is also possible.

To date, many different DFC precursors have been reported and these can be categorised based on how they are activated to release DFC (Figure 2.8).[46]

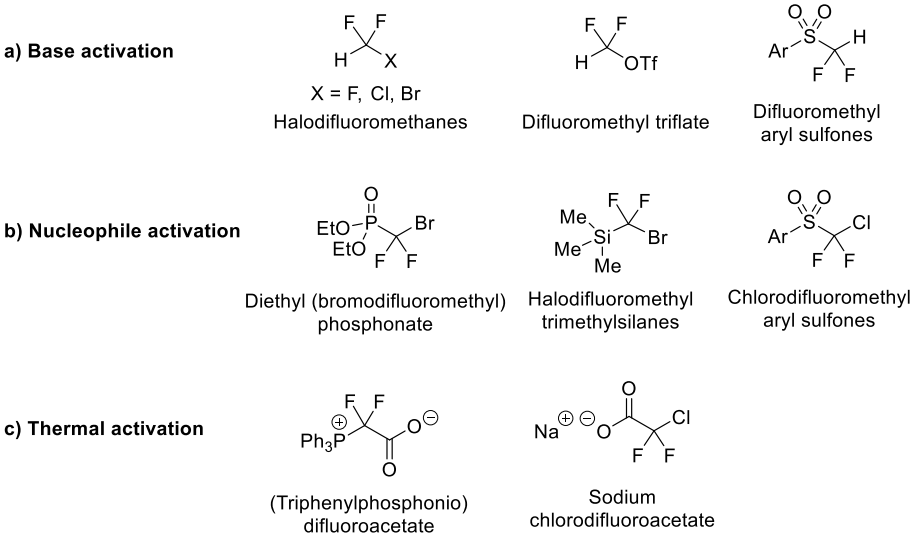


Figure 2.8. *Selected difluorocarbene reagents. a) Base-activated reagents, b) Nucleophile-activated reagents, c) Thermally activated reagents.*

Several reagents have been developed that release DFC upon deprotonation. This either eliminates a leaving group in a concerted fashion or gives an anion, from which a leaving group is eliminated (α-elimination) in a stepwise manner, to release DFC. Reagents of this type include chlorodifluoromethane ($ClCF_2H$), an ozone-depleting gas, difluoromethyl triflate (HCF_2OTf), which was developed by Hartwig and co-workers, as well as difluoromethyl (hetero)aryl sulfones.[48-50] These reagents (in radiolabelled form) are the subject of the work described in this chapter.

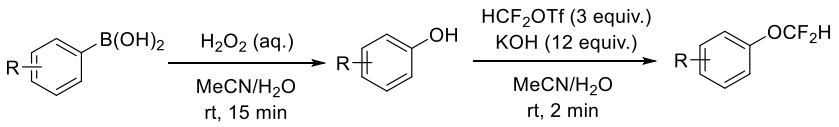
Another category of DFC precursors require activation with a nucleophile before DFC is eliminated. These reagents include Hu's $TMSCF_2Br$, which can be activated with various Lewis bases, including fluoride, hydroxide or acetate anions,[51] as well as diethyl (bromodifluoromethyl)phosphonate (**2.13**) and chlorodifluoromethyl aryl sulfones (e.g.

2.14), which are most often activated by the hydroxide anion attacking at the phosphorus or sulfur atom and eliminating DFC and a halide anion in the process.[52]

The final class of DFC reagents are those that degrade to DFC thermolytically. Upon heating, reagents such as sodium chlorodifluoroacetate (**2.15**) and (triphenylphosphonio) difluoroacetate (PDFA, **2.16**) release an equivalent of CO_2 to form DFC, providing an entropic driving force.[53,54]

As an electrophilic difluoromethyl synthon, DFC is most commonly applied in reactions with nucleophiles. Key advances in this area are described in this section.

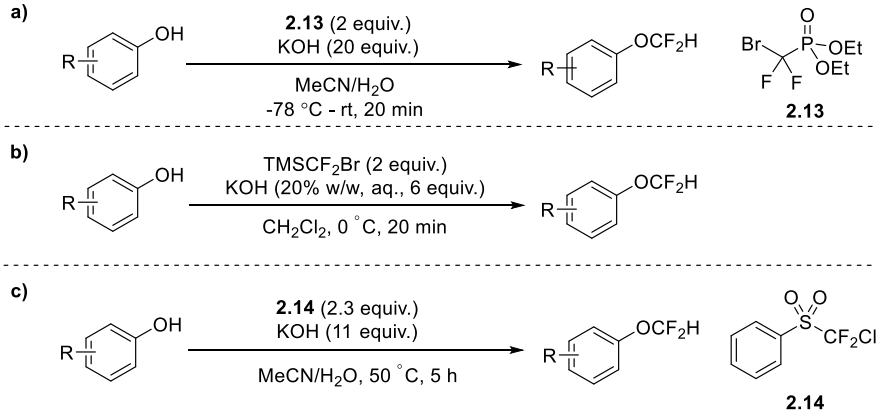
The difluoromethylation of *O*, *S*, *N*-nucleophiles is well reported with numerous DFC sources. Early reports showed that the ozone-depleting $ClCF_2H$ was competent in such reactions, after kinetic data from Hine and Porter suggested it was a DFC source upon activation with aqueous base.[48] Several groups have since attempted to develop non-ozone depleting substitutes for this reagent. For example, Hartwig and co-workers suggested HCF_2OTf as a new base-activated DFC reagent for the difluoromethylation of phenols (Scheme 2.6). They also demonstrated that crude phenols obtained from the oxidation of aryl boron species as the product of catalytic borylation processes could be successfully difluoromethylated.[50] A similar concept is applied to a series of complex aryl boronic acids in a two-step ^{18}F-difluoromethoxylation protocol described in this chapter.



Scheme 2.6. *Difluoromethylation of phenols formed in situ from aryl boronic acids with HCF_2OTf.*

A further significant report emerged in 2009; Zafrani and co-workers reported non-ozone depleting diethyl (bromodifluoromethyl)phosphonate **2.13** and its reactivity towards (thio)phenols under nucleophilic activation with aqueous KOH (Scheme 2.7 a).[55] Hu and co-workers have also reported various protocols for the difluoromethylation of various

substrates, including (thio)phenols and *N*-heterocycles. They successfully applied numerous Lewis-base activated DFC reagents, including the non-ozone depleting $TMSCF_2Br$,[51] 2-chloro-2,2-difluoroacetophenone[56] and chlorodifluoromethyl aryl sulfone reagents (e.g. **2.14**) (Scheme 2.7 b, c).[52] Gouverneur and co-workers also recently used these reagents for mechanochemical difluoromethylation of (thio)phenols and *N*-heterocycles.[57] Hu investigated the effect of substitution of the 4-position of the phenyl ring of this latter class of reagents on their difluoromethylation reactivity, observing that electron-withdrawing chloro- and nitro-substituents gave the highest yields of difluoromethylated product.[58] A similar study is described for the class of difluoromethyl aryl sulfones used for ^{18}F-difluoromethylation described in this chapter (section 2.2.1), in which the effect of the 4-substituent on reactivity and A_m is investigated.

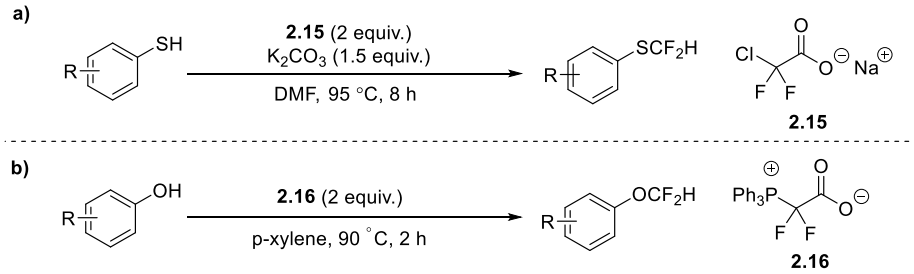


Scheme 2.7 *Difluoromethylation of phenols with nucleophile-activated DFC reagents: a) Zafrani and co-workers' conditions with* ***2.13****, b) Hu and co-workers' conditions with* $TMSCF_2Br$*, c) Hu and co-workers' conditions with* ***2.14****.*

Thermally activated sodium chlorodifluoroacetate (**2.15**) was first applied to the difluoromethylation of thiophenols and *N*-heterocycles by Greaney and co-workers (Scheme 2.8 a).[59] Further application of such reagents was disclosed in 2015 when Xiao and co-workers reported the application of PDFA (**2.16**) to *O*, *S*, *N*-difluoromethylation (Scheme 2.8 b).[54]

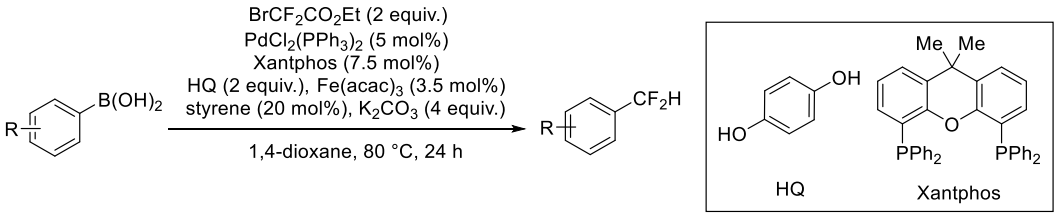
Several groups have studied the reactivity of DFC with transition metals, with low valent, nucleophilic transition metal centres being shown to be competent in the capture of DFC.[60]

These complexes have been leveraged in catalytic cross-coupling protocols, primarily in aromatic difluoromethylation.



Scheme 2.8 *Difluoromethylation of phenols with thermally-activated DFC reagents: a) Greaney and co-workers' conditions with* ***2.15****, b) Xiao and co-workers' conditions with* ***2.16****.*

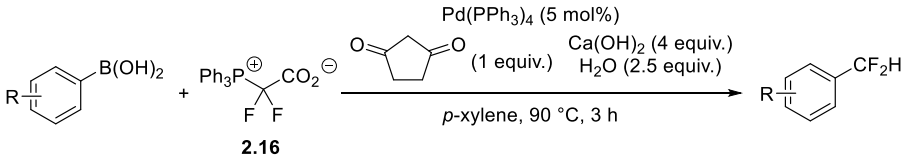
Seminal reports of Pd-catalysed difluoromethylation with DFC emerged in 2016, with the Zhang and Xiao groups both reporting conditions for the difluoromethylation of aryl boronic acids.[61,62] Zhang and co-workers used $PdCl_2(PPh_3)_2$ as a pre-catalyst in combination with the bidentate phosphine Xantphos as a ligand (Scheme 2.9). The DFC reagent employed was ethyl bromodifluoroacetate, which was activated with a K_2CO_3 base, likely first by hydrolysis of the ethyl ester and then decarboxylation. A selection of additives was also employed in Zhang's first report: 2 equivalents of hydroquinone (HQ) were used, while $Fe(acac)_3$ and styrene were added in catalytic amounts. The exact role of HQ was initially unclear, but it was an essential additive and was suggested to assist in the hydrolysis of ethyl bromodifluoroacetate. The reaction conditions required heating to 80 °C using 1,4-dioxane as a solvent. Zhang and co-workers also isolated a homologated C_2F_4H product that was suggested to arise from DFC insertion into the Pd^{II}-CF_2H complex (*vide infra*).



Scheme 2.9. *Pd-catalysed difluoromethylation of aryl boronic acids by Zhang and co-workers (2016)*

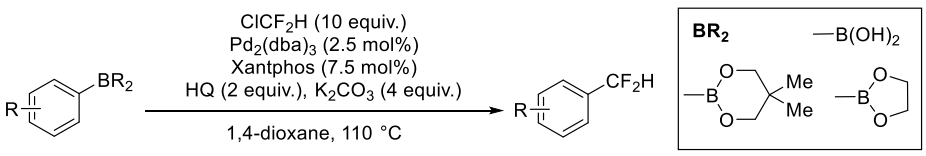
Xiao and co-workers used a $Pd(PPh_3)_4$ catalyst system with thermally-activated PDFA as a DFC reagent (Scheme 2.10).[62] They used $Ca(OH)_2$ as a base, along with added water. Similar to Zhang and co-workers, they added 1,3-cyclopentadione as a stoichiometric additive, which

they suggested behaved as a proton shuttle in the reaction. The optimal conditions required heating at 90 °C in *p*-xylene solvent. Under their conditions, electron-rich and neutral substrates, including substrates derived from heterocycles were converted to the difluoromethylarene.



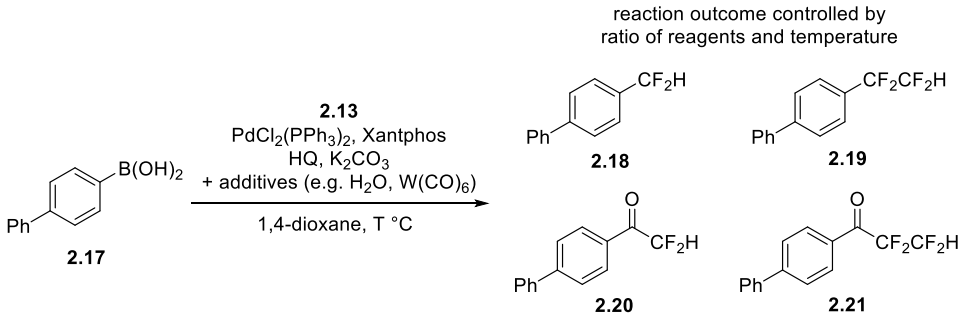
Scheme 2.10. *Pd-catalysed difluoromethylation of aryl boronic acids by Xiao and co-workers (2016).*

Zhang and co-workers further explored Pd-catalysed difluoromethylation using $ClCF_2H$ and diverse (hetero)aryl boron reagents (Scheme 2.11).[63] Under their standard conditions, $Pd_2(dba)_3$ was used in combination with Xantphos as a ligand, in the presence of HQ and K_2CO_3 as a base, and the reaction was performed in 1,4-dioxane at 110 °C. In their exploration of aryl boronate coupling partners, they discovered that aryl boronic acids and boronic esters of ethylene glycol and neopentyl glycol reacted very efficiently, while prevalent pinacol boronates reacted very sluggishly, even when these were pre-activated as the KOH adduct. A broad scope of difluoromethylated compounds, including numerous heterocycles and an array of common functional groups, was accessible using this method. Several difluoromethylated analogues of bioactive and complex molecules were also prepared, suggesting the value of the method for late-stage difluoromethylation of pharmaceutically relevant targets. As in their previous studies, HQ was required as an additive for the reaction to proceed and the authors suggested it can behave as a proton shuttle, required for the protonation of the Pd^0-DFC complex, or as a ligand for Pd. The authors state that oxidised benzoquinone was observed in these reactions.



Scheme 2.11. *Pd-catalysed difluoromethylation of aryl boron reagents with $ClCF_2H$.*

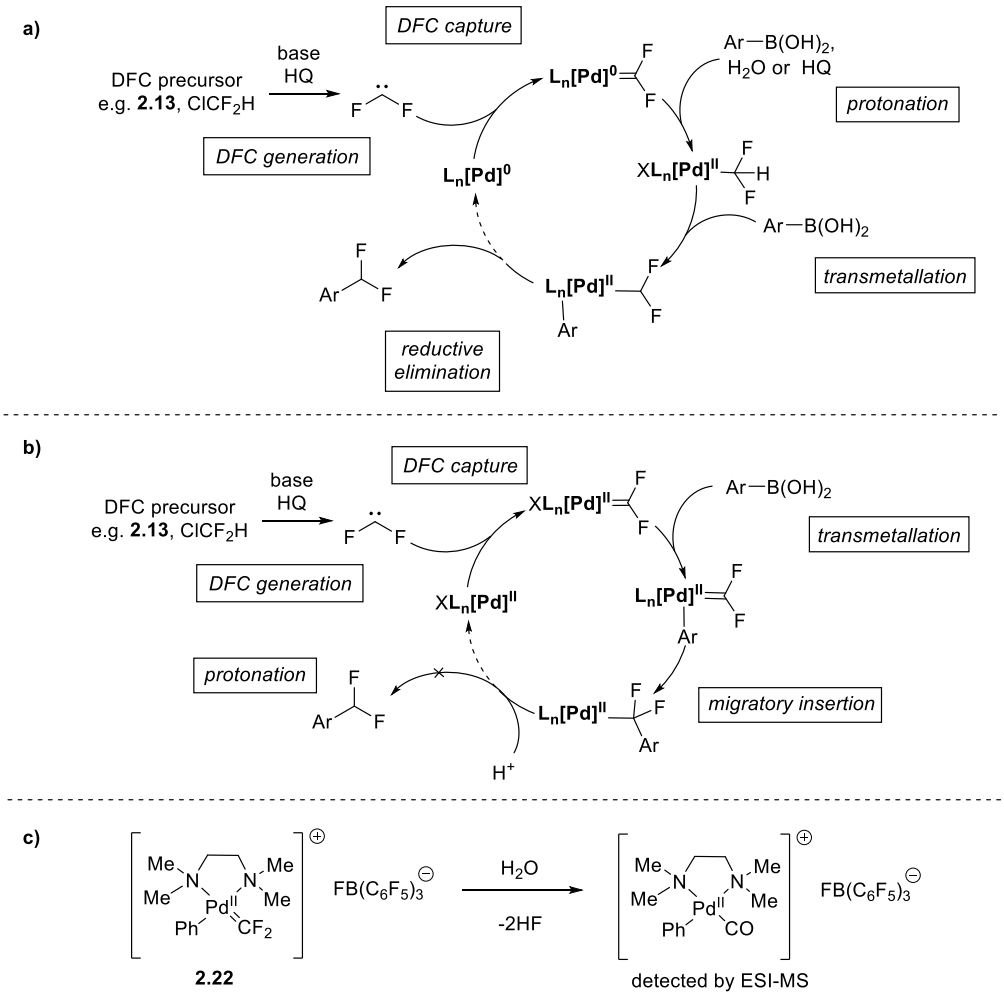
They further expanded their difluoromethylation platform in 2019 to the synthesis of diverse fluoroalkylated compounds.[64] They noted that a model reaction, using a $PdCl_2(PPh_3)_2$-Xantphos catalyst system **2.13** as a DFC reagent, a K_2CO_3 base and a model aryl boronic acid ([1,1'-biphenyl]-4-ylboronic acid, **2.17**) at varying temperature and amounts of water and HQ, gave mixtures of different products (Scheme 2.12). Along with the difluoromethyl arene (**2.18**), the tetrafluoroethyl arene (**2.19**), the difluoromethyl aryl ketone (**2.20**) and tetrafluoroethyl aryl ketone (**2.21**) could also form. They surmised that CO could evolve from DFC by defluorination of the Pd^0-DFC complex. Zhang and co-workers optimised multiple sets of reaction conditions to control the outcome of the reaction. Using more equivalents of DFC reagent and HQ at higher temperature favoured the production of tetrafluoroethyl arenes in preference to difluoromethylarenes. Using a tungsten hexacarbonyl as a CO surrogate, difluoromethyl aryl ketones were obtained, and tetrafluoroethyl aryl ketones could also be obtained.



Scheme 2.12. *Pd-catalysed formation of diverse difluoromethylated products from* ***2.17*** *with* ***2.13****.*

Based on Houk, Zhang and co-workers' mechanistic and computational studies into these conceptually similar reactions, a prevailing Pd^0/Pd^{II} mechanistic proposal has emerged for this type of Pd-catalysed difluoromethylation (Scheme 2.13 a).[64] First, DFC is generated under the reaction conditions from the DFC reagent. In all cases, this is a base-mediated process and it is suggested that HQ (which is likely deprotonated under the reaction conditions) may play a key role as a soluble base. Indeed, computational analysis has shown this is within reach and is also illustrated experimentally by the slower consumption of DFC sources in the absence of HQ. Once generated, DFC is then subsequently captured by a Pd^0 complex. This yields a Pd^0-

DFC complex, which is next suggested to be protonated as it has substantial nucleophilic character at the carbon atom. This protonation event could be mediated by various electrophiles, including water and HQ, but it is suggested computationally that a lower energy pathway proceeds *via* protonation from the aryl boronic acid substrate. Transmetallation of an X-type ligand at Pd with an aryl boronic acid then furnishes a [(Xantphos)Pd^{II}(Ar)(CF_2H)] complex, which can undergo reductive elimination to yield the difluoromethyl arene product and a Pd^0-complex. Xantphos is hypothesised to be a privileged ligand for the reductive elimination of aryl and CF_2H substituents based on prior studies by Grushin *et al* on Xantphos-promoted Ar–CF_3 reductive elimination, due to its wide bite angle (111°) and its nature as a both *cis*- and *trans*-chelating ligand.[65]

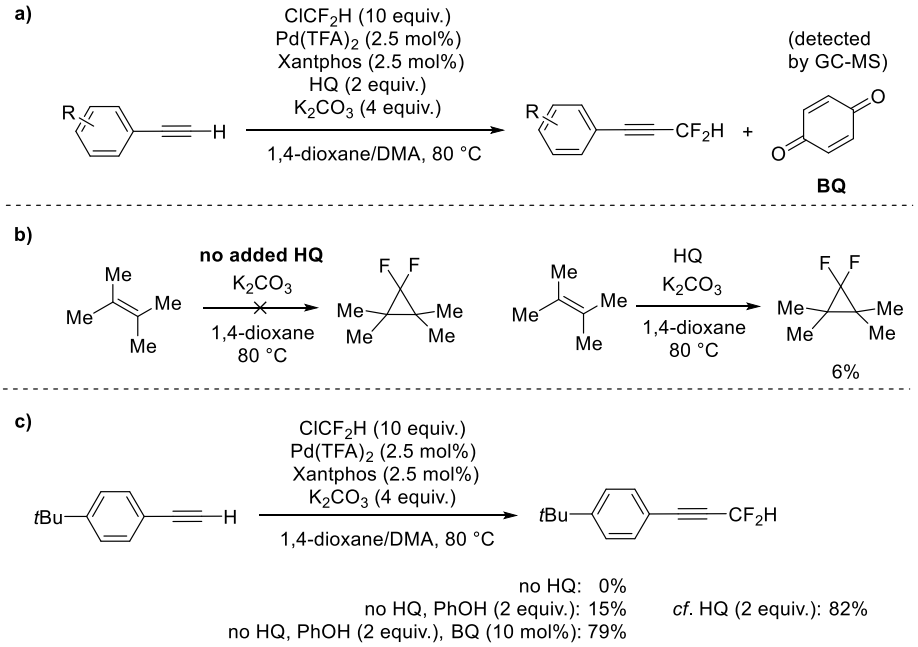


Scheme 2.13. *a) Proposed mechanism for the Pd-catalysed difluoromethylation of aryl boronic acids via a Pd(0)/Pd(II) cycle. b) Unlikely mechanistic proposal for the Pd-catalysed difluoromethylation of aryl boronic acids via a Pd(II)/Pd(II) cycle. c) Proposed mechanism of the hydrolysis of DFC at Pd^{II} centres.*

Where Zhang and co-workers demonstrated the diversification of their product with CO and/or DFC insertion, this is proposed to proceed *via* the interception of their Pd cycle with CO and/or DFC, which could ligate to intermediate Pd^{II} complexes and undergo migratory insertion. These processes are suggested to be competitive with transmetallation of the aryl boron reagent. A Pd^{II} cycle was also ruled out (Scheme 2.13 b); a synthesised $[(Xantphos)Pd^{II}(CF_2Ph)][FB(C_6F_5)_3]$ complex also did not react with proton sources to generate $PhCF_2H$, which only formed in the presence of excess $NaBH_4$. Additionally, a possible mechanism of formation of CO in such reactions was proposed. Zhang and co-workers suggest Pd^{II}-DFC complexes may also form in the reaction, and synthesised Pd^{II}-DFC complex **2.22** was hydrolysed and defluorinated rapidly in the presence of water to produce a Pd^{II}-carbonyl complex that was detected by MS (Scheme 2.13 c). This contrasts with the much slower rate of hydrolysis expected for the more nucleophilic zero-valent Pd^0-DFC complex.[66] This process would lead to degradation of DFC to fluoride and will be considered later in this chapter when the development of a Pd-mediated ^{18}F-difluoromethylation is described.

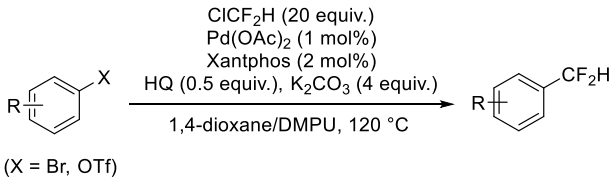
Zhang and co-workers next extended their Pd-catalysed difluoromethylation platform to terminal alkyne substrates (Scheme 2.14 a).[67] Using a $Pd(TFA)_2$-Xantphos catalyst system, $ClCF_2H$ was used as a DFC reagent with HQ as an additive and K_2CO_3 as a base. Terminal alkenes bearing aryl, heteroaryl and alkyl groups were well tolerated and the difluoromethyl alkyne products proved to be a useful handle for functionalisation, being successfully engaged in Au and Pd-catalysed reactions, as well as cyclisations and azide-alkyne click reactions.[67] HQ was suggested to play a crucial role in the generation of DFC from $ClCF_2H$, which was shown in the model difluorocyclopropanation of tetramethylethylene (Scheme 2.14 b). The use of K_2CO_3 alone gave no difluorocyclopropanation. In contrast to their previous studies, Zhang and co-workers suggested HQ could also act as a reductant, as benzoquinone (BQ) was detected by GC-MS analysis in crude reactions (Scheme 2.14 a). Indeed, HQ was competent at reducing $Pd(TFA)_2$ in the presence of Xantphos to a Pd(0) complex with

Xantphos and BQ ligands. The use of a catalytic amount of BQ in combination with phenol in place of HQ enabled the reaction to proceed in similar yield to the standard reaction conditions, while a dramatic reduction in yield was observed when phenol was used in isolation (Scheme 2.14 c).



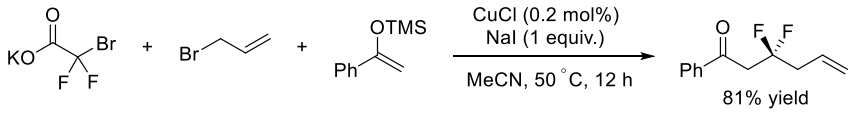
Scheme 2.14. *a) Pd-catalysed difluoromethylation of terminal alkynes. b) Difluorocyclopropanation of tetramethylethylene with and without HQ. c) Effect of HQ, phenol and phenol/BQ additives on the Pd-catalysed difluoromethylation of terminal alkynes.*

Further developments emerged after the work described in this chapter was completed. A reductive, Pd-catalysed difluoromethylation of aryl bromides and triflates was reported by Zhang and co-workers, an interesting departure from their previous redox neutral cross-couplings with nucleophilic aryl boron reagents and alkynes (Scheme 2.15).[68] This cross-electrophile coupling used remarkably similar conditions to their previous reactions, using $ClCF_2H$ as a DFC reagent with a $Pd(OAc)_2$-Xantphos catalyst system, HQ as an additive and K_2CO_3 as a base, in a 1,4-dioxane/DMPU solvent mixture. They suggested HQ could act as a reductant towards Pd^{II} after oxidative addition of the aryl (pseudo)halide partner.



Scheme 2.15. *Pd-catalysed difluoromethylation of (hetero)aryl bromides and triflates.*

Zhang and co-workers disclosed a further DFC transfer reaction under copper catalysis.[69] Despite many literature reports on the chemistry of copper carbenoids, this study comprised the first report of an isolated copper-DFC complex. Along with their structural studies of these isolable complexes, a catalytic reaction was also developed, in which a nucleophilic silyl enol ether was difluoroalkylated with DFC and an allyl/propargyl halide partner, *via* a Cu^{I}-DFC complex. Unlike their Pd^{0}-DFC complexes, which were nucleophilic and reacted readily with electrophiles (e.g. H^{+}), they suggested that the Cu^{I}-DFC complex was electrophilic and thus readily reacted with a silyl enol ether nucleophile. The resulting difluoroalkyl Cu species could then react as a nucleophile with allyl and propargyl halide electrophiles, which gave the desired β-difluorinated ketones (Scheme 2.16).



Scheme 2.16. *Cu-catalysed DFC transfer reported by Zhang and co-workers.*

These catalytic reactions have been shown to be highly valuable methods for the preparation of difluoromethylated compounds from synthetically convenient precursors, such as aryl boron reagents and aryl halides. For this reason, their translation to radiochemistry would be of interest. The development of a Pd-mediated ^{18}F-difluoromethylation of aryl boronic acids with an [^{18}F]DFC reagent is described in this chapter.

2.1.3. Radiosynthetic Approaches to the ^{18}F-Difluoromethyl Group

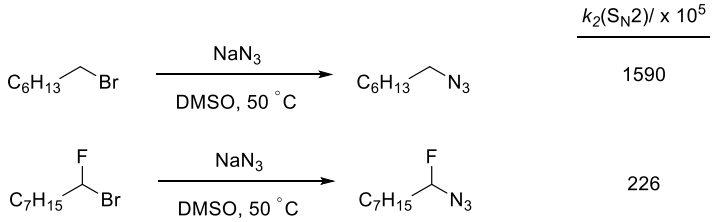
Radiochemists have developed numerous unique strategies to access the difluoromethyl group in radiolabelled form.[70] The constraints of F-18 radiochemistry imposed a set of demands upon the development of any synthesis of [^{18}F]CF_2H compounds, which has rendered this a challenging prospect. For example, such reactions should be compatible with automated radiosynthesis and not require the exclusion of air and moisture. A_m also presents a key challenge in the synthesis of ^{18}F-difluoromethylated compounds (Chapter 1, section 1.3.1).[71] The nature of the difluoromethyl group demands the presence of at least one ^{19}F

atom per labelled molecule and due to the nano-to-picomolar concentration of the ^{18}F-labelled reagent, the concentration of ^{19}F will always vastly exceed the concentration of ^{18}F atoms. Defluorination side-reactions of pre-fluorinated radiolabelling substrates may also produce fluoride anions, which can either compete with [^{18}F]fluoride for the substrate, or participate in undesired ^{19}F/^{18}F-isotopic exchange processes under the reaction conditions. Both processes produce the ^{19}F-compound, which will reduce the A_m of the product. Due to the importance of A_m in the preparation of PET radiotracers, this account will only consider the non-carrier-added radiosynthesis of [^{18}F]CF_2H compounds.

2.1.3.1. Radiosynthesis via ^{18}F-Fluorination

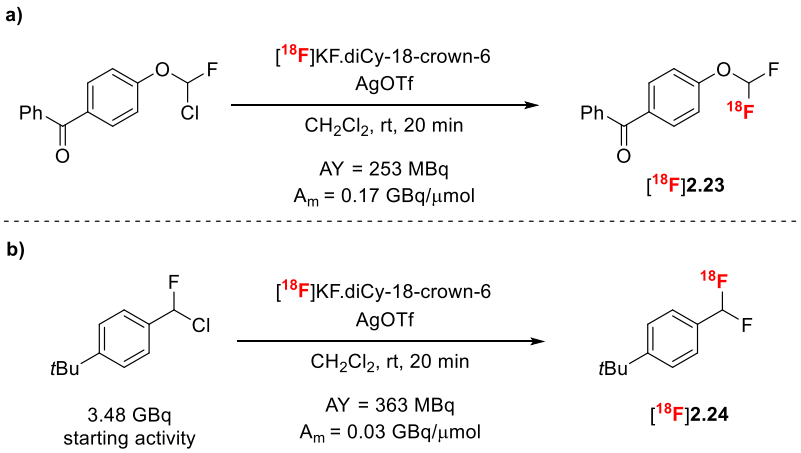
Several groups have demonstrated that ^{18}F-fluorination is an effective approach to [^{18}F]CF_2H compounds. It allows for the direct use of [^{18}F]fluoride and therefore does not necessitate multiple radiosynthetic steps. However, this strategy, in general, requires a pre-fluorinated radiolabelling substrate, also bearing a leaving group. The synthesis of such bespoke substrates can be a bottleneck to PET radioligand discovery, especially for complex targets, or if multi-step synthetic routes are required. Another challenge is the detrimental effect α-fluorine atom-substitution at carbon has on the rate of nucleophilic substitution of leaving groups. This was studied by Dolbier and co-workers, who analysed the effect of fluorine substitution on nucleophilic substitution kinetics (Scheme 2.17).[72] They compared the second-order rate constants ($k_2(S_N2)$) for a series of nucleophilic substitution reactions of primary alkyl bromides and the mono-α-fluorinated analogue and found that the rate of substitution with sodium azide was approximately 7 times slower for the α-fluoro compound. It is suggested this effect arises from the electrostatic repulsion of the nucleophile by the fluorine atom's lone pairs and the inductively withdrawing fluorine atom can also destabilise any positive charge build-up at carbon during substitution. The α-fluorine atom has also been shown to promote competitive elimination. This may lead to the degradation of the radiolabelling substrate, as radiofluorination is often conducted in the presence of bases,

such as K_2CO_3. To tackle this, radiochemists have developed strategies to activate their radiolabelling substrate towards [^{18}F]fluoride or have designed substrates with improved substitution reactivity in ^{18}F-fluorination.



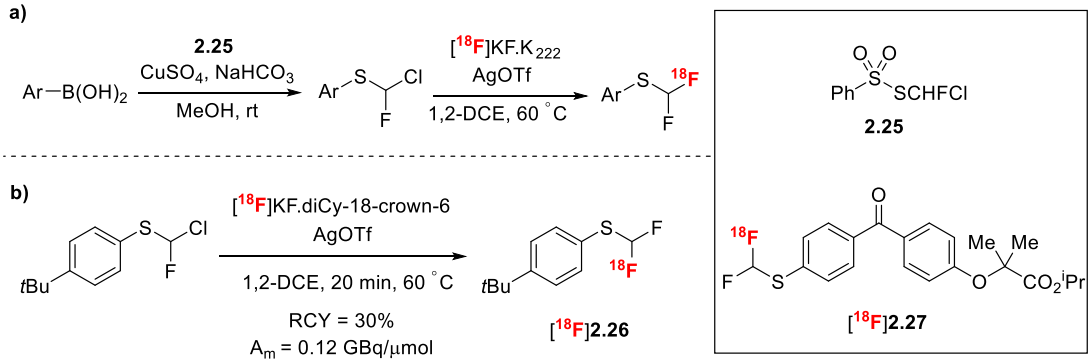
Scheme 2.17. *Effect of α-fluorination on nucleophilic substitution kinetics.*

In a first example, Gouverneur and co-workers demonstrated that a halophilic $Ag^{I}OTf$ additive could activate chlorofluoromethylated substrates to 'halex' (halogen exchange) substitution with [^{18}F]fluoride, while control experiments performed in the absence of this gave no desired radiofluorinated product (Scheme 2.18).[73,74] They suggested that the halophilic Ag^{I} cation polarises the C–Cl bond, which facilitates substitution processes. They were able to access aryl-[^{18}F]CF_2H and aryl-[^{18}F]OCF_2H compounds using this method, delivering 8 examples in up to 39% RCY and 9 examples in up to 79% RCY, respectively. They also demonstrated that the products could be isolated by semi-preparative HPLC, preparing aryl-[^{18}F]OCF_2H compound [^{18}F]**2.23** in an AY of 253 MBq and an A_m of 0.17 GBq/µmol (Scheme 2.18 a) and aryl-[^{18}F]CF_2H compound [^{18}F]**2.24** in an AY of 363 MBq and an A_m of 0.03 GBq/µmol (Scheme 2.18 b). This work served as a proof-of-concept that such precursors could be activated towards nucleophilic substitution with [^{18}F]fluoride. However, there are several limitations of the wider application of this radiochemistry. The first being that the obtained A_m values are low (< 1 GBq/µmol), which could limit the use of the products in some PET imaging applications. Another important consideration is the preparation of the chlorofluoromethyl labelling substrates, which require multi-step synthesis from either aryl acetic acids or phenols. This could limit the application of this method to the preparation of more elaborate or structurally complex targets.



Scheme 2.18. *Gouverneur and co-workers' Ag-mediated halex radiofluorination for the preparation of a) aryl-[^{18}F]OCF$_2$H and b) aryl-[^{18}F]CF$_2$H.*

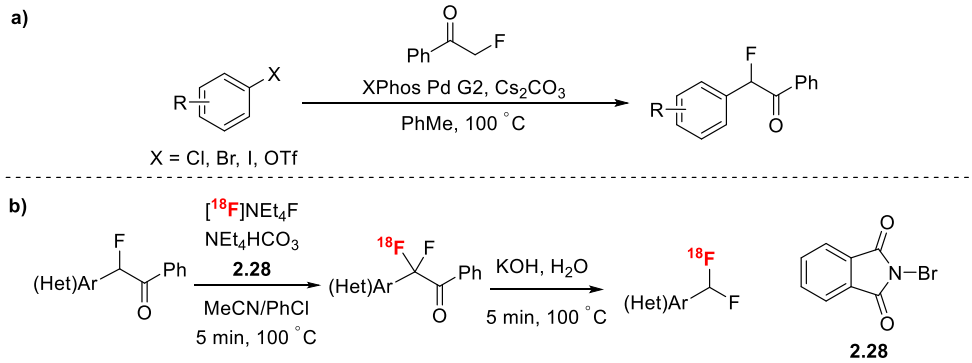
Shen, Gouverneur and co-workers later demonstrated that the same strategy could also be applied to the radiosynthesis of aryl-[^{18}F]SCF$_2$H compounds, in 14 examples (Scheme 2.19 a).[75] The chlorofluoromethyl sulfide labelling precursors were prepared in a single step synthesis *via* a Cu-catalysed cross-coupling, using a novel chlorofluoromethylthiolation reagent (**2.25**). This enabled extension of the Ag-halex methodology to more complex molecules, including a ^{18}F-difluoromethylthiolated derivative of the hypolipidemic agent fenofibrate ([^{18}F]**2.27**), which was prepared in 51% RCY. Using starting activities of up to 4 GBq, the model aryl-[^{18}F]SCF$_2$H compound ([^{18}F]**2.26**) was prepared in an A_m of 0.12 GBq/μmol (Scheme 2.19 b).



Scheme 2.19. *Shen, Gouverneur and co-workers' Ag-mediated halex radiofluorination for the preparation of aryl-[^{18}F]SCF$_2$H compounds. a) Reaction blueprint. b) Isolation of compound [^{18}F]**2.26**.*

Ritter, Vasdev, Liang and co-workers disclosed a ^{18}F-fluorination approach to access ^{18}F-difluoromethyl arenes in 2016 (Scheme 2.20).[76] They proposed the preparation of 2-fluoro-2-arylacetophenones as radiolabelling substrates using Pd-catalysed enolate coupling of aryl

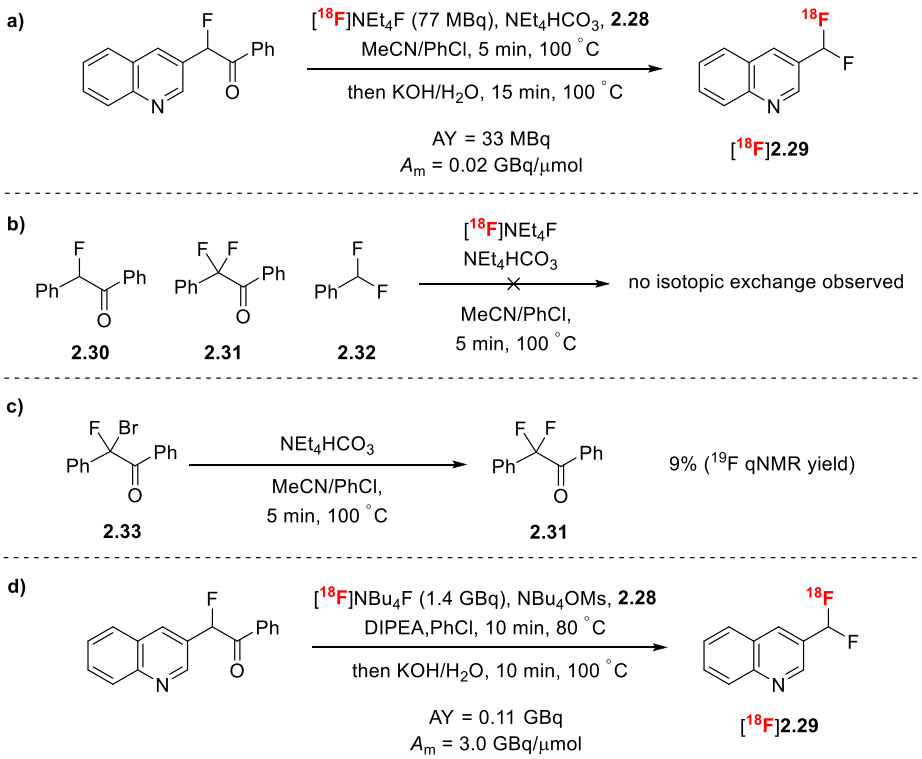
halides and triflates and 2-fluoroacetophenone (Scheme 2.20 a).[77] The reactivity of these substrates hinged on the benzoyl auxiliary group. These substrates are easily brominated at the α-carbon, to yield an intermediate that is reactive towards halex ^{18}F-fluorination. The benzoyl group likely also activates the substrate towards nucleophilic substitution at the α-carbon and this group can also be conveniently cleaved with aqueous base in a Haller-Bauer reaction.[78] Ritter and co-workers demonstrated that all of these steps could occur in a one-pot fashion from the 2-fluoro-2-arylacetophenone: [^{18}F]fluoride in the presence of *N*-bromophthalimide (**2.28**) gave an intermediate [^{18}F]2,2-difluoro-2-arylacetophenone in an MeCN and chlorobenzene solvent mixture at 100 °C (Scheme 2.20 b). An aqueous KOH solution was then added, and the mixture again heated to 100 °C to facilitate the cleavage of the benzoyl group. This method was used in the preparation of 25 examples of ^{18}F-difluoromethyl arenes in up to 60% RCY, including derivatives of bioactive molecules. They also found that side-reactions of **2.28** with substrates containing tertiary amines, a common structural motif in pharmaceuticals, could be avoided by the pre-bromination of a Li-enolate with *N*-bromosuccinimide. This enolate could be formed by deprotonation of the 2-fluoro-2-arylacetophenone substrates with LiHMDS.



Scheme 2.20. *Ritter, Vasdev, Liang and co-workers' radiosynthesis of ^{18}F-difluoromethyl arenes. a) Synthesis of α-aryl-α-fluoroacetophenone labelling precursors from* ***2.27.*** *b) One-pot bromination with* ***2.28****, ^{18}F-fluorination and benzoyl group cleavage.*

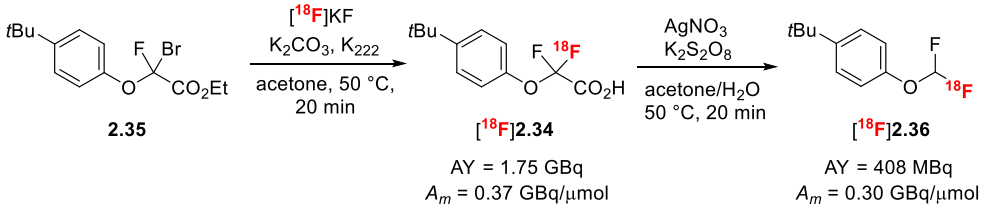
Ritter and co-workers also optimised for the A_m of their isolated radioproducts (Scheme 2.21). Isolation of a ^{18}F-difluoromethylated quinoline ([^{18}F]**2.29**) from 77 MBq starting activity gave 33 MBq of the desired product with low A_m of 0.02 GBq/µmol (Scheme 2.21 a). The authors investigated potential sources of isotopic dilution. Isotopic exchange with [^{18}F]fluoride under

the reaction conditions was not observed for the substrate **2.30**, nor for ^{19}F-products **2.31** and **2.32** (Scheme 2.21 b). This suggested that these fluorinated species were likely not sources of ^{19}F-fluoride, as they were stable to substitution. In an subsequent experiment, however, under the reaction conditions, **2.33** was revealed to form to the difluorinated product **2.31** in 9% yield (determined by ^{19}F qNMR); a possible pathway for this could be the leaching of ^{19}F-fluoride from **2.33**, which can then fluorinate another molecule of **2.33** (Scheme 2.21 c). Changing the elution conditions to use a less basic elution reagent, tetrabutylammonium mesylate, in place of tetraethylammonium hydrogencarbonate, proved instrumental. As these conditions resulted in lower reactivity, DIPEA was used an additive, as the addition of tertiary amine bases has been suggested to aid substitutions at fluorinated carbon atoms.[79] Under this set of conditions, starting with 1.4 GBq of [^{18}F]fluoride gave [^{18}F]**2.29** in an improved A_m of 3.0 GBq/μmol and an AY of 0.11 GBq (Scheme 2.21 d).



Scheme 2.21. *Optimisation for A_m in Ritter and co-workers' radiosynthesis of aryl-[^{18}F]CF_2H compounds. a) Original conditions for the radiosynthesis of [^{18}F]**2.29**. b) Isotopic exchange study for ^{19}F-fluorinated intermediates **2.30**, **2.31** and **2.32**. c) Degradation of **2.33** under the reaction conditions in the absence of [^{18}F]fluoride to yield non-radioactive fluorination product **2.31**. d) Optimised conditions for the radiosynthesis of [^{18}F]**2.29** in higher A_m.*

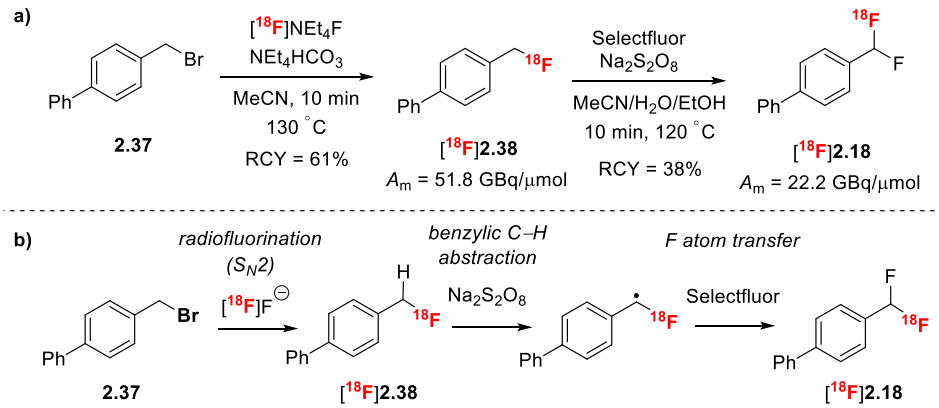
In 2017, the ^{18}F-fluorination of ethyl α-bromo-α-fluoro(aryloxy)acetates for the preparation of ^{18}F-difluoromethoxyarenes was described by Gouverneur and co-workers (Scheme 2.22).[80] ^{18}F-Fluorination of these substrates yielded ^{18}F-α,α-difluoro(aryloxy)acetic acids. For example, an AY of 1.75 GBq of [^{18}F]**2.34** (A_m = 0.37 GBq/μmol) was prepared from bromide **2.35** and a starting activity of 5.13 GBq. The telescoped synthesis of ^{18}F-difluromethyl aryl ether [^{18}F]**2.36** with cartridge-purified [^{18}F]**2.34** (1.75 GBq) proceeded in an AY of 408 MBq and A_m = 0.30 GBq/μmol. This was a two-step radiosynthetic protocol, which required the oxidative cleavage of the carboxylic acid group, for which a combination of $AgNO_3$ and $K_2S_2O_8$ was effective.



Scheme 2.22. *^{18}F-Fluorination of ethyl α-bromo-α-fluoro(aryloxy)acetates and radiosynthesis of ^{18}F-difluoromethoxyarene [^{18}F]**2.36**.*

Liang and co-workers next disclosed a two-step protocol for the preparation of ^{18}F-difluoromethyl arenes.[81] Instead of using a pre-fluorinated labelling precursor, they instead applied a post-labelling ^{19}F-fluorination strategy. This allowed them to use primary benzylic halides and sulfonates as labelling precursors, which mitigates any detrimental effect of α-fluorine substitution on reactivity. These substrates were converted to the benzylic ^{18}F-fluorides in high RCY using [^{18}F]TEAF in MeCN solvent at 130 °C. These materials could then be ^{19}F-fluorinated *via* a benzylic C–H fluorination with Selectfluor and $K_2S_2O_8$. For example, starting from bromide **2.37**, benzylic ^{18}F-fluoride [^{18}F]**2.38** was prepared in 61% RCY, and this was then fluorinated to produce [^{18}F]**2.18** in 38% RCY and a good A_m of 22.2 GBq/μmol (Scheme 2.23 a). The benzylic C–H fluorination was proposed to proceed *via* a radical mechanism: firstly, the authors propose that sulfate radical anions form from persulfate.[82] These can abstract the benzylic H atom, leaving a benzyl C-centred radical. Selectfluor can then transfer an F-atom to this radical, furnishing the ^{18}F-difluoromethyl arene (Scheme 2.23

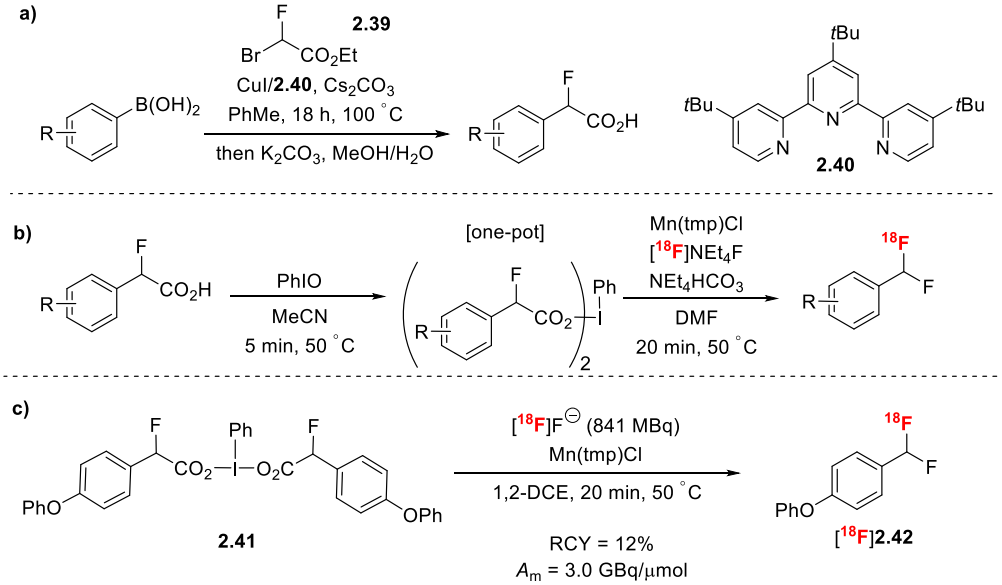
b). Liang and co-workers demonstrated that their method gave products with higher A_m than the other syntheses of ^{18}F-difluoromethyl arenes disclosed at the time. This is likely as the ^{18}F-fluorination is performed on a benzyl bromide substrate that is not fluorine-containing. The authors also suggest that there is limited isotopic exchange with Selectfluor, which possesses tetrafluoroborate counteranions. Despite the high A_m of the radiolabelled products, a drawback of this protocol is the need for two semi-preparative HPLC purifications. This results in a longer synthesis, increasing activity losses to radioactive decay and during purification. This protocol has also not been extended to substrates derived from complex molecules, likely due to challenges associated with precursor synthesis and/or the functional group tolerance of the C–H fluorination step.



Scheme 2.23. *Liang and co-workers' two-step radiosynthesis of ^{18}F-difluoromethyl arenes. a) Radiosynthesis of [^{18}F]**2.18** from benzyl bromide **2.37**. b) Proposed mechanism for the formation of [^{18}F]**2.18**.*

In 2019, Gouverneur and co-workers disclosed a decarboxylative ^{18}F-fluorination approach towards ^{18}F-difluoromethyl arenes, building on previous studies by Groves and co-workers' into Mn-mediated aliphatic radiofluorination.[83,84] The radiolabelling substrates required for this protocol were α-fluoro carboxylic acids, for which a convenient synthesis *via* a Cu-catalysed cross-coupling was reported (Scheme 2.24 a). This cross-coupling used widely available aryl boronic acids as starting materials in combination with ethyl bromofluoroacetate (**2.39**), a CuI catalyst and a terpyridine ligand (2,6-bis[4-(tert-butyl)pyridin-2-yl)-4-(*tert*-butyl)pyridine, **2.40**). The synthesised 2-fluoro-2-arylacetic acids were then applied in the Mn-mediated decarboxylative radiofluorination, which was carried

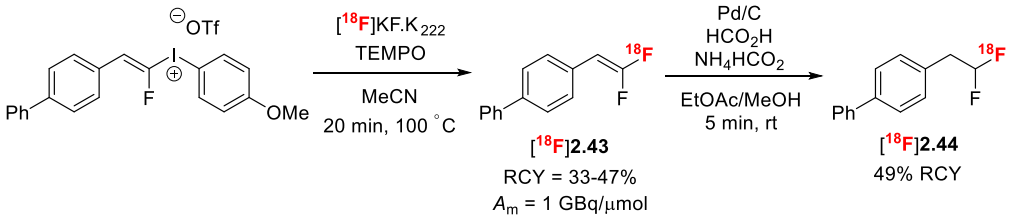
out in a two-step, one-pot protocol (Scheme 2.24 b). Firstly, the acid was combined with iodosylbenzene, which afforded an iodine(III) carboxylate intermediate. A Mn^{III}-porphyrin catalyst (Mn(tmp)Cl) was then added, along with a solution of [^{18}F]NEt_4F in DMF, after which heating at 50 °C for 20 min afforded the ^{18}F-difluoromethyl arene. This reaction was used for the preparation of 19 examples in up to 40% RCY, including ^{18}F-difluoromethylated derivatives of bioactive and complex molecules. Mechanistically, this reaction is suggested to proceed *via* an *in situ* formed [^{18}F]Mn(tmp)F complex, which could act as a F-atom transfer reagent to carbon-centred radicals generated by the decarboxylation of the iodine(III) carboxylate species. Using a pre-formed iodine(III) carboxylate derived from 2-fluoro-2-(4-phenoxyphenyl)acetic acid (**2.41**), and a modified elution protocol using Mn(tmp)Cl to elute [^{18}F]fluoride from the QMA cartridge, [^{18}F]**2.42** was prepared in 12% RCY and an A_m of 3.0 GBq/µmol (Scheme 2.24 c).



Scheme 2.24. *Gouverneur and co-workers' radiosynthesis of ^{18}F-difluoromethyl arenes via Mn^{III}-porphyrin mediated decarboxylative ^{18}F-fluorination of α-fluoro carboxylic acids. a) Cu-catalysed cross coupling of (hetero)aryl boronic acids and **2.39**. b) Decarboxylative ^{18}F-fluorination of α-fluoro carboxylic acids with Mn(tmp)Cl catalyst. c) Isolation of ^{18}F-difluoromethylarene [^{18}F]**2.42**.*

Tredwell and co-workers have discovered a route to ^{18}F-1,1-difluoroalkenes, which can also be exploited for the radiosynthesis of ^{18}F-difluoromethyl-containing compounds (Scheme 2.25).[85] From a fluoroalkenyl(aryl)iodonium triflate precursor, radiofluorination with [^{18}F]fluoride in the presence of TEMPO as an additive gave the ^{18}F-1,1-difluoroalkene upon

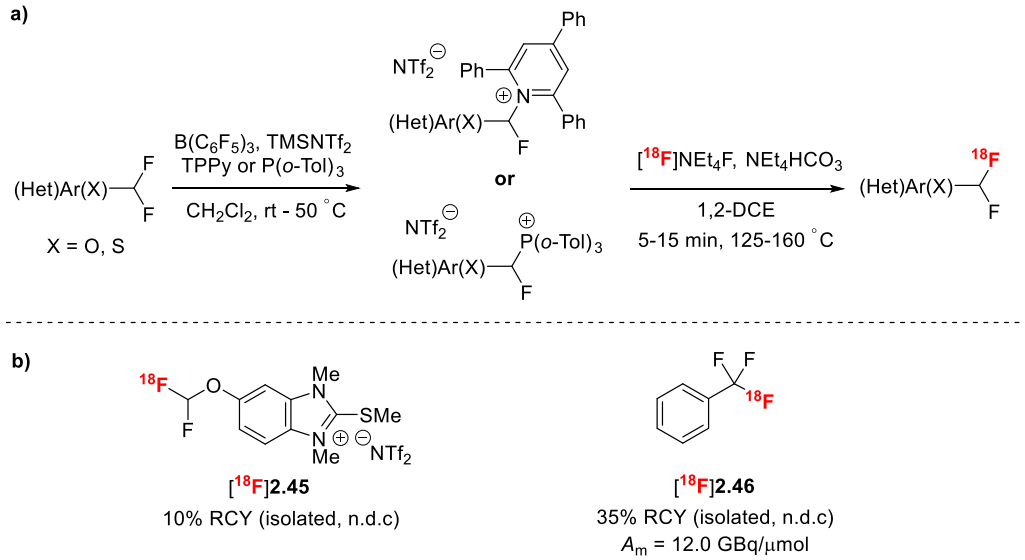
heating for 20 minutes at 100 °C in MeCN solvent. For example, [^{18}F]**2.43** was prepared in an automated radiosynthesis in up to 47% RCY and in A_m of 1 GBq/µmol. These products can then act as versatile intermediates to access various ^{18}F-difluorinated compounds. For example, the reduction of [^{18}F]**2.43** with Pd/C and ammonium formate/formic acid to form ^{18}F-difluoromethyl compound [^{18}F]**2.44** was possible in 49% RCY.



Scheme 2.25. *Tredwell and co-workers' radiosynthesis and derivatisation of ^{18}F-1,1-difluoroalkenes.*

Most recently, Young and co-workers reported a novel radiofluorination approach to various [^{18}F]CF_2H compounds, as well as ^{18}F-trifluoromethylated molecules (Scheme 2.26 a).[86] Using their Frustrated Lewis Pair-mediated C–F activation platform, they prepared pyridinium and phosphonium radiolabelling precursors that delivered the ^{18}F-isotopologue of the starting compounds upon reaction with [^{18}F]fluoride. Their 'on-demand' radiosynthetic strategy allowed for the synthesis of the labelling substrate in a single step from the ^{19}F-reference compound, obviating the need for multi-step precursor synthesis. To prepare the pyridinium or phosphonium substrates, difluoromethyl-containing substrates are combined with a $B(C_6F_5)_3$ catalyst and $TMSNTf_2$, in the presence of either 2,4,6-triphenylpyridine (TPPy) or tri(*o*-tolyl)phosphine (P(*o*-Tol)$_3$). These C–F activation conditions have been demonstrated for activated benzylic and α-heteroatom positions, but Young and co-workers have also shown that tetrahydrothiophene can be effective as an alternative Lewis base to access less activated substrates.[87] They showed that these onium substrates are reactive to substitution with [^{18}F]fluoride, reporting 7 examples of [^{18}F]CF_2H compounds in RCY up to 93%. Young and co-workers also isolated Pantaprazole fragment [^{18}F]**2.45** in 10% RCY (Scheme 2.26 b). While they did not measure the A_m of an isolated ^{18}F-difluoromethyl compound, [^{18}F]trifluorotoluene ([^{18}F]**2.46**) could be isolated in A_m of 12 GBq/µmol, suggesting that products in up to good A_m

would be readily accessible with this method. This was an optimised value, improved from an original value of 3 GBq/µmol, after 10-fold reduction of the loading of the labelling precursor. They also investigated sources of isotopic dilution and found that the triflimide counteranion was not significant as a ^{19}F-source in the reaction, as similar quantities of ^{19}F-trifluorotoluene formed in ^{19}F NMR experiments where a series of precursors with different counterions (both fluorine-containing and non-fluorine containing) were subjected to the reaction conditions.



Scheme 2.26. *Young and co-workers' radiosynthesis of ^{18}F-difluoromethylated compounds. a) Reaction overview. b) Isolation of [^{18}F]**2.45** and [^{18}F]**2.46**.*

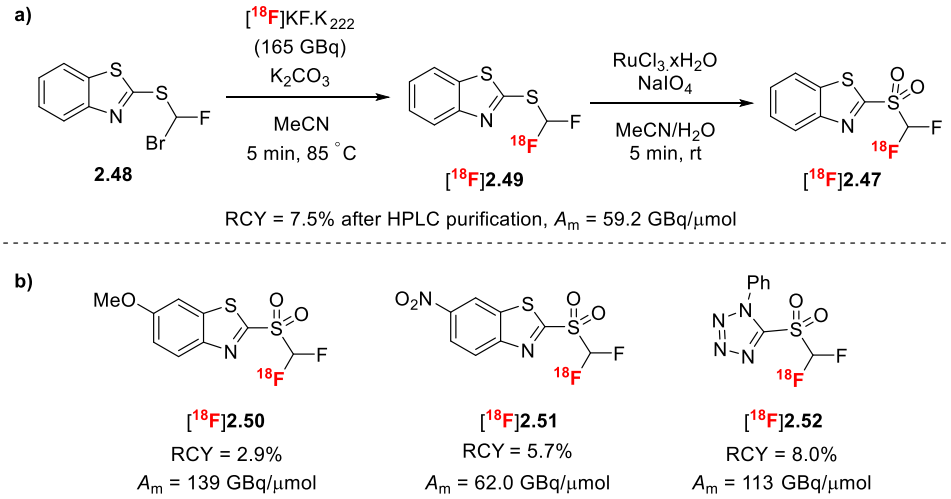
2.1.3.2. Radiosynthesis via ^{18}F-Difluoromethylation

Compared to ^{18}F-fluorination approaches, ^{18}F-difluoromethylation has attracted less attention for the radiosynthesis of ^{18}F-difluoromethylated compounds, however, as noted in section 2.1.2, it has proved a highly effective strategy for the late-stage introduction of unlabelled difluoromethyl groups.[2] As noted previously, such an approach requires a reagent to transfer the ^{18}F-difluoromethyl unit to a substrate, and as with ^{19}F-difluoromethylation, this invokes reagents that release reactive intermediates or act as equivalents of these species. Thus far, two key reports have emerged. One approach hinges on a ^{18}F-difluoromethyl radical intermediate and the second, which is the object of the work described in this chapter, harnesses [^{18}F]DFC as a reactive intermediate for ^{18}F-difluoromethylation.

In 2019, Lemaire, Luxen, Genicot and co-workers disclosed a ^{18}F-difluoromethylation platform that proceeded *via* the [^{18}F]CF_2H radical.[88] As highlighted in section 2.1.2.3, this is a versatile synthetic intermediate that can be engaged either directly in reactions with substrates, or indirectly using transition metal catalysts. The reagent chosen for their work was a ^{18}F-difluoromethyl heteroaryl sulfone, as this class of reagents offers several advantages. Firstly, their radiosynthesis is within reach using [^{18}F]fluoride, as several methods have been reported for the preparation of [^{18}F]SCF_2H compounds, and oxidation of sulfides to sulfones should be facile. They have been shown to be reactive as difluoromethyl radical sources in difluoromethylation reactions previously.[89] They are also non-volatile solids, rendering them easy to handle, and are easily characterised and purified by HPLC methods, due to the heteroarene substituent and their nature as neutral molecules. They have also been demonstrated to be compatible with automated radiosynthesis platforms, such as the Trasis AllinOne and GE FastLab.[88,90]

The authors first prepared the benzothiazole-derived ^{18}F-difluoromethyl sulfone reagent ([^{18}F]**2.47**) *via* a two-step radiosynthesis. Firstly, a halex ^{18}F-fluorination of a

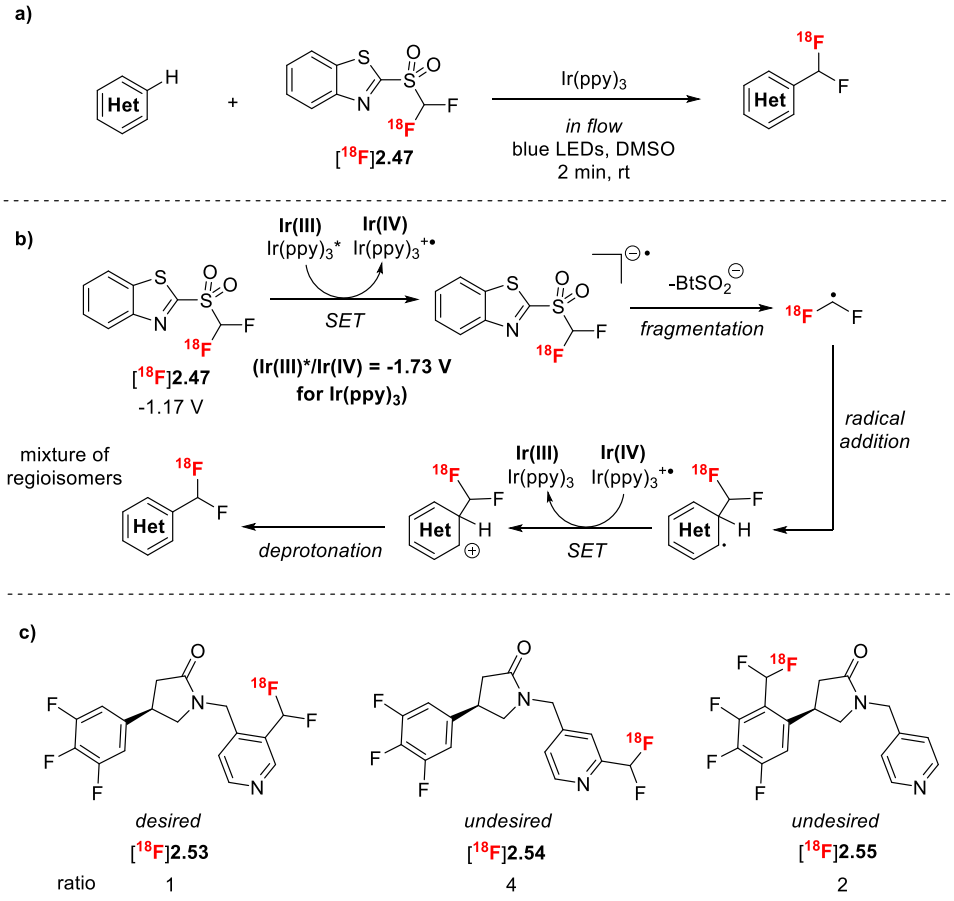
bromofluoromethyl sulfide precursor (**2.48**) was carried out, followed by oxidation of the crude ^{18}F-difluoromethyl thioether ([^{18}F]**2.49**) with $RuCl_3$ hydrate and $NaIO_4$. Over two steps, isolated [^{18}F]**2.47** was prepared in 7.5% RCY from 165 GBq starting activity, with A_m of 59.2 GBq/μmol using a Trasis AllinOne radiosynthesiser (Scheme 2.27 a).[90] The same authors later studied the effect of modifications to the heteroaryl scaffold on the radiosynthesis of the ^{18}F-sulfone reagents (Scheme 2.27 b).[91] These analogues [^{18}F]**2.50**, [^{18}F]**2.51** and [^{18}F]**2.52** were found to be similarly reactive as ^{18}F-difluoromethylating reagents and these could be prepared in up to 8% RCY and in A_m of up to 139 GBq/μmol.



Scheme 2.27. *Radiosynthesis of ^{18}F-difluoromethyl heteroaryl sulfones a) Radiosynthesis of [^{18}F]**2.47**. b) Comparison of ^{18}F-difluoromethyl heteroaryl sulfones [^{18}F]**2.50**, [^{18}F]**2.51** and [^{18}F]**2.52**.*

The application of these reagents in photoredox Minisci-type ^{18}F-difluoromethylation reactions with *N*-heterocycles was demonstrated in 27 examples and in RCY up to 75% (Scheme 2.28 a). The reaction was conducted in flow in DMSO solvent under blue light irradiation in the presence of an $Ir(ppy)_3$ photocatalyst, which in its photoexcited state was capable of reducing [^{18}F]**2.47** (Scheme 2.28 b). This was proposed to deliver a radical anion, which fragmented to a sulfinate anion and the CF_2H radical, which could then add to an *N*-heterocycle. Due to the innate reactivity of the CF_2H radical, however, where a substrate possessed multiple reactive sites, mixtures of regioisomeric ^{18}F-difluoromethylated products were obtained. This is exemplified in the authors' radiosynthesis of an ^{18}F-difluoromethylated analogue of the PET radiotracer [^{11}C]UCB-J ([^{18}F]**2.53**), where 3 regioisomeric radiolabelled

products were obtained ([^{18}F]**2.53**, [^{18}F]**2.54** and [^{18}F]**2.55**), the desired regioisomer being formed in the lowest RCY (Scheme 2.28 c). This illustrates a limitation of this method, as reactivity and regioselectivity is intrinsically substrate-controlled and regioisomeric product mixtures are likely to be time-consuming to separate by HPLC methods.



Scheme 2.28. *^{18}F-Difluoromethylation with [^{18}F]**2.47**. a) Minisci-type ^{18}F-difluoromethylation of heteroarenes with [^{18}F]**2.47** b) Proposed mechanism. First reduction potentials indicated are relative to the standard calomel electrode. c) Regioselectivity in the radiosynthesis of ^{18}F-difluoromethylated analogues of UCB-J.*

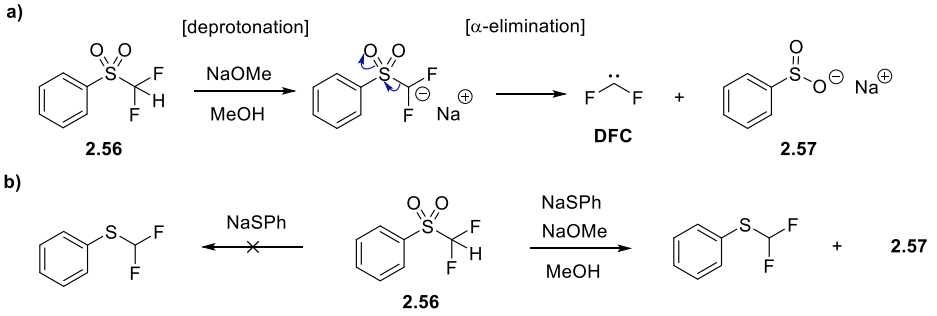
Development of radiochemistry with the [^{18}F]CF_2H radical currently remains limited to the reports of Minisci-type radical addition by Lemaire, Luxen, Genicot and co-workers. However, as described in section 2.1.2.3, there exists a wide array of promising difluoromethylation reactions that would expand the radiochemical space if these were translated to ^{18}F-radiochemistry.

The second reactive intermediate that has been explored for ^{18}F-difluoromethylation is [^{18}F]difluorocarbene ([^{18}F]DFC).[92] This was disclosed by Gouverneur and co-workers in 2022 and this work will also be presented in this chapter. The next section will summarise the state-of-play before the work described in this thesis commenced.

2.1.4. [^{18}F]Difluorocarbene Radiochemistry

As described in section 2.1.2.4, DFC is a powerful and versatile reactive intermediate for difluoromethylation.[46] Therefore, harnessing [^{18}F]DFC and the translation of its diverse reactivity profile to ^{18}F-radiochemistry was a promising and attractive prospect. The work described in this section was carried out by Dr. J. Sap, Dr. C. Meyer and Dr. N. Straathof, prior to the work disclosed in this chapter. Computational studies were conducted by Dr. A. Dürr.[92]

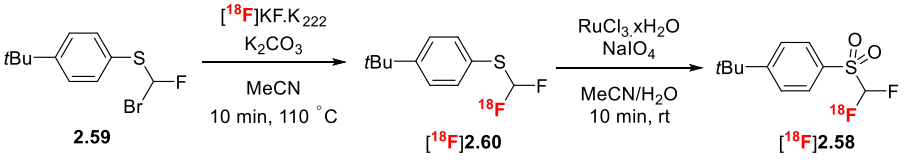
^{18}F-Difluoromethyl aryl sulfones were identified as a class of [^{18}F]DFC reagents that was promising for ^{18}F-difluoromethylation. Hine and Porter had suggested in 1960 that difluoromethyl phenyl sulfone (**2.56**) was a source of DFC; the rate of reaction of **2.56** with sodium methoxide was faster than would be expected for an S_N2 mechanism, suggesting another degradation pathway was in operation, namely *via* stepwise deprotonation and α-elimination to yield DFC and sodium benzenesulfinate (**2.57**) (Scheme 2.29).[49] This is in contrast to the behaviour observed in their studies on haloforms, which undergo concerted deprotonation and α-elimination to produce DFC.[48] They also found that while sodium thiophenoxide did not react with **2.56** directly, it rapidly reacted when sodium methoxide was added, giving difluoromethyl phenyl sulfide, difluoromethyl methyl ether and **2.57**.[49]



Scheme 2.29. *Formation of DFC from **2.56** by stepwise mechanism, proposed by Hine and Porter.*

Since Hine and Porter's report, such reagents have been largely overlooked as DFC precursors, as new reagents were developed, but for radiolabelling their properties rendered them well-suited. Similarly to the reagents prepared by Luxen, Genicot and co-workers, difluoromethyl aryl sulfones can be prepared *via* established radiosynthetic methods and have also been shown to be compatible with automation on commercial radiosynthesis platforms.[88] As with heteroaryl sulfones, difluoromethyl aryl sulfones are non-volatile, which allows for easier handling than gaseous reagents. As they are neutral, rather than ionic compounds, absorb UV light and are chemically stable, they are also readily characterised by radio-TLC and HPLC methods. This is convenient for the measurement of A_m, as it allows for the direct evaluation of the reagent's A_m, rather than requiring its derivatisation to a product. They can also be conveniently purified by (semi)-preparative HPLC methods, which is a standard purification method for ^{18}F-radiotracers. Their modular nature and presence of an aromatic ring, which can be functionalised with various groups, allows for structural optimisation and the comparison of properties across a series of analogues. This aspect is investigated in detail in this chapter.

Initial studies proceeded with a first generation [^{18}F]DFC reagent ([^{18}F]**2.58**), which featured a 4-*tert*-butyl phenyl substituent. A radiosynthesis for this compound was first developed from a bromofluoromethyl sulfide precursor (**2.59**) (Scheme 2.30).



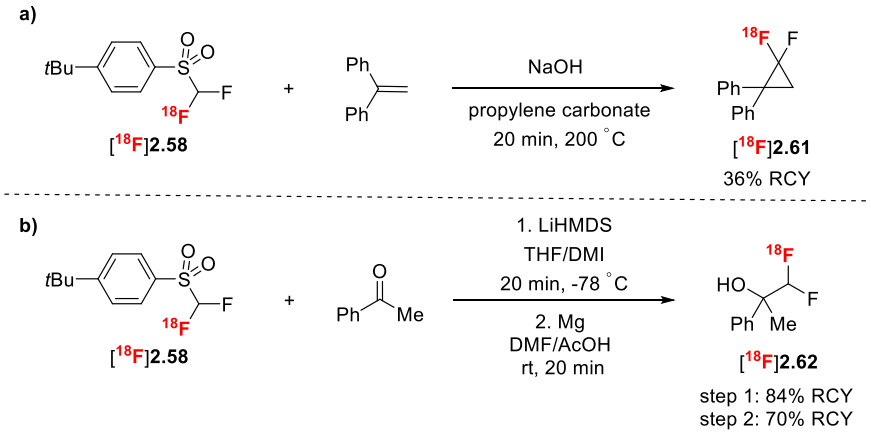
RCY = 10% (isolated, from 4.1–6.3 GBq starting radioactivity)
A_m (from 150 GBq starting radioactivity) = 12 GBq/μmol

Scheme 2.30. *Radiosynthesis of [^{18}F]**2.58**.*

Applying the same synthetic route as Lemaire, Luxen, Genicot and co-workers, **2.59** was radiofluorinated to give an ^{18}F-difluoromethyl sulfide ([^{18}F]**2.60**), which could then be oxidised with *in situ* generated RuO_4 to give the ^{18}F-difluoromethyl sulfone ([^{18}F]**2.58**).[88] In a manual

radiosynthesis, this was obtained in up to 0.76 GBq starting from up to 6.3 GBq activity. In a high activity production using 148 GBq of [^{18}F]fluoride, [^{18}F]**2.58** was obtained in an A_m of 12 GBq/μmol.

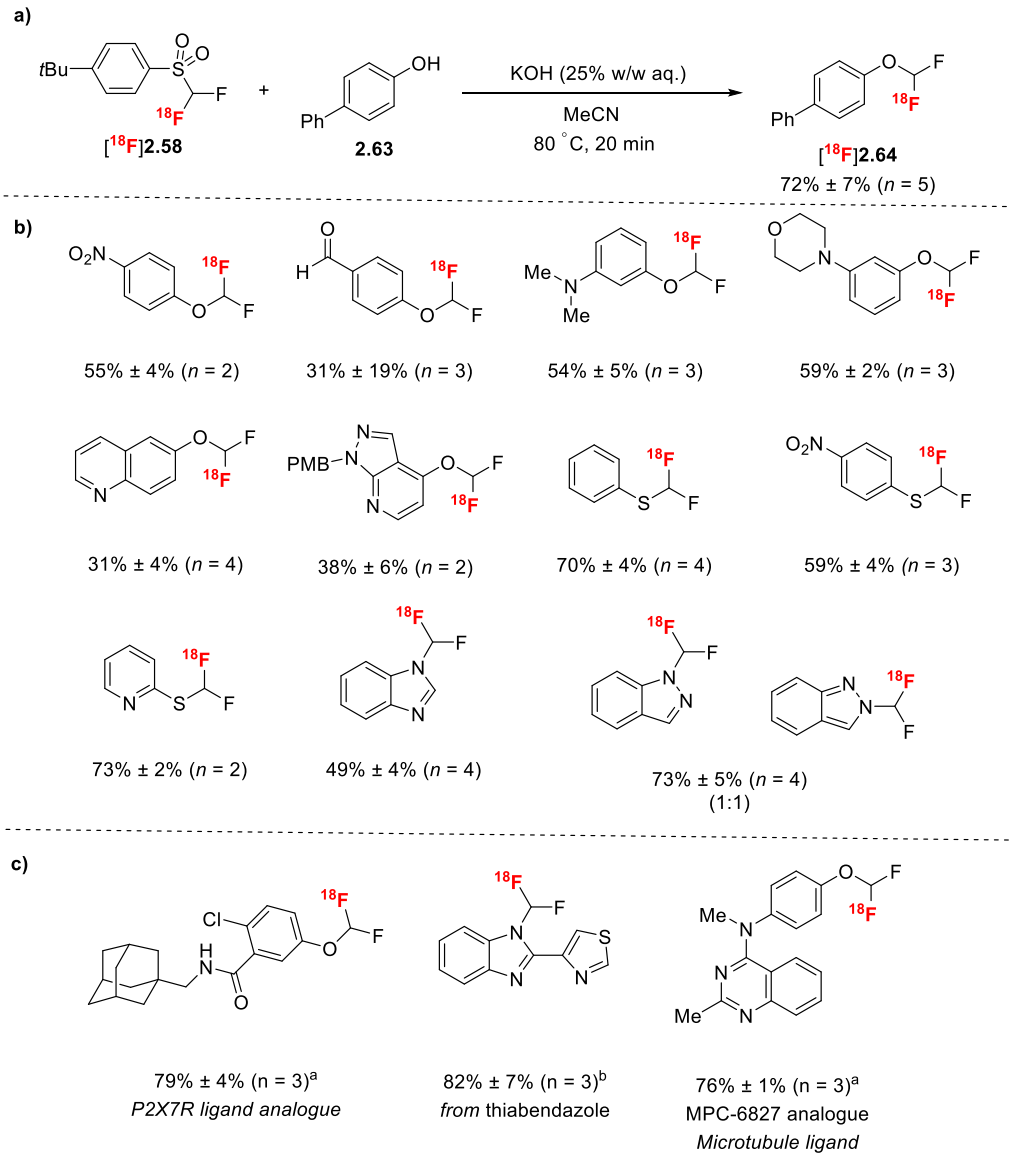
The reactivity of [^{18}F]**2.58** was also explored (Scheme 2.31). Initial studies looked to test the hypothesis that [^{18}F]**2.58** could act as a source of [^{18}F]DFC. To demonstrate this, 1,1-diphenylethylene was reacted with [^{18}F]**2.58** in the presence of NaOH as a base in a [2+1] cycloaddition (Scheme 2.31 a). ^{18}F-Difluorocyclopropanated product [^{18}F]**2.61** was thus observed in 36% RCY. Computational studies also probed the mechanism of formation of [^{18}F]DFC from [^{18}F]**2.58**, finding this was within reach and also proceeded *via* a stepwise process, as suggested by Hine and Porter's study. It was also noted that such reagents could act as an equivalent of the ^{18}F-difluoromethyl anion, if they were deprotonated at low temperature, such that α-elimination of aryl sulfinate did not occur (Scheme 2.31 b). In the presence of acetophenone as a model substrate, this yielded ^{18}F-difluoromethylated alcohol [^{18}F]**2.62** after the sulfonyl group was removed by reductive cleavage.



Scheme 2.31. *a) ^{18}F-Difluorocyclopropanation with [^{18}F]**2.58** ([^{18}F]DFC reactivity); b) ^{18}F-Difluoromethylation of acetophenone with [^{18}F]**2.58** ([^{18}F]CF_2H^- reactivity). Indicated yields are RCY_{HPLC} values obtained from analysis of crude reaction mixtures.*

The ^{18}F-difluoromethylation of phenols, thiophenols and *N*-heterocycles was selected as the initial focus. The reaction proceeded with KOH as a base, in an MeCN/H_2O solvent mixture at 80 °C for 20 min. Under these conditions, KOH was suggested to deprotonate [^{18}F]**2.58** to release [^{18}F]DFC, which could then react with the nucleophilic substrate to yield an *O*-, *S*- or

N-^{18}F-difluoromethylated product. For example, with model phenol **2.63**, the ^{18}F-difluoromethylated product ([^{18}F]**2.64**) was obtained in 72% RCY_{HPLC} (Scheme 2.32 a). The functional group tolerance of the reaction was shown to be excellent in an additive-based robustness screening and additionally by the broad scope of products accessible (Scheme 2.32 b). Such tolerance is ideal for the application of late-stage ^{18}F-difluoromethylation of complex targets (Scheme 2.32 c). This reaction was applied in 40 examples to obtain *O*-, *S*-, *N*-^{18}F-difluoromethylated products.



Scheme 2.32. *a) ^{18}F-Difluoromethylation of model phenol **2.63** with [^{18}F]**2.58**; b) Selected scope examples of ^{18}F-difluoromethylation of O, S, N-nucleophiles with [^{18}F]**2.58**; c) Selected complex molecule scope examples of the ^{18}F-difluoromethylation of O, S, N-nucleophiles. Indicated yields are RCY_{HPLC} values obtained from analysis of crude reaction mixtures.*

2.1.5. Project Outline

In the light of the prior work presented in section 2.1.4, there are several directions of further investigation that would extend [^{18}F]DFC radiochemistry. This chapter will describe advancements in three areas.

The first generation reagent [^{18}F]**2.58** has proven very effective in establishing the utility of [^{18}F]DFC radiochemistry. A key limitation remains the A_m of [^{18}F]**2.58**, as the value measured in a high starting activity production of 12 GBq/µmol, while promising, requires substantial improvement to enable general application as a reagent to prepare radiotracers for PET imaging. The optimisation of A_m will be the initial focus of the work presented in this chapter.

A second focus that would add value to [^{18}F]DFC radiochemistry would be the radiosynthesis and isolation of a PET radiotracer, which can then be used in a proof-of-concept preclinical imaging study. Radiosynthetic work towards this goal as well as a comparative PET imaging study conducted in collaboration with Cardiff University is disclosed in this chapter.

Finally, as [^{18}F]**2.58** has so far only been radiosynthetically applied in the ^{18}F-difluoromethylation of heteroatoms and DFC can be engaged in various difluoromethylation processes, it is of interest to expand the reactivity of [^{18}F]**2.58** to other ^{18}F-difluoromethylation reactions. Due to the interest in difluoromethyl arenes in medicinal chemistry, and the numerous reports of metal-mediated processes that can engage DFC in the difluoromethylation of arenes, this chapter will disclose the discovery of a novel Pd-mediated [^{18}F]DFC-cross coupling to expand the scope of accessible radiochemistry with [^{18}F]DFC.

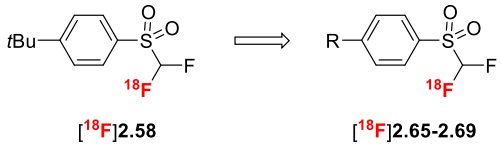
2.2. Results and Discussion

2.2.1. Radiosynthetic Studies Towards an Improved [^{18}F]DFC Reagent

As described in section 2.1.4, the 4-*tert*-butylphenyl substituted reagent ([^{18}F]**2.58**) was initially used in the development of [^{18}F]DFC radiochemistry, however due to its modest A_m, it was an appealing prospect to determine whether structural optimisation could furnish an analogous reagent with improved A_m. To achieve this, we elected to undertake a comparison study between various analogues of [^{18}F]**2.58**.

Prior work suggested such a study could be promising. Hu and co-workers previously demonstrated that installing electron-withdrawing substituents at the 4-position of their chlorodifluoromethyl aryl sulfone DFC reagents led to improved yields of difluoromethylated products (section 2.2.1.4),[58] as well as Luxen and co-workers' demonstration that structurally related ^{18}F-difluoromethyl heteroaryl sulfones were available in different A_m, which varied both with heteroarene scaffold and with substituents (section 2.1.3.2).[91]

We therefore opted to modify the 4-substituent of the ^{18}F-difluoromethyl aryl sulfone, as this could allow for the preparation of a series of structurally related, electronically differentiated reagents, that could possess different reactivity profiles and that were possibly accessible in different A_m. For initial consideration, six ^{18}F-difluoromethyl aryl sulfones were evaluated (Figure 2.9). At their 4-position, these were substituted with a methoxy group ([^{18}F]**2.65**), a proton ([^{18}F]**2.66**), a chlorine atom ([^{18}F]**2.67**), a cyano group ([^{18}F]**2.68**), and a nitro group ([^{18}F]**2.69**), as well as the original reagent [^{18}F]**2.58** bearing a *tert*-butyl substituent. These were appealing as the electronic properties of each substituent differed, e.g. inductively and mesomerically withdrawing or donating. This series represented a range of Hammett σ_p values across the various substituents.[93] We also prioritised reagents that could be prepared from commercial thiophenols, as this would encourage implementation of our [^{18}F]DFC radiochemistry by practitioners in other centres.

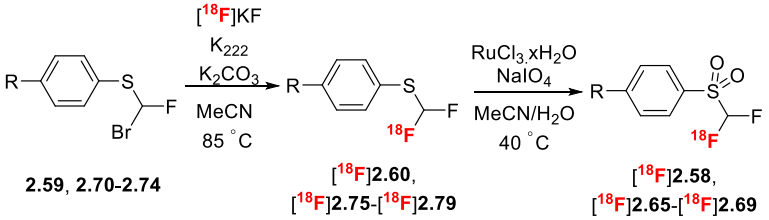


R	σ_p	
OMe	-0.27	[^{18}F]**2.65**
*t*Bu	-0.20	[^{18}F]**2.58**
H	0.00	[^{18}F]**2.66**
Cl	0.23	[^{18}F]**2.67**
CN	0.66	[^{18}F]**2.68**
NO_2	0.78	[^{18}F]**2.69**

Figure 2.9. *Outline for the comparison study between ^{18}F-difluoromethyl aryl sulfones.*

2.2.1.1. Preparation of ^{18}F-Difluoromethyl Aryl Sulfones and Evaluation of their A_m

The reagents ([^{18}F]**2.58**, [^{18}F]**2.65**-[^{18}F]**2.69**) to be evaluated in this chapter were prepared using the same radiosynthetic strategy described for [^{18}F]**2.58** in section 2.1.4. This relied on an initial radiofluorination of a bromofluoroaryl sulfide precursor (**2.59**, **2.70**-**2.74**) with [^{18}F]fluoride to yield ^{18}F-difluoromethyl aryl sulfide ([^{18}F]**2.60**, [^{18}F]**2.75**-[^{18}F]**2.79**), followed by an oxidation to the desired sulfone ([^{18}F]**2.58**, [^{18}F]**2.65**-[^{18}F]**2.69**) (Scheme 2.33).

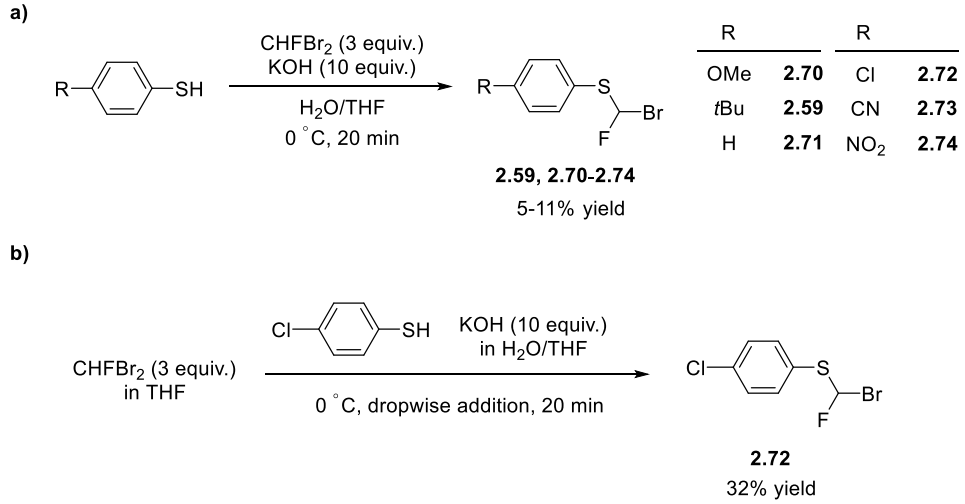


R	-SCFHBr	-SCF$_2$H	-SO$_2$CF$_2$H
*t*Bu	**2.59**	[^{18}F]**2.60**	[^{18}F]**2.58**
OMe	**2.70**	[^{18}F]**2.75**	[^{18}F]**2.65**
H	**2.71**	[^{18}F]**2.76**	[^{18}F]**2.66**
Cl	**2.72**	[^{18}F]**2.77**	[^{18}F]**2.67**
CN	**2.73**	[^{18}F]**2.78**	[^{18}F]**2.68**
NO_2	**2.74**	[^{18}F]**2.79**	[^{18}F]**2.69**

Scheme 2.33. *General radiosynthetic approach to ^{18}F-difluoromethyl aryl sulfones ([^{18}F]**2.58**, [^{18}F]**2.65**-[^{18}F]**2.69**).*

These radiolabelling precursors were prepared adapting an established synthesis, whereby a thiophenol is reacted with dibromofluoromethane in the presence of KOH (Scheme 2.34). This yields a bromofluoromethyl aryl sulfide (**2.59**, **2.70**-**2.74**), which can then be used for the radiosynthesis of [^{18}F]**2.58**, [^{18}F]**2.65**-[^{18}F]**2.69**. In these reactions, the addition of dibromofluoromethane was performed slowly over 20 minutes, and the reaction was then immediately quenched. This furnished the desired product, albeit in low isolated yields (5–11%). We suspected that the low yields of bromofluoromethyl aryl sulfide could result from the over-reaction of the product with further equivalents of the thiophenol. Furthermore, Shen and co-workers had reported that fluoromethyl aryl sulfides formed in a catalytic fluoromethylation of aryl boronic acids could degrade to bis(arylthio)methanes at prolonged

reaction times, which could also lead to reduced yields of the desired bromofluoromethyl aryl sulfide.[94] Inverting the addition order of reagents, such that a solution of thiophenol and KOH in a THF/water mixture is added to a stirred solution of dibromofluoromethane over 20 minutes delivered a threefold improvement in the isolated yield of **2.72** to 32% from 11% (Scheme 2.34 b). Once isolated, these materials were stored neat in a freezer at -20 °C until required, to avoid degradation of the labelling precursor, as described by Shen and co-workers.[94]



Scheme 2.34. *a) Synthesis of bromofluoromethyl sulfides (**2.59**, **2.70**-**2.74**). b) Synthesis of **2.72** in improved yield.*

With these radiolabelling precursors in hand, we next investigated factors that might cause reduction in A_m. We supposed that a significant cause of lower A_m values could be ^{19}F-isotopic dilution, which originated from the large excess of pre-fluorinated labelling precursors **2.59**, **2.70**-**2.74** present in the radiosynthesis of [^{18}F]**2.58**. Ritter and co-workers had previously observed that the degradation of a bromofluoromethyl intermediate led to formation of a ^{19}F-difluoromethyl compound under the reaction conditions in the absence of an external fluoride source (section 2.1.3.1).[76] If ^{19}F-fluoride were formed in the reaction from degradation of the substrate, this would engage **2.59**, **2.70**-**2.74** in parallel ^{19}F-fluorination and yield the difluoromethyl sulfide **2.60**, **2.75**-**2.79**, which would reduce the A_m of the final product. A similar observation had also been made during the development of the Ag-mediated halex radiofluorination in our laboratories, whereby the degradation of a

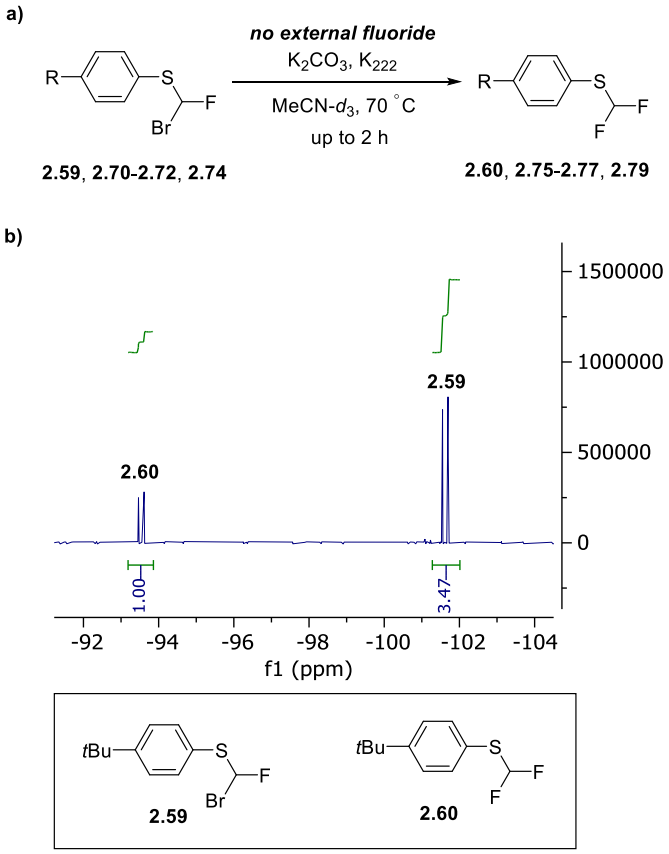
halofluoromethyl precursor led to the formation of the ^{19}F-difluoromethyl compound, as observed by ^{19}F NMR.[73,95] We therefore looked to investigate whether this was in operation for **2.59**, **2.70**-**2.74**, and whether the extent to which it took place differed with the identity of the 4-substituent.

In a series of NMR experiments, five precursors (**2.59**, **2.70, 2.71, 2.72** and **2.74**) representing *para*-substituents of varying nature were combined with the elution reagents K_2CO_3 and K_{222} and dissolved in MeCN-d_3 in an NMR tube (Scheme 2.35 a). These were then heated at 70 °C over a 2 h period and quantitative ^{19}F NMR spectra were acquired over a series of time points (Scheme 2.35 b).

In these experiments, the formation of the difluoromethyl thioether (**2.60**, **2.75-2.77, 2.79**) was observed in all cases. The ^{19}F NMR signals corresponding to the bromofluoromethyl precursor (**2.59**, **2.70-2.72, 2.74**) and the difluoromethyl compound (**2.60**, **2.75-2.77, 2.79**) were integrated and the ratio of the concentrations of these species was calculated; the data from the 30 minute and 120 minute time points are tabulated in Table 2.1. Full experimental details are available in Chapter 4. An internal standard was not used for this study to ensure that fluoride leaching from other species was not responsible for the formation of the difluoromethyl thioether (**2.60**, **2.75-2.77, 2.79**). It is noteworthy that when no elution reagents were added, no formation of **2.60** was observed from **2.59**, suggesting the crucial role that these additives play in the degradation of the bromofluoromethyl aryl sulfide precursor to ^{19}F-fluoride. This was also observed in the study of Ritter and co-workers and perhaps suggests that optimisation of the [^{18}F]fluoride elution conditions could also be leveraged to improve A_m, as an alternative strategy to the structural optimisation described herein.[76]

Based on the data from the NMR study, there is a good indication that varying the 4-substituent leads to the varying formation of the difluoromethyl thioethers **2.60**, **2.75-2.77,**

2.79. Therefore, selecting a substituent, which causes the bromofluoromethyl precursor to be less susceptible to degradation, could be exploited to prepare a ^{18}F-difluoromethyl aryl



Scheme 2.35. *^{19}F-fluoride leaching experiments. a) Reaction of bromofluoromethyl sulfide precursors (**2.59, 2.70-2.72, 2.74**) with elution reagents; b) Example ^{19}F NMR spectrum taken from the experiment using **2.59** showing the formation of difluoromethyl thioether **2.60** (δ_F = -93.5 ppm) at 120 min timepoint.*

Entry	R	[ArSCF$_2$H] : [ArSCFHBr]	[ArSCF$_2$H] : [ArSCFHBr]
		t = 30 min	t = 120 min
1	-*t*Bu	0.0219	0.1440
2	-OMe	0.0897	0.3763
3	-H	0.0554	0.1474
4	-Cl	0.0049	0.0812
5	-NO$_2$	0.0233	0.0491

Table 2.1. *Ratios of the concentrations of difluoromethyl aryl sulfide (**2.60, 2.75-2.77, 2.79**) and bromofluoromethyl sulfide precursors (**2.59, 2.70-2.72, 2.74**) formed in ^{19}F-fluoride leaching experiments determined by ^{19}F qNMR (N = 16, d1 = 10 s).*

sulfone reagent in higher A_m. Compared to the *t*Bu substituent, the chloro and nitro groups are the most promising for further implementation and are suggested by the outcome of the NMR study to lead to less fluoride leaching under the reaction conditions, while the precursors bearing proton and methoxy substituents were likely more susceptible to isotopic dilution, and may lead to lower A_m. It should also be noted that this study considers only a single factor that may contribute to reduced A_m, and others, such as radiolysis, may also play a role.

Following this study, the reagents ([^{18}F]**2.58**, [^{18}F]**2.65**-[^{18}F]**2.69**) were next prepared in an automated radiosynthesis using a Trasis AllInOne synthesiser. The automated programme encoded all of the operations required for its radiosynthesis and the same programme in combination with a single-use cassette was used for the preparation of each reagent (cassette layout shown in Figure 2.10). This began with the trapping of [^{18}F]fluoride (135–148 GBq) in [^{18}O]water on an anion exchange cartridge, followed by its elution with a solution of K_2CO_3 and K_{222} in MeCN and H_2O mixed solvent, and drying at elevated temperature for 12 minutes. The relevant precursor (**2.59**, **2**.**70**-**2.74**) in MeCN was added to the dry [^{18}F]fluoride and was then reacted for 3 minutes. To this crude mixture, a solution of oxidant ($RuCl_3$ hydrate and $NaIO_4$) was added and reacted for 5 minutes. The organics were then separated from the [^{18}F]fluoride in a cartridge purification (C18 phase), and these were purified by semi-preparative HPLC. The reagent ([^{18}F]**2.58**, [^{18}F]**2.65**-[^{18}F]**2.69**) was then reformulated with a second C18 cartridge and was obtained as a solution in MeCN. The activity yield was measured in a dose calibrator and A_m was determined using a radio-HPLC method.

In order to maximise A_m, the loadings of the bromofluoromethyl precursors **2.59**, **2**.**70**-**2.74** were reduced to 0.02 mmol in these experiments, relative to the amount (0.04 mmol) that was used in the manual radiosynthesis of [^{18}F]**2.58**. This can be expected to improve A_m, as the concentration of leached ^{19}F-fluoride from the precursor should scale with precursor

loading.[71] For the same reason, a high starting radioactivity (135–150 GBq) was used for each experiment; A_m should scale with the amount of starting radioactivity. These amounts of activity are in line with the starting activities used in clinical PET radiotracer productions, so would also provide an indication whether the radiosynthesis is amenable to multi-GBq productions and whether radiolysis is problematic at high activity.

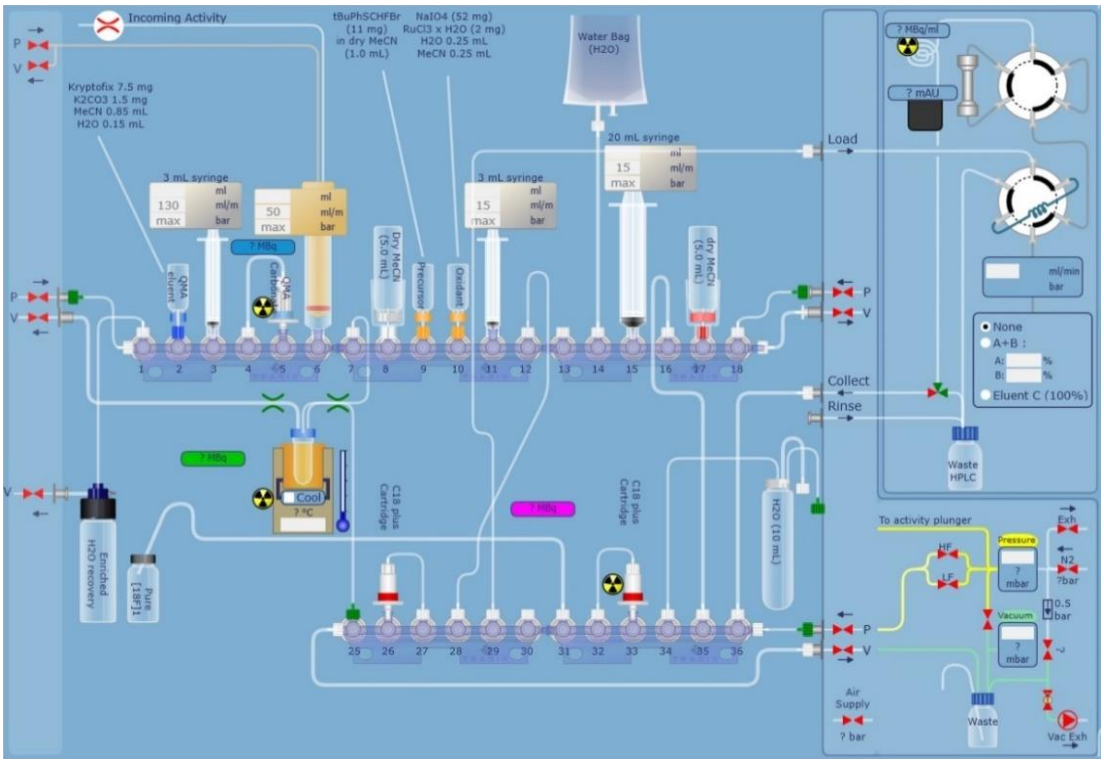
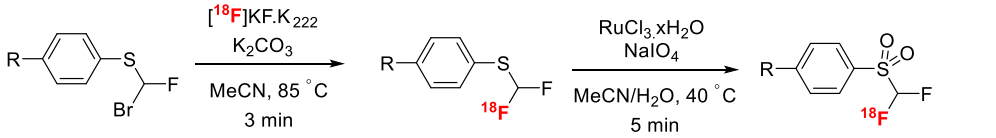


Figure 2.10. *Cassette set-up for the automated radiosynthesis of ^{18}F-difluoromethyl aryl sulfone reagents ([^{18}F]**2.58**, [^{18}F]**2.65**-[^{18}F]**2.69**) using a Trasis AllInOne synthesiser.*

The radiosynthetic data (AY and A_m) for these experiments (completed in duplicate) is given in Table 2.2, sorted by ascending A_m. Full experimental details are available in Chapter 4. As suggested by the NMR experiments, these data also imply that altering the 4-substituent results in reagents that are accessible in varying A_m (and AY). Promisingly, several of these are accessible in higher A_m than the first-generation reagent [^{18}F]**2.58**. Based on these data, the 4-chloro-substituted reagent [^{18}F]**2.67** is accessible in the highest A_m (131 GBq/μmol, d.c. EOS), in line with the data from the NMR experiments (Table 2.1) and therefore was carried forward as the optimal reagent. Cyano-substituted reagent [^{18}F]**2.68** is available in the second highest AY and A_m of those assessed, which also render it an appealing choice as an [^{18}F]DFC

reagent. Nitro-substituted reagent [^{18}F]**2.69** is also of interest, as it available in the highest AY of those prepared in this study. This reagent would therefore be best applied to the radiosynthesis of tracers for PET applications where high A_m is not required.

In general, substitution of electron-withdrawing substituents (Cl, NO_2 and CN) led to reagents available in higher A_m than for those substituted with electron donating groups (*t*Bu, OMe). However, as a strong correlation with the Hammett σ_p parameter was not observed, this is unlikely to be instructive in the design of such reagents for high A_m. To address the limitation associated with the lower AY obtained for the chloro-substituted reagent [^{18}F]**2.67** that had the highest A_m, further optimisation of the automated radiosynthesis programme for higher radiochemical yields of [^{18}F]**2.67** is described in section 2.2.1.3.



2.59, **2.70-2.74** [^{18}F]**2.60**, [^{18}F]**2.75**-[^{18}F]**2.79** [^{18}F]**2.58**, [^{18}F]**2.65**-[^{18}F]**2.69**

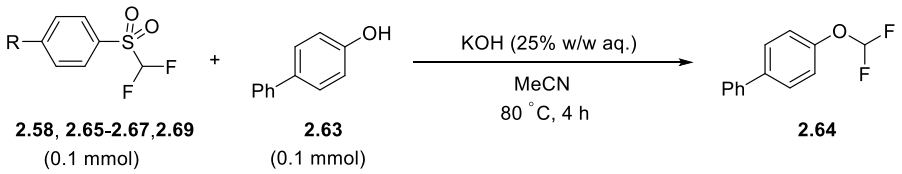
Entry	Reagent	R	AY	A_m
1	[^{18}F]**2.66**	-H	1.12 GBq	5 GBq/µmol
2	[^{18}F]**2.58**	-*t*Bu	1.77 GBq	10 GBq/µmol
3	[^{18}F]**2.65**	-OMe	2.21 GBq	18 GBq/µmol
4	[^{18}F]**2.69**	-NO_2	4.07 GBq	46 GBq/µmol
5	[^{18}F]**2.68**	-CN	2.43 GBq	109 GBq/µmol
6	[^{18}F]**2.67**	-Cl	1.68 GBq	131 GBq/µmol

Table 2.2. *Radiosynthetic data for the preparation of ^{18}F-difluoromethyl aryl sulfone reagents ([^{18}F]**2.58**, [^{18}F]**2.65**-[^{18}F]**2.69**). AY and A_m values are averages over two runs. A_m is decay-corrected to the EOS. For entries 1,2,4 and 6, 135 GBq starting activity was used, for entries 3 and 5, 148 GBq starting activity was used.*

2.2.1.2. Substituent Effects on the Reactivity of ^{18}F-Difluoromethyl Aryl Sulfones

In addition to their differing A_m, the structure of a ^{18}F-difluoromethyl aryl sulfone should also be expected to affect its reactivity in ^{18}F-difluoromethylation. Analogous to the study disclosed by Hu and co-workers, our investigation into this effect first began with a reactivity study for a series of 4-substituted ^{19}F-difluoromethyl aryl sulfones in a difluoromethylation of model phenol **2.63** (Table 2.3).[58] In these experiments, a 4 h reaction time was chosen to avoid full consumption of **2.58**, **2.65**-**2.69** and a single equivalent of difluoromethyl sulfone was used, as under radiochemical conditions, this component would be expected to be the limiting reagent, present in only nano- to picomolar concentrations.

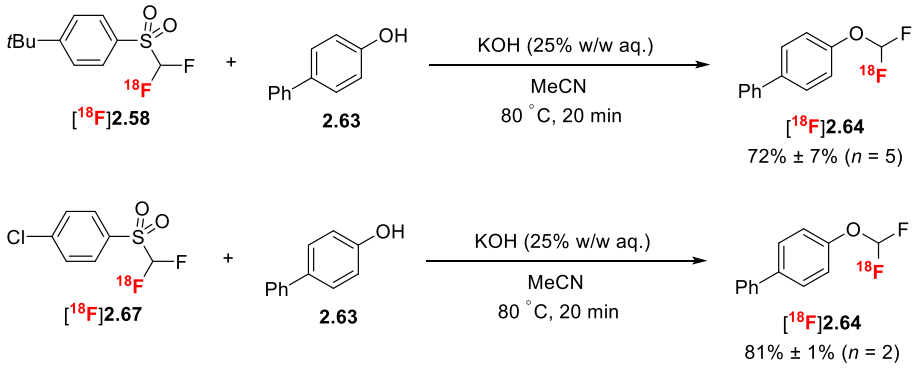
There is a moderate positive correlation (r^2 = 0.75) between the yield of the difluoromethylated product **2.64** and σ_p. This suggests that difluoromethyl aryl sulfones with more electron-withdrawing *para*-substituents are more reactive and are activated more readily under basic conditions to release DFC. This is consistent with the stepwise mechanism for DFC formation proposed for this class of reagents both by Hine and Porter and by the DFT calculations conducted by Dr. A. Dürr.[49] A more electron-deficient arene is better able to stabilise negative charge build-up in the α-elimination transition state, resulting in a lower energy and more rapid formation of DFC. Based on these experiments, it is suggested that [^{18}F]DFC reagents bearing electron-withdrawing groups are hypothesised to display improved reactivity in ^{18}F-difluoromethylation. This suggests that lead reagent [^{18}F]**2.67** bearing a chloro substituent could be more reactive than first-generation reagent [^{18}F]**2.58**. However, more rapid formation of [^{18}F]DFC could also be accompanied by increased side-reactivity, so care must also be taken to optimise reaction parameters that could affect the rate of [^{18}F]DFC release, including base identity and concentration, and reaction temperature.



Entry	Reagent	R	σ_p	NMR yield
1	**2.65**	-OMe	-0.27	42% ± 0% (*n* = 2)
2	**2.58**	-*t*Bu	-0.20	54% ± 1% (*n* = 2)
3	**2.66**	-H	0.00	61% ± 1% (*n* = 2)
4	**2.67**	-Cl	0.23	64% ± 0% (*n* = 2)
6	**2.69**	-NO_2	0.78	70% ± 1% (*n* = 2)

Table 2.3. *Reactivity study for a series of difluoromethyl aryl sulfones in the difluoromethylation of a model phenol. NMR yields estimated by ^{19}F qNMR using 4-fluoroanisole (1 equiv.) as internal standard.*

We were next interested to determine whether this observation translated to ^{18}F-radiochemistry. In a side-by-side comparison, model phenol **2.63** was reacted with the first-generation reagent [^{18}F]**2.58** and the lead reagent [^{18}F]**2.67** (approx. 10 MBq) under the optimised reaction conditions for *O*-^{18}F-difluoromethylation (Scheme 2.36). A higher RCY_{HPLC} was obtained for chloro-substituted reagent [^{18}F]**2.67** (81%), compared to *tert*-butyl-substituted reagent [^{18}F]**2.58** (72%), suggesting that [^{18}F]**2.67** was more reactive as a source of [^{18}F]DFC. This was consistent with the observations from the reactions on non-radioactive material (Table 2.3).

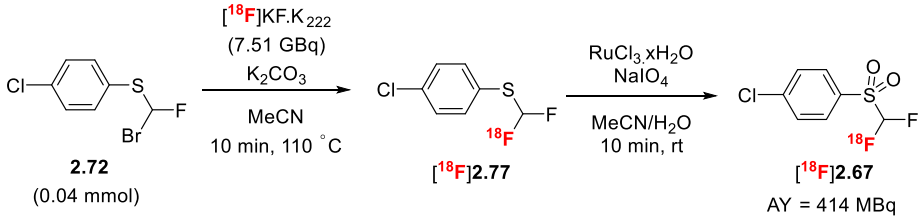


Scheme 2.36. *^{18}F-Difluoromethylation of model phenol **2.63** with [^{18}F]**2.58** and [^{18}F]**2.67**. Indicated yields are RCY_{HPLC} values obtained from analysis of crude reaction mixtures.*

The effect of the substituent on reactivity in a Pd-mediated ^{18}F-difluoromethylation of aryl boronic acids will be described later in this chapter (section 2.2.3.3), in a comparison of the reactivity of [^{18}F]**2.58** and [^{18}F]**2.67**.

2.2.1.3. Radiosynthesis of ^{18}F-Difluoromethyl Aryl Sulfones in Improved AY

While structural optimisation of the ^{18}F-difluoromethyl sulfone reagents had successfully increased the A_m by 13-fold to up to 131 GBq/μmol for [^{18}F]**2.67**, the AY of 1.68 GBq from a starting radioactivity of 135 GBq in an automated radiosynthesis was an apparent limitation. Meanwhile, a manual radiosynthesis of [^{18}F]**2.67** provided up to 0.41 GBq from 7.5 GBq starting activity (Scheme 2.37). This represents a much more efficient radiosynthesis, although it should be noted that it cannot be necessarily expected that AY would scale linearly at high starting activities, and a higher loading of precursor **2.72** was also used in the manual synthesis. This improved AY however highlighted that the automated programme could be further improved to deliver [^{18}F]**2.67** in higher AY.



Scheme 2.37. *Manual radiosynthesis of [^{18}F]**2.67**.*

A key difference between the manual and automated procedures was the use of an azeotropic drying method for the [^{18}F]fluoride in the manual protocol, where additional MeCN is added three times to ensure the azeotropic removal of H_2O. Meanwhile, the initial automated protocol instead dried the [^{18}F]fluoride in a single step without the addition of further MeCN. We supposed improper drying could lead to reduced reactivity, as hydrogen bonding of fluoride to water renders it a poorer nucleophile.[96] Therefore, an improved version of the automated programme was developed, which implemented an azeotropic drying programme. The C18 cartridge purification before the HPLC purification was also removed as

this proved unnecessary and increased the duration of the programme. Removing this sequence also made additional positions available on the cassette for the possible integration of the ^{18}F-difluoromethylation step (Figure 2.11).

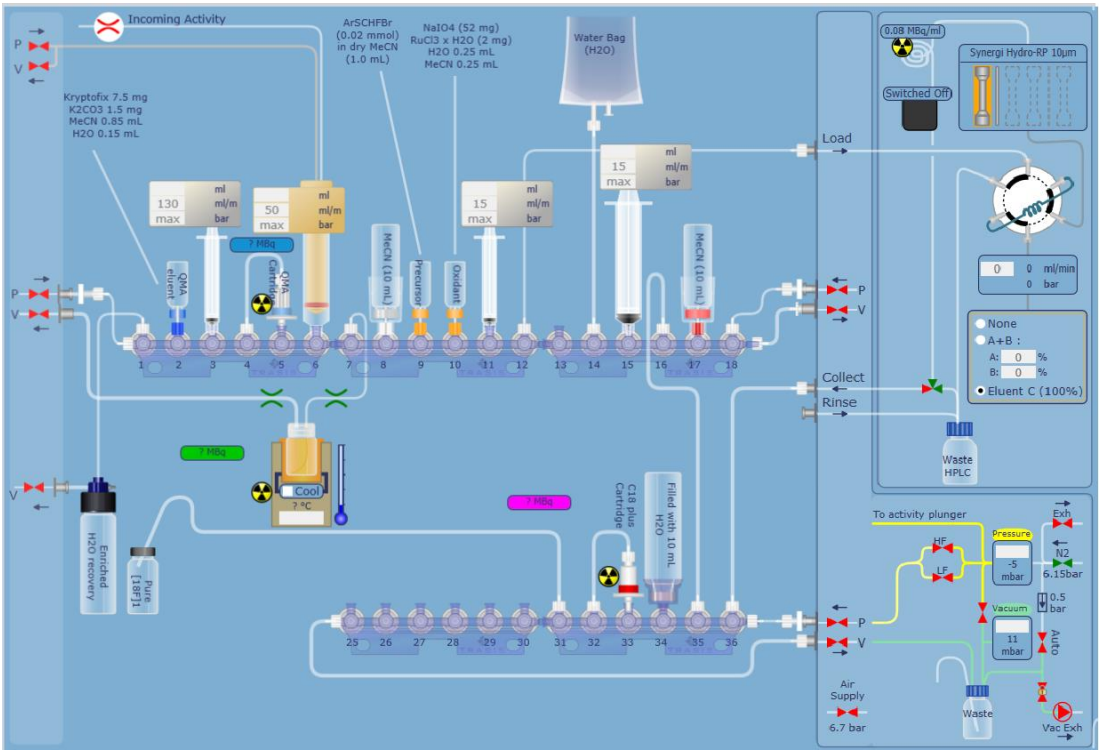
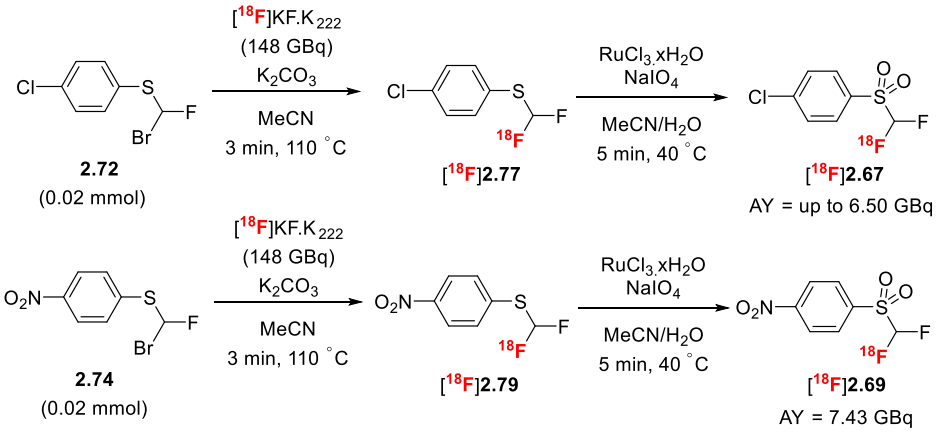


Figure 2.11. *Cassette set-up for the improved automated radiosynthesis of [^{18}F]**2.67** and [^{18}F]**2.69** using a Trasis AllInOne synthesiser.*

Applying this new programme, the AY of [^{18}F]**2.67** could thus be improved and up to 6.50 GBq of [^{18}F]**2.67** could be prepared from 148 GBq of [^{18}F]fluoride (Scheme 2.38). We also ran the same programme for the synthesis of nitro-substituted [^{18}F]**2.69**, which was the reagent previously available in the highest AY from the series considered, however the increase in AY (7.43 GBq) was more modest than the significant improvement observed for [^{18}F]**2.67** (Scheme 2.38). Other parameters that could deliver further improvements in AY or A_m, such as an alternative radiosynthesis (e.g. *via* another route with a different radiolabelling precursor), the use of activators (such as DIPEA or DBU) and alternative elution conditions, remain under consideration.



Scheme 2.38. *Automated, improved radiosynthesis of [^{18}F]**2.67** and [^{18}F]**2.69**.*

2.2.2. Application of [^{18}F]DFC Radiochemistry to PET Radiotracer Production

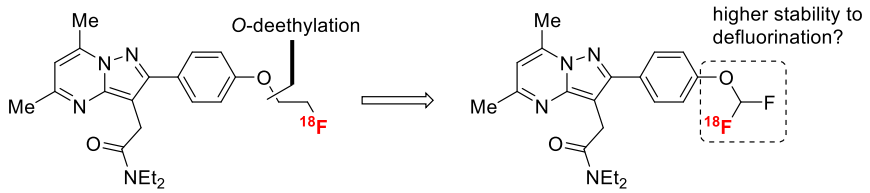
With the work described in the previous section to identify an improved [^{18}F]DFC reagent ([^{18}F]**2.67**) that was accessible in high A_m and displayed improved reactivity, it was of interest to apply this to the preparation of a ^{18}F-difluoromethylated PET radiotracer. While not widely used in PET ligand design currently, ^{18}F-difluoromethylation could be a viable alternative to ^{11}C-methylation and ^{18}F-fluoroalkylation reactions that are regularly applied in the preparation of preclinical and clinical radiotracers.[97] Such groups can be more vulnerable to metabolic instability, especially ^{18}F-fluoromethyl compounds, which can require deuteration to improve their stability to ^{18}F-defluorination.[19] This, along with other attractive properties of difluoromethylated compounds, was introduced in section 2.1.1, which suggest that the ^{18}F-difluoromethylated analogues of existing (pre)clinical radiotracers could be of interest to radiochemistry practitioners.

2.2.2.1. Target Identification

Several possible radiotracers were considered as possible targets for our study. Due to the prevalence of ^{18}F-fluoroethyl ethers in (pre)clinical PET radiopharmaceuticals we opted to apply our *O*-^{18}F-difluoromethylation reaction for the synthesis of an ^{18}F-difluoromethyl ether analogue of an existing ^{18}F-fluoroethylated tracer. Of numerous possible options, we selected

[^{18}F]DPA-714 ([^{18}F]**2.80**) as a model radiotracer. This compound is used as a PET ligand for the 18 kDa translocator protein (TSPO), which is considered as a biomarker for microglial activation and neuroinflammation.[98,99] TSPO is overexpressed in neurodegenerative disease states, such as Alzheimer's disease, and following brain injury. It has therefore attracted attention for brain PET imaging.

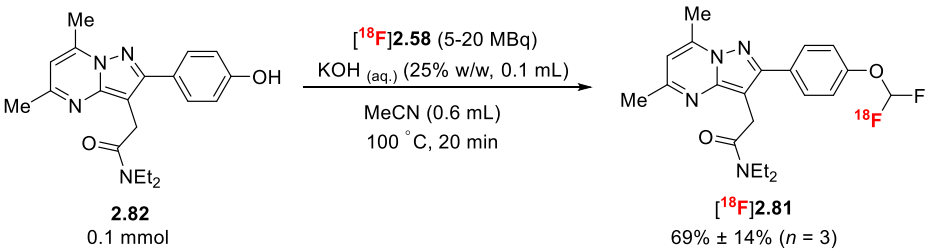
The radiometabolite profile of [^{18}F]DPA-714 has been previously studied in several species.[100-102] *In vitro* studies revealed the formation of metabolites corresponding to *O*-defluoroethylation by LC-MS analysis, among others. An *in vitro* radiometabolite study suggested that the cleavage of this reporter group could lead to the formation of [^{18}F]fluoroacetaldehyde, [^{18}F]fluoroacetate and [^{18}F]fluoride as radiometabolites, which could engage in non-specific binding or be uptaken undesirably (e.g. in bone), resulting in lower quality images.[100] We therefore proposed that modification of this tracer with a ^{18}F-difluoromethyl group ([^{18}F]DPA-OCF$_2$H, [^{18}F]**2.81**) could offer possible improvements in its stability profile, making [^{18}F]**2.81** an interesting target for PET imaging (Scheme 2.39).



[^{18}F]**2.80** [^{18}F]DPA-714 [^{18}F]**2.81** [^{18}F]DPA-OCF$_2$H

Scheme 2.39. *Structures of [^{18}F]DPA-714 ([^{18}F]**2.80**) and its ^{18}F-difluoromethylated analogue [^{18}F]DPA-OCF$_2$H ([^{18}F]**2.81**).*

Finally, in prior work by Dr J. Sap and Dr C. Meyer, the radiosynthesis of [^{18}F]**2.81** was established from phenol **2.82** and [^{18}F]**2.58** (Scheme 2.40). The high RCY of [^{18}F]**2.81** observed in these reactions was encouraging for its further consideration as a model PET radioligand for imaging studies.

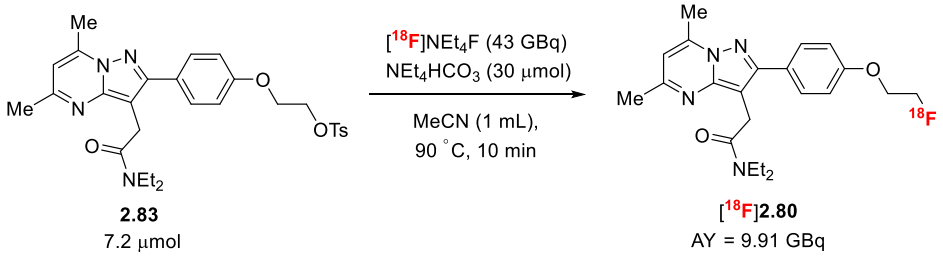


Scheme 2.40. *^{18}F-Difluoromethylation of phenol **2.82** with [^{18}F]**2.58** for the radiosynthesis of [^{18}F]**2.81** Indicated yields are RCY_{HPLC} values obtained from analysis of crude reaction mixtures.*

2.2.2.2. Radiosynthesis of [^{18}F]DPA-714 and [^{18}F]DPA-OCF_2H

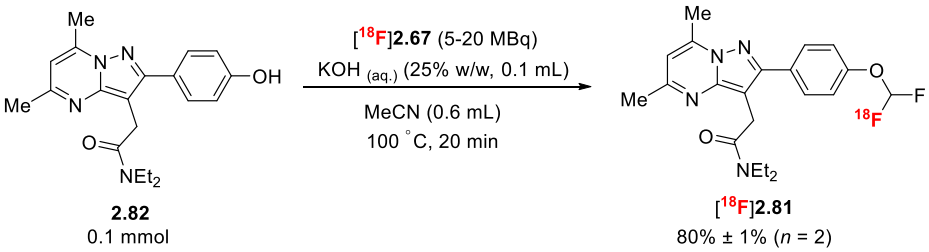
We next turned our attention to the preparation of [^{18}F]DPA-714 ([^{18}F]**2.80**) and [^{18}F]DPA-OCF_2H ([^{18}F]**2.81**) on larger scale for subsequent PET imaging and *in vivo* studies; this would require the preparation of these radiotracers in AY of at least 0.1 GBq.

The radiosynthesis of the former ([^{18}F]**2.80**) has been reported, so this was carried out using the established conditions from tosylate precursor **2.83** and an automated programme for its preparation on a Trasis AllinOne synthesiser was thus prepared (Scheme 2.41).[98]



Scheme 2.41. *Preparation of [^{18}F]DPA-714 ([^{18}F]**2.81**).*

Having already established a radiosynthetic route to [^{18}F]**2.81** from first-generation reagent ([^{18}F]**2.58**), the effect on the RCY with chloro-substituted reagent [^{18}F]**2.67** was next assessed. In line with observations made on the reactivity of ^{18}F-difluoromethyl aryl sulfones in section 2.2.1.2, when the radiosynthesis of [^{18}F]**2.81** was later repeated with [^{18}F]DFC reagent [^{18}F]**2.67**, this was pleasingly obtained in an increased average RCY_{HPLC} of 80% compared to 69% (Schemes 2.40 and 2.42).



Scheme 2.42. *^{18}F-Difluoromethylation of phenol **2.82** with [^{18}F]**2.67** for the radiosynthesis of [^{18}F]**2.81** Indicated yields are RCY$_{HPLC}$ values obtained from analysis of crude reaction mixtures.*

The reaction time for the ^{18}F-difluoromethylation step was also investigated in a time course experiment (Figure 2.12). After 5 minutes the reaction reached completion (RCY$_{HPLC}$ = 81% (*n* = 1)), after which time RCY$_{HPLC}$ remained constant, so the reaction time could be confidently shortened from 20 minutes to 10 minutes (RCY$_{HPLC}$ = 81% (*n* = 1)). While the reaction time could likely have been further shortened to 5 minutes, this would leave less time available for cassette cleaning steps, which ran during the ^{18}F-difluoromethylation reaction.

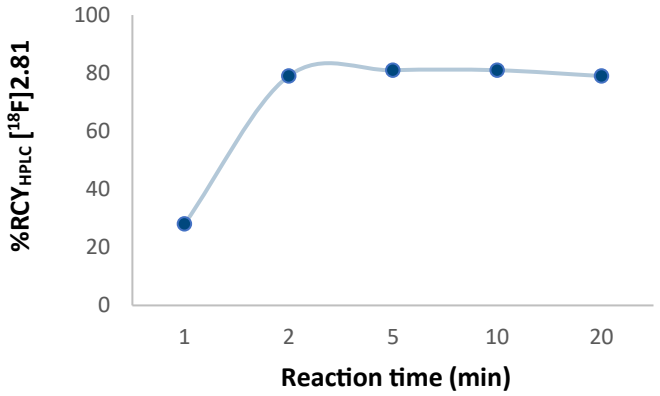


Figure 2.12. *Time course for the radiosynthesis of [^{18}F]**2.81**. Conditions are as Scheme 2.42. Indicated yields are RCY$_{HPLC}$ values obtained from analysis of crude reaction mixtures.*

Further to this, the development of an automated programme for both the preparation of [^{18}F]**2.67** and the ^{18}F-difluoromethylation step was next considered. The protocol described herein represents a semi-automated radiosynthesis, where the synthesis and purification of [^{18}F]**2.67** and the purification of the ^{18}F-difluoromethylated product were conducted with a TrasisAllinOne synthesiser, while the [^{18}F]DFC reaction took place on an external hotplate and [^{18}F]**2.67** was dispensed and crude [^{18}F]**2.81** was taken up in lines that connected to the Trasis cassette. Minor manual operations were therefore still required. This was achieved by

modifying the existing automated radiosynthesis programme for the Trasis AllinOne for the synthesis of [^{18}F]**2.67** to include additional steps for the purification of the crude ^{18}F-difluoromethylated product.

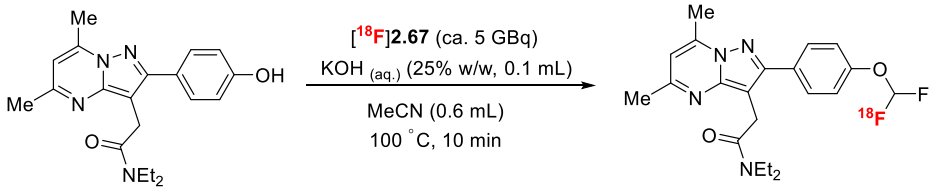
In summary, this semi-automated protocol comprised the following steps: 1) [^{18}F]fluoride was received from the cyclotron and trapped on a QMA cartridge; 2) the cartridge is eluted and the eluate is dried azeotropically at elevated temperature; 3) **2.72** is transferred to the reactor for the ^{18}F-fluorination (85 °C, 3 minutes); 4) once cooled, the $RuCl_3$ hydrate/$NaIO_4$ solution is transferred to the reactor for the oxidation step (5 minutes); 5) once the reaction time elapsed, the crude mixture was transferred to the HPLC and thus purified; 6) the fraction containing [^{18}F]**2.67** was collected in a falcon tube containing water (10 mL); 7) [^{18}F]**2.67** was reformulated using a C18 cartridge and eluted in MeCN into an externally mounted vial containing phenol **2.82** and a stirrer bar; 8) a prepared syringe containing KOH (aq., 25% w/w, 0.1 mL) solution was added; 9) the line from the Trasis cassette was removed and the vial was moved to a hot plate at 100 °C for 10 minutes; 10) during the reaction, the HPLC load and collect lines and the 20 mL syringe at position 15 were washed with MeCN, to ensure that any remaining [^{18}F]**2.67** did not contaminate the final product; 11) after 10 minutes elapsed, the vial was cooled and once cooled, a line from the Trasis was added to the reaction vial; 12) the crude reaction mixture was transferred to the HPLC and purified; 13) the fraction containing [^{18}F]**2.81** was collected in a falcon tube containing water (10 mL); 14) [^{18}F]**2.81** was reformulated using a C18 cartridge; 15) the cartridge was removed and eluted manually with a minimum volume of Et_2O (first 0.3 mL fraction was discarded, second 0.6 mL fraction was retained); 16) the Et_2O solvent was evaporated to dryness under a stream of N_2; 17) [^{18}F]**2.81** was redissolved in an ethanolic (12.5%) solution of saline to render it injectable for preclinical studies.

The set-up (excluding hot plate, placed in an adjacent hot cell) is shown in Figure 2.13.



Figure 2.13. *Set-up for the semi-automated radiosynthesis of [^{18}F]**2.81** using a Trasis AllInOne synthesiser. (Taken by J. Ford)*

Starting from 148 GBq of [^{18}F]fluoride using this method, [^{18}F]**2.81** was obtained in AY up to 903 MBq, with a [^{18}F]**2.67** starting activity of 5.36 GBq after the reagent synthesis (Scheme 2.43). In one run, the A_m of [^{18}F]**2.81** was measured to be 40 GBq/µmol at EOS. This represents a good A_m and the AY is sufficient for PET imaging and *in vivo* experiments, which were conducted by collaborators at Cardiff University and described in the next section. This is also the highest A_m value reported to date for the radiosynthesis of a [^{18}F]OCF_2H compound.



Scheme 2.43. *^{18}F-Difluoromethylation of phenol **2.82** with [^{18}F]**2.67** in the semi-automated radiosynthesis of [^{18}F]**2.81**.*

2.2.2.3. Comparative Imaging and In Vivo Experiments

The following PET imaging and *in vivo* experiments were conducted by Dr S. Paisey and Dr M. Lelos (Cardiff University). All experiments were conducted in compliance with the UK Animals (Scientific Procedures) Act 1986 under Home Office Licence No. P49E8C976 and with the

approval of the Cardiff University Ethics Review Committee. The radiotracers used in these experiments were prepared by J. Ford and Dr J. Sap. HPLC analysis of tissue samples was conducted by J. Ford and Dr J. Sap. These data are presented here to demonstrate a potential application of [^{18}F]**2.81** as a PET radiotracer for neuroinflammation and microglial activation, with a comparison to the existing tracer DPA-714 ([^{18}F]**2.80**).

PET imaging experiments were conducted using an excitotoxic model of Huntington's disease, which was prepared surgically using a solution of quinolinic acid to produce a unilateral lesion in the brain in C57BL/6J mice.[103] This model was expected to cause neuroinflammation and microglial activation and thus upregulated production of TSPO, for which [^{18}F]**2.80** has been shown to be a radioligand. We therefore hypothesised the modified version of this tracer [^{18}F]**2.81** should also exhibit similar behaviour. Two weeks after the surgical preparation of the lesion model, [^{18}F]**2.80** and [^{18}F]**2.81** were administered on consecutive days to the mice *via* tail vein injection. The mice then were scanned for 60 minutes. This process is summarised in Figure 2.14.

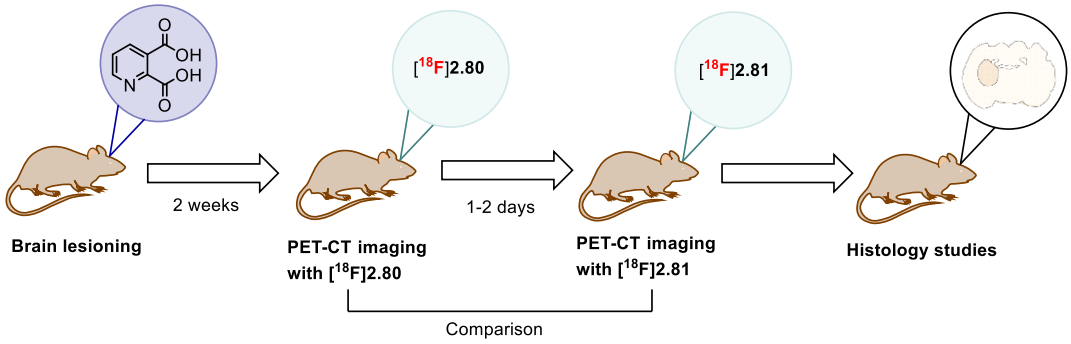
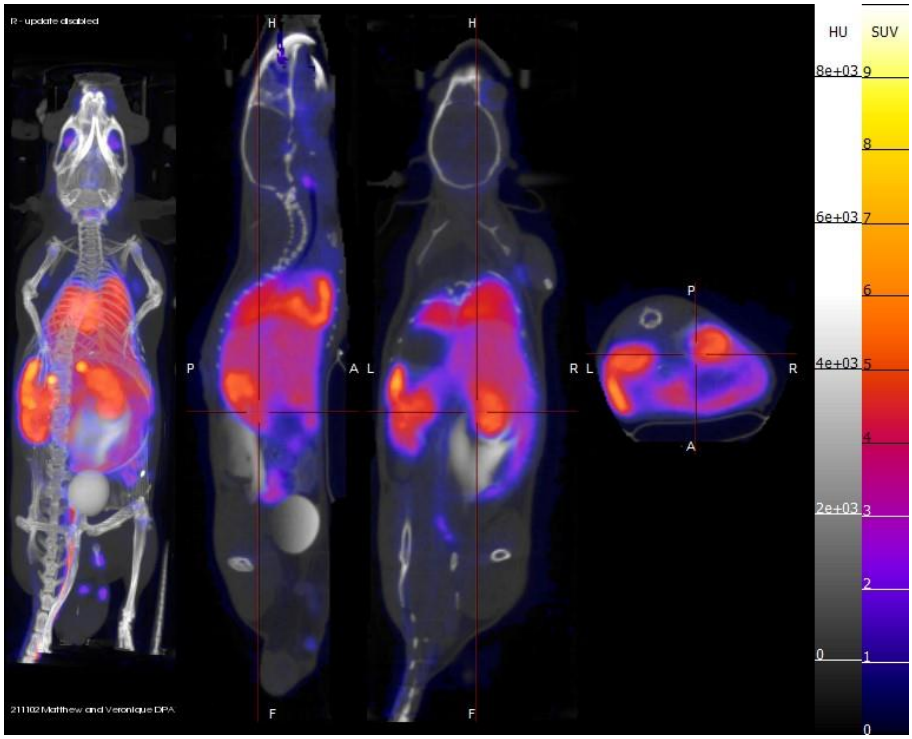


Figure 2.14. *Overview of PET-CT imaging experiments with [^{18}F]**2.80** and [^{18}F]**2.81** in quinolinic acid lesion mouse model of Huntington's Disease.*

PET-CT images were reconstructed from scanning data acquired between 40 and 60 minutes of the 60-minute scans. Figure 2.15 shows the whole-body PET-CT images obtained from a single mouse injected with [^{18}F]**2.80** (Figure 2.15 a) and [^{18}F]**2.81** (Figure 2.15 b), consecutively. The scanning data is expressed as Standard Uptake Values (SUVs), which compensates for the mass and size of the mouse, the injected dose of radiotracer and

radioactive decay during the scan. As these images have the same SUV thresholding and were conducted with the same mouse, the scanning data can be expected to be comparable.

a) [^{18}F]**2.80**



b) [^{18}F]**2.81**

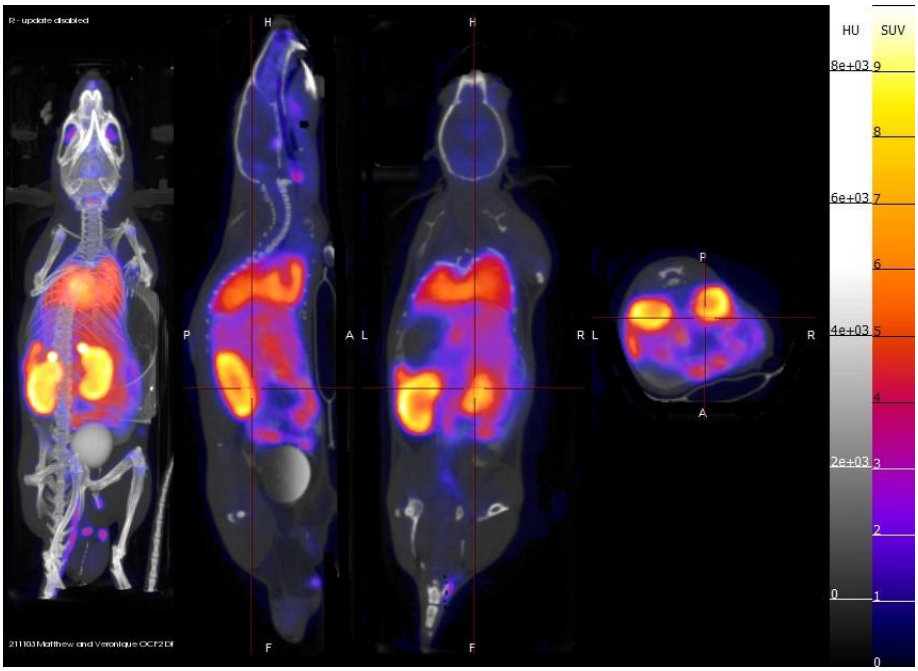


Figure 2.15. *Whole-body PET-CT images of a quinolinic acid lesion model mouse injected with a) [^{18}F]**2.80**; b) [^{18}F]**2.81**.*

From the PET-CT images, it is apparent that the distribution of modified tracer [^{18}F]**2.81** is similar to the existing tracer [^{18}F]**2.80**, with both tracers predominantly accumulating in the adrenal glands, kidneys, spleen, heart and lungs, with lower uptake observed in the liver and intestines. This is promising as the structural modification between [^{18}F]**2.80** and [^{18}F]**2.81** is the introduction of a single fluorine atom. Despite this similar profile, based on the higher SUVs observed, it appears that [^{18}F]**2.81** is more strongly taken up in the adrenal glands and kidneys than [^{18}F]**2.80**, whilst [^{18}F]**2.80** exhibits a higher spleen uptake and a higher background in the liver and intestines than [^{18}F]**2.81**. Based on the higher SUVs observed for the rest of the body compared to the head, [^{18}F]**2.80** and [^{18}F]**2.81** appear to be more strongly taken up in the organs of the body compared to the brain, however close inspection of the image for [^{18}F]**2.81** shows faint uptake in the cerebellum and the lesioned area of the brain which is not visible for [^{18}F]**2.80** when displayed with the same intensity threshold. Figure 2.16 shows images from the same scans that are cropped to the head region and expanded, showing that both tracers were capable of binding to the intended TSPO target that was present in elevated concentrations in the brain lesion, due to upregulation from microglial activation in the mouse model. To better highlight the difference in activity uptake in the brain between the 2 tracers the scans are shown with 2 SUV threshold settings. In the images on the left, the threshold was adjusted to best highlight the brain uptake of tracer [^{18}F]**2.81** (SUV 0-5). By contrast, the lesion is barely visible at this same threshold setting in the same mouse scanned on the previous day after injection with [^{18}F]**2.80**. The images on the right show the same scans but with the SUV thresholds adjusted to best highlight the lesion in the [^{18}F]**2.80** scan (SUV 0–2.5). At this lower SUV threshold, the [^{18}F]**2.81** scan is over-exposed, which highlights the increased brain uptake of tracer [^{18}F]**2.81** over tracer [^{18}F]**2.80**. Furthermore, closer inspection of these scans reveals that tracer [^{18}F]**2.81** exhibits sharper contrast with a better lesion to background brain tissue uptake ratio. This pattern was repeated across four

quinolinic acid lesioned model mice, with higher uptake in the brain lesion observed for the [^{18}F]OCF_2H containing tracer [^{18}F]**2.81** scans than for those with existing tracer [^{18}F]**2.80**.

a) [^{18}F]**2.80**

b) [^{18}F]**2.81**

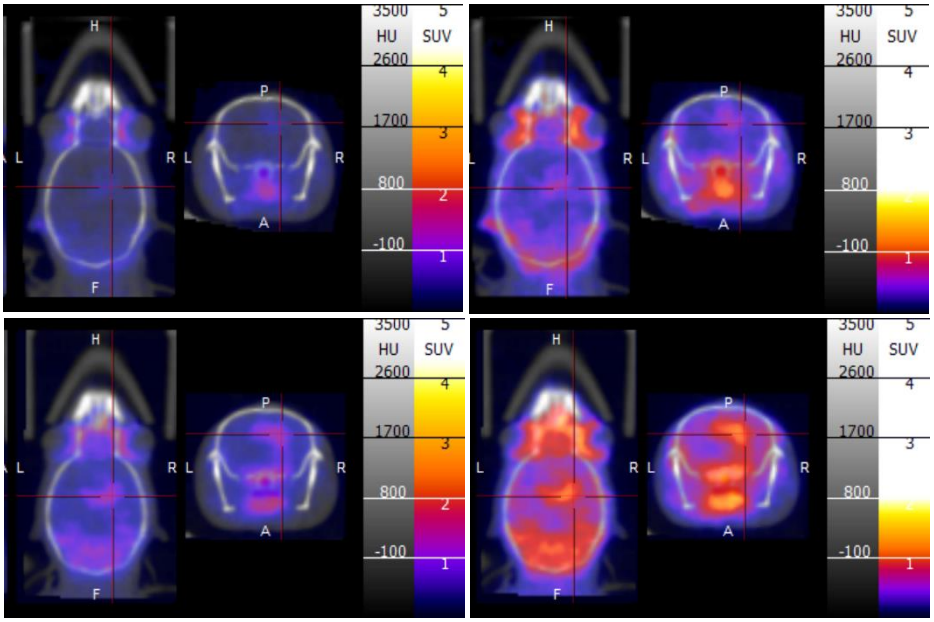


Figure 2.16. *PET-CT images of the head of a quinolinic acid lesion model mouse injected with a) [^{18}F]**2.80**; b) [^{18}F]**2.81**. The site of the induced brain lesion is indicated by the red crosshair.*

As these experiments suggested that there may be a difference in the brain uptake profile between [^{18}F]**2.80** and [^{18}F]**2.81**, a blocking study was also conducted to provide evidence that the observed brain uptake corresponded to specific target binding. PK-11195 (**2.84**) was used as a blocking agent, as it has been demonstrated to have high affinity for TSPO.[104] This was administered to naïve C57BL/6J mice, before [^{18}F]**2.81** was injected. Images obtained in these experiments show that no brain uptake of [^{18}F]**2.81** was observed in mice that had been previously administered with **2.84** (Figure 2.17 b), while brain uptake was observed in the absence of the blocking agent (Figure 2.17 a). This suggests that [^{18}F]**2.81** likely binds to the desired target TSPO. Histology studies to further confirm that [^{18}F]**2.81** binds specifically to the intended TSPO target are ongoing.

a) [^{18}F]**2.81, no 2.84**

b) [^{18}F]**2.81, blocked with 2.84**

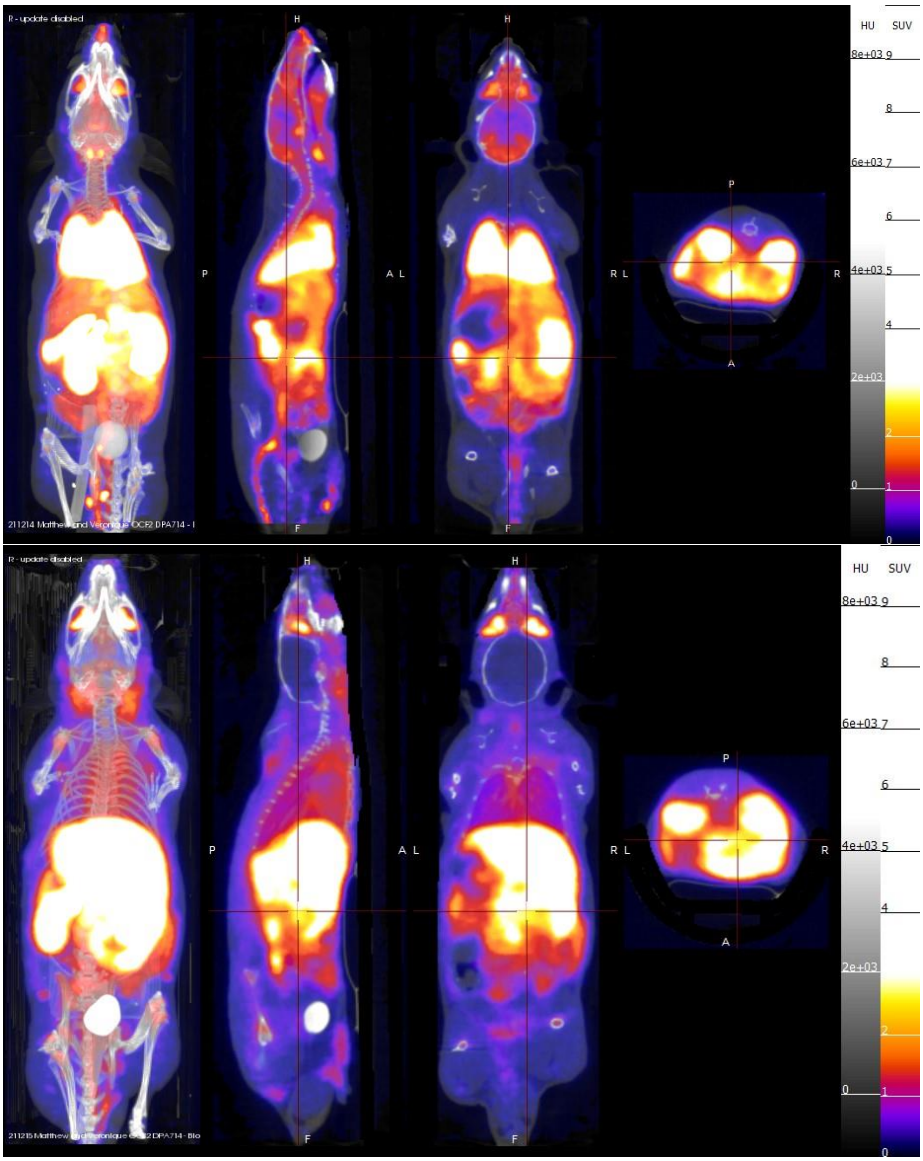


Figure 2.17. *Blocking study for [^{18}F]**2.81**. PET-CT images of a naïve C57BL/6J mouse injected with [^{18}F]**2.81**; b) [^{18}F]**2.81** and **2.84** (blocking agent).*

A radiometabolite study was also conducted to provide preliminary information about the differences in the metabolic stability of [^{18}F]**2.81** (containing a [^{18}F]CF_2H group) and [^{18}F]**2.80** (containing an [^{18}F]CH_2CH_2F group). Based on the superior stability profile of difluoromethylated compounds compared to their fluoromethylated analogues, we hypothesised that [^{18}F]**2.81** may be more chemically resistant to metabolic processes, such as oxidation. Naïve C57BL/6J mice were administered with either [^{18}F]**2.80** or [^{18}F]**2.81**. After 5 minutes, blood plasma and brain extracts were harvested and these were analysed by radio-HPLC. In the case of [^{18}F]**2.81**, no radioactive metabolites were observed, and intact [^{18}F]**2.81**

was observed by radio-HPLC (Figure 2.18). Meanwhile, for [^{18}F]**2.80**, polar radioactive metabolites were formed, in line with previous studies, which observed the formation of species such as [^{18}F]fluoride, [^{18}F]fluoroacetate or [^{18}F]fluoroacetaldehyde (Figure 2.19).[100] Furthermore, no intact [^{18}F]**2.80** was observed by radio-HPLC. This may indicate that the [^{18}F]OCF_2H group in [^{18}F]**2.81** has greater stability to defluorination compared to the [^{18}F]OCH_2CH_2F group in [^{18}F]**2.80**, however additional studies will be required to provide further evidence to test this hypothesis and to investigate whether this trend is applicable to other ^{18}F-radiotracers beyond those considered here.

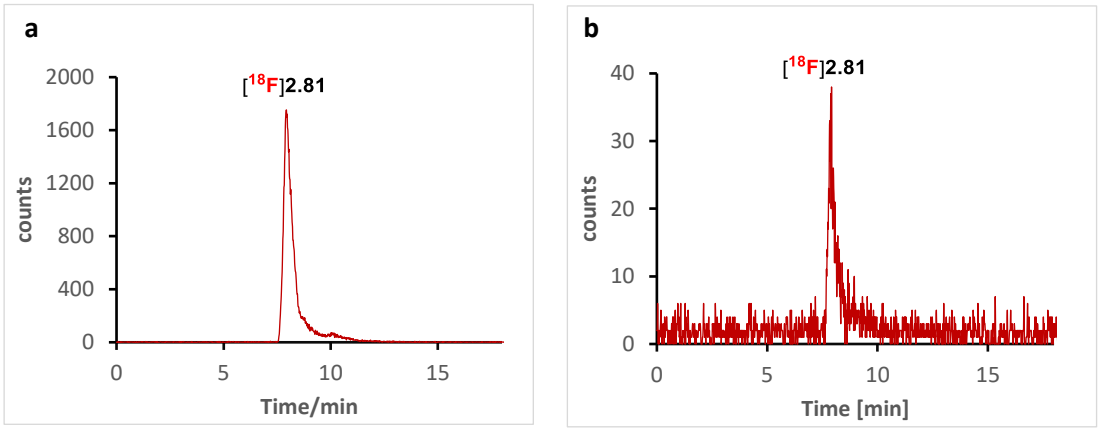


Figure 2.18. *Radio-HPLC traces from the radiometabolite study using [^{18}F]**2.81**. Samples taken from a) brain tissue, b) blood. t_R ([^{18}F]**2.81**) = 7.9 min.*

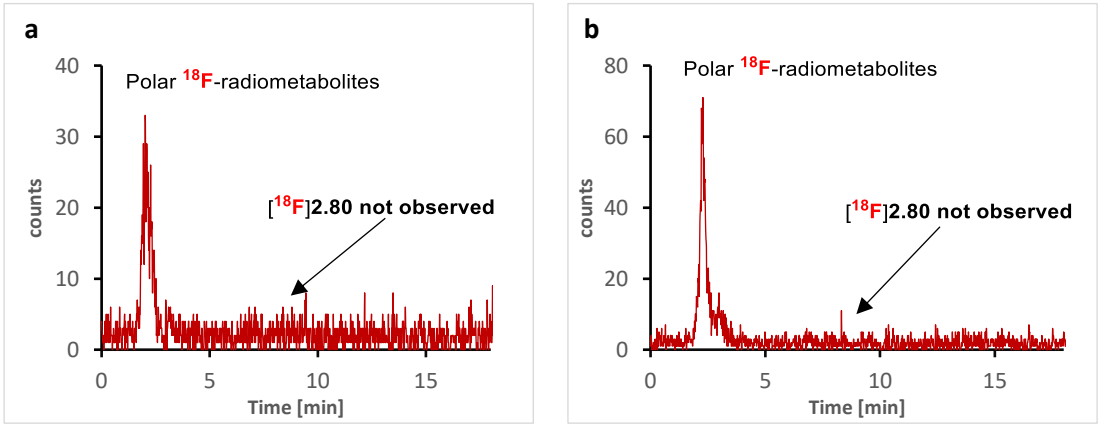
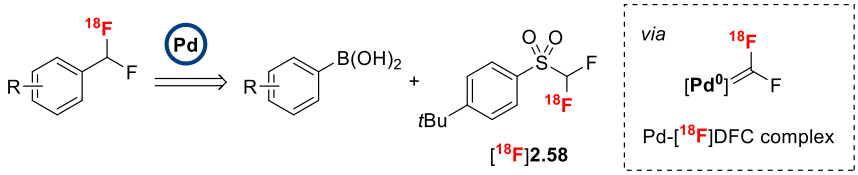


Figure 2.19. *Radio-HPLC traces from the radiometabolite study using [^{18}F]**2.80**. Samples taken from a) brain tissue, b) blood.*

2.2.3. ^{18}F-Difluoromethylation of Aryl Boronic Acids

As outlined in section 2.1.3, prior to the work disclosed herein, there had been only a single report of ^{18}F-difluoromethylation of aromatic scaffolds. Lemaire, Luxen, Genicot and co-workers engaged a benzothiazole-derived ^{18}F-difluoromethyl sulfone ([^{18}F]**2.47**) in a photoredox-mediated Minisci-type ^{18}F-difluoromethylation of heteroarenes.[88] While effective, this reaction could lead to mixtures of regioisomeric products that would be challenging and time-consuming to separate, requiring longer preparative HPLC runs. The efficiency of their reaction also depends on the philicity match between the ^{18}F-difluoromethyl radical and the heteroarene, which limited the reaction scope to essentially selected heteroaromatic scaffolds and the site of reaction to the most activated positions.[31]

We therefore sought to address these limitations with the development of the first direct and regioselective aromatic ^{18}F-difluoromethylation. Taking inspiration from the reports of Pd-catalysed difluorocarbene transfer from the Zhang and Xiao groups, we hypothesised that [^{18}F]DFC could also be captured by Pd^0, forming a key Pd^0-[^{18}F]DFC complex that could then engage in cross-coupling with a suitable aryl partner (Scheme 2.44).[60-64] In addition to providing a new route to complex ^{18}F-difluoromethylarenes, such a protocol would be the first demonstration that our [^{18}F]DFC platform was compatible with transition metals and would represent the most complex application of [^{18}F]DFC radiochemistry to date. We therefore developed a Pd-mediated ^{18}F-difluoromethylation of aryl borons using reagents [^{18}F]**2.58** and [^{18}F]**2.67**. The design for this reaction is outlined in Scheme 2.44. As this work began in 2020 before Zhang's difluoromethylation of aryl halides had been reported, these were not considered as coupling partners.[68]

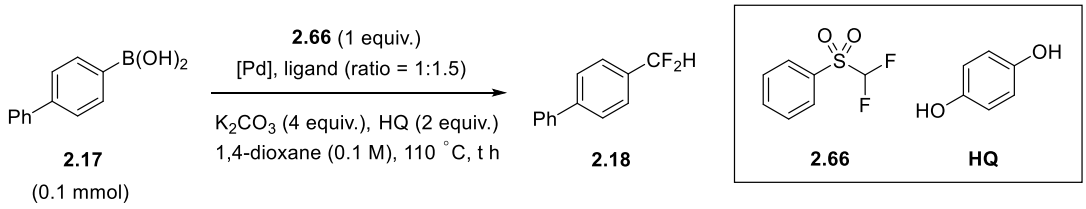


Scheme 2.44. *Pd-mediated ^{18}F-difluoromethylation of aryl boronic acids with [^{18}F]**2.58**.*

However, as difluoromethyl aryl sulfone reagents had not applied in such DFC cross-couplings previously, proof-of-concept studies were first required to demonstrate feasibility. Indeed, difluoromethyl phenyl sulfone (**2.66**) has been engaged in Cu-mediated cross-coupling with aryl boronic acids, yielding (phenylsulfonyl)difluoromethylated products, rather than the desired difluoromethyl arenes,[105] while the cross-coupling of another DFC reagent diethyl bromodifluoromethylphosphonate (**2.13**) under Pd-catalysis could lead to either the difluoromethyl arene or the undesired aryldifluoromethyl phosphonate.[106] The formation of such products could therefore be a possible challenge. It is worth noting that we were not concerned with the formation of products observed by Zhang corresponding to multiple [^{18}F]DFC insertions and/or CO insertion, as the concentration of Pd complexes would vastly exceed that of [^{18}F]DFC, and no CO surrogates were to be employed. We therefore first sought to establish whether difluoromethyl aryl sulfones could be viable DFC reagents in Pd-catalysed difluoromethylation with experiments on non-radioactive material.

2.2.3.1. Preliminary Experiments on Non-Radioactive Material

For preliminary experiments, as aryl boronic acids have been shown to be effective across a number of reports, we elected commercially available 4-biphenylboronic acid (**2.17**) as a model substrate.[61-64] As reactivity differences between ^{18}F-difluoromethyl aryl sulfones would be assessed on radioactive material, commercially available **2.66** was selected as a DFC reagent. We also opted to use a single equivalent of **2.66** in these reactions, as under radiochemical conditions, all other reagents will be present in vast excess compared to the ^{18}F-labelled component. Initial conditions were taken from Zhang's report of Pd-catalysed difluoromethylation with $ClCF_2H$, which is also a base-activated DFC reagent, whereby a Pd to ligand ratio of 1:1.5 was used, 4 equivalents of K_2CO_3 was used as a base and 2 equivalents of HQ were used as an additive.[63] The reactions were conducted in 1,4-dioxane solvent (0.1 M) and were heated at 110 °C. The first parameters to be varied were the identity of the Pd-catalyst and ligands (Table 2.4).

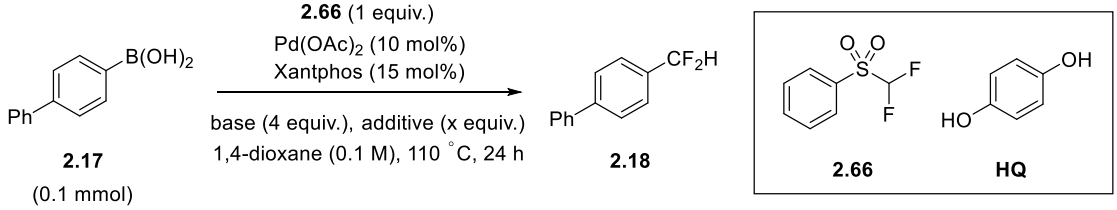


Entry	[Pd]	[Pd] loading	Ligand	Degassed?	t	NMR yield
1	$PdCl_2$	5 mol%	Xantphos	N	4 h	n.d.
2	$PdCl_2(PPh_3)_2$	5 mol%	Xantphos	N	4 h	n.d.
3	$PdCl_2(PhCN)_2$	5 mol%	Xantphos	N	4 h	5%
4	$PdCl_2(PPh_3)_2$	5 mol%	Xantphos	N	4 h	n.d.
5	$Pd(OAc)_2$	5 mol%	Xantphos	N	4 h	2%
6	$Pd(OAc)_2$	5 mol%	Xantphos	Y	4 h	12%
7	$Pd(OAc)_2$	5 mol%	Xantphos	Y	24 h	17%
8	$Pd(OAc)_2$	10 mol%	Xantphos	Y	24 h	27%
9	$Pd(OAc)_2$	20 mol%	Xantphos	Y	24 h	31%
10	$Pd(OAc)_2$	10 mol%	dppf	Y	24 h	1%
11	$Pd(OAc)_2$	10 mol%	(±)-BINAP	Y	24 h	n.d.
12	$Pd(OAc)_2$	10 mol%	dppp	Y	24 h	13%
13	$Pd(OAc)_2$	10 mol%	dppb	Y	24 h	n.d.
14	$Pd(OAc)_2$	10 mol%	dppm	Y	24 h	n.d.
15	$Pd(OAc)_2$	10 mol%	dppe	Y	24 h	1%
16	$Pd(OAc)_2$	10 mol%	DPEPhos	Y	24 h	2%

***Table 2.4**. Preliminary optimisation of the catalyst system for the Pd-catalysed difluoromethylation of model aryl boronic acid **2.17** with **2.66**. NMR yields estimated by ^{19}F qNMR using 4-fluoroanisole (1 equiv.) as internal standard. n.d. = not determined.*

Of those considered, $Pd(OAc)_2$ and $PdCl_2(PhCN)_2$ were found be the most promising catalysts when used in combination with a Xantphos ligand (Table 2.4, entries 3 and 5). The yield of

2.18 was improved to 12% by degassing the reaction mixture with N_2 prior to heating (Table 2.4, entry 6). Increasing the reaction time to 24 h from 4 h gave a further small improvement in yield (Table 2.4, entry 7). Higher loadings of $Pd(OAc)_2$ of 10 and 20 mol% delivered **2.18** in up to 31% ^{19}F NMR yield (Table 2.4, entries 8 and 9). A range of other bidentate bis-phosphines were evaluated and were found to be inferior to Xantphos (Table 2.4, entries 10-16). This is consistent with Zhang's optimised conditions, and in line with Grushin's findings of improved reductive elimination from [(Xantphos)Pd(Ph)(CF_3)] complexes.[65] Therefore, we proceeded with a $Pd(OAc)_2$- Xantphos catalyst system for further studies.



Entry	Base	Additive	x equiv.	NMR yield
1	K_2CO_3	HQ	2 equiv.	27%
2	KO*t*Bu	HQ	2 equiv.	12%
3	K_3PO_4	HQ	2 equiv.	1%
4	NaOPh	HQ	2 equiv.	5%
5	KOAc	HQ	2 equiv.	n.d.
6	K_2CO_3	dimedone	2 equiv.	n.d.
7	K_2CO_3	1,3-cyclopentadione	2 equiv.	n.d.
8	K_2CO_3	none	-	n.d.
9	KO*t*Bu	none	-	n.d.
10	NaOPh	none	-	n.d.

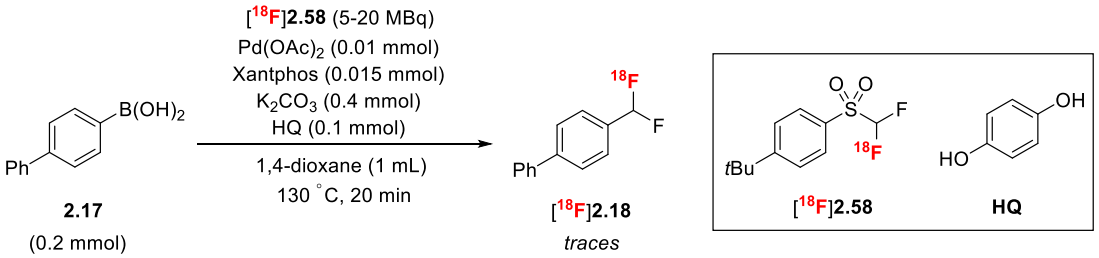
***Table 2.5**. Preliminary optimisation of bases and additives for the Pd-catalysed difluoromethylation of model aryl boronic acid **2.17** with **2.66**. NMR yields estimated by ^{19}F qNMR using 4-fluoroanisole (1 equiv.) as internal standard. n.d. = not determined.*

Next, the identity of the base and additive used were assessed (Table 2.5). K_2CO_3 remained the most effective base of those trialled, but the stronger base KO*t*Bu was also able to activate **2.66** (Table 2.5, entry 2). When weaker bases, such as KOAc, K_3PO_4 or NaOPh were used, this gave no or reduced yields of the desired product **2.18** and full recovery of **2.66** (Table 2.5, entries 3-5). The application of alternative additives to HQ gave no desired product, while the removal of HQ from the reaction also resulted in no **2.18** formation (Table 2.5, entries 6-10). The presence of the HQ additive appears to be essential for an efficient reaction and this was also observed with NaOPh and KO*t*Bu bases. Interestingly, the use of the HQ additive did not lead to formation of *O*-difluoromethylated products by ^{19}F NMR analysis in any of these experiments investigating the ^{19}F-difluoromethylation of aryl boronic acids with **2.66**.

2.2.3.2. Optimisation of the Pd-Mediated ^{18}F-Difluoromethylation

Having established a proof-of-concept that **2.66** is a viable DFC reagent for Pd-catalysed difluoromethylation of aryl boronic acid **2.17**, we next proceeded to conduct first radiochemistry experiments with [^{18}F]**2.58**. In the development of this reaction, no attempt was made to exclude air or moisture, as these variables are challenging to control with commercial radiosynthesis equipment.

Initial attempts to replicate the conditions that were effective in experiments with non-radioactive material gave only traces of desired product ([^{18}F]**2.18**) (Scheme 2.45); radio-HPLC analysis showed that [^{18}F]**2.58** was not consumed under these conditions (Figure 2.20). We surmised that the reaction conditions were too mild to activate [^{18}F]**2.58** to generate [^{18}F]DFC even at temperatures up to 130 °C. We therefore decided to explore the use of stronger bases than K_2CO_3, marking a further point of divergence from Zhang and co-workers' system.[61,63,64] This is in line with the previous work on ^{18}F-difluoromethylation of *O*,*S*,*N*-nucleophiles with [^{18}F]**2.58**, where aqueous KOH is used as a base at a reaction temperature of 80 °C.



Scheme 2.45. *Initial attempts towards Pd-mediated ^{18}F-difluoromethylation of* ***2.17*** *with [^{18}F]****2.58****.*

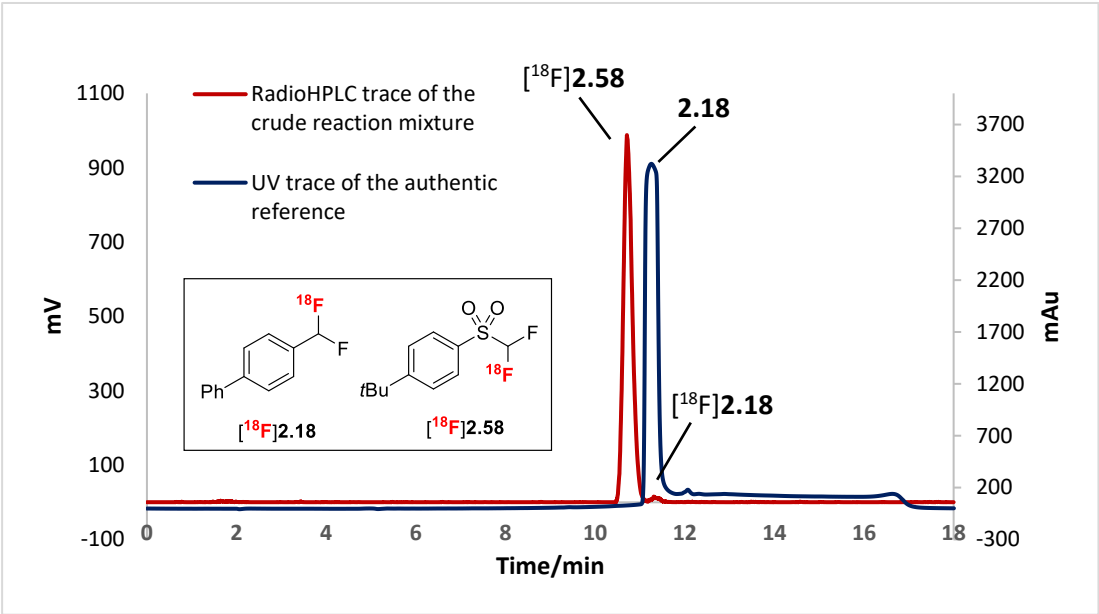


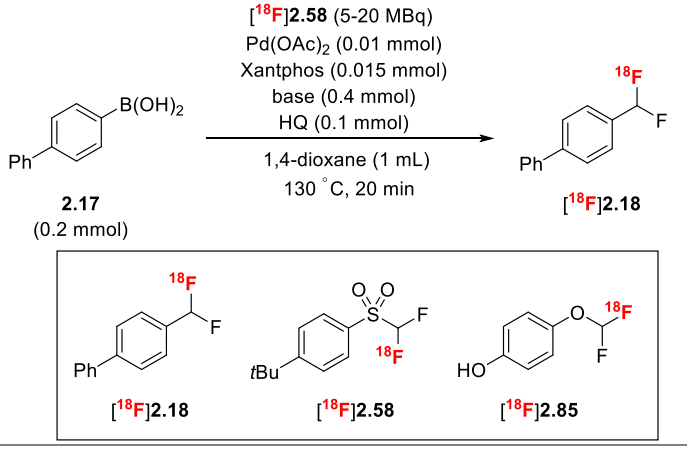
Figure 2.20. *Radio/UV-HPLC trace overlays for: 1) Radio-HPLC trace for the initial conditions attempted for the ^{18}F-difluoromethylation of* ***2.17*** *with [^{18}F]****2.58****, using K_2CO_3 as a base, 2) UV-HPLC trace for authentic reference* ***2.18****.*

We first opted to explore various bases as alternatives to K_2CO_3, as we hypothesised that this was too weak to deprotonate [^{18}F]**2.58** and generate [^{18}F]DFC. We therefore assessed a range of stronger bases to determine whether this would lead to an increased in RCY_{HPLC} of [^{18}F]**2.18** beyond the traces observed with K_2CO_3. We therefore assessed a range of hydroxide bases in next experiments. These data are summarised in Table 2.6. Of all the bases assessed, KOH appeared to be the most promising (Table 2.6, entry 2), with [^{18}F]**2.18** formed in RCY_{HPLC} of 5%. We also trialled aqueous KOH solution as a base, as this had proven effective for the activation of [^{18}F]**2.58** previously. This delivered [^{18}F]**2.18** in higher RCY_{HPLC} of 13% (Table 2.6, entry 5). The formation of a new product ([^{18}F]**2.85**) in 12% RCY_{HPLC} was also observed. This was found to be *O*-^{18}F-difluoromethylated HQ by radio-HPLC analysis (Figure 2.21). This is in

contrast to our studies on non-radioactive material, where **2.85** was not observed as a side product in the ^{19}F-difluoromethylation reaction. Indeed, numerous attempts to difluoromethylate HQ directly failed (e.g. with DFC reagents **2.13**, **2.15** and **2.16**), and a two-step synthetic route, starting from 4-(benzyloxy)phenol was necessary to prepare **2.85** as an authentic reference for HPLC analysis (see Chapter 4 for further details). This highlights a potential mechanistic difference between the ^{18}F- and ^{19}F-reactions.

Furthermore, the major product of the reaction yielding [^{18}F]**2.18** in an RCY_{HPLC} of 13% (Table 2.6, entry 5) was a highly polar species; we surmised that this species was likely [^{18}F]fluoride. This could be formed from the hydrolysis of [^{18}F]DFC by aqueous KOH, which would yield potassium formate and [^{18}F]KF as reaction products, or, as suggested by Zhang and co-workers, the hydrolysis of a Pd^{II}-[^{18}F]DFC complex in the presence of water.[64] As addition of water when weaker K_2CO_3 was used as a base did not lead to any formation of [^{18}F]**2.18** or [^{18}F]fluoride, this suggested base strength was a more significant parameter compared to the presence of water for both the formation of desired product and also degradation of [^{18}F]DFC to [^{18}F]fluoride (Table 2.6, entry 6). The formation of [^{18}F]fluoride is also observed during the ^{18}F-difluoromethylation of *O*,*S*,*N*-nucleophiles with [^{18}F]**2.58** and aqueous KOH as a base, in the absence of a Pd additive. This indicates a mechanistic difference between the formation of fluoride between the ^{18}F- and ^{19}F-reactions, likely caused by the stronger hydroxide base required under radiochemical conditions.

Next, the effect of the loadings of KOH and the HQ additive was assessed (Table 2.7); to allow for easier calculation of the amount of KOH added, aqueous KOH solutions were prepared with known molar concentrations (M), rather than weight concentration (w/w).



Entry	Base	RCY_{HPLC} of [^{18}F]2.18
1	K_2CO_3	traces
2	KOH (solid)	5%
3	LiOH	n.d.
4	$Ca(OH)_2$	n.d.
5	KOH (aq.)[a]	13%
6	K_2CO_3[b]	n.d.

***Table 2.6**. Optimisation of base identity for the Pd-catalysed ^{18}F-difluoromethylation of **2.17** with [^{18}F]**2.58**. RCY_{HPLC} determined by radio-HPLC analysis of the crude reaction mixture. [a] 50 µL KOH solution used was a 40% w/w aqueous solution. [b] 80 µL water added. n.d. = not detected.*

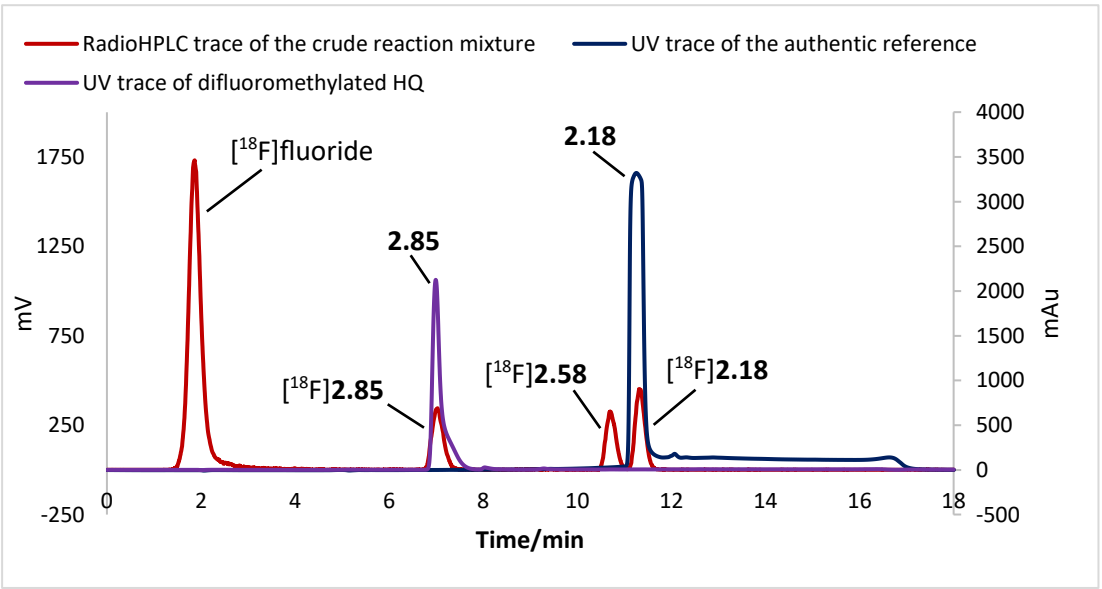
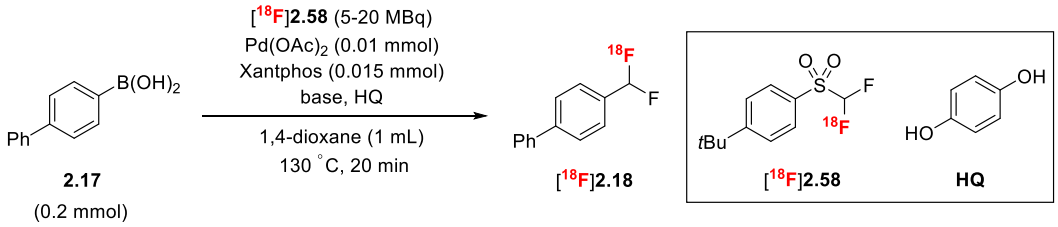


Figure 2.21.** Radio/UV-HPLC trace overlays for: 1) Radio-HPLC trace for the ^{18}F-difluoromethylation of **2.17** with [^{18}F]**2.58**, using KOH (aq.) as a base, 2) UV-HPLC trace for authentic reference **2.18**, 3) UV-HPLC trace for difluoromethylated HQ **2.85.



Entry	HQ loading	KOH $_{(aq.)}$ concentration	KOH $_{(aq.)}$ volume	RCY_{HPLC} of [^{18}F]**2.18**
1	0.1 mmol	5 M	80 µL	26%
2	0.1 mmol	10 M	40 µL	26%
3	0.1 mmol	20 M	20 µL	16%
4	0.05 mmol	10 M	40 µL	29% ± 2 % (*n* = 2)
5	0.05 mmol	10 M	80 µL	1%
6	none	10 M	40 µL	9%
7	none[a]	10 M	40 µL	11%

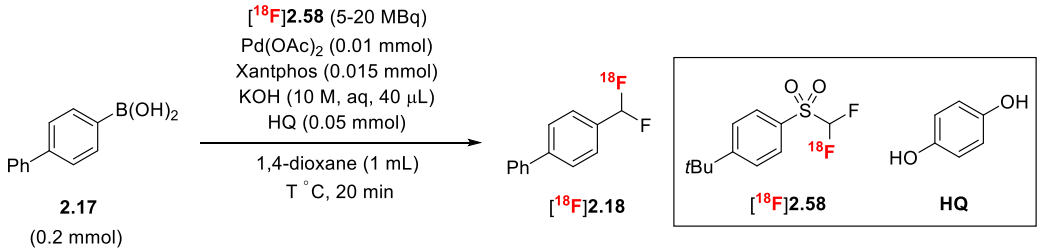
***Table 2.7**. Optimisation of base and HQ loading for the Pd-catalysed ^{18}F-difluoromethylation of **2.17** with [^{18}F]**2.58**. RCY_{HPLC} determined by radio-HPLC analysis of the crude reaction mixture. [a] 0.1 mmol 4-methyl-2,6-bis(t-butyl)phenol and 0.01 mmol benzoquinone were added.*

Based on these experiments, various concentrations of KOH solution are effective and lead to the formation of [^{18}F]**2.18** and small differences in the volume of water added are not significant when the total loading of KOH remains constant (Table 2.7, entries 1-3). The use of 5 M or 10 M KOH solutions pleasingly led to an increase in RCY_{HPLC} to 26%. The RCY_{HPLC} of [^{18}F]**2.18** could be further improved to 29%, when the loading of HQ was halved to 0.05 mmol; in this reaction, a 3% RCY_{HPLC} of side-product [^{18}F]**2.85** was observed, representing a significant improvement in selectivity for *C*-^{18}F-difluoromethylation over *O*-^{18}F-difluoromethylation (Table 2.7, entry 4). When the amount of base was doubled, this led to a loss in reactivity, likely as [^{18}F]DFC was more readily hydrolysed to [^{18}F]fluoride under these conditions (Table 2.7, entry 5). The exclusion of the HQ additive was next investigated. If HQ is not added, the side reactivity is avoided and a RCY_{HPLC} of up to 9 % was obtained (Table 2.7, entry 6). This is in contrast to Zhang and co-workers' observation that an absence of HQ

causes the reaction to fail, suggesting mechanistic and/or kinetic differences between the ^{18}F-reaction and ^{19}F-reactions.[61,63-64] Due to the large excess of $Pd(OAc)_2$ relative to [^{18}F]DFC, the potential role of HQ as a reductant is perhaps less significant than under catalytic ^{19}F-reaction conditions. As in Zhang's study on the difluoromethylation of alkynes, a phenol with a catalytic amount of benzoquinone was shown to be a viable alternative to the HQ additive, a bulky phenol in combination with benzoquinone were next trialled as additives in place of HQ.[67] This resulted in a similar RCY_{HPLC} of [^{18}F]**2.18** (11%) compared to when HQ was not added (Table 2.7, entry 7). Furthermore, under these conditions, [^{18}F]**2.58** was completely consumed and the major species observed by radio-HPLC was [^{18}F]fluoride. On this basis, the addition of 40 µL of 10 M aqueous KOH as a base and 0.05 mmol of HQ as an additive were selected as optimal conditions to be carried forwards, as these delivered desired product [^{18}F]**2.18** in superior RCY_{HPLC}, with a low RCY_{HPLC} of side-product [^{18}F]**2.85**.

The effect of reaction temperature was next assessed. Varying this parameter had a significant effect on the outcome of the reaction, suggesting a high sensitivity of the reaction to temperature. For model substrate **2.17**, reducing the temperature to 125 °C improved the RCY_{HPLC} of [^{18}F]**2.18** to 45% from 29% at the original temperature of 130 °C (Table 2.8, entry 3, and Table 2.7, entry 4). Further increasing the reaction temperature to 135 °C led to increased formation of [^{18}F]fluoride, resulting in complete consumption of [^{18}F]**2.58** (Table 2.8, entry 4). Meanwhile, at 120 °C and 115 °C, the RCY_{HPLC} of [^{18}F]**2.18** was lower, perhaps suggesting that the release and/or transfer of [^{18}F]DFC operate less efficiently at lower temperatures, while [^{18}F]**2.58** was left unreacted in the reaction mixture, with less formation of [^{18}F]fluoride observed (Table 2.8, entries 1, 2).

The reaction solvent was next considered in our optimisation study. First, we varied the solvent identity. We prioritised water-miscible solvents, as ^{18}F-radiotracers are most commonly purified using reverse-phase HPLC and remaining non-polar solvents may reduce

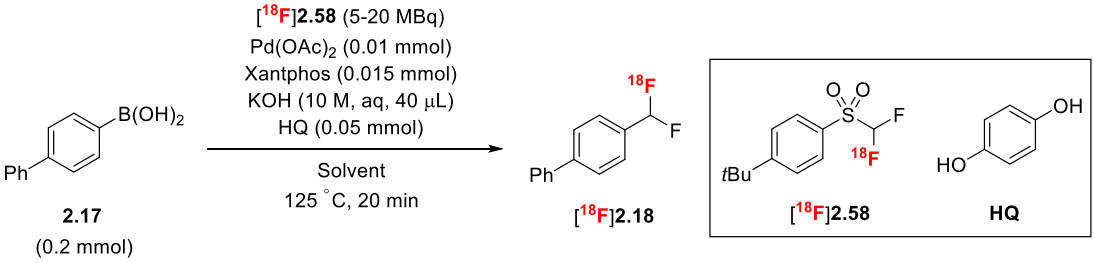


Entry	Temperature	RCY_{HPLC} of [^{18}F]2.18	RCY_{HPLC} of [^{18}F]fluoride	RCY_{HPLC} of unreacted [^{18}F]2.58
1	115 °C	10%	10%	80%
2	120 °C	32% ± 12% (*n* = 2)	30% ± 2% (*n* = 2)	37% ± 12% (*n* = 2)
3	125 °C	45% ± 10% (*n* = 3)	51% ± 9% (*n* = 3)	2% ± 1% (*n* = 3)
4	135 °C	14%	86%	n.d.

***Table 2.8**. Optimisation of temperature for the Pd-catalysed ^{18}F-difluoromethylation of **2.17** with [^{18}F]**2.58**. RCY_{HPLC} determined by radio-HPLC analysis of the crude reaction mixture. n.d. = not detected.*

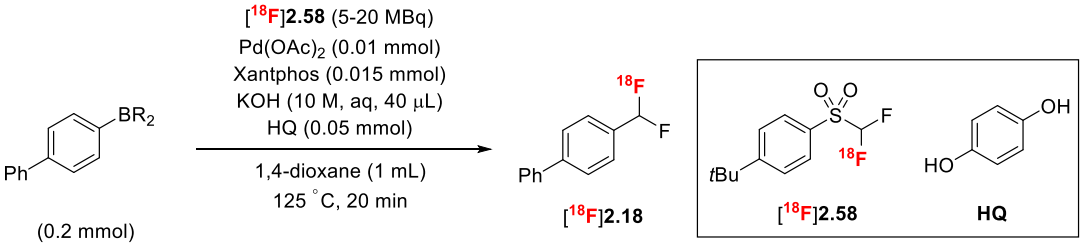
the efficiency of purification using this method. The removal of non-polar solvents can necessitate an additional cartridge purification and/or the evaporation of the solvent, prior to HPLC purification. For this reason, *p*-xylene, which previously proved effective in Xiao and co-workers' Pd-catalysed difluoromethylation of aryl boronic acids, was not considered.[62] Instead, two alternative high boiling and water-miscible solvents, DMF and DMSO, were trialled (Table 2.9, entries 1 and 2). Neither of these proved to be superior to 1,4-dioxane and this remained the optimal solvent in our study, in line with Zhang and co-workers' conditions.[61,63-64] Solvent volume was also evaluated (Table 2.9, entries 3-5). This also affected the RCY_{HPLC} of [^{18}F]**2.18**, with the highest value for model substrate **2.17** obtained at the intermediate volume of 1 mL. Similarly to the trend observed with increasing temperature, at increasing concentration, the formation of [^{18}F]fluoride increased, and consumption of [^{18}F]**2.58** increased. This did not necessarily correlate with increased RCY_{HPLC}, but the effect of solvent volume and reaction temperature could exploited in optimisation.

The effect of using a pinacol boronic ester (Bpin) precursor in place of a boronic acid was also assessed. This gave a lower RCY_{HPLC} of [^{18}F]**2.18** compared to boronic acid **2.17** (Table 2.10).



Entry	Solvent	Solvent volume	RCY_{HPLC} of [^{18}F]2.18
1	DMF	1.0 mL	2%
2	DMSO	1.0 mL	n.d.
3	1,4-dioxane	0.5 mL	11%
4	1,4-dioxane	1.0 mL	45% ± 10% (*n* = 3)
5	1,4-dioxane	1.5 mL	30%

***Table 2.9**. Optimisation of solvent for the Pd-catalysed ^{18}F-difluoromethylation of **2.17** with [^{18}F]**2.58**. RCY_{HPLC} determined by radio-HPLC analysis of the crude reaction mixture. n.d. = not detected.*



Entry	BR_2	RCY_{HPLC} of [^{18}F]2.18
1	$B(OH)_2$	45% ± 10% (*n* = 3)
2	Bpin	12%

***Table 2.10**. Optimisation of aryl boron partner for the Pd-catalysed ^{18}F-difluoromethylation with [^{18}F]**2.58**. RCY_{HPLC} determined by radio-HPLC analysis of the crude reaction mixture.*

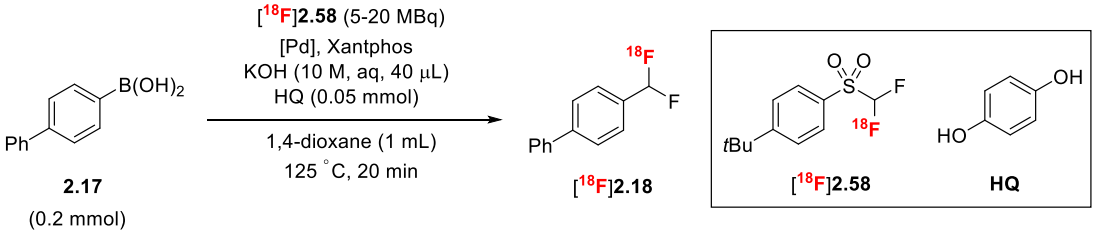
Further designer aryl boron reagents were not assessed, as their commercial availability is lower than that of aryl boronic acid and aryl-Bpin substrates.[63] Libraries of these compounds are often available due to their prevalent use in cross-coupling reactions, and we were aiming towards a protocol that was readily implementable by practitioners, relying on a convenient

substrate class. Aryl boronic acids therefore remained the substrate of choice for this reaction.

Finally, the loading and identity of the palladium catalyst was considered (Table 2.11). The Pd-to-ligand ratio was maintained at 1:1.5 in these experiments. $Pd(PPh_3)_2Cl_2$ gave a lower RCY_{HPLC} of [^{18}F]**2.18** (Table 2.11, entry 2), while Pd_2dba_3 proved more effective (Table 2.11, entry 3). The use of a commercial precatalyst (Xantphos Pd G3) was not effective, leading to significantly reduced RCY_{HPLC} of [^{18}F]**2.18** (Table 2.11, entry 4). When the loading of $Pd(OAc)_2$ was altered, this did not change the RCY_{HPLC} of [^{18}F]**2.18** significantly (Table 2.11, entries 5 and 6). $Pd(OAc)_2$ had proven effective so far, however we preferred to use a neutral catalyst that was more soluble in 1,4-dioxane. This would render possible translation to automated platforms in future studies more facile, as these require any reagents to be transferred in solution. We ultimately found that [^{18}F]**2.18** could be obtained in the same RCY_{HPLC} with Pd_2dba_3 as $Pd(OAc)_2$ with a minor reoptimisation of the reaction temperature to 130 °C (Table 2.11, entry 7). The lowest loading of Pd catalyst was carried forward, as this would render its removal from the desired product during purification more facile. This is an important consideration in the development of PET radiochemistry, as concentrations of residual transition metals in pharmaceutical products to be used in humans must be below thresholds set out in (inter)national pharmacopeia guidelines.[107]

This gave us an optimised set of conditions that could next be applied to a scope of aryl boronic acids. In combination with reagent [^{18}F]**2.58**, 10 M aqueous KOH solution would be used as a base. A Pd_2dba_3/Xantphos catalyst system would be used. HQ would be added as an additive, albeit in reduced quantity to suppress the formation of side product [^{18}F]**2.85**. The optimal reaction solvent was found to be 1,4-dioxane. It was observed that the volume of this solvent affected the consumption of [^{18}F]**2.58**. A similar observation was made for

reaction temperature. As it was found to have a significant effect on the RCY_{HPLC} of [^{18}F]**2.18**, this parameter should be carefully evaluated for other substrates.



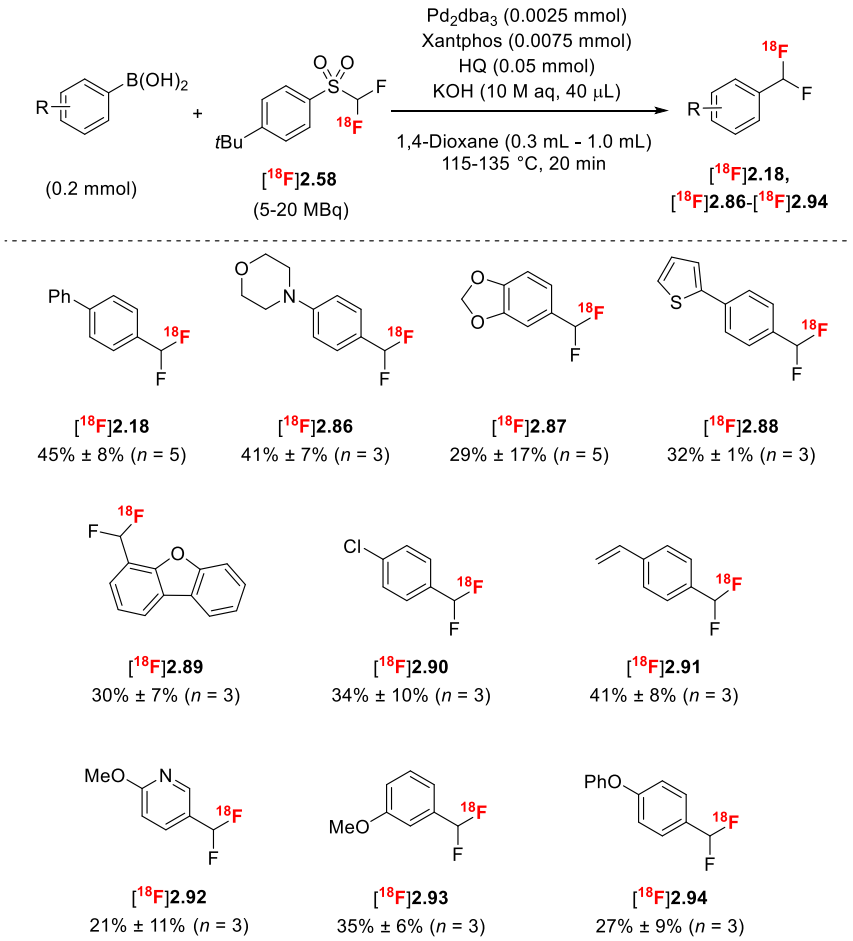
Entry	[Pd] source	Loading of [Pd]	RCY_{HPLC} of [^{18}F]2.18
1	$Pd(OAc)_2$	0.01 mmol	45% ± 10% (*n* = 3)
2	$Pd(PPh_3)_2Cl_2$	0.01 mmol	12%
3	Pd_2dba_3	0.005 mmol	34%
4	Xantphos Pd G3	0.01 mmol	4%
5	$Pd(OAc)_2$	0.02 mmol	31%
6	$Pd(OAc)_2$	0.005 mmol	36%
7[a]	Pd_2dba_3	0.0025 mmol	45% ± 8% (*n* = 5)

Table 2.11. *Optimisation of Pd additive identity and loading for the Pd-catalysed ^{18}F-difluoromethylation of* ***2.17*** *with [^{18}F]**2.58**. RCY_{HPLC} determined by radio-HPLC analysis of the crude reaction mixture. [a]Reaction temperature = 130 °C.*

2.2.3.3. Scope of the Pd-Mediated ^{18}F-Difluoromethylation

With optimised conditions in hand we next proceeded to assess the generality and scope of the Pd-mediated ^{18}F-difluoromethylation of aryl boronic acids. In each case, the effect of reaction temperature (and solvent volume, where appropriate) was first assessed to obtain a set of optimal conditions, which were used for the scope entry. These were found to be substrate dependent and a range of temperatures (115 °C–135°C) and solvent volumes (0.3 mL–1.0 mL) were used in the experiments described in this section. Full details of the conditions used for each substrate are available in the Experimental section (Chapter 4).

Numerous small molecule (hetero)aryl boronic acids, featuring various functional groups, were first considered and subjected to our ^{18}F-difluoromethylation conditions (Scheme 2.46).



***Scheme 2.46**. Small molecule scope of the Pd-catalysed ^{18}F-difluoromethylation with [^{18}F]**2.58**. Yields are RCY$_{HPLC}$ values determined by radio-HPLC analysis of the crude reaction mixture.*

Products featuring medicinally relevant heterocycles, such as [^{18}F]**2.86** bearing a morpholine, [^{18}F]**2.87** featuring a 1,3-dioxolane, [^{18}F]**2.88** that was substituted with a thiophene and dibenzofuran-derived [^{18}F]**2.89**, were obtained in up to 41 %, 31 %, 45 % and 30 % RCY$_{HPLC}$, respectively. Functional groups that could display competing reactivity, such as aryl chloride [^{18}F]**2.90**, which could undergo competing C–Cl oxidative addition in the presence of Pd^0, and alkene [^{18}F]**2.91**, which may undergo ^{18}F-difluorocyclopropanation with [^{18}F]DFC, were well tolerated and prepared in 34% and 41% RCY$_{HPLC}$, respectively. In both cases, no such side-reactivity was observed. (6-Methoxypyridin-3-yl)-boronic acid underwent site-selective ^{18}F-difluoromethylation at the 3-position in up to 27% RCY$_{HPLC}$ ([^{18}F]**2.92**). This reactivity complemented the Minisci-type ^{18}F-difluoromethylation disclosed by Lemaire, Luxen,

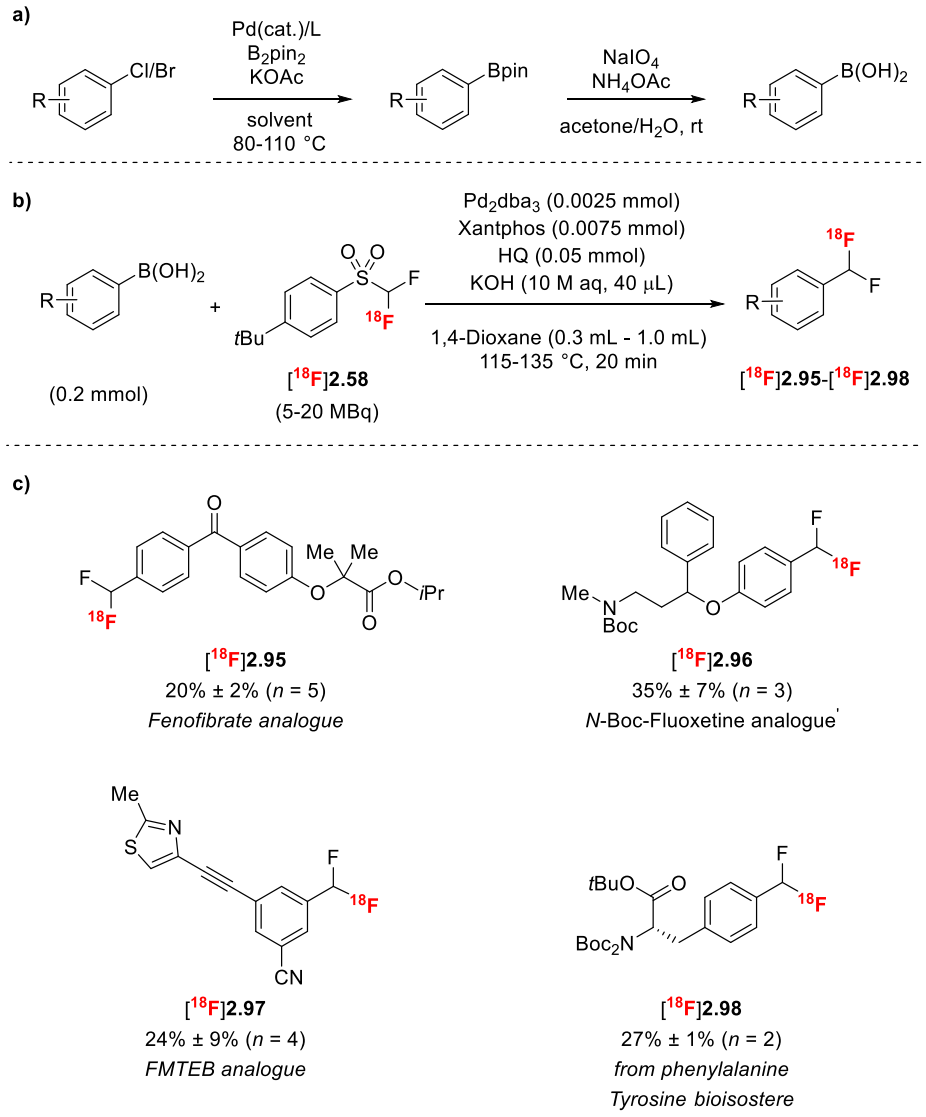
Genicot and co-workers, which, as a radical addition, favoured the activated 2- and 4-positions.[88] In contrast, the regioselectivity of our system was driven by the site at which the boronic acid group was substituted. The reaction operated well on electron rich and neutral substrates. The presence of methoxy and phenoxy groups, for example, was well tolerated, with [^{18}F]**2.93** and [^{18}F]**2.94** obtained in 35% and 27% RCY_{HPLC}, respectively.

Aryl boronic acids derived from biorelevant molecules were next prepared for evaluation as substrates for the Pd-mediated ^{18}F-difluoromethylation (Scheme 2.47 a). These included derivatives of pharmaceuticals and PET radiotracers. This was achieved in a two-step sequence from aryl halide precursors, in which a first-step Miyaura borylation yielded an aryl pinacol boronic ester,[108] followed by oxidative cleavage with $NaIO_4$ to furnish the aryl boronic acid.[109] Further details relating to the synthesis of these molecules is available in Chapter 4.

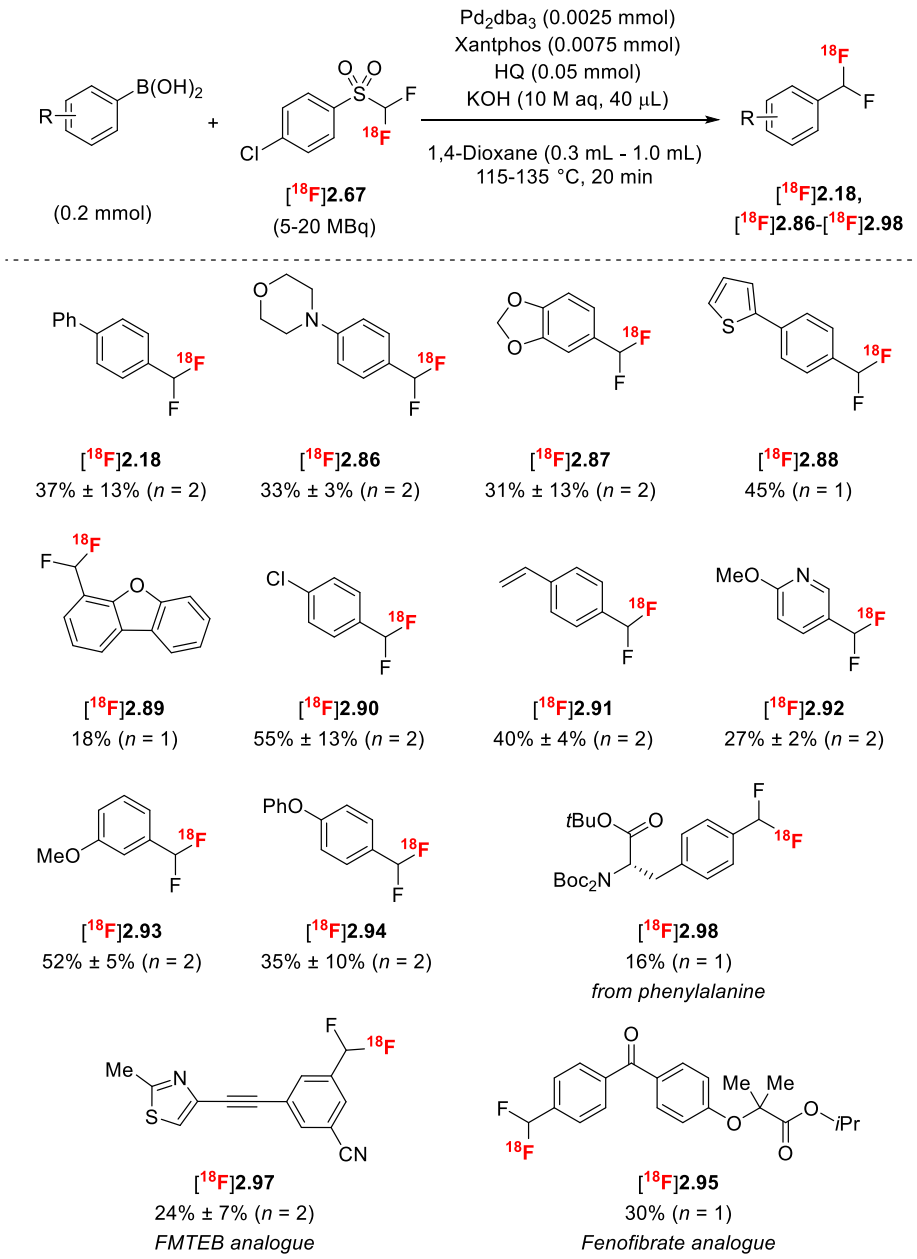
These aryl boronic acids were next subjected to the optimised conditions for the Pd-mediated ^{18}F-difluoromethylation with [^{18}F]**2.58** (Scheme 2.47 b, c). A ^{18}F-difluoromethylated derivative of the hypolipidemic agent fenofibrate ([^{18}F]**2.95**) was available in 20% RCY_{HPLC}. An *N*-Boc protected boronic acid derivative of the antidepressant fluoxetine ([^{18}F]**2.96**) was successfully prepared in 35% RCY_{HPLC}. A ^{18}F-difluoromethylated analogue of the PET radiotracer FMTEB ([^{18}F]**2.97**) was achieved in 24% RCY_{HPLC}. Finally, a phenylalanine derivative and bioisostere of the amino acid tyrosine ([^{18}F]**2.98**) was prepared in 27% RCY_{HPLC}

As described in section 2.2.1, structural optimisation of the *tert*-butyl substituted [^{18}F]DFC reagent [^{18}F]**2.58** was achieved with the discovery of chloro-substituted [^{18}F]**2.67** that was available in higher A_m and also was shown to be more reactive as an [^{18}F]DFC reagent in the ^{18}F-difluoromethylation of (thio)phenols and *N*-heterocycles. We next looked to assess how [^{18}F]**2.67** compared with [^{18}F]**2.58** in the Pd-mediated ^{18}F-difluoromethylation of aryl boronic acids (Scheme 2.48). [^{18}F]**2.67** proved similarly effective to [^{18}F]**2.58**, with ^{18}F-difluoromethylated products being obtained in up to 55% RCY_{HPLC} (Scheme 2.48). In general,

reactions using [^{18}F]**2.67** as a reagent operated optimally at lower reaction temperatures, such as 120 °C instead of 125 °C for [^{18}F]**2.93** and 120 °C instead of 130 °C for [^{18}F]**2.92**. This is in line with higher reactivity expected for this reagent, observed in our studies (section 2.2.1) and by Hu and co-workers.[58] However, due to the complex nature of the reaction, the increased reactivity of [^{18}F]**2.67** as a [^{18}F]DFC precursor did not necessarily correlate with higher RCY_{HPLC} for all substrates.



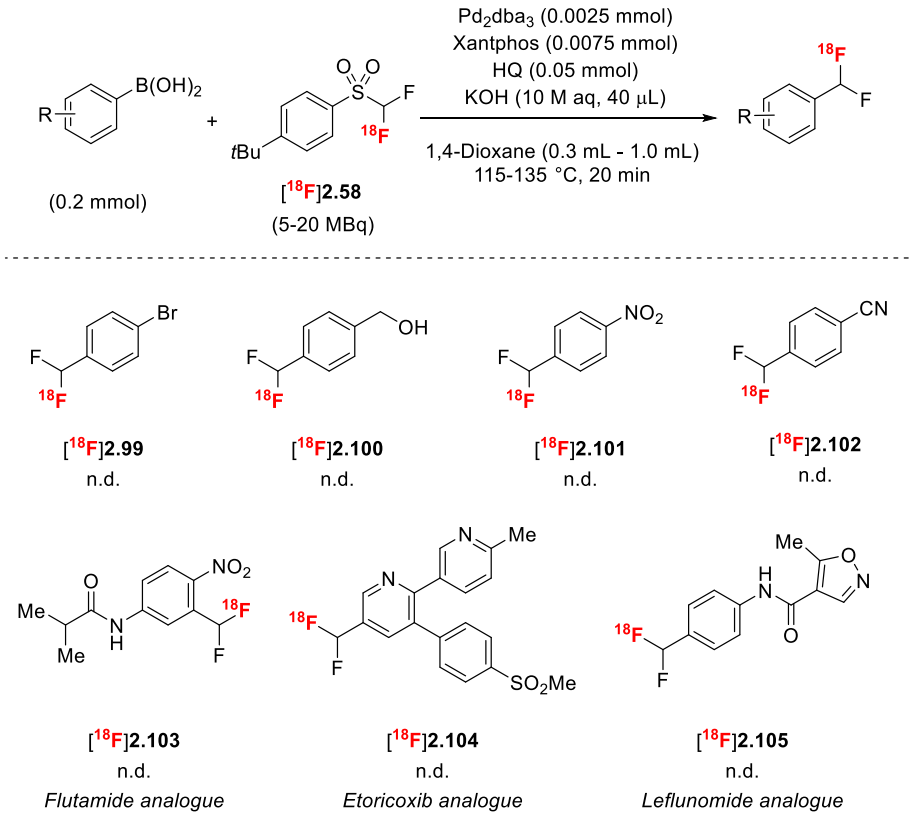
***Scheme 2.47**. Bioactive molecule scope of the Pd-catalysed ^{18}F-difluoromethylation with [^{18}F]**2.58**. Yields are RCY_{HPLC} values determined by radio-HPLC analysis of the crude reaction mixture.*



***Scheme 2.48**. Scope of the Pd-catalysed ^{18}F-difluoromethylation with [^{18}F]**2.67**. Yields are RCY$_{HPLC}$ values determined by radio-HPLC analysis of the crude reaction mixture.*

During our investigation of the scope of this reaction with reagent [^{18}F]**2.58**, several unsuccessful substrates were identified (Scheme 2.49). For these substrates, only traces or no RCY$_{HPLC}$ was observed under the standard reaction conditions. Substrates bearing reactive groups such as Pd-reactive bromide [^{18}F]**2.99** or competing nucleophilic groups (e.g. [^{18}F]**2.100**) were not amenable to ^{18}F-difluoromethylation. Substrates bearing electron-withdrawing groups or otherwise electron deficient substrates did not perform well in the reaction (e.g. [^{18}F]**2.101**, [^{18}F]**2.102**, [^{18}F]**2.103**, [^{18}F]**2.104**). In the case of 4-cyano substituted

[^{18}F]**2.102**, this was obtained in low and irreproducible RCY_{HPLC} and thus was excluded from our scope study. Groups that could be deprotonated under the reaction conditions also proved problematic, such as secondary amides (e.g. [^{18}F]**2.103**, [^{18}F]**2.105**).



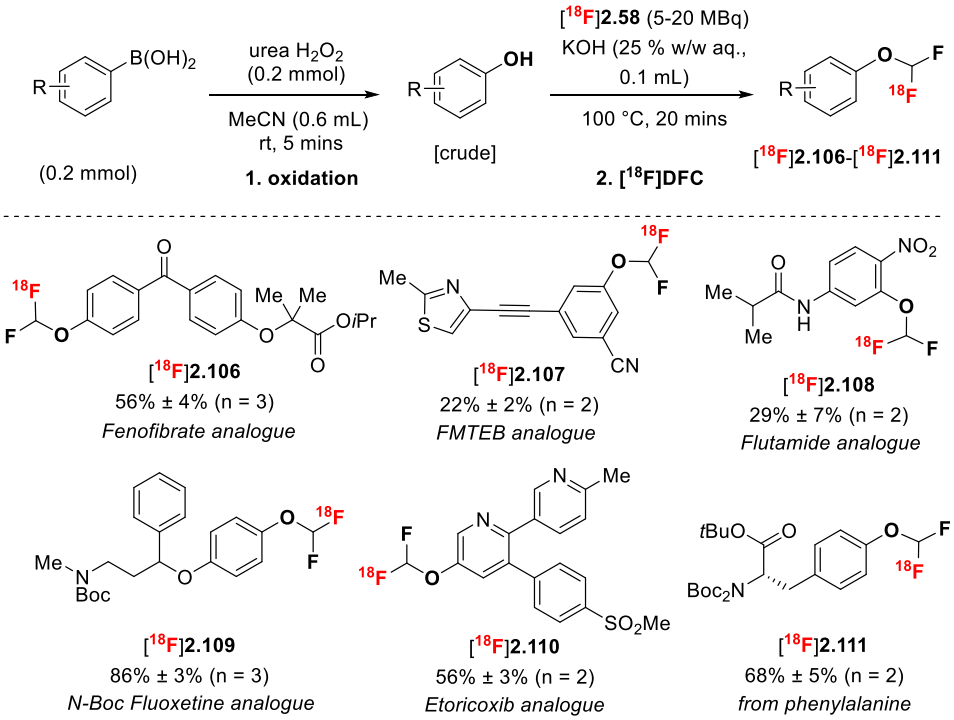
***Scheme 2.49**. Unsuccessful scope molecule examples for the Pd-catalysed ^{18}F-difluoromethylation with [^{18}F]**2.58**. n.d. = not determined.*

Finally, as this method requires a Pd additive and $RuCl_3$ hydrate is used in the radiosynthesis of [^{18}F]**2.58** and [^{18}F]**2.67**, it is important to determine whether these transition metal additives can be suitably purified from the radiolabelled products. In order to be usable for human PET imaging applications, the residual concentration of transition metals must fall below certain thresholds.[107] To investigate this, a sample of [^{18}F]**2.18** was purified by semi-preparative reverse-phase HPLC, and the collected product was analysed for the concentration of residual Ru and Pd. The amount of residual ^{101}Ru and ^{105}Pd were found to be 242.18 µg/L and 18.53 µg/L by ICP-MS analysis. Both of these values fall below the maximum thresholds allowed by the ICH Q3D(R2) guidelines for in-human injection, suggesting the use

of transition-metal additives does not preclude the use of this method for the preparation of PET radiotracers. [107]

2.2.3.4. Two-step, One-pot ^{18}F-Difluoromethoxylation of Aryl Boronic Acids

In addition to their transmetallation reactivity with Pd^{II} complexes, aryl boron reagents are also easily oxidised to phenols.[110] Given that [^{18}F]DFC can also be engaged in the ^{18}F-difluoromethylation of phenols, aryl boron precursors could therefore enable access to ^{18}F-difluoromethoxylated products if subjected to a two-step oxidation-^{18}F-difluoromethylation sequence. [50] The proof-of-concept for such a protocol was established by Dr J. Sap using model boronic acid **2.17**. Given the array of complex molecule aryl boronic acids we had in hand, we were interested to extend the scope of this ^{18}F-difluoromethoxylation protocol to derivatives of bioactive molecules and radiotracers. Such an approach is also synthetically convenient. As aryl borons can be easily prepared in catalytic processes from aryl halides or *via* C–H borylation, this allows for convenient access to an [^{18}F]OCF_2H product where a phenol is not already in place.[50] Efficient ^{18}F-difluoromethylation was observed of various crude phenols derived from complex molecules, which were rapidly obtained from the relevant aryl boronic acid after 5 minutes using solid urea hydrogen peroxide as an oxidant (Scheme 2.50). This included [^{18}F]OCF_2H analogues of fenofibrate ([^{18}F]**2.106**), the PET tracer FMTEB ([^{18}F]**2.107**) and the antiandrogen flutamide ([^{18}F]**2.108**). A Boc-protected boronic acid derivative of fluoxetine was an excellent substrate and was ^{18}F-difluoromethylated in 86% RCY_{HPLC} ([^{18}F]**2.109**). Finally, ^{18}F-difluoromethoxylated analogues of COX-2 inhibitor etoricoxib ([^{18}F]**2.110**) and a protected phenylalanine ([^{18}F]**2.111**) were prepared in up to 68% RCY_{HPLC}. In general, this method demonstrates the applicability of our *O*-^{18}F-difluoromethylation platform with [^{18}F]DFC beyond phenolic substrates, extending it to aryl boron reagents and beyond, as these are readily obtained from numerous substrate classes.

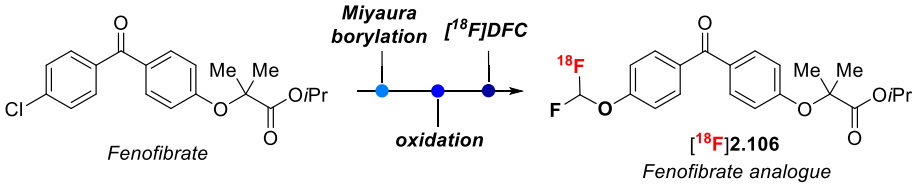


***Scheme 2.50**. Bioactive molecule scope two-step, one-pot ^{18}F-difluoromethoxylation with [^{18}F]**2.58**. Yields are RCY$_{HPLC}$ values determined by radio-HPLC analysis of the crude reaction mixture.*

Finally, we aimed to determine whether this protocol could be extended to a three-step ^{18}F-difluoromethoxylation of aryl halides, where a crude aryl-Bpin is first obtained in a Miyaura borylation of an aryl chloride, followed by the protocol developed above. An analogous reaction has been developed by Scott, Sanford and co-workers, where a crude aryl-Bpin is first prepared *via* Ir-catalysed C–H borylation, and then subjected to Cu-mediated radiofluorination to obtain the ^{18}F-fluoroarene.[111] The bioactive molecule fenofibrate was taken as a model substrate for this transformation as it features an aryl chloride. Firstly, it was subjected to a Miyaura borylation with a Pd_2dba_3/XPhos catalyst system, B_2pin_2 and KOAc. The loading of B_2pin_2 was reduced as 3 equivalents were not required to obtain the aryl Bpin in high yield and an excess boron-containing species may reduce the concentration of hydroxide, which may be detrimental for the activation of [^{18}F]**2.58** (Table 2.11, entries 1-2).

We also observed that passing this crude mixture through a syringe filter before being subjected to oxidation with urea hydrogen peroxide was productive and [^{18}F]**2.106** formed in low RCY$_{HPLC}$. We found that a reaction time of 5 minutes remained sufficient for the oxidation

step (Table 2.11, entries 3 and 5). The volume of 25% w/w aqueous KOH solution was also varied; increasing the volume of base was productive, perhaps due to the presence of boron impurities (Table 2.11, entries 3 and 4). This reaction proved challenging to develop and the highest RCY_{HPLC} of [^{18}F]**2.106** obtained was 14%, relative to 56% for the two-step protocol from the aryl boronic acid (Table 2.12, entry 7).



Fenofibrate *Fenofibrate analogue*

Entry	B_2pin_2 loading	Volume of KOH solution	$t_{oxidation}$	Filtered after borylation?	RCY_{HPLC} of [^{18}F]2.106
1	3 equiv.	100 µL	5 mins	N	n.d.
2	1 equiv.	100 µL	5 mins	N	n.d.
3	1 equiv.	100 µL	5 mins	Y	3 %
4	1 equiv.	200 µL	5 mins	Y	10 %
5	1 equiv.	100 µL	60 mins	Y	3 %
6[a]	1 equiv.	200 µL	5 mins	Y	10 %
7[a]	1 equiv.	150 µL	5 mins	Y	14 %

Table 2.12. *Optimisation data for the three step sequential borylation-oxidation-^{18}F-difluoromethylation of fenofibrate with [^{18}F]**2.58**. RCY_{HPLC} determined by radio-HPLC analysis of the crude reaction mixture. [a]Reagent [^{18}F]**2.67** was used. n.d. = not detected.*

2.3. Conclusion and Outlook

This chapter has disclosed several advances in the area of ^{18}F-difluoromethylation, which is an emerging radiosynthetic strategy for the preparation of compounds containing [^{18}F]CF_2H or [^{18}F]CF_2R groups. This work has focused on the application of [^{18}F]DFC as a reactive intermediate for late-stage ^{18}F-difluoromethylation of various precursor classes that are commonly used in pharmaceutical discovery.

The first part of this chapter demonstrates that ^{18}F-difluoromethyl aryl sulfones can be prepared in high A_m (131 GBq/μmol) when the 4-position of the arene is substituted with chlorine ([^{18}F]**2.67**), which we suggest minimises leaching of ^{19}F-fluoride that results in isotopic dilution based on a ^{19}F NMR study. This represents a substantial improvement from the moderate A_m of first-generation reagent [^{18}F]**2.58.** The automated radiosynthesis was reoptimised to deliver [^{18}F]**2.67** in higher AY, which is crucial for practitioners seeking to apply this methodology. Improvements in RCY of ^{18}F-difluoromethylated products in line with the higher reactivity of [^{18}F]**2.67** were also demonstrated. This work therefore represents the first radiosynthesis of a [^{18}F]DFC reagent with properties that are highly desirable for end-users. Further investigation in this area could entail examination of the effect of further (hetero)aromatic scaffolds, as this study has demonstrated the impact of structural modifications on A_m and reactivity. The use of different S(VI) hubs, such as sulfoximines, could also be considered. The effect of additives, such as organic bases and/or elution reagents used in the preparation of reactive [^{18}F]fluoride, is a further aspect for future investigation, and these could be leveraged to deliver further improvements in AY or A_m. Finally, the application of alternative radiolabelling precursors is another important consideration for future work, especially due to the recent reduced commercial availability of dibromofluoromethane used to prepare the bromofluoromethyl aryl sulfide radiolabelling substrates.

In the second part of this chapter, [^{18}F]DFC radiochemistry was extended to the preparation of a radiotracer that was used in PET imaging experiments for the first time. A process for the preparation of a ^{18}F-difluoromethylated analogue ([^{18}F]**2.81**) of existing TSPO radiotracer DPA-714 ([^{18}F]**2.80**) was designed, resulting in the development of a semi-automated radiosynthesis that delivered [^{18}F]**2.81** in sufficient activity yield and A_m for a preliminary PET imaging and *in vivo* radiometabolite study. This proof-of-concept work acts as a demonstration to end-users that [^{18}F]DFC radiochemistry can deliver radiotracers suitable for

preclinical work, which should inspire its uptake by the community to access this unexplored radiochemical space. PET imaging experiments indicated that [^{18}F]**2.81** was a suitable radiotracer for TSPO and may have advantages over existing tracer [^{18}F]**2.80**, such as improved metabolic stability. In future work, further data should be collected to test the hypothesis that [^{18}F]**2.81** is an improved TSPO radiotracer, as well as probing the effect of ^{18}F-difluoromethylation on other PET radiotracers. Furthermore, improved protocols (including full automation) for the radiosynthesis of [^{18}F]**2.81** would further extend the value of the work presented herein to radiochemistry practitioners, and this is actively under consideration for future work.

In the final part of this chapter, the development of a novel Pd-mediated ^{18}F-difluoromethylation of (hetero)aryl boronic acids using [^{18}F]**2.58** and [^{18}F]**2.67** was disclosed. This represented the most complex extension of the reactivity of [^{18}F]DFC to date and enabled access to high-value ^{18}F-difluoromethyl arenes using this platform for the first time. In preliminary studies, proof-of-concept data was secured, demonstrating that difluoromethyl aryl sulfones were amenable to Pd-catalysed DFC cross-couplings. The translation of this reactivity to ^{18}F-radiochemistry was successful, with the identity and loading of the base, reaction temperature and concentration requiring significant optimisation. The ability of the method to access ^{18}F-difluoromethylarenes from the relevant boronic acid was demonstrated, with 14 examples, including heteroarenes and derivatives of bioactive molecules and PET radiotracers. The same (hetero)aryl boronic acid substrates could also be engaged in a one-pot, two-step ^{18}F-difluoromethoxylation, which was demonstrated on a further 6 examples. Attempts were also made to extend this protocol to aryl halides and arenes using well-established catalytic borylation protocols, however this was limited to a single example in 14% RCY. Future work could look to further optimise these conditions to deliver ^{18}F-difluoromethoxyarenes in higher RCY from arenes and aryl halides. Demonstration of the application of the Pd-mediated ^{18}F-difluoromethylation of boronic acids to the

preparation of a preclinical PET radiotracer should also be considered, to highlight the value of the method to practitioners.

The work disclosed in this chapter provides an extension of [^{18}F]DFC radiochemistry, in the optimisation of the properties of the [^{18}F]DFC reagents, its first application to PET imaging and the discovery of novel ^{18}F-radiochemistry to expand the accessible radiochemical space. We anticipate these further developments should result in increased interest in [^{18}F]DFC radiochemistry from the community and encourage its uptake by practitioners in the preparation of ^{18}F-difluoromethylated radiotracers.

2.4. References

1 O'Hagan, D. Understanding organofluorine chemistry. An introduction to the C–F bond. *Chem. Soc. Rev.* **2008**, *37* (2), 308–319.

2 Sap, J. B. I.; Meyer, C. F.; Straathof, N. J. W.; Iwumene, N.; am Ende, C. W.; Trabanco, A. A.; Gouverneur, V. Late-stage difluoromethylation: concepts, developments and perspective. *Chem*. *Soc*. *Rev*. **2021**, *50*, 8214–8247.

3 Purser, S.; Moore, P. R.; Swallow, S.; Gouverneur, V. Fluorine in medicinal chemistry. *Chem*. *Soc*. *Rev*. **2008**, *37* (2), 320–330.

4 Inoue, M.; Sumii, Y.; Shibata, N. Contribution of Organofluorine Compounds to Pharmaceuticals. *ACS Omega* **2020**, *5* (19), 10633–10640.

5 Ogawa, Y.; Tokunaga, E.; Kobayashi, O.; Hirai, K.; Shibata, N. Current Contributions of Organofluorine Compounds to the Agrochemical Industry. *iScience* **2020**, *23* (9), 101467.

6 Shin, J. M.; Cho, Y. M.; Sachs, G. Chemistry of Covalent Inhibition of the Gastric (H^+, K^+)-ATPase by Proton Pump Inhibitors. *J. Am*. *Chem*. *Soc*. **2004**, *126* (25), 7800–7811.

7 Erickson, J. A.; McLoughlin, J. I. Hydrogen Bond Donor Properties of the Difluoromethyl Group *J*. *Org*. *Chem*. **1995**, *60* (6), 1626–1631.

8 Sessler, C. D.; Rahm, M.; Becker, S.; Goldberg, J. M.; Wang, F.; Lippard, S. CF_2H, a Hydrogen Bond Donor. J. *J. Am. Chem. Soc.* **2017**, *139* (27), 9325–9332.

9 Malquin, N.; Rahgoshay, K.; Lensen, N.; Chaume, G.; Miclet, E.; Brigaud, T. CF_2H as a hydrogen bond donor group for the fine tuning of peptide bond geometry with difluoromethylated pseudoprolines. *Chem*. *Commun*. **2019**, *55* (83), 12487–12490.

10 Bhal, S. K.; Kassam, K.; Peirson, I. G.; Pearl, G. M. The Rule of Five Revisited: Applying Log D in Place of Log P in Drug-Likeness Filters. *Mol*. *Pharmaceutics* **2007**, *4* (4), 556–560.

11 Zafrani, Y.; Sod-Moriah, G.; Yeffet, D.; Berliner, A.; Amir, D.; Marciano, D.; Elias, S.; Katalan, S.; Ashkenazi, N.; Madmon, M.; Gershonov, E.; Saphier, S. CF_2H, a Functional Group-Dependent Hydrogen-Bond Donor: Is It a More or Less Lipophilic Bioisostere of OH, SH, and CH_3? *J*. *Med*. *Chem*. **2019**, *62* (11), 5628–5637.

12 Xing, L.; Blakemore, D. C.; Narayanan, A.; Unwalla, R.; Lovering, F.; Denny, R. A.; Zhou, H.; Bunnage, M. E. Fluorine in Drug Design: A Case Study with Fluoroanisoles. *ChemMedChem* **2015**, *10* (4), 715–726.

13 Huchet, Q. A.; Kuhn, B.; Wagner, B.; Kratochwil, N. A.; Fischer, H.; Kansy, M.; Zimmerli, D.; Carreira, E. M.; Müller, K. Fluorination Patterning: A Study of Structural Motifs That Impact Physicochemical Properties of Relevance to Drug Discovery. *J. Med. Chem.* **2015**, *58* (22), 9041–9060.
14 Zafrani, Y.; Saphier, S.; Gershonov, E. Utilizing the CF_2H moiety as a H-bond-donating group in drug discovery. *Future Med. Chem.* **2020**, *12* (5), 361–365.
15 Meanwell, N. A. Applications of Bioisosteres in the Design of Biologically Active Compounds. *J. Agric. Food Chem.* **2023**, *71* (47), 18087–18122.
16 Wang, L.; Wei, J.; Wu, R.; Cheng, G.; Li, X.; Hu, J.; Hu, Y.; Sheng, R. The stability and reactivity of tri-, di-, and monofluoromethyl/methoxy/methylthio groups on arenes under acidic and basic conditions. *Org. Chem. Front.* **2017**, *4* (2), 214–223.
17 Brand, S.; Norcross, N. R.; Thompson, S.; Harrison, J. R.; Smith, V. C.; Robinson, D. A.; Torrie, L. S.; McElroy, S. P.; Hallyburton, I.; Norval, S.; Scullion, P.; Stojanovski, L.; Simeons, F. R. C.; van Aalten, D.; Frearson, J. A.; Brenk, R.; Fairlamb, A. H.; Ferguson, M. A. J.; Wyatt, P. G.; Gilbert, I. H.; Read, K. D. Lead Optimization of a Pyrazole Sulfonamide Series of Trypanosoma brucei*N*-Myristoyltransferase Inhibitors: Identification and Evaluation of CNS Penetrant Compounds as Potential Treatments for Stage 2 Human African Trypanosomiasis. *J. Med. Chem.* **2014**, *57* (23), 9855–9869.
18 Ghosh, K. K.; Padmanabhan, P.; Yang, C.-T.; Mishra, S.; Halldin, C.; Gulyás, B. Dealing with PET radiometabolites. *EJNMMI* Res. **2020**, *10* (1), 109.
19 Shetty, H. U.; Zoghbi, S. S.; Siméon, F. G.; Liow, J.-S.; Brown, A. K.; Kannan, P.; Innis, R. B.; Pike, V. W. Radiodefluorination of 3-Fluoro-5-(2-(2-[^{18}F](fluoromethyl)-thiazol-4-yl)ethynyl) benzonitrile ([^{18}F]SP203), a Radioligand for Imaging Brain Metabotropic Glutamate Subtype-5 Receptors with Positron Emission Tomography, Occurs by Glutathionylation in Rat Brain. *J. Pharmacol. Exp. Ther.* **2008**, *327* (3), 727–735.
20 Terry, G. E.; Hirvonen, J.; Liow, J.-S.; Zoghbi, S. S.; Gladding, R.; Tauscher, J. T.; Schaus, J. M.; Phebus, L.; Felder, C. C.; Morse, C. L.; Donohue, S. R.; Pike, V. W.; Halldin, C.; Innis, R. B. Imaging and Quantitation of Cannabinoid CB1 Receptors in Human and Monkey Brains Using ^{18}F-Labeled Inverse Agonist Radioligands. *J. Nucl. Med.* **2010**, *51* (1), 112–120.
21 Osman, S.; Lundkvist, C.; Pike, V. W.; Halldin, C.; McCarron, J. A.; Swahn, C. G.; Farde, L.; Ginovart, N.; Luthra, S. K.; Gunn, R. N.; Bench, C. J.; Sargent, P. A.; Grasby, P. M. Characterisation of the appearance of radioactive metabolites in monkey and human plasma from the 5-HT1A receptor radioligand, [carbonyl-^{11}C]WAY-100635-explanation of high signal contrast in PET and an aid to biomathematical modelling. *Nucl. Med. Biol.* **1998**, *25* (3), 215–223.
22 Singh, R. P.; Shreeve, J. M. Recent Advances in Nucleophilic Fluorination Reactions of Organic Compounds Using Deoxofluor and DAST. *Synthesis* **2002**, *2002* (17): 2561–2578.
23 Yan, G. Photochemical and Electrochemical Strategies for Hydrodefluorination of Fluorinated Organic Compounds. *Chem. Eur. J.* **2022**, *28* (29), e202200231.
24 Fier, P. S.; Hartwig, J. F. Copper-Mediated Difluoromethylation of Aryl and Vinyl Iodides. *J. Am. Chem. Soc.* **2012**, *134* (12), 5524–5527.
25 Prakash, G. K. S.; Ganesh, S. K.; Jones, J.-P.; Kulkarni, A.; Masood, K.; Swabeck, J. K.; Olah, G. A. Copper-Mediated Difluoromethylation of (Hetero)aryl Iodides and β-Styryl Halides with Tributyl(difluoromethyl)stannane *Angew. Chem. Int. Ed.* **2012**, *51* (48), 12090–12094.
26 Gu, Y.; Leng, X.; Shen, Q. Cooperative dual palladium/silver catalyst for direct difluoromethylation of aryl bromides and iodides. *Nat. Commun.* **2014**, *5*, 5405.

27 Ferguson, D. M.; Malapit, C. A.; Bour, J. R.; Sanford, M. S. Palladium-Catalyzed Difluoromethylation of Aryl Chlorides and Bromides with $TMSCF_2H$. *J. Org. Chem.* **2019**, *84* (6), 3735–3740.
28 Xu, L.; Vicic, D. A. Direct Difluoromethylation of Aryl Halides *via* Base Metal Catalysis at Room Temperature. *J. Am. Chem. Soc.* **2016**, *138* (8), 2536–2539.
29 Pan, F.; Boursalian, G. B.; Ritter, T. Palladium-Catalyzed Decarbonylative Difluoromethylation of Acid Chlorides at Room Temperature. *Angew. Chem. Int. Ed.* **2018**, *57* (51), 16871–16876.
30 Zhao, Y.; Huang, W.; Zheng, J.; Hu, J. Efficient and Direct Nucleophilic Difluoromethylation of Carbonyl Compounds and Imines with Me_3SiCF_2H at Ambient or Low Temperature. *Org. Lett.* **2011**, *13* (19), 5342–5345.
31 Duan, M.; Shao, Q.; Zhou, Q.; Baran, P. S.; Houk, K. N. Why $\bullet CF_2H$ is nucleophilic but $\bullet CF_3$ is electrophilic in reactions with heterocycles. *Nat. Commun.* **2024**, *15*, 4630.
32 Fujiwara, Y. Dixon, J. A.; Rodriguez, R. A.; Baxter, R. D.; Dixon, D. D.; Collins, M. R.; Blackmond, D. G.; Baran, P. S. A New Reagent for Direct Difluoromethylation. *J. Am. Chem. Soc.* **2012**, *134* (3), 1494–1497.
33 Tung, T. T.; Christensen, S. B.; Nielsen, J. Difluoroacetic Acid as a New Reagent for Direct C–H Difluoromethylation of Heteroaromatic Compounds. *Chem. Eur. J.* **2017**, *23* (72), 18125–18128.
34 Sakamoto, R.; Kashiwagi, H.; Maruoka, K. The Direct C–H Difluoromethylation of Heteroarenes Based on the Photolysis of Hypervalent Iodine(III) Reagents That Contain Difluoroacetoxy Ligands. *Org. Lett.* **2017**, *19* (19), 5126–5129.
35 Sun, A. C.; McClain, E. J.; Beatty, J. W.; Stephenson, C. R. J. Visible Light-Mediated Decarboxylative Alkylation of Pharmaceutically Relevant Heterocycles. *Org. Lett.* **2018**, *20* (12), 3487–3490.
36 Tang, X.-J. Zhang, Z.; Dolbier Jr., W. R. Direct Photoredox-Catalyzed Reductive Difluoromethylation of Electron-Deficient Alkenes. *Chem. Eur. J.* **2015**, *21* (52), 18961–18965.
37 Lin, Q.-Y.; Xu, X.-H.; Zhang, Ke.; Qing, F. L. Visible-Light-Induced Hydrodifluoromethylation of Alkenes with a Bromodifluoromethylphosphonium Bromide. *Angew. Chem. Int. Ed.* **2016**, *55* (4), 1479–1483.
38 Meyer, C. F.; Hell, S. M.; Misale, A.; Trabanco, A. A.; Gouverneur, V. Hydrodifluoromethylation of Alkenes with Difluoroacetic Acid. *Angew. Chem. Int. Ed.* **2019**, *58* (26) 8829–8833.
39 Merchant, R. R.; Edwards, J. T.; Qin, T.; Kruszyk, M. M.; Bi, C.; Che, G.; Bao, D.-H.; Qiao, W.; Sun, L.; Collins, M. R.; Fadeyi, O. O.; Gallego, G. M.; Mousseau, J. J.; Nuhant, P.; Baran, P. S. Modular radical cross-coupling with sulfones enables access to sp^3-rich (fluoro)alkylated scaffolds. *Science* **2018**, *360* (6384), 75–80.
40 Miao, W.; Zhao, Y.; Ni, C.; Gao, B.; Zhang, W.; Hu, J. Iron-Catalyzed Difluoromethylation of Arylzincs with Difluoromethyl 2-Pyridyl Sulfone. *J. Am. Chem. Soc.* **2018**, *140* (3), 880–883.
41 Bacauanu, V.; Cardinal, S.; Yamauchi, M.; Kondo, M.; Fernández, D. F.; Remy, R.; MacMillan, D. W. C. Metallaphotoredox Difluoromethylation of Aryl Bromides. *Angew. Chem. Int. Ed.* **2018**, *57* (38), 12543–12548.
42 Xu, C.; Guo, W.-H.; He, X.; Guo, Y.-L.; Zhang, X.-Y.; Zhang, X. Difluoromethylation of (hetero)aryl chlorides with chlorodifluoromethane catalyzed by nickel. *Nat. Commun.* **2018**, *9*, 1170.

43 Du, W.; Luo, Q.; Wei, Z.; Wang, X.; Ni. C.; Hu, J. Switching from 2-pyridination to difluoromethylation: ligand-enabled nickel-catalyzed reductive difluoromethylation of aryl iodides with difluoromethyl 2-pyridyl sulfone. Sci. China Chem. **2023**, *66*, 2785–2790.
44 Prakash, G. K. S.; Zhang, Z.; Wang, F.; Ni, C.; Olah, G. A. *N*,*N*-Dimethyl-*S*-difluoromethyl-S-phenylsulfoximinium tetrafluoroborate: A versatile electrophilic difluoromethylating reagent. *J*. *Fluorine Chem*. **2011**, *132* (10), 792–798.
45 Zhu, J.; Liu, Y.; Shen, Q. Direct Difluoromethylation of Alcohols with an Electrophilic Difluoromethylated Sulfonium Ylide. *Angew*. *Chem*. *Int*. *Ed*. **2016**, *55* (31), 9050–9054.
46 Ni, C.; Hu, J. Recent Advances in the Synthetic Application of Difluorocarbene. *Synthesis* **2014**, 46 (7), 842–863.
47 Brahms, D. L. S.; Dailey, W. P. Fluorinated Carbenes. *Chem*. *Rev*. **1996**, *96* (5), 1585–1632.
48 Hine, J.; Porter, J. J. Methylene Derivatives as Intermediates in Polar Reactions. VIII. Difluoromethylene in the Reaction of Chlorodifluoromethane with Sodium Methoxide. *J*. *Am*. *Chem*. *Soc*. **1957**, *79* (20), 5493–5496.
49 Hine, J.; Porter, J. J. The formation of difluoromethylene from difluoromethyl phenyl sulfone and sodium methoxide. *J*. *Am*. *Chem*. *Soc*. **1960**, *82* (23), 6178–6181.
50 Fier, P. S.; Hartwig, J. F. Synthesis of Difluoromethyl Ethers with Difluoromethyltriflate. *Angew*. *Chem*. *Int*. *Ed*. **2013**, *52* (7), 2092–2095.
51 Synthesis of gem-Difluorocyclopropa(e)nes and *O*-, *S*-, *N*-, and *P*-Difluoromethylated Compounds with $TMSCF_2Br$. *Angew*. *Chem*. *Int*. *Ed*. **2013**, *52* (47), 12390–12394.
52 Zheng, J.; Li, Y.; Zhang, L.; Hu, J.; Meuzelaarb, G. J.; Federsel, H.-J. Chlorodifluoromethyl phenyl sulfone: a novel non-ozone-depleting substance-based difluorocarbene reagent for *O*- and *N*-difluoromethylations. *Chem*. *Commun*. **2007**, *2007* (48), 5149–5151.
53 Birchall, J. M.; Cross, G. E.; Haszeldine, R. N. Difluorocarbene. *Proc*. *Chem*. Soc. **1960**, 81.
54 Deng, X.-Y.; Lin, J.-H.; Zheng, J.; Xiao, J.-C. Difluoromethylation and gem-difluorocyclopropenation with difluorocarbene generated by decarboxylation. *Chem. Commun.* **2015**, *51* (42), 8805–8808.
55 Zafrani, Y.; Sod-Moriah, G.; Segall, Y. Diethyl bromodifluoromethylphosphonate: a highly efficient and environmentally benign difluorocarbene precursor. *Tetrahedron* **2009**, *65* (27), 5278–5283.
56 Zhang, L.; Zheng, J.; Hu, J. 2-Chloro-2,2-difluoroacetophenone: A Non-ODS-Based Difluorocarbene Precursor and Its Use in the Difluoromethylation of Phenol Derivatives. *J*. *Org*. *Chem*. **2006**, *71* (26), 9845–9848.
57 Ford, J.; Hopkin, B.; Sap, J. B. I.; Gouverneur, V. Mechanochemical difluoromethylation of (thio)phenols and *N*-heterocycles. *Isr*. *J*. *Chem*. **2023**, *63* (10–11), e202300109.
58 Wang, F.; Zhang, L.; Zheng, J.; Hu, J. Chlorodifluoromethyl aryl ketones and sulfones as difluorocarbene reagents: The substituent effect. *J*. *Fluorine Chem*. **2011**, *132* (8), 521–528.
59 Mehta, V. P.; Greaney, M. F. *S*-, *N*-, and *Se*-Difluoromethylation Using Sodium Chlorodifluoroacetate. *Org*. *Lett*. **2013**, *15* (19), 5036–5039.
60 Zhou, W.; Pan, W.-J.; Chen, J.; Zhang, M.; Lin, J.-H.; Cao, W.; Xiao, J. C. Transition-metal difluorocarbene complexes. *Chem*. *Commun*. **2021**, *57* (74), 9316–9329.
61 Feng, Z.; Min, Q.; Zhang, X. Access to difluoromethylated arenes by Pd-catalyzed reaction of arylboronic acids with bromodifluoroacetate. *Org*. *Lett*. **2016**, *18* (1), 44–47.
62 Deng, X.; Lin, J.; Xiao, J. Pd-catalyzed transfer of difluorocarbene. *Org*. *Lett*. **2016**, *18* (17), 4384–4387.
63 Feng, Z.; Min, Q.; Fu, X.; An, L.; Zhang, X. Chlorodifluoromethane-triggered formation of difluoromethylated arenes catalysed by palladium. *Nat*. *Chem*. **2017**, *9* (9), 918–923.

64 Fu, X.; Xue, X.-S.; Zhang, X.-Y.; Xiao, Y.-L.; Zhang, S.; Guo, Y.-L.; Leng, X.; Houk, K. N.; Zhang, X. Controllable catalytic difluorocarbene transfer enables access to diversified fluoroalkylated arenes. *Nat*. *Chem*. **2019**, *11* (10), 948–956.
65 Grushin, V. V.; Marshall, W. Facile Ar−CF_3 Bond Formation at Pd. Strikingly Different Outcomes of Reductive Elimination from [$(Ph_3P)_2Pd(CF_3)Ph$] and [(Xantphos)Pd(CF_3)Ph]. J. *Am*. *Chem*. *Soc*. **2006**, *128* (39), 12644–12645.
66 Brothers, P. J.; Roper, W. R. Transition-metal dihalocarbene complexes. *Chem*. *Rev*. **1988**, *88* (7), 1293–1326.
67 Zhang, X.-Y.; Fu, X.-P.; Zhang, S.; Zhang, X. Palladium Difluorocarbene Involved Catalytic Coupling with Terminal Alkynes. *CCS Chem*. **2020**, *2* (5), 293–304.
68 Zhang, X.-Y.; Sun, S.-P.; Sang, Y.-Q.; Xue, X.-S.; Min, Q.-Q.; Zhang, X. Reductive Catalytic Difluorocarbene Transfer *via* Palladium Catalysis. *Angew*. *Chem*. *Int*. *Ed*. **2023**, *62* (37), e202306501.
69 Zeng, X.; Li, Y.; Min, Q.-Q.; Xue, X.-S.; Zhang, X. Copper-catalysed difluorocarbene transfer enables modular synthesis. *Nat*. *Chem*. **2023**, *15* (8), 1064–1073.
70 Ford, J.; Ortalli, S.; Gouverneur, V. The ^{18}F-Difluoromethyl Group: Challenges, Impact and Outlook. *Angew. Chem. Int. Ed.* **2024**, *63* (26), e202404957.
71 Luurtsema, G.; Pichler, V.; Bongarzone, S.; Seimbille, Y.; Elsinga, P.; Gee, A.; Vercouillie, J. EANM guideline for harmonisation on molar activity or specific activity of radiopharmaceuticals: impact on safety and imaging quality. *EJNMMI Radiopharm. Chem.* **2021**, *6*, 34.
72 Martinez, H.; Rebeyrol, A.; Nelms, T. B.; Dolbier Jr, W. R. Impact of fluorine substituents on the rates of nucleophilic aliphatic substitution and β-elimination. *J*. *Fluorine Chem*. **2012**, *135*, 167–175.
73 Khotavivattana, T.; Verhoog, S.; Tredwell, M.; Pfeifer, L.; Calderwood, S.; Wheelhouse, K.; Collier, T. L.; Gouverneur, V. ^{18}F-Labeling of Aryl-SCF_3, -OCF_3 and -$OCHF_2$ with [^{18}F]Fluoride. *Angew*. *Chem*. *Int*. *Ed*. **2015**, *54* (34), 9991–9995.
74 Verhoog, S.; Pfeifer, L.; Khotavivattana, T.; Calderwood, S.; Collier, T. L.; Wheelhouse, K.; Tredwell, M.; Gouverneur, V. Silver-Mediated ^{18}F-Labeling of Aryl-CF_3 and Aryl-CHF_2 with ^{18}F-Fluoride. *Synlett* **2016**, *27* (1), 25–28.
75 Zhao, Q.; Isenegger, P. G.; Wilson, T. C.; Sap, J. B. I.; Guibbal, F.; Lu, L.; Gouverneur, V.; Shen, Q. Radiosynthesis of [^{18}F]ArylSCF_2H Using Aryl Boronic Acids, *S*-(Chlorofluoromethyl)benzenesulfonothioate and [^{18}F]Fluoride. *CCS Chem*. **2020**, *2* (7), 1921–1928.
76 Shi, H.; Braun, A.; Wang, L.; Liang, S. H.; Vasdev, N.; Ritter, T. Synthesis of ^{18}F-Difluoromethylarenes from Aryl (Pseudo) Halides. *Angew*. *Chem*. *Int*. *Ed*. **2016**, *55* (36), 10786–10790.
77 Ge, S.; Chaładaj, W.; Hartwig, J. F. Pd-Catalyzed α-Arylation of α,α-Difluoroketones with Aryl Bromides and Chlorides. A Route to Difluoromethylarenes. *J. Am. Chem. Soc.* **2014**, *136* (11), 4149–4152.
78 Kost, D.; Aviram, K. The S_N2 Transition State. 6: Breakdown of the Reactivity–Selectivity Principle in the S_N2 Reaction of α-Halocarbonyl Compounds. A Molecular Orbital Analysis. *Isr. J. Chem.* **1985**, *26* (4), 349–353.
79 Bermejo-Gómez, A.; Cortés-González, M. A.; Lübcke, M.; Johansson, M. J.; Halldin, C.; Szabó, K. J.; Schou, M. Efficient DBU accelerated synthesis of ^{18}F-labelled trifluoroacetamides. *Chem*. *Commun*. **2016**, *52* (97), 13963–13966.

80 Khotavivattana, T.; Calderwood, S.; Verhoog, S.; Pfeifer, L.; Preshlock, S.; Vasdev, N.; Collier, T. L.; Gouverneur, V. Synthesis and Reactivity of ^{18}F-Labeled α,α-Difluoro-α-(aryloxy)acetic Acids. *Org*. *Lett*. **2017**, 19 (3), 568–571.
81 Yuan, G.; Wang, F.; Stephenson, N. A.; Wang, L.; Rotstein, B. H.; Vasdev, N.; Tang, P.; Liang, S. H. Metal-free ^{18}F-labeling of aryl-CF_2H *via* nucleophilic radiofluorination and oxidative C–H activation. *Chem*. *Commun*. **2017**, *53* (1), 126–129.
82 Xu, P.; Guo, S.; Wang, L.; Tang, P. Silver-Catalyzed Oxidative Activation of Benzylic C–H Bonds for the Synthesis of Difluoromethylated Arenes. *Angew*. *Chem*. *Int*. *Ed*. **2014**, *53* (23), 5955–5958.
83 Huang, X.; Liu, W.; Hooker, J. M.; Groves, J. T. Targeted Fluorination with the Fluoride Ion by Manganese-Catalyzed Decarboxylation. *Angew*. *Chem*. *Int*. *Ed*. **2015**, *54* (17), 5241–5245.
84 Sap, J. B. I.; Wilson, T. C.; Kee, C. W.; Straathof, N. J. W.; am Ende, C. W.; Mukherjee, P.; Zhang, L.; Genicot, C.; Gouverneur, V. Synthesis of ^{18}F-difluoromethylarenes using aryl boronic acids, ethyl bromofluoroacetate and [^{18}F]fluoride. *Chem*. *Sci*. **2019**, *10* (11), 3237–3241.
85 Frost, A. B.; Brambilla, M.; Exner, R. M.; Tredwell, M. Synthesis and Derivatization of 1,1-[^{18}F]Difluorinated Alkenes. *Angew*. *Chem*. *Int*. *Ed*. **2019**, *58* (2),472–476.
86 Khanapur, S.; Lye, K.; Mandal, D.; Wee, X. J.; Robins, E. J.; Young, R. D. Fluorine-18 Labeling of Difluoromethyl and Trifluoromethyl Groups *via* Monoselective C−F Bond Activation. *Angew*. *Chem*. *Int*. *Ed*. **2022**, *61* (49), e202210917.
87 Mandal, D.; Gupta, R.; Jaiswal, A. K.; Young, R. D. Frustrated Lewis-Pair-Meditated Selective Single Fluoride Substitution in Trifluoromethyl Groups. *J. Am. Chem. Soc.* **2020**, *142* (5), 2572–2578.
88 Trump, L.; Lemos, A.; Lallemand, B.; Pasau, P.; Mercier, J.; Lemaire, C.; Luxen, A.; Genicot, C. Late-Stage ^{18}F-Difluoromethyl Labeling of *N*-Heteroaromatics with High Molar Activity for PET Imaging. *Angew*. *Chem*. *Int*. *Ed*. **2019**, *58* (37), 13149–13154.
89 Rong, J.; Deng, L.; Tan, P.; Ni, C.; Gu, Y.; Hu, J. Radical Fluoroalkylation of Isocyanides with Fluorinated Sulfones by Visible-Light Photoredox Catalysis. *Angew*. *Chem*. *Int*. *Ed*. **2016**, *55* (8), 2743–2747.
90 Trump, L.; Lemos, A.; Jacq, J.; Pasau, P.; Lallemand, B.; Mercier, J.; Genicot, C.; Luxen, A.; Lemaire, C. Development of a General Automated Flow Photoredox ^{18}F-Difluoromethylation of *N*-Heteroaromatics in an AllinOne Synthesizer. *Org*. *Process Res*. *Dev*. **2020**, *24* (5), 734–744.
91 Lemos, A. L. P.; Trump, L.; Lallemand, B.; Pasau, P.; Mercier, J.; Lemaire, C.; Monbaliu, J,-C.; Genicot, C.; Luxen, A. Radical C–H ^{18}F-Difluoromethylation of Heteroarenes with [^{18}F]Difluoromethyl Heteroaryl-Sulfones by Visible Light Photoredox Catalysis. *Catalysts* **2020**, *10* (3), 275.
92 Sap, J. B. I.; Meyer, C. F.; Ford, J.; Straathof, N. J. W.; Dürr, A. B.; Lelos, M. J.; Paisey, S. J.; Mollner, T. A.; Hell, S. M.; Trabanco, A. A.; Genicot, C.; am Ende, C. W.; Paton, R. S.; Tredwell, M.; Gouverneur, V. [^{18}F]Difluorocarbene for positron emission tomography. *Nature* **2022**, *606* (7912), 102–108.
93 Hansch, C.; Leo, A; Taft, R. W. A survey of Hammett substituent constants and resonance and field parameters. *Chem*. *Rev*. **1991**, *91* (2), 165–195.
94 Zhao, Q.; Lu, L.; Shen, Q. Direct Monofluoromethylthiolation with *S*-(Fluoromethyl) Benzenesulfonothioate. *Angew*. *Chem*. *Int*. *Ed*. **2017**, *56* (38), 11575–11578.
95 Verhoog, S. Late-Stage Trifluoromethylation. Ph.D. Thesis, University of Oxford, Oxford, U.K., 2016.

96 Cai, L.; Lu, S.; Pike, V. W. Chemistry with [^{18}F]Fluoride Ion. *Eur*. *J*. *Org*. *Chem*. **2008**, *2008* (17), 2853–2873.
97 van der Born, D.; Pees, A.; Poot, A. J.; Orru, R. V. A.; Windhorst, A. D.; Vugts, D. J. Fluorine-18 labelled building blocks for PET tracer synthesis. *Chem*. *Soc*. *Rev*. **2017**, *46* (15), 4709–4773.
98 James, M. L.; Fulton, R. R.; Vercoullie, J.; Henderson, D. J.; Garreau, L.; Chalon, S.; Dollé, F.; Selleri, S.; Guilloteau, D.; Kassiou, M. DPA-714, a New Translocator Protein–Specific Ligand: Synthesis, Radiofluorination, and Pharmacologic Characterization. *J*. *Nucl*. *Med*. **2008**, *49* (5), 814–822.
99 Zheng, J.; Winkeler, A.; Peyronneau, M. A.; Dollé, F.; Boisgard, R. Evaluation of PET Imaging Performance of the TSPO Radioligand [^{18}F]DPA-714 in Mouse and Rat Models of Cancer and Inflammation. *Mol*. *Imaging Biol*. **2016**, *18* (1), 127–134.
100 Peyronneau, M. A.; Saba, W.; Goutal, S.; Damont, A.; Dollé, F.; Kassiou, M.; Bottlaender, M.; Valette, H. Metabolism and Quantification of [^{18}F]DPA-714, a New TSPO Positron Emission Tomography Radioligand. *Drug Metab*. *Dispos*. **2013**, *41* (1), 122–131.
101 Keller, T.; López-Picón, F. R., Krzyczmonik, A.; Forsback, S.; Kirjavainen, A. K.; Takkinen, J. S.; Alzghool, O.; Rajander, J.; Teperi, S.; Cacheux, F.; Damont, A.; Dollé, F.; Rinne, J. O.; Solin, O.; Haaparanta-Solin, M. [^{18}F]F-DPA for the detection of activated microglia in a mouse model of Alzheimer's disease. *Nucl*. *Med*. *Biol*. **2018**, *67*, 1–9.
102 Keller, T.; López-Picón, F. R.; Krzyczmonik, A.; Forsback, S.; Takkinen, J. S.; Rajander, J.; Teperi, S.; Dollé, F.; Rinne, J. O.; Haaparanta-Solin, M.; Solin O. Comparison of high and low molar activity TSPO tracer [^{18}F]F-DPA in a mouse model of Alzheimer's disease. *J*. *Cereb*. *Blood Flow Metab*. **2020**, *40* (5), 1012–1020.
103 Lelos, M. J.; Dunnett, S. B. Generating Excitotoxic Lesion Models of Huntington's Disease. *Methods Mol*. *Biol*. **2018**, *1780*, 209–220.
104 Pike, V. W.; Halldin, C.; Crouzel, C.; Barré, L.; Nutt, D. J.; Osman, S.; Shah, F.; Turton, D. R.; Waters, S. L. Radioligands for PET studies of central benzodiazepine receptors and PK (peripheral benzodiazepine) binding sites. *Nucl*. *Med*. *Biol*. **1993**, *20* (4), 503–525.
105 Li, X.; Zhao, J.; Hu, M.; Chen, D.; Ni, C.; Wang, L.; Hu, J. Copper-mediated aerobic (phenylsulfonyl)difluoromethylation of arylboronic acids with difluoromethyl phenyl sulfone. *Chem*. *Commun*. **2016**, 52 (18), 3657–3660.
106 Feng, Z.; Min, Q.-Q.; Xiao, Y.-L.; Zhang, B.; Zhang, X. Palladium-Catalyzed Difluoroalkylation of Aryl Boronic Acids: A New Method for the Synthesis of Aryldifluoromethylated Phosphonates and Carboxylic Acid Derivatives. *Angew*. *Chem*. *Int*. *Ed*. **2014**, *53* (6), 1669–1673.
107 International Council For Harmonisation Of Technical Requirements For Pharmaceuticals For Human Use, *ICH Harmonised Guideline: Guideline For Elemental Impurities Q3D(R2).* International Council for Harmonisation of Technical Requirements for Pharmaceuticals for Human Use, 2022. https://database.ich.org/sites/default/files/Q3D-R2_Guideline_Step4_2022_0308.pdf (accessed 2024-07-09).
108 Billingsley, K.; Barder, T.; Buchwald, S. Palladium-Catalyzed Borylation of Aryl Chlorides: Scope, Applications, and Computational Studies. *Angew*. *Chem*. *Int*. *Ed*. **2007**, *46* (28), 5359–5363.
109 Coutts, S. J.; Adams, J.; Krolikowski, D.; Snow, R. J. Two efficient methods for the cleavage of pinanediol boronate esters yielding the free boronic acids. *Tetrahedron Lett*. **1994**, *35* (29), 5109–5112.

110 Gupta, S.; Chaudhary, P.; Srivastava, V.; Kandasamy, J. A chemoselective ipso-hydroxylation of arylboronic acids using urea-hydrogen peroxide under catalyst free condition. *Tetrahedron Lett*. **2016**, *57* (23), 2506–2510.

111 Wright, J. S.; Sharninghausen, L. S.; Preshlock, S.; Brooks, A. F.; Sanford, M. S.; Scott, P. J. H. Sequential Ir/Cu-Mediated Method for the Meta-Selective C–H Radiofluorination of (Hetero)Arenes. *J*. *Am*. *Chem*. *Soc*. **2021**, *143* (18), 6915–6921.

Chapter 3: Deaminative ^{18}F-Fluorination of Heteroaryl Pyridinium Salts

This chapter first summarises key advances in nucleophilic aromatic substitution (S_NAr) reactivity with both ^{19}F-fluoride and [^{18}F]fluoride, with a focus on the latter and the utility of such reactions to radiochemists. Next, an account of the synthesis and reactivity of pyridinium salts is provided. The development of a pyridinium-based radiofluorination of heteroarenes is the object of the work presented in this chapter. Reaction design considerations and preliminary experiments are first described, followed by an evaluation of key reaction parameters. The utility of the reaction is demonstrated in scope and additive-based robustness screening studies. Further extension to an ^{18}F-fluorodeamination of crude pyridinium substrates and the application of the charged substrates to elution of [^{18}F]fluoride are next disclosed. Finally, the reaction is scaled-up and translated to multi-GBq automated radiosynthesis and a preliminary comparison to existing methods is provided.

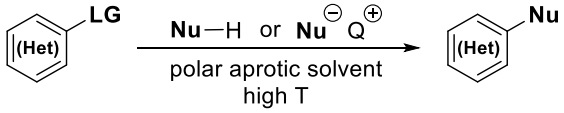
The work presented in this chapter has been published (J. Ford, S. Ortalli, Z. Chen, J. B. I. Sap, M. Tredwell, V. Gouverneur. Expedient Access to ^{18}F-Fluoroheteroarenes *via* Deaminative Radiofluorination of Aniline-Derived Pyridinium Salts. *Angew. Chem. Int. Ed.* **2024**, *63* (26), e202404945).

All ^{18}F-radiolabelling experiments described in section 3.2 were conducted by J. Ford, with assistance from Dr. J. Sap, S. Ortalli and Dr. Z. Chen. Synthesis of materials was conducted by J. Ford, S. Ortalli and Dr. J. Sap. Further details are available in the Experimental section (Chapter 4).

3.1. Introduction

3.1.1. Nucleophilic Aromatic Substitution with Fluoride

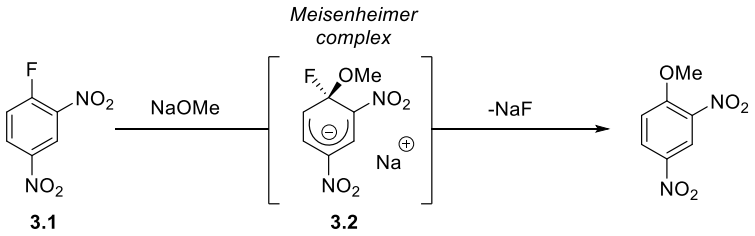
Nucleophilic aromatic substitution (S_NAr) is a highly exploited reaction type in synthetic organic chemistry and is the second most used reaction in medicinal chemistry after amide coupling.[1] Fundamentally, it involves the substitution of a leaving group by a nucleophile at an aromatic or heteroaromatic framework (Scheme 3.1). It relies on the direct reactivity of a given nucleophile and as it is not assisted by transition metal additives or catalysts, in general its application is limited to electron-deficient arenes (usually substituted with groups that are electron-withdrawing by resonance at the *ortho*- and *para*-positions) and heteroarenes, i.e., sufficiently electrophilic substrates.[2]



Scheme 3.1 *Nucleophilic aromatic substitution (S_NAr) of (hetero)arenes. LG = leaving group, Nu = nucleophile, Q = countercation.*

The most typical leaving groups for S_NAr reactions include halide anions, with leaving group ability descending down group 17.[3,4] This observation correlates with the classical mechanistic hypothesis for S_NAr reactivity.[5] For example, the reaction of Sanger's reagent **3.1** with sodium methoxide proceeds *via* a stepwise addition-elimination mechanism, with formation of a negatively charged intermediate **3.2**, commonly referred to as the Meisenheimer complex (Scheme 3.2).[5-7] Such complexes have been chemically isolated for the addition of various nucleophiles to arenes. The stabilisation of this negatively charged intermediate is proposed to be greatest for the strongly inductively electron-withdrawing fluoride, compared to less electron-withdrawing chloride, bromide and iodide.[3,4] However, it is noteworthy that comparable Meisenheimer complexes for heteroaromatics have only been isolable in the case of poor leaving groups, while those of good leaving groups have not been detected.[5,6]

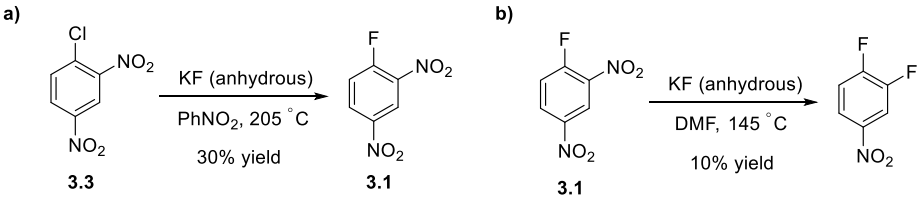
Despite its common application as a leaving group in S_NAr reactions, as highlighted in the above example, fluorination is also accessible in S_NAr reactions with a fluoride nucleophile. This account of S_NAr reactivity will be restricted to such reports.



3.1 3.2

Scheme 3.2 *Reaction of* ***3.1*** *with NaOMe via Meisenheimer complex* ***3.2****.*

Fluorination *via* S_NAr was first reported by Gottlieb in 1936 for the synthesis of **3.1** from KF and 1-chloro-2,4-dinitrobenzene (**3.3**) (Scheme 3.3 a).[8] Further advances were disclosed by Kruse and Finger in 1956, who found that electron-deficient aryl chlorides less activated than **3.3** could also be fluorinated in an S_NAr reaction with anhydrous KF at high temperature.[9] Key to their discovery was the use of polar aprotic solvents, such as DMSO and DMF, which proved much more effective than the nitrobenzene solvent trialled previously. In the same study, fluorodenitration of **3.1** was also reported, with NO_2 evolved as a gas, demonstrating the effectiveness of nitro groups as nucleofuges in S_NAr processes with fluoride (Scheme 3.3 b).[9] Nonetheless, fluorination *via* S_NAr still required anhydrous and harsh conditions, such as high temperatures.



3.3 3.1 3.1

Scheme 3.3 *a) Gottlieb's initial conditions for the S_NAr fluorination of* ***3.3****. b) Fluorodenitration of* ***3.1*** *observed by Finger and Kruse.*

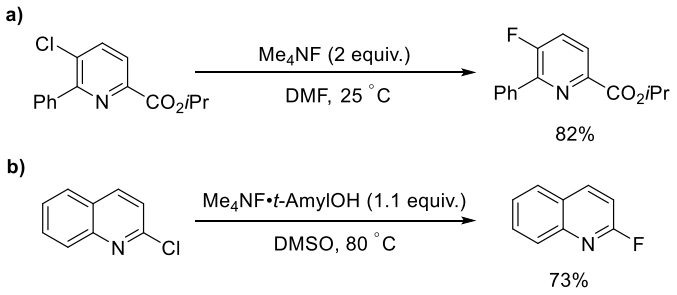
Later, other groups explored the use of alternative fluoride sources other than KF, which suffers from low solubility in organic solvents.[10] In 1991, Scorrano and co-workers found that KF could be used in combination with a tetramethylammonium chloride phase transfer reagent for the effective fluorination of electron-deficient arenes *via* denitration.[11] Clark and co-workers reported in 1993 that tetramethylammonium fluoride (TMAF) could also be used

directly for the fluorination of nitroarenes.[12] Later in 2005, Kuduk *et al.* reported that various nitroheteroarenes could be readily fluorinated with a solution of TBAF in THF at temperatures as low as room temperature.[13] These findings were corroborated in 2006 by DiMagno and co-workers, who used their conditions for the anhydrous preparation of TBAF in various halex and fluorodenitrations of (hetero)arene substrates.[14] In line with previous studies, DMSO proved effective as a polar aprotic solvent and they also observed an inverse correlation between reaction time and the presence of electron-withdrawing functionality.

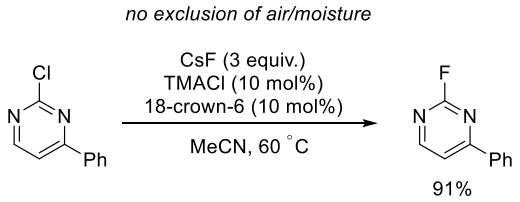
More recently, Sanford and co-workers have extensively studied halex fluorination *via* S_NAr with TMAF, reporting numerous advances (Scheme 3.4).[15] They advocate for the use of TMAF, as it can be prepared from inexpensive KF and tetramethylammonium chloride, and unlike TBAF, can be dried at high temperatures for extended periods without competing Hofmann elimination. In 2015, they first reported the halex and denitration reactions of (hetero)aromatic substrates with TMAF, and in many cases the desired (hetero)aromatic fluoride was accessible in good to excellent yield at room temperature in DMF solvent (Scheme 3.4 a).[16] They later found that TMAF-alcohol complexes were also effective fluoride sources in S_NAr processes, which removed the need for rigorously dried, anhydrous TMAF (Scheme 3.4 b).[17] A TMAF complex with *tert*-amyl alcohol proved to be the optimal reagent for various halex fluorination and fluorodenitration reactions of heteroarenes and aromatic substrates substituted with electron-withdrawing groups.

In 2021, Hong *et al.* also disclosed that the superior reactivity of TMAF could be exploited, without the need for the synthesis of a bespoke complex and/or rigorous drying (Scheme 3.5).[18] Using catalytic amounts of commercial tetramethylammonium chloride and 18-crown-6, CsF could be used directly for the fluorination of heteroaryl chlorides and aryl triflates in MeCN solvent. Advantageously, the reaction could also be performed without the exclusion of air or moisture. The authors proposed that tetramethylammonium chloride and 18-crown-

6 behave co-operatively in the solubilisation of CsF, with the formation of a small amount of soluble TMAF, which they observed by ^{19}F NMR spectroscopy.

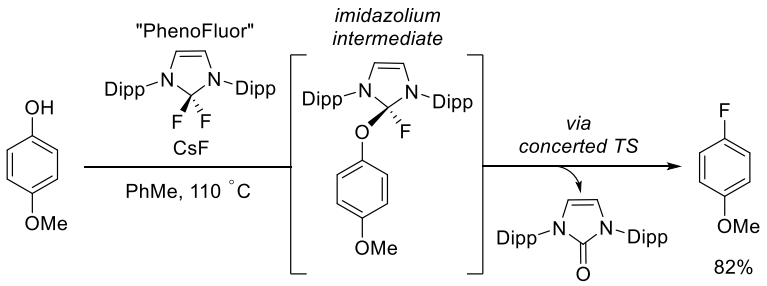


Scheme 3.4 *S_NAr fluorination with TMAF using a) anhydrous TMAF, b) TMAF-alcohol complexes.*



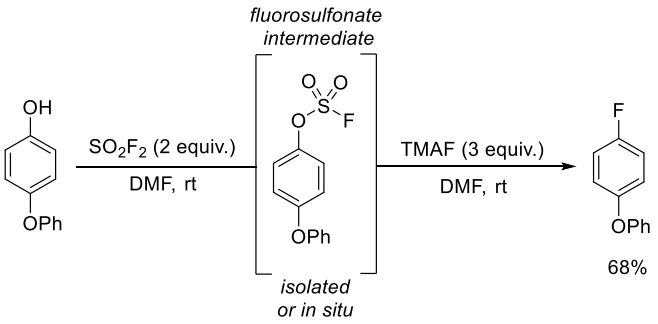
Scheme 3.5 *Nucleophilic fluorination of heteroaryl chlorides with CsF under co-operative catalysis.*

A significant departure from the stepwise mechanistic hypothesis (Scheme 3.2) was reported in aromatic fluorination by Ritter and co-workers, who disclosed a deoxygenative fluorination of phenols that was proposed to proceed *via* a concerted nucleophilic aromatic substitution (cS_NAr) mechanism.[19] The reaction of phenol and a reagent (1,3-bis(2,6-diisopropylphenyl)-2,2-difluoro-4-imidazoline, PhenoFluor™) proceeded *via* the formation of an imidazolium species, which was then reactive towards an external fluoride nucleophile (CsF). The scope of their reaction was broader than could be expected from a stepwise S_NAr mechanism, which they rationalised by the limited delocalisation of negative charge onto the aromatic ring in the cS_NAr transition state. Therefore, electron-rich substrates such as 4-methoxyphenol could be readily fluorinated (Scheme 3.6). Computational data also corroborated the mechanistic hypothesis, with a low energy cS_NAr transition state being located and the calculation of a reaction coordinate for the deoxyfluorination.[20]



Scheme 3.6 *Deoxyfluorination of 4-hydroxyanisole with PhenoFluor and CsF. Dipp = 2,6-diisopropylphenyl.*

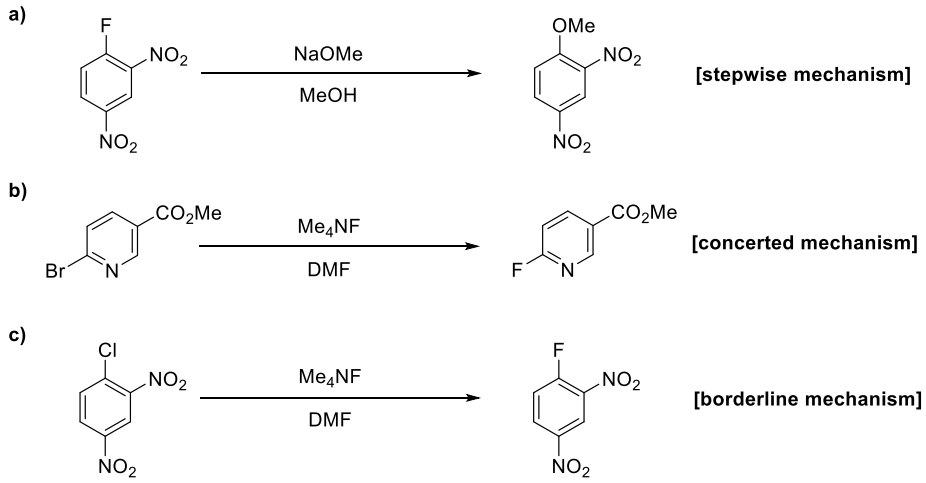
In a further development, Sanford and co-workers discovered another deoxyfluorination of phenols that was also proposed to proceed *via* a cS_NAr mechanism (Scheme 3.7).[21] Sulfuryl fluoride (SO_2F_2) first reacted with phenol substrates to generate aryl fluorosulfonates. In the presence of an external fluoride nucleophile (TMAF), the fluorosulfonate could undergo fluorodeoxygenation in a cS_NAr-type process that did not proceed *via* a Meisenheimer-type intermediate to deliver the aryl fluoride. Various electronically differentiated phenols, including those bearing electron-donating substituents, were well tolerated. Sanford and co-workers also performed electronic structure calculations finding that a stable Meisenheimer intermediate could not be located and observed only a concerted transition state in their computational analysis of the deoxyfluorination of aryl fluorosulfonates.



Scheme 3.7. *Deoxyfluorination of phenols via aryl fluorosulfonates.*

The Jacobsen laboratory have further studied the mechanism of S_NAr and cS_NAr reactions, including those with fluoride nucleophiles.[22] They used a blended computational and experimental approach to investigate the mechanisms of various S_NAr reactions. This included the measurement using ^{13}C NMR experiments and *ab initio* calculation of $^{12}C/^{13}C$ kinetic isotope effects. It was found that there were three distinct cases, either a stable

Meisenheimer complex exists and the reaction proceeds in a stepwise manner (Scheme 3.8 a), or the reaction is concerted, with a Meisenheimer complex-like transition state (Scheme 3.8 b), or a borderline case, where a longer-lived Meisenheimer-type transition state exists in a shallow potential energy surface (Scheme 3.8 c). In the two model reactions where a fluoride nucleophile was considered, these proceed either as concerted reactions or *via* longer-lived Meisenheimer-type transition states, i.e. not *via* stable Meisenheimer intermediates (Scheme 3.8 b, c).



Scheme 3.8. *Model S_NAr reactions considered by Jacobsen and co-workers, proposed to proceed via a) a stepwise mechanism with stable Meisenheimer intermediate, b) concerted mechanism with a Meisenheimer-like transition state, c) borderline stepwise-concerted mechanism with a longer lived Meisenheimer-like transition state.*

3.1.2. Nucleophilic Aromatic Substitution with [^{18}F]Fluoride

Radiofluorination by S_NAr with [^{18}F]fluoride is a highly prominent reaction in ^{18}F-radiochemistry, well used by radiochemistry practitioners.[23] It offers several key advantages, which have rendered it well suited to ^{18}F-radiochemistry. Firstly, it allows for the direct use of cyclotron-produced [^{18}F]fluoride. This is the most widely available ^{18}F-synthon and is available in the majority of PET radiopharmacies. It is also a simple reaction to implement, only requiring the combination of substrate and [^{18}F]fluoride, and therefore it is readily amenable to automated radiosynthesis using commercial platforms. Furthermore, as it relies on the innate nucleophilicity of [^{18}F]fluoride towards an electrophilic substrate, it does not require the use of transition metal additives to promote reactivity, which simplifies quality control for

the production of clinical radiotracers. S_NAr reactions also allow access to various heteroaromatic scaffolds in radiolabelled form, and such structures are highly prevalent in pharmaceutical drugs.[24] Indeed, analysis from a 2021 systematic review of UK PET radiopharmacy capabilities indicated that 55% of the 20 available clinical PET ^{18}F-radiotracers were accessible *via* an S_NAr route with [^{18}F]fluoride.[25] Several examples of these are given in Figure 3.1.

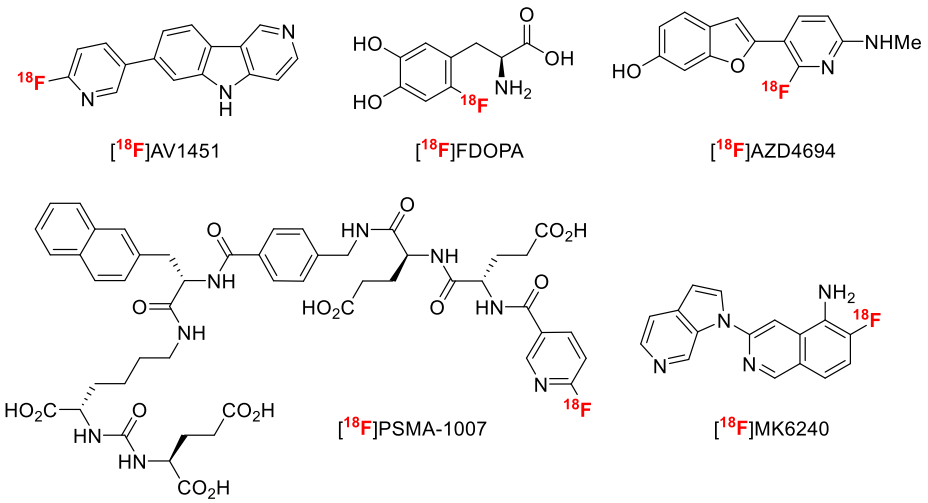


Figure 3.1. *Examples of radiotracers available from UK PET radiopharmacies that are prepared via an S_NAr radiosynthetic route (correct 2021).*

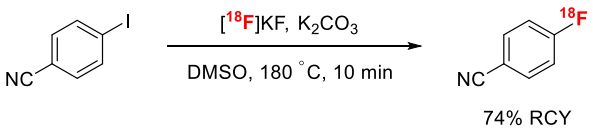
This section will provide an account of the progress made to date to access ^{18}F-fluoro(hetero)arenes *via* the S_NAr reactivity of [^{18}F]fluoride. While reports of ^{18}F-fluorination *via* aromatic substitution have emerged relying on transition metal catalysis and/or photochemical activation, such as the recent halex ^{18}F-fluorination of electron-rich arenes under oxidative photocatalysis from the Nicewicz and Li laboratories, this account will focus on classical S_NAr-type reactivity under thermal conditions.[26] Various substrate classes have been applied to S_NAr reactions with [^{18}F]fluoride and the summary in this section will distinguish these reports by leaving group identity.

3.1.2.1. ^{18}F-S_NAr from Halide Precursors

(Hetero)aryl halides being arguably the most well established class of S_NAr precursors,[2] there has therefore been significant effort to apply these precursors in S_NAr reactions with [^{18}F]fluoride.[27] As they are commonly used in the synthesis of pharmaceuticals, small

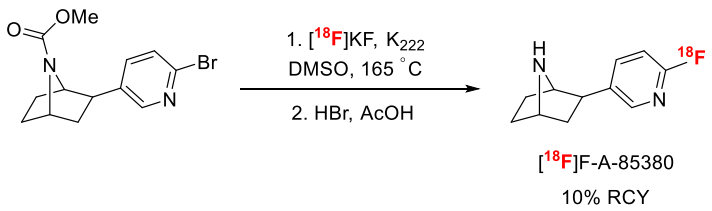
molecule (hetero)aryl halides (chlorides in particular) are often commercially available. Otherwise, they are most often installed *via* the chlorination of hydroxy groups using reagents, such as phosphoryl chloride, in the case of heteroarenes or by direct chlorination for arenes.[28] While their availability and well-established synthesis is an advantage, a limitation of their application to radiochemistry is their lower reactivity compared to other commonly used labelling precursors.[27] Therefore, radiofluorination often demands very high temperatures, which could be problematic for sensitive substrates. Furthermore, the separation of hetero(aryl) chloride labelling substrates and ^{18}F-fluoride products can be challenging for complex molecules, as these species would be expected to behave chromatographically similarly in reverse-phase HPLC purification due to their similar polarity.

An early example of the use of aryl iodides to access aryl ^{18}F-fluorides was reported in 1985 by Crouzel and co-workers (Scheme 3.9).[29] At 180 °C in DMSO solvent, [^{18}F]4-fluorobenzonitrile could be obtained from the iodide precursor in up to 74% RCY, for example (Scheme 3.9). In the same report, they also compared aryl iodides to triazenes prepared from diazonium precursors under the same conditions, finding that such substrates were less viable in reactions with [^{18}F]fluoride.



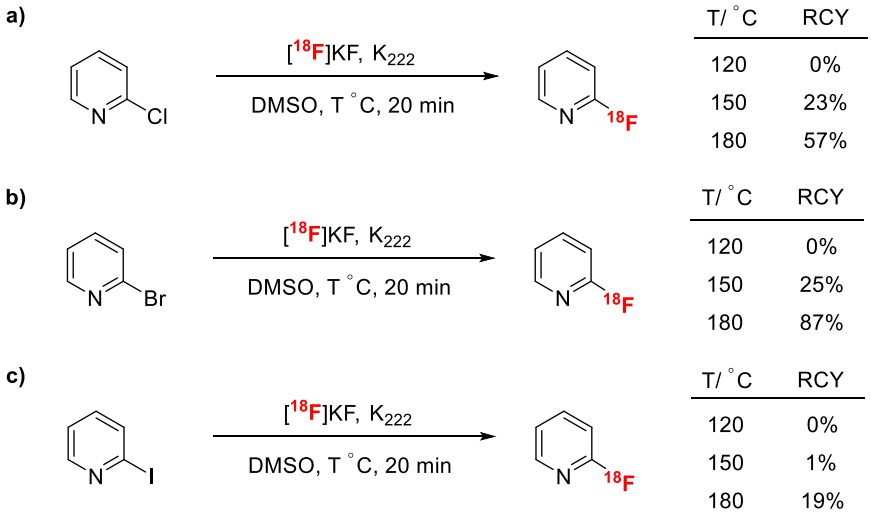
Scheme 3.9. *Halex ^{18}F-fluorination of 4-iodobenzonitrile.*

After this report, over the next decade, several ^{18}F-radiotracer syntheses exploited an S_NAr route using (hetero)aryl halide precursors. One such example was the radiosynthesis of [^{18}F]F-A-85380 from a 2-bromopyridine precursor disclosed in 1996 by Horti *et al.* (Scheme 3.10). The desired tracer was obtained in an RCY of 10%.[30]



Scheme 3.10. *Radiosynthesis of [^{18}F]F-A-85380 via an S_NAr route.*

In 1999, Dollé and co-workers disclosed a comparative study, in which they compared the reactivity of 2-halopyridines towards [^{18}F]fluoride to other S_NAr precursors of the same scaffold under various conditions (Scheme 3.11).[31] Using a K_2CO_3-K_{222} elution system, it was found that 2-halopyridines were entirely unreactive towards ^{18}F-fluorination in DMSO at 120 °C over 20 minutes, however, at higher temperatures above 150 °C, the desired product was formed. ^{18}F-Fluorination also took place under 100 W microwave irradiation, while 50 W irradiation proved insufficient. In these experiments, 2-bromopyridine was the most effective halide S_NAr precursor (Scheme 3.11 b), followed by 2-chloropyridine (Scheme 3.11 a) and finally 2-iodopyridine, which proved to be a significantly poorer substrate (Scheme 3.11 c).

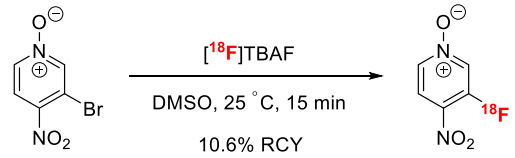


Scheme 3.11. *Comparison of the reactivity of a series of 2-halopyridine precursors in ^{18}F-fluorination with [^{18}F]KF, a) 2-chloropyridine, b) 2-bromopyridine, c) 2-iodopyridine.*

In a subsequent study from 2003, Dollé and co-workers also investigated the reactivity differences between different isomers of bromopyridines in radiofluorination.[32] Compared to the good reactivity observed above 150 °C for 2-bromopyridine, no reactivity was observed for 3-bromopyridine under any of the radiofluorination conditions trialled, as it was a less activated substrate for S_NAr.

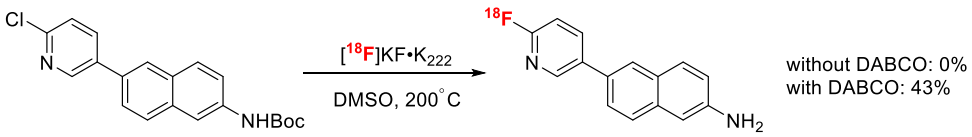
This challenge was later studied by Brugarolas and co-workers, who proposed a solution exploiting the different electronics of pyridine *N*-oxides (Scheme 3.12).[33] In these compounds, the 3-position would be expected to be the most activated towards S_NAr, compared to the 2-

and 4-positions for pyridines. Focusing their attention on model compound 3-bromo-4-nitropyridine *N*-oxide, they were able to prepare the 3-^{18}F-fluoropyridine-*N*-oxide in an isolated RCY of 10.6%. They also showed 3-bromopyridine *N*-oxide was a viable radiolabelling substrate, suggesting there is not a requirement for a nitro group or another electron-withdrawing group at the 4-position.



Scheme 3.12. *Radiofluorination of 3-bromopyridine N-oxides.*

In 2017, Pike and co-workers looked to address the reactivity challenges associated with S_NAr radiofluorination of 5-substituted-2-halopyridine substrates (Scheme 3.13).[34] They proposed an additive-based solution using quinuclidine and DABCO, which likely substitute the chloride reversibly to form quaternary ammonium intermediates *in situ* that were more reactive towards [^{18}F]fluoride. This approach enabled the superior reactivity of ammonium radiolabelling substrates to be exploited, without the need to prepare them in a lengthy synthesis, as the synthetically convenient 2-chloropyridine could be used directly. For example, 2-chloropyridine substrate **3.4** gave product [^{18}F]**3.5** in up to 43% RCY in the presence of the DABCO additive, while no [^{18}F]**3.5** formed when no DABCO was added.

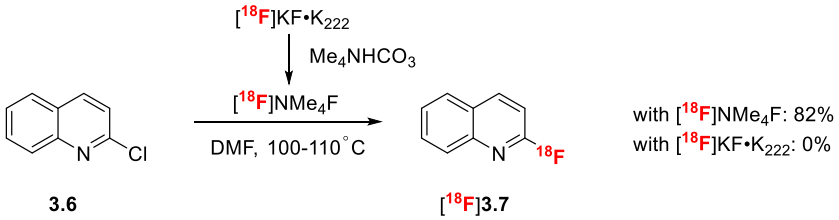


3.4 **[^{18}F]3.5**

Scheme 3.13. *DABCO and quinuclidine-assisted radiofluorination of 5-substituted-2-halopyridines.*

Inspired by the excellent reactivity of TMAF in fluorination *via* S_NAr, Scott, Sanford and co-workers reported that it could also be harnessed in radiolabelled form.[35] In 2021, they disclosed a protocol for the preparation of [^{18}F]TMAF from [^{18}F]KF (obtained in a standard [^{18}F]fluoride elution and azeotropic drying procedure), and a tetramethylammonium salt additive. This obviated challenges with drying [^{18}F]TMAF and/or elution with non-aqueous solutions. [^{18}F]TMAF displayed excellent reactivity in S_NAr reactions of various electrophiles,

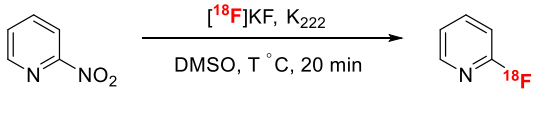
predominantly heteroaryl halides, but also aryl triflates and nitro compounds. Its reactivity was contrasted with [^{18}F]KF, which in 18 out of 27 examples studied gave no or low RCY of the desired product (e.g. the radiofluorination of **3.6**, Scheme 3.14).



Scheme 3.14. *S_NAr radiofluorination of heteroaryl halides (e.g.* ***3.6****) with [^{18}F]TMAF.*

3.1.2.2. ^{18}F-S_NAr from Nitro Precursors

Based on the reactivity of nitro compounds towards fluoride described in section 3.1.1, it is unsurprising that nitroarenes are also a well exploited substrate class for S_NAr reactions with [^{18}F]fluoride.[9,13,14] In general, these precursors display improved reactivity over (hetero)aryl halides, which Dollé and co-workers investigated in their comparative study of different S_NAr precursors towards [^{18}F]2-fluoropyridine (*vide supra*-Scheme 3.11) (Scheme 3.15).[31]



T/ °C	RCY
120	82%
150	92%
180	89%

Scheme 3.15. *S_NAr ^{18}F-fluorodenitration of 2-nitropyridine, c.f. Scheme 3.11.*

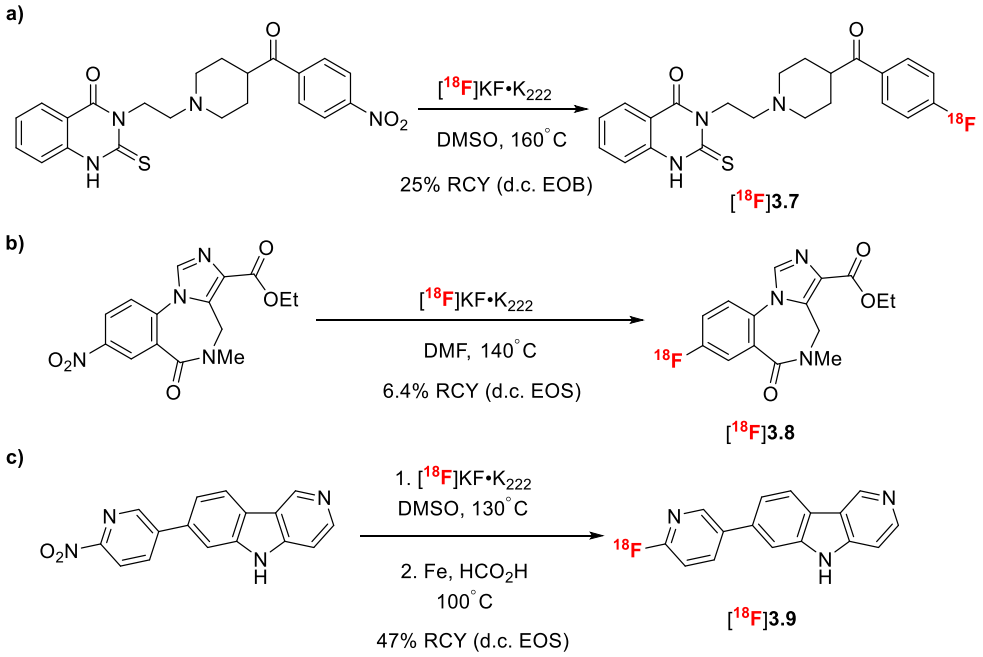
In 1983, Wolf and co-workers disclosed first conditions for the ^{18}F-fluorodenitration of nitroarenes, whereby these were reacted with [^{18}F]RbF in DMSO at 150 °C (Scheme 3.15).[36] These precursors were found to provide efficient access to various small molecule aryl ^{18}F-fluorides.



Scheme 3.16. *S_NAr ^{18}F-fluorodenitration of nitroarenes with [^{18}F]RbF.*

Since this seminal publication, ^{18}F-fluorodenitration has been well explored for the synthesis of PET radiotracers. [^{18}F]Altanserin ([^{18}F]**3.7**) could be conveniently prepared in a single-step radiosynthesis *via* an S_NAr of a nitro precursor with [^{18}F]fluoride (Scheme 3.17 a).[37] An early radiosynthesis of [^{18}F]flumazenil ([^{18}F]**3.8**) also proceeded *via* a nitro precursor (Scheme 3.17

b).[38] However, this precursor could be challenging to separate from the labelled product ([^{18}F]**3.8**). A similar challenge was observed for the first-generation radiosynthesis of [^{18}F]AV-1451 ([^{18}F]**3.9**) from a nitro precursor and post-labelling reduction of the nitro group to an amine facilitated purification (Scheme 3.17 c).[39]

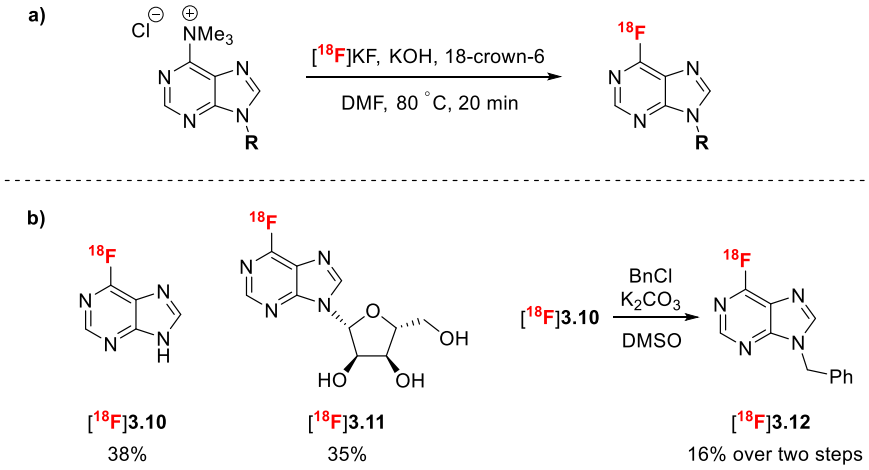


Scheme 3.17. *S_NAr ^{18}F-fluorodenitration routes to radiotracers, a) [^{18}F]altanserin, b) [^{18}F]flumazenil, c) [^{18}F]AV-1451. d.c = decay-corrected, EOS = end-of-synthesis, EOB = end-of-bombardment.*

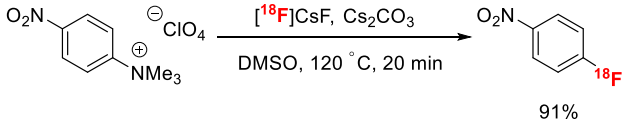
3.1.2.3. ^{18}F-S_NAr from Ammonium Precursors

The use of ammonium precursors for S_NAr with [^{18}F]fluoride was first established in the 1980s, when Irie and co-workers showed that ^{18}F-fluorinated purines could be accessed from radiofluorination of trimethylammonium chloride precursors in superior RCY to the comparable halex process with [^{18}F]AgF (Scheme 3.18 a).[40,41] Across two studies, they disclosed radiosyntheses of ^{18}F-6-fluoropurines [^{18}F]**3.10**, [^{18}F]**3.11** and [^{18}F]**3.12**, the latter of which they were able to access in a two-step sequence and was proposed to have utility as a radiotracer for brain PET imaging (Scheme 3.18 b).

A later report from Angelini *et al.* in 1985 showed that various aryl ^{18}F-fluorides were accessible from trimethylammonium perchlorate substrates upon heating in DMSO at temperatures up to 140 °C (Scheme 3.19).[42] While these displayed good reactivity, perchlorate salts are also potentially explosive, which could limit their possible application.

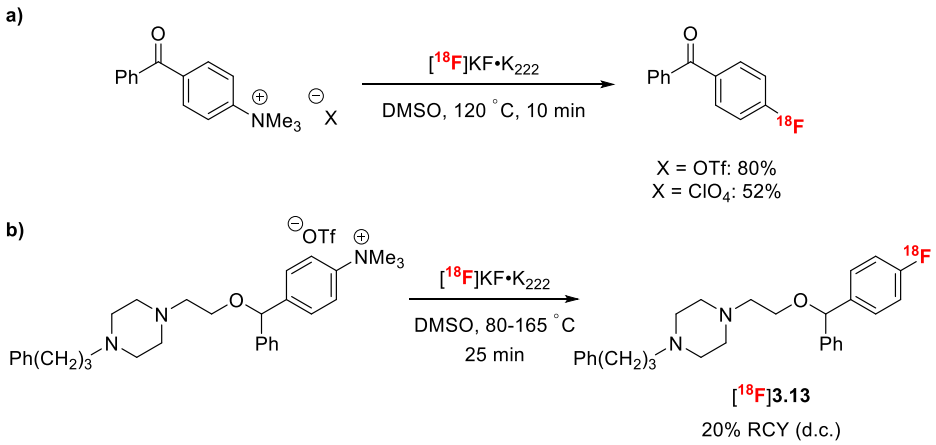


Scheme 3.18. *Radiosynthesis of ^{18}F-fluoropurines via S_NAr of trimethylammonium chlorides with [^{18}F]fluoride; a) reaction overview, b) reaction scope.*



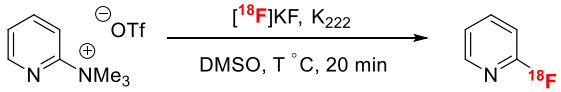
Scheme 3.19. *S_NAr of trimethylammonium perchlorates with [^{18}F]fluoride.*

This was followed by a study from Haka and co-workers, where the reactivity of aryl trimethylammonium triflates towards [^{18}F]fluoride was studied.[43] These substrates displayed improved reactivity relative to the nitro or trimethylammonium perchlorate precursor of the same scaffold (Scheme 3.20 a). Their results also suggested that the use of very high reaction temperatures could also be detrimental, leading to substrate degradation and side reactions in some cases. They were able to use their method for the preparation of a PET radiotracer for dopamine uptake ([^{18}F]GBR-13119, [^{18}F]**3.13**) (Scheme 3.20 b).



Scheme 3.20. *S_NAr of trimethylammonium triflates with [^{18}F]fluorides. a) Comparison of triflate and perchlorate salts, b) Radiosynthesis of [^{18}F]GBR-13119 ([^{18}F]**3.13**).*

The superior reactivity profile of trimethylammonium salts as S_NAr precursors in ^{18}F-fluorination was further investigated by Dollé and co-workers.[31] In their 1999 study into the radiosynthesis of [^{18}F]2-fluoropyridine (*vide supra*, Schemes 3.11 and 3.15), the trimethylammonium triflate substrate performed best of all considered, providing the highest RCY relative to the nitro and halide precursors also under consideration (Scheme 3.21).



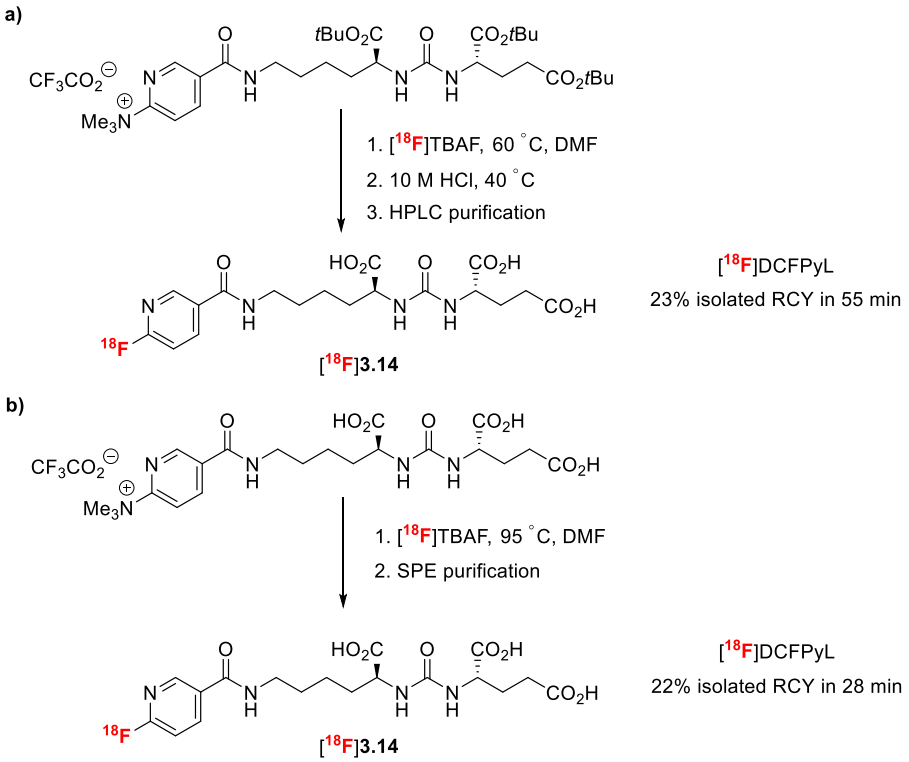
T/ °C	RCY
120	91%
150	90%
180	92%

Scheme 3.21. *S_NAr ^{18}F-fluorodenitration of (2-pyridyl)trimethylammonium triflate, c.f. Scheme 3.11 and Scheme 3.15.*

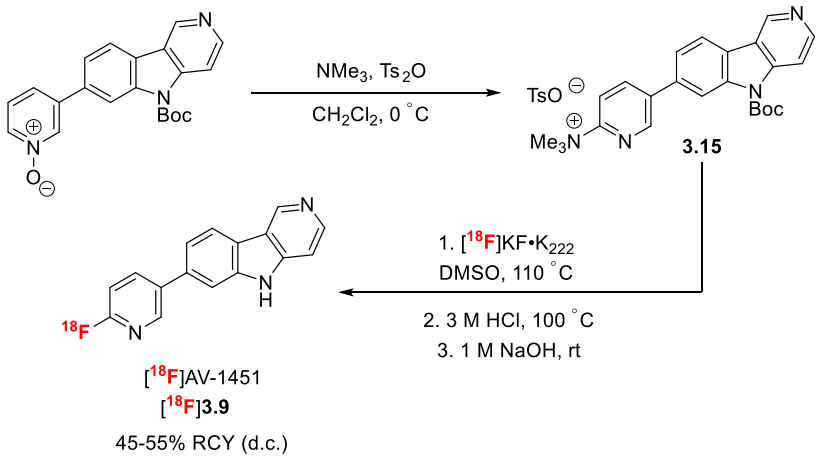
This key advantage has rendered ammonium precursors attractive for radiotracer synthesis *via* nucleophilic (hetero)aromatic radiofluorination. As a charged precursor, it can also be more easily purified from neutral ^{18}F-products. While HPLC purification is still routinely used for tracer radiosynthesis, there are several reports of HPLC-free purification using solid-phase extraction cartridges in reactions of trimethylammonium salts. For example, the radiosynthesis of prostate cancer tracer [^{18}F]DCFPyL ([^{18}F]**3.14**) from a trimethylammonium salt has been reported using both conventional HPLC purification and later with a HPLC free, cartridge-based purification, exploiting the lower affinity of charged and polar molecules for C18 phases compared to neutral molecules. (Scheme 3.22).[44,45] A post-labelling *tert*-butyl ester deprotection step could also be avoided (Scheme 3.22 b). With the removal of HPLC purification and deprotection, [^{18}F]**3.14** could be obtained in approximately 50% faster synthesis time.

Despite these advantages, the synthesis of trimethylammonium salts can limit their application, particularly for complex targets bearing sensitive functional groups. The preparation of these precursors often requires late-stage methylation of a dimethyl (hetero)aryl amine.[46] Such protocols often require electrophilic methylating reagents, usually iodomethane or methyl triflate, which could react unselectively with other nucleophilic

groups present in the target. Another route requires the use of nucleophilic trimethylamine in an S_NAr reaction, which could present challenges at late synthetic stage.[47] Electrophilic reagents such as trimethylsilyl triflate are often used to promote the anion metathesis of chloride to triflate and this may also be reactive towards nucleophilic groups. A recent study disclosed a route to 2-pyridyltrialkylammonium salts from pyridine-*N*-oxides that could be applied in radiolabelling.[48] The conditions reported used an excess of trimethylamine in combination with acetic or sulfonic acid anhydrides to activate the pyridine *N*-oxide. The value of the method was demonstrated with the radiosynthesis of the radiotracer [^{18}F]AV-1451 ([^{18}F]**3.9**) *via* trimethylammonium tosylate **3.15** (Scheme 3.23). As this approach exploits the reactivity of pyridine *N*-oxide substrates, it should be noted that these conditions are limited to the synthesis of ^{18}F-2-fluoropyridines and is likely not amenable to other classes of *N*-heterocycles.

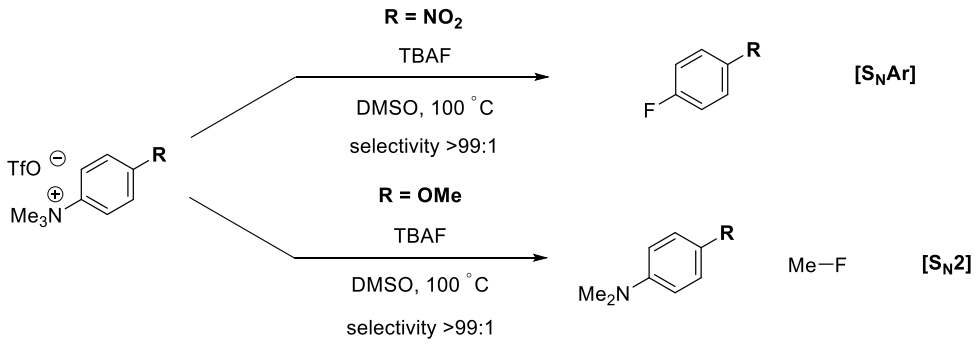


Scheme 3.22. *Radiosynthesis of PET radiotracer [^{18}F]DCFPyL ([^{18}F]**3.14**) via S_NAr radiofluorination of a trimethylammonium precursor, with a) preparative HPLC purification and b) SPE cartridge-based purification.*



Scheme 3.23. *Radiosynthesis of PET radiotracer [^{18}F]AV-1451 ([^{18}F]**3.15**).*

A further challenge with the use of trimethylammonium precursors for S_NAr radiofluorination has been the possibility of these substrates to engage in competing S_N2 side-reactivity with [^{18}F]fluoride.[49] Such processes liberate gaseous [^{18}F]fluoromethane, which could lead to reduced AY of the desired product and also presents safety concerns from the liberation of radioactive gas. DiMagno and Sun studied this side-reactivity on a range of aryl trimethylammonium salts and found that higher selectivity for S_NAr reactivity was observed when the arene was substituted with electron-withdrawing groups, but for electron-neutral or electron-rich groups fluoromethane was the major product (Scheme 3.24).[50]



Scheme 3.24. *Reactivity of aryl trimethylammonium triflates with TBAF via S_NAr or S_N2 pathways.*

3.1.2.4. ^{18}F-S_NAr from Other Precursors

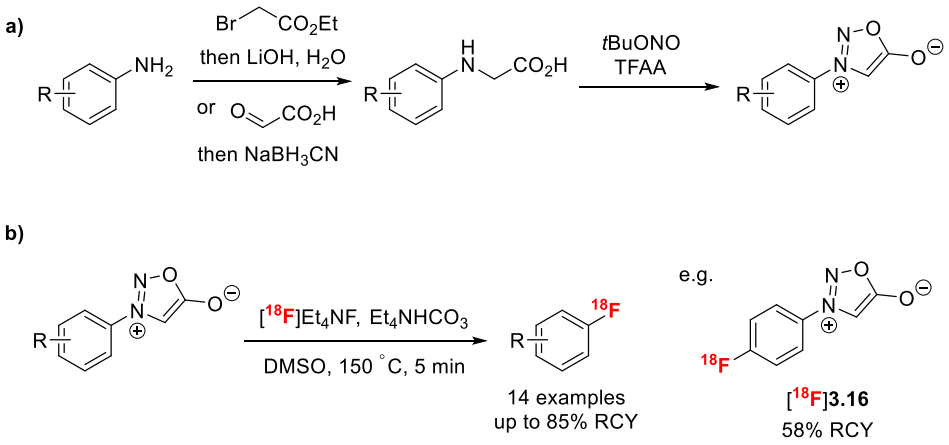
As discussed in Chapter 1, various other precursor types have been disclosed that are sufficiently activated to engage in substitution reactivity with [^{18}F]fluoride. Successful substrate classes have included (hetero)aryl sulfonium and iodonium salts, however it has been suggested that these do not proceed *via* a classical S_NAr mechanism, rather *via* an

associative mechanism at the heteroatom.[51] Ritter and co-workers also translated their aromatic deoxyfluorination platform described in section 3.1.1 to ^{18}F-fluorination, however they found the scope of this transformation was limited to electron-deficient substrates.[20] They were successful extending the scope of their reaction using RuCp(cod)Cl as an additive, which reacts with the phenol to form an η^6-complex, removing electron density from arene and thus activating it towards S_NAr.[52]

As described in section 3.1.2.3, ammonium functional groups display excellent reactivity in S_NAr radiofluorination and the substitution of aniline-derived nitrogen-based functionality has also been demonstrated to be a viable approach to aryl ^{18}F-fluorides. Such deaminative transformations are of interest for ^{18}F-radiochemistry, as anilines and aminoheterocycles are commonly encountered in natural products and used as synthetic/functional handles in synthetic chemistry. As such, many amines are commercially available, which renders them well suited as starting materials for radiochemical transformations. They also display orthogonal reactivity to conventional functional handles commonly used for pharmaceutical discovery, which means their substitution reactivity can be unmasked late-stage by (poly)alkylation or pyridinium salt formation.[53]

Murphy and co-workers reported the aromatic substitution of aniline-derived aryl sydnones with [^{18}F]fluoride in 2017.[54] Aryl sydnones are most commonly used as starting materials in 1,3-dipolar cycloaddition and can be obtained in two steps from the aniline (Scheme 3.25 a). Firstly, the aniline is converted to an *N*-aryl glycine by either reductive amination with glyoxylic acid or alkylation with ethyl bromoacetate. This intermediate is then cyclised with *tert*-butyl nitrite and trifluoroacetic anhydride to yield the aryl sydnone. These substrates are then reacted with [^{18}F]fluoride in DMSO solvent at 150 °C. This gave access to an array of small molecule (hetero)aryl ^{18}F-fluorides (Scheme 3.25 b). It is noteworthy that the majority of the reported examples featured arenes substituted with electron-withdrawing groups,

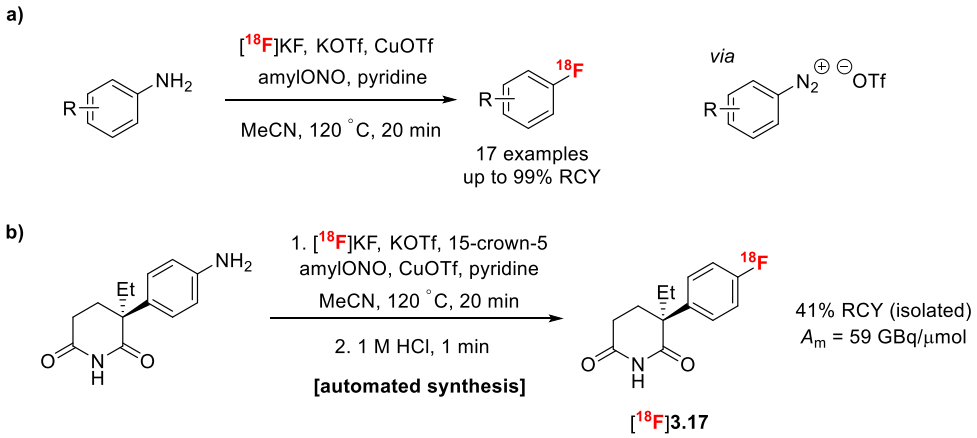
such as nitro, cyano, sulfonyl or carbonyl groups. A bis(sydnone) precursor was then used to prepare [^{18}F]4-fluorophenyl sydnone [^{18}F]**3.16**, which was isolated in good A_m of 48 GBq/µmol. [^{18}F]**3.16** could then be applied in cycloaddition reactions with alkynes for bioconjugation. Murphy and co-workers also demonstrated the radiosynthesis of an ^{18}F-labelled enkephalin peptide with applications in neuroscience. When the mechanism of the reaction was examined using electronic structure calculations, it was found that the ^{18}F-fluorination of aryl sydnones proceeded *via* a stepwise addition-elimination S_NAr mechanism (see section 3.1.1 for further discussion) with a high energy Meisenheimer intermediate.



Scheme 3.25. *Murphy and co-workers radiosynthesis of ^{18}F-fluoroarenes via aryl sydnones. a) Preparation of aryl sydnones, b) Radiofluorination of aniline-derived aryl sydnones, e.g. [^{18}F]**3.16**.*

A further report of deaminative radiofluorination, complementary to the report from Murphy and co-workers, emerged in 2021 (Scheme 3.26).[55] Rather than exploiting S_NAr reactivity of nitrogen-based leaving groups, Riss and co-workers instead disclosed conditions for a ^{18}F-fluoro-Sandmeyer reaction that enabled access to ^{18}F-fluoroarenes from the relevant aniline (Scheme 3.26 a). This proceeded *via* a diazotisation-^{18}F-fluorination sequence, where an aryl diazonium salt was first formed from amyl nitrite and the aniline in MeCN solvent. The crude diazonium salt and a separate solution of CuOTf and pyridine could then be added to azeotropically dried [^{18}F]fluoride and upon heating at 120 °C, this yielded the desired aryl ^{18}F-product. The reaction was amenable to various small molecule arenes, as well as a complex molecule tracer, (−)-4-[^{18}F]fluorogluthetimide ([^{18}F]**3.17**), the radiosynthesis of which was

successfully automated on a Synthra RN plus module (Scheme 3.26 b). A key limitation of this reaction was that it could not be applied to heteroaromatic substrates. The reaction of such substrates trialled by Riss and co-workers failed, for example 2-aminopyridine was not amenable to radiofluorination with this method. This could be due to the coordination of nitrogen-containing heterocycles to the Cu-complex, in line with our group's observations for the Cu-mediated ^{18}F-fluorodeboronation of aryl boronic esters.[56]



Scheme 3.26. *Sandmeyer ^{18}F-fluorination of anilines a) Reaction overview, b) Application to the radiosynthesis of [^{18}F]**3.17**.*

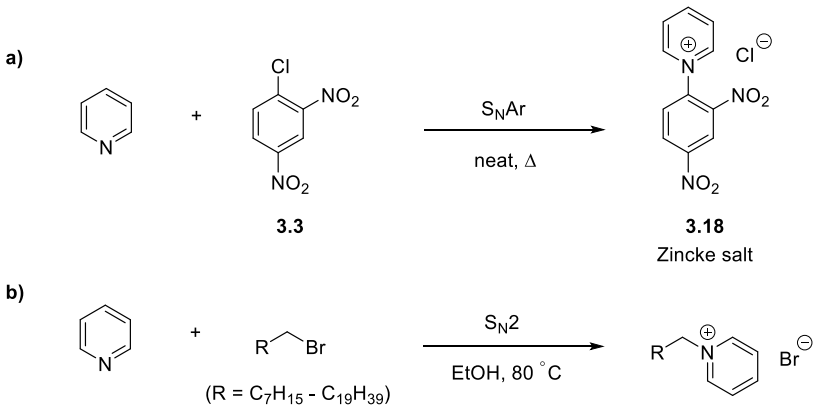
3.1.3. The Synthesis and Reactivity of Pyridinium Salts

Over the past century, pyridinium salts have emerged as synthetically useful intermediates, and also feature in natural products as well as in bioactive molecules.[57] They are ionic compounds, with the pyridinium moiety bearing a positive charge, which is formally localised on the pyridine nitrogen. This property has significant implications on the reactivity of pyridinium salts, which can be engaged as substrates in both one and two-electron chemistries. This section will consider their preparation and application in organic synthesis.

3.1.3.1. Synthetic Approaches towards Pyridinium Salts

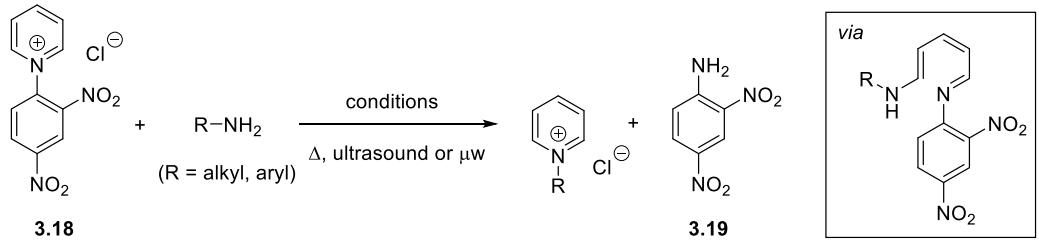
At the start of the 20th century, Theodor Zincke reported the reaction of pyridine with **3.3**, which led to the synthesis of an aryl pyridinium chloride salt **3.18**, *via* the displacement of a chloride leaving group (Scheme 3.27 a).[58,59] The product **3.18** is commonly referred to as a Zincke salt. Beyond this example of an S_NAr-type reaction, the reactivity of pyridine

nucleophiles with electrophiles represents a general route to pyridinium salts. For example, reaction partners, such as alkyl halides, can be applied in S_N2-type reactions with pyridine to access alkyl pyridinium salts (Scheme 3.27 b).[60]



Scheme 3.27. *Synthesis of pyridinium salts via a) S_NAr-type reactivity of pyridine, b) S_N2-type reactivity of pyridine.*

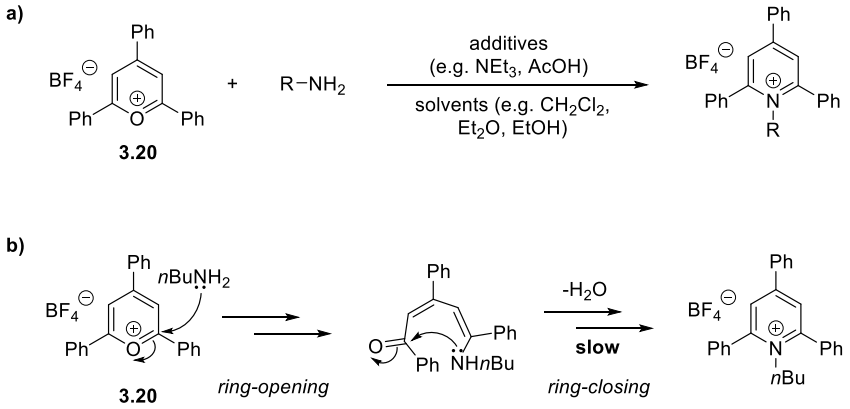
Zincke found that **3.18** displayed interesting reactivity towards primary amines (Scheme 3.28). The reaction (the Zincke reaction) gave a second pyridinium salt and aniline **3.19**, which were formed in an 'ANRORC' (Addition of the Nucleophile-Ring Opening-Ring Closure) mechanism, where the nucleophilic amine adds to the Zincke salt to affect a ring-opening, followed by a ring-closing cyclisation, which eliminates aniline **3.19**.[59,61]



Scheme 3.28. *The Zincke reaction with primary amine nucleophiles.*

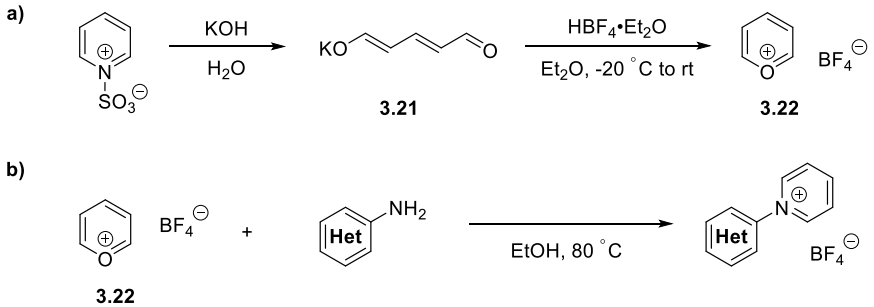
In addition to the Zincke reaction, primary amines can also be converted to pyridinium salts by condensation with pyrylium salts (Scheme 3.29 a).[62] This represents a highly convenient approach to pyridinium salts, as primary amines are a common class of substrates, and many are available commercially. Various pyrylium reagents are also available commercially or can be conveniently prepared *via* single-step condensation reactions of carbonyl compounds.[62,63] For example, 2,4,6-triphenylpyrylium tetrafluoroborate (**3.20**) can be prepared from the condensation of acetophenone and benzaldehyde with boron trifluoride etherate.[63] The

reaction of primary amines with pyrylium salts has been investigated extensively; Katritzky conducted many key studies in the field. This reaction is also suggested to proceed *via* an ANRORC-type mechanism; in a ^{13}C NMR study of the reaction of *n*-butylamine and 2,4,6-triphenylpyrylium tetrafluoroborate (**3.20**), rapid formation of ring-opened divinylogous amide intermediates was observed.[64] Katritzky and co-workers suggested that these intermediates then cyclise slowly to furnish the desired pyridinium salt (Scheme 3.29 b).



Scheme 3.29. *The synthesis of pyridinium salts from primary amines and pyrylium salts. a) General reaction conditions, b) Proposed ANRORC mechanism by Katritzky and co-workers.*

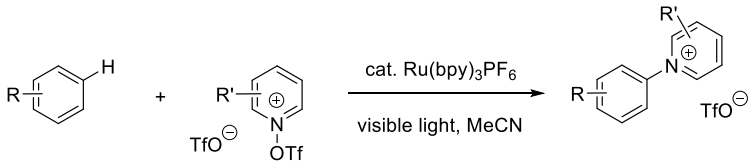
Cornella and co-workers also reported a synthesis of pyrylium tetrafluoroborate (**3.22**) from the acid-mediated cyclisation of enolate **3.21**, which was obtained by the hydrolysis of pyridine sulfur trioxide with KOH (Scheme 3.30 a).[53,65] This pyrylium reagent was shown to be reactive towards anilines at 80 °C in EtOH solvent with (hetero)aryl pyridinium tetrafluoroborates being obtained as the product (Scheme 3.30 b).



Scheme 3.30. *a) Synthesis of pyrylium tetrafluoroborate (**3.22**); b) Overview of condensation reactivity of **3.22** with anilines.*

In addition to these approaches, several groups have also reported conditions for the pyridination of arenes. The Ritter laboratory and the groups of Togni and Carreira

simultaneously reported that pyridyl radical cations generated by the reduction of *N*-sulfonyloxypyridinium triflates were reactive towards arenes, to yield aryl pyridinium triflate salts (Scheme 3.31).[66,67] Zincke aminolysis of these products could then furnish the C–H aminated product. In a separate approach, Sanford and co-workers demonstrated that aryl radical cations generated photocatalytically from arenes and aryl halides were also reactive towards pyridine, yielding aryl pyridinium hexafluorophosphate salts.[68] They later demonstrated that the use of an external photocatalyst was not required, as pyridine-arene electron donor-acceptor complexes could be excited directly with visible light under acidic conditions.[69]

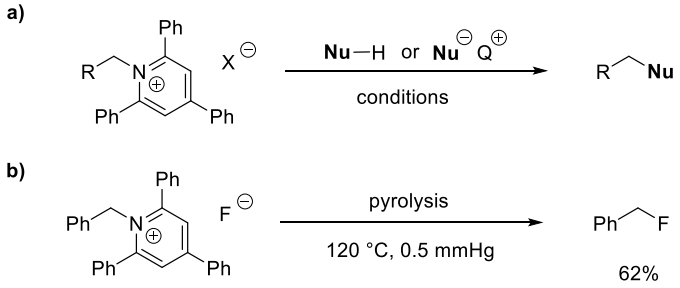


Scheme 3.31. *Ritter's and Carreira's approach to aryl pyridinium salts from N-trifyl pyridinium reagents.*

3.1.3.2. The Reactivity of Pyridinium Salts

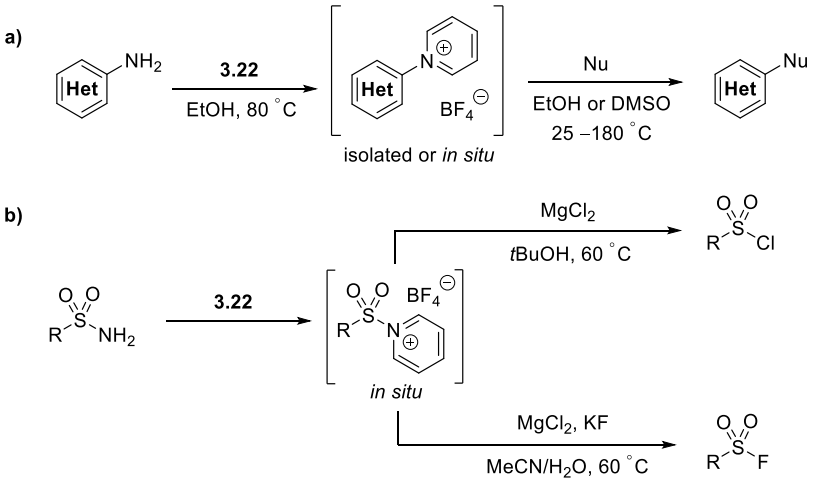
As positively charged species, pyridinium salts are electrophilic and can thus be readily engaged by nucleophiles. A prevalent application of pyridinium salts in organic synthesis is the use of 4-dimethylaminopyridine (DMAP) as a nucleophilic catalyst in acylation reactions.[70] Acyl halides, acid anhydrides and other activated carboxylic acids react with DMAP to give an *N*-acyl pyridinium intermediate that reactive towards nucleophiles.[71]

Katritzky studied the reactivity of pyridinium salts towards various nucleophiles extensively.[63,72] His group reported the conversion of primary amines into myriad functionalities (including halides, esters, azides, (thio)ethers, sulfones, nitrates *etc*.) *via* S_N2-type reactions of pyridinium salt intermediates (Scheme 3.32 a). Fluorination of alkyl pyridinium salts was notably challenging, requiring pyrolytic conditions for the formation of the desired alkyl fluoride product (Scheme 3.32 b).[73]



Scheme 3.32. *Katritzky's work on the reactivity of alkyl pyridinium salts with nucleophiles. a) Reaction overview; b) Pyrolysis of pyridinium fluoride salts for fluorination.*

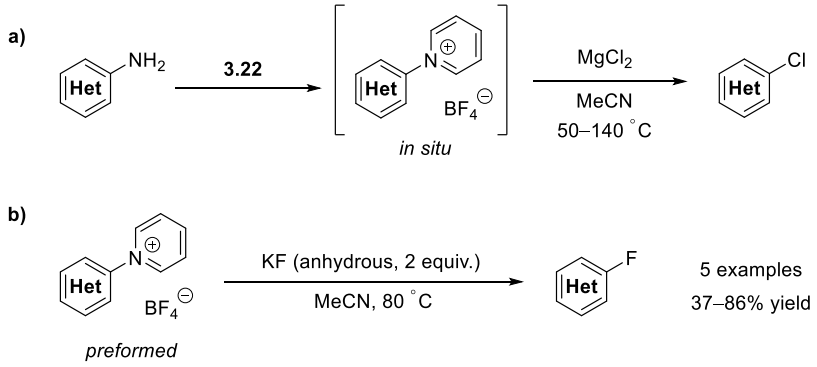
Cornella and co-workers have recently disclosed several deaminative transformations of (hetero)anilines, relying on the use of pyridinium salts formed from pyrylium reagent **3.22** as electrophiles. Firstly, in 2018, they demonstrated that heteroaryl pyridinium salts were reactive towards primary and secondary aniline, alcohol, phenol, thiophenol and sulfinate nucleophiles in a two-step, one-pot deaminative process from the relevant heteroaryl amine (Scheme 3.33 a).[53] In addition, they found that sulfonamides could also be converted to sulfonyl chlorides using **3.22** and $MgCl_2$ and sulfonyl fluorides could also be obtained with the addition of KF (Scheme 3.33 b).[74,75]



Scheme 3.33. *Cornella and co-workers' deaminative functionalisation platform using **3.22**. a) Deaminative functionalisation of aminoheterocycles with O,S,N-nucleophiles (Nu); b) Deaminative chlorination and fluorination of sulfonamides.*

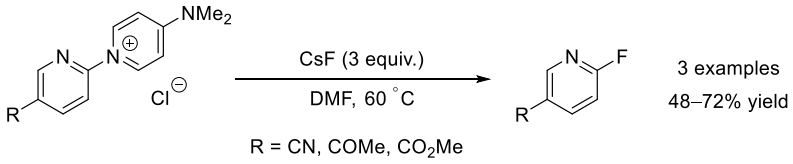
In 2022, Cornella and co-workers extended this reactivity to deaminative chlorination.[76] Using $MgCl_2$ as a chloride source and in the presence of **3.22**, aminoheterocycles were converted to heteroaryl chlorides with the formation of heteroaryl pyridinium tetrafluoroborates *in situ* (Scheme 3.34 a). The same strategy could also be applied to bromination with LiBr or $MgBr_2$

as bromide sources. However, fluorination was found to be more challenging; the formation of heteroaryl fluorides only proceeded using rigorously dried KF and when the preformed pyridinium tetrafluoroborate was used as a substrate (Scheme 3.34 b). Nonetheless, this demonstration that fluoride nucleophiles were reactive towards heteroaryl pyridinium salts was of significant interest.



Scheme 3.34. *Cornella and co-workers' deaminative halogenation platform using* ***3.22****. a) Deaminative chlorination of aminoheterocycles; b) Fluorination of pyridinium tetrafluoroborate salts with KF.*

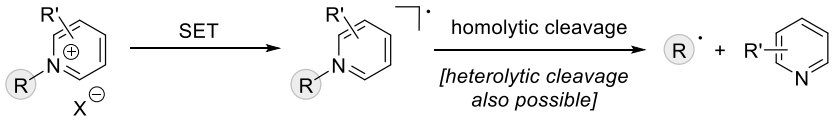
Osborne and co-workers also disclosed a study into the reactivity of heteroaryl pyridinium salts derived from DMAP with fluoride nucleophiles (Scheme 3.35).[77] Firstly, 2-chloropyridines were reacted with DMAP in THF to yield pyridinium chloride salts. However, this synthesis was found only to be effective for the preparation of pyridinium salts derived from electron-deficient pyridines. In a subsequent fluorination step, the isolated pyridinium salts could then be converted to the requisite fluoride using an excess of CsF in DMF solvent at 60 °C, in three examples.



Scheme 3.35. *Osborne and co-workers' fluorination of DMAP-derived pyridinium chloride salts with CsF.*

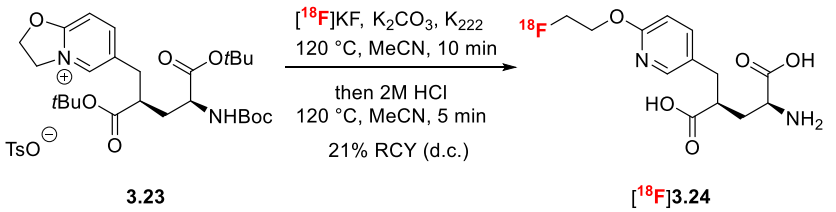
As redox-active species, pyridinium salts can also be readily exploited to generate radicals.[78,79] This occurs by the reduction of the pyridinium salt, which produces a neutral radical that can fragment either homolytically or heterolytically (Scheme 3.36). Homolytic cleavage produces

a second radical that can be engaged, for example, in Minisci or Giese-type reactivity, as well as in transition metal catalysed cross-coupling.



Scheme 3.36. *Radical generation from pyridinium salts via single-electron transfer (SET).*

The application of pyridinium salts as substrates in F-18 radiochemistry is limited and only two examples have been reported. In a first example, cyclic pyridinium tosylate **3.23** was reactive towards [^{18}F]fluoride to yield the alkyl ^{18}F-fluoride **3.24** (Scheme 3.37).[80] Secondly, Young and co-workers demonstrated the application of α-(di)fluorinated alkyl pyridinium salts in the radiosynthesis of ^{18}F-fluoroalkyl compounds (see Chapter 2, section 2.1.3.2 for a full discussion of this method).[81]



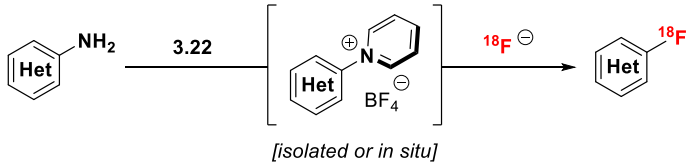
Scheme 3.37. *^{18}F-Fluorination of alkyl pyridinium tosylate **3.23** to [^{18}F]**3.24**.*

3.1.4. Project Outline

The limited application of pyridinium salts in radiofluorination described in section 3.1.3.2 is surprising, as they possess numerous advantageous properties which render them well suited as substrates for radiofluorination. For example, as ionic molecules, they are able to participate in ion pairing with [^{18}F]fluoride, which could enable elution of [^{18}F]fluoride from ion exchange cartridges used in the separation of [^{18}F]fluoride from target water (Chapter 1, section 1.3.2). Furthermore, their charged nature should facilitate the separation of neutral radiofluorinated products from the excess of charged labelling substrates. In contrast, the separation of neutral products and starting materials has been shown to present challenges on complex targets (e.g. [^{18}F]**3.9**). Finally, as illustrated in section 3.1.3.1, pyridinium salts are

easily prepared by an array of different methods; most conveniently by the late-stage condensation of readily available aniline precursors with pyrylium reagents.

Inspired by these advantages, as well as the promising reactivity of pyridinium salts towards nucleophiles and their underutilisation in radiochemistry, the work described in this chapter aims to open the field of pyridinium-based radiolabelling, with the development of novel radiofluorination methodology using pyridinium salts as substrates. Specifically, this chapter discloses the discovery, optimisation and evaluation of a deaminative ^{18}F-fluorination of heteroaryl pyridinium tetrafluoroborates (Scheme 3.38).



Scheme 3.38. *Project overview.*

In doing so, we proposed to expand the current utility of ^{18}F-fluorodeamination for the preparation of structurally diverse and complex ^{18}F-fluoroheteroarenes. In order to maximise the value of the method to radiochemistry practitioners, we aimed to design an operationally simple reaction that provided ^{18}F-fluoroheteroarenes in good RCY that could be readily translated to automated synthesis, while ensuring the method did not require transition metal additives that would complicate quality control protocols. Such advantages reduce the barrier to (pre)clinical translation and will encourage the adoption of the novel radiochemistry disclosed herein by radiochemists.

3.2. Results and Discussion

3.2.1. Reaction Design

3.2.1.1. Initial Considerations

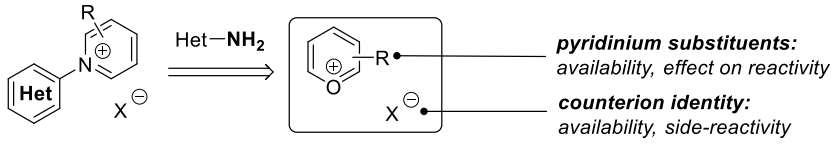
As the groups of Cornella and Osborne had demonstrated that the fluorination of heteroaryl pyridinium salts was within reach using alkali metal fluoride salts (section 3.1.3.1),[76,77] as a starting point for our studies we opted to investigate the reactivity of heteroaryl pyridinium salts with [^{18}F]KF.

The nature of the pyridinium salts that we proposed to use as substrates was first considered. As we aimed to develop a reaction that was valuable to radiochemistry practitioners, we decided to prepare all substrates from anilines, which could be readily condensed with pyrylium reagents to yield the desired pyridinium salt in a single step, chromatography-free synthesis that would be applicable at late-stage. As the choice of pyrylium reagent could affect the reactivity of the pyridinium salts towards [^{18}F]fluoride, this was first carefully considered (Scheme 3.39).

Firstly, as Cornella and co-workers disclosed in reactions of pyridinium salts with aniline nucleophiles, the substitution of the pyridinium scaffold with functional groups was suggested to have a detrimental effect on reactivity.[53] For this reason, substituted pyrylium reagents, such as 2,4,6-triphenylpyrylium tetrafluoroborate (**3.20**), were avoided. Protocols for the preparation of 4-substituted pyrylium salts are scarce, and where available, these are predominantly limited to alkyl, alkoxy or aryl groups. For these reasons, we focused our attention on the use of unsubstituted pyrylium reagents.

Secondly, nucleophilic counterions, such as chloride and bromide, were avoided. We surmised that these might compete with [^{18}F]fluoride for the pyridinium substrate and therefore non-nucleophilic anions would be preferred. As we aimed to prioritise substrate

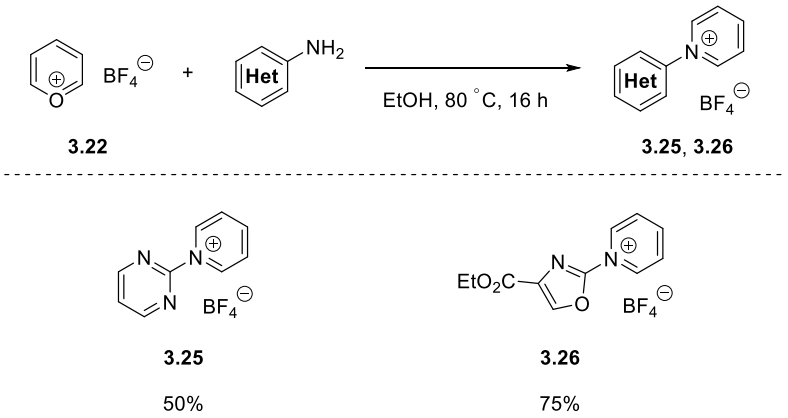
accessibility by applying a synthetic route from heteroanilines, the commercial availability and/or synthetic accessibility of the pyrylium reagent should also be taken into account. For example, a synthesis of pyrylium triflate has not been disclosed. A synthesis of pyrylium perchlorate has been reported, however the use of perchlorate salts presents potential safety hazards, as perchlorate salts can be explosive.[82] Pyrylium tetrafluoroborate (**3.22**) was an appealing candidate; the reagent is commercial or easily prepared *via* a well-precedented route (Scheme 3.30).[65] Its condensation reactivity with amines is also well-established in numerous reports.[53,76]



Scheme 3.39. *Substrate design strategy and key considerations.*

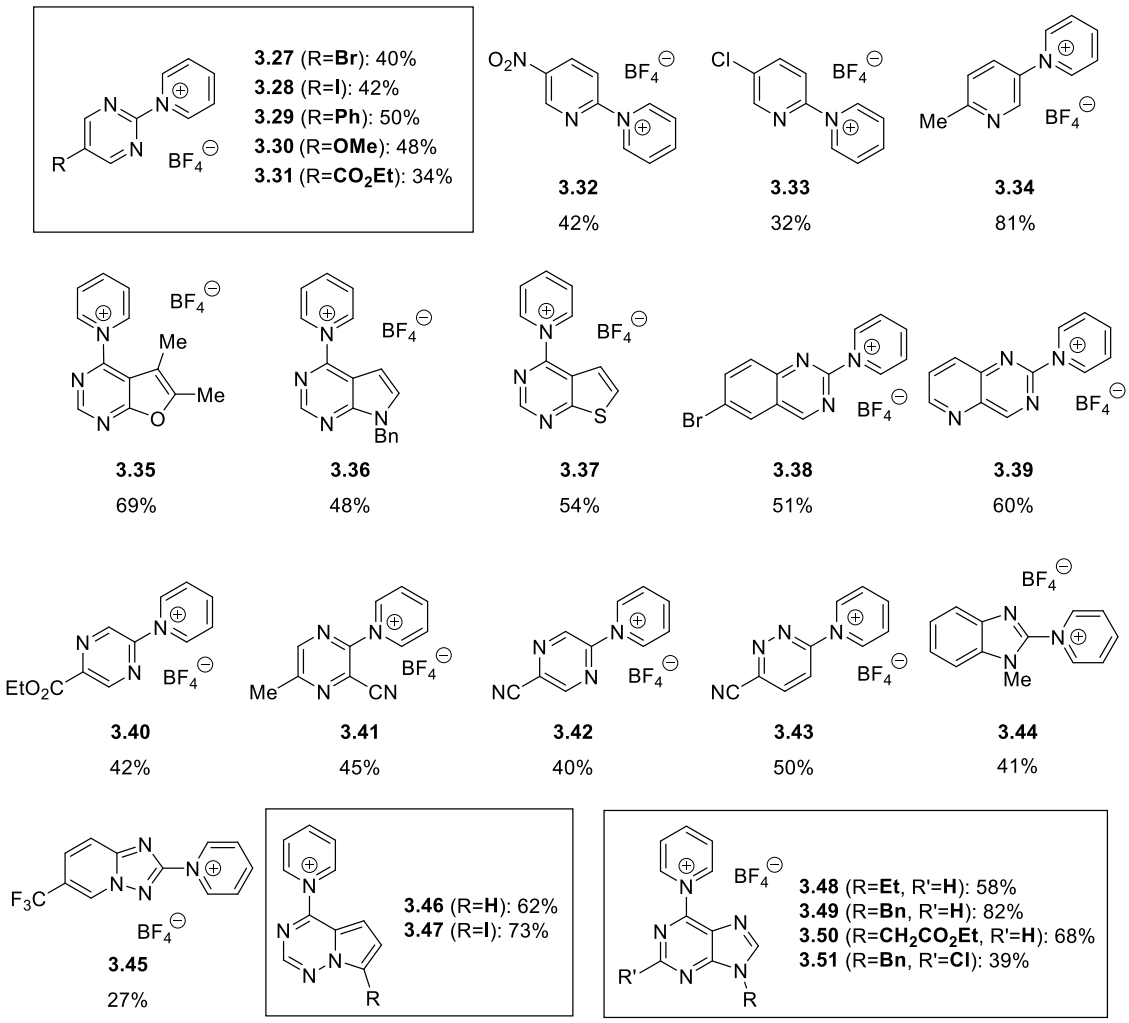
3.2.1.2. Synthesis of Pyridinium Tetrafluoroborate Substrates

For initial studies, two pyridinium tetrafluoroborates derived from small molecule heteroaromatic amines were selected as model substrates (**3.25** and **3.26**). These were obtained by condensation of the relevant amine with 1 equiv. of pyrylium salt **3.22**, which were heated overnight at 80 °C in EtOH solvent. Further experimental details are available in Chapter 4.



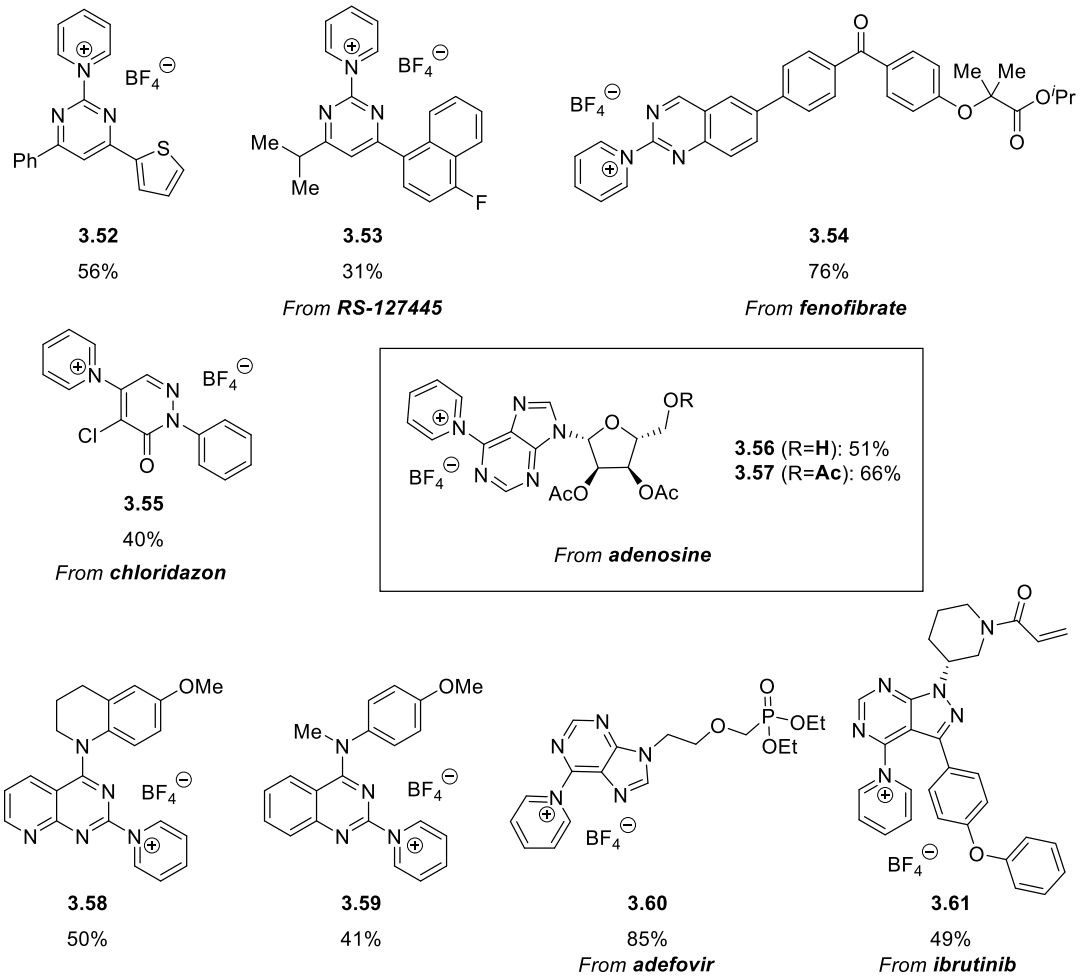
Scheme 3.40. *Synthesis of model pyridinium tetrafluoroborates **3.25** and **3.26**. Yields given are isolated yields.*

Later, a scope of small molecule heteroaryl pyridinium salts were also isolated using the same procedure. These were to be used in assessing the scope and limitations of the method (Scheme 3.41) (section 3.2.4).



Scheme 3.41. *Synthesis of small molecule pyridinium tetrafluoroborates* ***3.27–3.51****. Yields given are isolated yields. Further experimental details are available in Chapter 4.*

In order to highlight the value of the method to radiochemistry practitioners, an important consideration is that the method tolerates molecules representative of the complexity of pharmaceutical compounds. To this end, further examples of heteroaryl pyridinium tetrafluoroborate salts derived from complex and/or bioactive molecules were also prepared following this procedure (Scheme 3.42).



Scheme 3.42. *Synthesis of bioactive molecule-derived pyridinium tetrafluoroborates* ***3.52–3.61****. Yields given are isolated yields. Further experimental details are available in Chapter 4.*

3.2.2. Reaction Discovery and Optimisation

3.2.2.1. Initial Experiments

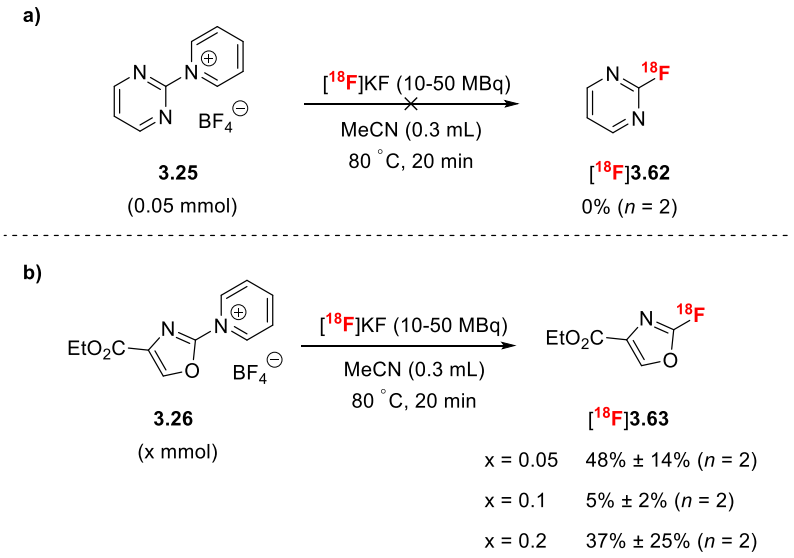
In first experiments, we aimed to assess whether heteroaryl pyridinium salts were sufficiently electrophilic to react with [^{18}F]fluoride. We anticipated that translation of ^{19}F-fluorination conditions to ^{18}F-fluorination could present challenges, as there are several significant differences when working under radiochemical conditions. Firstly, as solutions of reactive [^{18}F]fluoride are prepared by eluting ion exchange resins with solutions of inorganic bases in organic solvents, the concentration and identity of this inorganic base has been shown to be a key parameter in ^{18}F-radiochemical reaction development. As discussed in Chapter 1, stronger bases have been shown to be detrimental in reactions of substrates prone to

elimination, for example.[83] Secondly, as the concentration of [^{18}F]fluoride is significantly lower than the concentration of substrate, reagents and additives, radiolabelling reactions often proceed under pseudo-first order kinetics, with the radiofluorinated species as the limiting reagent.[84] Therefore, the reaction can be expected to proceed under a substantially different kinetic regime under radiochemical conditions. This perturbation can be detrimental for or even prohibit reactivity in some cases.

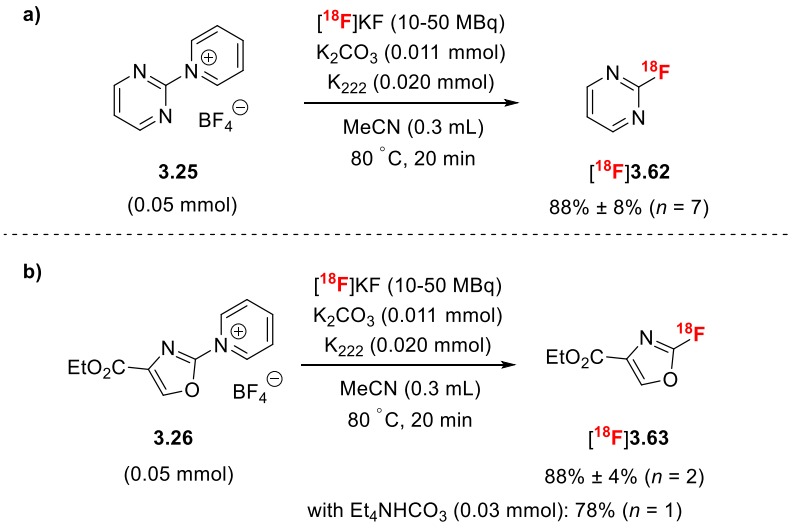
With these potential challenges in mind, model substrates **3.25** and **3.26** were selected for preliminary studies, as both of these had been demonstrated to display excellent reactivity towards nucleophiles in reports from Cornella and co-workers. For these experiments, a solution of [^{18}F]KF.K_{222} was prepared by the trapping of the target water solution of [^{18}F]fluoride on a Waters Sep-Pak QMA Carbonate cartridge, followed by elution with a solution of K_2CO_3 and K_{222} in an MeCN/H_2O mixture. The eluate was then azeotropically dried at elevated temperature under a stream of N_2 gas, before being redissolved in MeCN. Aliquots of this solution were used for our preliminary experiments.

Reacting **3.25** with an aliquot of [^{18}F]KF under model conditions gave no RCY_{HPLC} of the desired radiofluorinated product [^{18}F]**3.62** (Scheme 3.43 a). Meanwhile, reacting **3.26** under the same conditions did furnish the desired product in up to 48% RCY_{HPLC}. However, upon conducting further optimisation experiments, such as varying the loading of substrate **3.26**, it was found that the yield could vary significantly, leading to irreproducible reactivity (Scheme 3.43 b). We surmised that the concentration of elution reagents could be an important factor, as this could vary between aliquots.

In order to probe this further, the addition of the elution reagents K_2CO_3 and K_{222} was next trialled in quantities representative of those used during the preparation of reactive [^{18}F]fluoride in PET radiotracer production (Scheme 3.44).[83] This appeared to have two effects. Firstly, the presence of K_2CO_3 and K_{222} in higher concentration led to increases in the



Scheme 3.43. *Preliminary ^{18}F-fluorination experiments using a) substrate **3.25**, b) substrate **3.26**. Indicated yields are RCY$_{HPLC}$ values, determined by radio-HPLC analysis of the crude reaction mixture.*



Scheme 3.44. *Preliminary ^{18}F-fluorination experiments in the presence of elution additives using a) substrate **3.25**, b) substrate **3.26**. Indicated yields are RCY$_{HPLC}$ values, determined by radio-HPLC analysis of the crude reaction mixture.*

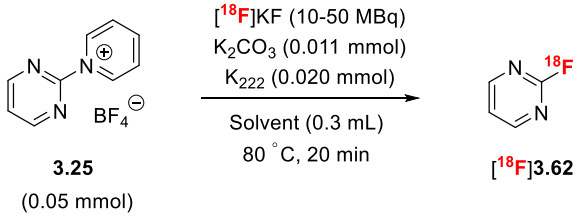
RCY$_{HPLC}$ of desired product in both cases. In the case of [^{18}F]**3.62**, RCY$_{HPLC}$ increased from 0% to 88% with this single modification, and for [^{18}F]**3.63**, RCY$_{HPLC}$ increased from 48% to 88%. Secondly, the standard deviation in the RCY$_{HPLC}$ was also smaller for [^{18}F]**3.63** when the elution reagents were added, suggesting that reactivity was more reproducible in the presence of these additives (Scheme 3.44 b). Finally, the use of an alternative elution base Et_4NHCO_3 was considered in reactions with substrate **3.26** and while this also proved to be effective (RCY$_{HPLC}$ = 78%), the K_2CO_3-K_{222} system was found to be superior (RCY$_{HPLC}$ = 88%) (Scheme 3.44 b). Furthermore, as K_2CO_3 and K_{222} are already very well used for the preparation of [^{18}F]fluoride

in clinical radiotracer production and quality control protocols for residual quanities of these eluents are established, the K_2CO_3-K_{222} system was used for the remainder of the study.[83] The tolerance to these additives also was promising for the scale-up of the reaction, as these will be present in mM concentrations in the reaction mixture, applying a conventional basic [^{18}F]fluoride elution protocol.

3.2.2.2. Effect of Reaction Parameters

With an initial set of conditions in hand, we next assessed the effect of other reaction parameters on the ^{18}F-fluorination of heteroaryl pyridinium salts.

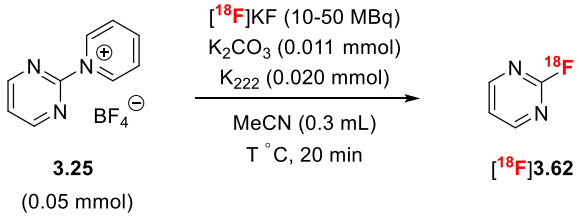
Firstly, various alternative solvents were screened using substrate **3.25** (Table 3.1). As expected for an S_NAr-type ^{18}F-fluorination (see sections 3.1.1 and 3.1.2), polar aprotic solvents performed best. DMSO, DMF and MeCN proved to be excellent candidates for the reaction solvent and all performed similarly well providing [^{18}F]**3.62** in RCY_{HPLC} of over 85% (Table 3.1, entries 1–3). 1,4-dioxane was also an effective solvent, but gave desired product [^{18}F]**3.62** in a slightly lower RCY_{HPLC} of 71% (Table 3.1, entry 4). Polar protic solvents delivered [^{18}F]**3.62** in lower RCY_{HPLC}, with EtOH (56% RCY_{HPLC}) proving superior to MeOH (7% RCY_{HPLC}) (Table 3.1, entries 5–6). The solubility of **3.25** in EtOH was also lower than observed for the other solvents considered, rendering this a poor candidate for the reaction solvent. As ^{18}F-radiotracers are conventionally purified using semi-preparative reverse-phase HPLC, non-polar solvents, such as toluene and dichloromethane, were not assessed, as these may complicate purification. MeCN was carried forward as the preferred solvent, although as is evident from Table 3.1, several viable alternatives exist and could be considered in future application of this method to radiotracer synthesis.



Entry	Solvent	RCY_{HPLC} of [^{18}F]3.62
1	MeCN	88% ± 8% (*n* = 7)
2	DMSO	94% (*n* = 1)
3	DMF	85% (*n* = 1)
4	1,4-dioxane	71% (*n* = 1)
5	EtOH	56% (*n* = 1)
6	MeOH	7% (*n* = 1)

***Table 3.1**. Optimisation of solvent for the ^{18}F-fluorination of **3.25**. RCY_{HPLC} determined by radio-HPLC analysis of the crude reaction mixture.*

The effect of reaction temperature was next evaluated. The reaction was found to operate best at the higher temperature of 80 °C, but [^{18}F]**3.62** still formed efficiently at 50 °C in 67% RCY_{HPLC} (Table 3.2, entries 1–2). Even at 30 °C, formation of [^{18}F]**3.62** was still observed, albeit in a substantially lower RCY_{HPLC} of 13% (Table 3.2, entry 3). This is in line with other S_NAr-type ^{18}F-fluorinations, although temperatures in excess of 100 °C are often required.



Entry	T °C	RCY_{HPLC} of [^{18}F]3.62
1	80 °C	88% ± 8% (*n* = 7)
2	50 °C	67% (*n* = 1)
3	30 °C	13% (*n* = 1)

***Table 3.2**. Optimisation of temperature for the ^{18}F-fluorination of **3.25**. RCY_{HPLC} determined by radio-HPLC analysis of the crude reaction mixture.*

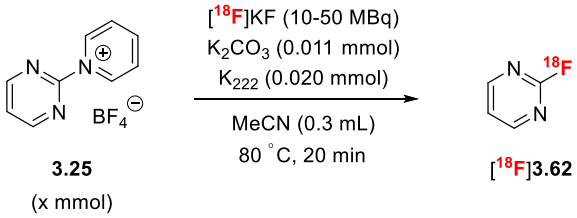
The effect of substrate loading was next assessed (Table 3.3, Figure 3.2). In order to maximise utility to end-users, the loading of substrate should be as low as possible. If smaller quantities of radiolabelling precursor are required per reaction, this reduces the synthesis burden for such precursors, and maximises the number of tracer radiosyntheses that that are possible from a single batch of precursor. Furthermore, it has also been demonstrated that product A_m often is improved at lower substrate loadings, particularly when the starting material contains fluorine (as is the case for pyridinium tetrafluoroborates). Measurement of A_m for products radiolabelled using this method and further discussion of these concepts can be found in section 3.2.7.

The reaction appears to tolerate loadings of **3.25** below 0.05 mmol and this can be reduced as low as 0.017 mmol without any apparent detrimental effect on the RCY_{HPLC} of [^{18}F]**3.62** (Table 3.3, entries 1–3). Beyond this, a reduction in the RCY_{HPLC} of [^{18}F]**3.62** to 29% is observed at a **3.25** loading of 0.01 mmol (Table 3.3, entry 4). Further decreases in **3.25** loading to 0.005 mmol and 0.001 mmol are shown to abolish reactivity (Table 3.3, entries 5–6)**.** Nonetheless, it was pleasing that the reaction operates well down to approximately 10 µmol scale, which is in line with quantities of labelling precursors used for the production of established (pre)clinical tracers (Figure 3.2).[37-39]

For the assessment of the reaction scope in section 3.2.6, it was decided to use the original substrate loading of 0.05 mmol, as it was not known whether the dependence of RCY on substrate loading was a substrate dependent effect. However, reduced substrate loadings were used for product isolation experiments, where A_m would be measured. These experiments are described in section 3.2.7.

Finally, the dependence of RCY_{HPLC} on reaction time was investigated in a time course experiment (Table 3.4, Figure 3.3). The reaction was shown to be rapid and approaches completion with a plateau in RCY_{HPLC} observed after just 10 minutes (Table 3.4, entries 4–6).

This short reaction time is highly suitable for F-18 radiolabelling and is in line with reaction times used in the routine production of (pre)clinical ^{18}F-radiotracers.



3.25
(x mmol)

[^{18}F]**3.62**

Entry	Loading of 3.25 (x)	RCY_{HPLC} of [^{18}F]3.62
1	0.050 mmol	88% ± 8% (*n* = 7)
2	0.025 mmol	92% (*n* = 1)
3	0.017 mmol	91% (*n* = 1)
4	0.010 mmol	29% (*n* = 1)
5	0.005 mmol	0% (*n* = 1)
6	0.001 mmol	0% (*n* = 1)

***Table 3.3**. Effect of substrate loading for the ^{18}F-fluorination of **3.25**. RCY_{HPLC} determined by radio-HPLC analysis of the crude reaction mixture.*

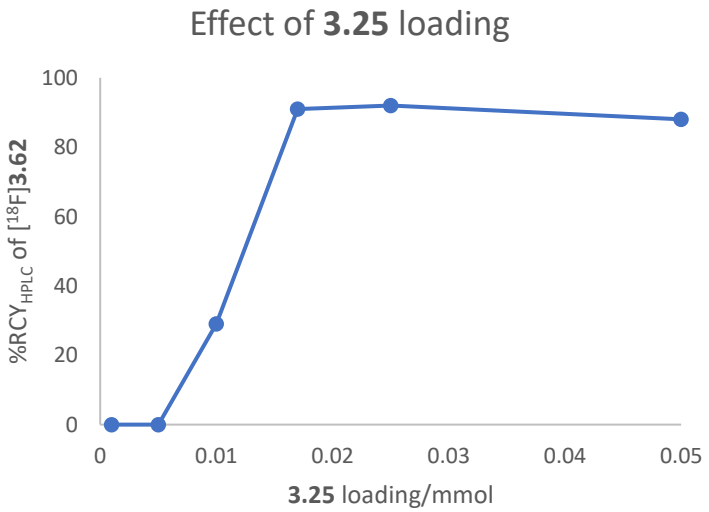
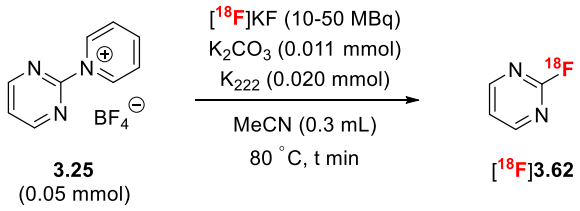


***Figure 3.2**. Graphical representation of the effect of substrate loading for the ^{18}F-fluorination of **3.25**.*



3.25
(0.05 mmol)

[^{18}F]**3.62**

Entry	Reaction time	RCY$_{HPLC}$ of [^{18}F]3.62
1	1 min	19% (*n* = 1)
2	2 min	49% (*n* = 1)
3	5 min	64% (*n* = 1)
4	10 min	82% (*n* = 1)
5	15 min	83% (*n* = 1)
6	20 min	88% ± 8% (*n* = 7)

Table 3.4. *Effect of reaction time for the ^{18}F-fluorination of* ***3.25****. RCY$_{HPLC}$ determined by radio-HPLC analysis of the crude reaction mixture.*

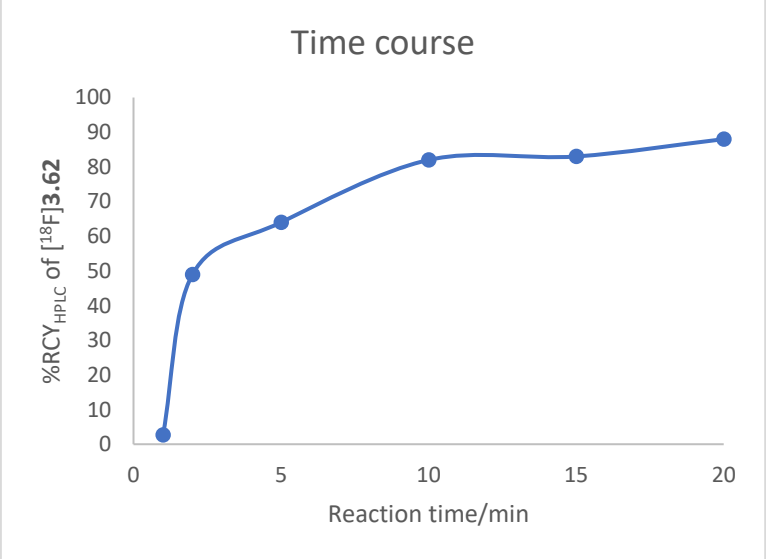


Figure 3.3*. Graphical representation of the time course of ^{18}F-fluorination of* ***3.25****. A separate reaction was run for each timepoint.*

3.2.3. Robustness Screening

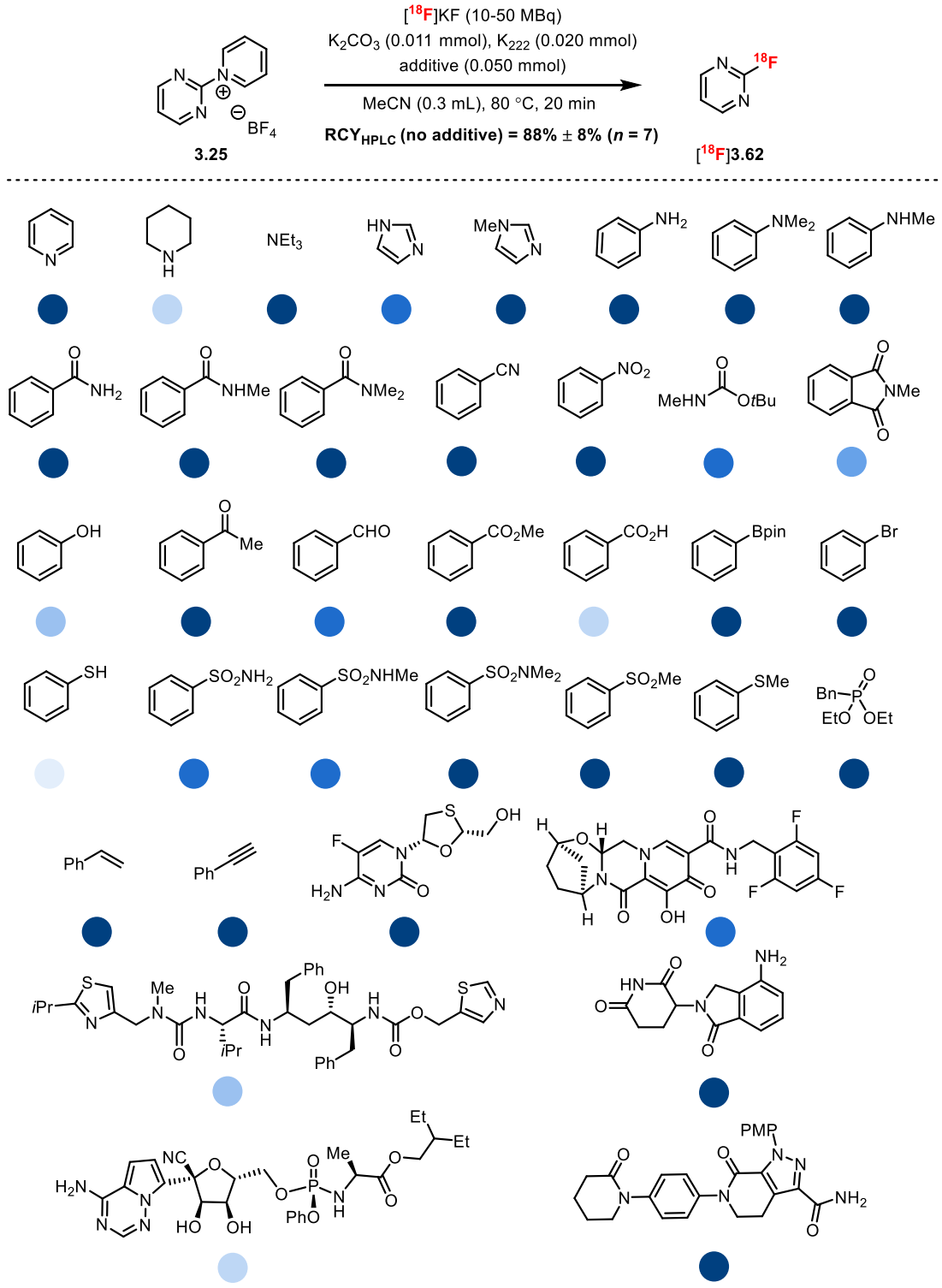
Additive-based robustness screening has emerged as a popular tool for assessing the tolerance of (radio)chemical reactions to common functional groups and heterocycles.[85] Gouverneur and co-workers have demonstrated this concept in PET radioligand synthesis for the Cu-mediated ^{18}F-fluorination of aryl boronic pinacol esters, in which tolerance to various functionalities was first assessed by robustness screening, before radiosynthetic routes to 7 complex bioactive molecules were designed.[86]

We were therefore interested to carry out a similar additive-based robustness screening to assess the tolerance of the radiofluorination of heteroaryl pyridinium salts to common and potentially reactive functionalities, as this would provide information about the possible limitations of our method in advance of evaluating the scope of the reaction. For this study, a diverse panel of 31 small molecule additives representative of those commonly encountered in medicinal and synthetic chemistry were selected. We were particularly interested to investigate the effect of nucleophilic functional groups, as these may consume the electrophilic pyridinium tetrafluoroborate substrate, leading to low/no reactivity. The effect of applying protecting groups to nucleophilic functionalities would also be evaluated, as this would be informative in the design of radiosynthetic routes towards complex ^{18}F-targets. 6 FDA-approved drugs were also selected as additives, to inform on how well structural complexity and complex targets are tolerated.

The additive-based robustness screening was completed by adding a single equivalent of each spiking additive to the ^{18}F-fluorination of model substrate **3.25** under the optimised reaction conditions (Scheme 3.45). [86] The RCY_{HPLC} of each reaction was then compared to that of the control reaction, where no spiking additive was added. The ratio of these RCY_{HPLC} values was then calculated to yield a robustness factor (here expressed as a percentage). This value gives an indication how well the functional group or motif is tolerated.

Firstly, an array of nitrogen-containing functional groups and scaffolds was evaluated. As suggested by the structure of substrates **3.25** and **3.26**, heteroarenes such as pyridine were well tolerated. Nucleophilic imidazole was moderately well tolerated as an additive, however the robustness improved upon substitution of the nitrogen atom with a methyl group. The secondary alkyl amine, piperidine, was not well tolerated, likely as it is sufficiently nucleophilic to react with **3.25** and/or [^{18}F]**3.62**. Basic tertiary alkyl amine triethylamine was completely tolerated. Less nucleophilic amines substituted with aromatic groups, such as aniline, *N*-methylaniline and *N*,*N*-dimethylaniline, were well tolerated, as were primary, secondary and tertiary amides. Derivatives of methylamine substituted with common nitrogen protecting groups, Boc and phthalimide, were next assessed, and were moderately well tolerated. Strongly nucleophilic thiophenol was not tolerated at all, and phenol, which was likely deprotonated and thus rendered more nucleophilic under the reaction conditions, was only poorly tolerated. Other functional groups, such as nitro, cyano, bromide, as well as alkene and alkyne functionalities were well tolerated. Acetophenone, benzaldehyde and methyl benzoate resulted in only small reductions in RCY_{HPLC} of the model reaction when these were used as spiking additives, while benzoic acid led to a much larger decrease in yield. We surmised that under the reaction conditions the excess of free carboxylic acid would easily consume the K_2CO_3 additive, which was earlier shown to be crucial for the radiofluorination (section 3.2.2). Sulfur functionalities, including sulfonamides, sulfones, thioethers, were in general well tolerated as spiking additives, as was a model phosphonate ester. Finally, when the FDA approved pharmaceuticals were trialled as spiking additives, this resulted in variable RCY_{HPLC} of [^{18}F]**3.62**. Three compounds were very well tolerated, while remdesivir resulted in the most significant reduction in the RCY_{HPLC} of the model reaction.

In general, the reaction displays good functional group tolerance to a broad range of functionalities, including those that occur frequently in bioactive molecules. Strong nucleophiles, such as thiols, proved to be the most significant limitation.

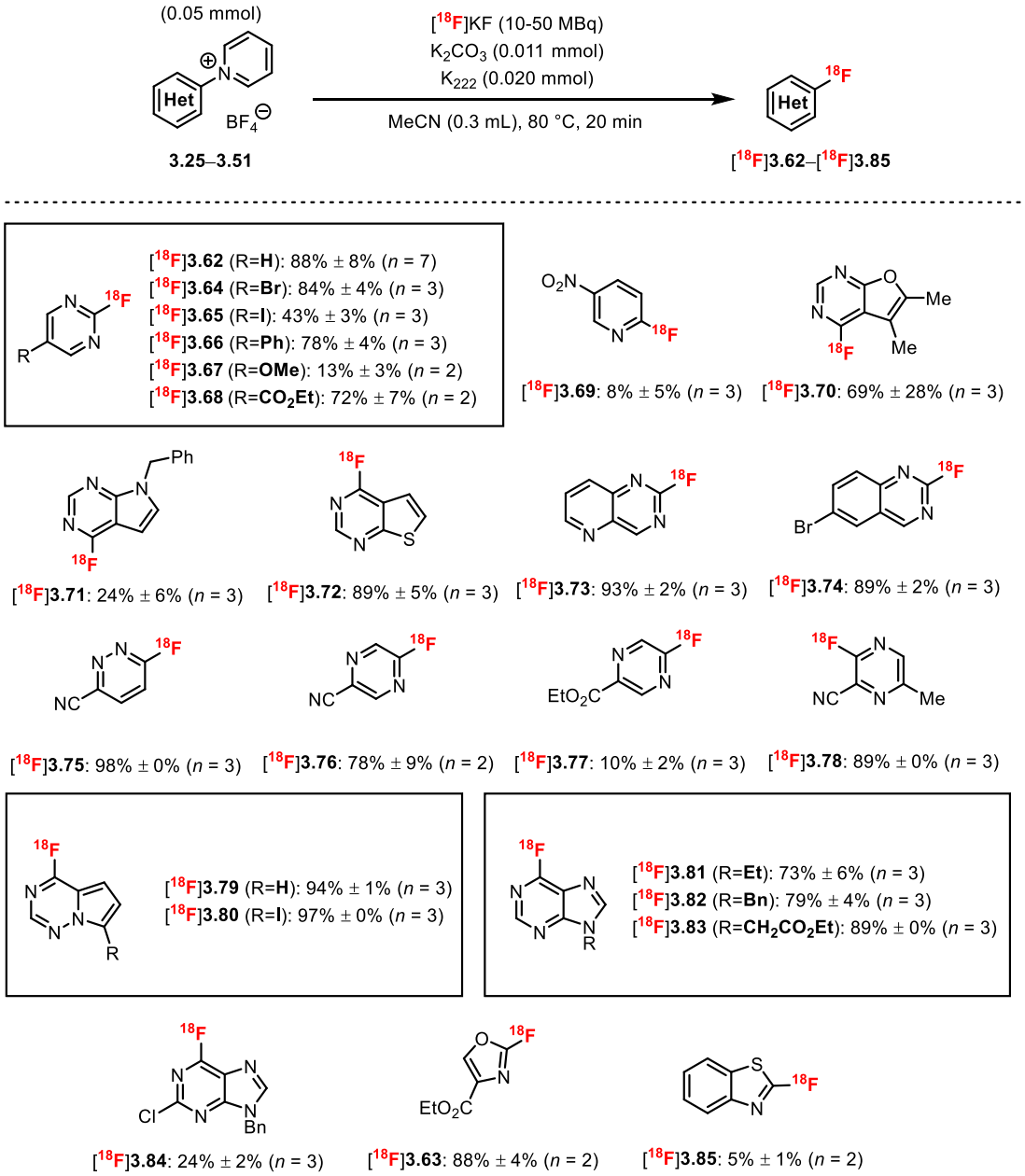


Scheme 3.45. *Robustness screening of the ^{18}F-fluorination of heteroaryl pyridinium salts using model substrate* ***3.25***. *RCY$_{HPLC}$ determined by radio-HPLC analysis of the crude reaction mixture.*

3.2.4. Reaction Scope

With information from the robustness screening on the functional group compatibility of the ^{18}F-fluorination of heteroaryl pyridinium tetrafluoroborate salts, we next looked to assess the scope of the reaction.

Firstly, a scope of small molecule heteroaryl pyridinium tetrafluoroborates (**3.25**-**3.51**) was evaluated (Scheme 3.46).

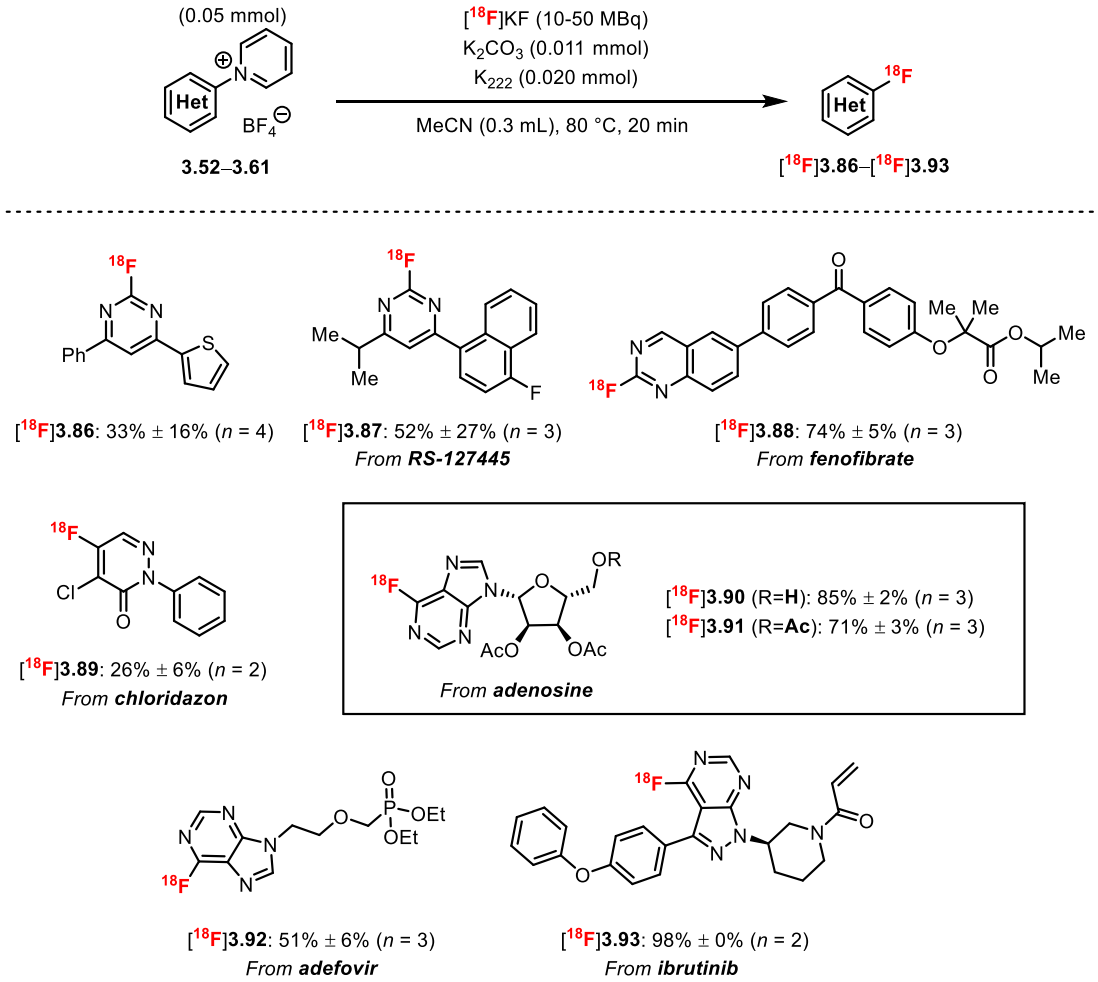


Scheme 3.46. *Small molecule scope of the ^{18}F-fluorination of heteroaryl pyridinium tetrafluoroborate salts. RCY_{HPLC} determined by radio-HPLC analysis of the crude reaction mixture.*

In line with the excellent reactivity observed for 2-aminopyrimidine-derived model substrate **3.25**, substrates derived from pyrimidine substituted at the 5-position with various functional groups were successfully converted to the relevant ^{18}F-fluoride ([^{18}F]**3.64**-[^{18}F]**3.68**). Inductively electron-withdrawing substituents, such as bromo ([^{18}F]**3.64**) and iodo groups ([^{18}F]**3.65**), were well tolerated and the desired product was obtained in excellent (84%) and moderate (43%) RCY_{HPLC}, respectively. Electron-neutral substituents performed equally well, e.g. [^{18}F]**3.66** was formed in 78% RCY_{HPLC}. The electron-donating methoxy substituent led to a decrease in RCY_{HPLC} to 13%, likely as the increased electron density rendered this substrate less electrophilic. Similar reactivity was not observed for pyridines, with the highest RCY_{HPLC} obtained for a pyridine-derived substrate obtained for 5-nitro-substituted [^{18}F]**3.69** (8% RCY_{HPLC}). Several fused heteroaromatic substrates were trialled next. First, a 5,6-dimethylated furo[2,3-*d*]pyrimidine substrate could be ^{18}F-fluorinated in 69% RCY_{HPLC} ([^{18}F]**3.70**). A similar N^7-benzylated pyrrolo[2,3-*d*]pyrimidine-derived pyridinium tetrafluoroborate was reactive in a lower RCY_{HPLC} of 29% ([^{18}F]**3.71**). A thieno-fused pyrimidine substrate also delivered the desired 4-^{18}F-fluorinated product [^{18}F]**3.72** in 89% RCY_{HPLC} when subjected to the optimised reaction conditions. Finally, a substrate derived from 2-aminopyrido[3,2-*d*]pyrimidine displayed excellent reactivity ([^{18}F]**3.73**, 93% RCY_{HPLC}). Quinazolines were also amenable to our ^{18}F-fluorination conditions, with [^{18}F]6-bromo-2-fluoroquinazoline ([^{18}F]**3.74**) accessible in 89% RCY_{HPLC}. Other diazine scaffolds were next considered. A 6-cyanopyridazine could be readily radiofluorinated at the 2-position in excellent RCY_{HPLC} ([^{18}F]**3.75**, 98%). Furthermore, pyrazine-derived substrates also proved to be amenable to radiolabelling, in 3 examples up to 89% RCY_{HPLC} ([^{18}F]**3.76**-[^{18}F]**3.78**). Pyridinium salts prepared from two pyrrolo[2,1-*f*][1,2,4]triazin-4-amines displayed excellent reactivity, and were ^{18}F-fluorinated in up to 97% RCY_{HPLC} ([^{18}F]**3.79**-[^{18}F]**3.80**). This scaffold is also present in the antiviral compound remdesivir and has not been labelled with F-18 previously. Several pyridinium tetrafluoroborates derived from adenine were found to be excellent substrates and reacted in up to 89% RCY_{HPLC}

([^{18}F]**3.81**-[^{18}F]**3.83**). For this series of substrates, the 9-position could be substituted with various groups, including an ester that could be susceptible to hydrolysis in the presence of K_2CO_3. No cleavage of this group was observed by radio-HPLC analysis. Furthermore, when a 2-chlorinated purine substrate was prepared, no product arising from substitution of chloride was observed, and only the 6-^{18}F-fluorinated product formed from displacement of pyridine was observed ([^{18}F]**3.84**, 24% RCY_{HPLC}). 5-Membered heterocycles beyond model compound **3.26** were also assessed, however, an ^{18}F-fluorinated benzothiazole ([^{18}F]**3.85**) formed in only 5% RCY_{HPLC} from the requisite pyridinium tetrafluoroborate.

Following this initial scope study, a selection of heteroaryl pyridinium tetrafluoroborates derived from bioactive molecules (**3.52**–**3.61**) were next evaluated (Scheme 3.47).

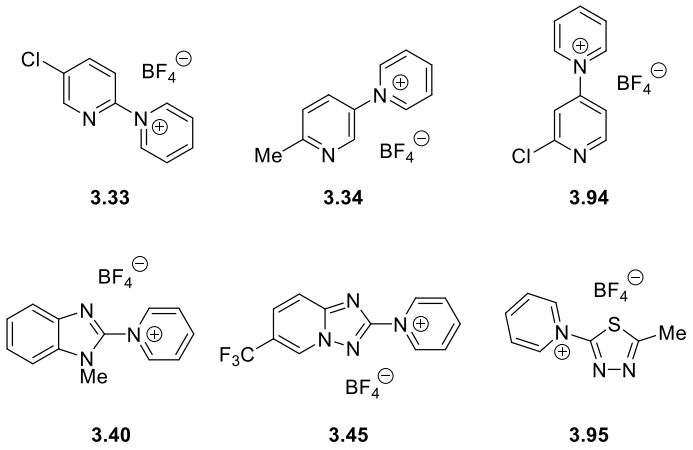


***Scheme 3.47**. Bioactive molecule scope of the ^{18}F-fluorination of heteroaryl pyridinium tetrafluoroborate salts. RCY_{HPLC} determined by radio-HPLC analysis of the crude reaction mixture.*

Firstly, two bioactive 2-aminopyrimidines underwent ^{18}F-fluorodeamination under our optimised conditions. For example, [^{18}F]**3.86** derived from an amine with antimicrobial activity was obtained in 33% RCY_{HPLC}, while [^{18}F]**3.87** derived from a 5-HT receptor antagonist (RS-127445) that can be used to treat gastrointestinal disorders was obtained in 52% RCY_{HPLC}. The antilipidemic compound fenofibrate was next modified with a 2-aminoquinazoline prosthetic group that could then be ^{18}F-fluorinated in 74% RCY_{HPLC} ([^{18}F]**3.88**). The agrochemical chloridazon was also successfully radiofluorinated in 26% RCY_{HPLC} ([^{18}F]**3.89**). In line with our small molecule scope studies, bioactive molecules containing purine scaffolds were readily amenable to ^{18}F-labelling. Pyridinium salts derived from di- and tri-acetylated adenosines were excellent substrates, with the ^{18}F-fluorinated products being obtained in 85% RCY_{HPLC} ([^{18}F]**3.90**) and 71% RCY_{HPLC} ([^{18}F]**3.91**), respectively. Adefovir, an antiviral compound used to treat HBV and also containing a purine aminoheterocycle, underwent ^{18}F-fluorodeamination *via* the pyridinium salt in 51% RCY_{HPLC} ([^{18}F]**3.92**). Finally, a pyridinium tetrafluoroborate derived from tyrosine kinase inhibitor ibrutinib, used in the treatment of cancers, including leukemia, could be ^{18}F-fluorinated in 98% RCY_{HPLC} ([^{18}F]**3.93**).

During the completion of our scope studies, we discovered several substrates that were not amenable to ^{18}F-fluorination under our optimised reaction conditions (Scheme 3.48). For example, substrates derived from 2-aminopyridines that were not substituted with sufficiently electron-withdrawing groups (e.g. **3.33**), were poor substrates and did not give any desired product. For this scaffold, the influence of electron-withdrawing groups is likely required to render substrates sufficiently electrophilic to react with [^{18}F]fluoride. Similarly, 4-aminopyridines were also not amenable to our ^{18}F-fluorodeamination protocol (e.g. **3.94**). ^{18}F-Fluorination at the 3-position of pyridine-derived substrates was also not within reach (e.g. **3.34**), likely due to this position being further deactivated to substitution compared to the 2- and 4-positions. In line with the observations made with pyridine-derived substrates, more electron-rich 5-membered heterocycles, such as benzimidazole-derived **3.40**, **3.45**,

which featured a [1,2,4]triazolo[1,5-a]pyridine core, and 1,3,4-thiadiazole-derived **3.95**, were also found to be poor substrates.

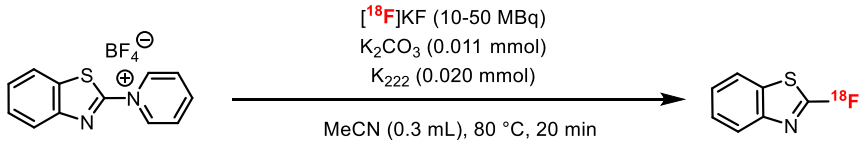


3.33 **3.34** **3.94**

3.40 **3.45** **3.95**

***Scheme 3.48**. Examples of unsuccessful substrates for the ^{18}F-fluorination of heteroaryl pyridinium tetrafluoroborate salts.*

We investigated whether alternative ^{18}F-fluorination conditions might improve the reactivity of poorly reactive substrates. For this study, a pyridinium tetrafluoroborate derived from benzo[*d*]thiazol-2-amine (**3.96**) was selected, as under the optimised conditions [^{18}F]**3.85** was obtained in a low RCY_{HPLC} of 5% (Table 3.5, entry 1).



3.96
(0.05 mmol)

[^{18}F]**3.85**

Entry	Deviation from standard conditions	RCY_{HPLC} of [^{18}F]**3.85**
1	none	5% ± 1% (*n* = 2)
2	MeCN as solvent, 120 °C	3% (*n* = 1)
3	PhCN as solvent, 120 °C	2% (*n* = 1)
4	NMP as solvent, 120 °C	<1% (*n* = 1)
5	DMSO as solvent, 150 °C	2% (*n* = 1)
6	NEt_4HCO_3 (0.03 mmol) instead of K_2CO_3 and K_{222}	<1% (*n* = 1)

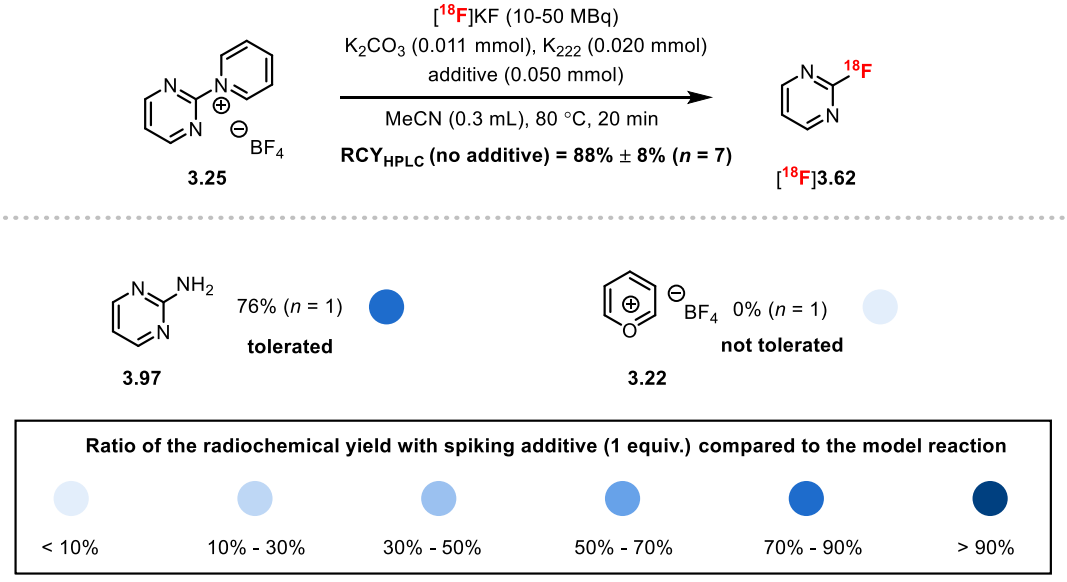
***Table 3.5**. Attempts to improve RCY for low-yielding [^{18}F]**3.85**. RCY_{HPLC} determined by radio-HPLC analysis of the crude reaction mixture.*

Alternative solvents and increased temperatures were assessed, however, no improvement in the RCY_{HPLC} of [^{18}F]**3.85** was observed (Table 3.5, entries 2–5). The use of Et_4NHCO_3 as an alternative elution additive also did not deliver any improvement in RCY_{HPLC} (Table 3.5, entry 6).

3.2.5. Studies towards the Development of a One-pot ^{18}F-Fluorodeamination of Crude Pyridinium Salts

As several studies had suggested deaminative functionalisations of crude pyridinium salts formed *in situ* from anilines and pyrylium reagents were accessible, we were interested to determine whether an ^{18}F-fluorination of crude heteroaryl pyridinium salts was within reach.[76,78-79] Riss and co-workers had also previously demonstrated in their ^{18}F-fluoro-Sandmeyer reaction that anilines could be activated to the relevant diazonium salt and then radiofluorinated directly in a one-pot protocol.[55]

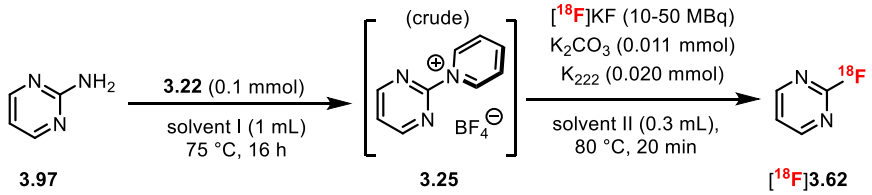
In order to assess the viability of a ^{18}F-fluorodeamination of heteroaryl amines *via* crude pyridinium tetrafluoroborate salts, the tolerance of the reaction to the reagents used to prepare model heteroaryl pyridinium salt **3.25** were assessed applying an additive-based robustness screening, in the same way as previously described in section 3.2.3 (Scheme 3.49).



***Scheme 3.49**. Robustness screening of the ^{18}F-fluorination of heteroaryl pyridinium salts using model substrate **3.25**. RCY_{HPLC} determined by radio-HPLC analysis of the crude reaction mixture.*

These experiments indicate that the aniline starting material **3.97** is well tolerated in this model reaction (76% RCY_{HPLC}), suggesting that unconverted **3.97** is unlikely to be problematic for the ^{18}F-fluorination of **3.25**. In contrast, the presence of an equivalent of pyrylium salt **3.22** was shown to result in no formation of [^{18}F]**3.62**, likely as **3.22** is strongly electrophilic and readily reacts with [^{18}F]fluoride.

When ^{18}F-fluorination of crude **3.25**, prepared from an equimolar amount of pyrylium reagent **3.22** and aniline **3.97**, was attempted, no desired product [^{18}F]**3.62** formed, consistent with the data obtained in the robustness screening (Table 3.6, entry 1).

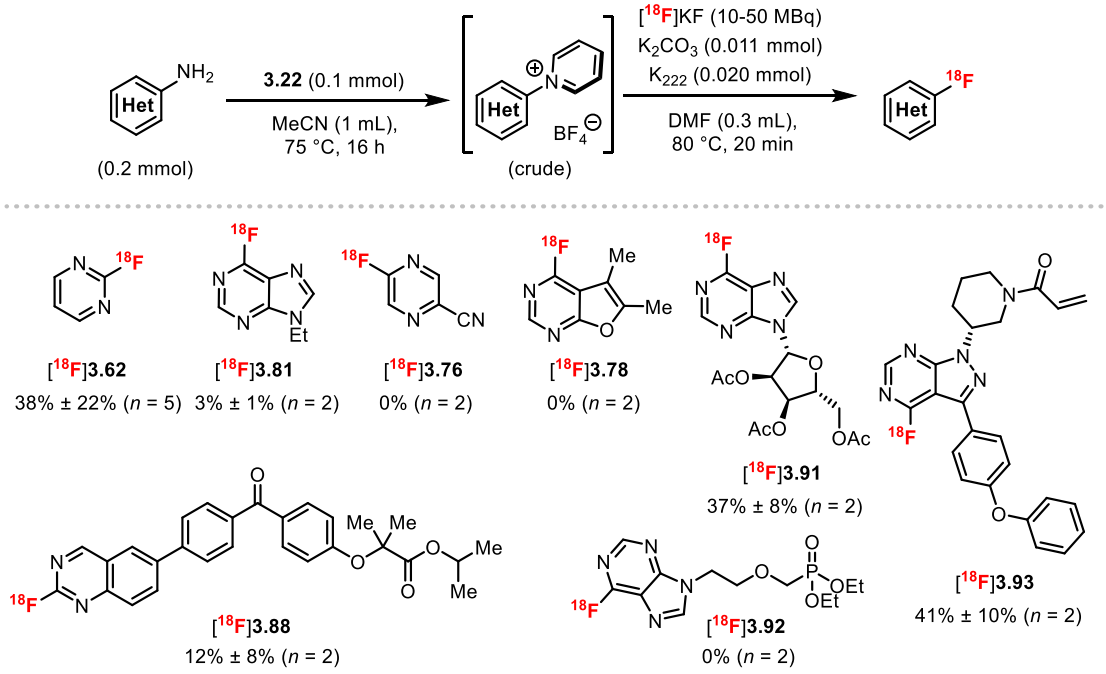


Entry	Loading of 3.97	Solvent I	Solvent II	RCY_{HPLC} of [^{18}F]3.62
1	0.10 mmol	MeCN	MeCN	0% (*n* = 1)
2	0.10 mmol	EtOH	MeCN	0% (*n* = 1)
3	0.20 mmol	MeCN	MeCN	32% ± 10% (*n* = 3)
4	0.20 mmol	EtOH	MeCN	22% ± 14% (*n* = 2)
5	0.20 mmol	1,4-dioxane	MeCN	9% (*n* = 1)
6	0.15 mmol	MeCN	MeCN	0% (*n* = 1)
7	0.25 mmol	MeCN	MeCN	22% (*n* = 1)
8	0.30 mmol	MeCN	MeCN	41% (*n* = 1)
9	0.40 mmol	MeCN	MeCN	31% (*n* = 1)
10	0.20 mmol	MeCN	DMF	38% ± 22% (*n* = 5)
11	0.20 mmol	MeCN	DMSO	35% (*n* = 1)

***Table 3.6**. Optimisation of the ^{18}F-fluorodeamination of heteroaryl amines, via crude pyridinium tetrafluoroborate salts. RCY_{HPLC} determined by radio-HPLC analysis of the crude reaction mixture.*

A solvent swap from EtOH to MeCN delivered no improvement (Table 3.6, entry 2). Based on our hypothesis that **3.22** was instead reacting with [^{18}F]fluoride and was therefore unavailable for the desired ^{18}F-fluorination, we next trialled increased loadings of **3.97**, to ensure that **3.22** was entirely consumed. In these experiments, conversion to [^{18}F]**3.62** was observed at **3.97** loadings from 0.2 mmol (2 equivalents) (Table 3.6, entries 3–9). Above this, however, no consistent trend was observed and all **3.97** loadings trialled above 0.2 mmol were within experimental error (Table 3.6, entries 3, 7–9). Deviation from MeCN as the solvent used for the condensation of **3.97** with **3.22** (solvent I) also delivered [^{18}F]**3.62** in lower RCY_{HPLC} (Table 3.6, entries 4–5). Varying the solvent used for the ^{18}F-fluorination (solvent II) from MeCN to other polar aprotic solvents DMSO and DMF gave [^{18}F]**3.62** in similar RCY_{HPLC} (Table 3.6, entries 3, 10–11). On the basis of its slightly higher average RCY_{HPLC} (38%), DMF was selected as solvent II (Table 3.6, entry 10).

Next, the generality of this protocol was assessed by subjecting an array of heteroanilines to the conditions (Scheme 3.50).



***Scheme 3.50**. Scope of the ^{18}F-fluorodeamination of heteroaryl amines, via crude pyridinium tetrafluoroborate salts. RCY_{HPLC} determined by radio-HPLC analysis of the crude reaction.*

These starting materials were selected from successful examples found during evaluation of the reaction scope; all were prepared in over 50% RCY_{HPLC} when assessed previously using the pyridinium tetrafluoroborate directly (Scheme 3.46 and Scheme 3.47). Two key general observations were made. Firstly, the scope of this ^{18}F-fluorodeamination of anilines is smaller compared to the ^{18}F-fluorination of the isolated and purified pyridinium tetrafluoroborate salt; across 8 anilines, only 5 were efficiently radiofluorinated. Secondly, the observed RCY_{HPLC} values for the 5 successful substrates were lower compared to the ^{18}F-fluorination of the pyridinium salt. In some cases, there was a substantial reduction observed, e.g., for ^{18}F-fluoropurine [^{18}F]**3.81**, RCY_{HPLC} reduced from 73% to 3%.

3.2.6. Elution of [^{18}F]Fluoride with Pyridinium Tetrafluoroborates

As ionic compounds, we were next interested to investigate whether pyridinium salts were efficient in the elution of [^{18}F]fluoride from ion exchange cartridges, which is a key step in the preparation of reactive [^{18}F]fluoride from the target [^{18}O]water.[83] As discussed in Chapter 1 (section 1.3.2), conventional protocols use inorganic bases, such as K_2CO_3, as elution reagents and the whole process can take up to 20 minutes, thereby resulting in activity losses to radioactive decay. However, other groups have pioneered methods that allow for the direct elution of [^{18}F]fluoride with ionic substrates, which can then be directly ^{18}F-fluorinated in a subsequent step.[20,87]

Model pyridinium salt **3.25** was selected for initial studies, along with the QMA cartridge used for the preparation of [^{18}F]fluoride in previous experiments. Firstly, the solvent used for the elution was varied (Table 3.7).

Polar protic solvents performed best, with MeOH giving 88% elution efficiency (EE), in line with established elution protocols used for the production of clinical radiotracers (Table 3.7, entry 1).[83] EtOH gave a moderate EE of 31%, however this data point may be influenced by the lower solubility of **3.25** in EtOH (Table 3.7 entry 2). Polar aprotic solvents MeCN and DMSO

gave no or very low EE values, respectively (Table 3.7, entries 3–4). EE recovered to 74% upon the use of an MeCN/MeOH mixture, suggesting the importance of a protic solvent to obtaining high EE (Table 3.7, entry 5). Therefore, MeOH was used as the solvent for future experiments.

Entry	Solvent	Elution efficiency
1	MeOH	88% ± 2% (*n* = 7)
2	EtOH	31% (*n* = 1)
3	MeCN	0% (*n* = 1)
4	DMSO	3% (*n* = 1)
5	MeOH:MeCN = 1:1	74% (*n* = 1)

***Table 3.7**. Effect of the elution solvent using a Waters Sep-Pak AccellPlus QMA Carbonate Plus Light SPE cartridge. Solvent volume = 1 mL. Loading of **3.25** = 0.025 mmol. Elution efficiency determined using a dose calibrator to measure loaded and eluted radioactivity.*

Next, the influence of the ion exchange cartridge was assessed (Table 3.8). Three commercial anion exchange SPE cartridges were assessed. These differ primarily in the identity of the counterion for the quaternary methyl ammonium phase.

Entry	Anion exchange cartridge	Elution efficiency
1	Waters Sep-Pak AccellPlus QMA Carbonate Plus Light	88% ± 2% (*n* = 7)
2	Waters Sep-Pak AccellPlus QMA Plus Light	<1% (*n* = 1)
3	Chromafix PS-HCO_3	87% (*n* = 1)

***Table 3.8**. Effect of the anion exchange cartridge. MeOH (1 mL) used as solvent. Loading of **3.25** = 0.025 mmol. Elution efficiency determined using a dose calibrator to measure loaded and eluted radioactivity.*

These data indicate that phases with hydrogen carbonate and carbonate counteranions are very effective, delivering up to 88% EE (Table 3.8, entry 1). In contrast, the QMA Plus Light

cartridge, which features a chloride counteranion, was not suitable, with only a trace of [^{18}F]fluoride eluted by a methanolic solution of **3.25**.

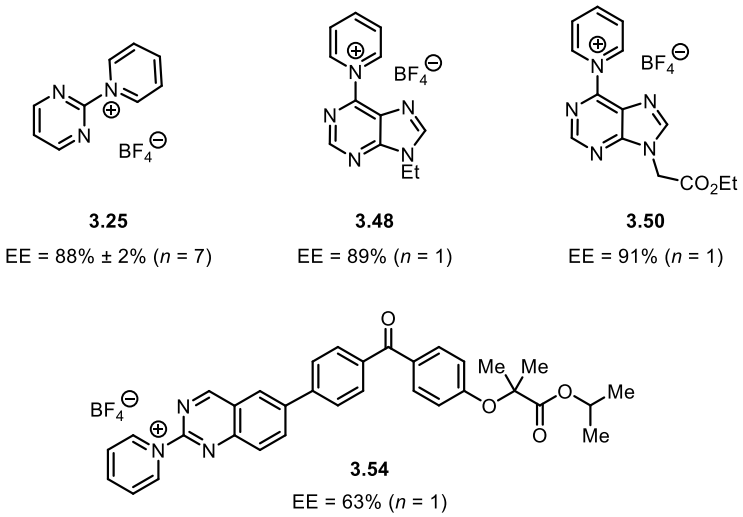
The next variable that was considered was the loading of pyridinium salt **3.25** required to elute [^{18}F]fluoride from the anion exchange cartridge (Table 3.9).

Entry	Loading of 3.25	Elution efficiency
1	0.025 mmol	88% ± 2% (*n* = 7)
2	0.020 mmol	84% (*n* = 1)
3	0.015 mmol	88% (*n* = 1)
4	0.010 mmol	84% (*n* = 1)

Table 3.9*. Effect of the anion exchange cartridge. MeOH (1 mL) used as solvent. Elution efficiency determined using a dose calibrator to measure loaded and eluted radioactivity.*

This series of experiments promisingly suggest that only low loadings of **3.25** are needed to obtain high EE values, with 84% being obtained using only 0.01 mmol of pyridinium salt (Table 3.9, entry 4). Despite this low quantity required for efficient elution, previous studies into the loading of substrate required for efficient radiofluorination suggested that reactivity was reduced at loadings below 0.017 mmol (Table 3.3). Therefore, to avoid any detrimental effect on reactivity, for the rest of the study a loading of 0.025 mmol was used, as some material is likely to be retained on the QMA cartridge.

Applying these optimised elution conditions, we next assessed whether other pyridinium tetrafluoroborate salts other than **3.25** were also proficient in eluting [^{18}F]fluoride from anion exchange cartridges (Figure 3.3). Pleasingly, the other pyridinium salts trialled were also able to elute [^{18}F]fluoride from the anion exchange cartridge, in good to excellent EE. A possible limitation is represented by fenofibrate derivative **3.54**, where lower than anticipated EE was obtained, likely due to the incomplete solubility of 0.025 mmol of **3.54** in 1 mL of MeOH.



3.25
EE = 88% ± 2% (*n* = 7)

3.48
EE = 89% (*n* = 1)

3.50
EE = 91% (*n* = 1)

3.54
EE = 63% (*n* = 1)

***Figure 3.3**. Pyridinium salt (0.025 mmol) scope for the elution of [^{18}F]fluoride. MeOH (1 mL) used as solvent. Elution efficiency determined using a dose calibrator to measure loaded and eluted radioactivity.*

With an optimised elution protocol in hand, we next turned our attention to the reactivity of the eluted mixtures of **3.25** and [^{18}F]fluoride. Firstly, eluates obtained from elution of anion exchange cartridges with **3.25** in various solvents were directly heated at 80 °C for 20 minutes (Table 3.10).

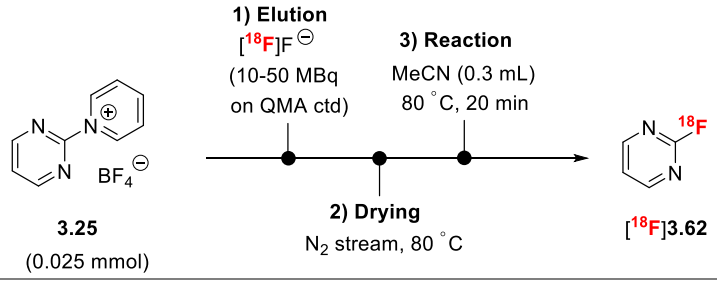
Entry	Solvent	RCY_{HPLC} of [^{18}F]**3.62**
1	MeOH	0% (*n* = 2)
2	EtOH	0% (*n* = 1)
3	MeOH:MeCN = 1:1	0% (*n* = 1)

***Table 3.10**. Direct reaction of the eluates when **3.25** is used to elute [^{18}F]fluoride from a QMA cartridge. RCY_{HPLC} determined by radio-HPLC analysis of the crude reaction mixture.*

In all cases, no [^{18}F]**3.62** was detected. MeOH is known to be a poor solvent for this reaction (Table 3.1), but the superior solvent EtOH also afforded no desired [^{18}F]**3.62** (Table 3.10, entries 1–2). The addition of MeCN also did not rescue reactivity (Table 3.10, entry 3).

As the direct use of solvents that were successful in eluting [^{18}F]fluoride proved problematic, MeOH was used for the elution and subsequently removed under a stream of N_2 at elevated temperature. A second solvent, such as MeCN, could then be added that would better promote the radiofluorination. Applying this strategy, reactivity was thus recovered and

[^{18}F]**3.62** formed in 40% RCY_{HPLC}, albeit in lower RCY_{HPLC} compared to the radiofluorination of **3.25** with separately prepared [^{18}F]KF.K_{222} (88%) (Table 3.11, entry 1). The obtained RCY_{HPLC} could be further improved up to 81% by the addition of further **3.25**, in combination with both K_2CO_3 and K_{222} additives (Table 3.11, entry 2). Despite this, the addition of further **3.25**, or K_2CO_3 and K_{222} in isolation, had a detrimental effect on the RCY_{HPLC} of [^{18}F]**3.62** (Table 3.11, entries 3–4).



Entry	Deviation from standard conditions (step 3)	RCY_{HPLC} of [^{18}F]3.62
1	none	40% ± 10% (*n* = 4)
2	**3.25** (0.025 mmol), K_2CO_3 (0.011 mmol), K_{222} (0.02 mmol)	81% (*n* = 1)
3	**3.25** (0.025 mmol)	9% (*n* = 1)
4	K_2CO_3 (0.011 mmol), K_{222} (0.02 mmol)	0% (*n* = 1)

***Table 3.11**. Effect of additional **3.25** and elution additives on the reactivity of an eluted mixture of **3.25** and [^{18}F]fluoride. RCY_{HPLC} determined by radio-HPLC analysis of the crude reaction mixture.*

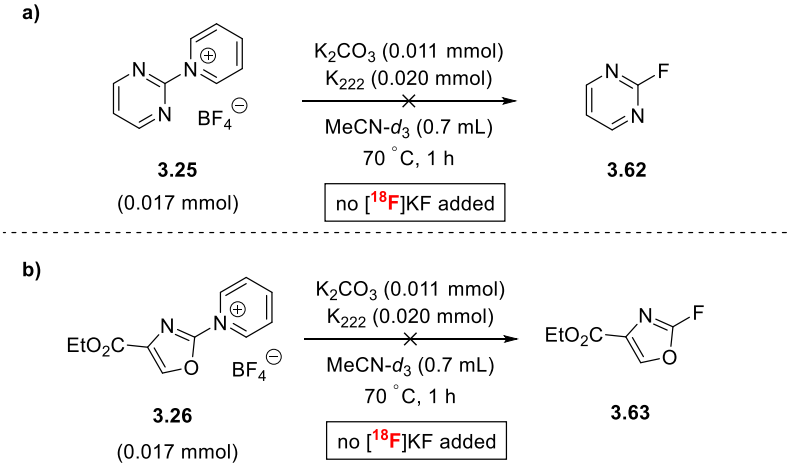
3.2.7. Reaction Automation, Product Isolation and A_m Measurement

With a good understanding of the reactivity of heteroaryl pyridinium tetrafluoroborates towards [^{18}F]fluoride in hand, we next turned our attention to reaction automation and scale-up to multi-GBq starting radioactivities. This is a crucial aspect of the work presented herein, as one of the primary success criteria for a novel PET radiochemistry method is its ability to provide radiotracers in sufficient AY for the desired application (e.g., PET imaging, *in vitro*/*vivo* studies etc.). Automation of the reaction on a commercial radiosynthesis platform will also encourage implementation by radiochemistry practitioners. Also, in completing this work, we are now able to determine the A_m of the radiolabelled products obtained from this method.

This was a key consideration, as all substrates used possess a tetrafluoroborate counterion that could be implicated in undesired ^{19}F-fluorination, as is the case in the Balz-Schiemann reaction of aryl diazonium tetrafluoroborates. There are contrasting reports in the literature concerning the reactivity of tetrafluoroborate with electrophiles less reactive than aryl diazonium salts. In a mechanochemical trifluoromethoxylation reported by Iaroshenko and co-workers, aryl pyridinium tetrafluoroborates have been shown to undergo fluorination in an undesired side reaction.[88] The authors suggest this is likely promoted by the presence of water and the mechanochemical reaction conditions, which can promote ^{19}F-fluoride release in substitution or dimerisation events. Meanwhile, in an ^{18}F-radiochemical scenario, Sanford, Scott and co-workers have shown that aryl iodonium tetrafluoroborates are amenable to Cu-mediated radiofluorination, yielding products in high A_m, suggesting ^{19}F-isotopic dilution from tetrafluoroborate is not competitive with ^{18}F-fluorination.[89]

3.2.7.1. Undesired ^{19}F-Fluorination of Heteroaryl Pyridinium Tetrafluoroborates

To assess the possibility of isotopic dilution originating from ^{19}F-fluorination from the tetrafluoroborate counterion, the stability of model substrates **3.25** and **3.26** in the presence of the K_2CO_3 and K_{222} additives was tested. This was achieved by combining the relevant pyridinium salt with the additives in an NMR tube with MeCN-d_3 and heating the tubes at 70 °C for 1 hour (Scheme 3.51).



***Scheme 3.51**. Stability testing of pyridinium salts a) **3.25** and b) **3.26** under the reaction conditions in the absence of [^{18}F]fluoride.*

Quantitative proton-decoupled ^{19}F NMR spectroscopic analysis of the resulting mixtures promisingly indicated the absence of the ^{19}F-fluorides **3.62** and **3.63** (Figure 3.4).

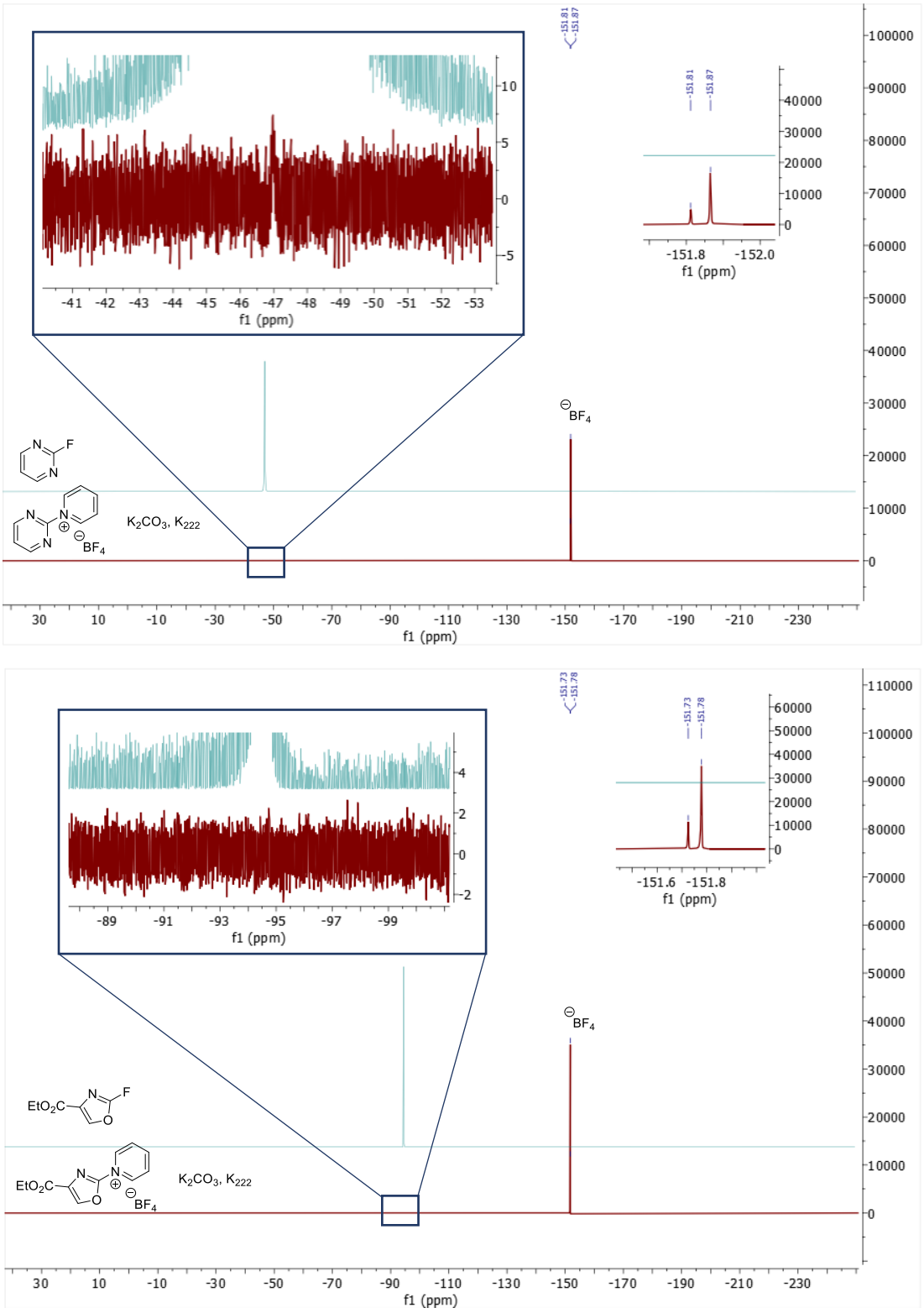


***Figure 3.4**. {^{1}H}^{19}F qNMR spectra (red) for the stability testing in the absence of [^{18}F]fluoride of a) **3.25**, b) **3.26**. ^{19}F NMR spectra of authentic references a) **3.62**, b) **3.63** (green).*

This suggested that competitive ^{19}F-fluorination of the pyridinium cation by tetrafluoroborate is not favourable and therefore that heteroaryl ^{18}F-fluorides prepared using this method should not suffer from extensive isotopic dilution from ^{19}F-fluoride (or surrogates thereof) and low A_m. This is in contrast to the report from Iaroshenko and co-workers, where this side-reactivity was observed under mechanochemical conditions.[88] However, the absence of water in significant quantities, the reaction taking place in solution rather than in the solid state, and the use of heating in our system rather than mechanical activation could explain the differences observed. Furthermore, Iaroshenko's report discloses only aryl pyridinium tetrafluoroborate salts as substrates, with no examples of heteroaromatic trifluoromethoxylation (or indeed fluorination) disclosed.

3.2.7.2. Automation of the ^{18}F-Fluorination of Heteroaryl Pyridinium Tetrafluoroborates

For initial automation and scale-up work, model pyridinium tetrafluoroborate **3.25** was selected in combination with a Trasis AllinOne automated radiosynthesiser. A programme and cassette configuration was designed that encoded all of the steps required for the radiosynthesis, including the elution and drying of [^{18}F]fluoride, the ^{18}F-fluorination of **3.25**, semi-preparative HPLC purification and reformulation of product [^{18}F]**3.62** (Figures 3.5, 3.6).

In summary, 1) [^{18}F]fluoride in [^{18}O]water is received from the cyclotron and loaded onto the QMA cartridge at position 5; 2) the [^{18}F]fluoride is eluted with a solution of K_2CO_3 and K_{222}; 3) this solution is dried azeotropically at 120 °C in the reactor with additions of further MeCN (position 8); 4) once dry, a solution of **3.25** in MeCN solvent (position 9) is added to the reactor; 5) the reaction mixture is heated for 20 minutes at 80 °C; 6) the reaction mixture is diluted with H_2O and transferred to the HPLC injection loop; 7) [^{18}F]**3.62** is purified by semi-preparative reverse-phase HPLC and the fraction corresponding to [^{18}F]**3.62** was collected in a vial charged with H_2O at position 34; 8) the solution containing [^{18}F]**3.62** is mixed with H_2O and passed over a C18 cartridge at position 33; 9) purified [^{18}F]**3.62** is eluted from the C18

cartridge into a vial at position 31 with MeCN. The activity of collected [^{18}F]**3.62** was then measured and the RCP and A_m determined by radio-HPLC analysis. Further experimental details are available in the Experimental section (Chapter 4).

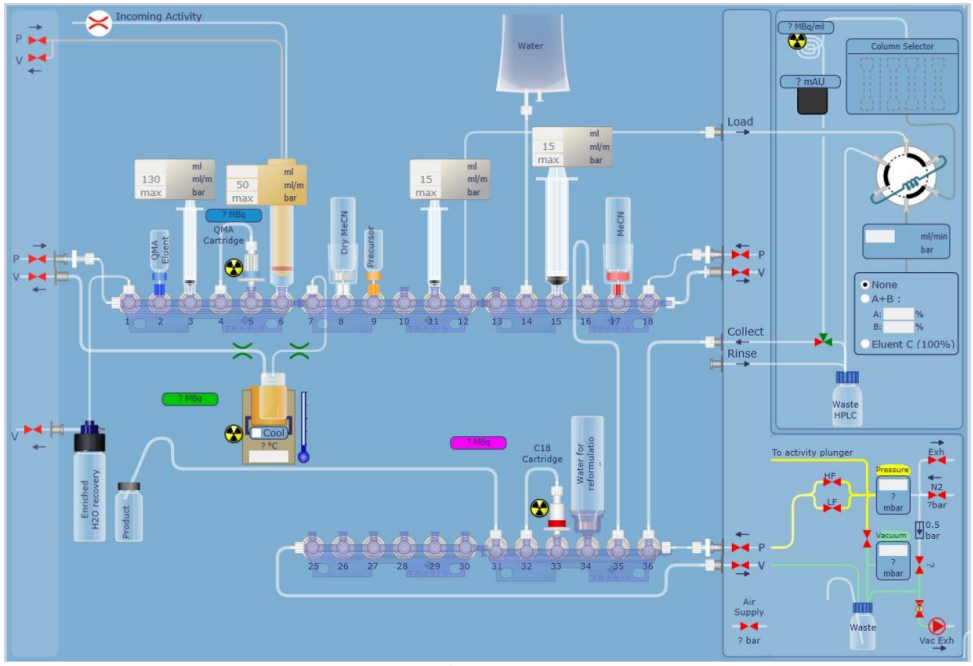
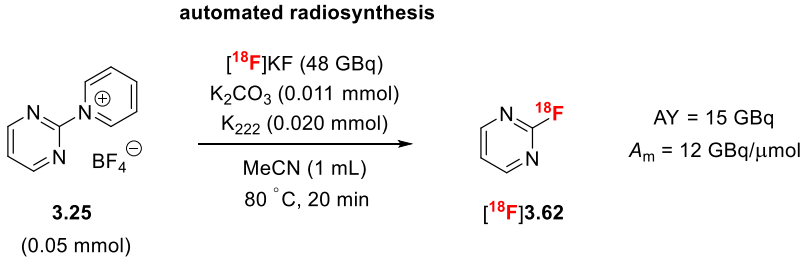


***Figure 3.5**. Cassette layout for the automated ^{18}F-fluorination of heteroaryl pyridinium tetrafluoroborates using a Trasis AllinOne automated radiosynthesiser.*



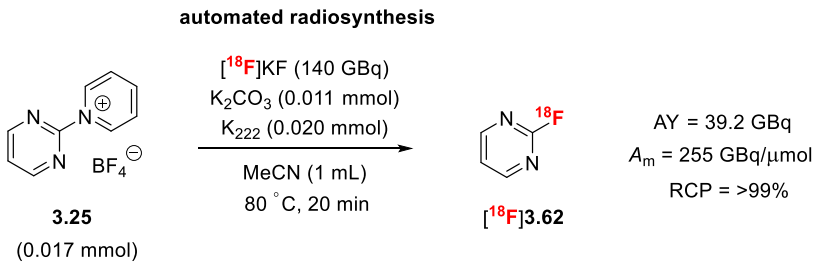
***Figure 3.6**. Set-up for the automated radiofluorination of heteroaryl pyridinium tetrafluoroborates using a Trasis AllInOne synthesiser. (Taken by J. Ford)*

For initial studies with [^{18}F]**3.62**, a **3.25** loading of 0.05 mmol was selected along with a 48 GBq starting radioactivity. Applying the automated radiosynthesis, [^{18}F]**3.62** was isolated in an AY of 15.2 GBq in a synthesis time of 55 minutes (Scheme 3.52). This experiment pleasingly demonstrated that the ^{18}F-fluorination of heteroaryl pyridinium salts was readily amenable to automated synthesis and could be successfully scaled up to multi-GBq starting activities. The A_m of [^{18}F]**3.62** isolated under these conditions was 12 ± 1.1 GBq/μmol. This modest A_m was promising, as the **3.25** loading of 0.05 mmol could be further reduced by a factor of 3 (Table 3.3) and starting radioactivity could also be increased to further deliver improvements in A_m.



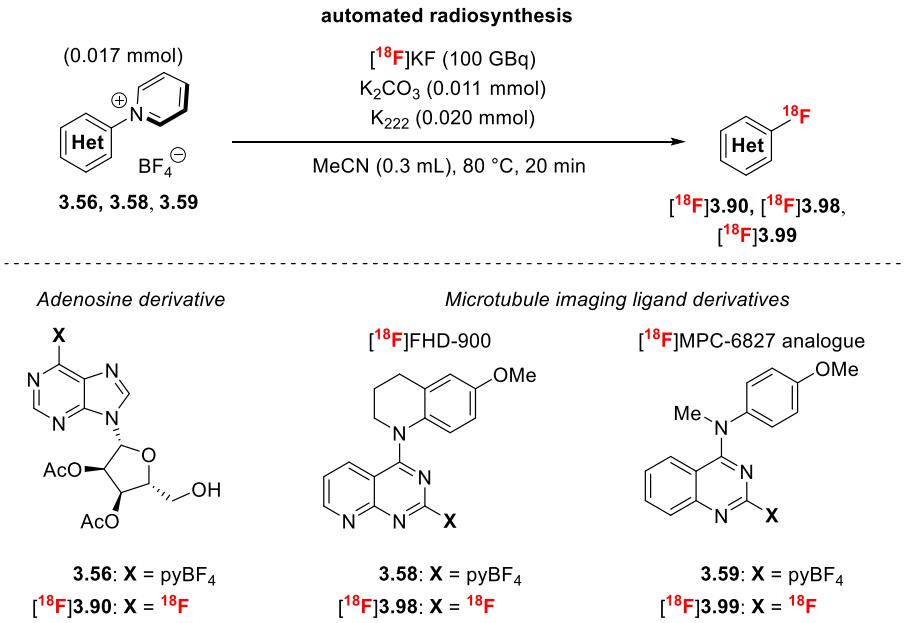
***Scheme 3.52**. Initial automated radiosynthesis of [^{18}F]**3.62**.*

Indeed, when the automated radiosynthesis of [^{18}F]**3.62** was repeated with a reduced loading of **3.25** (0.017 mmol) and higher starting radioactivity (140 GBq), [^{18}F]**3.62** could be prepared in an AY of 39.2 GBq in 52 minutes (Scheme 3.53). The isolated sample has an RCP of over 99% and the A_m reached an improved value of 255 GBq/μmol. Notably, the RCY remained similar between starting activities of 48 and 140 GBq (approximately 30% n.d.c. in both cases), suggesting the reaction of **3.25** is not negatively impacted by radiolysis at high starting activities (>0.1 TBq) routinely used for the production of PET radiotracers.



***Scheme 3.53**. Optimised, high activity automated radiosynthesis of [^{18}F]**3.62**.*

With this in hand, we next applied our automated radiosynthesis programme to the preparation of more complex targets that were representative of the functional group and structural diversity of (pre)clinical PET radiotracers (Table 3.12).



Entry	Substrate	AY	Synthesis time	RCP	A_m
1	**3.56**	33.8 GBq	72 min	>98%	322 GBq/µmol
2	**3.58**	11.9 GBq	74 min	>99%	110 GBq/µmol
3	**3.59**	2.2 GBq	75 min	>99%	142 GBq/µmol

***Table 3.12**. Radiosynthesis data for the automated radiosynthesis of [^{18}F]**3.90**, [^{18}F]**3.98** and [^{18}F]**3.99**.*

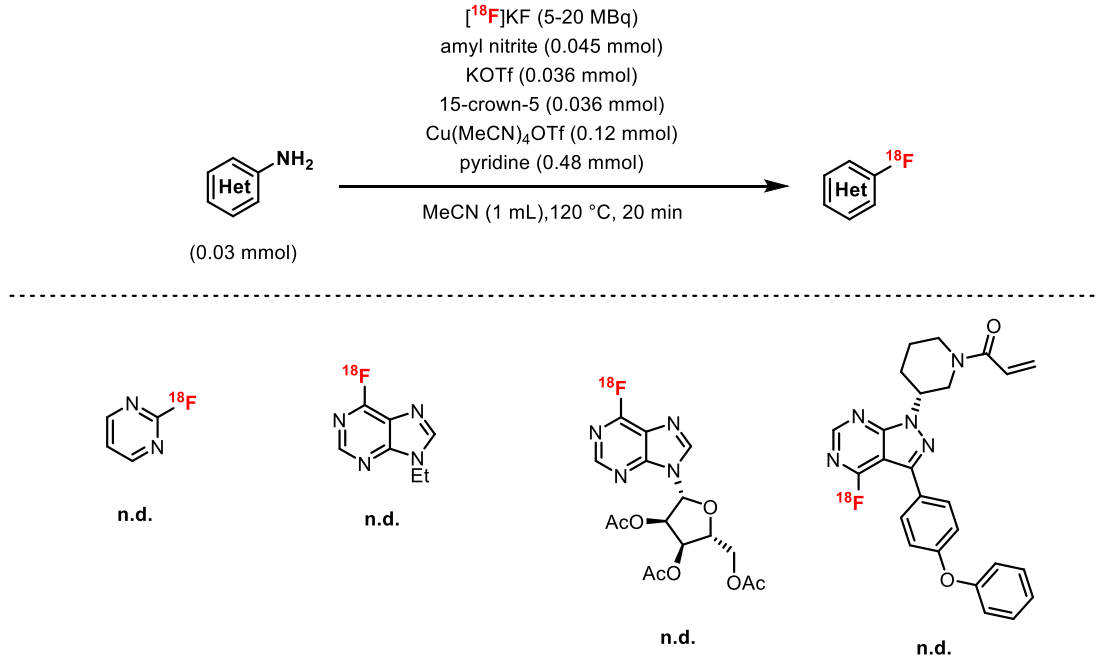
Firstly, a pyridinium tetrafluoroborate salt derived from the bioactive molecule adenosine (**3.56**) was evaluated (Table 3.12, entry 1). This had previously been demonstrated to be an excellent substrate under our radiofluorination conditions (Scheme 3.47). In line with the data obtained in our study of the reaction scope, [^{18}F]**3.90** was formed in a good AY of 33.8 GBq from 100 GBq starting activity, in a synthesis time of 72 minutes. The A_m of [^{18}F]**3.90** was high (322 GBq/µmol), in line with the high activity radiofluorination of model substrate **3.25** (Scheme 3.53). Finally, pyridinium salt derivatives of two preclinical heteroaromatic

radiotracers with potential for application in microtubule imaging (**3.58**, **3.59**) were subjected to automated radiofluorination with 100 GBq [^{18}F]fluoride. The relevant heteroaryl ^{18}F-fluorides ([^{18}F]**3.98** and [^{18}F]**3.99**) were prepared in AY sufficient for preclinical imaging studies and in high A_m (110 GBq/µmol and 142 GBq/µmol, respectively) (Table 3.12, entries 2 and 3).

3.2.8. Comparison with Other Methods

Finally, we looked to compare the ^{18}F-fluorination of aniline-derived pyridinium salts to alternative ^{18}F-fluorodeamination methods as well as those relying on other substrate types that can enable access to ^{18}F-fluoroheteroarenes.

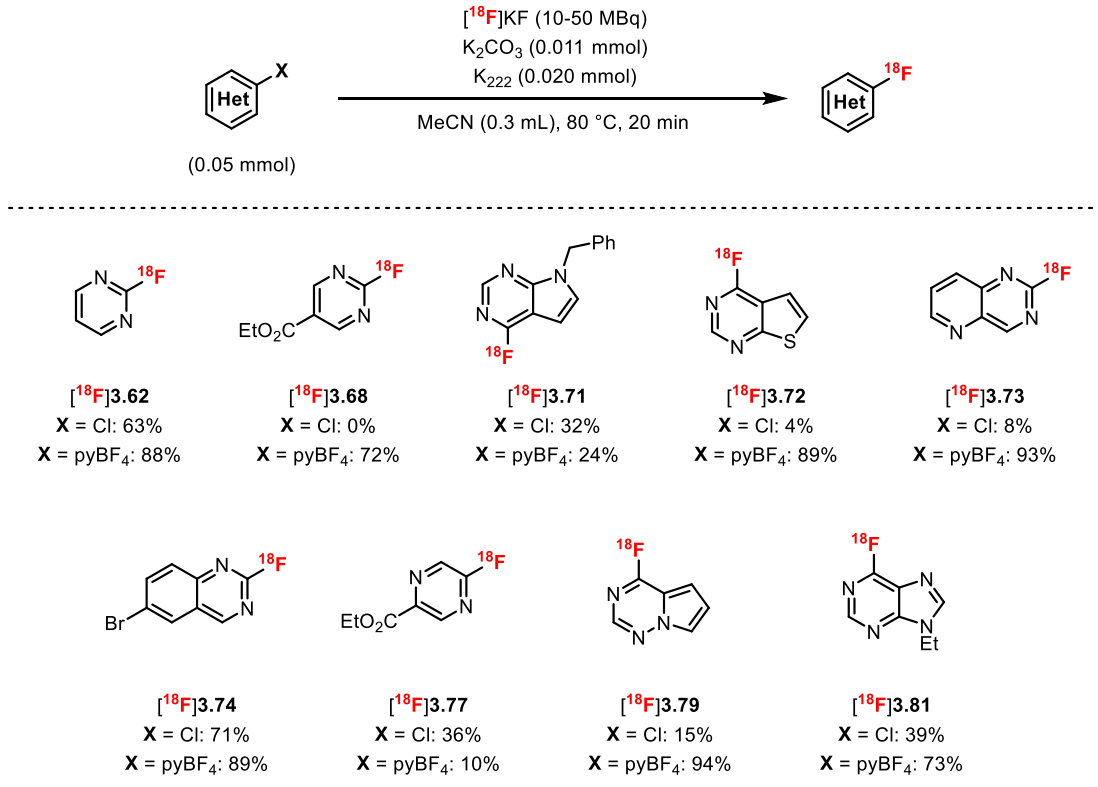
Firstly, the Sandmeyer-type ^{18}F-fluorodeamination developed by Riss and co-workers was examined.[55] As described in section 3.1.2.4, the authors of this study reported that a single heteroaromatic amine substrate was considered and was found not to be amenable to their ^{18}F-fluorodeamination conditions. In order to further investigate this, several of the anilines used to prepare the pyridinium tetrafluoroborate substrates were subjected to the conditions reported by Riss and co-workers (Scheme 3.54).



***Scheme 3.54**.[18]F-Fluorodeamination of heteroaromatic amines. RCY_{HPLC} determined by radio-HPLC analysis of the crude reaction mixture. n.d. = not detected.*

Of the four substrates trialled, none delivered the desired ^{18}F-fluoroheteroarene product. This suggests that there is good orthogonality between our pyridinium-based ^{18}F-fluorodeamination and existing methods for this transformation, thus highlighting the value of this method to radiosynthesis.

Next, alternative S_NAr precursors for the ^{18}F-fluorination of heteroarenes were considered. Of those commonly used for the radiosynthesis of such products, the heteroaryl chloride is the most widely available, both commercially and synthetically, so this was chosen for comparison to the pyridinium tetrafluoroborates used in this study. A panel of heteroaromatic chlorides were subjected to our ^{18}F-fluorination conditions (Scheme 3.55). These represented a diverse array of heteroaromatic scaffolds and the relevant ^{18}F-fluoride could be accessed from heteroaryl pyridinium tetrafluoroborates in variable yields (10–93%).



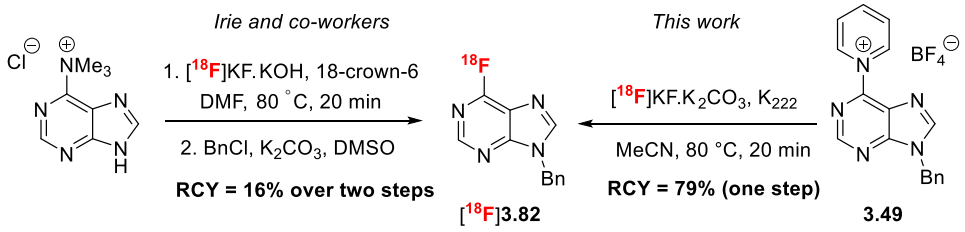
Scheme 3.55. *Comparison of heteroaryl chlorides and heteroaryl pyridinium tetrafluoroborates in ^{18}F-fluorination. RCY_{HPLC} determined by radio-HPLC analysis of the crude reaction mixture.*

Under these conditions, it can be seen that, in general, the RCY_{HPLC} of the radiofluorinated product is higher with the pyridinium tetrafluoroborate salt than is observed for the chloride

substrate. However, in two examples ([^{18}F]**3.71** and [^{18}F]**3.77**), the RCY_{HPLC} in the reaction using the chloride starting material exceeded that of the pyridinium salt. In several cases ([^{18}F]**3.68**, [^{18}F]**3.72**, [^{18}F]**3.73**, [^{18}F]**3.79** and [^{18}F]**3.81**), the pyridinium tetrafluoroborate substrate gave a much higher RCY_{HPLC} of the desired product than for the chloride. In other cases ([^{18}F]**3.62** and [^{18}F]**3.74**), the improvement in RCY_{HPLC} was only marginal.

It should be noted that a possible limitation of such a direct comparison of the two substrate classes could be that the optimal reaction conditions differ significantly between the substrates. For example, various solvents, elution reagents, temperatures and additives have been reported and these differ substantially across numerous literature reports.[31-35] It is therefore challenging to compare their reactivity directly, as such considerations (and others including precursor synthesis and other properties) are not captured, which may limit the value of such studies to radiochemistry practitioners.

We also noted that while trimethylammonium precursors are suggested to be the most reactive of all S_NAr radiofluorination precursors,[31] the RCY of potential brain PET tracer [^{18}F]**3.82** that was obtained in a single step using our method (79%), was higher than the original two-step radiosynthesis reported by Irie and co-workers (Scheme 3.56).[41] This highlights a benefit of heteroaryl pyridinium tetrafluoroborates as labelling precursors, as they are easily prepared late-stage from the relevant amine, removing the need for post-labelling transformations otherwise necessitated by challenging precursor synthesis or radiochemical limitations.



Scheme 3.56. *Comparison of the route to [^{18}F]**3.82** described herein and disclosed by Irie and co-workers.*

3.3. Conclusion and Outlook

This chapter has disclosed the development of a novel ^{18}F-fluorination protocol, whereby heteroaniline-derived pyridinium tetrafluoroborate salts are converted to the relevant ^{18}F-fluoroheteroarene in an S_NAr-type process with an [^{18}F]fluoride nucleophile.

A set of suitable ^{18}F-fluorination conditions was identified in initial experiments. Crucial to the success of the reaction was the presence of ionic elution reagents (in this case K_2CO_3), which delivered significant improvements to the yield and reproducibility of these reactions. The tolerance of the reaction to various functional groups and motifs was next evaluated using an additive-based robustness screening. A reaction scope study was completed, with 24 small molecule examples and 8 examples of bioactive molecules (and derivatives) shown to be accessible using this method. Diverse heteroaromatic scaffolds were successfully radiofluorinated, in contrast to previous studies focusing on pyridines and quinolines.[31-35] Several unsuccessful substrates were also identified. In future work, improvements in scope may be accessible applying an alternative strategy, perhaps with the use of alternative additives that promote reactivity or by exploiting the one-electron reactivity of pyridinium salts in combination with a transition metal catalyst. This reactivity may also unlock alternative transformations that are valuable to PET ligand discovery. Attempts to design a protocol for the ^{18}F-fluorination of crude pyridinium salts afforded a smaller scope of the desired ^{18}F-fluoride products and also in lower RCY. Future work could focus on the further optimisation of this protocol.

As ionic substrates, pyridinium tetrafluoroborate salts were found to be highly effective in the elution of [^{18}F]fluoride from anion exchange cartridges. The eluted mixtures of pyridinium salt and [^{18}F]fluoride displayed modest reactivity when subjected directly to the reaction conditions and this could be further improved with the addition of further substrate and the elution reagents, K_2CO_3 and K_{222}. Future work could integrate this property into the

automated radiosynthesis of a PET radiotracer and further optimise the radiofluorination in the absence of elution additives.

As it is vital that novel radiochemical transformations are capable of producing useful quantities of radiotracers for PET imaging, we next demonstrated that the ^{18}F-fluorination of pyridinium tetrafluoroborate salts was amenable to automated radiosynthesis using high [^{18}F]fluoride starting activities (up to 140 GBq [^{18}F]fluoride). The radiosynthesis of four heteroaryl ^{18}F-fluorides (three of which were complex and bioactive molecules) was automated and these were prepared in high A_m (up to 322 GBq/μmol) and in up to excellent AY in less than 75 minutes, demonstrating the value of the method to practitioners. This also corroborated early ^{19}F NMR experiments suggesting that ^{19}F-isotopic dilution from tetrafluoroborate was minimal under the reaction conditions.

Finally, a comparison of the ^{18}F-fluorination of pyridinium salts to an existing ^{18}F-fluorodeamination method, as well as other ^{18}F-S_NAr precursors was provided, which showed some complementarity between established substrate classes and heteroaryl pyridinium salts.

The work disclosed in this chapter provides an account of the development and application of a novel ^{18}F-S_NAr reaction, a reaction type that is applied worldwide by radiochemistry practitioners for the preparation of PET radiotracers. Heteroaryl pyridinium tetrafluoroborate salts are presented herein as an alternative to the well-established precursor types currently in use. They have been shown to offer several advantages, including good reactivity, precursor accessibility, amenability to automated PET tracer radiosynthesis and ability to be used as an [^{18}F]fluoride elution reagent. On this basis, we anticipate this method will be valuable to radiochemists seeking to prepare ^{18}F-fluoroheteroarenes.

3.4. References

1 Brown, D. G.; Boström, J. Analysis of Past and Present Synthetic Methodologies on Medicinal Chemistry: Where Have All the New Reactions Gone? *J*. *Med*. *Chem*. **2016**, *59* (10), 4443–4458.

2 Bunnett, J. F.; Zahler, R. E. Aromatic Nucleophilic Substitution Reactions. *Chem. Rev.* **1951**, *49* (2), 273–412.

3 Bunnett, J. F.; Garbisch Jr., E. W.; Pruitt, K. M. The "Element Effect" as a Criterion of Mechanism in Activated Aromatic Nucleophilic Substitution Reactions. *J. Am. Chem. Soc.* **1957**, *79* (2), 385–391.

4 Senger, N. A.; Bo, B.; Cheng, Q.; Keeffe, J. R.; Gronert, S.; Wu, W. The Element Effect Revisited: Factors Determining Leaving Group Ability in Activated Nucleophilic Aromatic Substitution Reactions. *J. Org. Chem.* **2012**, 77 (21), 9535–9540.

5 Terrier, F. Rate and equilibrium studies in Jackson-Meisenheimer complexes. *Chem. Rev.* **1982**, *82* (2), 77–152.

6 Artamkina, G. A.; Egorov, M. P.; Beletskaya, I. P. Some aspects of anionic σ-complexes. *Chem. Rev.* **1982**, *82* (4), 427–459.

7 Bowden, K.; Nadvi, N. S. Reactions in strongly basic media. Part 9. Correlation of the rates of methoxide-catalysed methanolysis of 1-substituted 2,4-dinitrobenzenes and 2-substituted 5-nitropyridines in methanolic dimethyl sulphoxide with an acidity function. Details of the mechanistic pathway. *J. Chem. Soc., Perkin Trans. 2* **1987***, 2*, 189–192.

8 Gottlieb, H. B. The Replacement of Chlorine by Fluorine in Organic Compounds. *J*. *Am*. *Chem*. *Soc*. **1936**, *58* (3), 532–533.

9 Finger, G. C.; Kruse, C. W. Aromatic Fluorine Compounds. VII. Replacement of Aromatic -Cl and -NO_2 Groups by -F. *J*. *Am*. *Chem*. *Soc*. **1956**, *78* (23), 6034–6037.

10 Adams, D. J.; Clark, J. H. Nucleophilic routes to selectively fluorinated aromatics. *Chem*. *Soc*. *Rev*. **1999**, *28* (4), 225–231.

11 Maggini, M.; Passudetti, M.; Gonzales-Trueba, G.; Prato, M.; Quintily, U.; Scorrano, G. A general procedure for the fluorodenitration of aromatic substrates. *J. Org. Chem.* **1991**, *56* (22), 6406–6411.

12 Boechat, N.; Clark, J. H. Fluorodenitrations using tetramethylammonium fluoride. *J*. *Chem*. *Soc*. *Chem*. *Commun*. **1993**, *1993* (11), 921–922.

13 Kuduk, S. D.; DiPardo, R. M.; Bock, M. G. Tetrabutylammonium Salt Induced Denitration of Nitropyridines: Synthesis of Fluoro-, Hydroxy-, and Methoxypyridines. *Org*. *Lett*. **2005**, *7* (4), 577–579.

14 Sun, H.; DiMagno, S. G. Room-Temperature Nucleophilic Aromatic Fluorination: Experimental and Theoretical Studies. *Angew*. *Chem*. *Int*. *Ed*. **2006**, *45* (17), 2720–2725.

15 See, Y. Y.; Morales-Colón, M. T.; Bland, D. C.; Sanford, M. S. Development of S_NAr Nucleophilic Fluorination: A Fruitful Academia-Industry Collaboration. *Acc. Chem. Res.* **2020**, *53* (10), 2372–2383.

16 Schimler, S. D.; Ryan, S. J.; Bland, D. C.; Anderson, J. E.; Sanford, M. S. Anhydrous Tetramethylammonium Fluoride for Room-Temperature S_NAr Fluorination. *J*. *Org*. *Chem*. **2015**, *80* (24), 12137–12145.

17 Morales-Colón, M. T.; See, Y. Y.; Lee, S. J.; Scott, P. J. H.; Bland, D. C.; Sanford, M. S. Tetramethylammonium Fluoride Alcohol Adducts for S_NAr Fluorination. *Org*. *Lett*. **2021**, *23* (11), 4493–4498.
18 Hong, C. M.; Whittaker, A. M.; Schultz, D. M. Nucleophilic Fluorination of Heteroaryl Chlorides and Aryl Triflates Enabled by Cooperative Catalysis. *J*. *Org*. *Chem*. **2021**, *86* (5), 3999–4006.
19 Tang, P.; Wang, W.; Ritter, T. Deoxyfluorination of Phenols. *J. Am. Chem. Soc.* **2011**, *133* (30), 11482–11484.
20 Neumann, C.; Hooker, J.; Ritter, T. Concerted nucleophilic aromatic substitution with $^{19}F^-$ and $^{18}F^-$. *Nature* **2016**, *534* (7607), 369–373.
21 Schimler, S. D.; Cismesia, M. A.; Hanley, P. S.; Froese, R. D. J.; Jansma, M. J.; Bland, D. C.; Sanford, M. S. Nucleophilic Deoxyfluorination of Phenols *via* Aryl Fluorosulfonate Intermediates. *J. Am. Chem. Soc.* **2017**, *139* (4), 1452–1455.
22 Kwan, E. E.; Zeng, Y.; Besser, H. A.; Jacobsen, E. N. Concerted nucleophilic aromatic substitutions. *Nat*. *Chem*. **2018**, *10* (9), 917–923.
23 Jacobson, O.; Kiesewetter, D. O.; Chen, X. Fluorine-18 Radiochemistry, Labeling Strategies and Synthetic Routes. *Bioconjugate Chem.* **2015**, *26* (1), 1–18.
24 Vitaku, E.; Smith, D. T.; Njardarson, J. T. Analysis of the Structural Diversity, Substitution Patterns, and Frequency of Nitrogen Heterocycles among U.S. FDA Approved Pharmaceuticals. *J. Med. Chem.* **2014**, *57* (24), 10257–10274.
25 Young, J. D.; Jauregui-Osoro, M.; Wong, W.-L.; Cooper, M. S.; Cook, G.; Barrington, S. F.; Ma, M. T.; Blower, P. J.; Aboagye, E. O. An overview of nuclear medicine research in the UK and the landscape for clinical adoption. *Nucl*. *Med*. *Commun*. **2021**, *42* (12), 1301–1312.
26 Chen, W.; Wang, H.; Tay, N. E. S.; Pistritto, V. A.; Li, K.-P.; Zhang, T.; Wu, Z.; Nicewicz, D. A.; Li, Z. Arene radiofluorination enabled by photoredox-mediated halide interconversion. *Nat. Chem*. **2022**, *14* (2), 216–223.
27 Ajenjo, J.; Destro, G.; Cornelissen, B.; Gouverneur, V. Closing the gap between ^{19}F and ^{18}F chemistry. *EJNMMI Radiopharm*. *Chem*. **2021**, *6*, 33.
28 Arnott, E. A.; Chan, L. C.; Cox, B. G.; Meyrick, B.; Phillips, A. Large-Scale Solvent-Free Chlorination of Hydroxy-Pyrimidines, -Pyridines, -Pyrazines and -Amides Using Equimolar $POCl_3$. *Molecules* **2012**, *17* (4), 4533–4544.
29 Berridge, M. S.; Crouzel, C.; Comar, D. Aromatic fluorination with N.C.A. F-18 fluoride: A comparative study. *J*. *Label*. *Compd*. *Radiopharm*. **1985**, *22* (7), 687–694.
30 Horti, A.; Ravert, H. T.; London, E. D.; Dannals, R. F. Synthesis of a radiotracer for studying nicotinic acetylcholine receptors: (+/−)-exo-2-(2-[^{18}F]fluoro-5-pyridyl)-7-azabicyclo[2.2.1]heptane. *J. Label*. *Compd*. *Radiopharm*. **1996**, *38* (4), 355–365.
31 Dolci, L.; Dollé, F.; Jubeau, S.; Vaufrey, F.; Crouzel, C. 2-[^{18}F]fluoropyridines by no-carrier-added nucleophilic aromatic substitution with [^{18}F]FK-K_{222}—a comparative study. *J*. *Label*. *Compd*. *Radiopharm*. **1999**, *42* (10), 975–985.
32 Karramkam, M.; Hinnen, F.; Vaufrey, F.; Dollé, F. 2-, 3- and 4-[^{18}F]Fluoropyridine by no-carrier-added nucleophilic aromatic substitution with K[^{18}F]F-K222 – a comparative study. *J*. *Label*. *Compd*. *Radiopharm*. **2003**, *46* (10), 979–992.

33 Brugarolas, P.; Freifelder, R.; Cheng, S.-H.; DeJesus, O. Synthesis of meta-substituted [^{18}F]3-fluoro-4-aminopyridine *via* direct radiofluorination of pyridine N-oxides. *Chem*. *Commun*. **2016**, *52* (44), 7150–7152.

34 Naumiec, G. R.; Cai, L.; Lu, S.; Pike, V. W. Quinuclidine and DABCO Enhance the Radiofluorination of 5-Substituted 2-Halopyridines. *Eur*. *J*. *Org*. *Chem*. **2017**, *2017* (45), 6593–6603.

35 Lee, S. J.; Morales-Colón, M. T.; Brooks, A. F.; Wright, J. S.; Makaravage, K. J.; Scott, P. J. H.; Sanford, M. S. S_NAr Radiofluorination with In Situ Generated [^{18}F]Tetramethylammonium Fluoride. *J*. *Org*. *Chem*. **2021**, *86* (20), 14121–14130.

36 Attiná, M.; Cacace, F.; Wolf, A. P. Labeled aryl fluorides from the nucleophilic displacement of activated nitro groups by $^{18}F\text{-}F^-$. *J*. *Label*. *Compd*. *Radiopharm*. **1983**, *20* (4), 501–514.

37 Massarweh, G.; Kovacevic, M.; Rosa-Neto, P.; Evans, A. C.; Diksic, M.; Schirrmacher, R. Time-efficient and convenient synthesis of [^{18}F]altanserin for human PET imaging by a new work-up procedure. *Appl*. *Radiat*. *Isot*. **2009**, *67* (11), 2040–2043.

38 Vaulina, D.; Nasirzadeh, M.; Gomzina, N. Automated radiosynthesis and purification of [^{18}F]flumazenil with solid phase extraction. *Appl*. *Radiat*. *Isot*. **2018**, *135*, 110–114.

39 Xia, C.-F.; Arteaga, J.; Chen, G.; Gangadharmath, U.; Gomez, L. F.; Kasi, D.; Lam, C.; Liang, Q.; Liu, C.; Mocharla, V. P.; Mu, F.; Sinha, A.; Su, H.; Szardenings, A. K.; Walsh, J. C.; Wang, E.; Yu, C.; Zhang, W.; Zhao, T.; Kolb, H. C. [^{18}F]T807, a novel tau positron emission tomography imaging agent for Alzheimer's disease. *Alzheimer's Dement.* **2013**, *9* (6), 666–676.

40 Irie, T.; Fukushi, K.; Ido, T. Synthesis of ^{18}F-6-fluoropurine and ^{18}F-6-fluoro-9-β-D-ribofuranosylpurine. *Int*. *J*. *Appl*. *Radiat*. *Isot*. **1982**, *33* (6), 445–448.

41 Irie, T.; Fukushi, K.; Inoue, O.; Yamasaki, T.; Ido, T.; Nozaki, T. Preparation of ^{18}F-labeled 6- and 2-fluoro-9-benzylpurine as a potential brain-scanning agent. *Int*. *J*. *Appl*. *Radiat*. *Isot*. **1982**, *33* (8), 633–636.

42 Angelini, G.; Speranza, M.; Wolf, A. P.; Shiue, C.-Y. Nucleophilic aromatic substitution of activated cationic groups by ^{18}F-labeled fluoride. A useful route to no-carrier-added (NCA) ^{18}F-labeled aryl fluorides. *J*. *Fluorine Chem*. **1985**, *27* (2), 177–191.

43 Haka, M. S.; Kilbourn, M. R.; Watkins, G. L.; Toorongian, S. A. Aryltrimethylammonium trifluoromethanesulfonates as precursors to aryl [^{18}F]fluorides: Improved synthesis of [^{18}F]GBR-13119. *J*. *Label*. *Compd*. *Radiopharm*. **1989**, *27* (7), 823–833.

44 Bouvet, V.; Wuest, M.; Jans, H.-S.; Janzen, N.; Genady, A. R.; Valliant, J. F.; Benard, F.; Wuest, F. Automated synthesis of [^{18}F]DCFPyL *via* direct radiofluorination and validation in preclinical prostate cancer models. *EJNMMI Res*. **2016**, *6*, 40.

45 Dornan, M. H.; Simard, J.-M.; Leblond, A.; Juneau, D.; Delouya, G.; Saad, F.; Ménard, C.; DaSilva. J. N. Simplified and robust one-step radiosynthesis of [^{18}F]DCFPyL *via* direct radiofluorination and cartridge-based purification. *J*. *Label*. *Compd*. *Radiopharm*. **2018**, *61* (10), 757–763.

46 Dollé, F.; Dolci, L.; Valette, H.; Hinnen, F.; Vaufrey, F.; Guenther, I.; Fuseau, C.; Coulon, C.; Bottlaender, M.; Crouzel, C. Synthesis and Nicotinic Acetylcholine Receptor in Vivo Binding Properties of 2-Fluoro-3-[2(*S*)-2-azetidinylmethoxy]pyridine: A New Positron Emission Tomography Ligand for Nicotinic Receptors. *J*. *Med*. *Chem*. **1999**, *42* (12), 2251–2259.

47 Olberg, D. E.; Arukwe, J. M.; Grace, D.; Hjelstuen, O. K.; Solbakken, M.; Kindberg, G. M.; Cuthbertson, A. One Step Radiosynthesis of 6-[^{18}F]Fluoronicotinic Acid 2,3,5,6-

Tetrafluorophenyl Ester ([^{18}F]F-Py-TFP): A New Prosthetic Group for Efficient Labeling of Biomolecules with Fluorine-18. *J*. *Med*. *Chem*. **2010**, *53* (4), 1732–1740.

48 Xiong, H.; Hoye, A. T.; Fan, K.-H.; Li, X.; Clemens, J.; Horchler, C. L.; Lim, N. C.; Attardo, G. Facile Route to 2-Fluoropyridines *via* 2-Pyridyltrialkylammonium Salts Prepared from Pyridine N-Oxides and Application to ^{18}F-Labeling. *Org*. *Lett*. **2015**, *17* (15), 3726–3729.

49 Hostetler, E. D.; Jonson, S. D.; Welch, M. J.; Katzenellenbogen, J. A. Synthesis of 2-[^{18}F]Fluoroestradiol, a Potential Diagnostic Imaging Agent for Breast Cancer: Strategies to Achieve Nucleophilic Substitution of an Electron-Rich Aromatic Ring with [^{18}F]F^{-}. *J. Org. Chem.* **1999**, *64* (1), 178–185.

50 Sun, H.; DiMagno, S. G. Competitive demethylation and substitution in *N*,*N*,*N*-trimethylanilinium fluorides. *J*. *Fluorine Chem*. **2007**, *128* (7), 806–812.

51 Rotstein, B.; Stephenson, N.; Vasdev, N.; Liang, S. H. Spirocyclic hypervalent iodine(III)-mediated radiofluorination of non-activated and hindered aromatics. *Nat. Commun.* **2014**, *5*, 4365.

52 Beyzavi, H.; Mandal, D.; Strebl, M. G.; Neumann, C. N.; D'Amato, E. M.; Chen, J.; Hooker, J. M.; Ritter, T. ^{18}F-Deoxyfluorination of Phenols *via* Ru π-Complexes. *ACS Cent. Sci.* **2017**, *3* (9), 944–948.

53 Moser, D.; Duan, Y.; Wang, F.; Ma, Y.; O'Neill, M. J.; Cornella, J. Selective Functionalization of Aminoheterocycles by a Pyrylium Salt. *Angew*. *Chem*. *Int*. *Ed*. **2018**, *57* (34), 11035–11039.

54 Narayanam, M. K.; Ma, G.; Champagne, P. A.; Houk, K. N.; Murphy, J. M. Synthesis of [^{18}F]Fluoroarenes by Nucleophilic Radiofluorination of *N*-Arylsydnones. *Angew*. *Chem*. *Int*. *Ed*. **2017**, *56* (42), 13006–13010.

55 Pérez-García, R. M.; Grønnevik, G.; J. Riss, P. J. A General Protocol for Cu-Mediated Fluoro-deamination: Sandmeyer Fluorination of Diverse Aromatic Substrates. *Org*. *Lett*. **2021**, *23* (3), 1011–1015.

56 Taylor, N. J.; Emer, E.; Preshlock, S.; Schedler, M.; Tredwell, M.; Verhoog, S.; Mercier, J.; Genicot, C.; Gouverneur, V. Derisking the Cu-Mediated ^{18}F-Fluorination of Heterocyclic Positron Emission Tomography Radioligands. *J*. *Am*. *Chem*. *Soc*. **2017**, *139* (24), 8267–8276.

57 Sowmiah, S.; Esperança, J. M. S. S.; Rebelo, L. P. N.; Afonso, C. A. M. Pyridinium salts: from synthesis to reactivity and applications. *Org*. *Chem*. *Front*. **2018**, *5* (3), 453-493.

58 Zincke, T. Ueber Dinitrophenylpyridiniumchlorid und dessen Umwandlungsproducte. *Justus Liebigs Ann*. *Chem*. **1904**, *330* (2), 361– 374.

59 Vanderwal, C. D. Reactivity and Synthesis Inspired by the Zincke Ring-Opening of Pyridines. *J*. *Org*. *Chem*. **2011**, *76* (23), 9555–9567.

60 Marek, J.; Stodulka, P.; Cabal, J.; Soukup, O.; Pohanka, M.; Korabecny, J.; Musilek, K.; Kamil Kuca, K. Preparation of the Pyridinium Salts Differing in the Length of the N-Alkyl Substituent. *Molecules* **2010**, *15* (3), 1967–1972.

61 Zincke, T.; Würker, W. Ueber Dinitrophenylpyridiniumchlorid und dessen Umwandlungsproducte (2. Mittheilung.). Ueber Dinitrophenylpyridiniumchlorid und dessen Umwandlungsproducte. *Justus Liebigs Ann*. *Chem*. **1904**, *338* (1), 107–141.

62 Balaban, A. T.; Schroth, W.; Fischer, G. Pyrylium Salts Part I. Syntheses. *Adv*. *Heterocyclic Chem*. **1969**, *10*, 241–326.

63 Katritzky, A. R. Conversions of primary amino groups into other functionality mediated by pyrylium cations. *Tetrahedron* **1980**, *36* (6), 679–699.

64 Katritzky, A. R.; Brownlee, R. T. C.; Musumarra, G. A C-13 study of the reaction of 2,4,6-triarylpyrylium cations with amines. *Tetrahedron* **1980**, *36* (11), 1643–1647.
65 Gómez-Palomino, A.; Ghiazza, C.; Busch, J.; Wagner, L.; Cornella, J. *Org*. *Synth*. **2023**, *100*, 361–381.
66 Ham, W. S.; Hillenbrand, J.; Jacq, J.; Genicot, C.; Ritter, T. Divergent Late-Stage (Hetero)aryl C−H Amination by the Pyridinium Radical Cation. *Angew*. *Chem*. *Int*. *Ed*. **2019**, *58* (2) 532–536.
67 Rössler, S. L.; Jelier, B. J.; Tripet, P. F.; Shemet, A.; Jeschke, G.; Togni, A.; Carreira, E. M. Pyridyl Radical Cation for C−H Amination of Arenes. *Angew*. *Chem*. *Int*. *Ed*. **2019**, *58* (2), 526–531.
68 Mantell, M. A.; Lasky, M. R.; Lee, M.; Remy, M.; Sanford, M. S. S_NAr and C–H Amination of Electron Rich Arenes with Pyridine as a Nucleophile Using Photoredox Catalysis. *Org*. *Lett*. **2021**, *23* (13), 5213–5217.
69 Lasky, M. R.; Salvador, T. K.; Mukhopadhyay, S.; Remy, M. S.; Vaid, T. P.; Sanford, M. S. Photochemical C(sp^2)−H Pyridination *via* Arene–Pyridinium Electron Donor–Acceptor Complexes. *Angew*. *Chem*. *Int*. *Ed*. **2022**, *61* (46), e202208741.
70 Spivey, A. C.; Arseniyadis, S. Nucleophilic Catalysis by 4-(Dialkylamino)pyridines Revisited—The Search for Optimal Reactivity and Selectivity. *Angew*. *Chem*. *Int*. *Ed*. **2004**, *43* (41), 5436–5441.
71 Xu, S.; Held, I.; Kempf, B.; Mayr, H.; Steglich, W.; Zipse, H. The DMAP-Catalyzed Acetylation of Alcohols—A Mechanistic Study. *Chem*. *Eur*. *J*. **2005**, *11* (16), 4751–4757.
72 Katritzky, A. R.; Marson, C. M. Pyrylium Mediated Transformations of Primary Amino Groups into Other Functional Groups. New Synthetic Methods. *Angew*. *Chem*. *Int*. *Ed*. **1984**, *23* (6), 420–429.
73 Katritzky, A. R.; Chermprapai, A.; Patel, R. C. The preparation of primary alkyl and benzyl fluorides from the corresponding primary amines. *J*. *Chem*. *Soc*. *Perkin Trans*. 1, **1980**, *1980* (0), 2901–2903.
74 Gómez-Palomino, A.; Cornella, J. Selective Late-Stage Sulfonyl Chloride Formation from Sulfonamides Enabled by Pyry-BF_4. *Angew*. *Chem*. *Int*. *Ed*. **2019**, *58* (50), 18235–18239.
75 Pérez-Palau, M.; Cornella, J. Synthesis of Sulfonyl Fluorides from Sulfonamides. *Eur*. *J*. *Org*. *Chem*. **2020**, *2020* (17), 2497–2500.
76 Ghiazza, C.; Faber, T.; Gómez-Palomino, A.; Cornella, J. Deaminative chlorination of aminoheterocycles. *Nat*. *Chem*. **2022**, *14* (1), 78–84.
77 Cressy, D.; Akula, M.; Frederick, A.; Shipley, K.; Osborne, D. A method for the nucleophilic fluorination of 4-dimethylaminopyridine (DMAP) pyridinium salts. *Results Chem*. **2023**, *5*, 100706.
78 Rössler, S. L.; Jelier, B. J.; Magnier, E.; Dagousset, G.; Carreira, E. M.; Togni, A. Pyridinium Salts as Redox-Active Functional Group Transfer Reagents. *Angew*. *Chem*. *Int*. *Ed*. **2019**, *59* (24), 9264–9280.
79 He, F.-S.; Ye, S.; Wu, J. Recent Advances in Pyridinium Salts as Radical Reservoirs in Organic Synthesis. *ACS Catal*. **2019**, *9* (10), 8943–8960.
80 Berndt, M.; Mueller, A.; Schmitt-Willich, H.; Stellfeld, T.; Kettschau, G.; Brumby, T.; Graham, K.; Lehmann L.; Hasfeld J.; Krueger M. Radiolabeled amino acids for diagnostic imaging. U.S. Patent WO2012150220A1, 2012.

81 Khanapur, S.; Lye, K.; Mandal, D.; Wee, X. J.; Robins, E. G.; Young, R. D. Fluorine-18 Labeling of Difluoromethyl and Trifluoromethyl Groups *via* Monoselective C−F Bond Activation. *Angew*. *Chem*. *Int*. *Ed*. **2022**, *61* (49), e202210917.
82 Greulich, T. W.; Daniliuc, C. G.; Studer, A. *N*-Aminopyridinium Salts as Precursors for N-Centered Radicals – Direct Amidation of Arenes and Heteroarenes. *Org*. *Lett*. **2015**, *17* (2), 254–257.
83 Haveman, L. Y. F.; Vugts, D. J.; Windhorst, A. D. State of the art procedures towards reactive [^{18}F]fluoride in PET tracer synthesis. *EJNMMI Radiopharm*. *Chem*. **2023**, *8*, 28.
84 Holland, J. P. Chemical Kinetics of Radiolabelling Reactions. *Chem. Eur. J.* **2018**, *24* (62), 16472–16483.
85 Collins, K. D.; Glorius, F. A robustness screen for the rapid assessment of chemical reactions. *Nat*. *Chem*. **2013**, *5* (7), 597–601.
86 Taylor, N. J.; Emer, E.; Preshlock, S.; Schedler, M.; Tredwell, M.; Verhoog, S.; Mercier, J.; Genicot, C.; Gouverneur, V. Derisking the Cu-Mediated ^{18}F-Fluorination of Heterocyclic Positron Emission Tomography Radioligands. *J*. *Am*. *Chem*. *Soc*. **2017**, *139* (24), 8267–8276.
87 Richarz, R.; Krapf, P.; Zarrad, F.; Urusova, E. A.; Neumaier, B.; Zlatopolskiy, B. D. Neither azeotropic drying, nor base nor other additives: a minimalist approach to ^{18}F-labeling. *Org*. *Biomol*. *Chem*. **2014**, *12* (40), 8094–8099.
88 Jakubczyk, M.; Mkrtchyan, S.; Shkoor, M.; Lanka, S.; Budzák, Š.; Iliaš, M.; Skoršepa, M.; Iaroshenko, V. O. Mechanochemical Conversion of Aromatic Amines to Aryl Trifluoromethyl Ethers. *J*. *Am*. *Chem*. *Soc*. **2022**, *144* (23), 10438–10445.
89 Ichiishi, N.; Brooks, A. F.; Topczewski, J. J.; Rodnick, M. E.; Sanford, M. S.; Scott, P. J. H. Copper-Catalyzed [^{18}F]Fluorination of (Mesityl)(aryl)iodonium Salts. *Org*. *Lett*. **2014**, *16* (12), 3224–3227.

Chapter 4: Experimental

Unless otherwise specified, the work described in this chapter was completed by J. Ford.

4.1. General Information (Chemistry)

All reagents used were obtained from commercial suppliers and used without further purification. Dry solvents were purchased from commercial suppliers or dried on a column of alumina. Dry conditions, where indicated, involved prior flame drying of reaction flasks and magnetic stir bars under high vacuum (<1 mbar) and then refilling the vessel with N_2. Reactions were followed by TLC (Merck Kieselgel 60 F254 plates) and visualised with UV light (λ = 254 nm), ceric ammonium molybdate, potassium permanganate or curcumin stains (for boronic acid derivatives). Silica gel (60, 40-63 μm) used for normal-phase flash column chromatography was obtained from commercial suppliers. NMR experiments were carried out at 298 K, unless otherwise specified. Deuterated solvents used for NMR experiments were purchased from commercial suppliers. All NMR spectra were recorded on Bruker AVIIIHD 400, AVIIIHD 500, AVII 500, AVIII 600 or AV NEO 600 spectrometers. ^{1}H and ^{13}C NMR spectral data are reported as chemical shifts (δ) in parts per million (ppm) to 2 d.p. and 1 d.p., respectively, relative to the solvent peak using the Bruker internal referencing procedure (edlock). ^{19}F and ^{31}P NMR spectra are reported as chemical shifts (δ) in parts per million (ppm) to 1 d.p. and are externally referenced relative to $CFCl_3$ and H_3PO_4, respectively. Coupling constants, *J*, are reported in Hz to the nearest 0.1 Hz. Unless otherwise stated, ^{13}C spectra are ^{1}H decoupled and reported coupling constants for ^{13}C spectra correspond to ^{19}F–^{13}C heteronuclear coupling, unless otherwise specified. Data are reported as follows: chemical shift, multiplicity (s = singlet, d = doublet, t = triplet, q = quartet, pent = pentet, hept = heptet, br = broad, m = multiplet), coupling constants (Hz) and integration. NMR spectra were processed with MestReNova 14.3.2. High resolution mass spectra were determined on a Thermo Exactive

mass spectrometer, for electrospray ionization (ESI-TOF), or an Agilent 7200 Accurate Mass Q-TOF GC-MS connected to a 7890 GC system, for electron ionization (GC-EI). Some compounds were found to be unstable under a variety of MS ionization methods (ESI, GC-EI, *etc*.) and therefore no HRMS could be obtained for them; this is stated for the relevant compounds. Infrared spectra were recorded as the neat compound (neat) or as an evaporated solution (thin layer film) using a Bruker Tensor 27 FT-IR spectrometer. Absorptions are reported in wavenumber (cm^{-1}). Optical rotations are reported as $[\alpha]_D^{T\,^\circ C}$ (units: ° cm^2 g^{-1}, herein ° for brevity) and were measured on a Schmidt-Haensch Autopol L 2000 polarimeter at 25 °C and λ_{max} = 589 nm. Concentrations have units g/100 mL). Melting points of solids were measured on a Stuart SMP10 apparatus and are uncorrected.

4.2. General Information (Radiochemistry)

For manual radiochemistry experiments described herein, [^{18}F]fluoride was produced by Alliance Medical (UK), Invicro (UK) or PETIC, Cardiff University (UK) *via* the $^{18}O(p,n)^{18}F$ reaction and delivered as [^{18}F]fluoride in [^{18}O]water. Radiosynthesis and azeotropic drying were performed on a NanoTek® automated microfluidic device (Advion) or on an AllinOne radiosynthesizer (TRASIS).

For automated radiochemistry experiments described herein, [^{18}F]fluoride was produced in an IBA Cyclon 18/9 cyclotron using the $^{18}O(p,n)^{18}F$ reaction in PETIC (UK). All experiments were performed on a Trasis AllinOne radiosynthesizer.

Radiochemistry terminology is as defined in Chapter 1. Briefly, radiochemical yields estimated by radio-HPLC analysis of the crude reaction mixture are referred to as RCY_{HPLC} and are decay corrected (d.c.). Isolated activity yields are non-decay corrected (n.d.c.). All molar activities are decay corrected to the end of synthesis (EOS), unless stated otherwise.

4.2.1. HPLC Conditions

Analytical HPLC runs were performed either with a Dionex Ultimate 3000 dual channel HPLC system equipped with shared autosampler, parallel UV-detectors and LabLogic NaI/PMT-radiodetectors with Flow-RAM analog output (Conditions A, approximate radio-UV detector offset = <0.1 min (pump 1) or 0.3-0.4 min (pump 2)), or on an Agilent 1200 equipped with a UV detector and LabLogic γ-RAM Model 4 detector (Conditions B, C, D: approximate radio-UV detector offset = 0.1 min).

Semi-preparative purification of radiolabelled products was achieved using the integrated HPLC system (conditions E, including UV and radio detectors) of a Trasis AllInOne synthesiser.

Conditions A: *Analytical*

Flow rate = 1.0 mL/min
Temperature = 25 °C
Wavelength = 220 nm (unless otherwise specified)
Column: Phenomenex Synergi™ 4 µm Hydro RP 80Å 150 x 4.6 mm LC column
HPLC gradient: water/MeCN

0-1 min (25% MeCN) isocratic
1-10 min (25% MeCN to 95% MeCN) linear increase
10-14 min (95% MeCN) isocratic
14-17 min (95% MeCN to 25% MeCN) linear decrease
17-19.4 min (25% MeCN) isocratic

Conditions B: *Analytical*

Flow rate = 1.0 mL/min
Temperature = 25 °C
Wavelength = 220 nm (unless otherwise specified)
Column: Phenomenex Synergi™ 4 µm Hydro RP 80Å 150 x 4.6 mm LC column
HPLC gradient: water/MeCN

0-1 min (25% MeCN) isocratic

1-10 min (25% MeCN to 95% MeCN) linear increase

10-16 min (95% MeCN) isocratic

16-18 min (95% MeCN to 25% MeCN) linear decrease

18-20 min (25% MeCN) isocratic

Conditions C: *Analytical*

Flow rate = 1.0 mL/min

Temperature = 25 °C

Wavelength = 220 nm (unless otherwise specified)

Column: Agilent C18 Eclipse Plus 80Å 150 x 4.6 mm LC column

HPLC gradient: water/MeCN

0-1 min (25% MeCN) isocratic

1-10 min (25% MeCN to 95% MeCN) linear increase

10-16 min (95% MeCN) isocratic

16-18 min (95% MeCN to 25% MeCN) linear decrease

18-20 min (25% MeCN) isocratic

Conditions D: *Analytical*

Flow rate = 1.0 mL/min

Temperature = 25 °C

Wavelength = 220 nm (unless otherwise specified)

Column: Agilent C18 Eclipse Plus 80Å 150 x 4.6 mm LC column

HPLC gradient: water/MeCN

0-1 min (5% MeCN) isocratic

1-10 min (5% MeCN to 95% MeCN) linear increase

10-14 min (95% MeCN) isocratic

14-15 min (95% MeCN to 5% MeCN) linear decrease

15-17 min (25% MeCN) isocratic

Conditions E: *Semi-preparative purification*

Flow rate = 4.0 mL/min

Temperature = room temperature

Wavelength = 254 nm

Column: Phenomenex Synergi™ 4 µm Hydro RP 80Å 250 x 10 mm LC column

Isocratic: water/MeCN

4.3. Experimental Details for Chapter 2

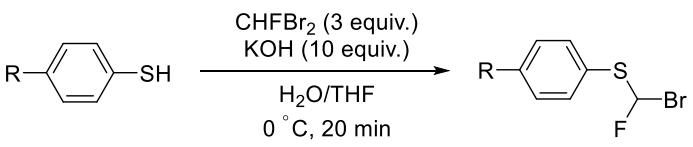
The experimental details presented in this section have been previously published (J. B. I. Sap, C. F. Meyer, J. Ford, N. J. W. Straathof, A. B. Dürr, M. J. Lelos, S. J. Paisey, T. A. Mollner, S. M. Hell, A. A. Trabanco, C. Genicot, C. W. am Ende, R. S. Paton, M. Tredwell, V. Gouverneur. [^{18}F]Difluorocarbene for positron emission tomography. *Nature* **2022**, *606* (7912), 102–108).

4.3.1. Preparation of Radiolabelling Substrates, Intermediates and Reference Compounds

4.3.1.1. Preparation of bromofluoromethyl sulfide radiolabelling precursors

Dibromofluoromethane, 4-*tert*-butylbenzenethiol, 4-methoxythiophenol, thiophenol, 4-chlorobenzenethiol, 4-mercaptobenzonitrile and 4-nitrobenzenethiol starting materials were purchased from commercial suppliers (Fluorochem, Sigma Aldrich, Biosynth) and used as received without further purification.

General Procedure 1



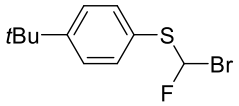
R		R	
OMe	**2.70**	Cl	**2.72**
*t*Bu	**2.59**	CN	**2.73**
H	**2.71**	NO_2	**2.74**

2.59, 2.70-2.74

The bromofluoromethyl sulfide radiolabelling precursors (**2.59**, **2.70**–**2.74**) were prepared according to a procedure adapted from the literature.[1] An aqueous solution of KOH (7.5 M, 4 mL) was added to a round-bottomed flask and cooled to 0 °C in an ice-water bath. A solution of the relevant thiophenol (3.0 mmol, 1.0 equiv.) in THF (3.0 mL) was then added to the

aqueous KOH solution and stirred for 20 minutes. Dibromofluoromethane (715 µL, 9.0 mmol, 3.0 equiv.) in THF (1.0 mL) was then added dropwise over a period of 15 minutes. The reaction mixture allowed to stir for a further 5 minutes at 0 °C, after which it was quenched by the addition of H_2O (20 mL). The crude product was extracted with CH_2Cl_2 (3 x 25 mL). The combined organic layers were washed with brine (25 mL) and dried over $MgSO_4$ and filtered. The volatiles were removed under reduced pressure. The crude product was purified by flash column chromatography.

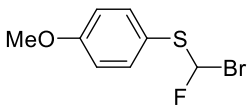
(Bromofluoromethyl)(4-(*tert*-butyl)phenyl)sulfane (2.59)



Prepared by J. Sap. This compound was prepared following General Procedure 1 using 4-*tert*-butylbenzenethiol (499 mg, 3 mmol). Flash chromatography conditions: pentane. Colourless oil, 80 mg, 10% yield.

^{1}H NMR (400 MHz, $CDCl_3$) δ 7.55 – 7.51 (m, 2H), 7.46 – 7.42 (m, 2H), 7.23 (d, J = 56.1 Hz, 1H) 1.35 (s, 9H); **^{13}C NMR** (101 MHz, $CDCl_3$) δ 153.5, 134.5, 127.3, 126.5, 92.9 (d, J = 293.9 Hz), 34.9, 31.2; **^{19}F NMR** (377 MHz, $CDCl_3$) δ -99.6 (d, J = 56.2 Hz); **HRMS** the compound did not ionise under various ionisation techniques; **IR** (neat) 2963, 2869, 1596, 1489, 1461, 1398, 1364, 1294, 1268, 1175, 1151, 1117, 995, 830.

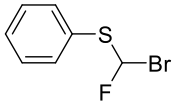
(Bromofluoromethyl)(4-methoxyphenyl)sulfane (2.70)



Prepared by J. Sap. This compound was prepared following General Procedure 1 using 4-methoxythiophenol (421 mg, 3 mmol). Flash column chromatography conditions: pentane/CH_2Cl_2 = gradient 100/0 to 80/20. Colourless oil, 38 mg, 5%.

^{1}H NMR (400 MHz, $CDCl_3$) δ 7.56 – 7.50 (m, 2H), 7.17 (d, J = 55.5 Hz, 1H), 6.96 – 6.90 (m, 2H), 3.85 (s, 3H); **^{19}F NMR** (377 MHz, $CDCl_3$) δ -100.3 (d, J = 55.7 Hz); **^{13}C NMR** (101 MHz, $CDCl_3$) δ 161.3, 137.1, 120.9, 114.9, 93.3 (d, J = 293.5 Hz), 55.4; **HRMS** the compound did not ionise under various ionisation techniques; **IR** (neat) 1591, 1572, 1494, 1462, 1441, 1290, 1249, 1173, 1151, 1107, 1029, 994, 830, 799, 770, 734.

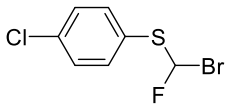
(Bromofluoromethyl)(phenyl)sulfane (2.71)



Prepared by J. Sap. This compound was prepared following General Procedure 1 using thiophenol (331 mg, 3 mmol). Flash chromatography conditions: pentane. Colourless oil, 44 mg, 7% yield.

^{1}H NMR (400 MHz, $CDCl_3$) δ 7.64 – 7.57 (m, 2H), 7.49 – 7.39 (m, 3H), 7.27 (d, J = 56.3 Hz, 1H); **^{19}F NMR** (377 MHz, $CDCl_3$) δ -99.4 (d, J = 55.8 Hz); **^{13}C NMR** (101 MHz, $CDCl_3$) δ 134.5, 130.7, 130.0, 129.4, 92.5 (d, J = 293.8 Hz); **HRMS** the compound did not ionise under various ionisation techniques; **IR** (neat) 1582, 1478, 1440, 1295, 1177, 1152, 991, 772, 736, 689, 666.

(Bromofluoromethyl)(4-chlorophenyl)sulfane (2.72)

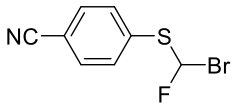


Prepared by J. Sap. This compound was prepared following General Procedure 1 using 4-chlorobenzenethiol (434 mg, 3 mmol). Flash chromatography conditions: pentane. Colourless oil, 84 mg, 11% yield.

*Alternatively, **2.72** was obtained in higher yield following General Procedure 1 using 4-chlorobenzenethiol (2 mmol) with the following deviation. The solution of 4-chlorobenzenethiol and KOH (10 equiv.) in a THF (3 mL) and H_2O (4 mL) solvent mixture was instead added dropwise over 20 minutes to a stirring solution of dibromofluoromethane (3 equiv.) in THF (1 mL) in a round bottomed flask at 0 °C. Colourless oil, 157 mg, 32% yield.*

^{1}H NMR (400 MHz, $CDCl_3$) δ 7.46 – 7.41 (m, 2H), 7.34 – 7.28 (m, 2H), 7.15 (d, *J* = 55.1 Hz, 1H); **^{19}F NMR** (377 MHz, $CDCl_3$) δ -100.0 (d, *J* = 55.2 Hz); **^{13}C NMR** (101 MHz, $CDCl_3$) δ 136.7, 136.0 (d, *J* = 1.7 Hz), 129.6, 128.7, 92.0 (d, *J* = 293.5 Hz); **HRMS** the compound did not ionise under various ionisation techniques; **IR** (neat) 1573, 1475, 1389, 1293, 1174, 1153, 1093, 1012, 820, 769, 748.

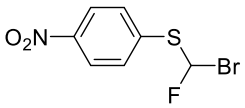
4-((Bromofluoromethyl)thio)benzonitrile (2.73)



Prepared by J. Sap. This compound was prepared following General Procedure 1 using 4-mercaptobenzonitrile (406 mg, 3 mmol). Flash chromatography conditions: pentane:CH_2Cl_2 = gradient 100/0 to 80/20. White solid, 45 mg, 6% yield.

^{1}H NMR (400 MHz, $CDCl_3$) δ 7.83 – 7.72 (m, 4H), 7.44 (d, *J* = 54.2 Hz, 1H); **^{19}F NMR** (377 MHz, $CDCl_3$) δ -100.2 (d, *J* = 54.9 Hz); **^{13}C NMR** (101 MHz, $CDCl_3$) δ 137.2 (d, *J* = 1.8 Hz), 133.4 (d, *J* = 2.0 Hz), 132.8, 118.0, 113.3, 90.6 (d, *J* = 293.9 Hz); **HRMS** the compound did not ionise under various ionisation techniques; **MP** 48 – 50 °C. **IR** (neat) 2993, 2228, 2031,1594, 1493, 1403, 1293, 1181, 1143, 1084, 1019, 960, 832, 812.

(Bromofluoromethyl)(4-nitrophenyl)sulfane (2.74)



This compound was prepared following General Procedure 1 using 4-nitrobenzenethiol (233 mg, 1.5 mmol). Flash chromatography conditions: pentane/toluene = 95/5 to 85/15. White solid, 34 mg, 9% yield.

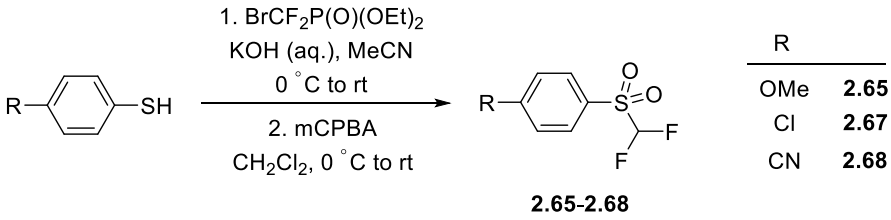
^{1}H NMR (400 MHz, $CDCl_3$) δ 8.29 – 8.23 (m, 2H), 7.75 – 7.67 (m, 2H), 7.38 (d, *J* = 54.9 Hz, 1H); **^{19}F NMR** (377 MHz, $CDCl_3$) δ -100.5 (d, *J* = 55.1 Hz); **^{13}C NMR** (101 MHz, $CDCl_3$) δ 148.2, 139.4 (d, *J* = 1.8 Hz), 133.1 (d, *J* = 2.1 Hz), 124.3, 90.3 (d, *J* = 294.0 Hz); **HRMS** the compound did not ionise under various ionisation techniques; **MP** 68 – 70 °C; **IR** (neat) 3104, 2919,

2360, 2160, 2031, 1593, 1576, 1504, 1480, 1401,1359, 1336, 1320, 1281, 1166, 1120, 1109, 1088, 1009, 976, 958, 851, 836, 780, 742.

4.3.1.2. Preparation of difluoromethyl aryl sulfone authentic references

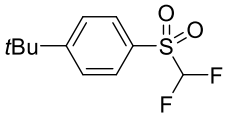
2.66 was obtained from a commercial supplier (Fluorochem) and used without further purification.

General Procedure 2



To a round bottomed flask, a solution of the relevant thiol (1 equiv.) in MeCN (5 mL) was added to an aqueous solution of KOH (2 M, 5 mL). The mixture was stirred and cooled to 0 °C, before diethyl bromodifluoromethylphosphonate (2 equiv.) was added. The ice-water bath was removed and the mixture was allowed to warm to room temperature and stirred for 30 min or until complete consumption of starting material. The reaction mixture was extracted with Et_2O (3 x 5 mL) and the combined organic layers were dried over $MgSO_4$, filtered and concentrated under reduced pressure. This mixture was redissolved in CH_2Cl_2 (20 mL) and *m*CPBA (3 equiv.) was added portionwise at 0 °C. The mixture was allowed to warm to room temperature and stirred until completion. The mixture was quenched by addition of $NaHCO_3$ (sat. aq., 20 mL), washed with brine (20 mL) and extracted with CH_2Cl_2 (3 x 10 mL). The mixture was dried over $MgSO_4$, filtered and concentrated *in vacuo* to yield crude sulfone which was purified by flash column chromatography.

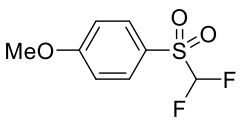
1-(*Tert*-butyl)-4-((difluoromethyl)sulfonyl)benzene (2.58)



Prepared by C. Meyer. 4-*Tert*-butylbenzenethiol (16.6 g, 100 mmol, 1 equiv.) was added to a suspension of K_2CO_3 (20.7 g, 150 mmol, 1.5 equiv.) and sodium chlorodifluoroacetate (30.5 g, 200 mmol, 2.0 equiv.) in dry DMF (250 mL). The mixture was heated to 80 °C behind a blast shield and stirred until completion (20 h). The mixture was cooled to room temperature, diluted with water (200 mL), extracted with EtOAc (3 x 150 mL) and washed with LiCl (10% aq., 200 mL). The organic layer was dried (Na_2SO_4), filtered and concentrated under reduced pressure (19.4 g crude product). The crude product (4-(*tert*-butyl) phenyl)(difluoromethyl) sulfane (9.0 g, 42 mmol, 1.0 equiv.) was dissolved in CH_2Cl_2 (180 mL) and *m*CPBA (21.5 g, 87 mmol, 2.1 equiv.) was added portionwise at 0 °C behind a blast shield. The mixture was allowed to warm to room temperature and stirred until completion. The mixture was quenched by addition of Na_2SO_3 (sat. aq., 200 mL) at 0 °C, basified (pH 10) with NaOH (1 M) and extracted with CH_2Cl_2 (3 x 200 mL). The mixture was dried over Na_2SO_4, filtered and concentrated under reduced pressure to yield **2.58**. White solid, 9.96 g, 96% yield.

^{1}H NMR (400 MHz, $CDCl_3$) δ 7.92 – 7.88 (m, 2H), 7.67 – 7.62 (m, 2H), 6.18 (t, J = 53.5 Hz, 1H), 1.36 (s, 9H); **^{13}C NMR** (101 MHz, $CDCl_3$) δ 160.3, 130.6, 128.7, 126.8, 114.8 (t, J = 285.4 Hz), 35.6, 31.0; **^{19}F NMR** (377 MHz, $CDCl_3$) δ -121.9 (d, J = 53.6 Hz); **MS** (ESI-TOF): 271.0 ($[M+Na]^+$). The recorded spectral data are in agreement with those reported in literature.[2]

1-((Difluoromethyl)sulfonyl)-4-methoxybenzene (2.65)

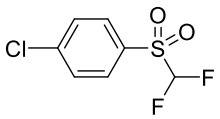


Prepared by C. Meyer. This compound was prepared following General Procedure 2 using 4-methoxybenzenethiol (140 mg, 1.0 mmol). Grey solid, 120 mg, 54% yield.

^{1}H NMR (400 MHz, $CDCl_3$) δ 7.96 – 7.79 (m, 2H), 7.13 – 6.99 (m, 2H), 6.17 (t, J = 53.6 Hz, 1H), 3.90 (s, 3H); **^{19}F NMR** (377 MHz, $CDCl_3$) δ -122.0 (d, J = 53.8 Hz); **^{13}C NMR** (101 MHz,

$CDCl_3$) δ 165.6, 132.9, 122.6, 115.0, 114.6 (t, J = 284.3 Hz), 55.9. The recorded spectral data are in agreement with those reported in literature.[2]

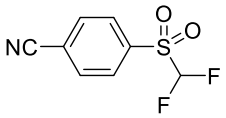
1-((Difluoromethyl)sulfonyl)-4-chlorobenzene (2.67)



Prepared by C. Meyer. This compound was prepared following General Procedure 2 using 4-chlorobenzenethiol (145 mg, 1.0 mmol). White solid, 158 mg, 70% yield.

^{1}H NMR (400 MHz, $CDCl_3$) δ 8.01 – 7.87 (m, 2H), 7.70 – 7.60 (m, 2H), 6.22 (t, J = 53.3 Hz, 1H); **^{19}F NMR** (377 MHz, $CDCl_3$) δ -121.3 (d, J = 53.5 Hz); **^{13}C NMR** (101 MHz, $CDCl_3$) [overlapping signals] δ 143.1, 132.1, 130.1, 114.6 (t, J = 285.9 Hz). The recorded spectral data are in agreement with those reported in literature.[2]

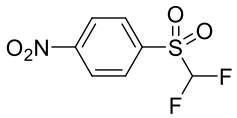
4-((Difluoromethyl)sulfonyl)benzonitrile (2.68)



This compound was prepared following General Procedure 2 using 4-mercaptobenzonitrile (68 mg, 0.5 mmol). White solid, 68 mg, 63% yield.

^{1}H NMR (500 MHz, $CDCl_3$) δ 8.18 – 8.12 (m, 2H), 8.01 – 7.94 (m, 2H), 6.27 (t, J = 53.1 Hz, 1H); **^{19}F NMR** (470 MHz, $CDCl_3$) δ -120.7 (d, J = 53.0 Hz); **^{13}C NMR** (126 MHz, $CDCl_3$) δ 136.0, 133.2, 131.4, 119.7, 116.7, 114.7 (t, J = 287.0 Hz); **HRMS** the compound did not ionise under various ionisation techniques; **IR** (neat) 3101, 3049, 2969, 2234, 1404, 1356, 1344, 1316, 1308, 1290, 1182, 1162, 1113, 1076, 1019, 843, 832, 716, 608; **MP** 110 – 112 °C.

1-((difluoromethyl)sulfonyl)-4-nitrobenzene (2.69)



4-Nitrobenzenethiol (2.3 g, 15 mmol, 1 equiv.) was added to a suspension of K_2CO_3 (3.1 g, 22.5 mmol, 1.5 equiv.) and sodium chlorodifluoroacetate (4.6 g, 30 mmol, 2.0 equiv.) in dry DMF (75 mL). The mixture was heated to 95 °C behind a blast shield and stirred until completion (0.75 h). The mixture was cooled to room temperature, diluted with water (40 mL), extracted with EtOAc (3 x 30 mL) and washed with LiCl (10% aq., 40 mL). The organic layer was dried (Na_2SO_4), filtered and concentrated under reduced pressure. The crude product was dissolved in CH_2Cl_2 (65 mL) and *m*CPBA (77% purity, 7.77 g, 2.3 equiv.) was added portionwise at 0 °C behind a blast shield. The mixture was allowed to warm to room temperature and stirred until completion. The mixture was quenched by addition of $NaHCO_3$ (sat. aq) at 0 °C and extracted with CH_2Cl_2 three times. The combined organics were washed with H_2O then with brine and the mixture was dried over Na_2SO_4, filtered and concentrated under reduced pressure. The mixture was then purified by flash column chromatography (pentane/CH_2Cl_2 = 1/1) to yield **2.69**. Pale yellow solid, 2.3 g, 65% yield.

^{1}H NMR (400 MHz, $CDCl_3$) δ 8.67 – 8.44 (m, 2H), 8.35 – 8.16 (m, 2H), 6.29 (t, *J* = 53.1 Hz, 1H); **^{19}F NMR** (377 MHz, $CDCl_3$) δ -120.7 (d, *J* = 53.2 Hz); **^{13}C NMR** (101 MHz, $CDCl_3$) δ 152.2, 137.4, 132.3, 124.7, 114.7 (t, *J* = 286.8 Hz). The recorded spectral data are in agreement with those reported in literature.[2]

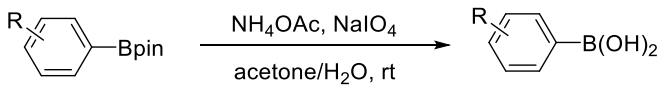
4.3.1.3. Preparation of radiolabelling substrates and related synthetic intermediates

4-Phenylphenol, 4-biphenylboronic acid, 4-(2-thienyl)phenylboronic acid, 4-chlorophenylboronic acid, 4-vinylphenylboronic acid, 4-morpholinophenylboronic acid, 4-(dibenzofuranyl)boronic acid, 4-phenoxyphenylboronic acid, 3,4-(methylenedioxy) phenylboronic acid, 2-methoxy-5-pyridinylboronic acid, 4-nitrophenylboronic acid, (4-

(hydroxymethyl)phenyl)boronic acid, (4-cyanophenyl)boronic acid, 4-bromophenylboronic acid and 3-methoxyphenylboronic acid were purchased from commercial suppliers (Fluorochem, Biosynth, CombiBlocks, Apollo Scientific, Sigma Aldrich) and used as received without further purification.

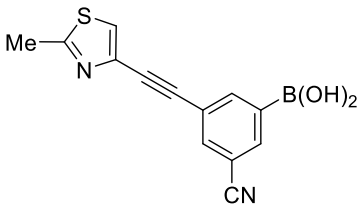
N,*N*-Diethyl-2-(2-(4-hydroxyphenyl)-5,7-dimethylpyrazolo[1,5-*a*]pyrimidin-3-yl)acetamide (**2.82**),[3] 2-(4-(3-(2-(diethylamino)-2-oxoethyl)-5,7-dimethylpyrazolo[1,5-*a*]pyrimidin-2-yl)phenoxy) ethyl 4-methylbenzenesulfonate (**2.83**),[4] Fenofibrate boronic acid,[5] 3-((2-methylthiazol-4-yl)ethynyl)-5-(4,4,5,5-tetramethyl-1,3,2-dioxaborolan-2-yl)benzonitrile,[6] 4-(5-methylisoxazole-4-carboxamido)phenylboronic acid[7] and *tert*-butyl (3-(4-bromophenoxy)-3-phenylpropyl)(methyl)carbamate[8] were prepared exactly as described in literature reports.

General Procedure 3



A single-necked round bottom flask was charged with boronic pinacol ester starting material (1 equiv.), acetone and water solvents. To the stirring solution was then added NH_4OAc (6 equiv.) and $NaIO_4$ (6 equiv.). The mixture was then left to stir at rt until TLC showed no starting material was remaining. The reaction mixture was filtered through a pad of celite, eluting EtOAc. The solvent was then removed under reduced pressure. This crude mixture was redissolved in EtOAc and transferred to a separatory funnel. The organics were washed twice with water and then with brine. The organics were then dried over $MgSO_4$ and were concentrated under reduced pressure.

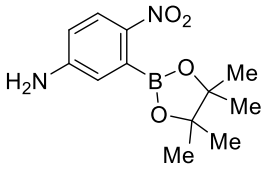
(3-cyano-5-((2-methylthiazol-4-yl)ethynyl)phenyl)boronic acid



The following is adapted from a literature procedure.[9] A 25 mL round bottom flask was charged with 3-((2-methylthiazol-4-yl)ethynyl)-5-(4,4,5,5-tetramethyl-1,3,2-dioxaborolan-2-yl) benzonitrile (705 mg, 2.0 mmol, 1 equiv.) and $NaIO_4$ (1.33 g, 6.2 mmol, 3.1 equiv.). Solvent (THF: water = 4:1, 16.8 mL) was added and the mixture was stirred at rt for 30 mins. After this time, 1 M aqueous HCl (1.5 mL) was added to the reaction mixture, and it was left to stir at rt for 24 h. The reaction was then diluted with EtOAc (30 mL) and transferred to a separatory funnel. The organics were washed with water (2 x 20 mL) and brine (20 mL), then dried over $MgSO_4$. The mixture was filtered, and the volatiles were removed under reduced pressure. The product was precipitated with heptane and the solid was washed with hexane. Beige solid, 315 mg, 58 % yield.

^{1}H NMR (400 MHz, DMSO-d_6) δ 8.20 – 8.15 (m, 1H), 8.13 – 8.08 (m, 1H), 8.04 (t, J = 1.7 Hz, 1H), 7.92 (s, 1H), 2.65 (s, 3H). **^{13}C NMR** (101 MHz, DMSO-d_6) δ 166.8, 141.4, 137.9, 136.1, 135.1, 125.8, 122.8, 118.6, 112.1, 86.6, 86.0, 19.0. *n.b*. C(Ar)-B was not observed. **HRMS** (ESI-TOF) calculated for $C_{13}H_9BN_2O_2S$ ([M-H]$^-$): 267.0405, found: 267.0401. **IR** (thin layer film) 2924, 2853, 2231, 1586, 1502, 1442, 1392, 1345, 1278, 1241, 1166, 892, 753. **MP** decomposed above 212 °C.

4-nitro-3-(4,4,5,5-tetramethyl-1,3,2-dioxaborolan-2-yl)aniline

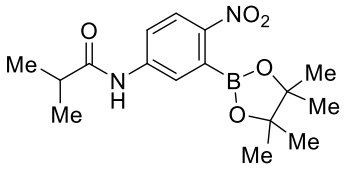


The following was adapted from a literature procedure.[10] A 250 mL two-necked round bottom flask under N_2 atmosphere was charged with 3-bromo-4-nitroaniline (2.17 g, 10 mmol, 1 equiv.), bis(pinacolato)diboron (3.81 g, 15 mmol, 1.5 equiv.), Pd(dppf)Cl_2 (220 mg, 0.3 mmol, 3 mol%) and KOAc (2.52 g, 25.7 mmol, 2.57 equiv.). The mixture was dissolved in dry DMSO (50 mL). This solution was then purged with N_2 for 15 mins. The reaction mixture was stirred at 80 °C for 24 h. The reaction mixture was transferred to a separatory funnel and partitioned

between toluene (50 mL) and water (50 mL). The organic layer was retained and the aqueous layer was washed with EtOAc (3 x 25 mL). The organics were combined and washed with brine (25 mL) and then dried over Na_2SO_4. The volatiles were then removed under reduced pressure and the crude mixture was purified by flash column chromatography (CH_2Cl_2/pentane = gradient 70/30 to 100/0). Yellow solid, 1.17 g, 44 % yield.

^{1}H NMR (400 MHz, $CDCl_3$) δ 8.08 – 7.92 (m, 1H), 6.63 – 6.55 (m, 2H), 4.37 (s, 2H), 1.41 (s, 12H). **^{13}C NMR** (101 MHz, $CDCl_3$) δ 152.1, 141.5, 126.2, 116.8, 114.2, 84.5, 24.9. *n.b*. C(Ar)-B was not observed. **HRMS** (ESI-TOF) calculated for $C_{12}H_{17}BN_2O_4$ ($[M+H]^+$): 265.1354, found: 265.1355. **IR** (thin layer film) 3363, 3246, 2980, 1634, 1582, 1478, 1442, 1364, 1314, 1255, 1142, 1047, 964, 851, 763, 702, 675, 628. **MP** 144 °C.

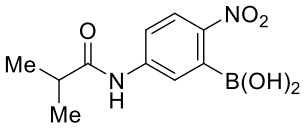
***N*-(4-nitro-3-(4,4,5,5-tetramethyl-1,3,2-dioxaborolan-2-yl)phenyl)isobutyramide**



The following was adapted from a literature procedure.[7] A 100 mL two-necked round bottom flask under N_2 atmosphere was charged with 23 (1.1 g, 4.17 mmol, 1 equiv.). 30 mL dry CH_2Cl_2 solvent was then added and after cooling to 0 °C, *i*Pr_2NEt (2.27 mL, 12.5 mmol, 3 equiv.) was slowly added *via* syringe. At 0°C, a solution of isobutyryl chloride (0.65 mL, 6.25 mmol, 1.5 equiv.) in 8 mL CH_2Cl_2 was added dropwise *via* syringe. Once the addition was complete, the ice-water bath was removed and the reaction mixture was left to stir overnight at rt The reaction mixture was diluted with 50 mL CH_2Cl_2 and transferred to a separatory funnel. The organics were washed with 1 M HCl (50 mL x 2), saturated $NaHCO_3$ solution (50 mL x 2), and brine (50 mL). The organics were dried over $MgSO_4$, filtered and the volatiles were subsequently removed under reduced pressure. The crude mixture was purified by flash column chromatography (CH_2Cl_2/Et_2O = gradient 100/0 to 90/10). Yellow solid, 921 mg, 66 % yield.

^{1}H NMR (600 MHz, $CDCl_3$) δ 8.14 (d, J = 9.0 Hz, 1H), 7.85 (dd, J = 9.0, 2.4 Hz, 1H), 7.56 (d, J = 2.4 Hz, 1H), 7.44 (s, 1H), 2.53 (sept, J = 6.9 Hz, 1H), 1.42 (s, 12H), 1.26 (d, J = 6.8 Hz, 6H). **^{13}C NMR** (151 MHz, $CDCl_3$) δ 175.7, 146.1, 143.4, 125.0, 122.2, 119.9, 84.9, 37.1, 24.9, 19.6. *n.b.* C(Ar)-B was not observed. **HRMS** (ESI-TOF) calculated for $C_{16}H_{23}BN_2O_5$ ($[M-H]^-$): 333.1628, found: 333.1625. **IR** (thin layer film) 3316, 2977, 1680, 1623, 1581, 1551, 1509, 1407, 1383, 1373, 1338, 1319, 1271, 1238, 1194, 1141, 1122, 1051, 965, 906, 842, 791, 764, 733, 699, 670, 647. **MP** 180 °C.

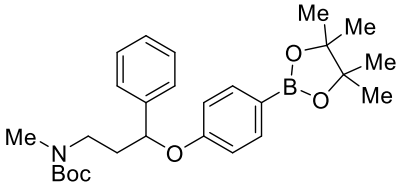
(5-isobutyramido-2-nitrophenyl)boronic acid



General Procedure 3 was followed using *N*-(4-nitro-3-(4,4,5,5-tetramethyl-1,3,2-dioxaborolan-2-yl)phenyl)isobutyramide (668 mg, 2 mmol), acetone (26 mL), water (13 mL), NH_4OAc (925 mg, 12 mmol), $NaIO_4$ (2.57 g, 12 mmol), and a reaction time of 48 h. The product was then precipitated from cold CH_2Cl_2 and washed with hexane. Yellow solid, 486 mg, 96 % yield.

^{1}H NMR (600 MHz, DMSO-d_6) δ 8.10 (d, J = 9.1 Hz, 1H), 7.78 (dd, J = 9.1, 2.3 Hz, 1H), 7.66 (d, J = 2.3 Hz, 1H), 2.62 (hept, J = 6.8 Hz, 1H), 1.09 (d, J = 6.8 Hz, 6H). **^{13}C NMR** (151 MHz, DMSO-d_6) δ 177.0, 145.0, 144.5, 124.9, 121.3, 118.8, 35.6, 19.7. *n.b.* C(Ar)-B was not observed. **HRMS** (ESI-TOF) calculated for $C_{10}H_{13}BN_2O_5$ ($[M+H]^+$): 251.0845, found: 251.0841. **IR** (thin layer film): 3309, 2923, 1682, 1552, 1508, 1404, 1335, 1243, 1155, 838, 767. **MP** decomposed above 165 °C.

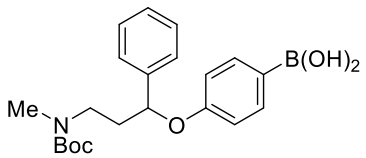
***Tert*-butyl methyl(3-phenyl-3-(4-(4,4,5,5-tetramethyl-1,3,2-dioxaborolan-2-yl)phenoxy)propyl)carbamate**



A 25 mL Schlenk tube under N_2 atmosphere was charged with bis(pinacolato)diboron (660 mg, 2.6 mmol, 1.3 equiv.), Pd(dppf)Cl_2 (73 mg, 0.1 mmol, 5 mol%) and KOAc (589 mg, 6 mmol, 3 equiv.). The Schlenk tube was evacuated and refilled with N_2 three times. In a separate Schlenk tube under N_2 atmosphere, *tert*-butyl (3-(4-bromophenoxy)-3-phenylpropyl)(methyl)carbamate (840 mg, 2 mmol, 1 equiv.) was dissolved in dry, degassed 1,4-dioxane (10 mL). This solution was then transferred to the other Schlenk tube *via* syringe. The tap was closed, and the reaction mixture was stirred at 80 °C for 14 h. The reaction mixture then diluted with EtOAc (10 mL) and filtered through celite, eluting EtOAc (30 mL). The volatiles were removed under reduced pressure and the crude mixture was purified by flash column chromatography (pentane/EtOAc = 90/10). Colourless viscous gel, 779 mg, 83 % yield.

^{1}H NMR (600 MHz, $CDCl_3$) δ 7.63 (d, J = 8.6 Hz, 1H), 7.30 (d, J = 6.3 Hz, 4H), 7.25 – 7.17 (m, 1H), 6.81 (d, J = 8.4 Hz, 2H), 5.35 – 4.95 (m, 1H), 3.39 (d, J = 44.5 Hz, 2H), 2.83 (s, 3H), 2.37 – 1.94 (m, 2H), 1.38 (broad s, 9H), 1.29 (s, 12H). **^{13}C NMR** (151 MHz, $CDCl_3$) δ 160.6, 155.9, 141.5, 136.5, 128.8, 127.7, 125.9, 115.3, 83.6, 79.5, 46.0, 37.4 (br), 34.7 (br), 28.6, 25.0, 24.9. *n.b*. C(Ar)-B was not observed. **HRMS** (ESI-TOF) calculated for $C_{27}H_{38}BNO_5$ ($[M+Na]^+$): 490.2738, found: 490.2731. **IR** (thin layer film) 2980, 2360, 1696, 1604, 1569, 1455, 1396, 1361, 1318, 1273, 1239, 1173, 1144, 1091, 1052, 1012, 963, 861, 831, 763, 701, 670, 655.

(4-(3-((*tert*-butoxycarbonyl)(methyl)amino)-1-phenylpropoxy)phenyl)boronic acid

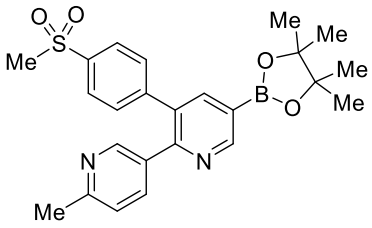


General Procedure 3 was followed using *tert*-butyl methyl(3-phenyl-3-(4-(4,4,5,5-tetramethyl-1,3,2-dioxaborolan-2-yl)phenoxy)propyl)carbamate (1.99 g, 4.26 mmol, 1 equiv.), acetone (160 mL), water (65 mL), NH_4OAc (1.97 g, 25.6 mmol, 6 equiv.), $NaIO_4$ (5.47 g, 25.6 mmol, 6 equiv.). The crude product was then purified by flash column chromatography

as described for this compound in the literature (CH_2Cl_2/*i*PrOH = 98/2).[8] White solid, 1.17 g, 71 % yield.

^{1}H NMR (400 MHz, DMSO-d_6) δ 7.59 (d, *J* = 8.1 Hz, 2H), 7.39 – 7.29 (m, 4H), 7.28 – 7.20 (m, 1H), 6.81 (d, *J* = 8.3 Hz, 2H), 5.30 (m, 1H), 3.30 (br m, 2H), 2.74 (s, 3H), 2.14 – 1.88 (m, 2H), 1.29 (br, 9H). **^{13}C NMR** (101 MHz, DMSO-d_6) *δ* 159.4, 155.0, 141.5, 135.8, 128.7, 127.7, 126.1, 114.9, 78.6, 76.1, 45.1, 36.4, 33.9, 28.1. *n.b*. C(Ar)-B was not observed. **HRMS** (ESI-TOF) calculated for $C_{21}H_{28}BNO_5Na$ ([M+Na]$^+$): 408.1954, found: 408.1952; **IR** (neat) 3658, 2981, 2889, 1666, 1604, 1462, 1382, 1241, 1154, 1073, 954, 830, 752, 699, 645; **MP** 105 – 110 °C. The recorded spectral data agree with those reported in the literature.[8]

6'-methyl-3-(4-(methylsulfonyl)phenyl)-5-(4,4,5,5-tetramethyl-1,3,2-dioxaborolan-2-yl)-2,3'-bipyridine

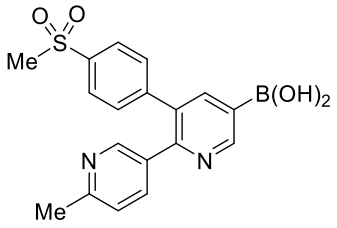


The following is adapted from a literature procedure.[11] A 15 mL Schlenk tube under N_2 atmosphere was charged with etoricoxib (900 mg, 2.51 mmol, 1 equiv.), bis(pinacolato)diboron (1.91 g, 7.5 mmol, 3 equiv.), $Pd_2(dba)_3$ (22.6 mg, 0.0025 mmol, 1 mol%), XPhos (47.7 mg, 0.1 mmol, 4 mol%) and KOAc (739 mg, 7.5 mmol, 3 equiv.). The Schlenk tube was evacuated and refilled with N_2, after which 5 mL dry, degassed 1,4-dioxane was added. The reaction mixture was then heated at 110 °C for 2 h. The reaction mixture was diluted with 10 mL EtOAc and then filtered through a pad of celite, eluting EtOAc (30 mL). The volatiles were removed under reduced pressure. The product was then triturated from hexane and washed with cold Et_2O. White solid, 1.01 g, 89 % yield.

^{1}H NMR (600 MHz, $CDCl_3$) *δ* 9.05 (d, *J* = 1.6 Hz, 1H), 8.41 (d, *J* = 2.3 Hz, 1H), 8.09 (d, *J* = 1.6 Hz, 1H), 7.86 (d, *J* = 8.3 Hz, 2H), 7.62 (dd, *J* = 8.0, 2.3 Hz, 1H), 7.41 (d, *J* = 8.3 Hz, 2H), 7.08 (d, *J* =

8.0 Hz, 1H), 3.06 (s, 3H), 2.53 (s, 3H), 1.37 (s, 12H). **^{13}C NMR** (151 MHz, $CDCl_3$) 158.5, 156.4, 155.3, 150.2, 145.5, 145.0, 139.7, 137.6, 133.8, 132.4, 130.7, 127.8, 122.9, 84.7, 44.7, 25.0, 24.4. *n.b*. C(Ar)-B was not observed. **HRMS** (ESI-TOF) calculated for $C_{24}H_{27}BN_2O_4S$ ($[M+H]^+$): 451.1859, found: 451.1857. **IR** (thin layer film) 2980, 1593, 1456, 1392, 1361, 1314, 1269, 1214, 1146, 1120, 1091, 1037, 1015, 961, 916, 879, 849, 780, 761, 729, 684. **MP** 212 °C.

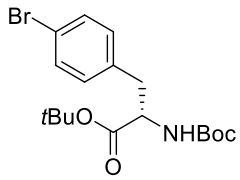
(6'-methyl-3-(4-(methylsulfonyl)phenyl)-[2,3'-bipyridin]-5-yl)boronic acid



General Procedure 3 was followed using 6'-methyl-3-(4-(methylsulfonyl)phenyl)-5-(4,4,5,5-tetramethyl-1,3,2-dioxaborolan-2-yl)-2,3'-bipyridine (867 mg, 1.93 mmol), acetone (30 mL), water (15 mL), NH_4OAc (1.12 g, 14.5 mmol, 7.5 equiv.), $NaIO_4$ (3.11 g, 14.5 mmol, 7.5 equiv.), and a reaction time of 67 h. The product was then washed with hexane and cold Et_2O. White solid, 245 mg, 33 % yield.

^{1}H NMR (600 MHz, DMSO-d_6) δ 8.99 (d, J = 1.7 Hz, 1H), 8.31 (d, J = 2.4 Hz, 1H), 8.17 (d, J = 1.7 Hz, 1H), 7.93 – 7.85 (m, 2H), 7.59 (dd, J = 8.0, 2.4 Hz, 1H), 7.52 – 7.45 (m, 2H), 7.19 (d, J = 8.1 Hz, 1H), 3.21 (s, 3H), 2.43 (s, 3H). **^{13}C NMR** (151 MHz, DMSO-d_6) δ 157.8, 154.8, 154.5, 149.6, 145.1, 144.6, 139.8, 137.7, 133.7, 132.5, 130.7, 127.4, 122.8, 43.7, 23.9. *n.b*. C(Ar)-B was not observed. **HRMS** (ESI-TOF) calculated for $C_{18}H_{17}BN_2O_4S$ ($[M+Na]^+$): 369.1076, found: 369.1073. **IR** (thin layer film) 2924, 1596, 1411, 1370, 1311, 1256, 1219, 1150, 1090, 1017, 959, 842, 773. **MP** decomposed above 202 °C.

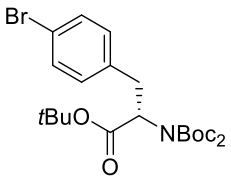
***tert*-butyl (*S*)-3-(4-bromophenyl)-2-((*tert*-butoxycarbonyl)amino)propanoate**



The following is adapted from a literature procedure.[12] To a two-necked round bottom flask under N_2 atmosphere, was added Boc-Phe(4-Br)-OH (4.13 g, 12 mmol, 1 equiv.), DMAP (147 mg, 1.2 mmol, 0.1 equiv.) and *tert*-butanol (34 mL). Boc_2O (3.14 g, 14.4 mmol, 1.2 equiv.) was then added as a solid and the resulting solution was stirred at 50 °C for 24 h. The solvent was then removed under reduced pressure and the crude mixture was purified directly by flash column chromatography (pentane/Et_2O = gradient 100/0 to 80/20). Colourless viscous oil, 3.03 g, 63 % yield.

^{1}H NMR (400 MHz, $CDCl_3$) δ 7.40 (d, J = 8.4 Hz, 2H), 7.04 (d, J = 8.4 Hz, 2H), 4.99 (d, J = 7.3 Hz, 1H), 4.42 (q, J = 6.2 Hz, 1H), 3.00 (m, 2H), 1.42 (s, 9H), 1.41 (s, 9H). **^{13}C NMR** (101 MHz, $CDCl_3$) δ 170.8, 155.2, 135.6, 131.5, 131.4, 120.9, 82.5, 79.9, 54.8, 38.1, 28.4, 28.1. **HRMS** (ESI-TOF) calculated for $C_{18}H_{26}BrNO_4$ ($[M+Na]^+$) 422.0937, found: 422.0937. **IR** (thin layer film) 3349, 2978, 2932, 1711, 1489, 1455, 1392, 1366, 1250, 1151, 1103, 1072, 1058, 1012, 844, 805, 780. 711. $\alpha_D^{25\,°C}$ + 35.5 ° (c = 0.50, $CHCl_3$).

***tert*-butyl (*S*)-2-(bis(*tert*-butoxycarbonyl)amino)-3-(4-bromophenyl)propanoate**

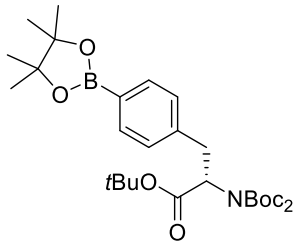


The following is adapted from a literature procedure.[12] To a two-necked round bottom flask under N_2 atmosphere, was added *tert*-butyl (*S*)-3-(4-bromophenyl)-2-((*tert*-butoxycarbonyl)amino)propanoate (2.80 g, 7 mmol, 1 equiv.), Boc_2O (12.2 g, 56 mmol, 8 equiv.), and acetonitrile (37 mL). DMAP (342 mg, 2.8 mmol, 0.4 equiv.) was then added and the resulting solution was stirred at rt for 43 h. The solvent was then removed under reduced

pressure and the crude mixture was purified directly by flash column chromatography (pentane/Et_2O = gradient 100/0 to 90/10). Colourless viscous oil, 3.50 g, 99 % yield.

^{1}H NMR (400 MHz, $CDCl_3$) δ 7.37 (d, J = 8.4 Hz, 2H), 7.05 (d, J = 8.4 Hz, 2H), 4.99 (dd, J = 10.2, 5.3 Hz, 1H), 3.33 (dd, J = 14.2, 5.3 Hz, 1H), 3.16 (dd, J = 14.2, 10.2 Hz, 1H), 1.46 (s, 9H), 1.42 (s, 18H). **^{13}C NMR** (101 MHz, $CDCl_3$) δ 169.3, 152.4, 137.3, 131.5, 131.4, 120.4, 82.9, 81.8, 59.9, 35.4, 28.1, 28.1. **HRMS** (ESI-TOF) calculated for $C_{23}H_{34}BrNO_6$ ([M+Na]$^+$): 522.1486, found: 522.1462. **IR** (thin layer film) 2979, 2934, 1734, 1700, 1489, 1457, 1382, 1366, 1310, 1287, 1254, 1234, 1139, 1119, 1072, 1012, 979, 852, 813, 784, 769. **$\alpha_D^{25\,°C}$** – 69.3 ° (c = 0.62, $CHCl_3$).

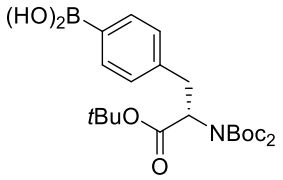
***tert*-butyl (*S*)-2-(bis(*tert*-butoxycarbonyl)amino)-3-(4-(4,4,5,5-tetramethyl-1,3,2-dioxaborolan-2-yl)phenyl)propanoate**



The following is adapted from a literature procedure.[11] In a Schlenk tube, $Pd_2(dba)_3$ (23 mg, 0.025 mmol, 1 mol%), XPhos (48 mg, 0.1 mmol, 4 mol%), bis(pinacolato)diboron (698 mg, 2.75 mmol, 1.1 equiv.) and KOAc (736 mg, 7.5 mmol, 3 equiv.) were added under N_2 atmosphere. A solution of *tert*-butyl (*S*)-2-(bis(*tert*-butoxycarbonyl)amino)-3-(4-bromophenyl)propanoate (1.25 g, 2.5 mmol, 1 equiv.) in dry, degassed 1,4-dioxane (5 mL) was then added *via* syringe. The tap was closed and the reaction mixture was heated to 110 °C for 20 h. The reaction mixture was diluted with EtOAc and filtered through a pad of celite, eluting EtOAc. The filtrate was concentrated under reduced pressure and purified directly by flash column chromatography (pentane/Et_2O = gradient 100/0 to 90/10). Colourless viscous oil, 1.22 g, 89 % yield.

^{1}H NMR (600 MHz, $CDCl_3$) δ 7.70 (d, *J* = 8.0 Hz, 2H), 7.18 (d, *J* = 7.9 Hz, 2H), 5.04 (dd, *J* = 10.2, 5.2 Hz, 1H), 3.39 (dd, *J* = 14.2, 5.2 Hz, 1H), 3.21 (dd, *J* = 14.2, 10.2 Hz, 1H), 1.46 (s, 9H), 1.40 (s, 18H), 1.32 (s, 12H). **^{13}C NMR** (151 MHz, $CDCl_3$) δ 169.5, 152.3, 141.7, 135.0, 129.0, 83.8, 82.8, 81.7, 60.1, 36.1, 28.1, 28.1, 25.0. *n.b*. C(Ar)-B was not observed. **HRMS** (ESI-TOF) calculated for $C_{29}H_{46}BNO_8$ ($[M+Na]^+$) 570.3212, found: 570.3205. **IR** (thin layer film) 2978, 2934, 1736, 1700, 1613, 1456, 1360, 1319, 1269, 1141, 1119, 1090, 1023, 979, 962, 860, 818, 781, 658. $\alpha_D^{25\,°C}$ – 49.8 ° (c = 0.78, $CHCl_3$).

(*S*)-(4-(2-(bis(*tert*-butoxycarbonyl)amino)-3-(*tert*-butoxy)-3-oxopropyl)phenyl)boronic acid



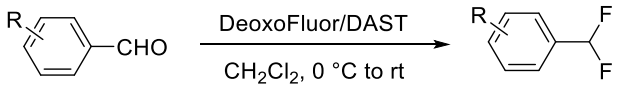
General Procedure 3 was followed using *tert*-butyl (*S*)-2-(bis(*tert*-butoxycarbonyl)amino)-3-(4-(4,4,5,5-tetramethyl-1,3,2-dioxaborolan-2-yl)phenyl)propanoate (1.09 g, 2 mmol), acetone (48 mL), water (24 mL), NH_4OAc (925 mg, 12 mmol), $NaIO_4$ (2.57 g, 12 mmol), and a reaction time of 39 h. The product was then precipitated from hexane. White solid, 595 mg, 64 % yield.

^{1}H NMR (400 MHz, DMSO-d_6) δ 7.66 (d, *J* = 7.7 Hz, 2H), 7.09 (d, *J* = 7.7 Hz, 2H), 3.25 (dd, *J* = 14.0, 5.1 Hz, 1H), 3.05 (dd, *J* = 14.0, 10.7 Hz, 1H), 1.39 (s, 9H), 1.32 (s, 18H). **^{13}C NMR** (101 MHz, DMSO-d_6) δ 169.1, 151.9, 139.9, 134.3, 128.6, 82.4, 81.3, 59.5, 35.2, 27.8, 27.7. *n.b*. C(Ar)-B was not observed**. HRMS** (ESI-TOF) calculated for $C_{23}H_{36}BNO_8$ ($[M+Na]^+$): 488.2428, found: 488.2425. **IR** (thin layer film) 2980, 2932, 1734, 1698, 1612, 1367, 1287, 1255, 1140, 981, 846, 759. **MP** 103 °C**.** $\alpha_D^{25\,°C}$ – 71.3 ° (c = 0.50, $CHCl_3$).

4.3.1.4. Preparation of authentic references and related synthetic intermediates

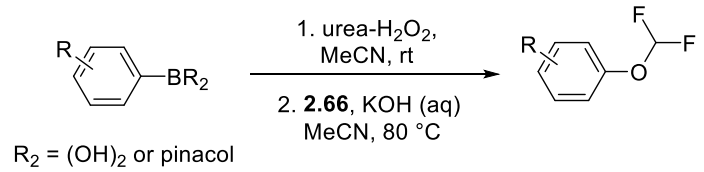
Authentic references **2.18**,[13] **2.64**,[14] **2.80**,[3] **2.86**,[15] **2.89**,[13] **2.93**,[13] **2.94**,[13] **2.95** [16] and **2.96** [17] were prepared exactly as described in literature reports.

General Procedure 4:



A single-necked round bottom flask was charged with the aldehyde starting material (1 equiv.) and dissolved in dry CH_2Cl_2 solvent. The reaction mixture was cooled to 0 °C and an excess of DeoxoFluor (50 % w/w in toluene) or DAST was added dropwise by syringe. The ice-water bath was then removed and the reaction was left to stir at rt until TLC analysis showed that the starting material was consumed. Saturated $NaHCO_3$ solution was then added to quench any unreacted DeoxoFluor/DAST and the mixture was stirred for 15 minutes at rt until gas evolution stopped. This was then transferred to a separatory funnel and extracted with CH_2Cl_2. The combined organic layers were washed with brine and then dried over $MgSO_4$ and filtered. The volatiles were evaporated, and the crude product was purified by flash column chromatography.

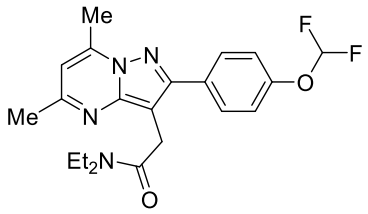
General Procedure 5:



The oxidation of aryl boronic acids is adapted from a literature procedure.[18] In a 7 mL vial, boronic acid or pinacol boronic ester starting material and urea hydrogen peroxide (1 equiv.) were dissolved in MeOH solvent (1 mL). Once TLC analysis showed that the starting material was fully consumed, H_2O was added (1 mL), and this was extracted with EtOAc (3 x 5 mL). The combined organic layers were dried over $MgSO_4$, filtered and concentrated under reduced pressure. The crude phenol was redissolved in MeCN and phenyl difluoromethyl sulfone (**2.66**) (2 equiv.) and KOH (aq., 25 % w/w) were added. The mixture was heated at 80 °C until TLC analysis showed that the starting material had been consumed. The reaction mixture was added to H_2O and extracted with CH_2Cl_2 (3 x). The combined organic layers were washed with

brine, dried over $MgSO_4$ and filtered. The volatiles were removed under reduced pressure and the crude product was purified by flash column chromatography.

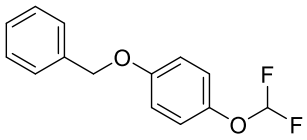
2-(2-(4-(difluoromethoxy)phenyl)-5,7-dimethylpyrazolo[1,5-*a*]pyrimidin-3-yl)-*N*,*N*-diethylacetamide (2.81)



Prepared by J. Sap and C. Meyer. Diethyl bromodifluoromethylphosphonate (71 µL, 0.4 mmol, 2 equiv.) was added to a stirred mixture of *N*,*N*-diethyl-2-(2-(4-hydroxyphenyl)-5,7-dimethylpyrazolo[1,5-*a*]pyrimidin-3-yl)acetamide (**2.82**) (0.2 mmol, 1.0 equiv.) in MeCN (1.0 mL) and KOH (aq., 2.0 M, 1.0 mL) at 0 °C. The mixture was allowed to warm to room temperature and stirred for 30 min. The mixture was extracted with Et_2O (3 x 5.0 mL), and the organic layer was dried over Na_2SO_4, filtered and concentrated under reduced pressure. The crude product was purified by flash column chromatography. Off-white solid, 55 mg, 68% yield.

^{1}H NMR (400 MHz, $CDCl_3$) δ 7.93 – 7.85 (m, 2H), 7.22 – 7.17 (m, 2H), 6.55 (t, *J* = 74.0 Hz, 1H), 6.53 (d, *J* = 1.0 Hz, 1H), 3.93 (s, 2H), 3.53 (q, *J* = 7.1 Hz, 2H), 3.40 (q, *J* = 7.1 Hz, 2H), 2.73 (d, *J* = 0.9 Hz, 3H), 2.55 (s, 3H), 1.23 (t, *J* = 7.1 Hz, 3H), 1.11 (t, *J* = 7.1 Hz, 3H); **^{19}F NMR** (377 MHz, $CDCl_3$) *δ* -80.7 (d, *J* = 74.3 Hz); **^{13}C NMR** (101 MHz, $CDCl_3$) *δ* 169.9, 157.7, 154.2, 151.4, 144.9, 147.5 131.2, 130.3, 119.4, 116.0 (t, *J* = 259.4 Hz), 108.5, 101.2, 42.4, 40.7, 28.0, 24.6, 16.9, 14.4, 13.1; **HRMS** (ESI-TOF) calculated for $C_{21}H_{25}F_2N_4O_2$ ($[M+H]^+$): 403.1940; found: 403.1941; **IR** (neat) 2924, 2521, 2159, 2030, 1977, 1643, 1624, 1591, 1481, 1442, 1397, 1229, 1109, 1036; **MP** 110 – 112 °C.

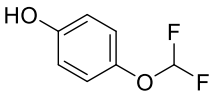
1-(benzyloxy)-4-(difluoromethoxy)benzene



The following was adapted from a literature procedure.[19] In a 50 mL 2-necked round bottom flask under inert atmosphere, 4-(benzyloxy)phenol (600 mg, 3 mmol, 1 equiv.), Cs_2CO_3 (1.95 g, 6 mmol, 2 equiv.) and sodium chlorodifluoroacetate (0.685 g, 4.5 mmol, 1.5 equiv.) were added, followed by DMF (6 mL). The mixture was heated to 120 °C and stirred for 1 h. After this time had passed, water (10 mL) was added, and the mixture was transferred to a separatory funnel. This was extracted with EtOAc (3 x 20 mL), and the combined organics were then washed with brine (20 mL) and dried over Na_2SO_4. The volatiles were then removed under reduced pressure. The crude product was then purified by flash column chromatography (pentane/EtOAc =19/1). White solid, 325 mg, 43 % yield.

^{1}H NMR (400 MHz, $CDCl_3$) δ 7.47 – 7.30 (m, 5H), 7.10 – 7.03 (m, 2H), 7.00 – 6.89 (m, 2H), 6.42 (t, J = 74.3 Hz, 1H), 5.05 (s, 2H). **^{13}C NMR** (101 MHz, $CDCl_3$) δ 156.5, 144.9 (t, J = 3.0 Hz), 136.8, 128.8, 128.2, 127.6, 121.5, 116.4 (t, J = 259.6 Hz), 115.9, 70.6. **^{19}F NMR** (377 MHz, $CDCl_3$) δ -80.4 (d, J = 74.8 Hz). **HRMS** the compound did not ionise under various ionisation techniques. **IR** (thin layer film): 2981, 1594, 1506, 1455, 1381, 1203, 1125, 1039, 830, 737, 697. **MP**: 54–56 °C.

4-(difluoromethoxy)phenol (2.85)

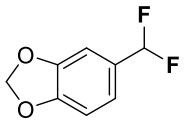


The following was adapted from a literature procedure.[19] In a 50 mL three-necked round bottom flask under N_2 atmosphere, 1-(benzyloxy)-4-(difluoromethoxy)benzene (300 mg, 1.28 mmol, 1 equiv.), 10 % Pd/C (34 mg, 0.32 mmol) and degassed MeOH solvent (12.8 mL) were sequentially added. The flask was then evacuated three times until solvent evaporation began and was refilled with a balloon of H_2. The mixture was left to stir at rt for 2 h. After this time,

the reaction mixture was filtered to remove the catalyst and the filtrate was collected. The volatiles were evaporated under reduced pressure to yield the product. Yellow oil, 176 mg, 86 % yield.

^{1}H NMR (400 MHz, $CDCl_3$) δ 7.09 – 6.96 (m, 2H), 6.85 – 6.75 (m, 2H), 6.41 (t, J = 74.3 Hz, 1H), 4.74 (s, 1H). **^{13}C NMR** (101 MHz, $CDCl_3$) δ 153.3, 144.8, 121.8, 116.3, 116.4 (t, J = 260.1 Hz). **^{19}F NMR** (377 MHz, $CDCl_3$) δ -80.5 (d, J = 74.4 Hz). **HRMS** the compound did not ionise under various ionisation techniques. **IR** (thin layer film) 3363, 2981, 1604, 1510, 1457, 1381, 1207, 1125, 1042, 834.

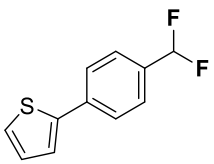
5-(difluoromethyl)benzo[*d*][1,3]dioxole (2.87)



Prepared by J. Sap. General Procedure 4 was followed for the synthesis of the title compound, using 3,4-(methylenedioxy)benzaldehyde (150 mg, 1 mmol, 1 equiv.), DAST (242 mg, 1.5 mmol, 1 equiv.) and CH_2Cl_2 (2 mL). The crude material was purified by flash column chromatography. Colourless oil, 96 mg, 56 % yield.

^{1}H NMR (400 MHz, $CDCl_3$) δ 7.04 – 6.92 (m, 2H), 6.91 – 6.78 (m, 1H), 6.54 (t, J = 56.6 Hz, 1H), 6.01 (s, 2H). **^{13}C NMR** (101 MHz, $CDCl_3$) δ 149.7, 148.2, 128.5 (t, J = 22.7 Hz), 120.3 (t, J = 7.2 Hz), 114.8 (t, J = 238.1 Hz), 108.4, 105.9 (t, J = 5.5 Hz), 101.7. **^{19}F NMR** (377 MHz, $CDCl_3$) δ -107.9 (d, J = 56.8 Hz). The recorded spectral data agree with those reported in the literature.[17]

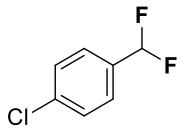
2-(4-(difluoromethyl)phenyl)thiophene (2.88)



Prepared by J. Sap. Thiophene-2-boronic acid (1.0 mmol, 128 mg, 1.5 equiv.), potassium carbonate (2.0 mmol, 415 mg, 3 equiv.) and Pd(dppf)Cl_2 (5 mol %, 24.5 mg) were added to a dry 25 mL Schlenk flask. 1-bromo-4-(difluoromethyl)benzene (0.67 mmol, 139 mg, 1 equiv.), dissolved in a 5:1 THF/H_2O (6.0 mL) mixture (sparged with N_2 beforehand) was then added to the Schlenk flask under nitrogen. The reaction was heated at 80 °C for 16 h under nitrogen. The reaction was cooled to rt, diluted with water (10 mL) and extracted with EtOAc (3 x 10 mL). The combined organics were dried over $MgSO_4$. The volatiles were evaporated under reduced pressure and the title compound was purified by flash column chromatography. White solid, 75 mg, 53% yield.

^{1}H NMR (500 MHz, $CDCl_3$) δ 7.69 (d, *J* = 8.2 Hz, 2H), 7.52 (d, *J* = 8.1 Hz, 2H), 7.37 (d, *J* = 3.6 Hz, 1H), 7.34 (d, *J* = 5.1 Hz, 1H), 7.11 (dd, *J* = 5.1, 3.6 Hz, 1H), 6.66 (t, *J* = 56.5 Hz, 1H).**^{13}C NMR** (126 MHz, $CDCl_3$) δ 143.3, 136.9, 133.4 (t, *J* = 22.5 Hz), 128.4, 126.4 (t, *J* = 6.1 Hz), 126.2, 125.9, 124.2, 114.7 (t, *J* = 238.5 Hz).**^{19}F NMR** (470 MHz, $CDCl_3$) δ -110.6 (d, *J* = 56.4 Hz). The recorded spectral data agree with those reported in the literature.[20]

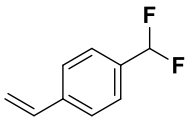
1-chloro-4-(difluoromethyl)benzene (2.90)



Prepared by J. Sap. General Procedure 4 was followed for the synthesis of the title compound, using 4-chlorobenzaldehyde (141 mg, 1 mmol, 1 equiv.), DAST (242 mg, 1.5 mmol, 1 equiv.) and CH_2Cl_2 (2 mL). The crude material was subjected to flash column chromatography (pentane). Colourless oil, 133 mg, 82 % yield.

^{1}H NMR (400 MHz, $CDCl_3$) δ 7.44 (s, 4H), 6.63 (t, *J* = 56.3 Hz, 1H). **^{13}C NMR** (101 MHz, $CDCl_3$) δ 136.9 (t, *J* = 2.3 Hz), 132.8 (t, *J* = 22.8 Hz), 127.0 (t, *J* = 6.0 Hz), 114.1 (t, *J* = 239.2 Hz). **^{19}F NMR** (377 MHz, $CDCl_3$) δ -110.8 (d, *J* = 56.5 Hz). The recorded spectral data agree with those reported in the literature.[21]

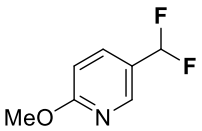
1-(difluoromethyl)-4-vinylbenzene (2.91)



The following is adapted from a literature procedure.[22] In a reaction tube was added potassium vinyltrifluoroborate (134 mg, 1 mmol, 1 equiv.), $PdCl_2$ (3.5 mg, 0.02 mmol, 2 mol %), PPh_3 (16 mg, 0.06 mmol, 6 mol %) and Cs_2CO_3 (978 mg, 3 mmol, 3 equiv.). A THF/H_2O solvent mixture (9/1 v/v, 10 mL) was then added, followed by 1-bromo-4-(difluoromethyl)benzene (207 mg, 1 mmol, 1 equiv.). The tube was sealed with a septum and purged with N_2. The reaction mixture was then heated for 21 h at 85 °C. H_2O (3 mL) was added and the mixture was then extracted with CH_2Cl_2 (3 x 10 mL). The combined organic layers were washed with brine (10 mL) and dried over $MgSO_4$. The volatiles were removed under reduced pressure and the crude material was purified by flash column chromatography (pentane). Colourless oil, 85 % yield (NMR yield, determined by quantitative ^{19}F NMR by addition of 1 equiv. 4-fluoroanisole internal standard to the crude mixture, as the product is volatile).

^{1}H NMR (400 MHz, $CDCl_3$) δ 7.48 (s, 4H), 6.75 (dd, J = 17.6, 10.9 Hz, 1H), 6.64 (t, J = 56.5 Hz, 1H), 5.83 (d, J = 17.6 Hz, 1H), 5.35 (d, J = 10.9 Hz, 1H). **^{13}C NMR** (101 MHz, $CDCl_3$) δ 140.1 (t, J = 2.0 Hz), 136.1, 133.8 (t, J = 22.4 Hz), 126.6, 125.9 (t, J = 6.1 Hz), 115.7, 114.8 (t, J = 238.3 Hz). **^{19}F NMR** (377 MHz, $CDCl_3$) δ -110.4 (d, J = 56.6 Hz). The recorded spectral data agree with those reported in the literature.[17]

5-(difluoromethyl)-2-methoxypyridine (2.92)

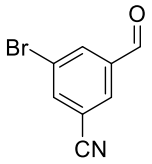


General Procedure 4 was followed for the synthesis of the title compound, using 5-formyl-2-methoxypyridine (274 mg, 2 mmol), DeoxoFluor solution (2.2 mL), CH_2Cl_2 (10 mL) and a

reaction time of 21 h. Flash column chromatography conditions: pentane/CH_2Cl_2 = 80/20. Colourless oil, 116 mg, 36 % yield.

^{1}H NMR (400 MHz, $CDCl_3$) δ 8.25 (s, 1H), 7.69 (d, *J* = 8.7 Hz, 1H), 6.78 (d, *J* = 8.7 Hz, 1H), 6.61 (t, *J* = 56.0 Hz, 1H), 3.94 (s, 3H). **^{13}C NMR** (101 MHz, $CDCl_3$) δ 165.7, 145.2 (t, *J* = 7.5 Hz), 135.7 (t, *J* = 4.5 Hz), 123.4 (t, *J* = 23.4 Hz), 113.8 (t, *J* = 237.4 Hz), 111.3, 53.7. **^{19}F NMR** (377 MHz, $CDCl_3$) δ -109.7 (d, *J* = 56.3 Hz). The recorded spectral data agree with those reported in the literature.[23]

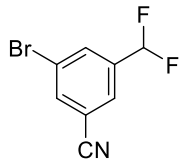
3-bromo-5-formylbenzonitrile



The following procedure was adapted from the literature.[24] Under N_2 atmosphere, concentrated H_2SO_4 (6 mL) was added dropwise to a stirring solution of 3-formylbenzonitrile (1.00 g, 7.6 mmol, 1 equiv.) in trifluoroacetic acid (4 mL) at 0 °C. NBS (1.35 g, 7.6 mmol, 1 equiv.) was then added portionwise at the same temperature. The mixture was then stirred at rt for 12 h. After this time, the reaction was poured into ice-water, and the precipated solid was collected by filtration, and dried in *vacuo*. This material was then dissolved in dry 1,4-dioxane (10 mL) in a 50 mL two necked round bottom flask. Trifluoroacetic anhydride (1.16 mL, 8.36 mmol, 1.1 equiv.) and anhydrous pyridine (1.23 mL, 15.2 mmol, 2 equiv.) were then added by syringe at 0 °C. The reaction mixture was stirred at rt overnight and the mixture was then diluted with chloroform (20 mL) and transferred to a separatory funnel. The organics were washed with water (2 x 10 mL) and brine (10 mL) and dried over Na_2SO_4 and filtered. The volatiles were removed under reduced pressure and the crude product was subsequently purified by flash column chromatography (hexane/EtOAc = 90/10). White solid, 460 mg, 29 % yield.

^{1}H NMR (400 MHz, $CDCl_3$) δ 9.99 (s, 1H), 8.23 (dd, *J* = 1.9, 1.4 Hz, 1H), 8.09 (t, *J* = 1.4 Hz, 1H), 8.08 – 7.98 (m, 1H). **^{13}C NMR** (101 MHz, $CDCl_3$) δ 188.5, 139.8, 138.3, 136.4, 131.7, 124.2, 116.3, 115.5. **HRMS** the compound did not ionise under various ionisation techniques. **IR** (thin layer film) 3070, 2981, 2915, 2889, 2848, 2237, 1697, 1566, 1442, 1376, 1255, 1237, 1152, 936, 884, 833, 808, 690, 669. **MP** 123 °C.

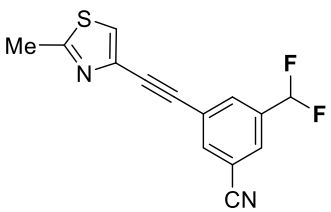
3-bromo-5-(difluoromethyl)benzonitrile



General Procedure 2 was followed for the synthesis of the title compound, using 3-bromo-5-formylbenzonitrile (300 mg, 1.43 mmol, 1 equiv.), DeoxoFluor solution (1.6 mL, 2.14 mmol, 3 equiv.), CH_2Cl_2 (10 mL) and a reaction time of 72 h. Flash column chromatography conditions: hexane: EtOAc = 100:0 to 80:20. White solid, 281 mg, 85 % yield.

^{1}H NMR (400 MHz, $CDCl_3$) δ 7.90 (dd, *J* = 4.3, 1.3 Hz, 1H), 7.74 (t, *J* = 1.3 Hz, 1H), 6.64 (t, *J* = 55.7 Hz, 1H). **^{13}C NMR** (101 MHz, $CDCl_3$) δ 137.5 (t, *J* = 23.7 Hz), 137.0, 133.4 (t, *J* = 6.0 Hz), 128.1 (t, *J* = 6.3 Hz), 123.6, 116.5, 115.0, 112.4 (t, *J* = 242.0 Hz). **^{19}F NMR** (377 MHz, $CDCl_3$) δ -113.1 (d, *J* = 55.9 Hz). **HRMS** (EI) calculated for $C_8H_4BrF_2N$ ($[M]^+$): 230.9495, 230.9482 found. **IR** (thin layer film) 3080, 2238, 1578, 1443, 1369, 1258, 1244, 1162, 1122, 1090, 1042, 882, 816, 728 670. **MP** 66–68 °C.

3-(difluoromethyl)-5-((2-methylthiazol-4-yl)ethynyl)benzonitrile (2.97)

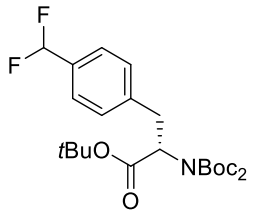


The following procedure was adapted from the literature.[6] To a solution of 2-methyl-4-((trimethylsilyl)-ethynyl)thiazole (129 mg, 0.66 mmol, 1 equiv.) in DMF (1.5 mL) were added

3-bromo-5-(difluoromethyl)benzonitrile (153 mg, 0.66 mmol, 1 equiv.), $PdCl_2(PPh_3)_2$ (46.5 mg, 0.066 mmol, 10 mol%), CuI (12.6 mg, 0.066 mmol, 10 mol%) and NEt_3 (0.37 mL, 2.65 mmol, 4 equiv.). To this mixture, TBAF (1M in THF, 0.79 mL, 0.79 mmol, 1.2 equiv.) was subsequently added dropwise over 30 mins. The reaction mixture was stirred at rt for 20 h, after which time no starting material was remaining. Following the addition of H_2O (5 mL), the mixture was transferred to a separatory funnel and extracted with EtOAc (4 x 10 mL). The combined organics were washed with an aqueous LiCl solution (10 % w/w; 2 x 15 mL) and then dried over $MgSO_4$ and filtered. The volatiles were removed under reduced pressure and the crude material was purified by flash column chromatography (CH_2Cl_2/pentane = 85/15). Orange-yellow solid, 93 mg, 51 % yield.

^{1}H NMR (500 MHz, $CDCl_3$) δ 7.90 (s, 1H), 7.89 (s, 1H), 7.75 (s, 1H), 7.47 (s, 1H), 6.66 (t, J = 55.8 Hz, 1H), 2.75 (s, 3H). **^{13}C NMR** (126 MHz, $CDCl_3$) δ 166.4, 136.7, 136.2 (t, J = 23.6 Hz), 135.6, 132.8 (t, J = 6.0 Hz), 128.7 (t, J = 6.2 Hz), 125.1, 124.1, 117.1, 113.8, 112.7 (t, J = 241.5 Hz), 87.0, 85.4, 19.3. **^{19}F NMR** (470 MHz, $CDCl_3$) δ -113.1 (d, J = 55.6 Hz). **HRMS** (ESI-TOF) calculated for $C_{14}H_8F_2N_2S$ ($[M+H]^+$): 275.0449, found: 275.0450. **IR** (thin layer film) 3076, 2925, 2237, 1601, 1497, 1448, 1378, 1320, 1271, 1196, 1174, 1119, 1092, 1039, 971, 889, 859, 746, 679. **MP** 113–114 °C.

tert-butyl (_S_)-2-(bis(_tert_-butoxycarbonyl)amino)-3-(4-(difluoromethyl)phenyl)propanoate (2.98)

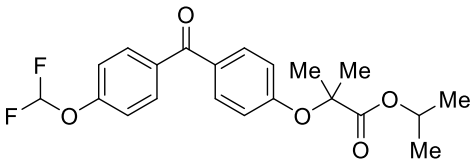


The following is adapted from a literature procedure.[16] In a Schlenk tube under N_2, $Pd(dba)_2$ (17.3 mg, 0.03 mmol, 3 mol %), di(1-adamantyl)-*n*-butylphosphine (14.3 mg, 0.04 mmol, 4 mol%) and $K_3PO_4 \cdot H_2O$ (921 mg, 4 mmol, 4 mol%) were added. Toluene (6 mL) was then added, followed by *tert*-butyl (*S*)-2-(bis(*tert*-butoxycarbonyl)amino)-3-(4-bromophenyl) propanoate

(500 mg, 1 mmol, 1 equiv.) and 2,2-difluoroacetophenone (264 µL, 2 mmol, 2 equiv.). The tap was closed and the mixture was heated at 100 °C for 24 h. After this time, KOH (500 mg, 8.91 mmol, 8.91 equiv.) and H_2O (250 µL) were added and the mixture was heated 100 °C for 18 h. The mixture was removed from the heat, diluted with toluene, and then filtered through a pad of celite, eluting EtOAc. The volatiles were removed under reduced pressure and the obtained material was purified by flash column chromatography (pentane/Et_2O = gradient 100/0 to 80/20). Colourless oil, 81 mg, 17 % yield.

^{1}H NMR (400 MHz, $CDCl_3$) δ 7.40 (d, *J* = 7.8 Hz, 2H), 7.27 (d, *J* = 7.8 Hz, 2H), 6.60 (t, *J* = 56.5 Hz, 1H), 5.04 (dd, *J* = 10.3, 5.2 Hz, 1H), 3.42 (dd, *J* = 14.2, 5.2 Hz, 1H), 3.25 (dd, *J* = 14.1, 10.3 Hz, 1H), 1.47 (s, 9H), 1.40 (s, 18H). **^{13}C NMR** (101 MHz, $CDCl_3$) δ 169.3, 152.3, 141.3, 132.7 (t, *J* = 22.3 Hz), 129.9, 125.7, 114.9 (t, *J* = 238.3 Hz), 83.0, 81.9, 59.9, 35.8, 28.1, 28.1. **^{19}F NMR** (377 MHz, $CDCl_3$) δ - 110.0 (d, *J* = 56.8 Hz). **HRMS** (ESI-TOF) calculated for $C_{24}H_{35}F_2NO_6$ ($[M+Na]^+$): 494.2325, found: 494.2323. **IR** (thin layer film) 2980, 2935, 1736, 1699, 1368, 1317, 1276, 1256, 1234, 1142, 1122, 1074, 1027, 981, 849, 819, 781. **$\alpha_D^{25\,°C}$** – 9.8 ° (c = 0.53, $CHCl_3$).

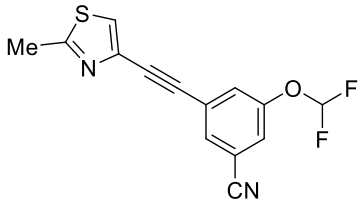
Isopropyl 2-(4-(4-(difluoromethoxy)benzoyl)phenoxy)-2-methylpropanoate (2.106)



General Procedure 5 was followed for the synthesis of the title compound, using fenofibrate boronic acid (185 mg, 0.5 mmol), urea hydrogen peroxide (47 mg, 0.5 mmol) and a 22 h reaction time, followed by difluoromethyl phenyl sulfone (**2.66**) (192 mg, 1.0 mmol), KOH (500 µL, 25 % w/w aq.), MeCN solvent (3 mL) and a 16 h reaction time. The crude product was then purified by flash column chromatography (pentane/EtOAc= gradient 100/0 to 90/10). White solid, 61 mg, 31 % yield.

^{1}H NMR (400 MHz, $CDCl_3$) δ 7.79 (d, J = 8.7 Hz, 2H), 7.73 (d, J = 8.8 Hz, 2H), 7.20 (d, J = 8.6 Hz, 2H), 6.87 (d, J = 8.8 Hz, 1H), 6.61 (t, J = 73.2 Hz, 1H), 5.09 (hept, J = 6.3 Hz, 1H), 1.66 (s, 6H), 1.20 (d, J = 6.3 Hz, 6H). **^{13}C NMR** (101 MHz, $CDCl_3$) δ 194.2, 173.3, 159.8, 154.1, 135.2, 132.1, 132.0, 130.5, 118.8, 117.4, 115.6 (t, J = 261.2 Hz), 79.6, 69.5, 25.5, 21.7. **^{19}F NMR** (377 MHz, $CDCl_3$) δ -81.6 (d, J = 73.2 Hz). **HRMS** (ESI-TOF) calculated for $C_{21}H_{22}F_2O_5$ ($[M+H]^+$): 393.1508, found: 393.1508. **IR** (thin layer film) 2982, 1730, 1654, 1600, 1506, 1467, 1385, 1281, 1249, 1174, 1146, 1103, 1050, 972, 929, 853, 768. **MP** 61–62 °C.

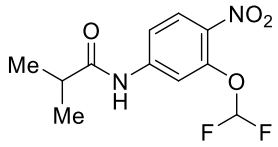
3-(Difluoromethoxy)-5-((2-methylthiazol-4-yl)ethynyl)benzonitrile (2.107)



General Procedure 5 was followed for the synthesis of the title compound, using 3-((2-methylthiazol-4-yl)ethynyl)-5-(4,4,5,5-tetramethyl-1,3,2-dioxaborolan-2-yl)benzonitrile (40 mg, 0.115 mmol), urea hydrogen peroxide (11.1 mg, 0.115 mmol) and a 45 min reaction time, followed by difluoromethyl phenyl sulfone (44.2 mg, 0.23 mmol), KOH (115 µL, 25 % w/w aq.), MeCN solvent (0.71 mL) and a 7 h reaction time. The crude product was then purified by flash column chromatography (pentane/EtOAc = 90/10). White solid, 9 mg, 27 % yield.

^{1}H NMR (600 MHz, $CDCl_3$) δ 7.66 (t, J = 1.4 Hz, 1H), 7.54 (t, J = 1.9 Hz, 2H), 7.47 (s, 1H), 7.39 (t, J = 1.8 Hz, 1H), 6.56 (t, J = 72.1 Hz, 1H), 2.75 (s, 3H). **^{13}C NMR** (151 MHz, $CDCl_3$) δ 166.5, 150.9, 135.8, 132.0, 127.2, 126.2, 124.2, 123.4, 117.1, 115.2 (t, J = 264.7 Hz), 114.4, 87.1, 85.4, 19.4. **^{19}F NMR** (565 MHz, $CDCl_3$) δ -81.99 (d, J = 72.0 Hz). **HRMS** (ESI-TOF): calculated for $C_{14}H_8F_2N_2OS$ ($[M+H]^+$): 291.0398, found: 291.0399. **IR** (thin layer film): 3079, 2234, 1588, 1507, 1425, 1388, 1326, 1272, 1197, 1175, 1141, 1113, 1054, 878, 749, 676. **MP**: 75 °C.

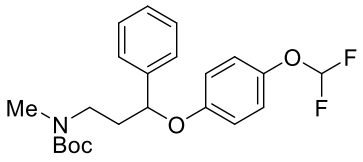
***N*-(3-(difluoromethoxy)-4-nitrophenyl)isobutyramide (2.108)**



General Procedure 5 was followed for the synthesis of the title compound, using (5-isobutyramido-2-nitrophenyl)boronic acid (176 mg, 0.5 mmol), urea hydrogen peroxide (47 mg, 0.5 mmol) and a 16 h reaction time, followed by difluoromethyl phenyl sulfone (192 mg, 1.0 mmol), KOH (0.5 mL, 25 % w/w aq.), MeCN solvent (3 mL) and a 2 h reaction time. The crude product was then purified by flash column chromatography (CH_2Cl_2/EtOAc = 100/0 to 97/3). Yellow solid, 45 mg, 33% yield.

^{1}H NMR (500 MHz, $CDCl_3$) δ 8.02 (d, J = 9.0 Hz, 1H), 7.85 – 7.74 (m, 1H), 7.50 (dd, J = 9.0, 2.3 Hz, 1H), 7.43 (s, 1H), 6.67 (t, J = 73.0 Hz, 1H), 2.57 (h, J = 6.9 Hz, 1H), 1.31 (d, J = 6.9 Hz, 7H). **^{13}C NMR** (126 MHz, $CDCl_3$) δ 175.6, 144.7 (t, J = 3.4 Hz), 143.6, 137.4, 127.2, 115.8, 115.7 (t, J = 264.9 Hz), 113.3, 36.9, 19.4. **^{19}F NMR** (470 MHz, $CDCl_3$) δ -82.2 (d, J = 72.9 Hz). **HRMS** (ESI-TOF) calculated for $C_{11}H_{12}F_2N_2O_4$ ([M-H]$^-$): 273.0692, found: 273.0690. **IR** (thin layer film) 3323, 2977, 1682, 1599, 1549, 1510, 1470, 1422, 1382, 1343, 1265, 1205, 1145, 1103, 1057, 845, 752. **MP** 93-94 °C.

***tert*-butyl (3-(4-(difluoromethoxy)phenoxy)-3-phenylpropyl)(methyl)carbamate (2.109)**

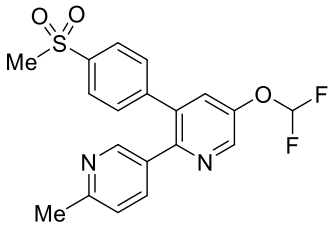


General Procedure 5 was followed for the synthesis of the title compound, using *tert*-butyl methyl(3-phenyl-3-(4-(4,4,5,5-tetramethyl-1,3,2-dioxaborolan-2-yl)phenoxy)propyl) carbamate (93 mg, 0.2 mmol), urea hydrogen peroxide (19 mg, 0.2 mmol) and a 1.5 h reaction time, followed by difluoromethyl phenyl sulfone (77 mg, 0.4 mmol), KOH (200 µL, 25 % w/w aq.), MeCN solvent (1.2 mL) and a 3 h reaction time. The crude product was then purified by

flash column chromatography (pentane/Et_2O = gradient 100/0 to 90/10). Colourless oil, 33 mg, 40 % yield.

^{1}H NMR (600 MHz, $CDCl_3$) 7.40 – 7.20 (m, 5H), 6.94 (d, *J* = 8.6 Hz, 2H), 6.78 (d, *J* = 9.1 Hz, 2H), 6.35 (t, *J* = 74.4 Hz, 1H), 5.06 (dd, *J* = 9.1, 4.0 Hz, 1H), 3.39 (d, *J* = 71.8 Hz, 2H), 2.84 (s, 3H), 2.32 – 1.93 (m, 2H), 1.37 (s, 9H). **^{13}C NMR** (151 MHz, $CDCl_3$) δ 155.9, 155.7, 144.8 (t, *J* = 2.8 Hz), 141.4, 128.9, 127.9, 125.9, 121.3, 116.8, 116.3 (t, *J* = 259.4 Hz), 79.6, 78.4 (br), 45.95, 37.19 (br), 34.6, 28.5. **^{19}F NMR** (377 MHz, $CDCl_3$) -80.4 (dd, *J* = 74.4, 71.2 Hz). **HRMS** (ESI-TOF) calculated for $C_{22}H_{27}F_2NO_4$ ($[M+Na]^+$): 430.1800, found: 430.1800. **IR** (thin layer film) 2976, 2929, 1689, 1505, 1454, 1394, 1366, 1304, 1207, 1172, 1127, 1048, 884, 832, 773, 702.

5-(Difluoromethoxy)-6'-methyl-3-(4-(methylsulfonyl)phenyl)-2,3'-bipyridine (2.110)

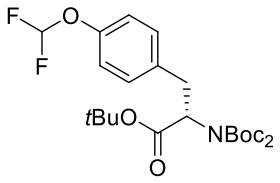


General Procedure 5 was followed for the synthesis of the title compound, using (6'-methyl-3-(4-(methylsulfonyl)phenyl)-[2,3'-bipyridin]-5-yl)boronic acid (294 mg, 0.8 mmol), urea hydrogen peroxide (76 mg, 0.8 mmol) and a 16 h reaction time, followed by difluoromethyl phenyl sulfone (384 mg, 0.8 mmol), KOH (0.8 mL, 25 % w/w aq.), MeCN solvent (6 mL) and a 2 h reaction time. The crude product was first purified by flash column chromatography (gradient DCM to DCM/EtOAc = 70/30) and then preparative HPLC. White solid, 22 mg, 7 % yield.

^{1}H NMR (400 MHz, $CDCl_3$) δ 8.64 (d, *J* = 2.6 Hz, 1H), 8.40 (s, 1H), 7.91 (d, *J* = 8.5 Hz, 2H), 7.60 (dd, *J* = 8.1, 2.3 Hz, 1H), 7.54 (d, *J* = 2.6 Hz, 1H), 7.43 – 7.37 (m, 2H), 7.11 (d, *J* = 8.1 Hz, 1H), 6.65 (t, *J* = 72.1 Hz, 1H), 3.08 (s, 3H), 2.56 (s, 3H). **^{13}C NMR** (101 MHz, $CDCl_3$) δ 158.2, 151.3, 149.5, 146.5, 144.0, 142.1, 140.4, 137.9, 135.4, 131.8, 130.6, 129.9, 128.1, 123.2, 115.3 (t, *J*

= 265.4 Hz), 44.7, 24.1. **^{19}F NMR** (377 MHz, $CDCl_3$) δ -81.6 (d, J = 72.3 Hz). **HRMS** (ESI-TOF): calculated for $C_{19}H_{16}F_2N_2O_3S$ ($[M+H]^+$) 391.0922, found: 391.0922. **IR** (thin layer film) 2925, 1600, 1444, 1393, 1311, 1204, 1150, 1113, 1056, 1014, 958, 917, 842, 779, 734. **MP** 135 °C.

tert-butyl-(_S_)-2-(bis(_tert_-butoxycarbonyl)amino)-3-(4-(difluoromethoxy)phenyl) propanoate (2.111)



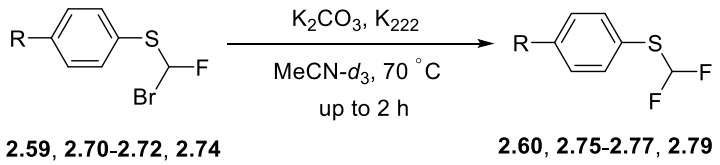
General Procedure 5 was followed for the synthesis of the title compound, using (*S*)-(4-(2-(bis(*tert*-butoxycarbonyl)amino)-3-(*tert*-butoxy)-3-oxopropyl)phenyl)boronic acid (47 mg, 0.1 mmol), urea hydrogen peroxide (9.4 mg, 0.1 mmol) and a 30 min reaction time, followed by difluoromethyl phenyl sulfone (38 mg, 0.2 mmol), KOH (100 µL, 25 % w/w aq.), MeCN solvent (1 mL) and a 5 h reaction time. The crude product was then purified by flash column chromatography (pentane/EtOAc = 98/2 to 95/5). Colourless oil, 27 mg, 55 % yield.

^{1}H NMR (600 MHz, $CDCl_3$) δ 7.17 (d, J = 8.6 Hz, 1H), 7.01 (d, J = 8.6 Hz, 1H), 6.45 (t, J = 74.2 Hz, 1H), 5.01 (dd, J = 10.3, 5.2 Hz, 1H), 3.36 (dd, J = 14.2, 5.2 Hz, 1H), 3.19 (dd, J = 14.2, 10.3 Hz, 1H), 1.47 (s, 8H), 1.41 (s, 17H). **^{13}C NMR** (151 MHz, $CDCl_3$) δ 169.4, 152.3, 149.9 (t, J = 2.7 Hz), 135.6, 131.0, 119.6, 116.1 (t, J = 259.6 Hz), 82.9, 81.8, 60.1, 35.2, 28.1, 28.1. **^{19}F NMR** (565 MHz, $CDCl_3$) δ -80.6 (d, J = 74.2 Hz). **HRMS** (ESI-TOF) calculated for $C_{24}H_{35}F_2NO_7$ ($[M+Na]^+$): 510.2274, found: 510.2273. **IR** (thin layer film) 2981, 2935, 1736, 1699, 1510, 1457, 1368, 1275, 1231, 1140, 1046, 980, 848. $\alpha_D^{25\,°C}$ -25.7 ° (c = 0.32, $CHCl_3$).

4.3.2. Experiments on Non-Radioactive Material

4.3.2.1. ^{19}F-Fluoride leaching experiments with bromofluoromethyl aryl sulfides

Procedure:



2.59, **2.70-2.72**, **2.74** → **2.60**, **2.75-2.77**, **2.79**

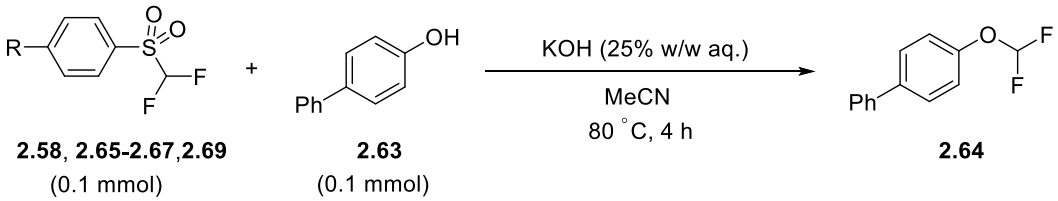
R	SCF_2H	SCFHBr
OMe	**2.75**	**2.70**
*t*Bu	**2.60**	**2.59**
H	**2.76**	**2.71**
Cl	**2.77**	**2.72**
NO_2	**2.79**	**2.74**

In an NMR tube were weighed Kryptofix 222 (K_{222}) (7.5 mg, 0.02 mmol) and K_2CO_3 (1.5 mg, 0.011 mmol). A solution of the relevant bromofluoromethyl aryl sulfide (**2.59, 2.70-2.72, 2.74**) (0.04 mmol) in MeCN-d_3 (0.7 mL) was then added. The NMR tube was sealed with a cap and heated at 70 °C in an oil bath for the relevant time. ^{19}F NMR experiments (16 scans, d1 = 10 s) were then conducted using a Bruker AVIIIHD 400 at various time points (10 min, 30 min, 60 min, 90 min, 120 min). At these time points, the NMR tube was removed from the oil bath and put in an ice bath (0 °C), heating was then resumed until the next time point. From these experiments, the ratio of the difluoromethyl aryl sulfide (**2.60**, **2.75–2.77, 2.79**) to bromofluoromethyl aryl sulfide (**2.59**, **2.70–2.72, 2.74**) was calculated. These experiments were conducted jointly by J. Ford and J. Sap.

Time (min)	$\frac{[2.60]}{[2.59]}$ (R = *t*Bu)	$\frac{[2.75]}{[2.70]}$ (R = OMe)	$\frac{[2.76]}{[2.71]}$ (R = H)	$\frac{[2.77]}{[2.72]}$ (R = Cl)	$\frac{[2.79]}{[2.74]}$ (R = NO_2)
10	0.0060	0.0385	0.0297	0.0046	0.0094
30	0.0219	0.0897	0.0554	0.0049	0.0233
60	0.0591	0.2040	0.0890	0.0335	0.0371
90	0.1089	0.3060	0.1250	0.0584	0.0466
120	0.1440	0.3763	0.1474	0.0812	0.0491

4.3.2.2. Comparison of ^{19}F-difluoromethylation reactivity of difluoromethyl aryl sulfones

Procedure:



2.58, **2.65-2.67**,**2.69** (0.1 mmol) + **2.63** (0.1 mmol) → **2.64**

A 7 mL vial was charged with phenol **2.63** (17 mg, 0.1 mmol) and the relevant difluoromethyl aryl sulfone (**2.58**, **2.65**, **2.66**, **2.67**, **2.69**, 0.1 mmol, 1 equiv.) and a stirrer bar. MeCN solvent (0.6 mL) was added, followed by an aqueous KOH solution (25% w/w, 0.1 mL). The vial was sealed with a cap and placed into a heating block, where the mixture was stirred at 80 °C for 4 h. After this time had passed, the vial was cooled to rt and the mixture was diluted with a solution of 4-fluoroanisole (0.1 mmol) internal standard in MeCN-d_3 (1 mL). This mixture was then analysed by quantitative ^{19}F NMR spectroscopy and the yield of the reaction was

estimated by integration of the peak corresponding to the difluoromethylated product. The reactions were run in duplicate for each difluoromethyl aryl sulfone.

4.3.2.3. ^{19}F-Difluoromethylation of aryl boronic acids

Procedure:

In a 7 mL vial, equipped with a stirrer bar, was added 4-biphenylboronic acid (**2.17**), a Pd additive, ligand, base and any further additives. Separately, a stock solution of [(difluoromethyl)sulfonyl]benzene (**2.66**, concentration = 0.1 M) was prepared and the required volume of this solution was dispensed into the reaction vials using a pipette. If degassing was to be applied, the mixture was sparged with a flow of N_2 for 1 minute. The reaction vials were closed tightly with a screw cap and heated to the desired temperature. After the desired reaction time had passed, the vial was placed in an ice-water bath. Chloroform-d_1 (1 mL) and 4-fluoroanisole internal standard (0.1 mmol) were added to the vials and the vial was shaken until well mixed. This mixture was then analysed by quantitative ^{19}F NMR spectroscopy and an NMR yield of the desired product **2.18** was determined.

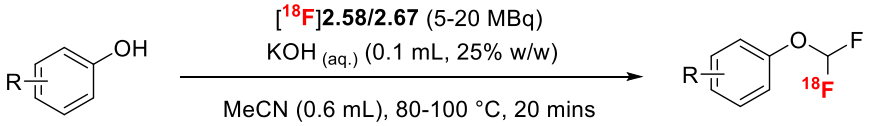
4.3.3. Radiochemistry

Radiochemistry experiments in this section were conducted jointly by J. Ford and J. Sap.

4.3.3.1. Manual radiochemistry experiments

^{18}F-Difluoromethylation of phenols

Procedure:

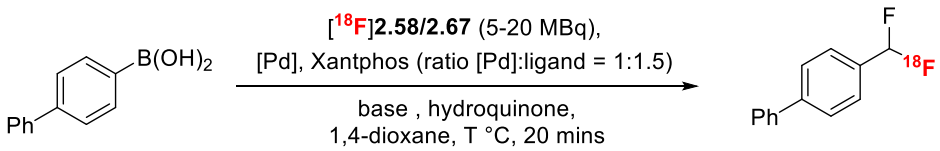


[^{18}F]**2.58** or [^{18}F]**2.67** in MeCN (<100 µL, 5–20 MBq) was added to a v-vial charged with a stir bar, the relevant phenol (0.2 mmol for **2.63**, 0.1 mmol for **2.82**), MeCN solvent (0.6 mL) and

an aqueous KOH solution (25% w/w, 0.1 mL). This mixture was heated at 80–100 °C (as relevant) for 20 minutes (*n.b.* for time course experiments, the reaction time was varied). The reaction mixture was allowed to cool and diluted with 300 µL of a 1:1 (v/v) mixture of EtOH and H_2O. This was filtered into a vial and was subsequently analysed by HPLC. The retention time of the product observed in the radio-HPLC trace was matched to the UV trace of an authentic reference and the radiochemical yield was determined by the integration of the radioactive species observed in the trace.

Optimisation experiments for the Pd-mediated ^{18}F-difluoromethylation of aryl boronic acids

Procedure:



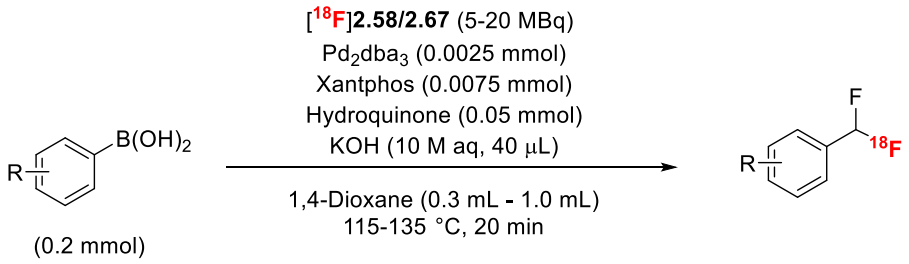
2.17
(0.2 mmol)

[^{18}F]**2.18**

[^{18}F]**2.58** or [^{18}F]**2.67** in 1,4-dioxane (<100 µL, 5–20 MBq) was added to a v-vial charged with a stir bar, 4-biphenylboronic acid (**2.17**, 0.2 mmol), hydroquinone (if being used), base, [Pd] additive, Xantphos and 1,4-dioxane solvent, to give the desired reaction volume. This mixture was heated at 115–135 °C for 20 minutes. The reaction mixture was allowed to cool and diluted with 300 µL of a 1:1 (v/v) mixture of EtOH and H_2O. This was filtered into a vial and was subsequently analysed by HPLC. The retention time of the product observed in the radio-HPLC trace was matched to the UV trace of an authentic reference and the radiochemical yield was determined by the integration of the radioactive species observed in the trace.

Pd-mediated ^{18}F-difluoromethylation of aryl boronic acids (reaction scope)

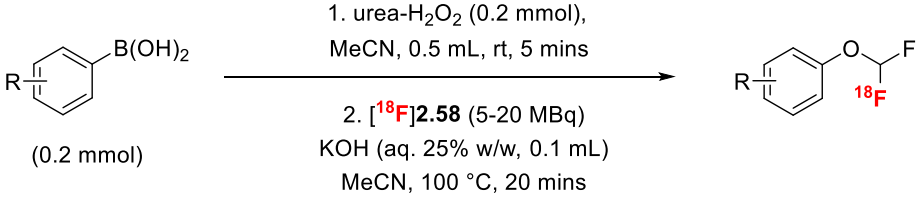
General Procedure 6:



In 7 mL vials, stock solutions of KOH (10 M, aqueous), Xantphos (43.4 mg in 3 mL 1,4-dioxane, 0.025 M) and Pd_2dba_3 (38.2 mg in 1 mL 1,4-dioxane, 0.042 M) were prepared. These were vortexed thoroughly to ensure that all material had dissolved. To a 5 mL v-vial charged with a stir bar were added aryl boronic acid (0.2 mmol) and hydroquinone (5.5 mg, 0.05 mmol) as solids. The solutions of KOH (40 µL, 0.4 mmol), Pd_2dba_3 (60 µL, 0.0025 mmol), Xantphos (300 µL, 0.0075 mmol) were then dispensed into the vial, followed by 1,4-dioxane solvent, to give the desired reaction volume. [^{18}F]**2.58** or [^{18}F]**2.67** in 1,4-dioxane (<100 µL, 5–20 MBq) were then added *via* syringe. This mixture was heated at 115–135 °C for 20 minutes. The reaction mixture was allowed to cool and diluted with 300 µL of a 1:1 (v/v) mixture of EtOH and H_2O. This was filtered into a vial and was subsequently analysed by radio-HPLC. The retention time of the product observed in the radio-HPLC trace was matched to the UV trace of an authentic reference and the radiochemical yield was determined by the integration of the radioactive species observed in the trace.

Two-step, one-pot net ^{18}F-difluoromethoxylation of aryl boronic acids (reaction scope)

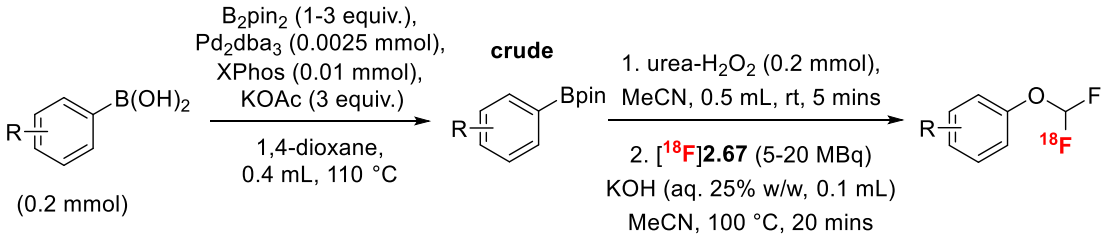
General Procedure 7:



In a v-vial, aryl boronic acid (0.2 mmol) was vortexed with urea hydrogen peroxide (0.2 mmol, 1 equiv.) in 0.5 mL MeCN for 5 minutes. To the vial was then added KOH (25% w/w, aq., 0.1 mL). 5-20 MBq of [^{18}F]**2.58** in approx. 0.1 mL MeCN was then added to this solution *via* syringe. The reaction was then stirred for 20 minutes at 100 °C. The reaction mixture was allowed to cool and diluted with 0.3 mL of a 1:1 (v/v) mixture of EtOH and H_2O. The retention time of the product observed in the radio-HPLC trace was matched to the UV trace of an authentic reference and the radiochemical yield was determined by the integration of the radioactive species observed in the trace.

Three step sequential borylation-oxidation-^{18}F-difluoromethylation of aryl chlorides

Procedure:



(0.2 mmol)

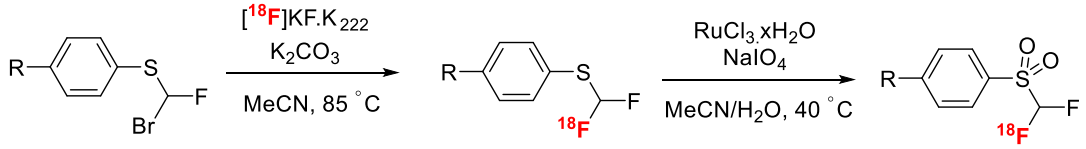
The borylation of aryl chlorides is adapted from a literature procedure.[11] A 7 mL vial was charged with aryl chloride substrate (0.2 mmol, 1 equiv.), Pd_2dba_3 (2.3 mg, 0.0025 mmol, 1.25 mol%), XPhos (4.8 mg, 0.01 mmol, 5 mol%), bis(pinacolato)diboron (1–3 equiv.) and KOAc (58.9 mg, 0.6 mmol, 3 equiv.). Degassed 1,4-dioxane solvent (0.4 mL) was added and the vial was sealed and heated to 110 °C for 20 mins. Once cooled, if the reaction mixture was to be filtered, this was diluted with EtOAc and drawn up in a syringe. Then this was passed through a syringe filter. The volatiles were removed under reduced pressure. If the mixture was not filtered, the volatiles were removed under reduced pressure directly. This mixture was dissolved in 0.5 mL MeCN and transferred to a v-vial containing urea hydrogen peroxide (0.2 mmol, 1 equiv.). This mixture was vortexed for 5 minutes, before the addition of KOH (25% w/w, aq., 0.1 mL). 5-20 MBq of [^{18}F]**2.67** in approx. 0.1 mL MeCN was then added to this solution *via* syringe. The reaction was then stirred for 20 minutes at 100 °C. The reaction mixture was allowed to cool and diluted with 0.3 mL of a 1:1 (v/v) mixture of EtOH and H_2O.

The retention time of the product observed in the radio-HPLC trace was matched to the UV trace of an authentic reference and the radiochemical yield was determined by the integration of the radioactive species observed in the trace.

4.3.3.2. Automated radiochemistry experiments

Automated radiosynthesis of [^{18}F]DFC reagents ([^{18}F]**2.58**, [^{18}F]**2.65**–[^{18}F]**2.69**)

General Procedure 8:



2.59, **2.70-2.74** [^{18}F]**2.60**, [^{18}F]**2.75**-[^{18}F]**2.79** [^{18}F]**2.58**, [^{18}F]**2.65**-[^{18}F]**2.69**

The automated radiosynthesis of [^{18}F]**2.58**, [^{18}F]**2.65**–[^{18}F]**2.69** was performed with a Trasis AllInOne synthesiser using an automated program and pre-built cassette (see Figure 2.10, Chapter 2 for the cassette layout). The vial in position 2 was charged with Kryptofix 222 (7.5 mg), K_2CO_3 (1.5 mg), H_2O (0.15 mL) and MeCN (0.85 mL). The vial in position 9 was charged with a solution of the relevant bromofluoromethyl aryl sulfide in dry MeCN (1.0 mL). The vial in position 10 was charged with $NaIO_4$ (52 mg), $RuCl_3{\cdot}xH_2O$ (2 mg), water (0.25 mL) and MeCN (0.25 mL). 10 mL vials were filled with MeCN and placed at positions 8 and 17. The reformulation vial was filled with water (10 mL) and placed at position 34. A Waters Sep-Pak AccellPlus QMA Carbonate cartridge (preactivated with 10 mL water) was installed at position 5. Waters SepPak C18 Plus cartridges (preactivated with 10 mL ethanol and 10 mL water) were installed at positions 26 and 33.

[^{18}F]Fluoride in [^{18}O]water was received directly from the cyclotron and passed over the QMA cartridge and eluted with the contents of vial 2 into the reactor. The contents of the reactor were then dried at 110 °C for 12 mins, after which the vessel was cooled. The contents of the vial at position 9 were added and the ^{18}F-fluorination reaction was run at 85 °C for 3 minutes.

Thereafter, the oxidation reaction was run in the same vessel at 40 °C for 5 minutes. The crude mixture was then purified by C18 cartridge followed by reverse-phase HPLC (HPLC conditions E, MeCN/H_2O = 55/45). The collected product was diluted with water and reformulated using a C18 cartridge. An aliquot of the isolated, chemically and radiochemically pure product was analysed in triplicate by radio-HPLC to determine A_m. (Radio-)HPLC analysis was performed under HPLC conditions B.

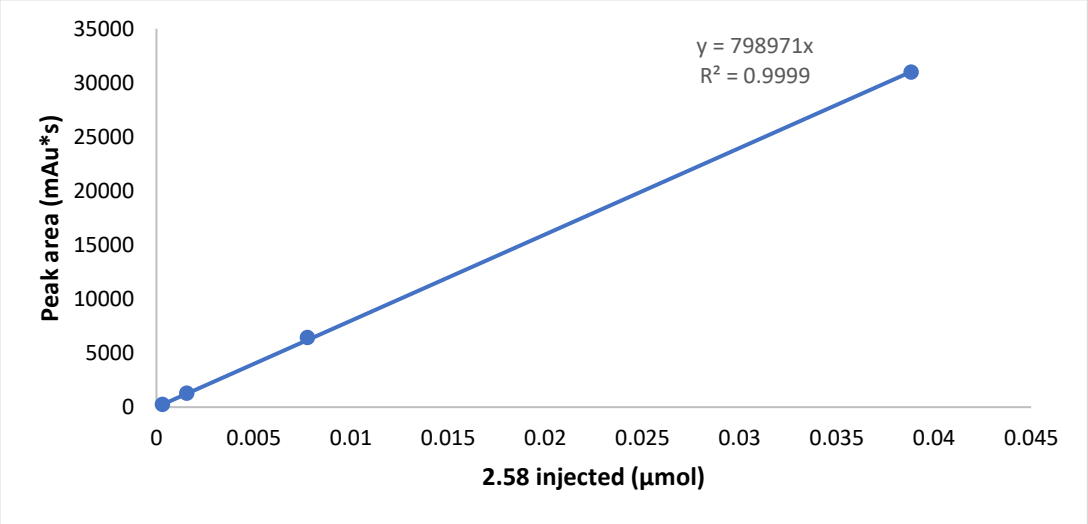
Separately, a calibration curve for the relevant difluoromethyl aryl sulfone authentic reference was recorded by preparing samples of a range of concentrations by serial dilution. These were injected onto an HPLC (10 µL injection volume from a 1.0 mL stock, HPLC conditions B) and the UV response was measured by integrating the peak of interest.

Automated radiosynthesis of [^{18}F]**2.58**

General Procedure 8 was followed using **2.59** (5.6 mg, 0.02 mmol).

Entry	Starting activity	RCP	%AY	A_m (GBq/μmol)
1	135 GBq	>99%	1.2%	10
2	135 GBq	>99%	1.4%	10
		Average (*n* = 2)	1.3% ± 0.1%	10 ± 0 GBq/μmol

Calibration curve for **2.58**



Prepared using HPLC conditions B.

Run 1

Measurement	Activity injected (MBq, d.c.)	2.58 injected (μmol)	Peak area (mAu*s)	A_m (GBq/μmol)
1	2.20	0.00024	191	9.22
2	2.26	0.00021	167	10.8
3	2.28	0.00024	188	9.67
			Average (*n* = 3)	9.9 GBq/μmol

Run 2

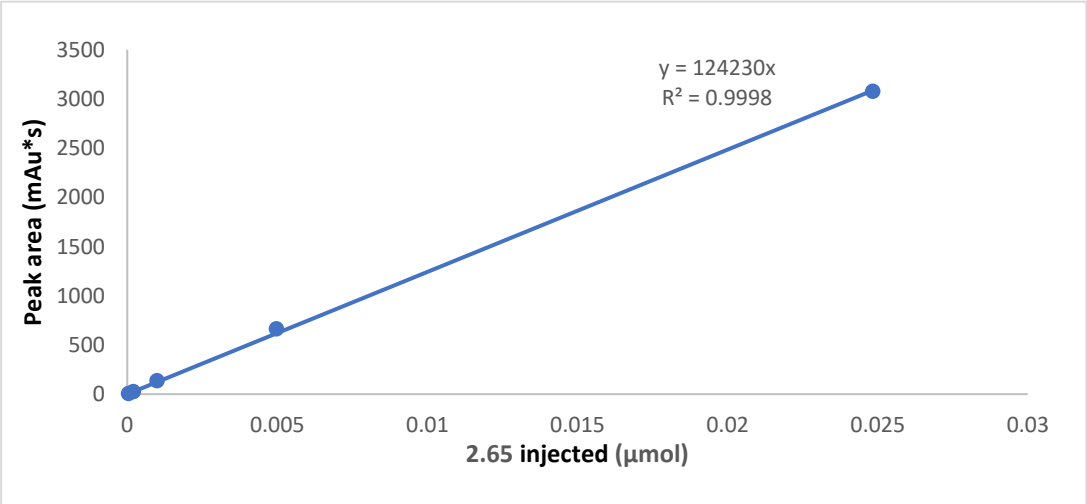
Measurement	Activity injected (MBq, d.c.)	2.58 injected (µmol)	Peak area (mAu*s)	A_m (GBq/µmol)
1	2.89	0.00023	186	12.4
2	1.59	0.00022	180	7.07
3	2.63	0.00022	178	11.8
			Average (*n* = 3)	10.4 GBq/µmol

Automated radiosynthesis of [^{18}F]**2.65**

General Procedure 8 was followed using **2.70** (5.0 mg, 0.02 mmol).

Entry	Starting activity	RCP	%AY	A_m (GBq/µmol)
1	148 GBq	>99%	1.4%	21
2	148 GBq	>99%	1.6%	15
		Average (*n* = 2)	1.5% ± 0.1%	18 ± 3 GBq/µmol

Calibration curve for **2.65**



Prepared using HPLC conditions B.

Run 1

Measurement	Activity injected (MBq, d.c.)	2.65 injected (µmol)	Peak area (mAu*s)	A_m (GBq/µmol)
1	1.31	5.2×10^{-5}	6.4	25
2	0.80	5.1×10^{-5}	6.3	16
3	1.14	5.3×10^{-5}	6.6	22
			Average (*n* = 3)	21 GBq/µmol

Run 2

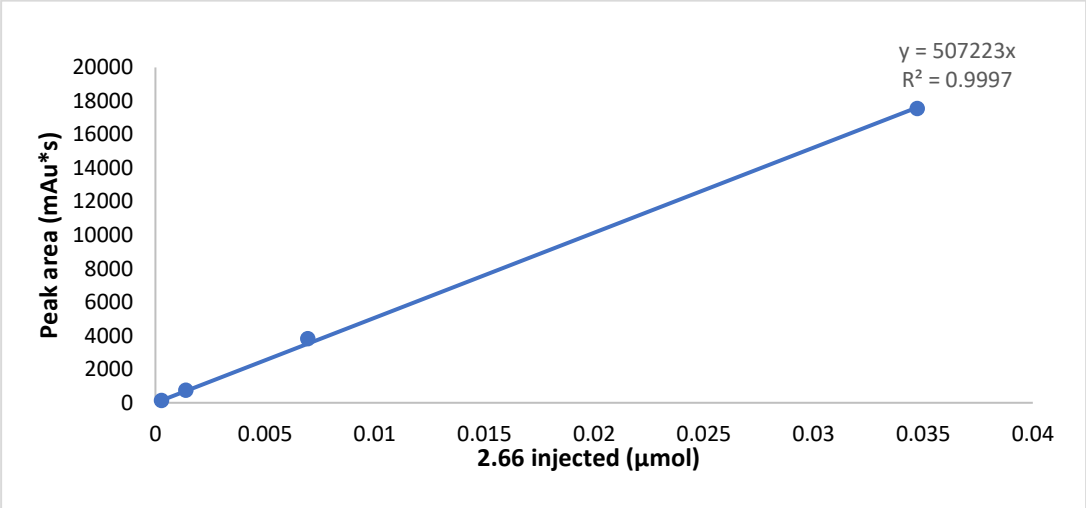
Measurement	Activity injected (MBq, d.c.)	2.65 injected (µmol)	Peak area (mAu*s)	A_m (GBq/µmol)
1	1.45	1.5×10^{-4}	18.1	10
2	1.64	8.4×10^{-5}	10.4	20
			Average (*n* = 2)	15 GBq/µmol

Automated radiosynthesis of [^{18}F]2.66

General Procedure 8 was followed using **2.71** (4.4 mg, 0.02 mmol).

Entry	Starting activity	RCP	%AY	A_m (GBq/µmol)
1	135 GBq	>99%	0.9%	3
2	135 GBq	>99%	0.8%	7
		Average (*n* = 2)	0.8% ± 0.1%	5 ± 2 GBq/µmol

Calibration curve for **2.66**



Prepared using HPLC conditions B.

Run 1

Measurement	Activity injected (MBq, d.c.)	2.66 injected (µmol)	Peak area (mAu*s)	A_m (GBq/µmol)
1	1.33	0.00057	289	2.33
2	1.36	0.00047	236	2.92
3	1.40	0.00044	225	3.15
			Average (*n* = 3)	2.8 GBq/µmol

Run 2

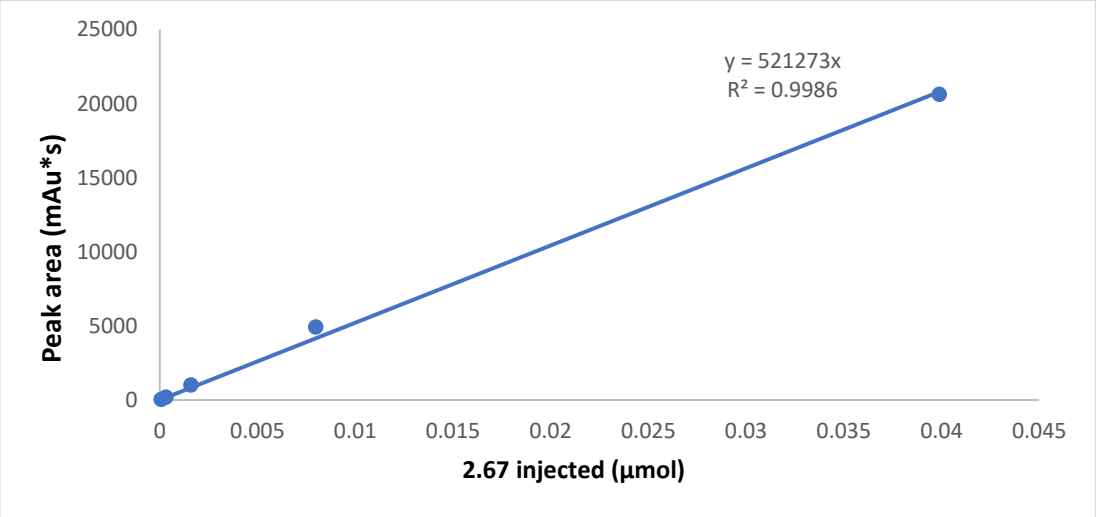
Measurement	Activity injected (MBq, d.c.)	2.66 injected (µmol)	Peak area (mAu*s)	A_m (GBq/µmol)
1	2.45	0.00027	137	9.09
2	1.83	0.00027	137	6.78
3	1.75	0.00027	137	6.46
			Average (*n* = 3)	7.4 GBq/µmol

Automated radiosynthesis of [^{18}F]**2.67**

General Procedure 8 was followed using **2.72** (5.5 mg, 0.02 mmol).

Entry	Starting activity	RCP	%AY	A_m (GBq/µmol)
1	135 GBq	>99%	1.0%	160
2	135 GBq	>99%	1.1%	102
		Average (*n* = 2)	1.0% ± 0.1%	131 ± 29 (GBq/µmol)

Calibration curve for **2.67**



Prepared using HPLC conditions B.

Run 1

Measurement	Activity injected (MBq, d.c.)	2.67 injected (µmol)	Peak area (mAu*s)	A_m (GBq/µmol)
1	2.07	1.67×10^{-5}	8.7	124
2	2.88	1.34×10^{-5}	7.0	214
3	2.08	1.48×10^{-5}	7.7	141
			Average (*n* = 3)	160 GBq/µmol

Run 2

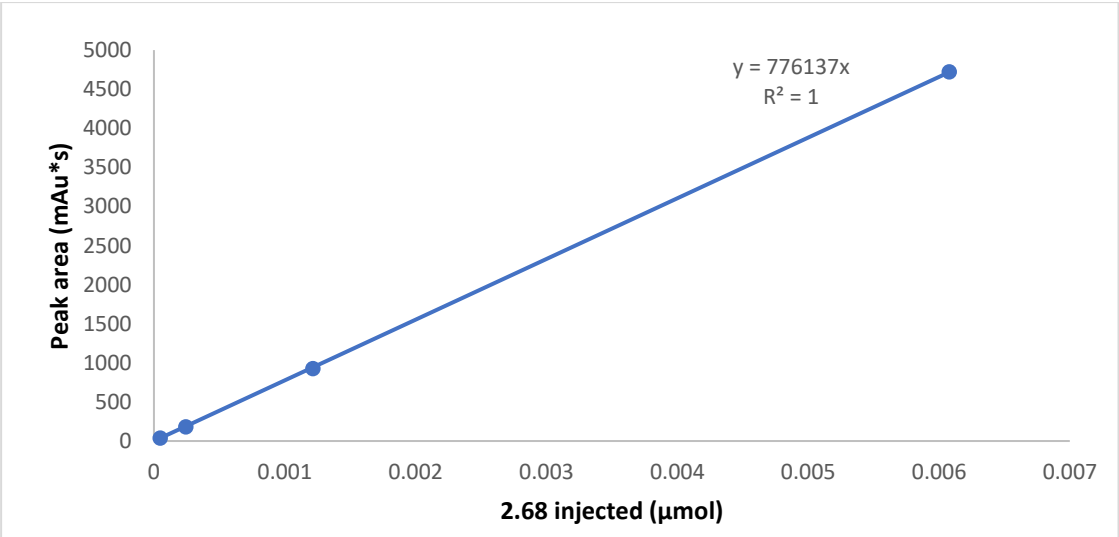
Measurement	Activity injected (MBq, d.c.)	2.67 injected (µmol)	Peak area (mAu*s)	A_m (GBq/µmol)
1	1.03	1.11×10^{-5}	5.8	93
2	1.57	1.38×10^{-5}	7.2	114
3	1.36	1.36×10^{-5}	7.1	100
			Average (*n* = 3)	102 GBq/µmol

Automated radiosynthesis of [^{18}F]**2.68**

General Procedure 8 was followed using **2.73** (4.9 mg, 0.02 mmol).

Entry	Starting activity	RCP	%AY	A_m (GBq/µmol)
1	148 GBq	>99%	2.0%	103
2	148 GBq	>99%	2.9%	114
		Average (*n* = 2)	2.5% ± 0.5%	108 ± 5 GBq/µmol

Calibration curve for **2.68**



Prepared using HPLC conditions B.

Run 1

Measurement	Activity injected (MBq, d.c.)	2.68 injected (µmol)	Peak area (mAu*s)	A_m (GBq/µmol)
1	0.76	7.86×10^{-6}	6.1	97
2	1.12	9.02×10^{-6}	7.0	124
3	0.85	9.66×10^{-6}	7.5	88
			Average (*n* = 3)	103 GBq/µmol

Run 2

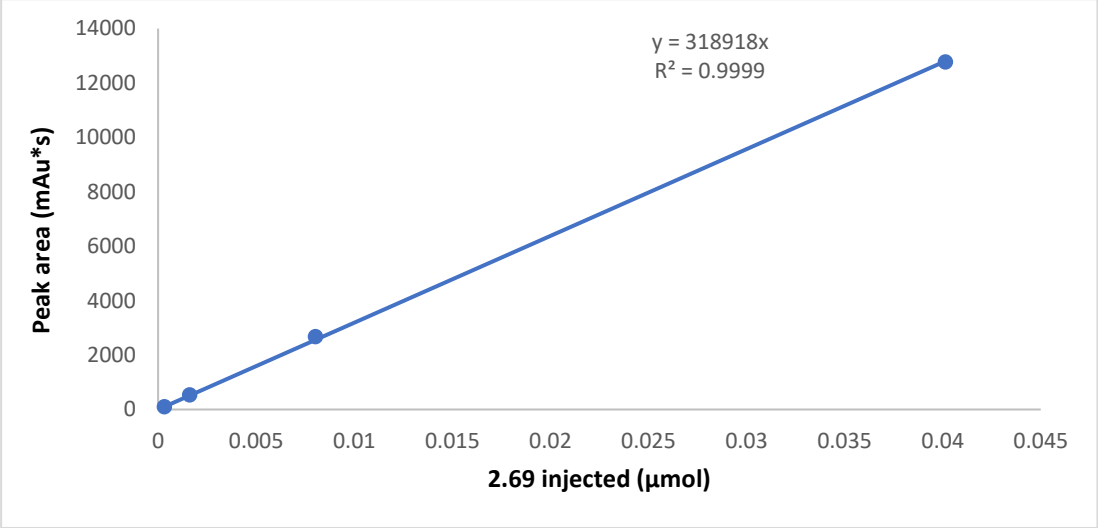
Measurement	Activity injected (MBq, d.c.)	2.68 injected (µmol)	Peak area (mAu*s)	A_m (GBq/µmol)
1	1.17	9.15×10^{-6}	7.1	128
2	1.17	1.00×10^{-5}	7.8	116
3	0.91	9.41×10^{-6}	7.3	97
			Average (*n* = 3)	114 GBq/µmol

Automated radiosynthesis of [^{18}F]2.69

General Procedure 8 was followed using **2.74** (5.5 mg, 0.02 mmol).

Entry	Starting activity	RCP	%AY	A_m (GBq/µmol)
1	135 GBq	>99%	4.5%	39
2	135 GBq	>99%	3.6%	53
		Average (*n* = 2)	4.1% ± 0.5%	46 ± 7 (GBq/µmol)

Calibration curve for **2.69**



Prepared using HPLC conditions B.

Run 1

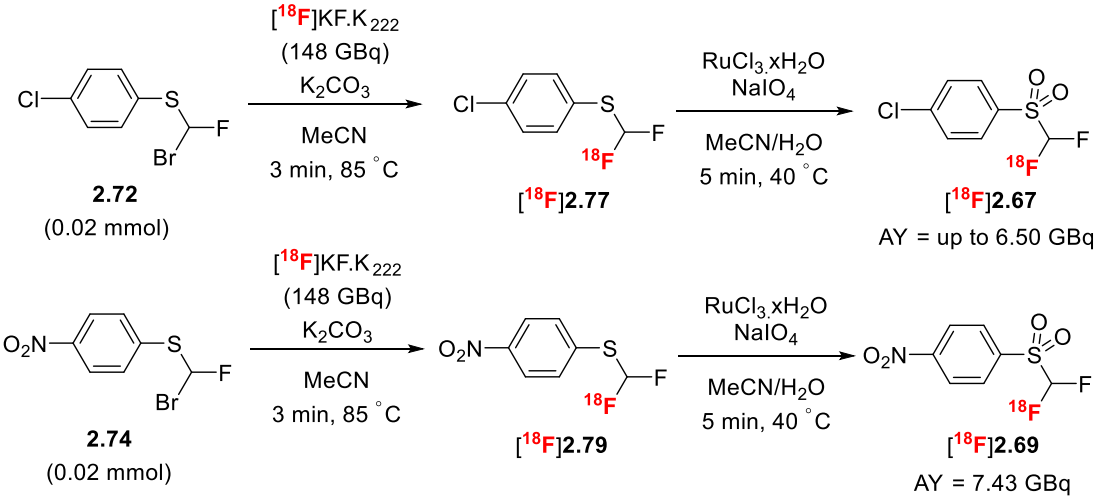
Measurement	Activity injected (MBq, d.c.)	2.69 injected (µmol)	Peak area (mAu*s)	A_m (GBq/µmol)
1	1.11	3.76×10^{-5}	12.0	29
2	1.77	3.73×10^{-5}	11.9	47
3	1.87	3.70×10^{-5}	11.8	39
			Average (n = 3)	39 GBq/µmol

Run 2

Measurement	Activity injected (MBq, d.c.)	2.69 injected (µmol)	Peak area (mAu*s)	A_m (GBq/µmol)
1	1.80	3.76×10^{-5}	12.0	48
2	2.20	3.73×10^{-5}	11.9	59
3	1.87	3.57×10^{-5}	11.4	52
			Average (n = 3)	53 GBq/µmol

Automated radiosynthesis of [^{18}F]**2.67** and [^{18}F]**2.69** in higher AY

Procedure:



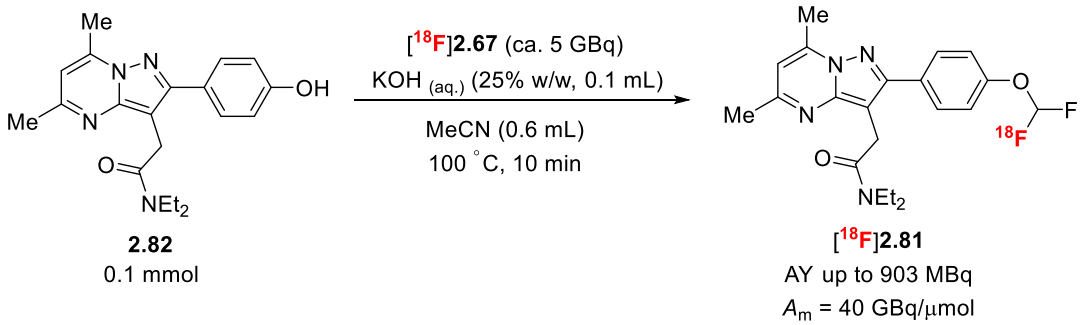
The automated radiosynthesis of [^{18}F]**2.67** and [^{18}F]**2.69** was performed with a Trasis AllInOne synthesiser using an automated program and pre-built cassette (see Figure 2.11, Chapter 2 for the cassette layout). The vial in position 2 was charged with Kryptofix 222 (7.5 mg), K_2CO_3 (1.5 mg), H_2O (0.15 mL) and MeCN (0.85 mL). The vial in position 9 was charged with a solution of the relevant bromofluoromethyl aryl sulfide (0.02 mmol) in dry MeCN (1.0 mL). The vial in position 10 was charged with $NaIO_4$ (52 mg), $RuCl_3{\cdot}xH_2O$ (2 mg), water (0.25 mL) and MeCN (0.25 mL). 10 mL vials were filled with MeCN and placed at positions 8 and 17. The reformulation vial was filled with water (10 mL) and placed at position 34. A Waters Sep-Pak AccellPlus QMA Carbonate cartridge (preactivated with 10 mL water) was installed at position 5. A Waters SepPak C18 Plus cartridge (preactivated with 10 mL ethanol and 10 mL water) was installed at position 33. The reactor at position 7 was made from glass, rather than the plastic reactor used in the previous synthesis.

[^{18}F]Fluoride in [^{18}O]water was received directly from the cyclotron and passed over the QMA cartridge and eluted with the contents of vial 2 into the reactor. A modified drying programme was used (azeotropic drying with MeCN); the contents of reactor were dried at 120 °C with further additions of MeCN from the vial at position 8, after which the vessel was cooled. The contents of the vial at position 9 were added and the ^{18}F-fluorination reaction was run at

85 °C for 3 minutes. Thereafter, the oxidation reaction was run in the same vessel at 40 °C for 5 minutes. The crude mixture was then purified by reverse-phase HPLC (HPLC conditions E, MeCN/H_2O = 55/45). The collected product was diluted with water and reformulated using a C18 cartridge, eluting with MeCN (2 mL).

Semi-automated radiosynthesis of [^{18}F]**2.81**

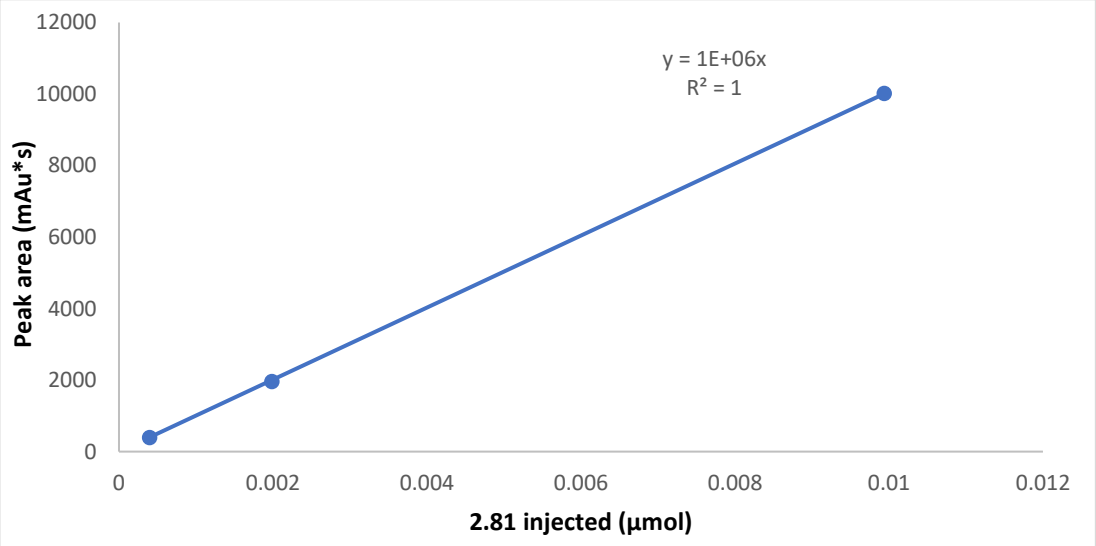
Procedure:



[^{18}F]**2.67** was first prepared as described above. HPLC-purified [^{18}F]**2.67** was eluted using MeCN into a vial containing phenol **2.82** (0.1 mmol) and a stirrer bar. KOH (aq., 25% w/w, 0.1 mL) solution was added by syringe. The line from the Trasis cassette was next removed and the vial was moved to a hot plate at 100 °C for 10 minutes. The vial was then allowed to cool, before a line from the Trasis was added to the vial and the crude reaction mixture was taken up in a syringe and transferred to the HPLC loop. The reaction mixture was purified using HPLC conditions E, eluent: 55/45=MeCN/H_2O. The fraction containing [^{18}F]**2.81** was collected in a falcon tube containing water (10 mL) and [^{18}F]**2.81** was reformulated using a C18 cartridge. The cartridge was removed and eluted manually with EtOH (2 mL). If [^{18}F]**2.81** was to be used for PET imaging, an alternative reformulation protocol was devised that maximised the activity concentration of [^{18}F]**2.81**: the C18 cartridge was eluted with minimum volume of Et_2O (first 0.3 mL fraction was discarded, second 0.6 mL fraction was retained). The Et_2O solvent was evaporated to dryness under a stream of N_2 and [^{18}F]**2.81** was redissolved in an ethanolic (12.5%) solution of saline to render it injectable.

For the measurement of A_m, an aliquot of the isolated, chemically and radiochemically pure product was analysed in triplicate by radio-HPLC. (Radio-)HPLC analysis was performed under HPLC conditions B. Separately, a calibration curve for the **2.81** authentic reference was recorded by preparing samples of a range of concentrations by serial dilution. These were injected onto an HPLC (10 µL injection volume from a 1.0 mL stock, HPLC conditions B) and the UV response was measured by integrating the peak of interest.

Calibration curve for **2.81**



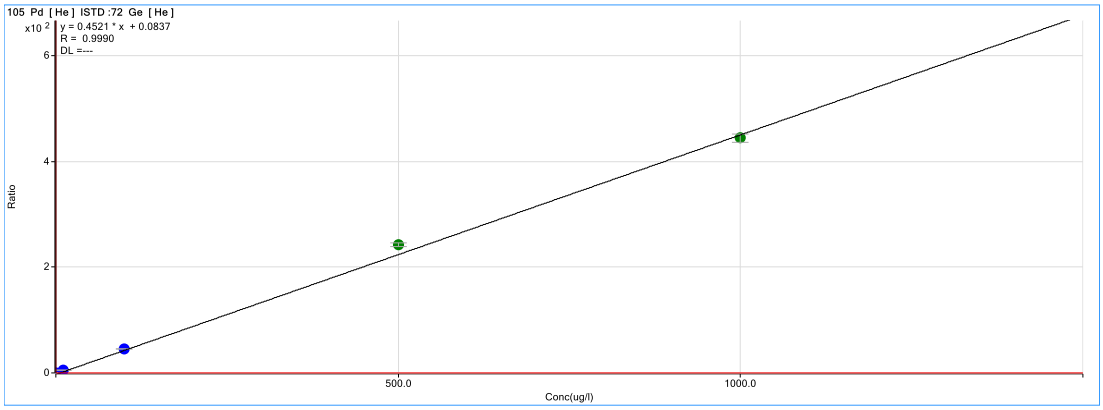
Measurement	Activity injected (MBq, d.c.)	2.81 injected (µmol)	Peak area (mAu*s)	A_m (GBq/µmol)
1	1.7	3.7E-05	37.0	46
2	2.1	5.6E-05	56.2	38
3	1.7	4.6E-05	46.3	37
			Average (n = 3)	40 GBq/µmol

4.3.3.3. ICP-MS analysis

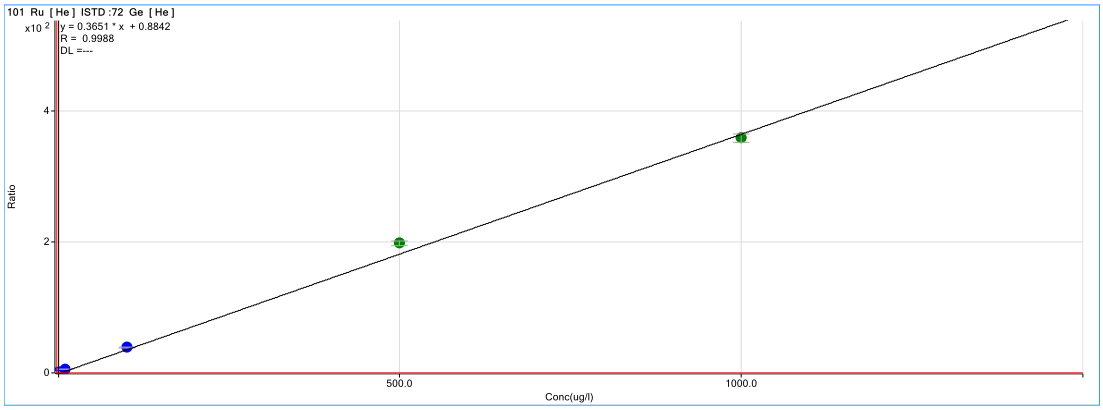
Procedure:

We thank Matthew Tredwell for assistance with ICP-MS analysis. A 5 mL V-vial was charged with **2.17** (0.2 mmol), hydroquinone (HQ) (0.05 mmol), Pd_2dba_3 (0.0025 mmol), Xantphos (0.0075 mmol) and a stirrer bar. [^{18}F]**2.67** in 1,4-dioxane (1.2 mL) and an aqueous KOH solution (10 M, 40 µL) were next added. The vial was heated on a hot plate at 120 °C for 20 minutes. The vial was then allowed to cool and the crude mixture was purified by semi-preparative HPLC (conditions E). Purified [^{18}F]**2.18** was collected and the sample was left to decay. ICP-MS analysis was used to determine the residual concentrations of Pd and Ru. Reference standards of known concentration were prepared by serial dilution and a calibration curve was prepared. The concentrations of residual ^{101}Ru and ^{105}Pd in the sample were found to be 242.18 µg/L and 18.53 µg/L.

Calibration curve for ^{105}Pd

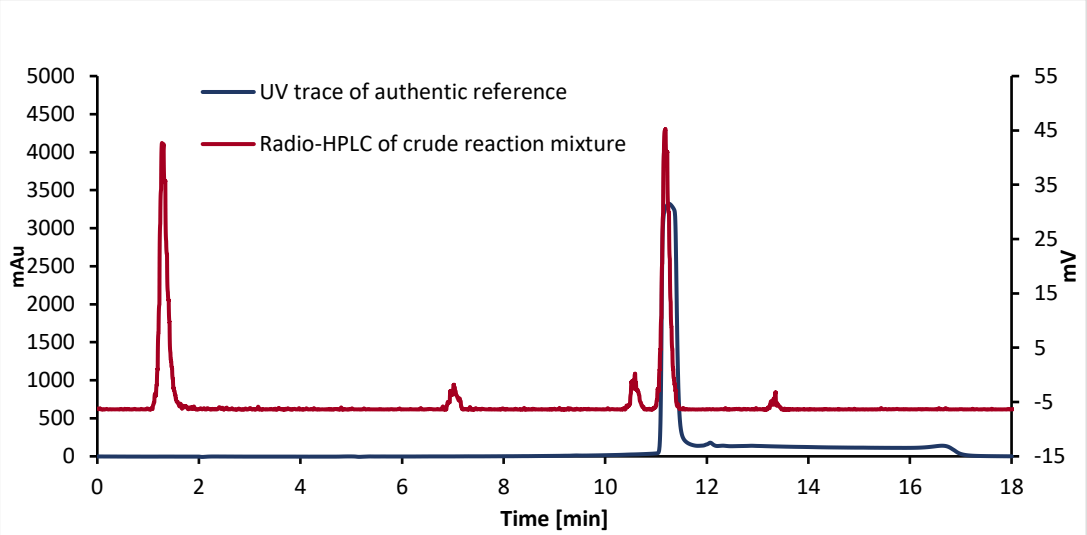


Calibration curve for ^{101}Ru



4.3.3.4. Radio and UV HPLC overlays and radiochemical yield calculations

UV/radio-HPLC trace overlay for [^{18}F]4-(difluoromethyl)-1,1'-biphenyl ([^{18}F]**2.18**)



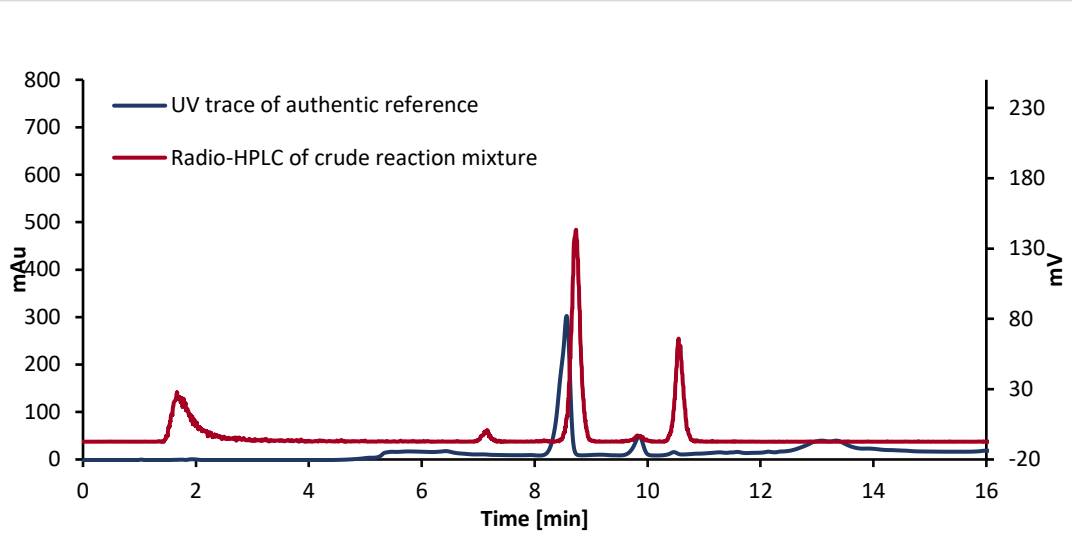
General Procedure 6 was followed, with:

- 1 mL reaction volume and 130 °C reaction temperature for [^{18}F]**2.58**.
- 1 mL reaction volume and 120 °C reaction temperature for [^{18}F]**2.67**.

Run	Reagent used	RCY of [^{18}F]2.18	
1	[^{18}F]**2.58**	61 %	
2	[^{18}F]**2.58**	44 %	
3	[^{18}F]**2.58**	45 %	
4	[^{18}F]**2.58**	41 %	
5	[^{18}F]**2.58**	36 %	
		Average RCY	**45 % ± 8 %** (n = 5), with [^{18}F]**2.58**
6	[^{18}F]**2.67**	24 %	
7	[^{18}F]**2.67**	49 %	
		Average RCY	**37 % ± 13 %** (n = 2), with [^{18}F]**2.67**

Analysed by (radio)HPLC using conditions A.

UV/radio-HPLC trace overlay for [^{18}F] 4-(4-(difluoromethyl)phenyl)morpholine ([^{18}F]**2.86**)



General Procedure 6 was followed, with:

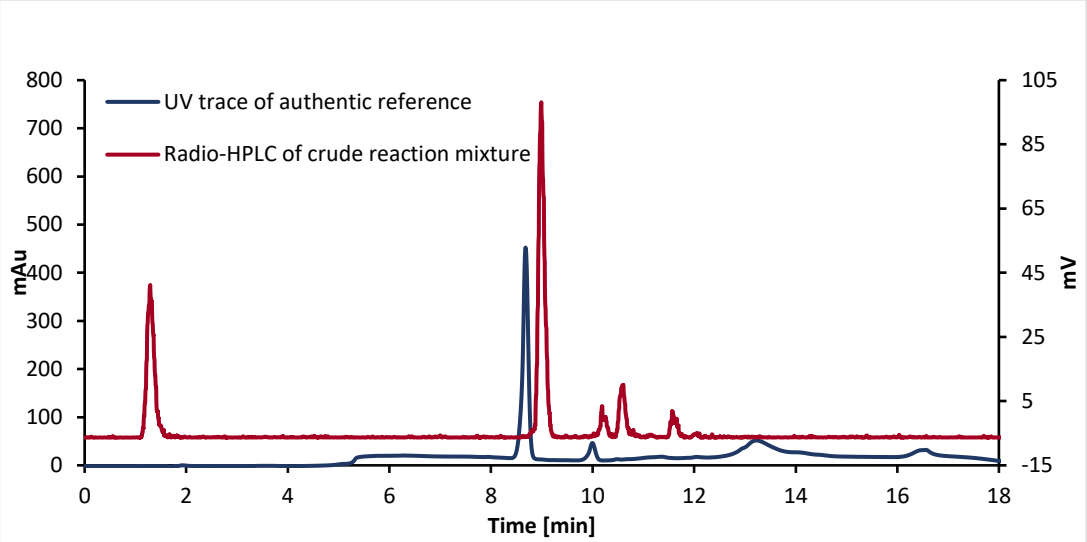
- 0.3 mL reaction volume and 130 °C reaction temperature for [^{18}F]**2.58**.
- 1 mL reaction volume and 120 °C reaction temperature for [^{18}F]**2.67**.

Run	Reagent used	RCY of [^{18}F]2.86	
1	[^{18}F]**2.58**	41 %	
2	[^{18}F]**2.58**	31 %	
3	[^{18}F]**2.58**	50 %	
		Average RCY	**41 % ± 8 %** (n = 3), with [^{18}F]**2.58**
4	[^{18}F]**2.67**	35 %	
5	[^{18}F]**2.67**	30 %	
		Average RCY	**33 % ± 3 %** (n = 2), with [^{18}F]**2.67**

n.b. A stock solution of 43.4 mg Xantphos was prepared in 2 mL 1,4-dioxane and 0.2 mL was dispensed to obtain a total reaction volume of 0.3 mL upon addition of other reagent stocks and additional solvent.

Analysed by (radio)HPLC using conditions A.

UV/radio-HPLC trace overlay for [^{18}F] 5-(difluoromethyl)benzo[*d*][1,3]dioxole ([^{18}F]**2.87**)



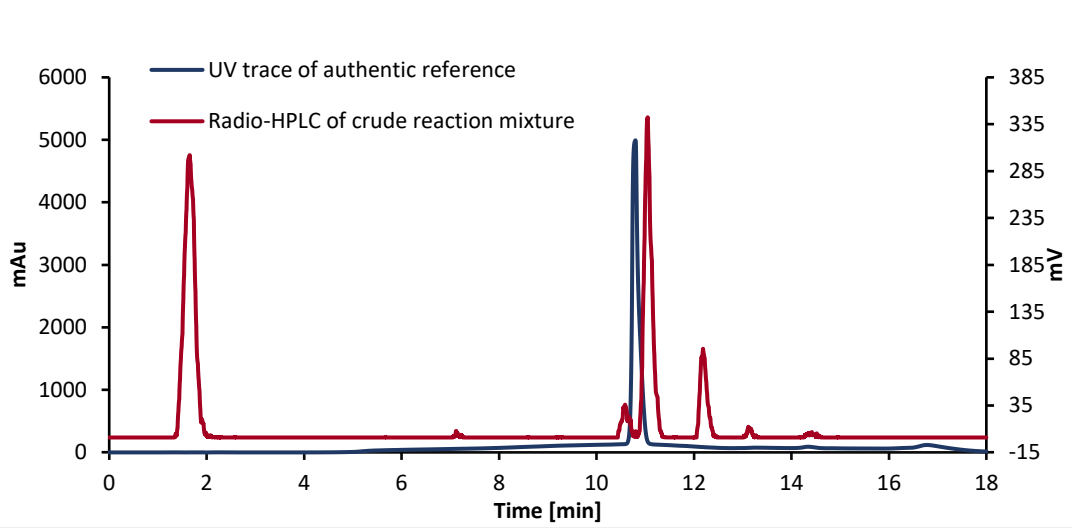
General Procedure 6 was followed, with:

- 1 mL reaction volume and 125 °C reaction temperature for [^{18}F]**2.58**.
- 1 mL reaction volume and 120 °C reaction temperature for [^{18}F]**2.67**.

Run	Reagent used	RCY of [^{18}F]2.87	
1	[^{18}F]**2.58**	11 %	
2	[^{18}F]**2.58**	55 %	
3	[^{18}F]**2.58**	44 %	
4	[^{18}F]**2.58**	22 %	
5	[^{18}F]**2.58**	15 %	
		Average RCY	**29 % ± 17 %** (n = 5), with [^{18}F]**2.58**
6	[^{18}F]**2.67**	18 %	
7	[^{18}F]**2.67**	43 %	
		Average RCY	**31 % ± 13 %** (n = 2), with [^{18}F]**2.67**

Analysed by (radio)HPLC using conditions A.

UV/radio-HPLC trace overlay for [^{18}F] 2-(4-(difluoromethyl)phenyl)thiophene ([^{18}F]**2.88**)



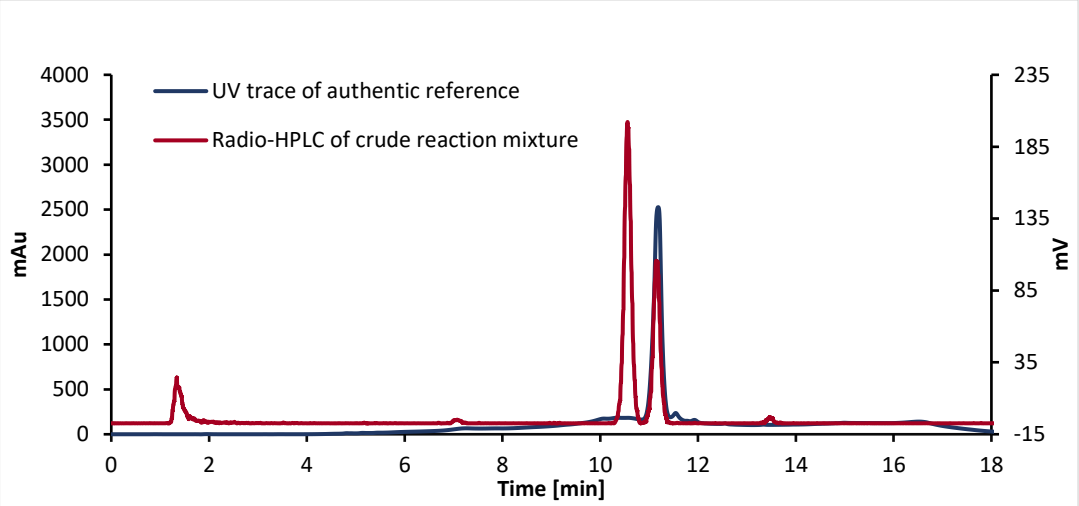
General Procedure 6 was followed, with:

- 1 mL reaction volume and 125 °C reaction temperature for [^{18}F]**2.58**.
- 1 mL reaction volume and 115 °C reaction temperature for [^{18}F]**2.67**.

Run	Reagent used	RCY of [^{18}F]2.88	
1	[^{18}F]**2.58**	32 %	
2	[^{18}F]**2.58**	33 %	
3	[^{18}F]**2.58**	30 %	
		Average RCY	**32 % ± 1 %** (n = 3), with [^{18}F]**2.58**
4	[^{18}F]**2.67**	45 %	
		Average RCY	**45 %** (n = 1), with [^{18}F]**2.67**

Analysed by (radio)HPLC using conditions A.

UV/radio-HPLC trace overlay for [^{18}F]4-(difluoromethyl)dibenzo[*b*,*d*]furan ([^{18}F]**2.89**)



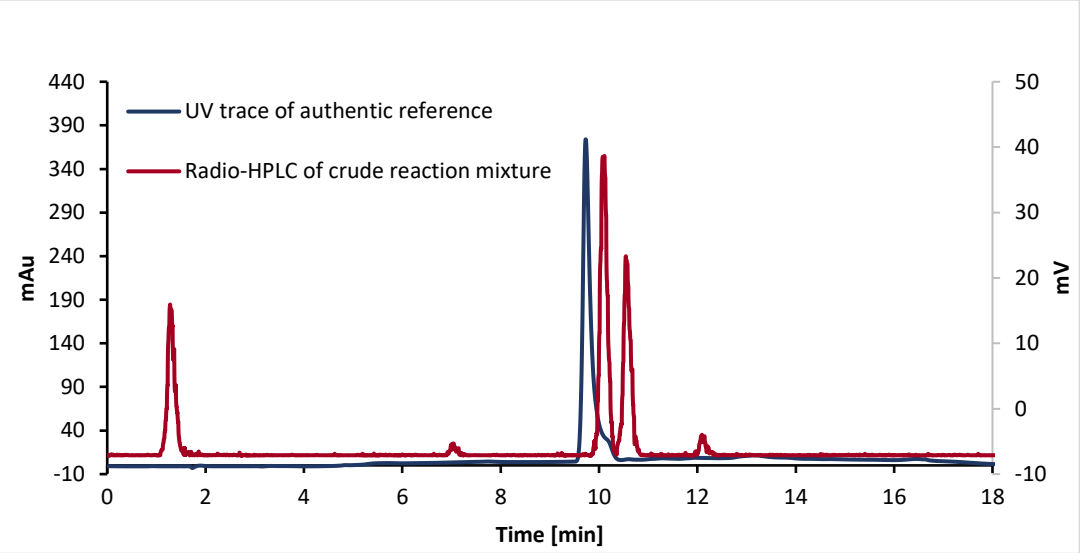
General Procedure 6 was followed, with:

- 1 mL reaction volume and 125 °C reaction temperature for [^{18}F]**2.58**.
- 1 mL reaction volume and 115 °C reaction temperature for [^{18}F]**2.67**.

Run	Reagent used	RCY of [^{18}F]2.89	
1	[^{18}F]**2.58**	31 %	
2	[^{18}F]**2.58**	22 %	
3	[^{18}F]**2.58**	38 %	
		Average RCY	**30 % ± 7 %** (n = 3), with [^{18}F]**2.58**
4	[^{18}F]**2.67**	18 %	
		Average RCY	**18 %** (n = 1), with [^{18}F]**2.67**

Analysed by (radio)HPLC using conditions A.

UV/radio-HPLC trace overlay for [^{18}F] 1-chloro-4-(difluoromethyl)benzene ([^{18}F]**2.90**)



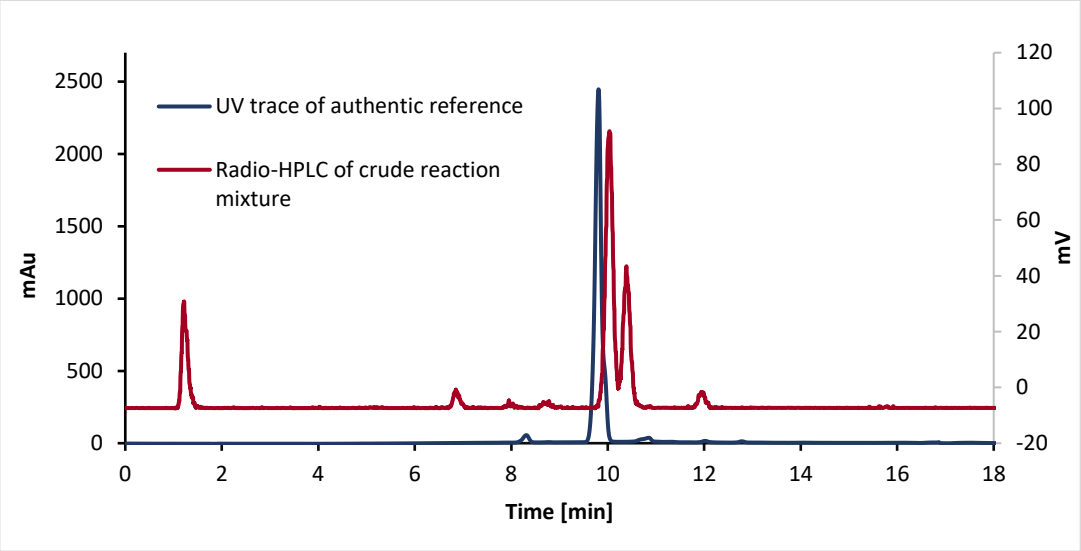
General Procedure 6 was followed, with:

- 1 mL reaction volume and 120 °C reaction temperature for [^{18}F]**2.58**.
- 1 mL reaction volume and 120 °C reaction temperature for [^{18}F]**2.67**.

Run	Reagent used	RCY of [^{18}F]2.90	
1	[^{18}F]**2.58**	45 %	
2	[^{18}F]**2.58**	36 %	
3	[^{18}F]**2.58**	21 %	
		Average RCY	**34 % ± 10 %** (n = 3), with [^{18}F]**2.58**
4	[^{18}F]**2.67**	67 %	
5	[^{18}F]**2.67**	42 %	
		Average RCY	**55 % ± 13 %** (n = 2), with [^{18}F]**2.67**

Analysed by (radio)HPLC using conditions A.

UV/radio-HPLC trace overlay for [^{18}F] 1-(difluoromethyl)-4-vinylbenzene ([^{18}F]**2.91**)



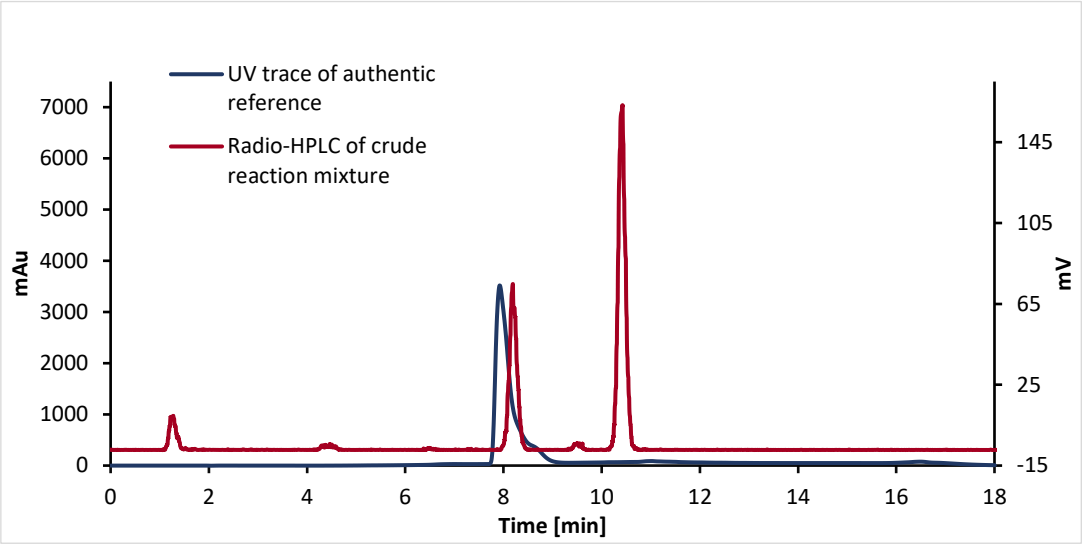
General Procedure 6 was followed, with:

- 1 mL reaction volume and 125 °C reaction temperature for [^{18}F]**2.58**.
- 1 mL reaction volume and 120 °C reaction temperature for [^{18}F]**2.67**.

Run	Reagent used	RCY of [^{18}F]2.91	
1	[^{18}F]**2.58**	52 %	
2	[^{18}F]**2.58**	39 %	
3	[^{18}F]**2.58**	32 %	
		Average RCY	**41 % ± 8 %** (n = 3), with [^{18}F]**2.58**
4	[^{18}F]**2.67**	36 %	
5	[^{18}F]**2.67**	43 %	
		Average RCY	**40 % ± 4 %** (n = 2), with [^{18}F]**2.67**

Analysed by (radio)HPLC using conditions A.

UV/radio-HPLC trace overlay for [^{18}F]5-(difluoromethyl)-2-methoxypyridine ([^{18}F]**2.92**)



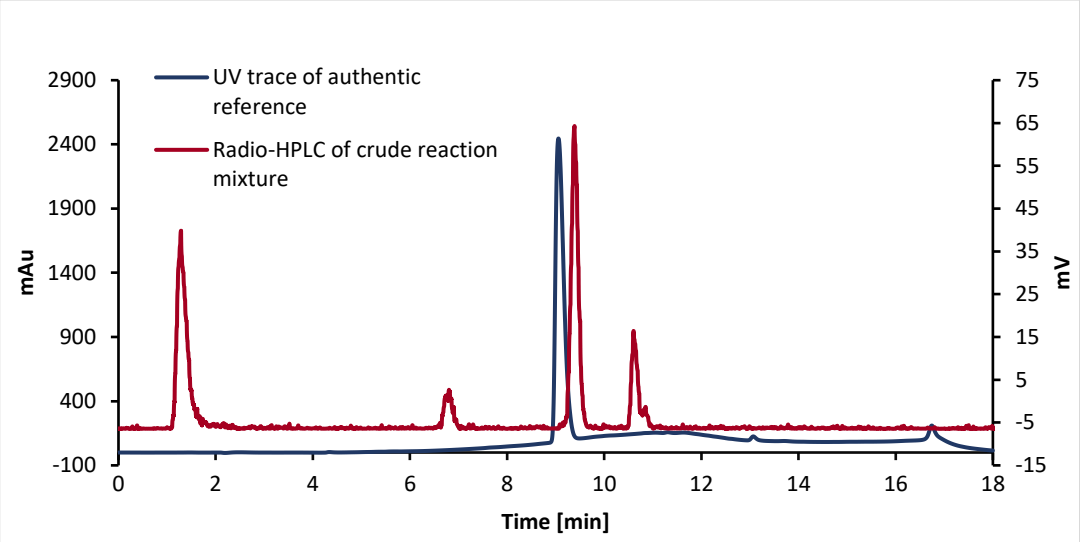
General Procedure 6 was followed, with:

- 1 mL reaction volume and 130 °C reaction temperature for [^{18}F]**2.58**.
- 1 mL reaction volume and 120 °C reaction temperature for [^{18}F]**2.67**.

Run	Reagent used	RCY of [^{18}F]2.92	
1	[^{18}F]**2.58**	6 %	
2	[^{18}F]**2.58**	31 %	
3	[^{18}F]**2.58**	26 %	
		Average RCY	**21 % ± 11 %** (n = 3), with [^{18}F]**2.58**
4	[^{18}F]**2.67**	25 %	
5	[^{18}F]**2.67**	28 %	
		Average RCY	**27 % ± 2 %** (n = 2), with [^{18}F]**2.67**

Analysed by (radio)HPLC using conditions A.

UV/radio-HPLC trace overlay for [^{18}F]1-(difluoromethyl)-3-methoxybenzene ([^{18}F]**2.93**)



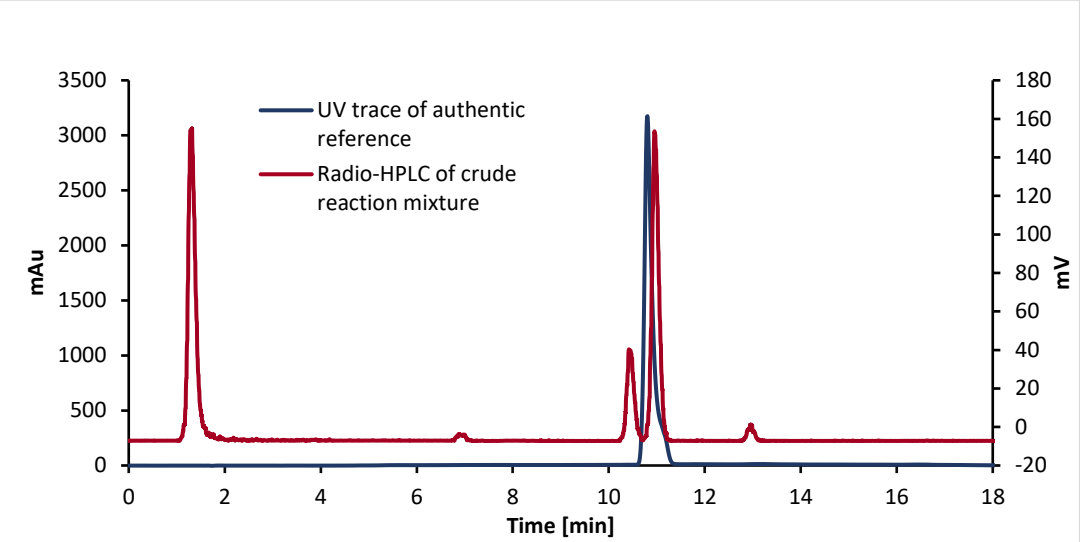
General Procedure 5 was followed, with:

- 1 mL reaction volume and 125 °C reaction temperature for [^{18}F]**2.58**.
- 1 mL reaction volume and 120 °C reaction temperature for [^{18}F]**2.67**.

Run	Reagent used	RCY of [^{18}F]2.93	
1	[^{18}F]**2.58**	43 %	
2	[^{18}F]**2.58**	30 %	
3	[^{18}F]**2.58**	32 %	
		Average RCY	**35 % ± 6 %** (n = 3), with [^{18}F]**2.58**
4	[^{18}F]**2.67**	56 %	
5	[^{18}F]**2.67**	47 %	
		Average RCY	**52 % ± 5 %** (n = 2), with [^{18}F]**2.67**

Analysed by (radio)HPLC using conditions A.

UV/radio-HPLC trace overlay for [^{18}F] 1-(difluoromethyl)-4-phenoxybenzene ([^{18}F]**2.94**)



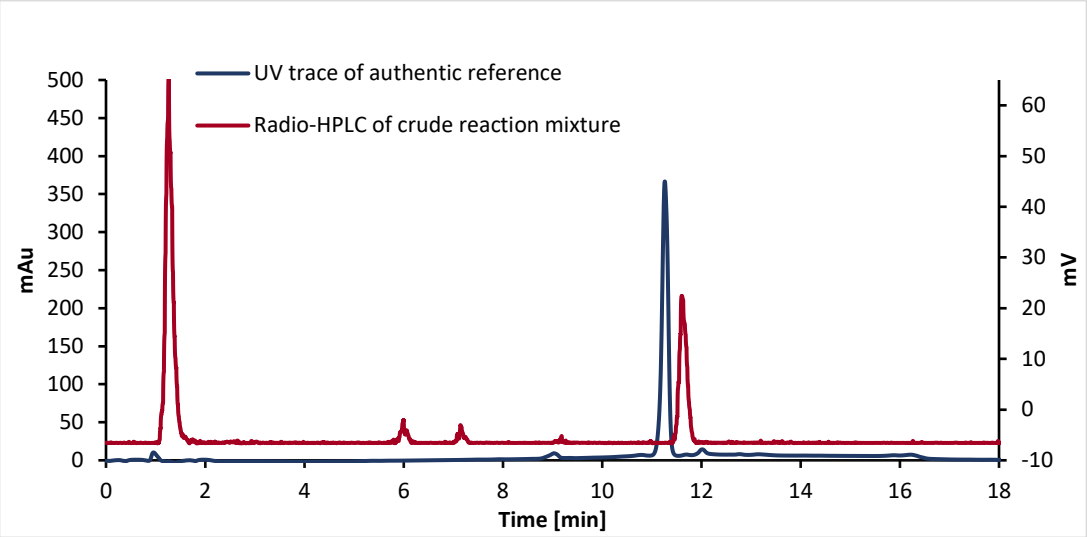
General Procedure 6 was followed, with:

- 1 mL reaction volume and 120 °C reaction temperature for [^{18}F]**2.58**.
- 1 mL reaction volume and 120 °C reaction temperature for [^{18}F]**2.67**.

Run	Reagent used	RCY of [^{18}F]2.94	
1	[^{18}F]**2.58**	41 %	
2	[^{18}F]**2.58**	18 %	
3	[^{18}F]**2.58**	23 %	
		Average RCY	**27 % ± 10 %** (n = 3), with [^{18}F]**2.58**
4	[^{18}F]**2.67**	45 %	
5	[^{18}F]**2.67**	25 %	
		Average RCY	**35 % ± 10 %** (n = 2), with [^{18}F]**2.67**

Analysed by (radio)HPLC using conditions A.

UV/radio-HPLC trace overlay for [^{18}F] isopropyl 2-(4-(4-(difluoromethyl)benzoyl)phenoxy)-2-methylpropanoate ([^{18}F]**2.95**)



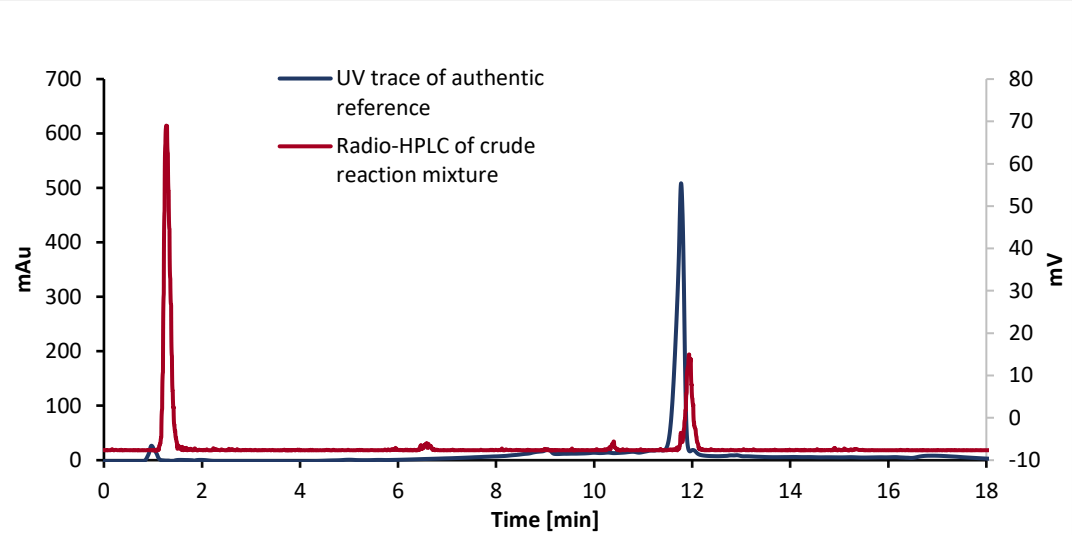
General Procedure 6 was followed, with:

- 0.5 mL reaction volume and 135 °C reaction temperature for [^{18}F]**2.58**.
- 1 mL reaction volume and 120 °C reaction temperature for [^{18}F]**2.67**.

Run	Reagent used	RCY of [^{18}F]2.95	
1	[^{18}F]**2.58**	20 %	
2	[^{18}F]**2.58**	18 %	
3	[^{18}F]**2.58**	22 %	
		Average RCY	**20 % ± 2 %** (n = 3), with [^{18}F]**2.58**
4	[^{18}F]**2.67**	30 %	
		Average RCY	**30 %** (n = 1), with [^{18}F]**2.67**

Analysed by (radio)HPLC using conditions A.

UV/radio-HPLC trace overlay for [^{18}F]*tert*-butyl (3-(4-(difluoromethyl)phenoxy)-3-phenylpropyl)(methyl)carbamate ([^{18}F]**2.96**)



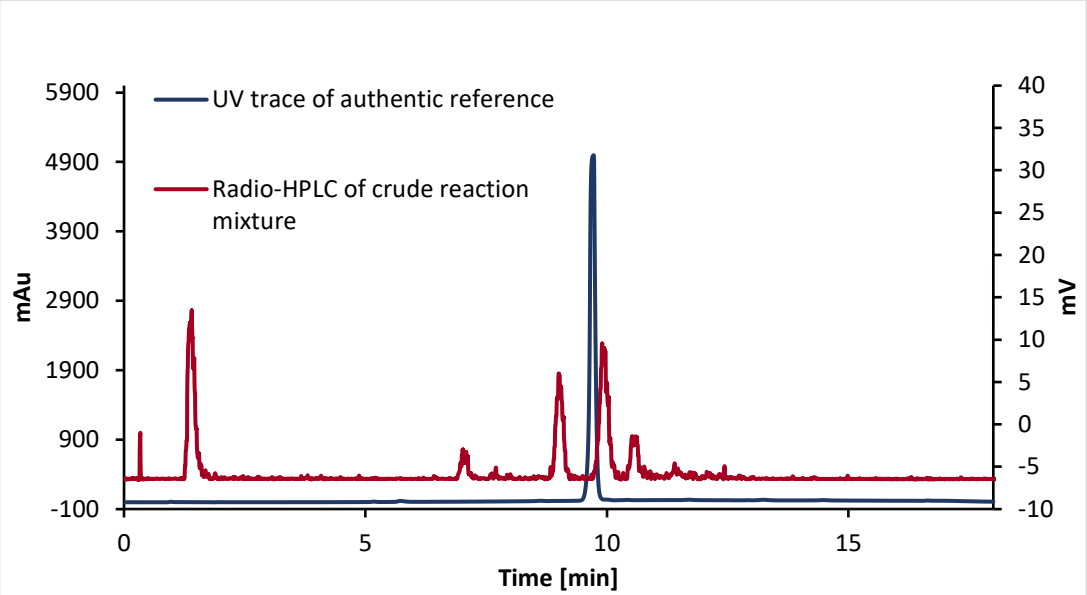
General Procedure 6 was followed, with:

- 0.7 mL reaction volume and 125 °C reaction temperature for [^{18}F]**2.58**.

Run	Reagent used	RCY of [^{18}F]2.96	
1	[^{18}F]**2.58**	27 %	
2	[^{18}F]**2.58**	45 %	
3	[^{18}F]**2.58**	33 %	
		Average RCY	**35 % ± 7 %** (n = 3), with [^{18}F]**2.58**

Analysed by (radio)HPLC using conditions A.

UV/radio-HPLC trace overlay for [^{18}F]3-(difluoromethyl)-5-((2-methylthiazol-4-yl)ethynyl)benzonitrile ([^{18}F]**2.97**)



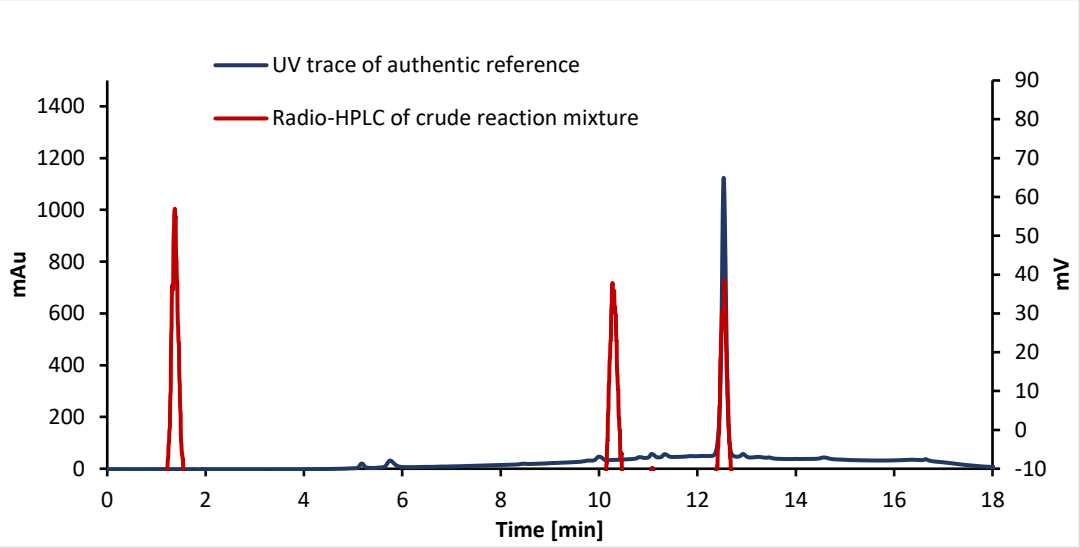
General Procedure 6 was followed, with:

- 1 mL reaction volume and 125 °C reaction temperature for [^{18}F]**2.58**.
- 1 mL reaction volume and 120 °C reaction temperature for [^{18}F]**2.67**.

Run	Reagent used	RCY of [^{18}F]2.97	
1	[^{18}F]**2.58**	37 %	
2	[^{18}F]**2.58**	18 %	
3	[^{18}F]**2.58**	25 %	
4	[^{18}F]**2.58**	14 %	
		Average RCY	**24 % ± 9 %** (n = 4), with [^{18}F]**2.58**
5	[^{18}F]**2.67**	31 %	
6	[^{18}F]**2.67**	17 %	
		Average RCY	**24 % ± 7 %** (n = 2), with [^{18}F]**2.67**

Analysed by (radio)HPLC using conditions A.

UV/radio-HPLC trace overlay for [^{18}F] tert-butyl (*S*)-2-(bis(tert-butoxycarbonyl)amino)-3-(4-(difluoromethyl)phenyl)propanoate ([^{18}F]**2.98**)



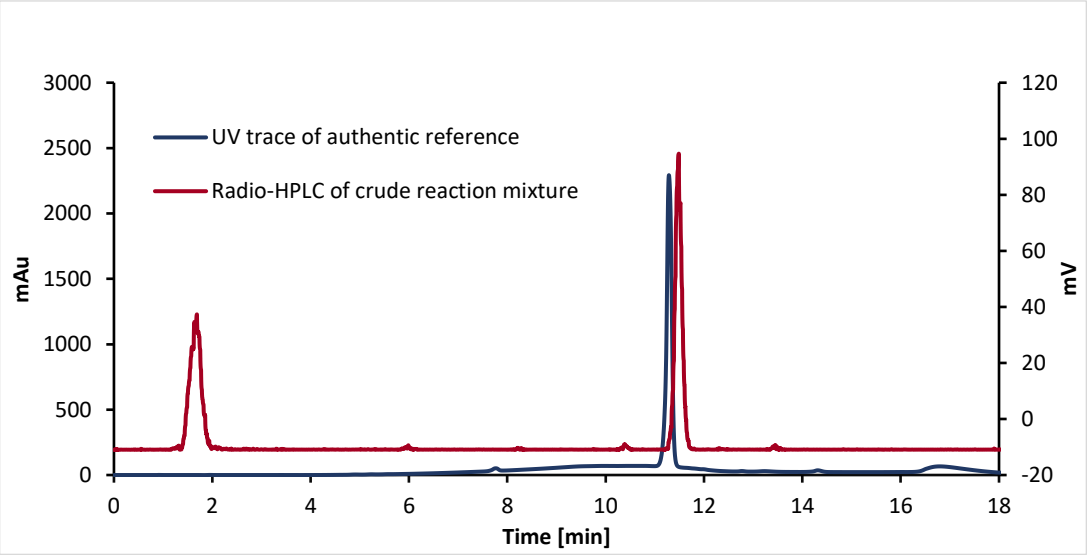
General Procedure 6 was followed, with:

- 0.5 mL reaction volume and 125 °C reaction temperature for [^{18}F]**2.58**.
- 1 mL reaction volume and 120 °C reaction temperature for [^{18}F]**2.67**.

Run	**Reagent used**	**RCY of [^{18}F]2.98**	
1	[^{18}F]**2.58**	26 %	
2	[^{18}F]**2.58**	27 %	
		Average RCY	**27 % ± 1 %** (n = 2), with [^{18}F]**2.58**
3	[^{18}F]**2.67**	16 %	
		Average RCY	**16 %** (n = 1), with [^{18}F]**2.67**

Analysed by (radio)HPLC using conditions A.

UV/radio-HPLC trace overlay for [^{18}F] isopropyl 2-(4-(4-(difluoromethoxy)benzoyl)phenoxy)-2-methylpropanoate ([^{18}F]**2.106**)

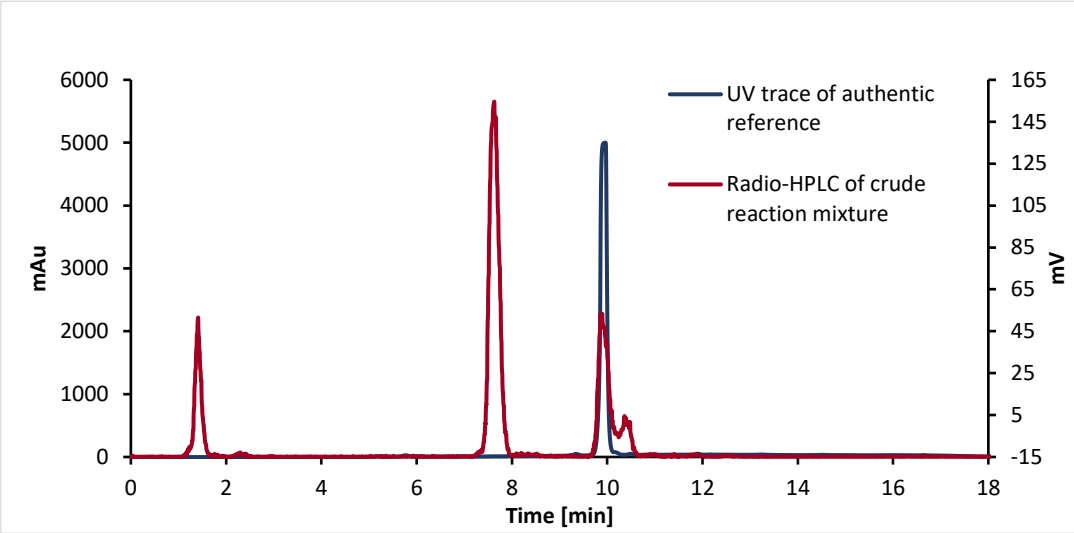


General Procedure 7 was followed.

Run	Reagent used	RCY of [^{18}F]**2.106**	
1	[^{18}F]**2.58**	60 %	
2	[^{18}F]**2.58**	58 %	
3	[^{18}F]**2.58**	50 %	
		Average RCY	**56 % ± 4 %** (n = 3), with [^{18}F]**2.58**

Analysed by (radio)HPLC using conditions A.

UV/radio-HPLC trace overlay for [^{18}F]3-(difluoromethoxy)-5-((2-methylthiazol-4-yl)ethynyl)benzonitrile ([^{18}F]**2.107**)

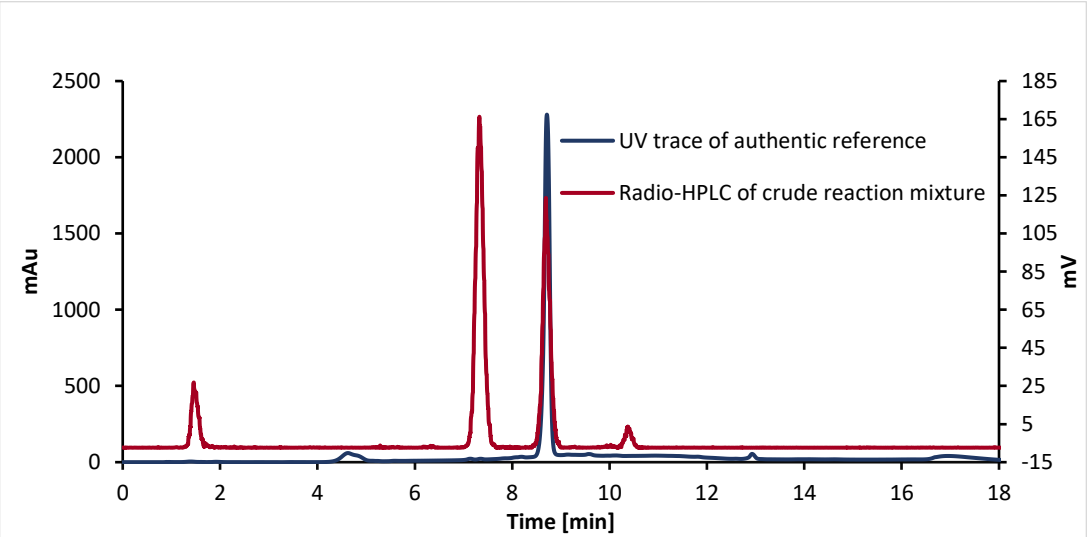


General Procedure 7 was followed.

Run	Reagent used	RCY of [^{18}F]**2.107**	
1	[^{18}F]**2.58**	20 %	
2	[^{18}F]**2.58**	24 %	
		Average RCY	**22 % ± 2 %** (n = 2), with [^{18}F]**2.58**

Analysed by (radio)HPLC using conditions A.

UV/radio-HPLC trace overlay for [^{18}F] *N*-(3-(difluoromethoxy)-4-nitrophenyl)isobutyramide ([^{18}F]**2.108**)

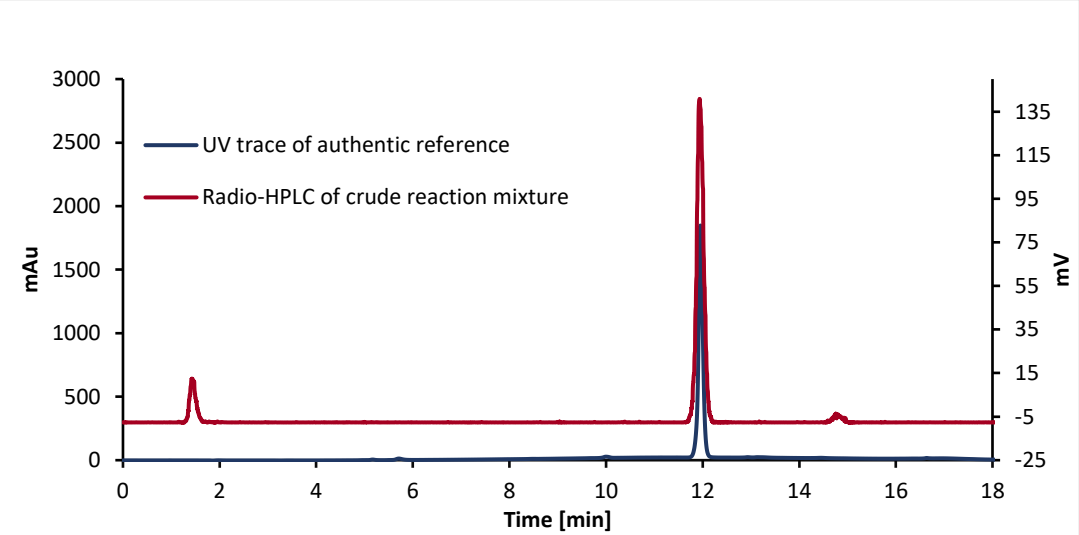


General Procedure 7 was followed.

Run	Reagent used	RCY of [^{18}F]**2.108**	
1	[^{18}F]**2.58**	36 %	
2	[^{18}F]**2.58**	22 %	
		Average RCY	**29 % ± 7 %** (n = 2), with [^{18}F]**2.58**

Analysed by (radio)HPLC using conditions A.

UV/radio-HPLC trace overlay for [^{18}F] *tert*-butyl (3-(4-(difluoromethoxy)phenoxy)-3-phenylpropyl)(methyl)carbamate ([^{18}F]**2.109**)

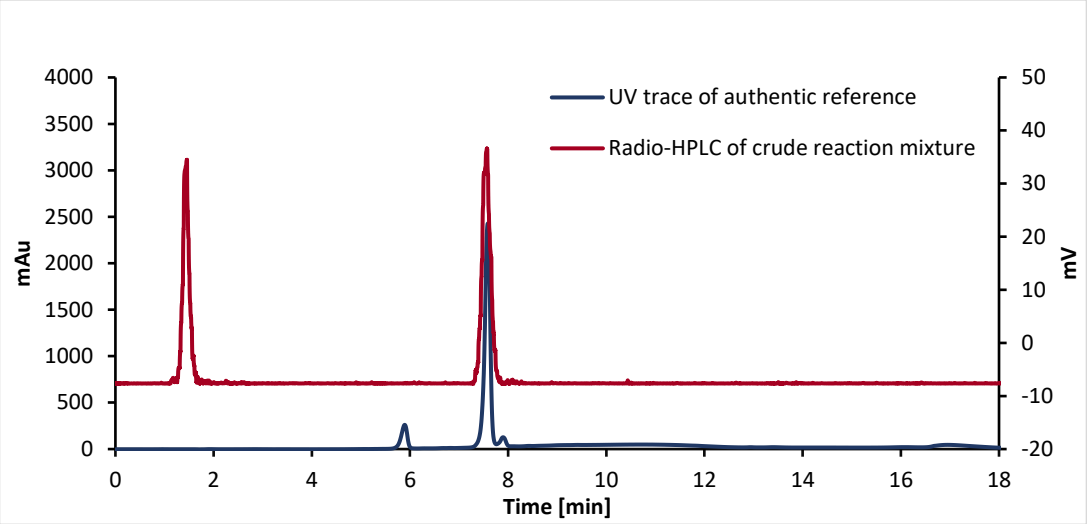


General Procedure 7 was followed.

Run	Reagent used	RCY of [^{18}F]2.109	
1	[^{18}F]**2.58**	83 %	
2	[^{18}F]**2.58**	88 %	
		Average RCY	**86 % ± 3 %** (n = 2), with [^{18}F]**2.58**

Analysed by (radio)HPLC using conditions A.

UV/radio-HPLC trace overlay for [^{18}F]5-(difluoromethoxy)-6'-methyl-3-(4-(methylsulfonyl)phenyl)-2,3'-bipyridine ([^{18}F]**2.110**)

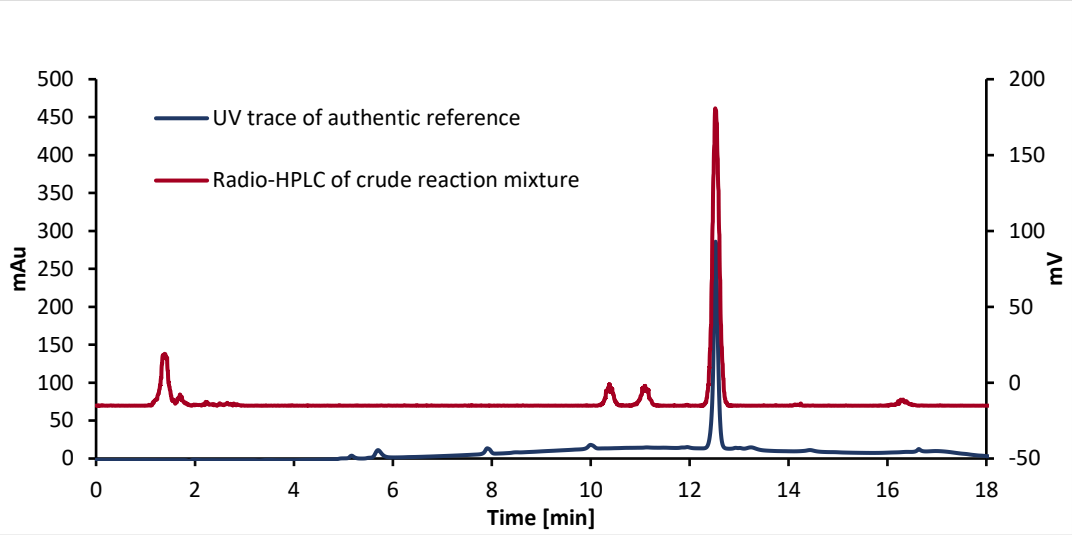


General Procedure 7 was followed, with the addition of 0.1 mL DMSO to the solvent mixture, as the substrate was poorly soluble in MeCN.

Run	Reagent used	RCY of [^{18}F]**2.110**	
1	[^{18}F]**2.58**	53 %	
2	[^{18}F]**2.58**	58 %	
		Average RCY	**56 % ± 3 %** (n = 2), with [^{18}F]**2.58**

Analysed by (radio)HPLC using conditions A.

UV/radio-HPLC trace overlay for [^{18}F] *tert*-butyl (*S*)-2-(bis(tert-butoxycarbonyl)amino)-3-(4-(difluoromethoxy)phenyl)propanoate ([^{18}F]**2.111**)



General Procedure 7 was followed.

Run	Reagent used	RCY of [^{18}F]2.111	
1	[^{18}F]**2.58**	73 %	
2	[^{18}F]**2.58**	63 %	
		Average RCY	**68 % ± 5 %** (n = 2), with [^{18}F]**2.58**

Analysed by (radio)HPLC using conditions A.

4.3.4. PET imaging and in vivo studies

These experiments were conducted in collaboration with Dr. S. Paisey, Dr. M. Lelos and Dr. M. Tredwell (Cardiff University). J. Ford and J. Sap prepared the radiotracers used in these studies and performed radio-HPLC analysis of samples generated from the *in vivo* studies by Dr. S. Paisey and Dr. M. Lelos. All experiments and animal care were conducted in Cardiff University in compliance with the UK Animals (Scientific Procedures) Act 1986 under Home Office Licence No. P49E8C976 and with the approval of the local Cardiff University Ethics Review Committee.

[^{18}F]**2.80** was prepared exactly as described in a literature report using a Trasis AllinOne synthesiser.[25] PK-11195 (**2.84**) was purchased from a commercial supplier (Axon Medchem) and used as received without further purification. [^{18}F]**2.81** was prepared as described in section 4.3.3.2.

Male C57BL/6 mice were purchased from Charles River. These were housed in individually ventilated cages in groups of 5 and maintained on a 12 h/12 h light/dark cycle. The excitotoxic quinolinic acid mouse model was prepared by Dr M. Lelos (Cardiff University) according to a protocol described in the literature.[26]

PET imaging with [^{18}F]**2.80** and [^{18}F]**2.81** was conducted by Dr. S. Paisey (Cardiff University). The disease model mouse was placed in an incubator set to 40 °C for 10 mins and then anaesthetised using 5% isoflurane with 100% oxygen (1 L/min) as a carrier gas. The mouse was immediately transferred to the Mediso multicell mouse bed of the Mediso nanoScan 122s PET/CT scanner (Mediso, Budapest, Hungary) and anaesthesia was maintained with 1-2% isoflurane in 100% oxygen (1 L/min) through an integral nose cone. Core body temperature of the mice was maintained at 37 °C and respiration rate was monitored and kept at 30-50 BPM for the duration of the imaging protocol. A 60 min single bed position whole body dynamic PET scan was prepared and acquisition was commenced immediately

upon tracer injection. The mouse was injected with [^{18}F]**2.80** and [^{18}F]**2.81**. Where pre-blocking with **2.84** was to be studied, a naïve C57BL/6 mouse was administered by injection 30 minutes prior to the injection of radiotracer (total dose = 1 mg, in DMSO), following a literature procedure.[27] PET scans were followed by a 3.5 minute semi-circular single FOV (96.6 mm) CT scan with a beam energy of 50 KVp applied over 480 projections with an exposure time of 300 ms per projection. The PET data was binned into 3 time frames of 20 minutes each and images were reconstructed with Mediso's Nucline NanoScan reconstruction software (v 3.04.010.0000) using the Tera-Tomo 3D reconstruction algorithm with 4 iterations and 6 subsets, on 0.4mm isotropic 3D voxel grids, with an energy-window of 400-600 KeV. Scatter correction, random correction, CT-based non-uniform attenuation correction, median and spike filters were applied. The CT scans were reconstructed using cone-beam filtered backprojection on a 0.25 mm voxel grid with cosine filter applied. The PET images were registered to the CT images and a quantification factor was applied to allow absolute quantitation of the PET data. The reconstructed image was converted to SUV and viewed and analysed using Vivoquant V 4.0 patch 3 (Invicro, Boston, Massachusetts, USA).

The radiometabolite study was conducted by Dr. S. Paisey and Dr. M. Lelos (Cardiff University). The mouse was placed in an incubator set to 40 °C for 10 mins and then anaesthetised using 5% isoflurane with oxygen as a carrier gas. Mice were injected *via* tail vein with either [^{18}F]**2.80** (*n* = 4) or [^{18}F]**2.81** (*n* = 4). Five minutes post-infusion, blood was collected in a heparin-coated syringe and centrifuged at 5500g for 5 minutes at 4°C. The plasma fraction was precipitated with MeCN (equal volume) and the resulting solution was centrifuged at 9000g for 5 mins at 4°C. The supernatant was removed and analysed by radio-HPLC. Brain tissues were extracted and homogenised in an MeCN/MeOH solution (200 µL, 95:5, v/v). The samples were then centrifuged at 13000g for 5 mins at 4 °C. The supernatant was removed and this was analysed by radio-HPLC. The experimental data are summarised in the table below.

Animal	Tracer	Tissue	RCP (polar radiometabolites)	RCP ([^{18}F]2.81/[^{18}F]2.80)
1	[^{18}F]**2.80**	Blood	100%	n.d.
1	[^{18}F]**2.80**	Brain	100%	n.d.
2	[^{18}F]**2.80**	Blood	100%	n.d.
2	[^{18}F]**2.80**	Brain	100%	n.d.
3	[^{18}F]**2.80**	Blood	100%	n.d.
3	[^{18}F]**2.80**	Brain	100%	n.d.
4	[^{18}F]**2.80**	Blood	100%	n.d.
4	[^{18}F]**2.80**	Brain	100%	n.d.
5	[^{18}F]**2.81**	Blood	n.d.	100%*
5	[^{18}F]**2.81**	Brain	n.d.	100%
6	[^{18}F]**2.81**	Blood	n.d.	100%*
6	[^{18}F]**2.81**	Brain	n.d.	100%
7	[^{18}F]**2.81**	Blood	n.d.	100%
7	[^{18}F]**2.81**	Brain	n.d.	100%
8	[^{18}F]**2.81**	Blood	n.d.	100%
8	[^{18}F]**2.81**	Brain	n.d.	100%

n.d. = not detected, * = HPLC trace weak in intensity. Radio-HPLC analysis was conducted using HPLC conditions B, albeit with a Chromolith Performance RP-18 endcapped 100 mm x 4.6 mm LC column.

4.4. Experimental details for Chapter 3

The experimental details presented in this section have previously been published (J. Ford, S. Ortalli, Z. Chen, J. B. I. Sap, M. Tredwell, V. Gouverneur. Expedient Access to ^{18}F-Fluoroheteroarenes *via* Deaminative Radiofluorination of Aniline-Derived Pyridinium Salts. *Angew. Chem. Int. Ed.* **2024**, *63* (26), e202404945).

4.4.1. Preparation of radiolabelling substrates, intermediates and reference compounds

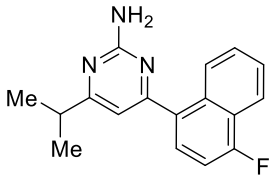
4.4.1.1. Preparation of starting materials and synthetic intermediates

2-Chloro-*N*-(4-methoxyphenyl)-*N*-methylquinazolin-4-amine,[28] 2-chloro-4-(6-methoxy-3,4-dihydro-quinolin-1(2*H*)-yl)pyrido[2,3-*d*]pyrimidine,[29] 4-phenyl-6-(thiophen-2-yl)pyrimidin-2-amine,[30] 5-phenyl-pyrimidin-2-amine,[31] pyrido[3,2-*d*]pyrimidin-2-amine,[32] *N*-ethyl adenine,[33] 9-benzyl-2-chloro-9*H*-purin-6-amine [34] were prepared exactly as described in literature.

2-aminopyrimidine (**3.97**), 2-amino-5-nitropyridine, 5-bromo-2-aminopyrimidine, 6-bromoquinazolin-2-amine, thieno[2,3-*d*]pyrimidin-4-amine, pyrrolo[2,1-*f*][1,2,4]triazin-4-amine, 7-iodopyrrolo[2,1-*f*] [1,2,4]triazin-4-amine, ibrutinib, chloridazon, fenofibrate, ethyl 2-aminopyrimidine-5-carboxylate, 2-amino-5-iodopyrimidine, 2-amino-5-methoxypyrimidine, 5,6-dimethylfuro[2,3-*d*]pyrimidin-4-amine, 7-benzyl-7*H*-pyrrolo[2,3-*d*]pyrimidin-4-amine, 5-aminopyrazine-2-carbonitrile, 3-amino-6-methyl-pyrazine-2-carbonitrile, ethyl 5-aminopyrazine-2-carboxylate, N^9-benzyl adenine, ethyl 2-(6-amino-9*H*-purin-9-yl)acetate, 6-aminopyridazine-3-carbonitrile, 9-[2-(diethylphosphonomethoxy)ethyl] adenine, (2*R*,*3R*,4*R*,5*R*)-2-(6-amino-9*H*-purin-9-yl)-5-(hydroxymethyl) tetrahydrofuran-3,4-diyl diacetate and (2*R*,3*R*,4*R*,5*R*)-2-(acetoxymethyl)-5-(6-amino-9*H*-purin-9-yl)tetrahydrofuran-3,4-diyl diacetate were purchased from commercial suppliers

(Fluorochem, Sigma Aldrich, TCI, BLDpharm, Apollo Scientific, Ambeed, Manchester Organics, Biosynth) and used as received, without further purification.

4-(4-Fluoronaphthalen-1-yl)-6-isopropylpyrimidin-2-amine

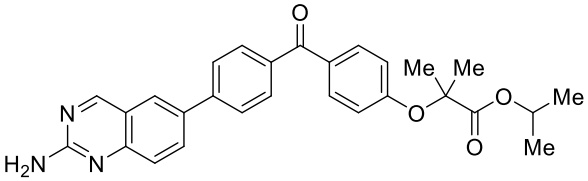


To an oven-dried Schlenk tube equipped with a condenser were added 4-chloro-6-isopropylpyrimidin-2-amine (343 mg, 2 mmol, 1 equiv.) and 4-fluoronaphthalen-1-yl)boronic acid (380 mg, 2 mmol, 1 equiv), as solids. The flask was evacuated under vacuum and refilled with N_2 three times. 1,4-Dioxane (anhydrous, 13 mL, 0.15 M) was next added by syringe, followed by the addition of a saturated aqueous solution of $NaHCO_3$ (3.25 mL). The tube was capped with a septum, and then degassed for 15 min by sparging with N_2. Tetrakis(triphenylphosphine)palladium(0) (130 mg, 0.11 mmol, 5.5 mol%) was then added as a solid and the septum was replaced with a glass stopper. The reaction mixture was stirred at 95 °C for 22 h. The reaction mixture was then cooled to rt and the contents of the flask were passed over a pad of celite, eluting EtOAc. This was concentrated under reduced pressure and the crude product was purified by flash column chromatography. Flash column chromatography conditions: CH_2Cl_2/Et_2O = gradient 20/1 to 5/1. Yellow solid, 513 mg, 91% yield.

^{1}H NMR (400 MHz, $CDCl_3$) δ 8.25 – 8.10 (m, 2H), 7.62 – 7.49 (m, 3H), 7.20 (dd, *J* = 10.1, 7.9 Hz, 1H), 6.76 (s, 1H), 5.27 (s, 2H), 2.89 (hept, *J* = 6.9 Hz, 1H), 1.31 (d, *J* = 6.9 Hz, 6H). **^{19}F NMR** (376 MHz, $CDCl_3$) δ -120.7 – -120.8 (m, 1F). **^{13}C NMR** (101 MHz, $CDCl_3$) δ 177.7, 167.2, 163.1, 159.5 (d, *J* = 254.3 Hz), 133.3 (d, *J* = 4.4 Hz), 132.3 (d, *J* = 5.1 Hz), 127.7, 127.2 (d, *J* = 8.7 Hz), 126.5 (d, *J* = 2.2 Hz), 125.6 (d, *J* = 2.6 Hz), 124.1 (d, *J* = 16.0 Hz), 121.0 (d, *J* = 5.8 Hz), 109.4, 109.1 (d, *J* = 20.3 Hz), 36.2, 21.9. **HRMS** (ESI-TOF) calculated for $C_{17}H_{17}FN_3$ ($[M+H]^+$): 282.1401,

found: 282.1396. **IR** (thin layer film) 3490, 3311. 3183, 2967, 1630, 1573, 1543, 1510, 1453, 1364, 1264, 1229, 1157, 1048, 1014, 962, 909, 830, 805, 765, 734. **MP** 113 °C.

Isopropyl 2-(4-(4-(2-aminoquinazolin-6-yl)benzoyl)phenoxy)-2-methylpropanoate

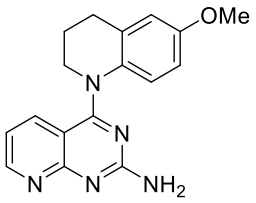


The title compound was prepared according to a procedure adapted from the literature.[11] To an oven-dried Schlenk flask equipped with a condenser were added fenofibrate (1.30 g, 3.6 mmol, 1.2 equiv.), bis(pinacolato)diboron (912 mg, 3.6 mmol, 1.2 equiv.), KOAc (588 mg, 6 mmol, 3 equiv.), Pd_2dba_3 (27 mg, 0.03 mmol, 1 mol%) and XPhos (98 mg, 0.21 mmol, 7 mol%) as solids. The flask was evacuated and refilled with N_2 3 times, before dry, degassed 1,4-dioxane (12 mL, 0.25 M) was added *via* syringe. The reaction mixture was then stirred at 110 °C for 4 h, at which point all fenofibrate was consumed. The reaction mixture was allowed to cool to rt, and 6-bromoquinazolin-2-amine (672 mg, 3 mmol, 1 equiv.) was then added as a solid. 3 mL of a K_3PO_4 solution (aq., 5 M) was then added *via* syringe. The reaction mixture was then heated at 110 °C for 20 h. The reaction mixture was allowed to cool to rt, and the contents of the flask were filtered over celite, eluting EtOAc. The collected filtrate was concentrated under reduced pressure. The crude product was purified by flash column chromatography. Flash column chromatography conditions: pentane/EtOAc = gradient 90/10 to 30/70. Yellow solid, 951 mg, 68% yield.

^{1}H NMR (500 MHz, $CDCl_3$) δ 9.14 (s, 1H), 8.04 (dd, *J* = 8.7, 2.1 Hz, 1H), 7.98 (d, *J* = 2.1 Hz, 1H), 7.87 (d, *J* = 8.2 Hz, 2H), 7.84 – 7.77 (m, 2H), 7.75 (d, *J* = 8.2 Hz, 2H), 7.70 (d, *J* = 8.7 Hz, 1H), 6.93 – 6.86 (m, 2H), 5.61 (s, 2H), 5.09 (hept, *J* = 6.3 Hz, 1H), 1.67 (s, 6H), 1.21 (d, *J* = 6.3 Hz, 6H). **^{13}C NMR** (126 MHz, $CDCl_3$) δ 195.1, 173.3, 163.5, 160.1, 159.8, 150.9, 143.4, 137.2, 135.4, 134.2, 132.1, 130.8, 130.7, 126.9, 125.9, 125.7, 120.5, 117.4, 79.5, 69.5, 25.5, 21.7. **HRMS** (ESI-TOF) calculated for $C_{28}H_{28}N_3O_4$ ($[M+H]^+$): 470.2074, found: 470.2065. **IR** (thin layer film)

3417, 3326, 3163, 2988, 2941, 1730, 1651, 1627, 1601, 1505, 1472, 1418, 1385, 1308, 1289, 1250, 1179, 1149, 1102, 1014, 974, 930, 913, 847, 828, 795, 770, 734, 689, 665, 634. **MP** 195–197 °C.

4-(6-Methoxy-3,4-dihydroquinolin-1(2*H*)-yl)pyrido[2,3-*d*]pyrimidin-2-amine

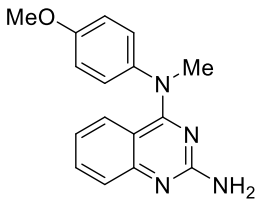


The title compound was prepared according to a procedure adapted from the literature.[35] To a flame-dried Schlenk flask under N_2 and equipped with a condenser were added 2-chloro-4-(6-methoxy-3,4-dihydroquinolin-1(2*H*)-yl)pyrido[2,3-*d*]pyrimidine (654 mg, 2 mmol, 1 equiv.), Pd_2dba_3 (182 mg, 0.2 mmol, 10 mol%) and CyJohnPhos (175 mg, 0.5 mmol, 25 mol%) as solids. Anhydrous THF (15 mL) was added *via* syringe. LiHMDS (1M in hexane, 5 mL, 5 mmol, 2 equiv.) was then added *via* syringe. The reaction mixture was then left to stir at 65 °C overnight for 16 h, at which point all starting material was consumed. The flask was cooled to rt and 1 M HCl (30 mL) was next added. This mixture was stirred at rt for 30 min. The contents of the flask were transferred to a separatory funnel and were partitioned between EtOAc (70 mL) and 1 M NaOH (aq., 70 mL). The organic layer was retained and the aqueous layer was washed twice more with EtOAc. The combined organics were dried over anhydrous Na_2SO_4, filtered and then concentrated under reduced pressure. The crude material was then purified by flash column chromatography. Flash column chromatography conditions: EtOAc/MeOH = 95/5. Orange solid, 455 mg, 74% yield.

^{1}H NMR (400 MHz, $CDCl_3$) δ 8.69 (dd, *J* = 4.4, 2.0 Hz, 1H), 7.52 (dd, *J* = 8.3, 2.0 Hz, 1H), 6.77 (d, *J* = 2.9 Hz, 1H), 6.74 (dd, *J* = 8.3, 4.4 Hz, 1H), 6.69 (d, *J* = 8.8 Hz, 1H), 6.54 (dd, *J* = 8.8, 2.9 Hz, 1H), 5.29 (s, 2H), 3.95 (t, *J* = 6.7 Hz, 2H), 3.79 (s, 3H), 2.83 (t, *J* = 6.7 Hz, 2H), 2.06 (pent, *J* = 6.7 Hz, 2H). **^{13}C NMR** (101 MHz, $CDCl_3$) δ 163.7, 162.4, 162.2, 156.6, 155.6, 135.5, 135.4, 133.3, 123.0, 116.3, 113.7, 112.3, 107.6, 55.6, 47.4, 27.3, 24.3. **HRMS** (ESI-TOF) calculated for

$C_{17}H_{18}N_5O$ ([M+H]$^+$): 308.1506, found: 308.1502. **IR** (thin layer film) 3331, 2950, 1594, 1568, 1542, 1501, 1463, 1392, 1353, 1265, 1231, 1202, 1162, 1110, 1058, 1038, 910, 783, 732, 647. **MP** 248 °C.

***N*^{4}-(4-Methoxyphenyl)-*N*^{4}-methylquinazoline-2,4-diamine**



The title compound was prepared according to a procedure adapted from the literature.[35] To a flame-dried Schlenk flask under N_2 and equipped with a condenser were added 2-chloro-*N*-(4-methoxyphenyl)-*N*-methylquinazolin-4-amine (750 mg, 2.5 mmol, 1 equiv.), Pd_2dba_3 (229 mg, 0.25 mmol, 10 mol%) and CyJohnPhos (210 mg, 0.60 mmol, 25 mol%) as solids. Anhydrous THF (11 mL) was added *via* syringe. LiHMDS (1M in hexane, 10 mL, 10 mmol, 4 equiv.) was then added *via* syringe. The reaction mixture was then left to stir at 65 °C overnight for 19 h, at which point all starting material was consumed. The flask was cooled to rt and 1 M HCl (50 mL) was next added. This mixture was stirred at rt for 30 min. The contents of the flask were transferred to a separatory funnel and were partitioned between EtOAc (100 mL) and 1 M NaOH (aq., 100 mL). The organic layer was retained and the aqueous layer was washed twice more with EtOAc (100 mL). The combined organics were dried over anhydrous Na_2SO_4, filtered and then concentrated under reduced pressure. The crude material was then purified by flash column chromatography. Flash column chromatography conditions: EtOAc/MeOH = 95/5. Yellow solid, 524 mg, 75% yield.

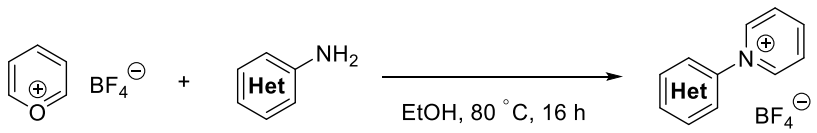
^{1}H NMR (400 MHz, $CDCl_3$) δ 7.44 – 7.34 (m, 2H), 7.14 – 7.07 (m, 2H), 6.92 – 6.86 (m, 3H), 6.71 (ddd, *J* = 8.3, 6.3, 2.0 Hz, 1H), 4.93 (br s, 2H), 3.82 (s, 3H), 3.50 (s, 3H).**^{13}C NMR** (101 MHz, $CDCl_3$) δ 163.3, 159.5, 158.0, 153.8, 141.6, 132.1, 127.5, 126.8, 125.6, 120.9, 115.2, 112.8, 55.6, 42.9. **HRMS** (ESI-TOF) calculated for $C_{16}H_{17}N_4O$ ([M+H]$^+$): 281.1397, found: 281.1393. **IR** (thin layer film) 3476, 3301, 3163, 2931, 2845, 1637, 1609, 1564, 1546, 1501, 1483, 1446,

1415, 1385, 1344, 1292, 1246, 1186, 1154, 1102, 1033, 911, 838, 812, 761, 730, 686, 656, 614. **MP** 195 °C.

4.4.1.2. Preparation of pyridinium tetrafluoroborate substrates

Pyrylium tetrafluoroborate (**3.22**), 1-(4-(ethoxycarbonyl)oxazol-2-yl)pyridin-1-ium tetrafluoroborate (**3.26**), 2'-chloro-[1,4'-bipyridin]-1-ium tetrafluoroborate (**3.94**), 1-(5-methyl-1,3,4-thiadiazol-2-yl)pyridin-1-ium tetrafluoroborate (**3.95**), 1-(benzo[*d*]thiazol-2-yl)pyridin-1-ium tetrafluoroborate (**3.96**) were prepared exactly as described in literature procedures.[33,36]

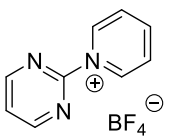
General Procedure 9:



3.22

The following is adapted from a literature procedure.[36] To a flame-dried Schlenk tube under N_2 were added the relevant heteroaryl amine (1 mmol, 1 equiv.) and pyrylium tetrafluoroborate (168 mg, 1 mmol, 1 equiv.) as solids. Anhydrous EtOH (5 mL) was then added *via* syringe. The flask was wrapped in aluminium foil and the mixture was stirred at 80 °C overnight for 16 h in an oil bath. The Schlenk tube was then removed from the oil bath and allowed to cool in an ice bath. If a solid did not precipitate, Et_2O was added. The solid was collected on a frit by filtration, washing with Et_2O to transfer any remaining solid, and then washed once with EtOAc (if the solubility of the product was not significant, otherwise Et_2O was used) and twice with Et_2O. The solid was then allowed to dry under reduced pressure.

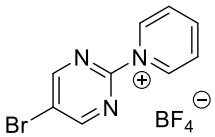
1-(Pyrimidin-2-yl)pyridin-1-ium tetrafluoroborate (3.25)



The title compound was prepared according to General Procedure 9, albeit on larger scale, using 2-aminopyrimidine (285 mg, 3 mmol). Light brown solid, 366 mg, 50% yield.

^{1}H NMR (400 MHz, DMSO-d_6) δ 10.07 – 9.98 (m, 2H), 9.24 (d, *J* = 4.8 Hz, 2H), 8.93 (tt, *J* = 7.6, 1.4 Hz, 1H), 8.41 – 8.32 (m, 2H), 7.99 (t, *J* = 4.9 Hz, 1H). **^{19}F NMR** (376 MHz, DMSO-d_6) δ -148.2 (s), -148.3 (s) (4F in total). **^{13}C NMR** (101 MHz, DMSO-d_6) δ 160.4, 155.1, 150.2, 141.2, 128.0, 124.0. **HRMS** (ESI-TOF) calculated for $C_9H_8N_3^+$ ([M-BF_4^-]$^+$): 158.0713, found: 158.0714. **IR** (neat) 1630, 1599, 1567, 1408, 1288, 1201, 1054, 1024, 841, 770, 673. **MP** 230 °C.

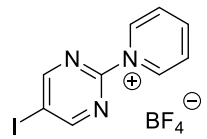
1-(5-Bromopyrimidin-2-yl)pyridin-1-ium tetrafluoroborate (3.27)



The title compound was prepared according to General Procedure 9, using 5-bromo-2-aminopyrimidine (174 mg, 1 mmol). Brown solid, 131 mg, 40% yield.

^{1}H NMR (400 MHz, CD_3CN) δ 9.93 – 9.85 (m, 2H), 9.19 (s, 2H), 8.84 (tt, *J* = 7.7, 1.4 Hz, 1H), 8.35 – 8.24 (m, 2H). **^{19}F NMR** (376 MHz, CD_3CN) δ -151.5 (s), -151.6 (s) (4F in total). **^{13}C NMR** (101 MHz, CD_3CN) δ 162.0, 154.6, 151.7, 141.9, 129.5, 123.7. **HRMS** (ESI-TOF) calculated for $C_9H_7{}^{79}BrN_3^+$ ([M-BF_4^-]$^+$): 235.9818, found: 235.9818. **IR** (neat) 1667, 1598, 1578, 1536, 1481, 1462, 1355, 1290, 1055, 860, 788, 760, 720, 676. **MP** no melting observed up to 320 °C.

1-(5-Iodopyrimidin-2-yl)pyridin-1-ium tetrafluoroborate (3.28)

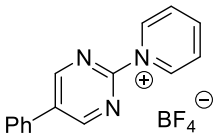


The title compound was prepared according to General Procedure 9, using 2-amino-5-iodopyrimidine (221 mg, 1 mmol). Light brown solid, 204 mg, 42% yield.

^{1}H NMR (600 MHz, CD_3CN) δ 9.92 – 9.86 (m, 2H), 9.30 (s, 2H), 8.83 (tt, *J* = 7.7, 1.4 Hz, 1H), 8.27 (t, *J* = 7.5 Hz, 2H). **^{19}F NMR** (565 MHz, CD_3CN) δ -151.6 (s), -151.7 (s) (4F in total). **^{13}C NMR** (151 MHz, CD_3CN) δ 166.8, 155.2, 151.7, 141.7, 129.5, 96.4. **HRMS** (ESI-TOF) calculated

$C_9H_7IN_3^+$ ([M-BF_4^-]$^+$): 283.9679, found: 283.9675. **IR** (thin layer film) 1749, 1632, 1560, 1476, 1410, 1337, 1286, 1207, 1060, 768, 674, 650. **MP** no melting observed up to 320 °C.

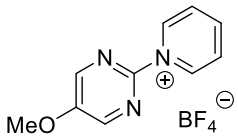
1-(5-Phenylpyrimidin-2-yl)pyridin-1-ium tetrafluoroborate (3.29)



The title compound was prepared according to General Procedure 9, using 5-phenylpyrimidin-2-amine (171 mg, 1 mmol). Beige solid, 160 mg, 50% yield.

^{1}H NMR (400 MHz, DMSO-d_6) δ 10.07 (dd, *J* = 7.0, 1.3 Hz, 2H), 9.60 (s, 2H), 8.94 (tt, *J* = 7.7, 1.3 Hz, 1H), 8.39 (t, *J* = 7.3 Hz, 2H), 8.02 (dd, *J* = 8.1, 1.2 Hz, 2H), 7.66 – 7.57 (m, 3H). **^{19}F NMR** (376 MHz, DMSO-d_6) δ -148.2 (s), -148.3 (s) (4F in total). **^{13}C NMR** (101 MHz, DMSO-d_6) δ 157.6, 154.2, 150.1, 141.1, 135.0, 131.9, 130.0, 129.5, 128.1, 127.4. **HRMS** (ESI-TOF) calculated for $C_{15}H_{12}N_3^+$ ([M-BF_4^-]$^+$): 234.1026, found: 234.1026. **IR** (neat) 1649, 1626, 1592, 1560, 1476, 1419, 1310, 1277, 1202, 1055, 775, 700, 671. **MP** 191–196 °C.

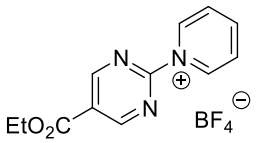
1-(5-Methoxypyrimidin-2-yl)pyridin-1-ium tetrafluoroborate (3.30)



Prepared by S. Ortalli. The title compound was prepared according to General Procedure 9, using 5-methoxypyrimidin-2-amine (125 mg, 1 mmol). Brown solid, 131 mg, 48% yield.

^{1}H NMR (500 MHz, CD_3CN) *δ* 9.88 – 9.84 (m, 2H), 8.75 (tt, *J* = 7.8, 1.4 Hz, 1H), 8.71 (s, 2H), 8.26 – 8.21 (m, 2H), 4.09 (s, 3H). **^{19}F NMR** (471 MHz, CD_3CN) *δ* -151.7 (s), -151.8 (s) (4F in total). **^{13}C NMR** (126 MHz, CD_3CN) *δ* 156.6, 150.2, 148.8, 146.7, 141.5, 129.3, 58.2. **HRMS** (ESI-TOF) calculated for $C_{10}H_{10}N_3O^+$ ([M-BF_4^-]$^+$): 188.0818, found: 188.0816. **IR** (neat) 3128, 1745, 1622, 1576, 1507, 1477, 1375, 1338, 1221, 1050, 906, 783, 679, 643. **MP** 141–143 °C.

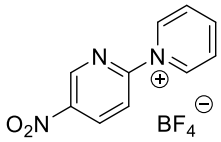
1-(5-(Ethoxycarbonyl)pyrimidin-2-yl)pyridin-1-ium tetrafluoroborate (3.31)



The title compound was prepared according to General Procedure 9, using ethyl 2-aminopyrimidine-5-carboxylate (167 mg, 1 mmol), with a modified purification procedure. Et_2O (15 mL) was added to the reaction mixture and this was sonicated for 15 min. The resulting solution was then cooled to 4 °C, after which time a precipitate had formed. This was transferred to a frit and washed with Et_2O and the collected solid was left to dry. Brown solid, 108 mg, 34% yield.

^{1}H NMR (400 MHz, CD_3CN) δ 10.02 – 9.93 (m, 2H), 9.53 (s, 2H), 8.87 (tt, *J* = 7.7, 1.4 Hz, 1H), 8.36 – 8.25 (m, 2H), 4.49 (q, *J* = 7.1 Hz, 2H), 1.43 (t, *J* = 7.1 Hz, 3H). **^{19}F NMR** (376 MHz, CD_3CN) δ -151.6 (s), -151.7 (s) (4F in total). **^{13}C NMR** (101 MHz, CD_3CN) δ 163.1, 162.2, 157.5, 152.2, 142.2, 129.6, 128.0, 63.6, 14.4. **HRMS** (ESI-TOF) calculated for $C_{12}H_{12}N_3O_2^+$ ($[M\text{-}BF_4^-]^+$): 230.0924, found: 230.0921. **IR** (thin layer film) 3623, 3136, 3084, 2988, 1726, 1652, 1630, 1597, 1587, 1478, 1423, 1393, 1371, 1284, 1202, 1139, 1061, 860, 776, 672. **MP** 128 °C.

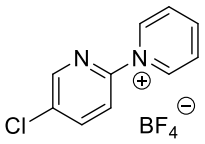
5'-Nitro-[1,2'-bipyridin]-1-ium tetrafluoroborate (3.32)



The title compound was prepared according to General Procedure 9, using 2-amino-5-nitropyridine (139 mg, 1 mmol). Dark brown solid, 120 mg, 42% yield.

^{1}H NMR (400 MHz, DMSO-d_6) δ 9.70 (d, *J* = 6.2 Hz, 2H), 9.61 – 9.56 (m, 1H), 9.15 (dd, *J* = 8.8, 2.0 Hz, 1H), 8.93 (t, *J* = 7.7 Hz, 1H), 8.52 (d, *J* = 8.9 Hz, 1H), 8.40 (t, *J* = 7.2 Hz, 2H). **^{19}F NMR** (376 MHz, DMSO-d_6) δ -148.2 (s), -148.3 (s) (4F in total). **^{13}C NMR** (101 MHz, DMSO-d_6) δ 154.5, 149.4, 145.8, 145.1, 143.4, 136.6, 128.1, 119.4. **HRMS** (ESI-TOF) calculated for $C_{10}H_8N_3O_2^+$ ($[M\text{-}BF_4^-]^+$): 202.0611, found: 202.0612. **IR** (neat) 1667, 1616, 1579, 1536, 1482, 1462, 1355, 1291, 1056, 860, 790, 759, 720, 677. **MP** 135–140 °C.

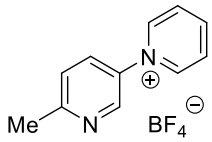
5'-Chloro-[1,2'-bipyridin]-1-ium tetrafluoroborate (3.33)



The title compound was prepared according to General Procedure 9, using 2-amino-5-chloropyridine (129 mg, 1 mmol). Light brown solid, 88 mg, 32% yield.

^{1}H NMR (500 MHz, CD_3CN) δ 9.31 – 9.25 (m, 2H), 8.79 – 8.72 (m, 2H), 8.30 – 8.21 (m, 3H), 7.95 (dd, *J* = 8.7, 0.7 Hz, 1H). **^{19}F NMR** (470 MHz, CD_3CN) δ -151.5 (s), -151.5 (s) (4F in total). **^{13}C NMR** (126 MHz, CD_3CN) δ 151.3, 149.7, 149.6, 143.6, 141.6, 136.2, 129.5, 120.1. **HRMS** (ESI-TOF) calculated for $C_{10}H_8ClN_2^+$ ([M-BF_4^-]$^+$): 191.0371, found: 191.0363. **IR** (neat) 1629, 1595, 1478, 1464, 1383, 1278, 1209, 1118, 1050, 1035, 1021, 839, 788, 745, 679, 628. **MP** 131–133 °C.

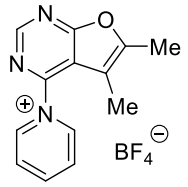
6'-Methyl-[1,3'-bipyridin]-1-ium tetrafluoroborate (3.34)



The title compound was prepared according to General Procedure 9, using 5-amino-2-methylpyridine (108 mg, 1 mmol). Light brown solid, 210 mg, 81% yield.

^{1}H NMR (500 MHz, CD_3CN) δ 8.94 – 8.89 (m, 2H), 8.76 (d, *J* = 2.8 Hz, 1H), 8.72 (tt, *J* = 7.9, 1.3 Hz, 1H), 8.26 – 8.19 (m, 2H), 7.99 (dd, *J* = 8.4, 2.8 Hz, 1H), 7.56 (d, *J* = 8.4 Hz, 1H), 2.67 (s, 3H). **^{19}F NMR** (470 MHz, CD_3CN) δ -151.5 (s), -151.6 (s) (4F in total). **^{13}C NMR** (126 MHz, CD_3CN) δ 163.5, 148.3, 145.8, 145.4, 138.5, 133.5, 129.6, 125.1, 24.5. **HRMS** (ESI-TOF) calculated for $C_{11}H_{11}N_2^+$ ([M-BF_4^-]$^+$): 171.0917, found: 171.0921. **IR** (neat) 1634, 1491, 1398, 1307, 1271, 1171, 1060, 1047, 920, 843, 781, 728, 690, 649, 629, 613. **MP** 186 °C.

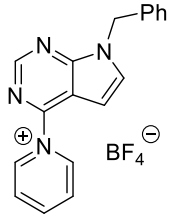
1-(5,6-Dimethylfuro[2,3-*d*]pyrimidin-4-yl)pyridin-1-ium tetrafluoroborate (3.35)



The title compound was prepared according to General Procedure 9, using 5,6-dimethylfuro[2,3-*d*]pyrimidin-4-amine (163 mg, 1 mmol), with a modified purification procedure. Et_2O (10 mL) was added to the crude reaction mixture, and the precipitated residue was transferred to a frit, where the material was washed with further Et_2O. The residue was then dissolved in MeOH and transferred to a vial, before the volatiles were removed under reduced pressure. A mixture of Et_2O and hexane (1:1, v/v, 5 mL) was then added to the vial, and subsequently removed under reduced pressure. This was repeated until the residue became solid. Red-brown solid, 217 mg, 69% yield.

^{1}H NMR (400 MHz, DMSO-d_6) δ 9.55 – 9.47 (m, 2H), 9.13 (s, 1H), 9.00 (tt, *J* = 7.9, 1.4 Hz, 1H), 8.49 – 8.44 (m, 2H), 2.58 (s, 3H), 1.92 (s, 3H). **^{19}F NMR** (376 MHz, DMSO-d_6) δ -148.2 (s), -148.3 (s) (4F in total). **^{13}C NMR** (101 MHz, DMSO-d_6) δ 167.8, 155.6, 151.7, 151.0, 149.7, 144.9, 128.2, 114.5, 107.4, 11.6, 8.9. **HRMS** (ESI-TOF) calculated for $C_{13}H_{12}N_3O^+$ ($[M\text{-}BF_4^-]^+$): 226.0975, found: 226.0975. **IR** (neat) 1667, 1598, 1578, 1536, 1481, 1462, 1355, 1290, 1055, 860, 788, 759, 720, 677. **MP** 104–106 °C.

1-(7-Benzyl-7*H*-pyrrolo[2,3-*d*]pyrimidin-4-yl)pyridin-1-ium tetrafluoroborate (3.36)

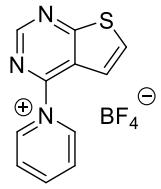


The title compound was prepared according to General Procedure 9, 7-benzyl-7*H*-pyrrolo[2,3-*d*]pyrimidin-4-amine (224 mg, 1 mmol), with a modified purification procedure. Once the reaction mixture had cooled, Et_2O (10 mL) was added to the crude reaction mixture, and this mixture was stirred, before the Et_2O was removed by pipette, leaving a sticky residue.

This was repeated three times, until the product precipitated as a solid. This material was transferred to a frit, where it was washed with EtOAc (5 mL) and Et_2O (10 mL). The solid was then allowed to dry under reduced pressure. Yellow solid, 181 mg, 48% yield.

^{1}H NMR (400 MHz, DMSO-d_6) δ 9.75 – 9.65 (m, 2H), 9.10 (s, 1H), 8.94 (tt, *J* = 7.9, 1.4 Hz, 1H), 8.47 – 8.38 (m, 2H), 8.22 (d, *J* = 3.7 Hz, 1H), 7.41 – 7.21 (m, 5H), 7.09 (d, *J* = 3.7 Hz, 1H), 5.65 (s, 2H). **^{19}F NMR** (376 MHz, DMSO-d_6) δ -148.2 (s), -148.3 (s) (4F in total). **^{13}C NMR** (101 MHz, DMSO-d_6) δ 153.5, 150.3, 149.9, 149.3, 143.7, 136.9, 134.5, 128.8, 128.4, 127.9, 127.6, 110.0, 98.5, 48.1. **HRMS** (ESI-TOF) calculated for $C_{18}H_{15}N_4^+$ ([M-BF_4^-]$^+$): 287.1291, found: 287.1291. **IR** (thin layer film) 1630, 1608, 1556, 1516, 1481, 1461, 1439, 1353, 1287, 1200, 1156, 1049, 923, 862, 775, 747, 725, 702, 681. **MP** 162 °C.

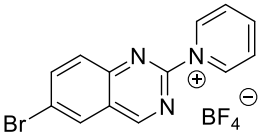
1-(Thieno[2,3-*d*]pyrimidin-4-yl)pyridin-1-ium tetrafluoroborate (3.37)



Prepared by J. Sap. The title compound was prepared according to General Procedure 9, using thieno[2,3-*d*]pyrimidin-4-amine (151 mg, 1 mmol). Grey-white solid, 162 mg, 54% yield.

^{1}H NMR (400 MHz, DMSO-d_6) δ 9.62 (dd, *J* = 6.8, 1.3 Hz, 2H), 9.40 (s, 1H), 9.00 (tt, *J* = 7.7, 1.4 Hz, 1H), 8.51 – 8.43 (m, 2H), 8.39 (d, *J* = 6.2 Hz, 1H), 7.78 (d, *J* = 6.2 Hz, 1H). **^{19}F NMR** (376 MHz, DMSO-d_6) δ -148.2 (s), -148.3 (s) (4F in total). **^{13}C NMR** (101 MHz, DMSO-d_6) δ 172.1, 153.0, 152.6, 149.7, 144.4, 132.9, 128.6, 123.3, 118.8. **HRMS** (ESI-TOF) calculated for $C_{11}H_8N_3S^+$ ([M-BF_4^-]$^+$): 214.0433, found: 214.0434. **IR** (neat) 1626, 1590, 1559, 1522, 1471, 1428, 1354, 1294, 1200, 1129, 1054, 957, 878, 852, 804, 779, 740, 681. **MP** 223 °C.

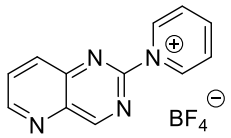
1-(6-Bromoquinazolin-2-yl)pyridin-1-ium tetrafluoroborate (3.38)



Prepared by J. Sap. The title compound was prepared according to General Procedure 9, using 6-bromoquinazolin-2-amine (224 mg, 1 mmol). Peach coloured solid, 190 mg, 51% yield.

^{1}H NMR (400 MHz, CD_3CN) δ 10.18 – 10.09 (m, 2H), 9.76 (d, *J* = 0.8 Hz, 1H), 8.85 (tt, *J* = 7.7, 1.4 Hz, 1H), 8.56 (dd, *J* = 2.2, 0.5 Hz, 1H), 8.36 – 8.29 (m, 3H), 8.16 (dt, *J* = 9.1, 0.7 Hz, 1H). **^{19}F NMR** (376 MHz, CD_3CN) δ -151.7 (s), -151.7 (s) (4F in total). **^{13}C NMR** (101 MHz, CD_3CN) δ 164.8, 151.4, 150.1, 142.1, 141.6, 131.8, 131.1, 129.5, 127.4, 124.8, *note: product peaks overlapping*. **HRMS** (ESI-TOF) calculated for $C_{13}H_9{}^{79}BrN_3{}^+$ ([M-BF_4^-]$^+$): 285.9974, found: 285.9975. **IR** (neat) 1667, 1615, 1597, 1579, 1536, 1482, 1462, 1355, 1290, 1054, 860, 759, 675. **MP** 274 °C.

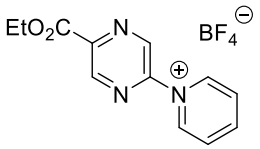
1-(Pyrido[3,2-*d*]pyrimidin-2-yl)pyridin-1-ium tetrafluoroborate (3.39)



The title compound was prepared according to General Procedure 9, using pyrido[3,2-*d*]pyrimidin-2-amine (146 mg, 1 mmol). Brown solid, 178 mg, 60% yield.

^{1}H NMR (400 MHz, CD_3CN) δ 10.19 – 10.12 (m, 2H), 9.92 (d, *J* = 0.6 Hz, 1H), 9.32 (dd, *J* = 4.2, 1.5 Hz, 1H), 8.87 (tq, *J* = 7.6, 1.1 Hz, 1H), 8.60 (d, *J* = 8.7 Hz, 1H), 8.41 – 8.29 (m, 2H), 8.16 (dd, *J* = 8.7, 4.1 Hz, 1H). **^{19}F NMR** (376 MHz, CD_3CN) δ -151.7 (s), -151.8 (s) (4F in total).**^{13}C NMR** (101 MHz, CD_3CN) δ 166.4, 156.6, 151.4, 148.5, 142.3, 141.6, 137.2, 132.4, 129.5, *note: a broad peak at 152.2 ppm was found by HMBC experiments.* **HRMS** (ESI-TOF) calculated for $C_{12}H_9N_4{}^+$ ([M-BF_4^-]$^+$): 209.0822, found: 209.0821. **IR** (neat) 1667, 1598, 1578, 1536, 1482, 1462, 1355, 1290, 1055, 860, 832, 759, 720, 675. **MP** 218 °C.

1-(5-(Ethoxycarbonyl)pyrazin-2-yl)pyridin-1-ium tetrafluoroborate (3.40)

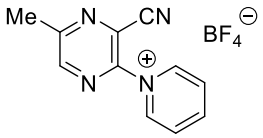


The title compound was prepared according to General Procedure 9 using ethyl 5-aminopyrazine-2-carboxylate (167 mg), with a modified purification procedure. The crude

mixture was briefly sonicated and then cooled to 0 °C, after which a brown precipitate formed. The liquid was decanted and the remaining brown solid was sonicated in Et_2O for 30 mins. This was then transferred to a frit and washed with further Et_2O, and subsequently left to dry. Brown solid, 132 mg, 42% yield.

^{1}H NMR 400 MHz, CD_3CN) δ 9.40 – 9.31 (m, 4H), 8.86 (tt, *J* = 7.8, 1.3 Hz, 1H), 8.38 – 8.29 (m, 2H), 4.51 (q, *J* = 7.1 Hz, 2H), 1.44 (t, *J* = 7.1 Hz, 3H). **^{19}F NMR** (376 MHz, CD_3CN) δ -151.1 (s), -151.2 (s) (4F in total). **^{13}C NMR** (101 MHz, CD_3CN) δ 163.5, 150.9, 150.6, 147.1, 145.9, 143.9, 140.1, 129.9, 63.7, 14.4. **HRMS** (ESI-TOF) calculated for $C_{12}H_{12}N_3O_2^+$ ([M-BF_4^-]$^+$): 230.0924, found: 230.0921. **IR** (thin layer film) 1747, 1723, 1649, 1632, 1474, 1373, 1277, 1213, 1144, 1057, 1014, 924, 861, 782, 728, 678, 615. **MP** 150–155 °C.

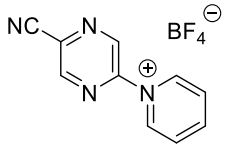
1-(3-Cyano-5-methylpyrazin-2-yl)pyridin-1-ium tetrafluoroborate (3.41)



The title compound was prepared according to General Procedure 9, with a modified purification procedure, using 3-amino-6-methyl-pyrazine-2-carbonitrile (134 mg, 1 mmol). To the crude reaction mixture, Et_2O (10 mL) was added, and a sticky solid formed. The liquid was decanted and the residue was dissolved in MeCN (2 mL). Et_2O (25 mL) was added, and the mixture was sonicated until a solid formed. The solid was collected on a frit and washed with EtOAc (3 x 5 mL) and Et_2O (2 x 5 mL). Brown solid, 128 mg, 45% yield.

^{1}H NMR (600 MHz, CD_3CN) δ 9.20 – 9.13 (m, 2H), 8.94 – 8.86 (m, 2H), 8.41 – 8.34 (m, 2H), 2.80 (s, 3H). **^{19}F NMR** (565 MHz, CD_3CN) δ -151.7 (s), -151.7 (s) (4F in total). **^{13}C NMR** (151 MHz, CD_3CN) δ 160.6, 151.6, 149.5, 148.6, 145.3, 130.1, 125.6, 113.8, 21.8. **HRMS** (ESI-TOF) calculated for $C_{11}H_9N_4^+$ ([M-BF_4^-]$^+$): 197.0822, found: 197.0820. **IR** (thin layer film) 3629, 3132, 3082, 1629, 1478, 1436, 1358, 1293, 1165, 1062, 794, 774, 683. **MP** 150–152 °C.

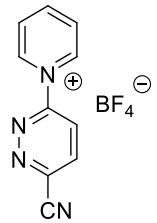
1-(5-Cyanopyrazin-2-yl)pyridin-1-ium tetrafluoroborate (3.42)



The title compound was prepared according to General Procedure 9, using 5-aminopyrazine-2-carbonitrile (120 mg, 1 mmol). Brown solid, 109 mg, 40% yield.

^{1}H NMR (400 MHz, DMSO-d_6) δ 9.74 – 9.66 (m, 3H), 9.53 (d, J = 1.4 Hz, 1H), 8.97 (tt, J = 7.8, 1.3 Hz, 1H), 8.50 – 8.39 (m, 2H). **^{19}F NMR** (376 MHz, DMSO-d_6) δ -148.2 (s), -148.3 (s) (4F in total).**^{13}C NMR** (101 MHz, DMSO-d_6) δ 150.1, 149.4, 147.5, 143.4, 141.2, 131.2, 128.3, 115.2. **HRMS** (ESI-TOF) calculated for $C_{10}H_7N_4^+$ ([M-BF_4^-]$^+$): 183.0665, found: 183.0666. **IR** (neat) 1727, 1646, 1594, 1571, 1522, 1470, 1419, 1380, 1336, 1283, 1173, 1057, 914, 769, 675. **MP** 197 °C.

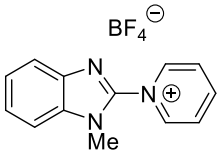
1-(6-Cyanopyridazin-3-yl)pyridin-1-ium tetrafluoroborate (3.43)



The title compound was prepared according to General Procedure 9, using 6-aminopyridazine-3-carbonitrile (120 mg, 1 mmol). Pale brown solid, 135 mg, 50% yield.

^{1}H NMR (500 MHz, CD_3CN) δ 9.38 – 9.35 (m, 2H), 8.90 (tt, *J* = 7.9, 1.4 Hz, 1H), 8.55 (d, *J* = 9.0 Hz, 1H), 8.47 (d, *J* = 9.2 Hz, 1H), 8.39 – 8.34 (m, 2H). **^{19}F NMR** (471 MHz, CD_3CN) δ -151.3 (s), -151.4 (s) (4F in total). **^{13}C NMR** (126 MHz, CD_3CN) δ 157.7, 151.3, 144.3, 142.8, 136.5, 129.8, 125.2, 115.5. **HRMS** (ESI-TOF) calculated for $C_{10}H_7N_4^+$ ([M-BF_4^-]$^+$): 183.0665, found: 183.0664. **IR** (neat) 3138, 3087, 1630, 1565, 1481, 1419, 1348, 1274, 1211, 1061, 1030, 956, 867, 820, 787, 765, 703, 675, 622. **MP** 100–102 °C.

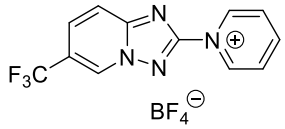
1-(1-methyl-1*H*-benzo[*d*]imidazol-2-yl)pyridin-1-ium tetrafluoroborate (3.44)



The title compound was prepared according to General Procedure 9, using 1-methyl-1*H*-benzo[*d*]imidazol-2-amine (147 mg, 1 mmol). Beige solid, 122 mg, 41% yield.

^{1}H NMR (500 MHz, CD_3CN) δ 9.16 – 9.10 (m, 2H), 8.88 (tt, *J* = 7.9, 1.4 Hz, 1H), 8.38 – 8.31 (m, 2H), 7.85 (dt, *J* = 8.2, 0.9 Hz, 1H), 7.70 (dt, *J* = 8.3, 0.9 Hz, 1H), 7.57 (ddd, *J* = 8.4, 7.2, 1.1 Hz, 1H), 7.48 (ddd, *J* = 8.3, 7.2, 1.1 Hz, 1H), 3.82 (s, 3H). **^{19}F NMR** (470 MHz, CD_3CN) δ -151.6 (s), -151.7 (s) (4F in total). **^{13}C NMR** (126 MHz, CD_3CN) δ 150.9, 146.3, 146.1, 141.1, 137.1, 130.0, 126.5, 125.3, 121.5, 112.6, 32.1. **HRMS** (ESI-TOF) calculated for $C_{13}H_{12}N_3^+$ ([M-BF_4^-]$^+$): 210.1026, found: 210.1023. **IR** (neat) 1629, 1519, 1288, 1207, 1049, 782, 749, 678, 613. **MP** 217 °C.

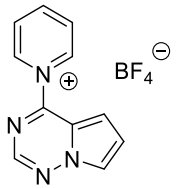
1-(6-(trifluoromethyl)-[1,2,4]triazolo[1,5-*a*]pyridin-2-yl)pyridin-1-ium tetrafluoroborate (3.45)



The title compound was prepared according to General Procedure 9, using 6-trifluoromethyl[1,2,4]triazolo[1,5-*a*]pyridin-2-amine (202 mg, 1 mmol). Brown solid, 95 mg, 27% yield.

^{1}H NMR ^{1}H NMR (400 MHz, CD_3CN) δ 9.78 – 9.64 (m, 2H), 9.37 – 9.31 (m, 1H), 8.86 (tt, *J* = 7.8, 1.4 Hz, 1H), 8.37 – 8.27 (m, 2H), 8.17 – 8.05 (m, 2H). **^{19}F NMR** (376 MHz, CD_3CN) δ -62.7 (s, 3F), -151.6 (s), -151.7 (s) (4F in total for the signals at -151 ppm).**^{13}C NMR** (101 MHz, CD_3CN) δ 160.5, 153.5, 151.8, 142.4, 130.6 (q, *J* = 5.6 Hz), 130.3 (q, *J* = 2.7 Hz), 130.0, 123.9 (q, *J* = 271.2 Hz), 121.4 (q, *J* = 35.2 Hz), 119.4. **HRMS** (ESI-TOF) calculated for $C_{12}H_8F_3N_4^+$ ([M-BF_4^-]$^+$): 265.0696, found: 265.0694. **IR** (neat) 1660, 1635, 1580, 1531, 1493, 1461, 1417, 1338, 1182, 1131, 1059, 941, 883, 829, 790, 762, 724, 677, 650, 617. **MP** 170–172 °C.

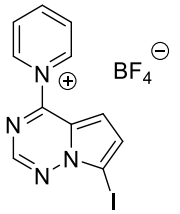
1-(Pyrrolo[2,1-*f*][1,2,4]triazin-4-yl)pyridin-1-ium tetrafluoroborate (3.46)



The title compound was prepared according to General Procedure 9, using pyrrolo[2,1-*f*][1,2,4]triazin-4-amine (134 mg, 1 mmol). Beige solid, 175 mg, 62% yield.

^{1}H NMR (400 MHz, DMSO-d_6) δ 9.70 – 9.63 (m, 2H), 9.02 (tt, *J* = 7.8, 1.4 Hz, 1H), 8.89 (s, 1H), 8.66 – 8.60 (m, 1H), 8.51 – 8.42 (m, 2H), 7.46 – 7.38 (m, 2H).**^{19}F NMR** (376 MHz, DMSO-d_6) δ -148.2 (s), -148.3 (s) (4F in total). **^{13}C NMR** (101 MHz, DMSO-d_6) δ 152.2, 150.7, 145.9, 143.7, 128.6, 123.5, 117.7, 115.9, 105.9. **HRMS** (ESI-TOF) calculated for $C_{11}H_9N_4^+$ ([M-BF_4^-]$^+$): 197.0822, found: 197.0823. **IR** (neat) 1612, 1505, 1481, 1454, 1429, 1357, 1318, 1240, 1208, 1145, 1053, 886, 846, 789, 769, 730, 674. **MP** decomposition observed at 235 °C.

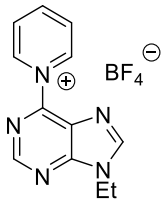
1-(7-Iodopyrrolo[2,1-*f*][1,2,4]triazin-4-yl)pyridin-1-ium tetrafluoroborate (3.47)



Prepared by S. Ortalli. The title compound was prepared according to General Procedure 9, using 7-iodopyrrolo[2,1-f][1,2,4]triazin-4-amine (260 mg, 1 mmol). Yellow solid, 299 mg, 73% yield.

^{1}H NMR (500 MHz, CD_3CN) δ 9.36–9.32 (m, 2H), 8.90 (tt, *J* = 7.9, 1.4 Hz, 1H), 8.78 (s, 1H), 8.38–8.31 (m, 2H), 7.54 (d, *J* = 4.9 Hz, 1H), 7.29 (d, *J* = 5.0 Hz, 1H). **^{19}F NMR** (471 MHz, CD_3CN) δ -151.8 (s), -151.9 (s) (4F in total). **^{13}C NMR** (151 MHz, CD_3CN) δ 152.5, 151.9, 147.3, 144.3, 130.2, 127.4, 120.6, 108.7, 78.9. **HRMS** (ESI-TOF) calculated for $C_{11}H_8IN_4^+$ ([M-BF_4^-]$^+$): 322.9788, found: 322.9782. **IR** (neat) 3120, 2358, 1748, 1605, 1482, 1450, 1390, 1298, 1254, 1207, 1139, 1095, 1056, 1025, 895, 853, 787, 728, 675. **MP** 277–279 °C.

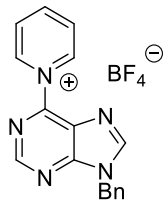
1-(9-Ethyl-9*H*-purin-6-yl)pyridin-1-ium tetrafluoroborate (3.48)



The title compound was prepared according to General Procedure 9, using *N*-ethyl adenine (163 mg, 1 mmol). Beige solid, 183 mg, 58% yield.

^{1}H NMR (400 MHz, DMSO-d_6) δ 10.29 – 10.22 (m, 2H), 9.24 (s, 1H), 9.11 (s, 1H), 8.97 (tt, *J* = 7.7, 1.4 Hz, 1H), 8.53 – 8.45 (m, 2H), 4.49 (q, *J* = 7.3 Hz, 2H), 1.54 (t, *J* = 7.3 Hz, 3H). **^{19}F NMR** (376 MHz, DMSO-d_6) δ -148.3 (s), -148.3 (s) (4F in total). **^{13}C NMR** (101 MHz, DMSO-d_6) δ 155.3, 151.2, 150.1, 149.9, 145.7, 143.2, 128.3, 124.6, 14.8*, note: product peak overlapping with solvent peak at 39.5 ppm.* **HRMS** (ESI-TOF) calculated for $C_{12}H_{12}N_5^+$ ([M-BF_4^-]$^+$): 226.1087, found: 226.1088. **IR** (neat) 1619, 1576, 1515, 1476, 1404, 1333, 1282, 1221, 1194, 1054, 1023, 932, 863, 781, 680, 646. **MP** 150 °C.

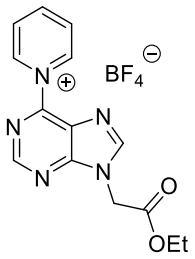
1-(9-Benzyl-9*H*-purin-6-yl)pyridin-1-ium tetrafluoroborate (3.49)



The title compound was prepared according to General Procedure 9, using *N*^{9}-benzyl adenine (225 mg, 1 mmol). Off-white solid, 307 mg, 82% yield.

^{1}H NMR (400 MHz, CD_3CN) δ 10.27 (dq, *J* = 6.7, 1.5 Hz, 2H), 9.12 (s, 1H), 8.84 (tt, *J* = 7.8, 1.4 Hz, 1H), 8.71 (s, 1H), 8.40 – 8.32 (m, 2H), 7.48 – 7.32 (m, 5H), 5.63 (s, 2H). **^{19}F NMR** (376 MHz, CD_3CN) δ -151.7 (s), -151.7 (s) (4F in total).**^{13}C NMR** (101 MHz, CD_3CN) δ 157.1, 152.4, 151.1, 150.5, 146.3, 143.9, 136.3, 129.9, 129.6, 129.5, 129.0, 125.9, 48.8. **HRMS** (ESI-TOF) calculated for $C_{17}H_{14}N_5^+$ ([M-BF_4^-]$^+$): 288.1244, found: 288.1239. **IR** (neat) 1667, 1578, 1537, 1481, 1355, 1289, 1055, 860, 760, 677. **MP** 149–151 °C.

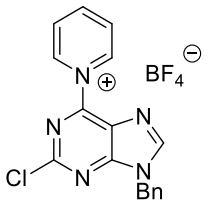
1-(9-(2-Ethoxy-2-oxoethyl)-9*H*-purin-6-yl)pyridin-1-ium tetrafluoroborate (3.50)



The title compound was prepared according to General Procedure 9, using ethyl 2-(6-amino-9*H*-purin-9-yl)acetate (221 mg, 1 mmol). Beige solid, 252 mg, 68% yield.

^{1}H NMR (600 MHz, CD_3CN) δ 10.30 – 10.25 (m, 2H), 9.12 (s, 1H), 8.85 (tt, *J* = 7.8, 1.4 Hz, 1H), 8.66 (s, 1H), 8.39 – 8.34 (m, 2H), 5.24 (s, 2H), 4.26 (q, *J* = 7.1 Hz, 2H), 1.28 (t, *J* = 7.1 Hz, 3H). **^{19}F NMR** (565 MHz, CD_3CN) δ -151.8 (s), -151.9 (s) (4F in total).**^{13}C NMR** (151 MHz, CD_3CN) δ 168.0, 157.3, 152.7, 151.3, 151.0, 146.5, 144.1, 129.6, 125.5, 63.3, 46.1, 14.4. **HRMS** (ESI-TOF) calculated for $C_{14}H_{14}N_5O_2^+$ ($[M\text{-}BF_4^-]^+$): 284.1142, found: 284.1138. **IR** (thin layer film) 3131, 1749, 1621, 1578, 1517, 1477, 1448, 1410, 1379, 1336, 1283, 1209, 1060, 974, 932, 861, 783, 678, 640. **MP** 165–167 °C.

1-(9-Benzyl-2-chloro-9*H*-purin-6-yl)pyridin-1-ium tetrafluoroborate (3.51)

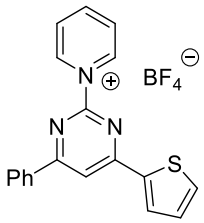


The title compound was prepared according to General Procedure 9, using 9-benzyl-2-chloro-9*H*-purin-6-amine (231 mg, 0.89 mmol), pyrylium tetrafluoroborate (150 mg, 0.89 mmol, 1 equiv.) and EtOH (4.5 mL) as solvent, with a modified purification procedure. The crude product was obtained as a sticky brown residue. This was washed from the frit with MeCN, which was concentrated to dryness under reduced pressure. The residue was redissolved in a minimal amount of MeCN (approx. 1 mL) and Et_2O was added until precipitation was observed. The liquid was decanted and the product was suspended in further Et_2O and

sonicated until a solid formed. This was then transferred to a frit and washed with Et_2O and allowed to dry. Brown solid, 141 mg, 39% yield.

^{1}H NMR (500 MHz, CD_3CN) δ 10.22 – 10.09 (m, 2H), 8.86 (tt, *J* = 7.8, 1.4 Hz, 1H), 8.69 (s, 1H), 8.41 – 8.31 (m, 2H), 7.43 – 7.40 (m, 5H), 5.58 (s, 2H). **^{19}F NMR** (471 MHz, CD_3CN) δ -151.5 (s), -151.6 (s) (4F in total). **^{13}C NMR** (126 MHz, CD_3CN) δ 158.5, 153.0, 151.5, 151.2, 146.5, 143.7, 135.5, 129.8, 129.5, 129.4, 128.8, 125.2, 48.8. **HRMS** (ESI-TOF) calculated for $C_{17}H_{13}{}^{35}ClN_5{}^+$ ([M-BF_4^-]$^+$): 322.0854, found: 322.0848. **IR** (thin layer film) 3088, 2260, 1757, 1695, 1670, 1620, 1573, 1563, 1514, 1456, 1419, 1392, 1357, 1325, 1264, 1217, 1191, 1054, 933, 881, 720, 676, 653, 631. **MP** no melting observed up to 320 °C.

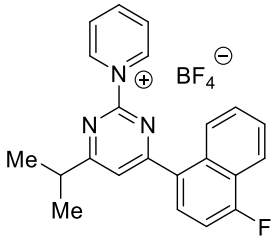
1-(4-Phenyl-6-(thiophen-2-yl)pyrimidin-2-yl)pyridin-1-ium tetrafluoroborate (3.52)



The title compound was prepared according to General Procedure 9, using 4-phenyl-6-(thiophen-2-yl)pyrimidin-2-amine (253 mg, 1 mmol). Brown solid, 226 mg, 56% yield.

^{1}H NMR (400 MHz, DMSO-d_6) δ 10.29 – 10.18 (m, 2H), 8.97 (tt, *J* = 7.6, 1.4 Hz, 1H), 8.91 (s, 1H), 8.62 – 8.57 (m, 3H), 8.45 – 8.38 (m, 2H), 8.10 (dd, *J* = 5.0, 1.2 Hz, 1H), 7.73 – 7.66 (m, 3H), 7.42 (dd, *J* = 5.0, 3.8 Hz, 1H). **^{19}F NMR** (376 MHz, DMSO-d_6) δ -148.2 (s), -148.3 (s) (4F in total). **^{13}C NMR** (101 MHz, DMSO-d_6) δ 166.1, 162.0, 155.3, 150.3, 141.2, 139.9, 134.3, 133.8, 132.7, 132.0, 129.6, 129.2, 128.1, 128.0, 112.0. **HRMS** (ESI-TOF) calculated for $C_{19}H_{14}N_3S^+$ ([M-BF_4^-]$^+$): 316.0903, found: 316.0904. **IR** (neat) 1605, 1572, 1536, 1516, 1440, 1354, 1319, 1255, 1197, 1143, 1051, 1000, 858, 758, 723, 690, 666, 644, 631. **MP** 239–241 °C.

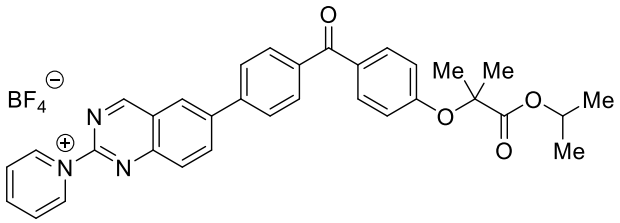
1-(4-(4-Fluoronaphthalen-1-yl)-6-isopropylpyrimidin-2-yl)pyridin-1-ium tetrafluoroborate (3.53)



The title compound was prepared according to General Procedure 9, using 4-(4-fluoronaphthalen-1-yl)-6-isopropylpyrimidin-2-amine (281 mg, 1 mmol) with a modified purification procedure. The reaction mixture was diluted with Et_2O (approx. 10 mL) and sonicated until a solid formed. This was then collected on a frit and washed with EtOAc and Et_2O. The solid was then dried. Yellow-beige solid, 134 mg, 31% yield.

^{1}H NMR (500 MHz, CD_3CN) δ 10.12 – 10.06 (m, 2H), 8.82 (tt, *J* = 7.7, 1.4 Hz, 1H), 8.39 (dt, *J* = 7.7, 2.0 Hz, 1H), 8.31 – 8.23 (m, 3H), 7.98 (s, 1H), 7.91 (dd, *J* = 8.0, 5.4 Hz, 1H), 7.79 – 7.69 (m, 2H), 7.45 (dd, *J* = 10.3, 8.1 Hz, 1H), 3.36 (hept, *J* = 6.9 Hz, 1H), 1.48 (d, *J* = 6.9 Hz, 6H). **^{19}F NMR** (471 MHz, CD_3CN) δ -119.2 – -119.3 (m, 1F), -151.8 (s), -151.8 (s) (4F for the two signals at -151 ppm combined). **^{13}C NMR** (151 MHz, CD_3CN) δ 181.6, 169.6, 161.3 (d, *J* = 255.6 Hz), 155.6, 151.3, 142.0, 132.9 (d, *J* = 5.4 Hz), 131.5 (d, *J* = 4.4 Hz), 130.8 (d, *J* = 9.8 Hz), 129.8, 129.3, 128.3 (d, *J* = 2.2 Hz), 126.0 (d, *J* = 2.7 Hz), 124.8 (d, *J* = 16.3 Hz), 122.8, 121.9 (d, *J* = 6.5 Hz), 110.4 (d, *J* = 21.3 Hz), 37.0, 21.8. **HRMS** (ESI-TOF) calculated for $C_{22}H_{19}FN_3^+$ ($[M\text{-}BF_4^-]^+$): 344.1558, found: 344.1557. **IR** (neat) 1604, 1569, 1517, 1445, 1371, 1320, 1296, 1233, 1198, 1051, 846, 784, 695, 665. **MP** 182 °C.

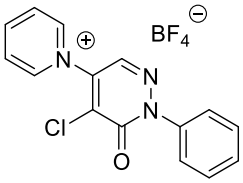
1-(6-(4-(4-((1-Isopropoxy-2-methyl-1-oxopropan-2-yl)oxy)benzoyl)phenyl)quinazolin-2-yl)pyridin-1-ium tetrafluoroborate (3.54)



The title compound was prepared according to General Procedure 9, using isopropyl 2-(4-(4-(2-aminoquinazolin-6-yl)benzoyl)phenoxy)-2-methyl-propanoate (469 mg, 1 mmol). Beige solid, 424 mg, 76% yield.

^{1}H NMR (600 MHz, CD_3CN) δ 10.21 – 10.14 (m, 2H), 9.87 (d, *J* = 0.8 Hz, 1H), 8.85 (tt, *J* = 7.7, 1.4 Hz, 1H), 8.65 (dd, *J* = 2.1, 0.7 Hz, 1H), 8.59 (dd, *J* = 8.8, 2.1 Hz, 1H), 8.37 – 8.31 (m, 3H), 8.02 – 7.97 (m, 2H), 7.94 – 7.89 (m, 2H), 7.82 – 7.78 (m, 2H), 6.95 – 6.91 (m, 2H), 5.05 (hept, *J* = 6.3 Hz, 1H), 1.65 (s, 6H), 1.21 (d, *J* = 6.2 Hz, 6H). **^{19}F NMR** (565 MHz, CD_3CN) δ -151.6 (s), -151.6 (s) (4F in total). **^{13}C NMR** (151 MHz, CD_3CN) δ 195.4, 173.7, 165.9, 160.7, 152.6, 151.2, 150.9, 142.7, 142.6, 142.1, 139.3, 137.7, 133.0, 131.5, 131.4, 129.9, 129.5, 128.5, 127.4, 126.8, 80.5, 70.3, 25.7, 21.7. *note: product peaks overlapping*. **HRMS** (ESI-TOF) calculated for $C_{33}H_{30}N_3O_4^+$ ([M-BF_4^-]$^+$): 532.2231, found: 532.2222. **IR** (thin layer film) 1732, 1648, 1598, 1567, 1506, 1473, 1427, 1402, 1289, 1252, 1180, 1149, 1102, 1060, 974, 931, 898, 838, 771, 719, 671, 616. **MP** 167–170 °C.

1-(5-Chloro-6-oxo-1-phenyl-1,6-dihydropyridazin-4-yl)pyridin-1-ium tetrafluoroborate (3.55)

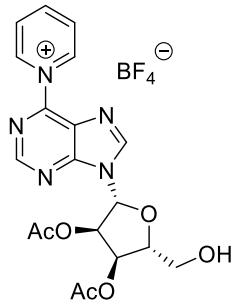


The title compound was prepared according to General Procedure 9, using chloridazon (222 mg, 1 mmol). Brown solid, 150 mg, 40% yield.

^{1}H NMR (400 MHz, CD_3CN) δ 8.94 – 8.83 (m, 3H), 8.41 – 8.30 (m, 2H), 8.23 (s, 1H), 7.65 – 7.53 (m, 5H). **^{19}F NMR** (376 MHz, CD_3CN) δ -151.4 (s), -151.5 (s) (4F in total). **^{13}C NMR** (101 MHz, CD_3CN) δ 157.3, 151.0, 145.8, 142.1, 140.9, 135.6, 133.6, 130.5, 130.3, 126.5, 125.8. **HRMS**

(ESI-TOF) calculated for $C_{15}H_{11}{}^{35}ClN_3O^+$ ([M-BF_4^-]$^+$): 284.0585, found: 284.0586. **IR** (neat) 1667, 1615, 1598, 1579, 1536, 1482, 1462, 1355, 1291, 1057, 860, 760, 677. **MP** no melting observed up to 320 °C.

1-(9-((2*R*,3*R*,4*R*,5*R*)-3,4-Diacetoxy-5-(hydroxymethyl)tetrahydrofuran-2-yl)-9*H*-purin-6-yl)pyridin-1-ium tetrafluoroborate (3.56)

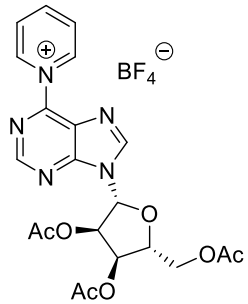


Prepared by S. Ortalli. The title compound was prepared according to General Procedure 9, using (2*R*,*3R*,4*R*,5*R*)-2-(6-amino-9*H*-purin-9-yl)-5-(hydroxymethyl)tetrahydrofuran-3,4-diyl diacetate (351 mg, 1 mmol), with a modified purification procedure. The crude product obtained was further diluted in a minimal amount of MeCN. Et_2O was then added, and the mixture was sonicated. The solvent was decanted and additional Et_2O was added. The mixture was sonicated until a solid precipitate was obtained. This was filtered and washed with Et_2O. Brown solid, 253 mg, 51% yield. *Note: residual starting material was still present in the product and this was used directly in the radiofluorination (ratio$_{starting\ material:product}$ = 1:11.1 by ^{1}H NMR analysis).*

^{1}H NMR (400 MHz, CD_3CN) δ 10.27–10.21 (m, 2H), 9.14 (s, 1H), 8.94 (s, 1H), 8.86 (tt, *J* = 7.7, 1.4 Hz, 1H), 8.37 (t, *J* = 7.5 Hz, 2H), 6.43 (d, *J* = 6.3 Hz, 1H), 5.93 (t, *J* = 5.8 Hz, 1H), 5.61 (dd, *J* = 5.5, 3.1 Hz, 1H), 4.40 (q, *J* = 2.7 Hz, 1H), 3.91 (dd, *J* = 12.6, 2.6 Hz, 2H), 3.81 (d, *J* = 11.9 Hz, 1H), 2.14 (s, 3H), 2.00 (s, 3H). **^{19}F NMR** (471 MHz, CD_3CN) δ -151.7 (s), -151.8 (s) (4F in total). **^{13}C NMR** (101 MHz, CD_3CN) δ 170.9, 170.6, 156.6, 152.6, 151.5, 149.1, 146.7, 144.0, 129.7, 126.9, 88.2, 85.9, 74.6, 72.3, 62.3, 20.9, 20.6. **HRMS** (ESI-TOF) calculated for $C_{19}H_{20}N_5O_6^+$ ([M-

$BF_4^-]^+$): 414.1408, found: 414.1398. **IR** (neat) 2360, 2341, 1746, 1622, 1577, 1507, 1476, 1376, 1337, 1246, 1212, 1051, 913, 783, 679, 642. **MP** 90–92 °C.

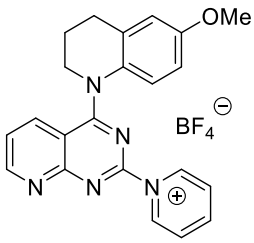
1-(9-((2*R*,3*R*,4*R*,5*R*)-3,4-Diacetoxy-5-(acetoxymethyl)tetrahydrofuran-2-yl)-9*H*-purin-6-yl)pyridin-1-ium tetrafluoroborate (3.57)



Prepared by S. Ortalli. The title compound was prepared according to General Procedure 9, using (2*R*,3*R*,4*R*,5*R*)-2-(acetoxymethyl)-5-(6-amino-9*H*-purin-9-yl)tetrahydrofuran-3,4-diyl diacetate (787 mg, 2 mmol), with a modified purification procedure. The crude product was further diluted in a minimal amount of MeCN. Et_2O was then added, and the mixture was sonicated. The solvent was decanted and additional Et_2O was added. The mixture was sonicated until a solid precipitate was obtained. This was filtered and washed with Et_2O. Brown solid, 714 mg, 66% yield. *Note: residual starting material was still present in the product and this was used directly in the radiofluorination (ratio$_{starting\ material:product}$ = 1:4.1 by ^{1}H NMR analysis).*

^{1}H NMR (500 MHz, CD_3CN) δ 10.23–10.20 (m, 2H), 9.15 (s, 1H), 8.85 (tt, *J* = 7.8, 1.4 Hz, 1H), 8.78 (s, 1H), 8.37 (t, *J* = 7.5 Hz, 2H), 6.40 (d, *J* = 4.7 Hz, 1H), 5.99 (t, *J* = 5.3 Hz, 1H), 5.69 (t, *J* = 5.6 Hz, 1H), 4.51 (td, *J* = 5.1, 3.2 Hz, 1H), 4.46 (dd, *J* = 12.4, 3.2 Hz, 1H), 4.35 (dd, *J* = 12.4, 4.9 Hz, 1H), 2.13 (s, 3H), 2.06 (s, 3H), 2.03 (s, 3H). **^{19}F NMR** (471 MHz, CD_3CN) δ -151.7 (s), -151.8 (s) (4F in total). **^{13}C NMR** (126 MHz, CD_3CN) δ 171.3, 170.8, 170.6, 156.4, 152.7, 151.4, 149.1, 146.8, 144.0, 129.7, 126.8, 88.5, 81.7, 74.0, 71.2, 63.7, 21.0, 20.8, 20.6. **HRMS** (ESI-TOF) calculated for $C_{21}H_{22}N_5O_7^+$ ([M-BF_4^-]$^+$): 456.1514, found: 456.1523. **IR** (neat) 3137, 2361, 1632, 1596, 1481, 1427, 1289, 1205, 1053, 1008, 934, 768, 676, 652. **MP** 85–87 °C.

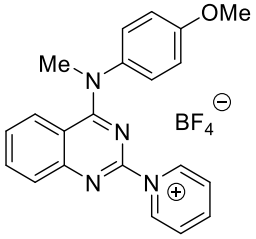
1-(4-(6-Methoxy-3,4-dihydroquinolin-1(2*H*)-yl)pyrido[2,3-*d*]pyrimidin-2-yl)pyridin-1-ium tetrafluoroborate (3.58)



The title compound was prepared according to General Procedure 9, using 4-(6-methoxy-3,4-dihydroquinolin-1(2*H*)-yl)pyrido[2,3-*d*]pyrimidin-2-amine (153 mg, 0.5 mmol), pyrylium tetrafluoroborate (84 mg, 0.5 mmol, 1 equiv.) and EtOH (2.5 mL) as solvent. Brown solid, 115 mg, 50% yield. *Note: residual starting material was still present in the product and this was used directly in the radiofluorination (ratio$_{starting\ material:product}$ = 1:5.5 by ^{1}H NMR analysis).*

^{1}H NMR (500 MHz, CD_3CN) δ 10.20 – 10.11 (m, 2H), 9.02 (dd, *J* = 4.3, 1.8 Hz, 1H), 8.81 (tt, *J* = 7.6, 1.4 Hz, 1H), 8.31 – 8.22 (m, 2H), 7.89 (dd, *J* = 8.5, 1.9 Hz, 1H), 7.30 (dd, *J* = 8.4, 4.3 Hz, 1H), 7.03 – 6.98 (m, 2H), 6.67 (dd, *J* = 8.8, 2.9 Hz, 1H), 4.24 (t, *J* = 6.8 Hz, 2H), 3.82 (s, 3H), 2.90 (t, *J* = 6.5 Hz, 2H), 2.15 – 2.12 (m, 2H, *overlapping with residual water peak in CD$_3$CN solvent*). **^{19}F NMR** (471 MHz, CD_3CN) δ -151.7 (s), -151.7 (s) (4F in total). **^{13}C NMR** (151 MHz, CD_3CN) δ 164.6, 161.1, 159.4, 158.1, 154.5, 151.1, 141.8, 137.3, 137.2, 134.0, 129.1, 124.3, 122.6, 114.7, 113.6, 113.0, 56.3, 49.6, 27.4, 24.7. **HRMS** (ESI-TOF) calculated for $C_{22}H_{20}N_5O^+$ ([M-BF_4^-]$^+$): 370.1662, found: 370.1657. **IR** (thin layer film) 1593, 1565, 1551, 1501, 1465, 1363, 1311, 1279, 1238, 1195, 1167, 1059, 791, 727, 671. **MP** 218 °C.

1-(4-((4-Methoxyphenyl)(methyl)amino)quinazolin-2-yl)pyridin-1-ium tetrafluoroborate (3.59)

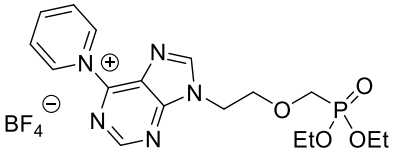


The title compound was prepared according to General Procedure 9, using *N*^{4}-(4-methoxyphenyl)-N^4-methylquinazoline-2,4-diamine (280 mg, 1 mmol), with a modified

purification procedure. Et_2O (approx. 15 mL) was added to the reaction mixture once it had cooled to rt. The mixture was then sonicated. The solvent was decanted and further Et_2O was added, and the mixture was sonicated until a solid formed. The solid was transferred to a frit and washed with EtOAc, then Et_2O. The crude solid (217 mg) was then transferred to a flask and redissolved in a minimum amount of MeCN (1 mL). Et_2O (5 mL) was added and the mixture agitated. The solid precipitate was collected on a frit and washed with Et_2O, then dried under vacuum. Brown solid, 175 mg, 41% yield.

^{1}H NMR (600 MHz, CD_3CN) δ 10.25 – 10.17 (m, 2H), 8.79 (tt, *J* = 7.7, 1.4 Hz, 1H), 8.26 (t, *J* = 7.3 Hz, 2H), 7.92 (dd, *J* = 8.3, 0.8 Hz, 1H), 7.78 (ddd, *J* = 8.3, 7.0, 1.4 Hz, 1H), 7.36 – 7.30 (m, 2H), 7.23 (ddd, *J* = 8.4, 7.0, 1.3 Hz, 1H), 7.11 – 7.06 (m, 2H), 7.04 (ddd, *J* = 8.6, 1.3, 0.6 Hz, 1H), 3.87 (s, 3H), 3.76 (s, 3H). **^{19}F NMR** (565 MHz, CD_3CN) δ -151.8 (s), -151.9 (s) (4F in total). **^{13}C NMR** (151 MHz, CD_3CN) δ 163.8, 160.6, 152.3, 151.7, 150.5, 141.6, 140.0, 135.0, 129.5, 129.0, 128.8, 128.0, 127.9, 117.0, 116.7, 56.4, 44.5. **HRMS** (ESI-TOF) calculated for $C_{21}H_{19}N_4O^+$ ([M-BF_4^-]$^+$): 343.1553, found: 343.1548. **IR** (thin layer film) 1601, 1567, 1549, 1509, 1491, 1472, 1388, 1316, 1283, 1250, 1198, 1059, 949, 844, 771, 714, 671. **MP** 193–194 °C.

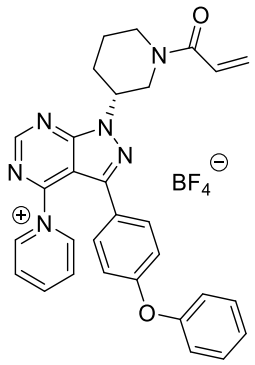
1-(9-(2-((Diethoxyphosphoryl)methoxy)ethyl)-9*H*-purin-6-yl)pyridin-1-ium tetrafluoroborate (3.60)



The title compound was prepared according to General Procedure 9, using 9-[2-(diethylphosphonomethoxy)ethyl] adenine (329 mg, 1 mmol), with a modified purification procedure. To the cooled reaction mixture was added Et_2O (15 mL). This mixture was sonicated and cooled to 4 °C. The liquid was then decanted, leaving a sticky residue. The residue was suspended in Et_2O and sonicated for 15 min. The liquid was decanted and this leaving a sticky orange solid behind. This was then dried under reduced pressure. Sticky orange solid, 407 mg, 85% yield.

^{1}H NMR (500 MHz, CD_3CN) δ 10.41 – 10.30 (m, 2H), 9.15 (s, 1H), 8.86 (tt, *J* = 7.8, 1.4 Hz, 1H), 8.75 (s, 1H), 8.42 – 8.36 (m, 2H), 4.67 – 4.63 (m, 2H), 4.08 – 4.00 (m, 6H), 3.85 (d, *J* = 8.4 Hz, 2H), 1.24 (t, *J* = 7.0 Hz, 6H). **^{19}F NMR** (471 MHz, CD_3CN) δ -151.7 (s), -151.8 (s) (4F in total). **^{31}P{^{1}H} NMR** (162 MHz, CD_3CN) δ 20.4 (s). **^{13}C NMR** (126 MHz, CD_3CN) δ 156.3, 151.3, 150.2, 150.2, 145.1, 142.9, 128.6, 124.7, 70.1 (d, J_{CP} = 11.2 Hz), 64.4 (d, J_{CP} = 165.1 Hz), 62.2 (d, J_{CP} = 6.3 Hz), 44.1, 15.8 (d, J_{CP} = 5.5 Hz). **HRMS** (ESI-TOF) calculated for $C_{17}H_{23}N_5O_4P^+$ ([M-BF_4^-]$^+$): 392.1482, found: 392.1477. **IR** (thin layer film) 1622, 1576, 1516, 1476, 1447, 1405, 1335, 1211, 1023, 977, 783, 680, 648. **MP** 179–180 °C.

(*R*)-1-(1-(1-Acryloylpiperidin-3-yl)-3-(4-phenoxyphenyl)-1*H*-pyrazolo[3,4-*d*]pyrimidin-4-yl)pyridin-1-ium tetrafluoroborate (3.61)



The title compound was prepared according to General Procedure 9, using ibrutinib (441 mg, 1 mmol), with a modified purification procedure. The crude reaction mixture was concentrated to dryness and was purified by flash column chromatography (conditions: gradient CH_2Cl_2: MeOH = 50:1 to 20:1). Yellow solid, 292 mg, 49% yield.

^{1}H NMR (400 MHz, $CDCl_3$) δ 8.99 (dd, *J* = 12.6, 6.2 Hz, 3H), 8.62 (t, *J* = 7.9 Hz, 1H), 7.97 (t, *J* = 7.1 Hz, 2H), 7.43 – 7.30 (m, 2H), 7.13 (d, *J* = 8.2 Hz, 3H), 6.97 (d, *J* = 8.0 Hz, 2H), 6.79 (d, *J* = 8.2 Hz, 2H), 6.59 (dd, *J* = 16.8, 10.6 Hz, 1H), 6.22 (t, *J* = 18.6 Hz, 1H), 5.67 (dd, *J* = 20.3, 10.4 Hz, 1H), 5.08 (s, 1H), 4.88 – 3.90 (m, 2H), 3.86 – 2.81 (m, 2H), 2.62 – 2.24 (m, 2H), 2.09 – 1.78 (m, 2H). **^{19}F NMR** (376 MHz, $CDCl_3$) δ -152.1 (s), -152.2 (s) (4F in total). **^{13}C NMR** (101 MHz, $CDCl_3$) δ 165.8, 159.1, 156.2, 156.0, 154.4, 152.5, 149.3, 144.1, 142.6, 130.4, 130.1, 128.3, 128.1, 127.5, 124.9, 124.3, 119.5, 118.7, 104.3, 54.7, 53.7, 49.8, 47.1, 46.0, 42.1, 29.9, 25.1, 23.8.

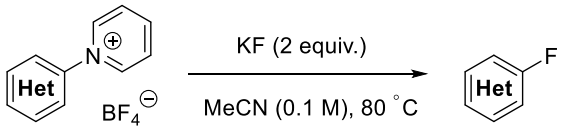
note: signal splitting/broad signals observed due to the piperidine ring in all NMR experiments. **HRMS** (ESI-TOF) calculated for $C_{30}H_{27}N_6O_2^+$ ([M-BF_4^-]$^+$): 503.2190, found: 503.2192. **IR** (neat) 1604, 1572, 1516, 1440, 1354, 1318, 1251, 1197, 1051, 857, 778, 758, 722, 690, 666, 644, 631. **MP** 117 °C.

4.4.1.3. Preparation of authentic references

2-fluoropyrimidine (**3.62**), 5-bromo-2-fluoropyrimidine (**3.64**), 2-fluoro-5-iodopyrimidine (**3.65**), 2-fluoro-5-methoxypyrimidine (**3.67**), 2-fluoro-5-nitropyridine (**3.69**) and 6-fluoropyridazine-3-carbonitrile (**3.75**), 2-fluorobenzothiazole (**3.85**) were purchased from commercial suppliers (Fluorochem, Manchester Organics, Biosynth, ThermoFisher) and used as received, without further purification.

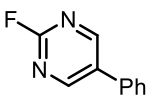
Ethyl 2-fluorooxazole-4-carboxylate (**3.63**) and 9-ethyl-6-fluoro-9*H*-purine (**3.81**) were prepared exactly as described in literature procedures.[33]

General Procedure 10:



The following is adapted from a literature procedure.[33] To a flame-dried Schlenk tube under N_2 were added heteroaryl pyridinium tetrafluoroborate (1 equiv.) and KF (2 equiv.) as solids. Anhydrous MeCN (0.1 M) was then added *via* syringe. The mixture was stirred at 80 °C overnight in an oil bath. The Schlenk tube was then removed from the oil bath and allowed to cool to rt. The reaction mixture was passed through a short SiO_2 plug, eluting EtOAc. The eluate was concentrated under reduced pressure and subsequently purified by flash column chromatography.

2-Fluoro-5-phenylpyrimidine (3.66)

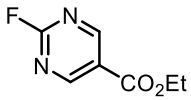


The title compound was prepared according to General Procedure 10, using 1-(5-phenylpyrimidin-2-yl)pyridin-1-ium tetrafluoroborate (**3.29**) (48 mg, 0.15 mmol), KF (17 mg, 0.3 mmol), MeCN (1.5 mL) and a reaction time of 17 h. Flash column chromatography conditions: hexane/EtOAc=90/10. Pale yellow solid, 13 mg, 50% yield.

^{1}H NMR (400 MHz, $CDCl_3$) δ 8.82 (d, *J* = 1.6 Hz, 2H), 7.59 – 7.43 (m, 5H). **^{19}F NMR** (376 MHz, $CDCl_3$) δ -47.7 (s). **^{13}C NMR** (101 MHz, $CDCl_3$) δ 162.6 (d, *J* = 219.8 Hz), 159.0 (d, *J* = 12.0 Hz), 133.2 (d, *J* = 1.8 Hz), 133.2 (d, J = 5.1 Hz), 129.7, 129.3, 127.1. **HRMS** (ESI-TOF) calculated for $C_{10}H_8FN_2$ ($[M+H]^+$): 175.0666, found: 175.0667.

The reported spectral data are in agreement with those reported in literature.[37]

Ethyl 2-fluoropyrimidine-5-carboxylate (3.68)

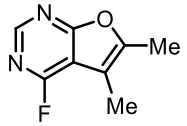


The title compound was prepared according to General Procedure 10, using 1-(5-(ethoxycarbonyl)pyrimidin-2-yl)pyridin-1-ium tetrafluoroborate (**3.31**) (48 mg, 0.15 mmol), KF (17 mg, 0.30 mmol), MeCN (1.5 mL). Flash column chromatography conditions: pentane/EtOAc = 90/10. Yellow solid, 10 mg, 39% yield.

^{1}H NMR (500 MHz, $CDCl_3$) δ 9.21 (d, *J* = 1.7 Hz, 2H), 4.46 (q, *J* = 7.1 Hz, 2H), 1.43 (t, *J* = 7.1 Hz, 3H). **^{19}F NMR** (470 MHz, $CDCl_3$) δ -38.9 (s). **^{13}C NMR** (126 MHz, $CDCl_3$) δ 164.7 (d, *J* = 225.6 Hz), 163.0 (d, *J* = 13.6 Hz), 162.7 (d, *J* = 1.7 Hz), 123.4 (d, *J* = 5.2 Hz), 62.3, 14.4.

The recorded spectral data are in agreement with those reported in literature.[38]

4-Fluoro-5,6-dimethylfuro[2,3-*d*]pyrimidine (3.70)

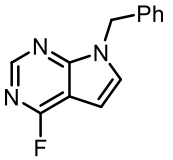


The title compound was prepared according to General Procedure 10, using 1-(5,6-dimethylfuro[2,3-*d*]pyrimidin-4-yl)pyridin-1-ium tetrafluoroborate (**3.35**) (62 mg, 0.2 mmol),

KF (23 mg, 0.4 mmol), MeCN (2 mL) and a reaction time of 16 h. Flash column chromatography conditions: hexane/EtOAc=95/5. White solid, 26 mg, 78% yield.

^{1}H NMR (400 MHz, $CDCl_3$) δ 8.52 (s, 1H), 2.44 (s, 3H), 2.27 (d, *J* = 0.9 Hz, 3H). **^{19}F NMR** (376 MHz, $CDCl_3$) δ -68.1 (s). **^{13}C NMR** (101 MHz, $CDCl_3$) δ 169.3 (d, *J* = 11.9 Hz), 162.8 (d, *J* = 252.6 Hz), 151.7 (d, *J* = 3.8 Hz), 151.7 (d, *J* = 14.5 Hz), 107.6 (d, *J* = 5.7 Hz), 107.1 (d, *J* = 31.4 Hz), 11.8, 9.1. **HRMS** (ESI-TOF) calculated for $C_8H_8FN_2O$ ($[M+H]^+$): 167.0615, found: 167.0616. **IR** (neat) 1733, 1637, 1579, 1459, 1409, 1390, 1355, 1323, 1262, 1189, 1071, 967, 819, 629. **MP** 85–88 °C.

7-Benzyl-4-fluoro-7*H*-pyrrolo[2,3-*d*]pyrimidine (3.71)

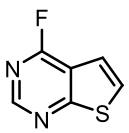


The title compound was prepared according to General Procedure 10, using 1-(7-benzyl-7*H*-pyrrolo[2,3-*d*]pyrimidin-4-yl)pyridin-1-ium tetrafluoroborate (**3.36**) (56 mg, 0.15 mmol), KF (18 mg, 0.3 mmol), MeCN (1.5 mL) and a reaction time of 14 h. Flash column chromatography conditions: hexane/EtOAc=90/10. Pale yellow solid, 29 mg, 85% yield.

^{1}H NMR (400 MHz, $CDCl_3$) δ 8.56 (d, *J* = 1.4 Hz, 1H), 7.36 – 7.29 (m, 3H), 7.25 – 7.20 (m, 2H), 7.18 (d, *J* = 3.6 Hz, 1H), 6.61 (d, *J* = 3.6 Hz, 1H), 5.48 (s, 2H). **^{19}F NMR** (376 MHz, $CDCl_3$) δ -65.9 (s). **^{13}C NMR** (101 MHz, $CDCl_3$) δ 162.6 (d, J = 252.9 Hz), 154.9 (d, J = 12.2 Hz), 150.8 (d, J = 14.5 Hz), 136.5, 129.1, 128.6 (d, J = 2.5 Hz), 128.3, 127.8, 104.5 (d, J = 33.3 Hz), 98.3 (d, J = 5.0 Hz), 48.9. **HRMS** (ESI-TOF) calculated for $C_{13}H_{11}FN_3$ ($[M+H]^+$): 228.0932, found: 228.0932.

The recorded spectral data are in agreement with those reported in literature.[39]

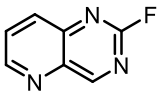
4-Fluorothieno[2,3-*d*]pyrimidine (3.72)



The title compound was prepared according to General Procedure 10, using 1-(thieno[2,3-*d*]pyrimidin-4-yl)pyridin-1-ium tetrafluoroborate (**3.37**) (75 mg, 0.25 mmol), KF (29 mg, 0.5 mmol), MeCN (2.5 mL) and a reaction time of 16 h. Flash column chromatography conditions: pentane/EtOAc=95/5. White solid, 27 mg, 71% yield.

^{1}H NMR (400 MHz, $CDCl_3$) δ 8.79 (s, 1H), 7.62 (d, *J* = 6.0 Hz, 1H), 7.44 (d, *J* = 6.0 Hz, 1H). **^{19}F NMR** (376 MHz, $CDCl_3$) δ -61.9 (s, 1F). **^{13}C NMR** (101 MHz, $CDCl_3$) δ 172.2 (d, *J* = 7.3 Hz), 163.7 (d, *J* = 258.9 Hz), 153.2 (d, *J* = 13.6 Hz), 128.0 (d, *J* = 1.4 Hz), 118.0 (d, *J* = 29.5 Hz), 117.3 (d, *J* = 5.5 Hz). **HRMS** (ESI-TOF) calculated for $C_6H_4FN_2S$ ($[M+H]^+$): 155.0074, found: 155.0075. **IR** (neat) 1601, 1580, 1523, 1474, 1439, 1417, 1360, 1315, 1262, 1150, 1087, 875, 793, 713, 633. **MP** 64 °C.

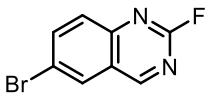
2-Fluoropyrido[3,2-*d*]pyrimidine (3.73)



The title compound was prepared according to General Procedure 10, using 1-(pyrido[3,2-*d*]pyrimidin-2-yl)pyridin-1-ium tetrafluoroborate (**3.39**) (59 mg, 0.2 mmol), KF (23 mg, 0.4 mmol), MeCN (2 mL) and a reaction time of 16 h. Flash column chromatography conditions: pentane/EtOAc = 80/20. Off-white solid, 26 mg, 87% yield.

^{1}H NMR (500 MHz, $CDCl_3$) δ 9.60 (d, *J* = 2.3 Hz, 1H), 9.07 (dd, *J* = 4.1, 1.5 Hz, 1H), 8.35 – 8.26 (m, 1H), 7.86 (dd, *J* = 8.6, 4.1 Hz, 1H). **^{19}F NMR** (471 MHz, $CDCl_3$) δ -45.2 (s). **^{13}C NMR** (126 MHz, $CDCl_3$) δ 167.2 (d, *J* = 15.0 Hz), 159.8 (d, *J* = 222.0 Hz), 152.2 (d, *J* = 2.7 Hz), 148.8 (d, *J* = 14.1 Hz), 139.7 (d, *J* = 3.6 Hz), 135.7 (d, *J* = 2.9 Hz), 129.5. **HRMS** (ESI-TOF) calculated for $C_7H_5FN_3$ ($[M+H]^+$): 150.0462, found: 150.0461. **IR** (neat) 1588, 1451, 1396, 1376, 1338, 1321, 1262, 1226, 1192, 1121, 1030, 973, 923, 828, 747, 721, 629. **MP** 119-121 °C.

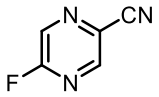
6-Bromo-2-fluoroquinazoline (3.74)



The title compound was prepared according to General Procedure 10, using 1-(6-bromoquinazolin-2-yl)pyridin-1-ium tetrafluoroborate (**3.38**) (75 mg, 0.2 mmol), KF (23 mg, 0.4 mmol), MeCN (2 mL) and a reaction time of 16 h. Flash column chromatography conditions: pentane/EtOAc=95/5. Pale yellow solid, 37 mg, 72% yield.

^{1}H NMR (400 MHz, $CDCl_3$) δ 9.30 (d, *J* = 2.1 Hz, 1H), 8.17 (d, *J* = 2.1 Hz, 1H), 8.02 (dd, *J* = 9.0, 2.0 Hz, 1H), 7.86 (d, *J* = 9.1 Hz, 1H). **^{19}F NMR** (376 MHz, $CDCl_3$) δ -45.2 (s). **^{13}C NMR** (101 MHz, $CDCl_3$) δ 164.5 (d, *J* = 14.2 Hz), 160.3 (d, *J* = 220.3 Hz), 151.1 (d, *J* = 13.2 Hz), 139.3, 129.6, 129.4 (d, *J* = 2.9 Hz), 124.9 (d, *J* = 3.3 Hz), 121.1 (d, *J* = 3.0 Hz). **HRMS** (ESI-TOF) calculated for $C_8H_5{}^{79}BrFN_2$ ($[M+H]^+$): 226.9615, found: 226.9615. **IR** (neat) 1732, 1614, 1580, 1558, 1485, 1427, 1375, 1343, 1300, 1276, 1267, 1236, 1184, 1137, 1055, 974, 923, 843, 809, 791, 760, 717, 650. **MP** 131–133 °C.

5-Fluoropyrazine-2-carbonitrile (3.76)

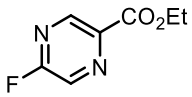


The title compound was prepared according to General Procedure 10, using 1-(5-cyanopyrazin-2-yl)pyridin-1-iumtetrafluoroborate (**3.42**) (54 mg, 0.2 mmol), KF (23 mg, 0.4 mmol), MeCN (2 mL) and a reaction time of 16.5 h. Flash column chromatography conditions: hexane/EtOAc=90/10. Colorless oil, 3 mg, 12% yield.

^{1}H NMR (400 MHz, CD_3CN) δ 8.73 (t, *J* = 1.4 Hz, 1H), 8.66 (dd, *J* = 8.0, 1.3 Hz, 1H). **^{19}F NMR** (376 MHz, CD_3CN) δ -72.1 – -72.2 (m, 1F).

The recorded spectral data are in agreement with those reported in literature.[40]

Ethyl 5-fluoropyrazine-2-carboxylate (3.77)

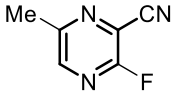


The title compound was prepared according to General Procedure 10, using 1-(5-(ethoxycarbonyl)pyrazin-2-yl)pyridin-1-ium tetrafluoroborate (**3.40**) (63 mg, 0.2 mmol), KF

(23 mg, 0.4 mmol), MeCN (2 mL) and a reaction time of 72 h. Flash column chromatography conditions: hexane/EtOAc = 90/10. White solid, 8 mg, 24% yield.

^{1}H NMR (600 MHz, $CDCl_3$) δ 8.98 (t, *J* = 1.4 Hz, 1H), 8.54 (dd, *J* = 8.3, 1.3 Hz, 1H), 4.51 (q, *J* = 7.1 Hz, 2H), 1.46 (t, *J* = 7.1 Hz, 3H). **^{19}F NMR** (565 MHz, $CDCl_3$) δ -73.6 (d, *J* = 8.0 Hz). **^{13}C NMR** (151 MHz, $CDCl_3$) δ 163.0, 161.5 (d, *J* = 260.0 Hz), 144.5 (d, *J* = 11.1 Hz), 141.5 (d, *J* = 4.5 Hz), 133.6 (d, *J* = 38.5 Hz), 62.7, 14.4. **HRMS** (ESI-TOF) calculated for $C_7H_8FN_2O_2$ ($[M+H]^+$): 171.0564, found: 171.0564. **IR** (thin layer film) 1749, 1729, 1653, 1550, 1474, 1374, 1341, 1309, 1283, 1190, 1136, 1027, 912, 866, 801, 775, 736, 647. **MP** 34 °C.

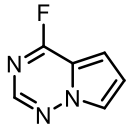
3-Fluoro-6-methylpyrazine-2-carbonitrile (3.78)



The title compound was prepared according to General Procedure 10, using 1-(3-cyano-5-methylpyrazin-2-yl)pyridin-1-ium tetrafluoroborate (**3.41**) (57 mg, 0.2 mmol), KF (23 mg, 0.4 mmol), MeCN (2 mL) and a reaction time of 16.5 h. Flash column chromatography conditions: hexane/EtOAc = 90/10. White solid, 18 mg, 66% yield.

^{1}H NMR (600 MHz, $CDCl_3$) δ 8.30 (s, 1H), 2.68 – 2.61 (d, *J* = 0.7 Hz, 3H). **^{19}F NMR** (565 MHz, $CDCl_3$) δ -76.9 (s). **^{13}C NMR** (151 MHz, $CDCl_3$) δ 159.8 (d, *J* = 258.6 Hz), 153.2 (d, *J* = 4.9 Hz), 145.1 (d, *J* = 8.7 Hz), 117.6 (d, *J* = 29.9 Hz), 112.2 (d, *J* = 9.2 Hz), 20.7 (d, *J* = 2.5 Hz). **HRMS** (GC-EI) calculated for $C_6H_4FN_3$ ($[M]^+$): 137.0384, found: 137.0389. **IR** (thin layer film) 2928, 2247, 1460, 1366, 1299, 1195, 1183, 1146, 952, 788, 740, 652, 635. **MP** 49–53 °C.

4-Fluoropyrrolo[2,1-*f*][1,2,4]triazine (3.79)

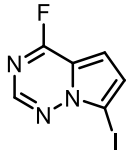


The title compound was prepared according to General Procedure 10, using 1-(pyrrolo[2,1-*f*][1,2,4]triazin-4-yl)pyridin-1-ium tetrafluoroborate (**3.46**) (227 mg, 0.8 mmol), KF (93 mg, 0.2

mmol), MeCN (8 mL) and a reaction time of 17 h. Flash column chromatography conditions: pentane/EtOAc = 95/5. Colorless oil, 67 mg, 61% yield.

^{1}H NMR (500 MHz, $CDCl_3$) δ 8.12 (s, 1H), 7.91 (ddd, *J* = 3.2, 2.5, 1.4 Hz, 1H), 6.99 – 6.90 (m, 2H). **^{19}F NMR** (471 MHz, $CDCl_3$) δ -62.8 (s). **^{13}C NMR** (126 MHz, $CDCl_3$) δ 162.2 (d, *J* = 253.9 Hz), 145.9 (d, *J* = 17.3 Hz), 121.9, 114.6 (d, *J* = 1.3 Hz), 113.3 (d, *J* = 49.0 Hz), 103.7 (d, *J* = 5.4 Hz). **HRMS** (ESI-TOF) calculated for $C_6H_5FN_3$ ($[M+H]^+$): 138.0462, found: 138.0461. **IR** (neat) 1622, 1524, 1476, 1433, 1361, 1337, 1264, 1229, 1148, 1090, 1059, 1019, 888, 745, 721, 695.

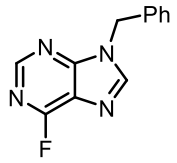
4-Fluoro-7-iodopyrrolo[2,1-f][1,2,4]triazine (3.80)



Prepared by S. Ortalli. The title compound was prepared according to General Procedure 10, using 1-(7-iodopyrrolo[2,1-*f*][1,2,4]triazin-4-yl)pyridin-1-ium tetrafluoroborate (**3.47**) (82 mg, 0.2 mmol), KF (23 mg, 0.4 mmol), MeCN (2 mL) and a reaction time of 16 h. Flash column chromatography conditions: EtOAc/pentane = gradient 0/100 to 4/96. White solid, 46 mg, 87% yield.

^{1}H NMR (500 MHz, $CDCl_3$) δ 8.28 (s, 1H), 7.13 (d, *J* = 4.6 Hz, 1H), 7.06 (d, *J* = 4.7 Hz, 1H). **^{19}F NMR** (471 MHz, $CDCl_3$) δ -65.2 (s). **^{13}C NMR** (126 MHz, $CDCl_3$) δ 161.5 (d, *J* = 254.8 Hz), 146.3 (d, *J* = 17.3 Hz), 123.1 (d, *J* = 1.8 Hz), 116.4 (d, *J* = 49.5 Hz), 105.7 (d, *J* = 5.4 Hz), 73.4. **HRMS** (ESI-TOF) calculated for $C_6H_4FIN_3$ ($[M+H]^+$): 263.9429, found: 263.9426. **IR** (neat) 3103, 2926, 2359, 1839, 1728, 1616, 1518, 1466, 1435, 1389, 1347, 1317, 1261, 1191, 1134, 1099, 1029, 926, 905, 887, 788, 720, 667, 642, 615. **MP** 113–115 °C.

9-Benzyl-6-fluoro-9*H*-purine (3.82)

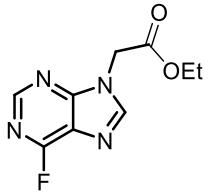


The title compound was prepared according to General Procedure 10, using 1-(9-benzyl-9*H*-purin-6-yl)pyridin-1-ium tetrafluoroborate (**3.49**) (75 mg, 0.2 mmol), KF (23 mg, 0.4 mmol), MeCN (2 mL) and a reaction time of 16 h. Flash column chromatography conditions: pentane/EtOAc = 80/20. Yellow solid, 35 mg, 75% yield.

^{1}H NMR (500 MHz, $CDCl_3$) δ 8.67 (s, 1H), 8.08 (s, 1H), 7.41 – 7.29 (m, 5H), 5.47 (s, 2H). **^{19}F NMR** (471 MHz, $CDCl_3$) δ -69.7 (s). **^{13}C NMR** (126 MHz, $CDCl_3$) δ 160.0 (d, *J* = 260.8 Hz), 155.8 (d, *J* = 11.4 Hz), 152.2 (d, *J* = 14.2 Hz), 144.9 (d, *J* = 3.1 Hz), 134.7, 129.4, 129.0, 128.1, 120.3 (d, *J* = 29.0 Hz), 48.2. **HRMS** (ESI-TOF) calculated for $C_{12}H_{10}FN_4$ ($[M+H]^+$): 229.0884, found: 229.0881.

The recorded spectral data are in agreement with those reported in literature.[39]

Ethyl 2-(6-fluoro-9*H*-purin-9-yl)acetate (3.83)

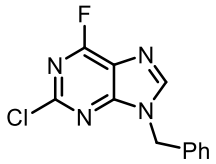


The title compound was prepared according to General Procedure 10, using 1-(9-(2-ethoxy-2-oxoethyl)-9*H*-purin-6-yl)pyridin-1-ium tetrafluoroborate (**3.50**) (93 mg, 0.25 mmol), KF (29 mg, 0.50 mmol), MeCN (2.5 mL) and a reaction time of 16 h. Flash column chromatography conditions: pentane/EtOAc=gradient 90/10 to 60/40. Yellow solid, 46 mg, 82% yield.

^{1}H NMR (600 MHz, $CDCl_3$) δ 8.64 (s, 1H), 8.20 (s, 1H), 5.08 (s, 2H), 4.28 (q, *J* = 7.1 Hz, 2H), 1.31 (t, *J* = 7.2 Hz, 3H). **^{19}F NMR** (565 MHz, $CDCl_3$) δ -69.5 (s). **^{13}C NMR** (151 MHz, $CDCl_3$) δ 166.6, 160.0 (d, *J* = 261.0 Hz), 155.8 (d, *J* = 11.4 Hz), 152.4 (d, *J* = 14.2 Hz), 145.4, 119.9 (d, *J* = 29.4 Hz), 62.8, 44.8, 14.2. **HRMS** (ESI-TOF) calculated for $C_9H_{10}FN_4O_2$ ($[M+H]^+$): 225.0782, found:

225.0781. **IR** (thin layer film) 1751, 1699, 1623, 1576, 1515, 1474, 1459, 1416, 1380, 1347, 1302, 1254, 1225, 1173, 1019, 969, 883, 795, 778, 642, 623. **MP** 83 °C.

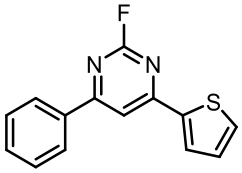
9-Benzyl-2-chloro-6-fluoro-9*H*-purine (3.84)



The title compound was prepared according to General Procedure 10, using 1-(9-benzyl-2-chloro-9*H*-purin-6-yl)pyridin-1-ium tetrafluoroborate (**3.51**) (82 mg, 0.2 mmol), KF (23 mg, 0.4 mmol), MeCN (2 mL) and a reaction time of 5 h. Flash column chromatography conditions: pentane/EtOAc = 75/25. Yellow solid, 11 mg, 21% yield.

^{1}H NMR (600 MHz, $CDCl_3$) δ 8.02 (s, 1H), 7.43 – 7.36 (m, 3H), 7.35 – 7.30 (m, 2H), 5.43 (s, 2H). **^{19}F NMR** (565 MHz, $CDCl_3$) δ -66.3 (s). **^{13}C NMR** (151 MHz, $CDCl_3$) δ 159.6 (d, *J* = 265.4 Hz), 157.0 (d, *J* = 11.6 Hz), 152.9 (d, *J* = 15.9 Hz), 145.5 (d, *J* = 3.3 Hz), 134.2, 129.6, 129.3, 128.3, 119.3 (d, *J* = 27.7 Hz), 48.3. **HRMS** (ESI-TOF) calculated for $C_{12}H_9ClFN_4$ ($[M+H]^+$): 263.0494, found: 263.0498. **IR** (thin layer film) 1622, 1585, 1564, 1511, 1457, 1429, 1411, 1366, 1324, 1308, 1259, 1221, 1202, 1180, 1145, 1029, 925, 809, 787, 737, 723, 698, 675, 639, 618. **MP** 102–103 °C.

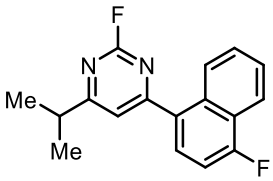
2-Fluoro-4-phenyl-6-(thiophen-2-yl)pyrimidine (3.86)



The title compound was prepared according to General Procedure 10, using 1-(4-phenyl-6-(thiophen-2-yl)pyrimidin-2-yl)pyridin-1-ium tetrafluoroborate (**3.52**) (121 mg, 0.3 mmol), KF (35 mg, 0.6 mmol), MeCN (3 mL) and a reaction time of 16 h. Flash column chromatography conditions: pentane/EtOAc=90/10. Off-white to yellow solid, 18 mg, 23% yield.

^{1}H NMR (400 MHz, $CDCl_3$) δ 8.17 – 8.11 (m, 2H), 7.93 (dd, *J* = 3.8, 1.2 Hz, 1H), 7.86 (d, *J* = 4.0 Hz, 1H), 7.60 (dd, *J* = 5.0, 1.1 Hz, 1H), 7.58 – 7.50 (m, 3H), 7.21 (dd, *J* = 5.0, 3.8 Hz, 1H). **^{19}F NMR** (376 MHz, $CDCl_3$) δ -44.7 (d, *J* = 4.2 Hz). **^{13}C NMR** (101 MHz, $CDCl_3$) δ 169.1 (d, *J* = 12.8 Hz), 163.8 (d, *J* = 13.1 Hz), 163.7 (d, *J* = 216.2 Hz), 141.1, 135.6, 131.9, 131.3, 129.2, 129.0, 128.8, 127.6, 108.8 (d, *J* = 4.5 Hz). **HRMS** (ESI-TOF) calculated for $C_{14}H_{10}FN_2S$ ($[M+H]^+$): 257.0543, found: 257.0543. **IR** (neat) 1729, 1594, 1578, 1530, 1514, 1499, 1454, 1443, 1422, 1361, 1334, 1304, 1244, 1215, 1099, 1077, 1044, 1002, 991, 925, 863, 841, 781, 766, 719, 704, 690, 656, 632. **MP** 125 °C.

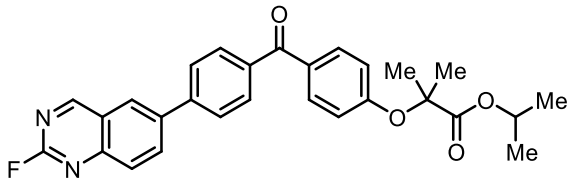
2-Fluoro-4-(4-fluoronaphthalen-1-yl)-6-isopropylpyrimidine (3.87)



The title compound was prepared according to General Procedure 10, using 1-(4-(4-fluoronaphthalen-1-yl)-6-isopropylpyrimidin-2-yl)pyridin-1-ium tetrafluoroborate (**3.53**) (59 mg, 0.2 mmol), KF (23 mg, 0.4 mmol), MeCN (2 mL) and a reaction time of 16 h. Flash column chromatography conditions: pentane/EtOAc = 80/20. Off-white solid, 7 mg, 12% yield.

^{1}H NMR (500 MHz, $CDCl_3$) δ 8.28 – 8.22 (m, 1H), 8.23 – 8.19 (m, 1H), 7.67 (dd, *J* = 8.0, 5.4 Hz, 1H), 7.63 (dt, *J* = 6.4, 3.4 Hz, 2H), 7.39 (d, *J* = 4.0 Hz, 1H), 7.26 – 7.22 (m, 1H), 3.13 (hept, *J* = 6.9 Hz, 1H), 1.39 (d, *J* = 6.9 Hz, 6H).**^{19}F NMR** (471 MHz, $CDCl_3$) δ -44.8 (d, *J* = 3.5 Hz, 1F), -118.35 – -118.40 (m, 1F). **^{13}C NMR** (126 MHz, $CDCl_3$) δ 181.4 (d, *J* = 11.6 Hz), 170.3 (d, *J* = 12.2 Hz), 163.1 (d, *J* = 217.7 Hz), 160.3 (d, *J* = 256.8 Hz), 132.1 (d, *J* = 5.1 Hz), 131.1 (d, *J* = 4.5 Hz), 128.7 (d, *J* = 9.2 Hz), 128.4, 126.9 (d, *J* = 2.1 Hz), 125.0 (d, *J* = 2.7 Hz), 124.2 (d, *J* = 16.3 Hz), 121.3 (d, *J* = 6.1 Hz), 116.9 (d, *J* = 4.7 Hz), 109.2 (d, *J* = 20.8 Hz), 36.2, 21.8. **HRMS** (ESI-TOF) calculated for $C_{17}H_{15}F_2N_2$ ($[M+H]^+$): 285.1198, found: 285.1195. **IR** (thin layer film) 1595, 1530, 1471, 1427, 1373, 1307, 1265, 1240, 1054, 1007, 969, 913, 833, 793, 765, 739, 707, 609. **MP** 159 °C.

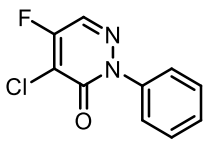
Isopropyl 2-(4-(4-(2-fluoroquinazolin-6-yl)benzoyl)phenoxy)-2-methylpropanoate (3.88)



The title compound was prepared according to General Procedure 10, 1-(6-(4-(4-((1-isopropoxy-2-methyl-1-oxopropan-2-yl)oxy)benzoyl)phenyl)quinazolin-2-yl)pyridin-1-ium tetrafluoroborate (**3.54**) (124 mg, 0.2 mmol), KF (23 mg, 0.4 mmol), MeCN (2 mL) and a reaction time of 16 h. Flash column chromatography conditions: pentane/EtOAc = gradient 90/10 to 75/25. Yellow solid, 60 mg, 63% yield.

^{1}H NMR (600 MHz, $CDCl_3$) δ 9.44 (d, *J* = 2.1 Hz, 1H), 8.30 – 8.20 (m, 2H), 8.08 (d, *J* = 8.7 Hz, 1H), 7.94 – 7.88 (m, 2H), 7.84 – 7.77 (m, 4H), 6.94 – 6.87 (m, 2H), 5.10 (hept, *J* = 6.3 Hz, 1H), 1.67 (s, 6H), 1.21 (d, *J* = 6.3 Hz, 6H).**^{19}F NMR** (565 MHz, $CDCl_3$) δ -45.6 (s).**^{13}C NMR** (151 MHz, $CDCl_3$) δ 194.9, 173.3, 165.8 (d, *J* = 14.1 Hz), 160.5 (d, *J* = 219.6 Hz), 159.9, 152.0 (d, *J* = 13.1 Hz), 142.6, 139.5 (d, *J* = 2.4 Hz), 138.1, 135.3, 132.2, 130.8, 130.6, 128.4 (d, *J* = 2.6 Hz), 127.4, 125.4, 124.2 (d, *J* = 3.1 Hz), 117.4, 79.6, 69.5, 25.5, 21.7. **HRMS** (ESI-TOF) calculated for $C_{28}H_{26}FN_2O_4$ ($[M+H]^+$): 473.1871, found: 473.1865. **IR** (thin layer film) 1731, 1651, 1588, 1506, 1433, 1406, 1375, 1350, 1291, 1251, 1180, 1148, 1103, 974, 927, 836, 793, 770, 733, 688, 665.**MP** 121–122 °C.

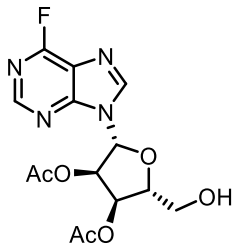
4-Chloro-5-fluoro-2-phenylpyridazin-3(2*H*)-one (3.89)



The title compound was prepared according to General Procedure 10, using 1- (5-chloro-6-oxo-1-phenyl-1,6-dihydropyridazin-4-yl)pyridin-1-ium tetrafluoroborate (**3.55**) (74 mg, 0.2 mmol), KF (23 mg, 0.4 mmol), MeCN (2 mL) and a reaction time of 16 h. Flash column chromatography conditions: pentane/EtOAc = 90/10. White solid, 13 mg, 29% yield.

^{1}H NMR (400 MHz, $CDCl_3$) δ 7.99 (s, 1H), 7.60–7.39 (m, 5H). **^{19}F NMR** (376 MHz, $CDCl_3$) δ -111.0 (s). **^{13}C NMR** (101 MHz, $CDCl_3$) δ 158.5 (d, *J* = 6.5 Hz), 157.7 (d, *J* = 280.5 Hz), 141.0, 129.8 (d, *J* = 28.3 Hz), 129.1, 129.1, 125.4, 120.0 (d, *J* = 9.1 Hz). **HRMS** (ESI-TOF) calculated for $C_{10}H_7{}^{35}ClFN_2O$ ($[M+H]^+$): 225.0225, found: 225.0227. **IR** (neat) 1655, 1624, 1598, 1517, 1495, 1458, 1388, 1320, 1278, 1197, 1146, 1078, 1049, 1005, 956, 901, 834, 760, 741, 687, 659. **MP** 138–141 °C.

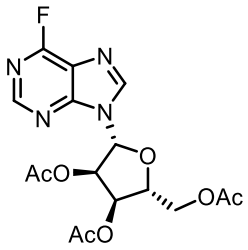
(2*R*,3*R*,4*R*,5*R*)-2-(6-Fluoro-9*H*-purin-9-yl)-5-(hydroxymethyl)tetrahydrofuran-3,4-diyl diacetate (3.90)



The title compound was prepared according to General Procedure 10, using 1-(9-((2*R*,3*R*,4*R*,5*R*)-3,4-diacetoxy-5-(hydroxymethyl)tetrahydrofuran-2-yl)-9*H*-purin-6-yl)pyridin-1-ium tetrafluoroborate (**3.56**) (102 mg, 0.2 mmol), KF (23 mg, 0.4 mmol), MeCN (2 mL) and a reaction time of 2 h. Flash column chromatography conditions: gradient pentane/EtOAc = 60/40 to 40/60. Yellow solid, 43 mg, 61% yield.

^{1}H NMR (600 MHz, $CDCl_3$) δ 8.69 (s, 1H), 8.21 (s, 1H), 6.14 (d, *J* = 7.5 Hz, 1H), 6.00 (dd, *J* = 7.5, 5.4 Hz, 1H), 5.69 (dd, *J* = 5.4, 1.6 Hz, 1H), 4.39 (q, *J* = 1.8 Hz, 1H), 4.00 (dd, *J* = 12.9, 1.9 Hz, 1H), 3.89 (dd, *J* = 12.9, 1.8 Hz, 1H), 2.18 (s, 3H), 2.02 (s, 3H). **^{19}F NMR** (565 MHz, $CDCl_3$) δ -66.7 (s). **^{13}C NMR** (151 MHz, $CDCl_3$) δ 169.8, 169.2, 160.4 (d, *J* = 262.7 Hz), 154.5 (d, *J* = 11.3 Hz), 152.2 (d, *J* = 14.8 Hz), 144.6 (d, *J* = 2.8 Hz), 122.3 (d, *J* = 29.0 Hz), 88.5, 86.3, 72.9, 72.5, 62.6, 20.9, 20.4. **HRMS** (ESI-TOF) calculated for $C_{14}H_{16}FN_4O_6$ ($[M+H]^+$): 355.1048, found: 355.1049. **IR** (thin layer film) 3381, 2980, 1752, 1624, 1578, 1505, 1479, 1466, 1418, 1372, 1353, 1326, 1289, 1208, 1140, 1109, 1084, 1049, 1025, 986, 951, 936, 913, 890, 859, 824, 794, 764, 642, 618. **MP** 101–102 °C.

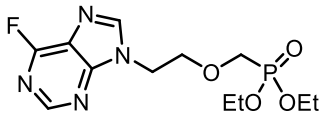
(2*R*,3*R*,4*R*,5*R*)-2-(Acetoxymethyl)-5-(6-fluoro-9*H*-purin-9-yl)tetrahydrofuran-3,4-diyl diacetate (3.91)



The title compound was prepared according to General Procedure 10, using 1-(9-((2*R*,3*R*,4*R*,5*R*)-3,4-diacetoxy-5-(acetoxymethyl)tetrahydrofuran-2-yl)-9*H*-purin-6-yl)pyridin-1-ium tetrafluoroborate (**3.57**) (82 mg, 0.15 mmol), KF (18 mg, 0.3 mmol), MeCN (1.5 mL) and a reaction time of 3 h. Flash column chromatography conditions: pentane/EtOAc = 50/50. Yellow sticky oil, 52 mg, 87% yield.

^{1}H NMR (600 MHz, $CDCl_3$) δ 8.67 (s, 1H), 8.26 (s, 1H), 6.24 (d, *J* = 5.1 Hz, 1H), 5.95 (t, *J* = 5.3 Hz, 1H), 5.65 (t, *J* = 5.1 Hz, 1H), 4.51 – 4.43 (m, 2H), 4.39 (dd, *J* = 12.3, 4.5 Hz, 1H), 2.16 (s, 3H), 2.13 (s, 3H), 2.09 (s, 3H). **^{19}F NMR** (565 MHz, $CDCl_3$) δ -68.4 (s). **^{13}C NMR** (151 MHz, $CDCl_3$) δ 170.4, 169.7, 169.5, 160.1 (d, *J* = 261.0 Hz), 155.1 (d, *J* = 10.9 Hz), 152.5 (d, *J* = 14.2 Hz), 143.5, 121.3 (d, *J* = 28.9 Hz), 87.1, 80.7, 73.3, 70.6, 63.1, 20.9, 20.7, 20.5. **HRMS** (ESI-TOF) calculated for $C_{16}H_{18}FN_4O_7$ ($[M+H]^+$): 397.1154, found: 397.1154. **IR** (thin layer film) 1749, 1623, 1575, 1506, 1461, 1378, 1224, 1176, 1066, 1021, 954, 795, 735, 644.

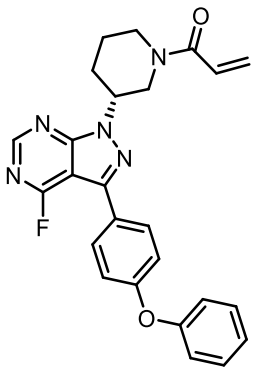
Diethyl ((2-(6-fluoro-9*H*-purin-9-yl)ethoxy)methyl)phosphonate (3.92)



The title compound was prepared according to General Procedure 10, using 1-(9-(2-((diethoxyphosphoryl)methoxy)ethyl)-9*H*-purin-6-yl)pyridin-1-ium tetrafluoroborate (**3.60**) (59 mg, 0.15 mmol), KF (18 mg, 0.3 mmol), MeCN (1.5 mL) and a reaction time of 3 h. Flash column chromatography conditions: EtOAc/MeOH = gradient 100/0 to 90/10. Light brown solid, 34 mg, 68% yield.

^{1}H NMR (600 MHz, $CDCl_3$) δ 8.63 (s, 1H), 8.35 (s, 1H), 4.57 – 4.51 (m, 2H), 4.10 (dq, *J* = 8.3, 7.1 Hz, 4H), 4.02 – 3.97 (m, 2H), 3.79 (d, *J* = 8.2 Hz, 2H), 1.29 (t, *J* = 7.1 Hz, 6H). **^{19}F NMR** (471 MHz, $CDCl_3$) δ -70.0 (s). **^{31}P NMR** (243 MHz, $CDCl_3$) δ 20.3 (hept, *J* = 8.2 Hz). **^{13}C NMR** (151 MHz, $CDCl_3$) δ 159.8 (d, *J* = 260.5 Hz), 155.5 (d, *J* = 11.4 Hz), 152.0 (d, *J* = 14.2 Hz), 146.1 (d, *J* = 2.7 Hz), 119.7 (d, *J* = 29.4 Hz), 70.8 (d, J_{CP} = 9.8 Hz), 65.4 (d, J_{CP} = 166.8 Hz), 62.7 (d, J_{CP} = 7.1 Hz), 44.3, 16.6 (d, J_{CP} = 5.7 Hz). **HRMS** (ESI-TOF) calculated for $C_{12}H_{19}FN_4O_4P$ ($[M+H]^+$): 333.1123, found: 333.1118. **IR** (thin layer film) 1623, 1573, 1511, 1475, 1462, 1409, 1344, 1301, 1221, 1165, 1124, 1027, 970, 794, 733, 646, 616. **MP** 59–61 °C.

(*R*)-1-(3-(4-Fluoro-3-(4-phenoxyphenyl)-1*H*-pyrazolo[3,4-*d*]pyrimidin-1-yl)piperidin-1-yl)prop-2-en-1-one (3.93)

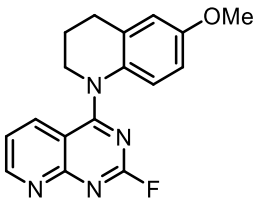


The title compound was prepared according to General Procedure 10, using (*R*)-1-(1-(1-acryloylpiperidin-3-yl)-3-(4-phenoxyphenyl)-1*H*-pyrazolo[3,4-*d*]pyrimidin-4-yl)pyridin-1-ium tetrafluoroborate (**3.61**) (118 mg, 0.2 mmol), KF (23 mg, 0.4 mmol), MeCN (2 mL) and a reaction time of 16 h. Flash column chromatography conditions: pentane/Et_2O= gradient 60/40 to 100/0. Off-white solid, 55 mg, 62% yield.

^{1}H NMR (600 MHz, $CDCl_3$) δ 8.66 (s, 1H), 7.98 (d, *J* = 8.5 Hz, 2H), 7.39 (td, *J* = 7.5, 1.9 Hz, 2H), 7.17 (t, *J* = 7.4 Hz, 1H), 7.14 – 7.11 (m, 2H), 7.09 (dt, *J* = 9.0, 1.7 Hz, 2H), 6.67 – 6.47 (m, 1H), 6.31 (t, *J* = 19.5 Hz, 1H), 5.70 (m, 1H), 4.99 (s, 1H), 4.93 – 4.52 (m, 1H), 4.26 – 3.98 (m, 1H), 3.89 – 3.39 (m, 1H), 3.33 – 2.91 (m, 1H), 2.52 – 2.33 (m, 1H), 2.32 – 2.25 (m, 1H), 2.10 – 2.00 (m, 1H), 1.82 – 1.71 (m, 1H). **^{19}F NMR** (565 MHz, $CDCl_3$) δ -51.0 (s), -51.4 (s). **^{13}C NMR** (151 MHz, $CDCl_3$) δ 165.9, 162.9 (d, *J* = 257.2 Hz), 158.9 (br m), 157.8 (d, *J* = 9.5 Hz), 156.6 (br

m), 155.1 (br m), 143.4 (br m), 130.1, 129.7 (d, *J* = 4.9 Hz), 128.4, 127.6, 126.1 (br), 125.8 (br), 124.1, 119.7, 118.8, 54.5, 53.5, 50.1, 46.2, 46.1, 42.3, 30.4, 30.2, 25.4, 23.9. *note:* signal splitting/broad signals observed due to the piperidine ring in all NMR experiments. **HRMS** (ESI-TOF) calculated for $C_{25}H_{23}FN_5O_2$ ($[M+H]^+$): 444.1830, found: 444.1829. **IR** (neat) 1650, 1608, 1548, 1523, 1489, 1439, 1419, 1366, 1343, 1287, 1236, 1200, 1169, 1155, 1130, 1096, 1025, 928, 870, 851, 794, 755, 722, 694, 659, 644, 636. **MP** 55 °C.

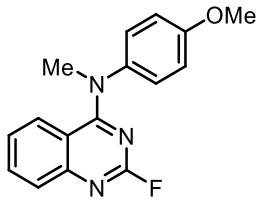
2-Fluoro-4-(6-methoxy-3,4-dihydroquinolin-1(2*H*)-yl)pyrido[2,3-*d*]pyrimidine (3.98)



The title compound was prepared according to General Procedure 10, using 1-(4-(6-methoxy-3,4-dihydroquinolin-1(2*H*)-yl)pyrido[2,3-d]pyrimidin-2-yl)pyridin-1-ium tetrafluoroborate (**3.58**) (91 mg, 0.2 mmol), KF (23 mg, 0.4 mmol), MeCN (2 mL) and a reaction time of 17 h. Flash column chromatography conditions: gradient pentane/EtOAc = 60/40 to 50/50. Yellow solid, 14 mg, 25% yield.

^{1}H NMR (600 MHz, $CDCl_3$) δ 8.91 (dd, *J* = 4.4, 1.9 Hz, 1H), 7.67 (dd, *J* = 8.5, 1.9 Hz, 1H), 7.01 (dd, *J* = 8.4, 4.3 Hz, 1H), 6.84 (d, *J* = 2.9 Hz, 1H), 6.78 (d, *J* = 8.8 Hz, 1H), 6.60 (dd, *J* = 8.8, 2.9 Hz, 1H), 4.08 (t, *J* = 6.9 Hz, 2H), 3.83 (s, 3H), 2.85 (t, *J* = 6.6 Hz, 2H), 2.12 (pent, *J* = 6.7 Hz, 2H). **^{19}F NMR** (565 MHz, $CDCl_3$) δ -41.8 (s). **^{13}C NMR** (151 MHz, $CDCl_3$) δ 164.9 (d, *J* = 19.6 Hz), 162.3 (d, *J* = 213.8 Hz), 162.2 (d, *J* = 19.1 Hz), 157.7, 156.3, 135.5, 135.0, 133.9, 123.1, 119.1, 113.8, 112.5, 110.0 (d, *J* = 3.8 Hz), 55.5, 47.7, 27.1, 24.1. **HRMS** (ESI-TOF) calculated for $C_{17}H_{16}FN_4O$ ($[M+H]^+$): 311.1303, found: 311.1314. **IR** (thin layer film) 1576, 1503, 1450, 1378, 1360, 1322, 1276, 1238, 1204, 1165, 1059, 1037, 998, 912, 789, 739, 647. **MP** 213-214 °C.

2-Fluoro-*N*-(4-methoxyphenyl)-N-methylquinazolin-4-amine (3.99)



The title compound was prepared according to General Procedure 10, using 1-(4-((4-methoxyphenyl)(methyl)amino)quinazolin-2-yl)pyridin-1-ium tetrafluoroborate (**3.59**) (72 mg, 0.167 mmol), KF (19 mg, 0.335 mmol), MeCN (1.6 mL) and a reaction time of 15 h. Flash column chromatography conditions: pentane/EtOAc = 60/40. Beige solid, 7 mg, 15% yield.

^{1}H NMR (600 MHz, $CDCl_3$) δ 7.83 (d, *J* = 8.4 Hz, 1H), 7.58 (t, *J* = 7.7 Hz, 1H), 7.17 (dd, *J* = 8.9, 0.9 Hz, 2H), 7.02 – 6.94 (m, 3H), 6.91 (d, *J* = 8.6 Hz, 1H), 3.87 (s, 3H), 3.64 (s, 3H). **^{19}F NMR** (565 MHz, $CDCl_3$) δ -47.9 (s). **^{13}C NMR** (151 MHz, $CDCl_3$) δ 164.8 (d, *J* = 18.5 Hz), 159.3, 158.9 (d, *J* = 214.7 Hz), 151.5, 139.4, 133.4, 127.7, 126.8, 126.7, 124.6, 115.8, 114.6, 55.8, 43.9. **HRMS** (ESI-TOF) calculated for $C_{16}H_{15}FN_3O$ ($[M+H]^+$): 284.1194, found: 284.1201. **IR** (thin layer film) 1587, 1558, 1509, 1473, 1458, 1388, 1252, 1153, 1072, 954, 768. **MP** 119 °C.

4.4.2. Radiochemistry

Radiochemistry experiments in this section were conducted by J. Ford, with assistance from J. Sap, S. Ortalli and Z. Chen.

4.4.2.1. Manual Radiochemistry Experiments

Manual [^{18}F]KF elution and drying

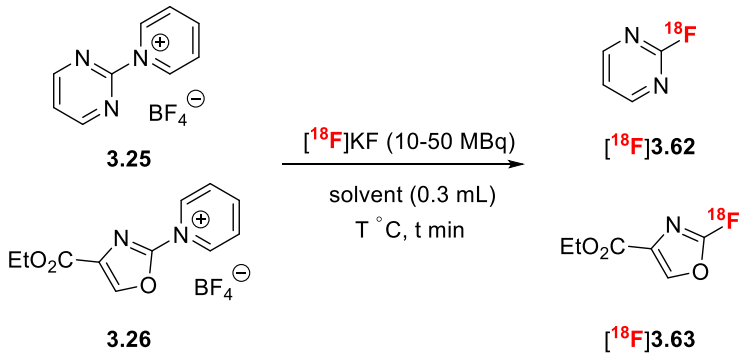
Procedure:

This procedure was used for the preparation of [^{18}F]KF solutions used in reaction optimisation, reaction scope and robustness screening experiments described in Chapter 3.

[^{18}F]fluoride was separated from ^{18}O-enriched-water using an anion exchange cartridge (Waters Sep-Pak AccellPlus QMA Carbonate Plus Light Cartridge, activated with H_2O (10 mL) prior to use) and released with a solution of K_{222} (7.5 mg) and K_2CO_3 (1.5 mg) in MeCN/H_2O (0.75 mL, 4:1 v/v). The solution was dried over a period of 20 min by azeotropic drying using dry MeCN (3 x 0.7 mL) under a flow of N_2 at 110 °C.

Optimisation experiments for the ^{18}F-fluorination of heteroaryl pyridinium salts

Procedure:



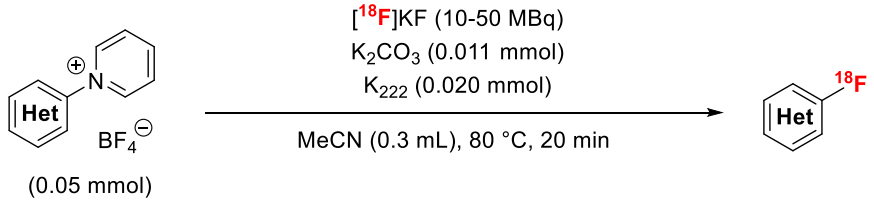
3.25 **3.26** [^{18}F]**3.62** [^{18}F]**3.63**

A 3 mL v-vial, capped with a septum, was charged with model heteroaryl pyridinium tetrafluoroborate substrate (**3.25** or **3.26**), K_2CO_3 (1.5 mg, 0.011 mmol), K_{222} (7.5 mg, 0.020 mmol), if these were to be added, and a stirrer bar. To this vial was added solvent (0.3 mL), [^{18}F]KF (10-50 MBq in 0.05-0.10 mL MeCN for screening reactions, prepared as described

above) was added to the vial and this mixture was heated at the relevant temperature (T °C) for the desired time (t min). Once this time had elapsed, the vial was allowed to cool to rt, before the addition of an EtOH-H_2O mixture (0.5 mL, 1:1 v/v). An aliquot of this mixture was taken and analysed by radio-HPLC (conditions A), and the radiochemical yield was determined by integration of the ^{18}F-product relative to the total peak area for all radioactive species observed.

^{18}F-Fluorination of heteroaryl pyridinium salts

General Procedure 11:

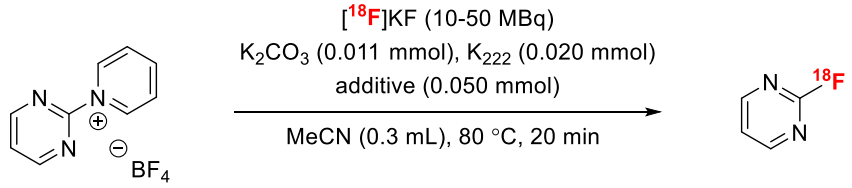


(0.05 mmol)

A 3 mL v-vial, capped with a septum, was charged with the relevant heteroaryl pyridinium tetrafluoroborate substrate (0.050 mmol), K_2CO_3 (1.5 mg, 0.011 mmol), K_{222} (7.5 mg, 0.020 mmol) and a stirrer bar. To this vial was added dry MeCN solvent (0.3 mL). [^{18}F]KF (10-50 MBq in 0.05-0.10 mL MeCN for screening reactions) prepared as described above was added to the vial and this mixture was heated at 80 °C for 20 min. Once this time had elapsed, the vial was allowed to cool to rt, before the addition of an EtOH-H_2O mixture (0.5 mL, 1:1 v/v). An aliquot of this mixture was taken and analysed by radio-HPLC (conditions A-C), and the radiochemical yield was determined by integration of the ^{18}F-product relative to the total peak area for all radioactive species observed.

Robustness screening of the ^{18}F-fluorination of heteroaryl pyridinium salts

Procedure:

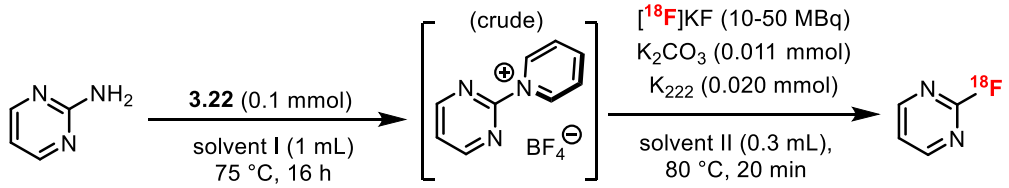


3.25 [^{18}F]**3.62**

A 3 mL v-vial, capped with a septum, was charged with **3.25** (0.050 mmol), K_2CO_3 (1.5 mg, 0.011 mmol), K_{222} (7.5 mg, 0.020 mmol), the relevant spiking additive (0.050 mmol, 1 equiv.) and a stirrer bar. To this vial was added dry MeCN solvent (0.3 mL). [^{18}F]KF (10-50 MBq in 0.05-0.1 mL MeCN for screening reactions) prepared as described above was added to the vial and this mixture was heated at 80 °C for 20 min. Once this time had elapsed, the vial was allowed to cool to rt, before the addition of an EtOH-H_2O mixture (0.5 mL, 1:1 v/v). An aliquot of this mixture was taken and analysed by radio-HPLC (conditions C), and the radiochemical yield of [^{18}F]**3.62** was determined by integration of the ^{18}F-product relative to the total peak area for all radioactive species observed. The robustness factor was calculated by dividing the RCY_{HPLC} observed in the presence of the spiking additive by the RCY_{HPLC} of the reference reaction in the absence of the spiking additive. This value was expressed as a percentage.

Optimisation of the one-pot radiofluorination of 2-aminopyrimidine

Procedure:



3.97 **3.25** [^{18}F]**3.62**

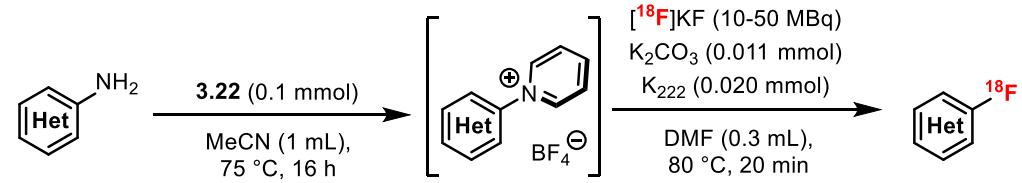
Step 1 (pyridinium salt formation): A 1.75 mL glass vial was charged with 2-aminopyrimidine (**3.97**, 0.1–0.4 mmol), pyrylium tetrafluoroborate (0.1 mmol) and a stirrer bar. Solvent (1 mL) was added and the vial was purged with N_2, before it was sealed with a screw cap. The vial was heated to 75 °C for 16 h. After this time had passed, the vial was cooled to rt and the

solvent was evaporated from the vial to dryness. The contents of the vial were dried further under high vacuum (0.1–1 mbar) for 30 min.

Step 2 (^{18}F-fluorination): A 3 mL v-vial, capped with a septum, was charged with K_2CO_3 (1.5 mg, 0.011 mmol), K_{222} (7.5 mg, 0.020 mmol) and a stirrer bar. The crude solid from the pyridinium salt formation step was dissolved in dry solvent (0.3 mL) and added to the vial. [^{18}F]KF (10-50 MBq in 0.05-0.1 mL MeCN) was added to the vial and this mixture was heated at 80 °C for 20 min. Once this time had elapsed, the vial was allowed to cool to rt, before the addition of an EtOH-H_2O mixture (0.5 mL, 1:1 v/v). An aliquot of this mixture was taken and analysed by radio-HPLC (conditions C), and the radiochemical yield was determined by integration of the ^{18}F-product relative to the total peak area for all radioactive species observed.

One-pot radiofluorination of heteroaromatic amines

Procedure:



Step 1 (pyridinium salt formation): A 1.75 mL glass vial was charged with the relevant amine substrate (0.2 mmol), pyrylium tetrafluoroborate (0.1 mmol) and a stirrer bar. MeCN (1 mL) was added and the vial was purged with N_2, before it was sealed with a screw cap. The vial was heated to 75 °C for 16 h. After this time had passed, the vial was cooled to rt and the solvent was evaporated from the vial to dryness. The contents of the vial were dried further under high vacuum (0.1–1 mbar) for 30 min.

Step 2 (^{18}F-fluorination): A 3 mL v-vial, capped with a septum, was charged with K_2CO_3 (1.5 mg, 0.011 mmol), K_{222} (7.5 mg, 0.020 mmol) and a stirrer bar. The crude solid from the pyridinium salt formation step was dissolved in dry solvent (0.3 mL) and added to the vial.

[^{18}F]KF (10-50 MBq in 0.05-0.10 mL MeCN) was added to the vial and this mixture was heated at 80 °C for 20 min. Once this time had elapsed, the vial was allowed to cool to rt, before the addition of an EtOH-H_2O mixture (0.5 mL, 1:1 v/v). An aliquot of this mixture was taken and analysed by radio-HPLC (conditions C), and the radiochemical yield was determined by integration of the ^{18}F-product relative to the total peak area for all radioactive species observed.

Elution of [^{18}F]fluoride with pyridinium tetrafluoroborates

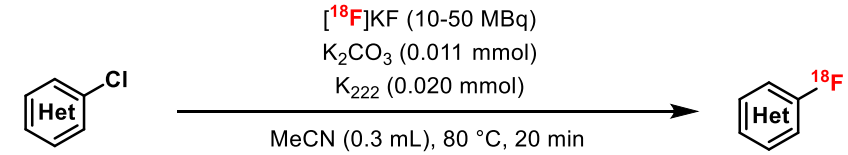
Procedure:

Step 1 (manual [^{18}F]fluoride elution): [^{18}F]Fluoride (10-50 MBq) was separated from ^{18}O-enriched-water using an anion exchange cartridge (activated with H_2O (10 mL) prior to use). The cartridge was dried by syringe with air (10 mL). The activity trapped on the cartridge was measured in a dose calibrator. The cartridge was moved to an empty vial (charged with a stirrer bar, as necessary) and eluted with a solution of the relevant pyridinium tetrafluoroborate salt in the relevant solvent. The cartridge was then dried by syringe with air (10 mL) to ensure none of the liquid remained trapped in the cartridge. The eluate was measured in a dose calibrator, as well as the activity trapped on the cartridge. Elution efficiency was thus calculated.

Step 2 (drying and reaction): Where the eluate was to be dried, this was done under a flow of N_2 at 80 °C with stirring over a period of approximately 5-10 min. Once dry, the residue was redissolved in the reaction solvent (0.3 mL). Where additives were used, these were next added as solids. The mixture was then heated at 80 °C for 20 min. Once this time had elapsed, the vial was allowed to cool to rt, before the addition of an EtOH-H_2O mixture (0.5 mL, 1:1 v/v). An aliquot of this mixture was taken and analysed by radio-HPLC (conditions C), and the radiochemical yield was determined by integration of the ^{18}F-product relative to the total peak area for all radioactive species observed.

^{18}F-Fluorination of heteroaryl chlorides

Procedure:

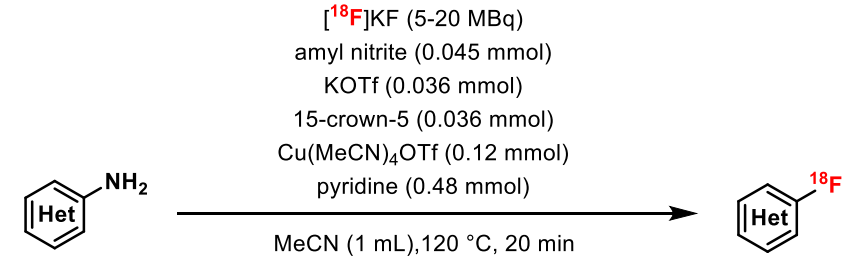


(0.05 mmol)

A 3 mL v-vial, capped with a septum, was charged with the relevant heteroaryl chloride (0.050 mmol), K_2CO_3 (1.5 mg, 0.011 mmol), K_{222} (7.5 mg, 0.020 mmol) and a stirrer bar. To this vial was added dry MeCN solvent (0.3 mL). [^{18}F]KF (10-50 MBq in 0.05-0.10 mL MeCN for screening reactions) prepared as described above was added to the vial and this mixture was heated at 80 °C for 20 min. Once this time had elapsed, the vial was allowed to cool to rt, before the addition of an EtOH-H_2O mixture (0.5 mL, 1:1 v/v). An aliquot of this mixture was taken and analysed by radio-HPLC (conditions C), and the radiochemical yield was determined by integration of the ^{18}F-product relative to the total peak area for all radioactive species observed.

^{18}F-Fluoro-Sandmeyer reaction of heteroaryl amines

Procedure:



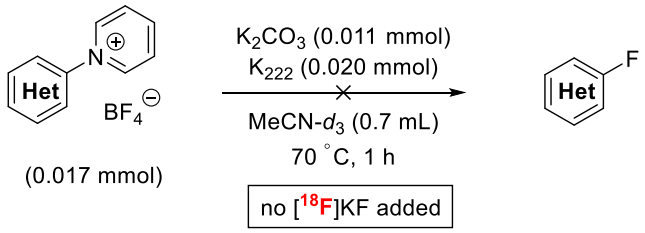
(0.03 mmol)

This procedure was adapted from a protocol disclosed by Riss and co-workers.[41] To a v-vial charged with potassium trifluoromethanesulfonate (0.036 mmol), 15-crown-5 (0.036 mmol) and a stirrer bar, was added a solution of [^{18}F]KF (5-20 MBq) in MeCN (0.05 mL). Separately, in an Eppendorf, the relevant aniline (0.03 mmol) was added. This was dissolved in MeCN (0.5 mL) and amyl nitrite (0.045 mmol) was then added with a pipette. This mixture was left to

react for 10 minutes. A solution of $Cu(MeCN)_4OTf$ (0.12 mmol) and pyridine (0.48 mmol) in MeCN (0.5 mL) was also prepared in an Eppendorf, no more than 10 minutes before the start of the reaction. Each solution was taken up in a 1 mL syringe and added sequentially to the v-vial. This mixture was then stirred at 120 °C for 20 minutes, after which time the mixture was allowed to cool to rt. A an EtOH-H_2O mixture (0.5 mL, 1:1 v/v) was added by syringe and an aliquot of the diluted reaction mixture was transferred to an HPLC vial for subsequent radio-HPLC analysis.

Stability testing of pyridinium tetrafluoroborate salts by ^{19}F NMR

Procedure:



An NMR tube was charged with the relevant heteroaryl pyridinium tetrafluoroborate (**3.25** or **3.26**) (0.017 mmol), K_2CO_3 (1.5 mg, 0.011 mmol) and K_{222} (7.5 mg, 0.020 mmol). MeCN-d_3 (0.7 mL) was added by syringe and the NMR tube was sealed with a cap. The NMR tube was placed in an oil bath and heated to 70 °C for 1 h. Once this time had elapsed, the tube was placed into an ice bath and then analysed by $\{^1H\}^{19}F$ qNMR (N=100 scans, d1 = 20 s, O1p = -100 ppm). $\{^1H\}^{19}F$ qNMR spectra for the authentic fluoroheteroarenes were also acquired in MeCN-d_3 and two spectra were superimposed for analysis of the formation of the fluoroheteroarene by degradation of the heteroaryl pyridinium tetrafluoroborate. For both **3.25** and **3.26**, no formation of the relevant fluoroheteroarene was observed.

4.4.2.2. Automated Radiochemistry Experiments

Automated radiosynthesis of heteroaryl ^{18}F-fluorides

General Procedure 12:

The automated radiosynthesis of [^{18}F]**3.62**, [^{18}F]**3.90**, [^{18}F]**3.98** and [^{18}F]**3.99** was performed with a Trasis AllInOne synthesiser using an automated program and pre-built cassette (Chapter 3, Figure 3.5). The vial in position 2 was charged with Kryptofix 222 (7.5 mg), K_2CO_3 (1.5 mg), H_2O (0.15 mL) and MeCN (0.85 mL). The vial in position 9 was charged with the relevant heteroaryl pyridinium tetrafluoroborate (0.017-0.050 mmol) and dry MeCN (1.0 mL). The solvent reservoirs (positions 8 and 17) were filled with dry MeCN (ca. 10 mL). The Waters Sep-Pak AccellPlus QMA Carbonate Plus Light Cartridge (position 5) was activated with water (10 mL) prior to use. The Waters Sep-Pak C18 Plus cartridge (position 33) was preconditioned with EtOH (10 mL), then water (10 mL).

After [^{18}F]fluoride in [^{18}O]water was received from the cyclotron, it was trapped on a Waters Sep-Pak AccellPlus QMA Carbonate Plus Light cartridge. [^{18}F]Fluoride was then eluted from the cartridge with a solution of K_{222} and K_2CO_3, and this was dried azeotropically with MeCN under a flow of air at 120 °C. Once drying was complete, the heteroaryl pyridinium tetrafluoroborate in MeCN (1 mL) was transferred to the reactor and the ^{18}F-fluorination reaction was run at 80 °C for 20 minutes. Thereafter, the mixture was diluted with water and transferred to the HPLC sample loop. The crude reaction mixture was purified by reverse-phase semi-preparative HPLC (MeCN/H_2O as eluent, Q = 4 ml/min, HPLC conditions E). The eluate was diluted with water (20 mL). This mixture was then loaded as a 1:1 mixture with additional water onto a Waters Sep-Pak C18 Plus cartridge and then washed with water (10 mL) and purged with air. The desired radiofluorinated product was eluted from the C18 cartridge with MeCN (2 mL) and transferred to a vial for analysis. The activity of the collected product was measured in a dose calibrator.

An aliquot of the isolated, chemically and radiochemically pure product was analysed in triplicate by radio-HPLC to determine A_m. (Radio-)HPLC analysis was performed under HPLC conditions C or D. The same sample was injected in triplicate, with the injected activity and time of injection recorded. The UV response corresponding to the desired radiofluorinated product was then integrated, to give the amount of non-radioactive product that was detected.

Separately, a calibration curve for the relevant authentic ^{19}F-reference was recorded by preparing samples of a range of concentrations by serial dilution. These were injected onto an HPLC (10 µL injection volume from a 1.0 mL stock, HPLC conditions C or D) and the UV response was measured by integrating the peak of interest.

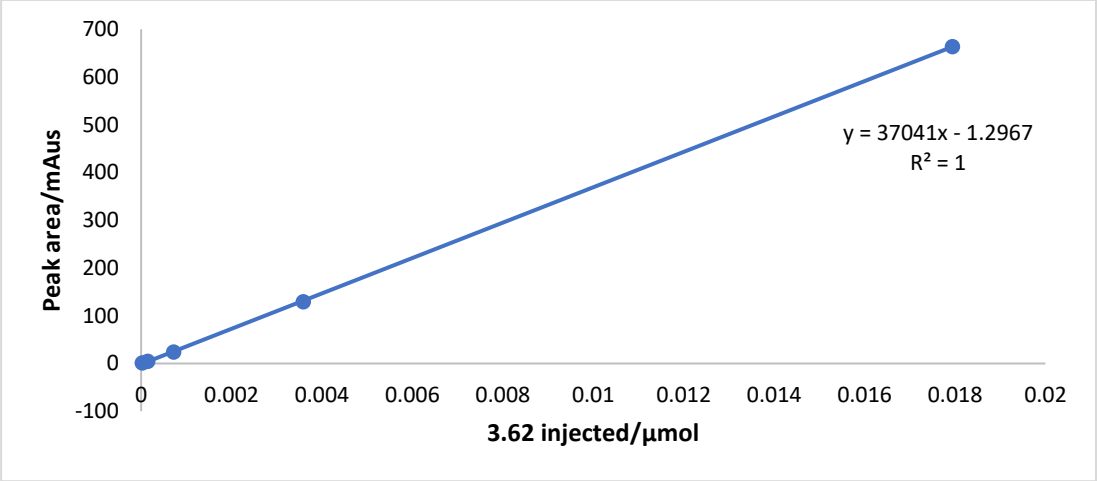
Automated radiosynthesis of [^{18}F]**3.62** (low starting activity)

General Procedure 12 was followed using **3.25** (12.2 mg, 0.05 mmol). HPLC purification was carried out using MeCN/H_2O = 35/65, v/v, as eluent, t_R([^{18}F]**3.62**) = 6 min. The product was not reformulated in this case and an aliquot of the collected HPLC eluate was taken directly for analysis.

Radiosynthetic data for [^{18}F]**3.62**:

Starting activity	**AY**	**Synthesis time**	**RCP**	A_m
48 GBq	15 GBq	55 min	>99%	12 GBq/µmol

Calibration curve for **3.62**



Prepared using HPLC conditions C.

Run 1

Measurement	**Activity injected (MBq, d.c.)**	**3.62 injected (µmol)**	**Peak area (mAu*s)**	A_m **(GBq/µmol)**
1	0.86	7.85×10^{-5}	2.9	11.0
2	0.99	7.31×10^{-5}	2.7	14.5
3	1.08	8.66×10^{-5}	3.2	12.5
			Average (*n* = 3)	12 GBq/µmol

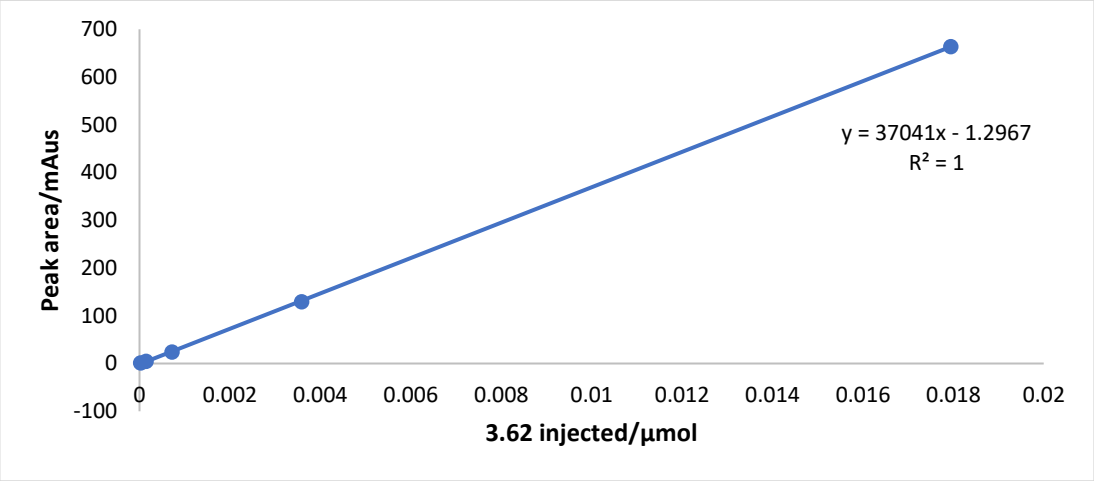
Automated radiosynthesis of [^{18}F]**3.62** (high starting activity)

General Procedure 12 was followed using **3.25** (4.1 mg, 0.017 mmol). HPLC purification was carried out using MeCN/H_2O = 35/65, v/v, as eluent, t_R([^{18}F]**3.62**) = 6 min. The product was not reformulated in this case and an aliquot of the collected HPLC eluate was taken directly for analysis.

Radiosynthetic data for [^{18}F]**3.62**:

Starting activity	**AY**	**Synthesis time**	**RCP**	A_m
140 GBq	39.7 GBq	52 min	>99%	255 GBq/µmol

Calibration curve for **3.62**

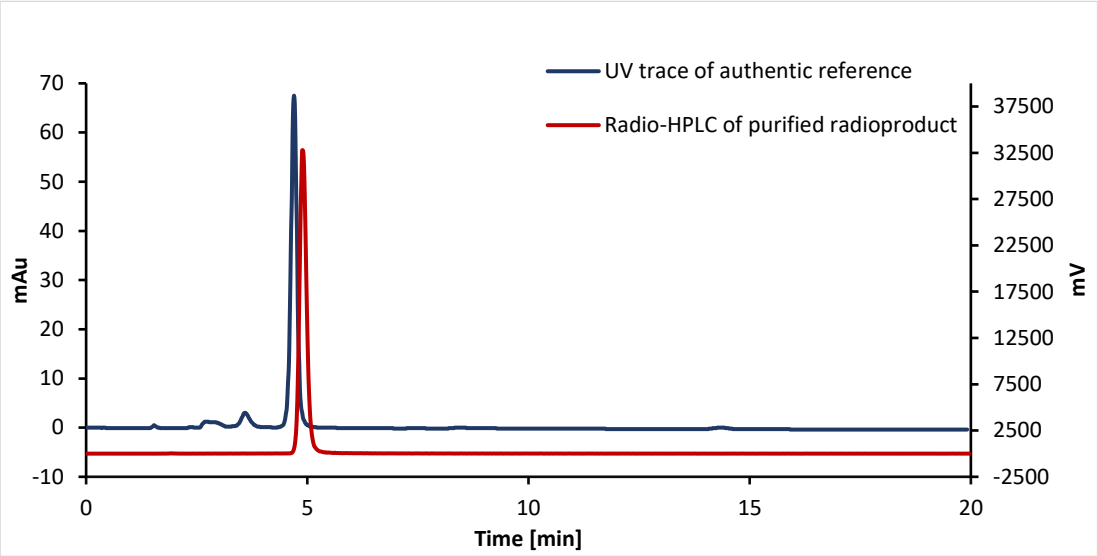


Prepared using HPLC conditions C.

Run 1

Measurement	**Activity injected (MBq, d.c.)**	**3.62 injected (µmol)**	**Peak area (mAu*s)**	A_m **(GBq/µmol)**
1	1.53	5.41×10^{-6}	0.2	281
2	1.86	8.12×10^{-6}	0.3	229
			Average (*n* = 2)	255 GBq/µmol

Radio/UV-HPLC overlay for isolated [^{18}F]**3.62** (HPLC conditions C)



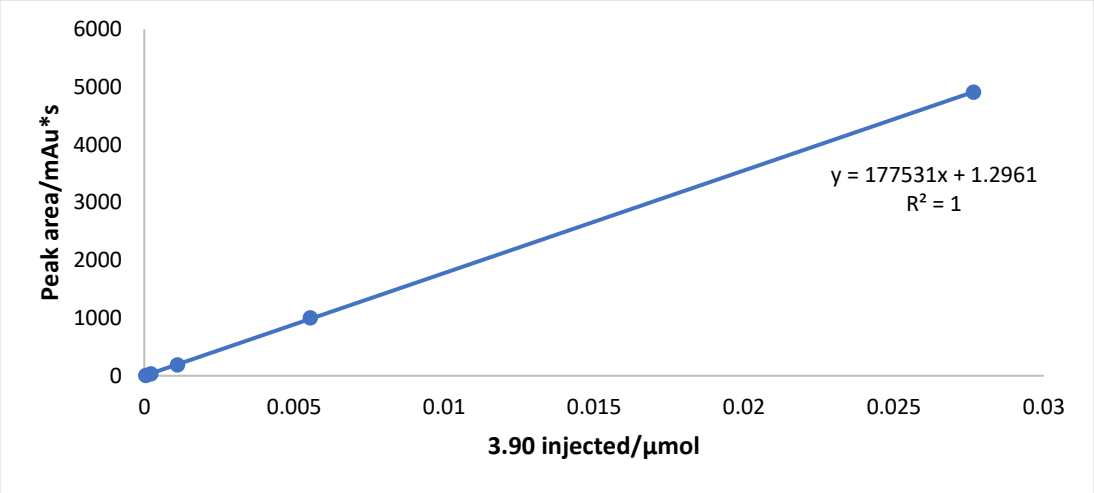
Automated radiosynthesis of [^{18}F]**3.90**

General Procedure 12 was followed using **3.56** (8.5 mg, 0.017 mmol). HPLC purification was carried out using MeCN/H_2O = 30/70, v/v, as eluent, t_R([^{18}F]**3.90**) = 9 min.

Radiosynthetic data for [^{18}F]**3.90**:

Starting activity	**AY**	**Synthesis time**	**RCP**	A_m
100 GBq	33.8 GBq	72 min	>98%	322 GBq/µmol

Calibration curve for **3.90**

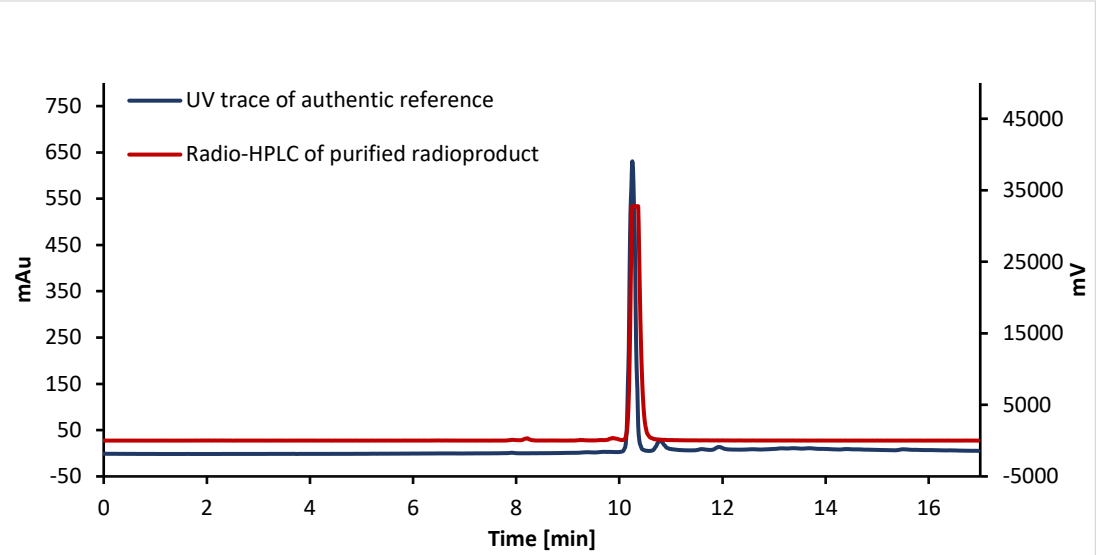


Prepared using HPLC conditions D.

Run 1

Measurement	**Activity injected (MBq, d.c.)**	**3.90 injected (µmol)**	**Peak area (mAu*s)**	**A_m (GBq/µmol)**
1	1.01	2.25 x 10^{-6}	0.4	448
2	1.01	3.38 x 10^{-6}	0.6	299
3	0.860	3.94 x 10^{-6}	0.7	218
			Average (*n* = 3)	322 GBq/µmol

Radio/UV-HPLC overlay for isolated [^{18}F]**3.90** (HPLC conditions D)



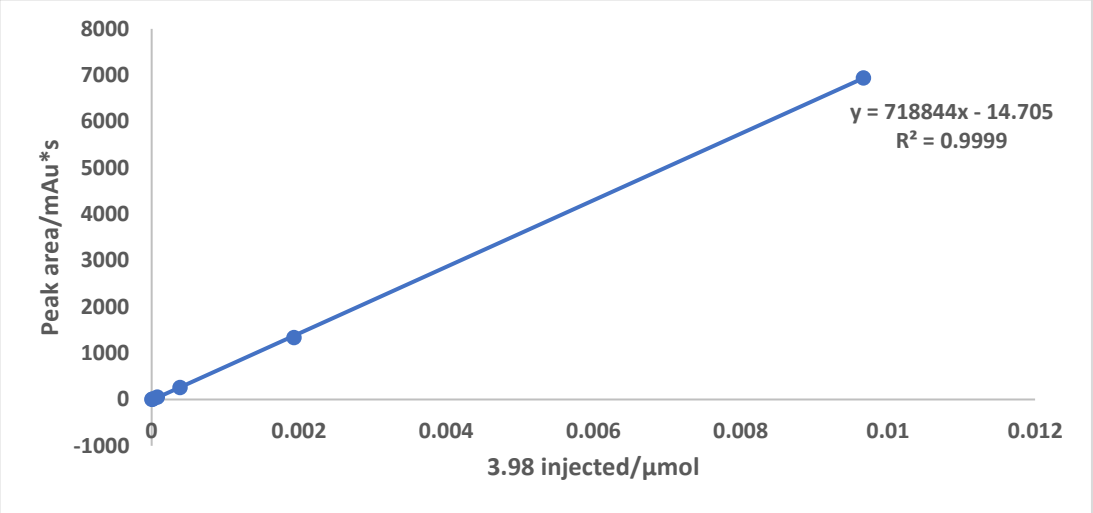
Automated radiosynthesis of [^{18}F]**3.98**

General Procedure 12 was followed using **3.58** (7.8 mg, 0.017 mmol). HPLC purification was carried out using MeCN/H_2O = 60/40, v/v, as eluent, t_R(**[^{18}F]3.98**) = 9 min.

Radiosynthetic data for [^{18}F]**3.98**:

Starting activity	AY	Synthesis time	RCP	A_m
100 GBq	11.9 GBq	74 min	>99%	110 GBq/µmol

Calibration curve for **3.98**

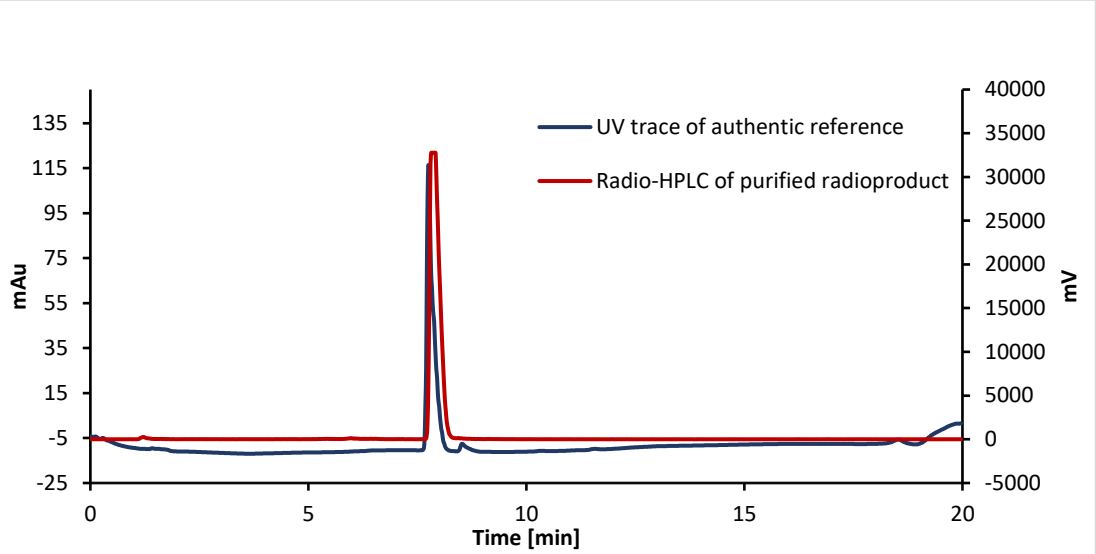


Prepared using HPLC conditions C.

Run 1

Measurement	Activity injected (MBq, d.c.)	3.98 injected (µmol)	Peak area (mAu*s)	A_m (GBq/µmol)
1	2.20	2.20 x 10^{-5}	15.8	100
2	1.50	1.89 x 10^{-5}	13.6	79.4
3	2.71	1.81 x 10^{-5}	13.0	150
			Average (*n* = 3)	110 GBq/µmol

Radio/UV-HPLC overlay for isolated [^{18}F]**3.98** (HPLC conditions C)



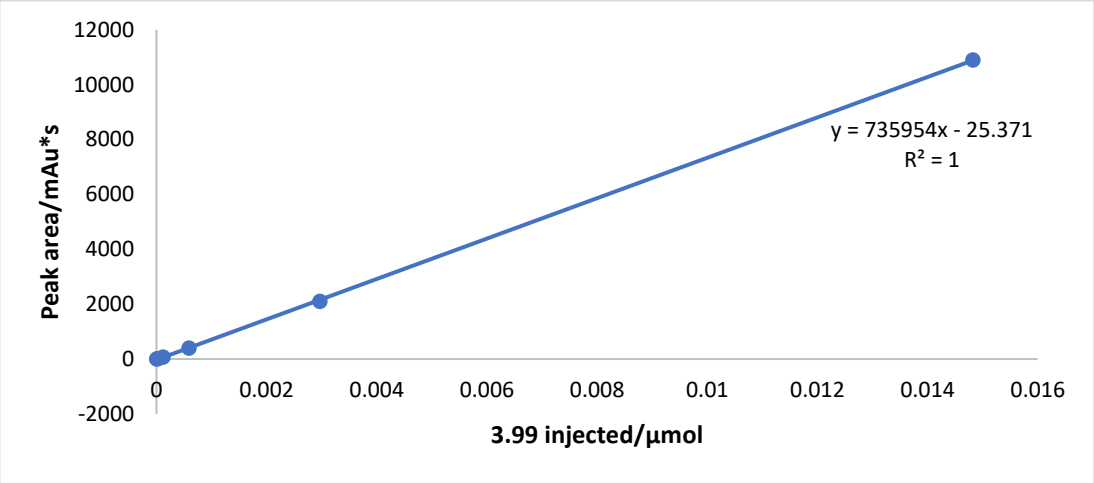
Automated radiosynthesis of [^{18}F]**3.99**

General Procedure 12 was followed using **3.59** (6.9 mg, 0.017 mmol). HPLC purification was carried out using MeCN/H_2O = 60/40, v/v, as eluent, t_R([^{18}F]**3.99**) = 11 min.

Radiosynthetic data for [^{18}F]**3.99**:

Starting activity	**AY**	**Synthesis time**	**RCP**	A_m
100 GBq	11.9 GBq	74 min	>99%	110 GBq/µmol

Calibration curve for **3.99**

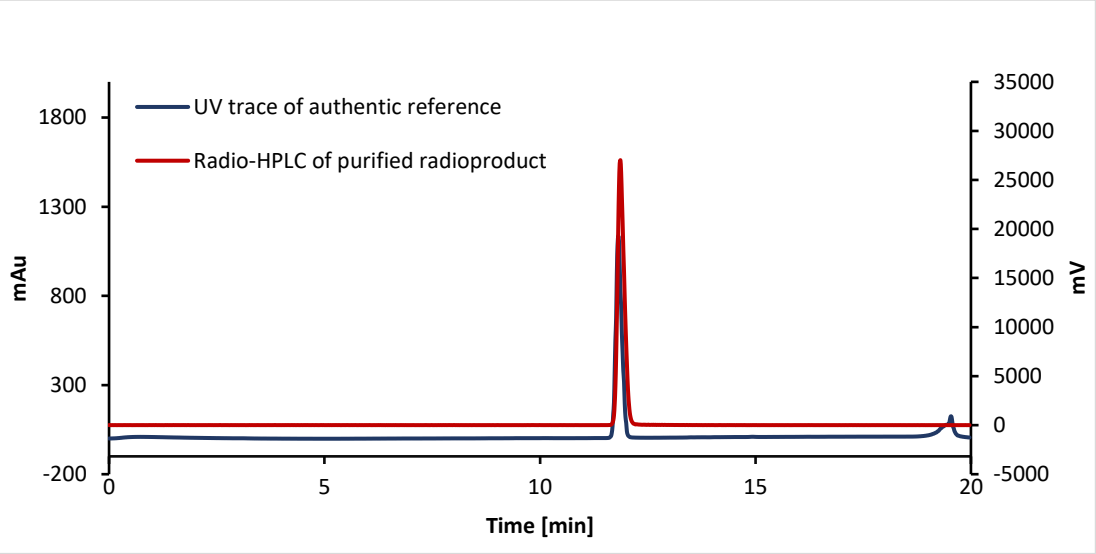


Prepared using HPLC conditions C.

Run 1

Measurement	**Activity injected (MBq, d.c.)**	**3.99 injected (µmol)**	**Peak area (mAu*s)**	A_m **(GBq/µmol)**
1	0.79	5.71×10^{-6}	4.2	138
2	0.73	5.98×10^{-6}	4.4	123
3	1.05	6.39×10^{-6}	4.7	165
			Average (*n* = 3)	142 GBq/µmol

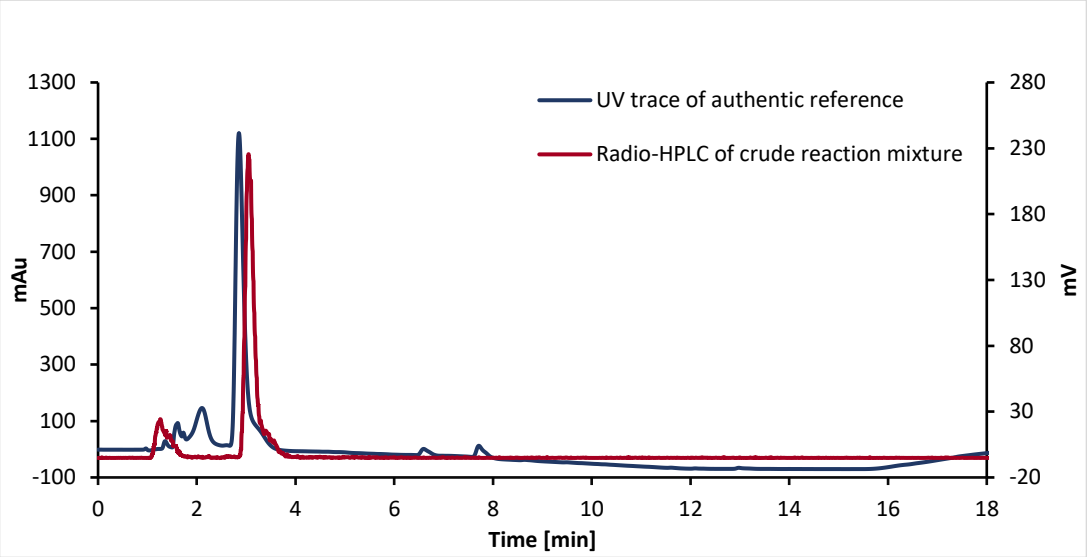
Radio/UV-HPLC overlay for isolated [^{18}F]**3.99 (**HPLC conditions C)



4.4.2.3. Radio and UV HPLC overlays and radiochemical yield calculations

UV/radio-HPLC trace overlay for [^{18}F]2-fluoropyrimidine ([^{18}F]**3.62**)

General Procedure 11 was followed using **3.25** as a substrate.

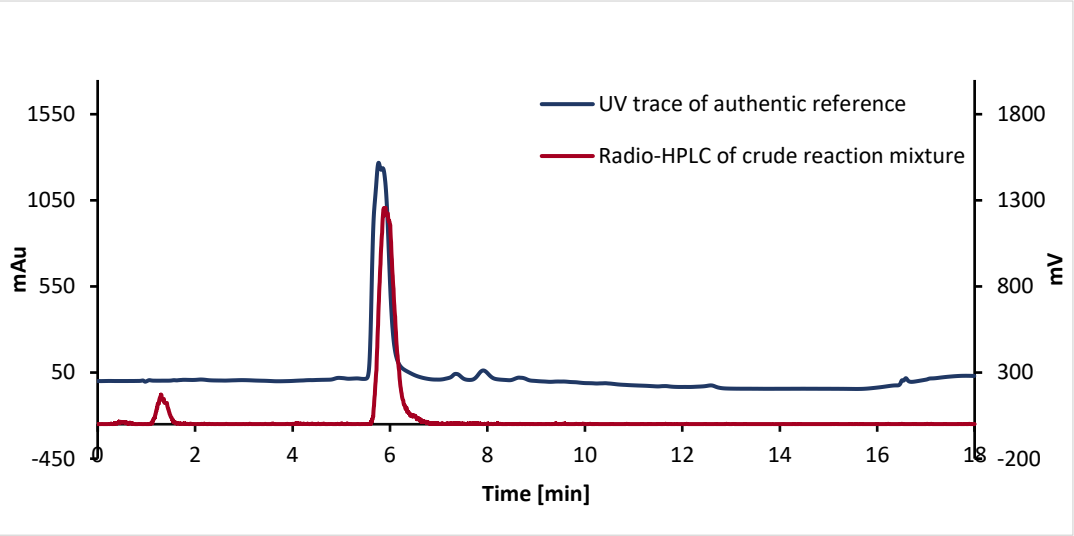


Analysed by (radio)HPLC using conditions A.

Run	**RCY of [^{18}F]3.62**	
1	85%	
2	89%	
3	94%	
4	93%	
5	87%	
6	71%	
7	94%	
	Average RCY	88% ± 8% (*n* = 7)

UV/radio-HPLC trace overlay for [^{18}F]ethyl 2-fluorooxazole-4-carboxylate ([^{18}F]**3.63**)

General Procedure 11 was followed using **3.26** as a substrate.

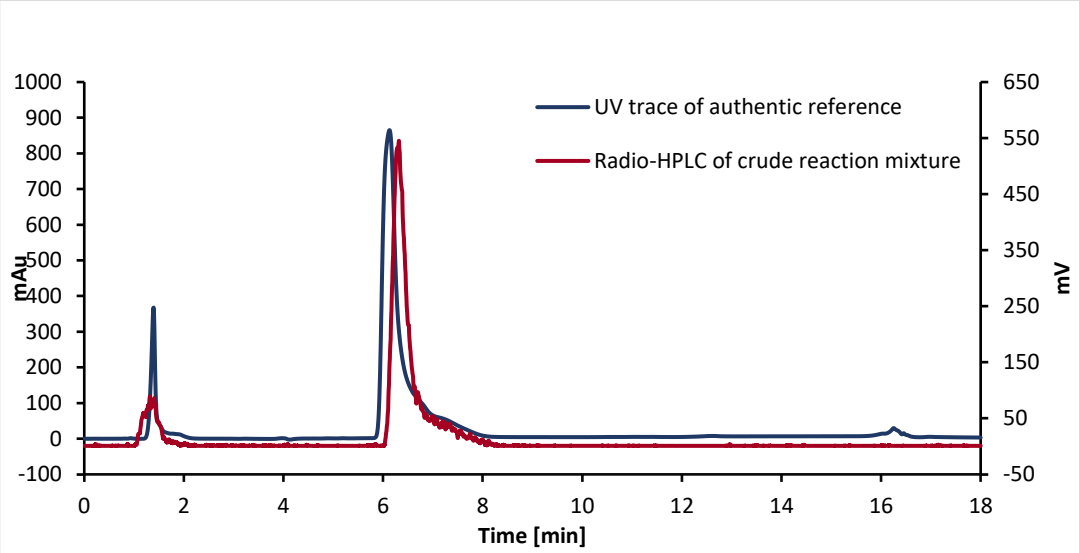


Analysed by (radio)HPLC using conditions A.

Run	RCY of [^{18}F]3.63	
1	92%	
2	84%	
	Average RCY	88% ± 4% (*n* = 2)

UV/radio-HPLC trace overlay for [^{18}F]5-bromo-2-fluoropyrimidine ([^{18}F]**3.64**)

General Procedure 11 was followed using **3.27** as a substrate.

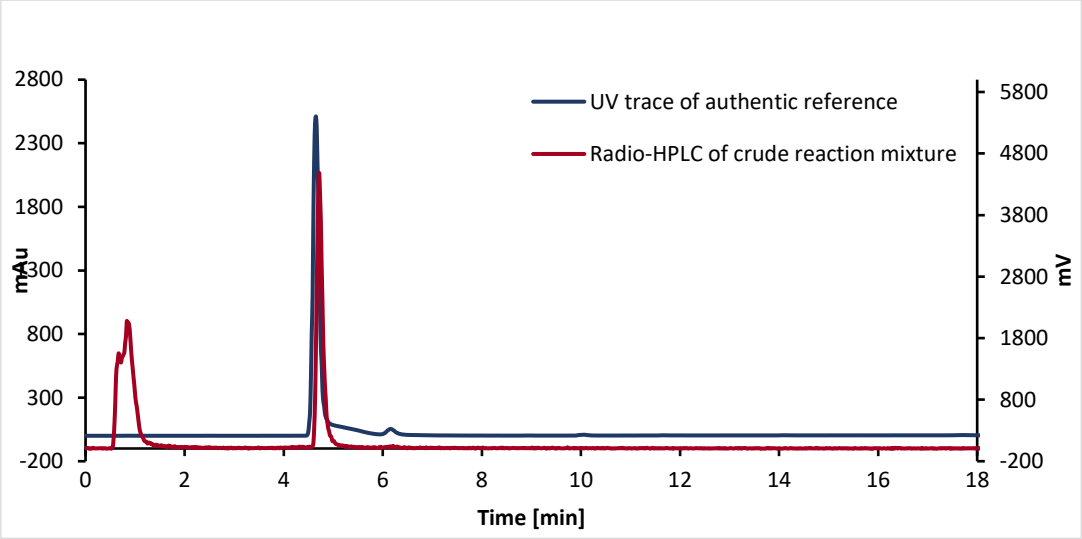


Analysed by (radio)HPLC using conditions A.

Run	**RCY of [^{18}F]3.64**	
1	88%	
2	85%	
3	78%	
	Average RCY	84% ± 4% (*n* = 3)

UV/radio-HPLC trace overlay for [^{18}F]5-iodo-2-fluoropyrimidine ([^{18}F]**3.65**)

General Procedure 11 was followed using **3.28** as a substrate.

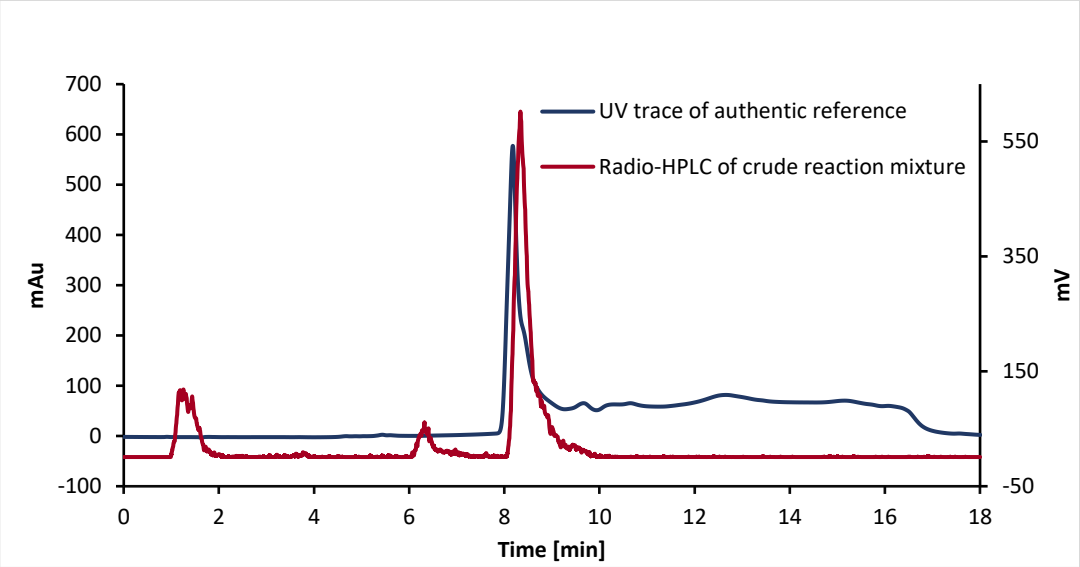


Analysed by (radio)HPLC using conditions B.

Run	**RCY of [^{18}F]3.65**	
1	47%	
2	42%	
3	39%	
	Average RCY	43% ± 3% (*n* = 3)

UV/radio-HPLC trace overlay for [^{18}F]2-fluoro-5-phenylpyrimidine ([^{18}F]**3.66**)

General Procedure 11 was followed using **3.29** as a substrate.

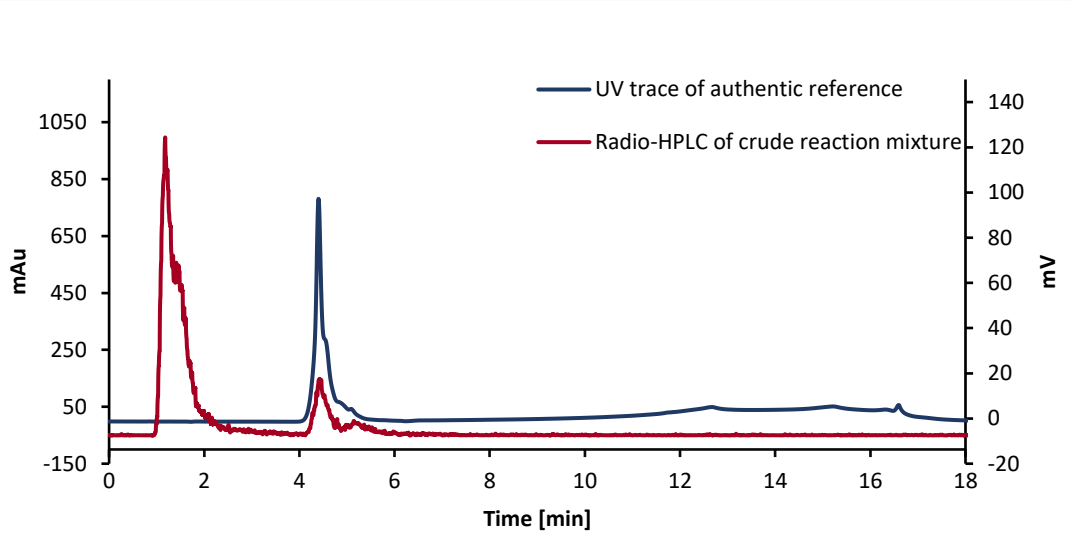


Analysed by (radio)HPLC using conditions A.

Run	**RCY of [^{18}F]3.66**	
1	83%	
2	78%	
3	72%	
	Average RCY	78% ± 4% (*n* = 3)

UV/radio-HPLC trace overlay for [^{18}F]5-methoxy-2-fluoropyrimidine ([^{18}F]**3.67**)

General Procedure 11 was followed using **3.30** as a substrate.

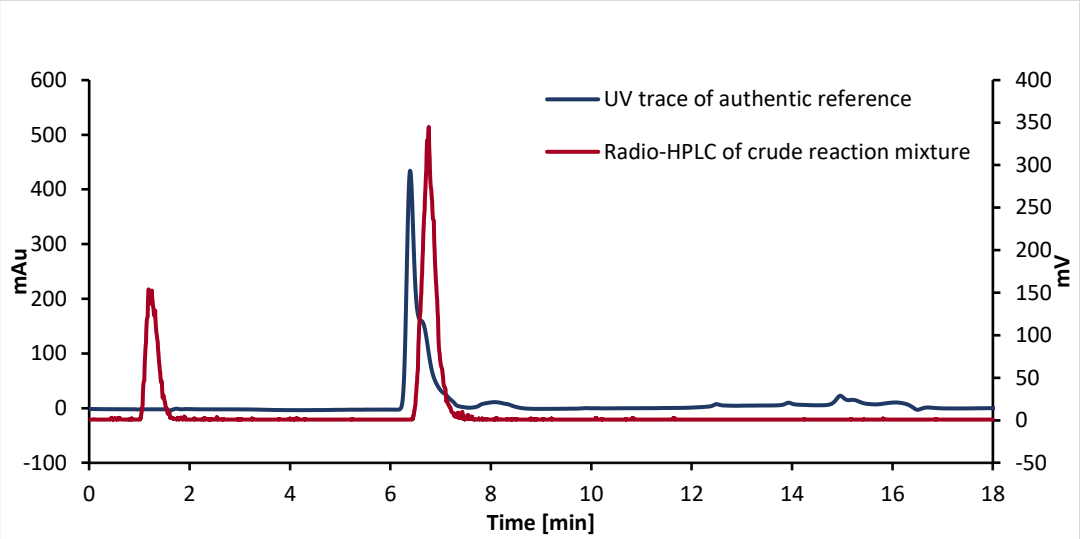


Analysed by (radio)HPLC using conditions A.

Run	RCY of [^{18}F]3.67	
1	10%	
2	16%	
	Average RCY	13% ± 3% (*n* = 2)

UV/radio-HPLC trace overlay for [^{18}F]ethyl-2-fluoropyrimidine-5-carboxylate ([^{18}F]**3.68**)

General Procedure 11 was followed using **3.31** as a substrate.

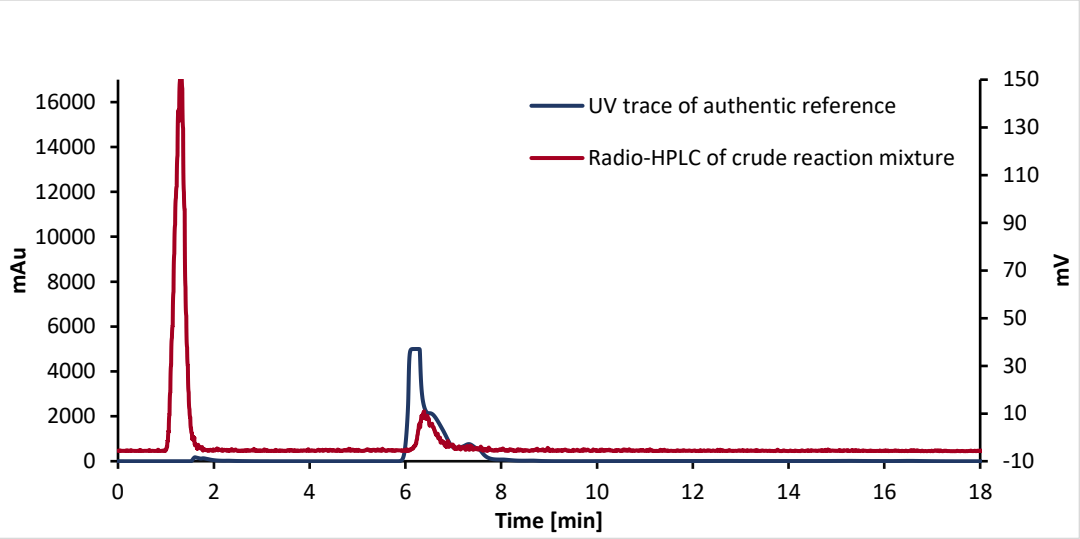


Analysed by (radio)HPLC using conditions A.

Run	**RCY of [^{18}F]3.68**	
1	65%	
2	78%	
	Average RCY	72% ± 7% (*n* = 2)

UV/radio-HPLC trace overlay for [^{18}F]2-fluoro-5-nitropyridine ([^{18}F]**3.69**)

General Procedure 11 was followed using **3.32** as a substrate.

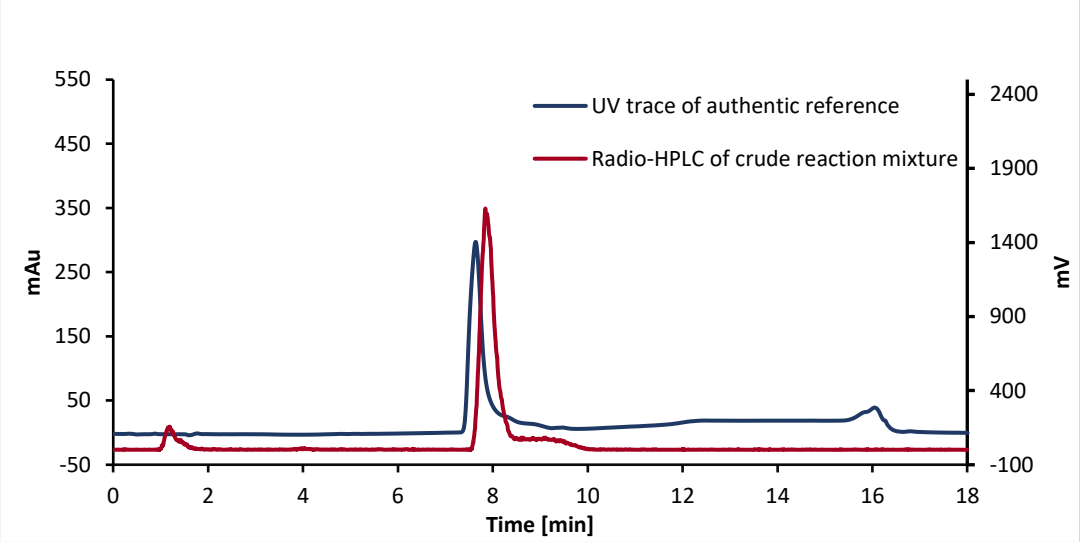


Analysed by (radio)HPLC using conditions A.

Run	**RCY of [^{18}F]3.69**	
1	14%	
2	7%	
3	3%	
	Average RCY	8% ± 5 % (*n* = 3)

UV/radio-HPLC trace overlay for [^{18}F]4-fluoro-5,6-dimethylfuro[2,3-*d*]pyrimidine ([^{18}F]**3.70**)

General Procedure 11 was followed using **3.35** as a substrate.

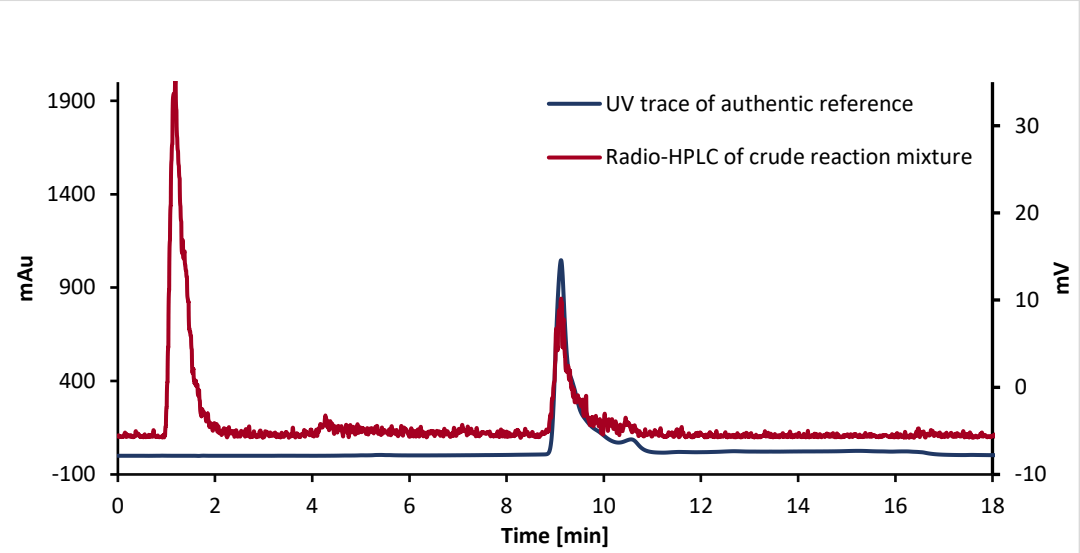


Analysed by (radio)HPLC using conditions A.

Run	RCY of [^{18}F]3.70	
1	93%	
2	30%	
3	85%	
	Average RCY	69% ± 28% (*n* = 3)

UV/radio-HPLC trace overlay for [^{18}F]7-benzyl-4-fluoro-7*H*-pyrrolo[2,3-*d*]pyrimidine ([^{18}F]**3.71**)

General Procedure 11 was followed using **3.36** as a substrate.

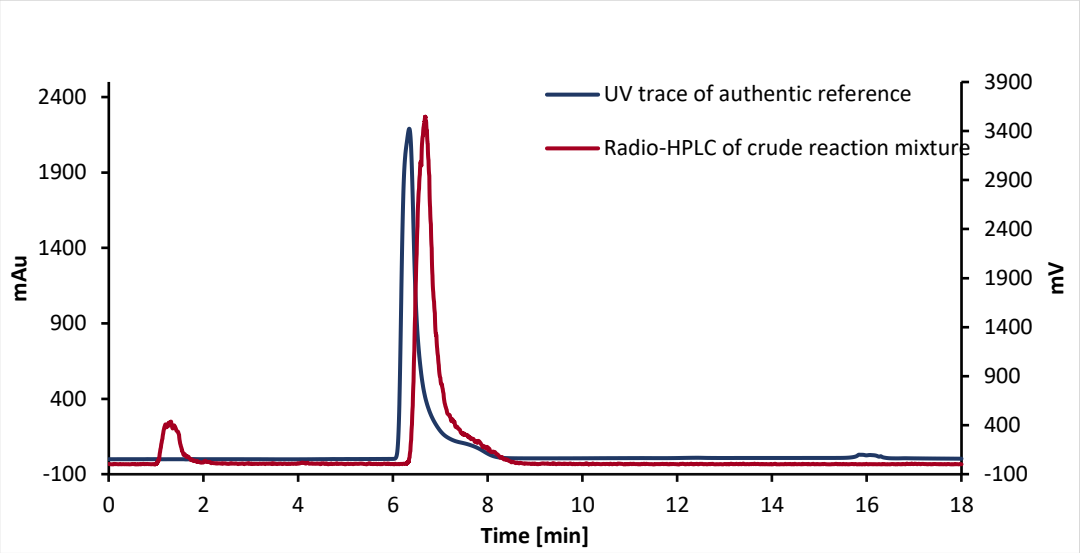


Analysed by (radio)HPLC using conditions A.

Run	RCY of [^{18}F]3.71	
1	22%	
2	32%	
3	17%	
	Average RCY	24% ± 6% (*n* = 3)

UV/radio-HPLC trace overlay for [^{18}F]4-fluorothieno[2,3-*d*]pyrimidine ([^{18}F]**3.72**)

General Procedure 11 was followed using **3.37** as a substrate.

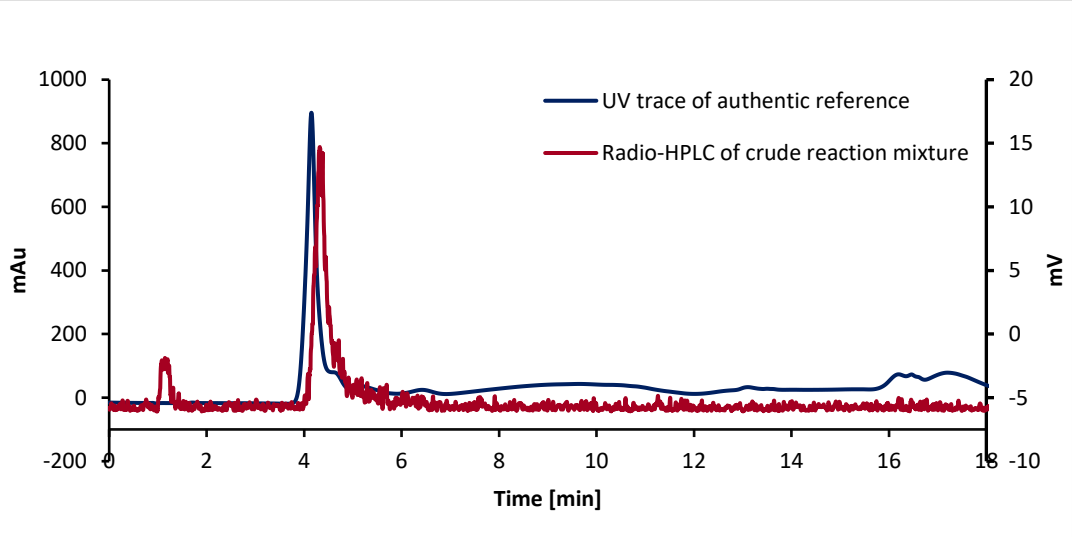


Analysed by (radio)HPLC using conditions A.

Run	**RCY of [^{18}F]3.72**	
1	90%	
2	83%	
3	94%	
	Average RCY	89% ± 5% (*n* = 3)

UV/radio-HPLC trace overlay for [^{18}F]2-fluoropyrido[3,2-*d*]pyrimidine ([^{18}F]**3.73**)

General Procedure 11 was followed using **3.39** as a substrate.

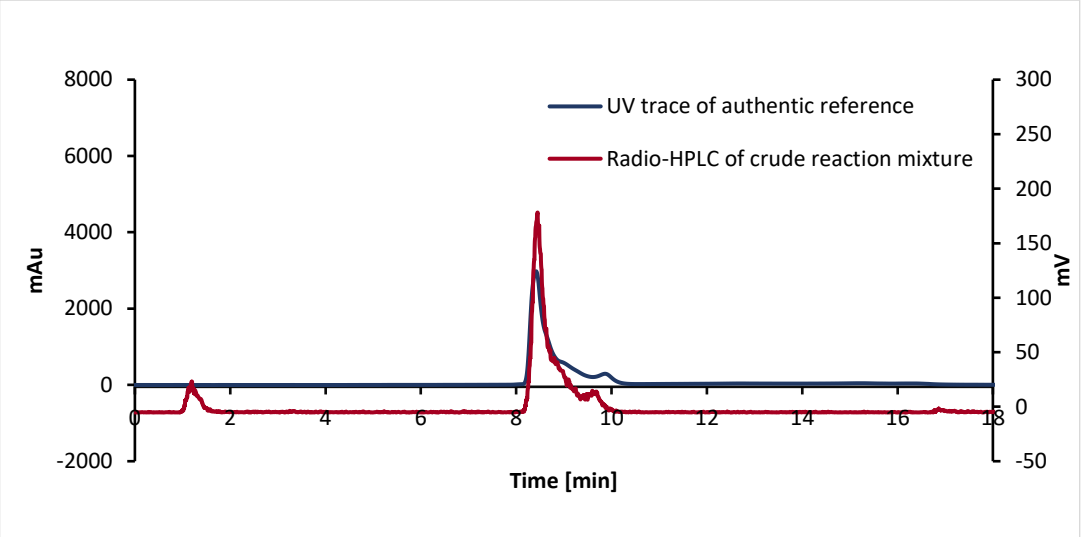


Analysed by (radio)HPLC using conditions A.

Run	RCY of [^{18}F]3.73	
1	95%	
2	95%	
3	90%	
	Average RCY	93% ± 2% (*n* = 3)

UV/radio-HPLC trace overlay for [^{18}F]6-bromo-2-fluoroquinazoline ([^{18}F]**3.74**)

General Procedure 11 was followed using **3.38** as a substrate.

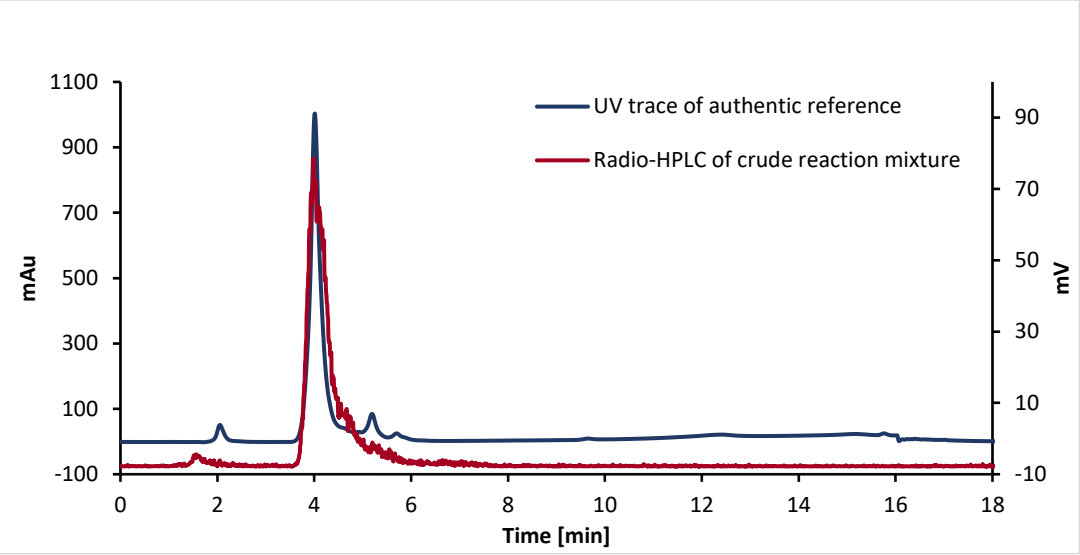


Analysed by (radio)HPLC using conditions A.

Run	RCY of [^{18}F]3.74	
1	86%	
2	91%	
3	91%	
	Average RCY	89% ± 2% (*n* = 3)

UV/radio-HPLC trace overlay for [^{18}F]6-fluoropyridazine-3-carbonitrile ([^{18}F]**3.75**)

General Procedure 11 was followed using **3.43** as a substrate.

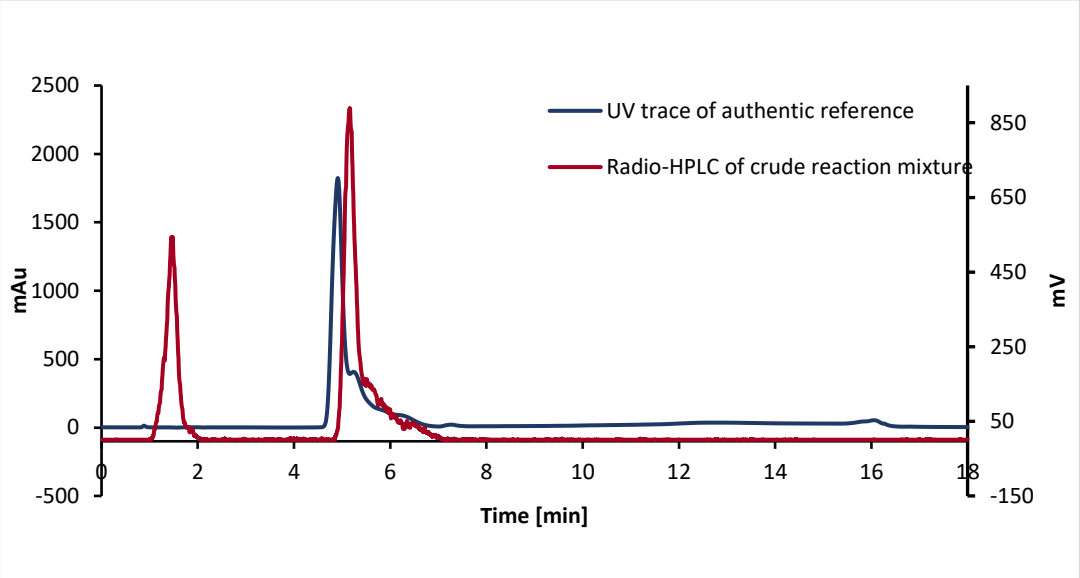


Analysed by (radio)HPLC using conditions A.

Run	RCY of [^{18}F]3.75	
1	98%	
2	98%	
3	98%	
	Average RCY	98% ± 0% (*n* = 3)

UV/radio-HPLC trace overlay for [^{18}F]5-fluoropyrazine-2-carbonitrile ([^{18}F]**3.76**)

General Procedure 11 was followed using **3.42** as a substrate.

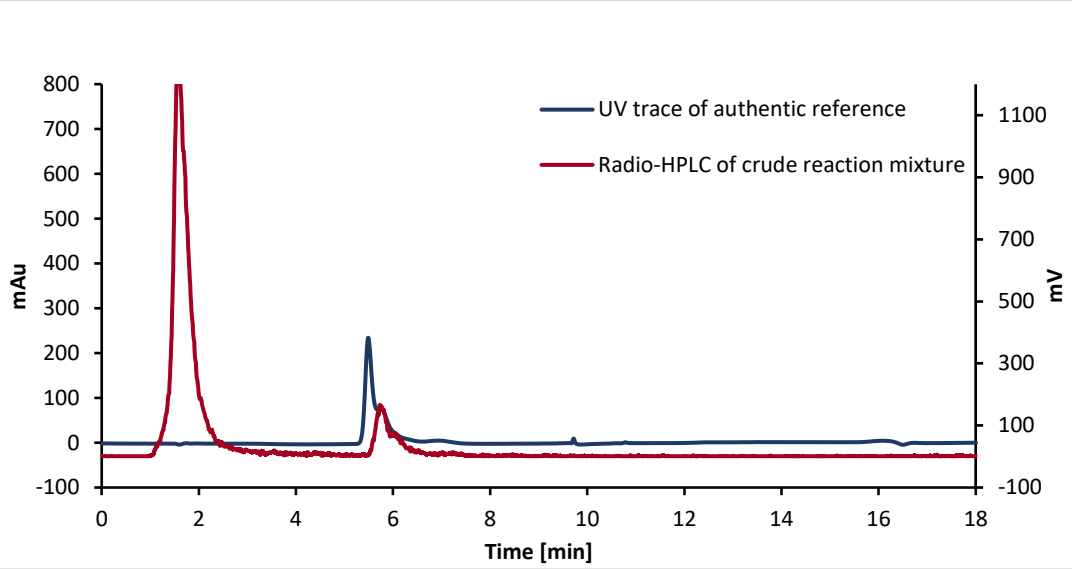


Analysed by (radio)HPLC using conditions A.

Run	**RCY of [^{18}F]3.76**	
1	69%	
2	87%	
	Average RCY	78% ± 9% (*n* = 2)

UV/radio-HPLC trace overlay for [^{18}F]ethyl-5-fluoropyrazine-2-carboxylate ([^{18}F]**3.77**)

General Procedure 11 was followed using **3.40** as a substrate.

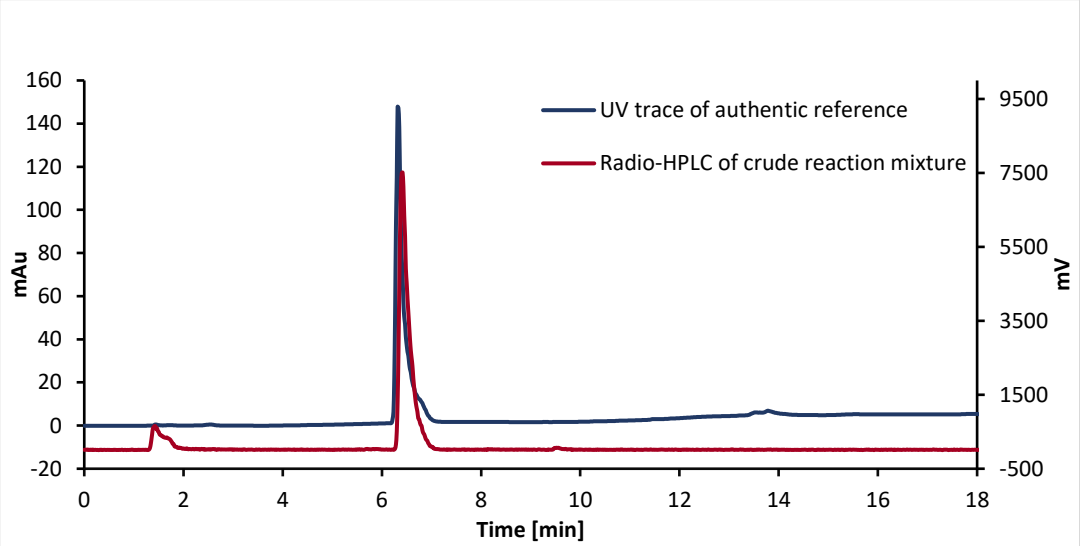


Analysed by (radio)HPLC using conditions A.

Run	**RCY of [^{18}F]3.77**	
1	11%	
2	11%	
3	7%	
	Average RCY	10% ± 2% (*n* = 3)

UV/radio-HPLC trace overlay for [^{18}F] 3-fluoro-6-methylpyrazine-2-carbonitrile ([^{18}F]**3.78**)

General Procedure 11 was followed using **3.41** as a substrate.

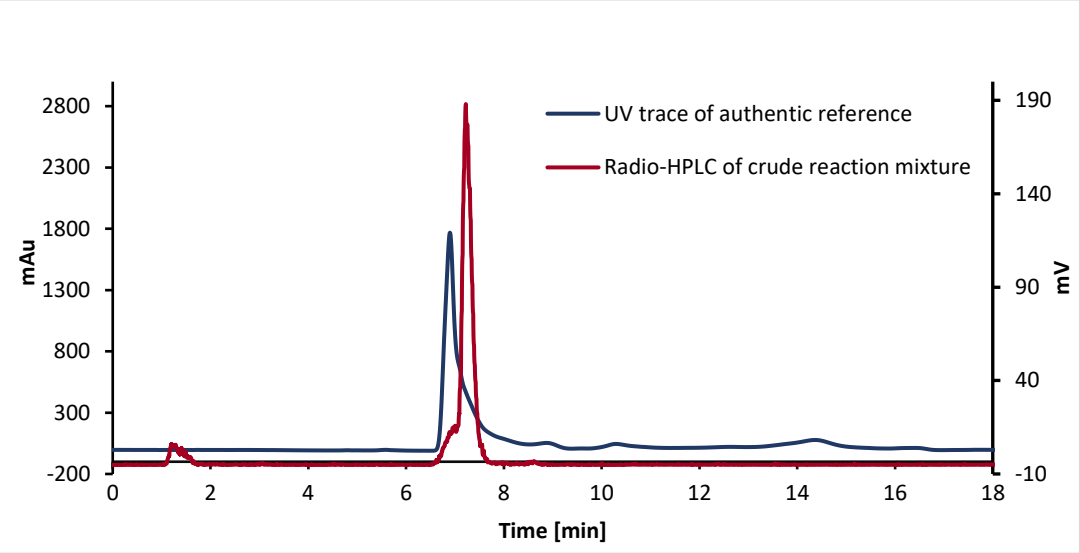


Analysed by (radio)HPLC using conditions C.

Run	**RCY of [^{18}F]3.78**	
1	89%	
2	88%	
3	89%	
	Average RCY	89% ± 0% (*n* = 3)

UV/radio-HPLC trace overlay for [^{18}F]4-fluoropyrrolo[2,1-*f*][1,2,4]triazine ([^{18}F]**3.79**)

General Procedure 11 was followed using **3.46** as a substrate.

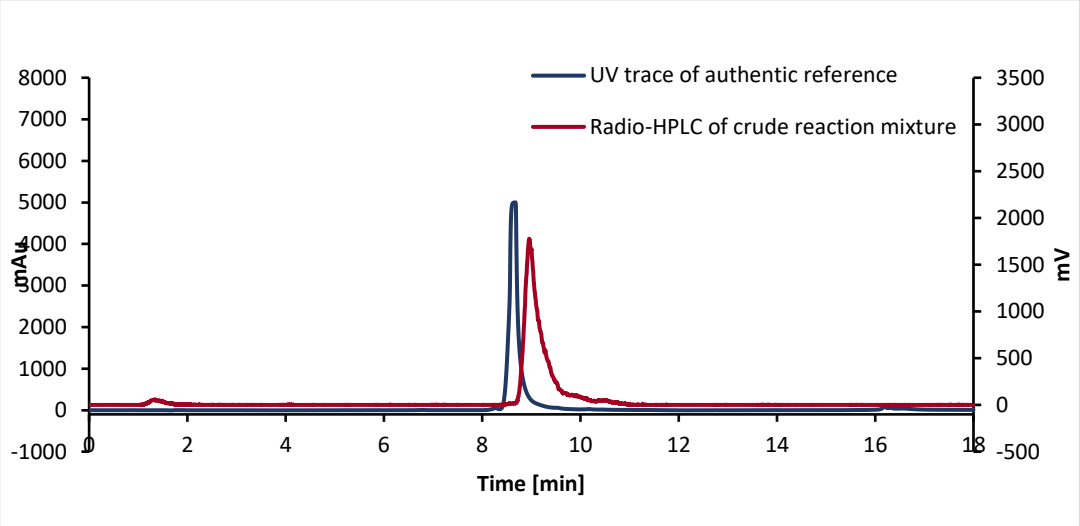


Analysed by (radio)HPLC using conditions A.

Run	**RCY of [^{18}F]3.79**	
1	95%	
2	94%	
3	93%	
	Average RCY	94% ± 1% (*n* = 3)

UV/radio-HPLC trace overlay for [^{18}F] 4-fluoro-7-iodopyrrolo[2,1-*f*][1,2,4]triazine ([^{18}F]**3.80**)

General Procedure 11 was followed using **3.47** as a substrate.

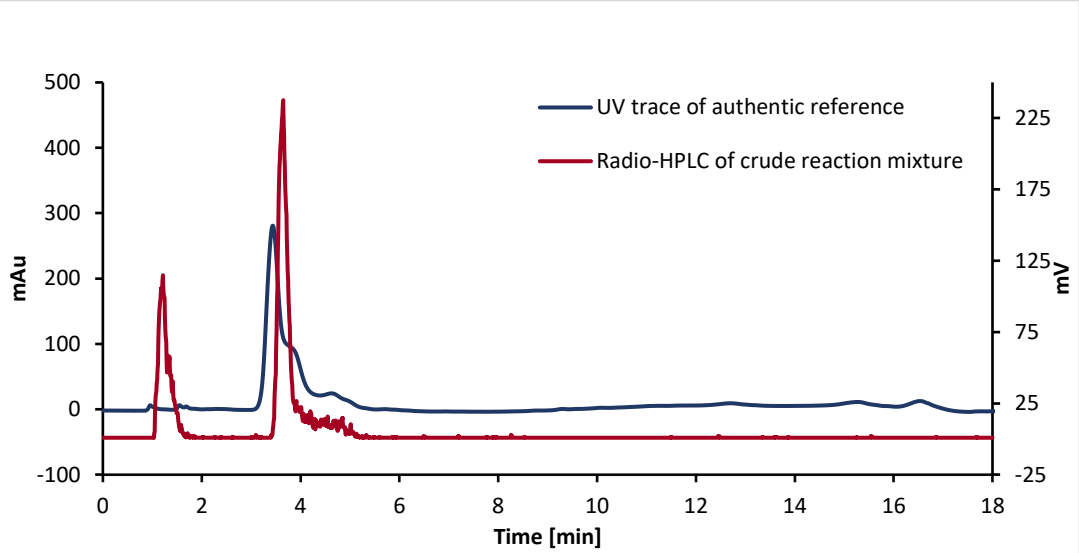


Analysed by (radio)HPLC using conditions A.

Run	**RCY of [^{18}F]3.80**	
1	97%	
2	97%	
3	98%	
	Average RCY	97% ± 0% (*n* = 3)

UV/radio-HPLC trace overlay for [^{18}F]9-ethyl-6-fluoro-9*H*-purine ([^{18}F]**3.81**)

General Procedure 11 was followed using **3.48** as a substrate.



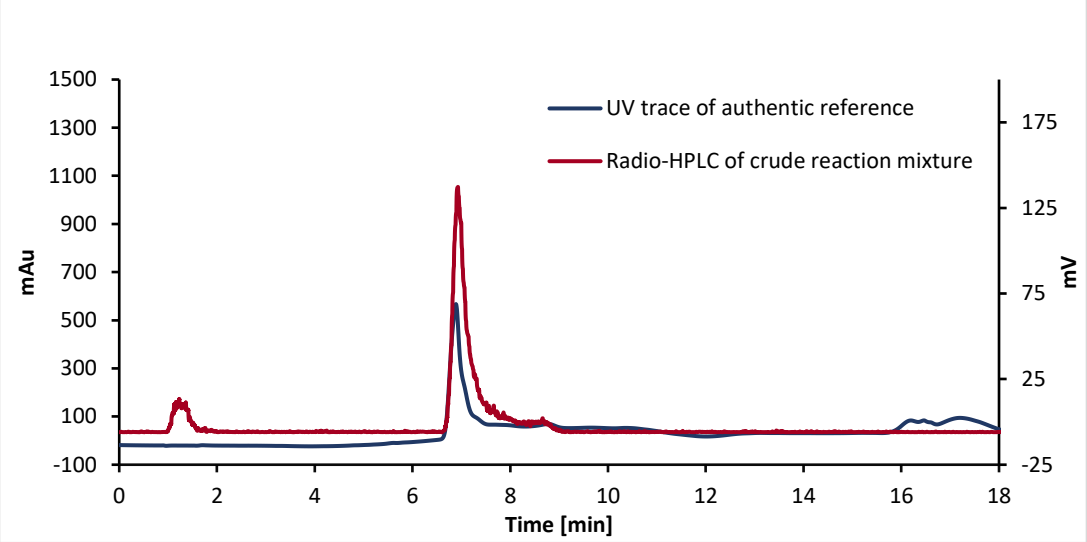
.

Analysed by (radio)HPLC using conditions A.

Run	RCY of [^{18}F]3.81	
1	67%	
2	70%	
3	81%	
	Average RCY	73% ± 6% (*n* = 3)

UV/radio-HPLC trace overlay for [^{18}F]9-benzyl-6-fluoro-9*H*-purine ([^{18}F]**3.82**)

General Procedure 11 was followed using **3.49** as a substrate.

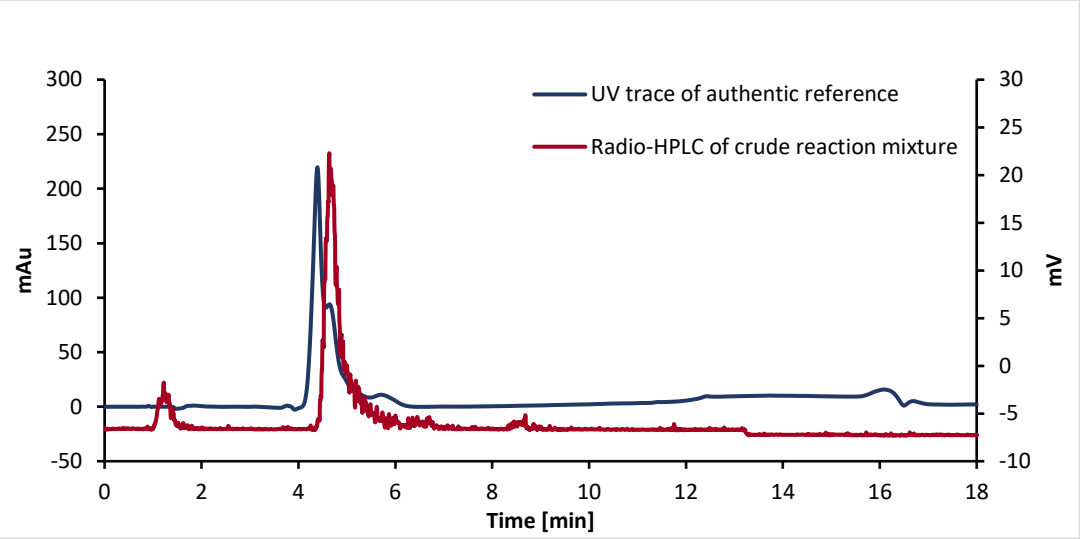


Analysed by (radio)HPLC using conditions A.

Run	RCY of [^{18}F]**3.82**	
1	75%	
2	78%	
3	85%	
	Average RCY	79% ± 4% (*n* = 3)

UV/radio-HPLC trace overlay for [^{18}F] ethyl-2-(6-fluoro-9*H*-purin-9-yl)acetate ([^{18}F]**3.83**)

General Procedure 11 was followed using **3.50** as a substrate.

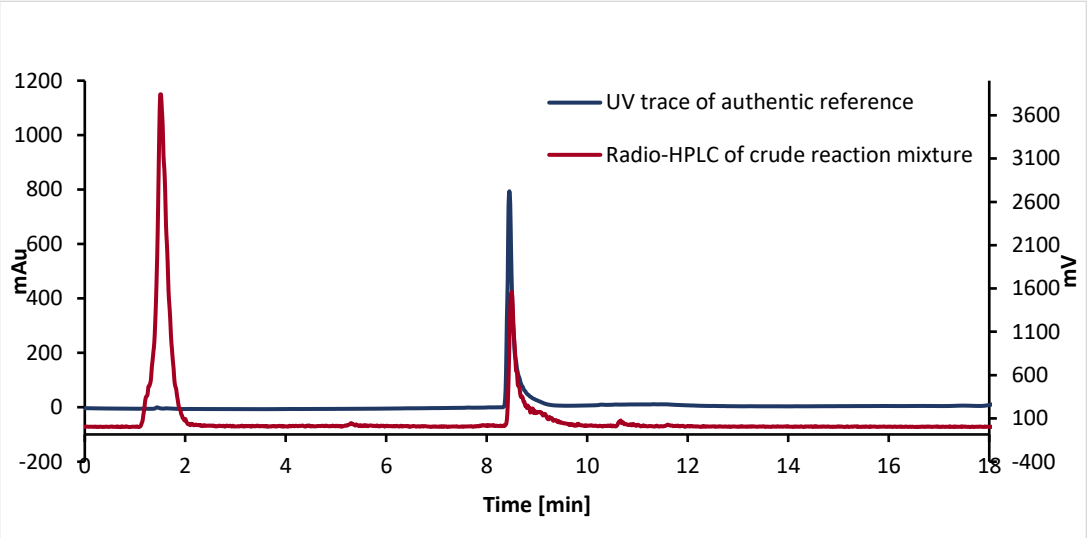


Analysed by (radio)HPLC using conditions A.

Run	RCY of [^{18}F]3.83	
1	89%	
2	88%	
3	89%	
	Average RCY	89% ± 0% (*n* = 3)

UV/radio-HPLC trace overlay for [^{18}F]9-benzyl-2-chloro-6-fluoro-9*H*-purine ([^{18}F]**3.84**)

General Procedure 11 was followed using **3.51** as a substrate.

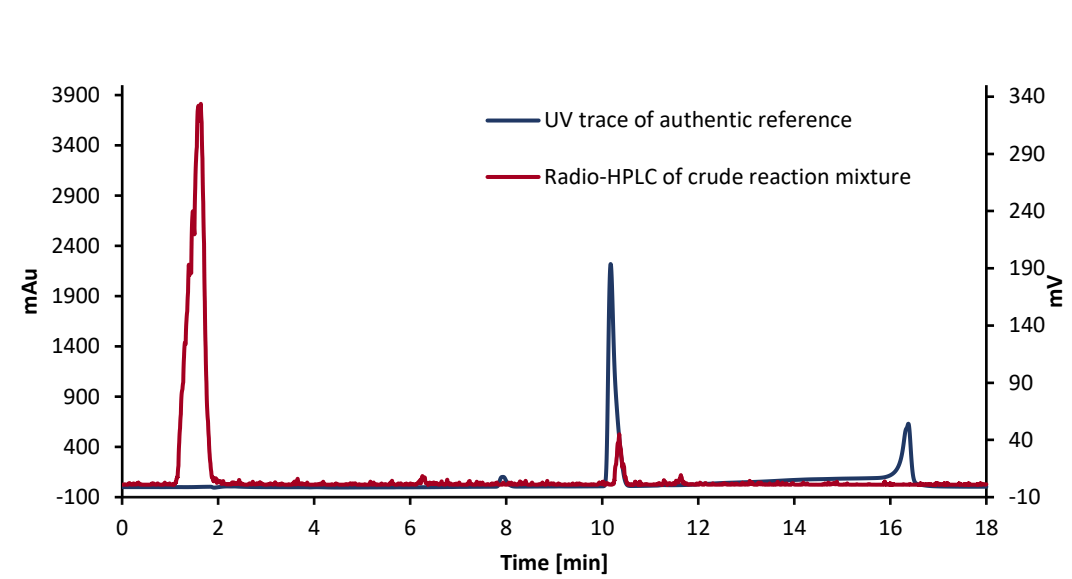


Analysed by (radio)HPLC using conditions C.

Run	RCY of [^{18}F]3.84	
1	23%	
2	26%	
3	22%	
	Average RCY	24% ± 2% (*n* = 3)

UV/radio-HPLC trace overlay for [^{18}F]2-fluorobenzo[*d*]thiazole ([^{18}F]**3.85**)

General Procedure 11 was followed using **3.96** as a substrate.

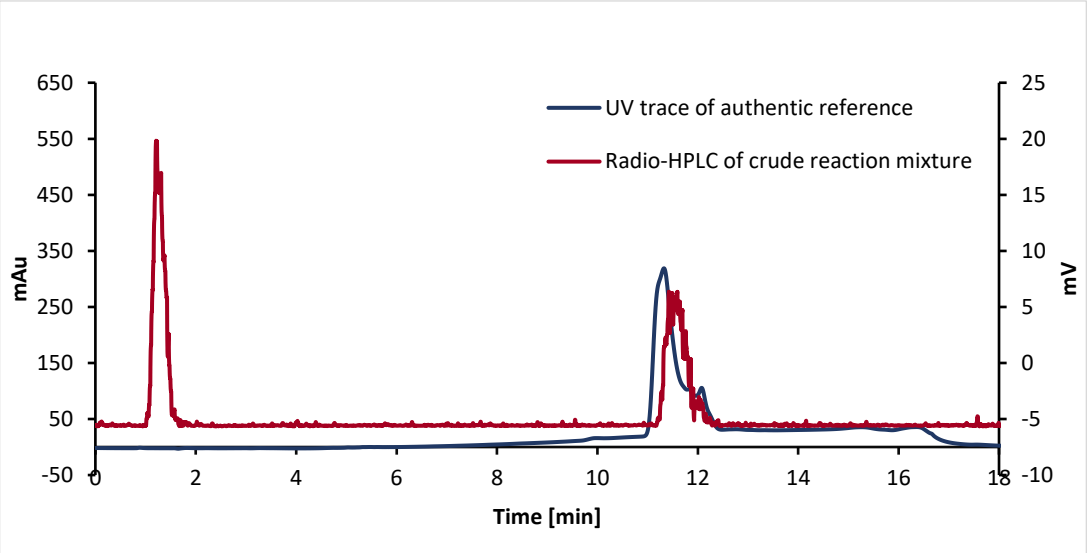


Analysed by (radio)HPLC using conditions A.

Run	**RCY of [^{18}F]3.85**	
1	5%	
2	4%	
	Average RCY	5% ± 1% (*n* = 2)

UV/radio-HPLC trace overlay for [^{18}F]2-fluoro-4-phenyl-6-(thiophen-2-yl)pyrimidine ([^{18}F]**3.86**)

General Procedure 11 was followed using **3.52** as a substrate.

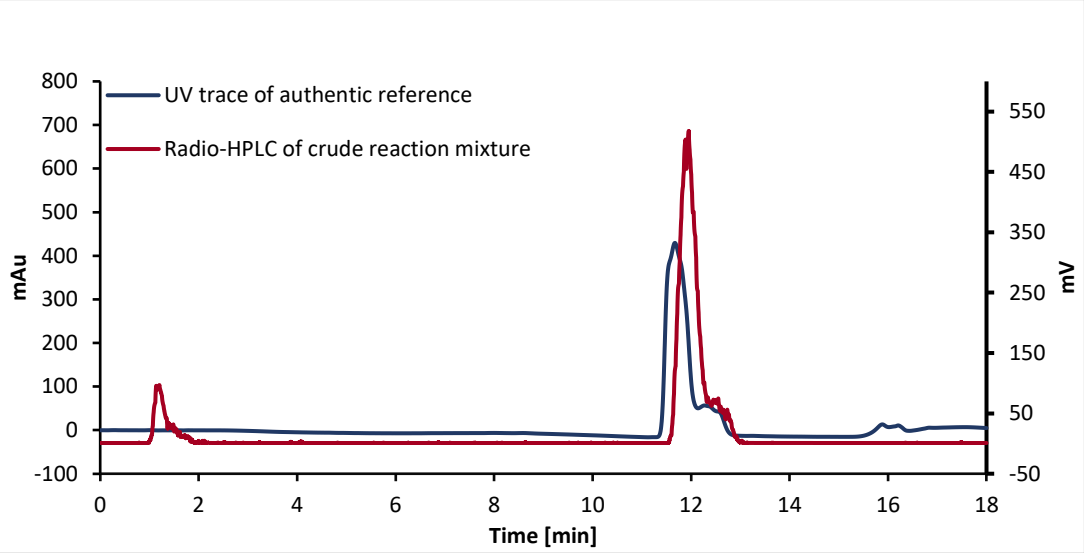


Analysed by (radio)HPLC using conditions A.

Run	RCY of [^{18}F]3.85	
1	48%	
2	46%	
3	8%	
4	30%	
	Average RCY	33% ± 16% (*n* = 4)

UV/radio-HPLC trace overlay for [^{18}F]2-fluoro-4-(4-fluoronaphthalen-1-yl)-6-isopropylpyrimidine ([^{18}F]**3.87**)

General Procedure 11 was followed using **3.53** as a substrate.

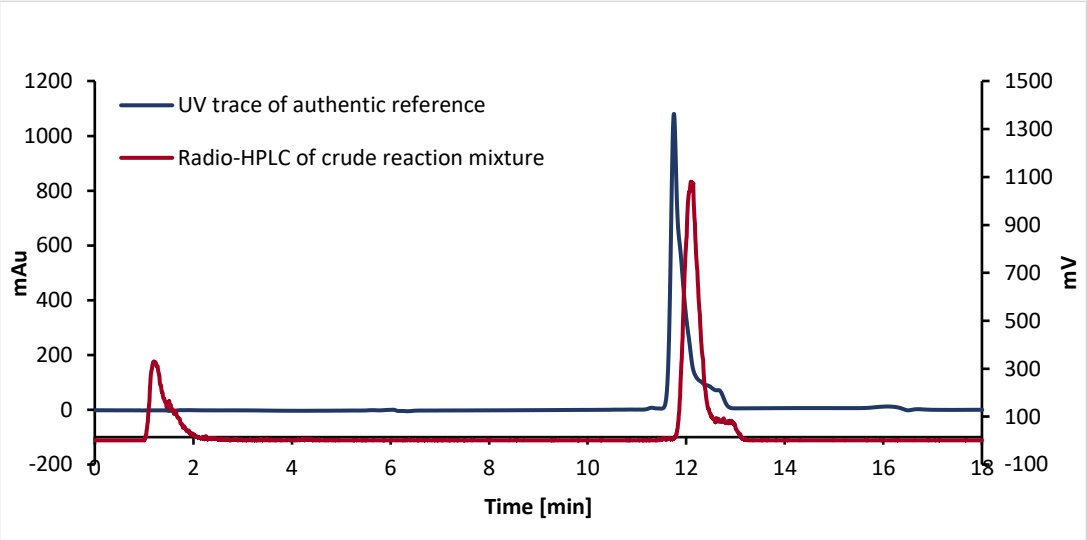


Analysed by (radio)HPLC using conditions A.

Run	**RCY of [^{18}F]3.87**	
1	22%	
2	88%	
3	46%	
	Average RCY	52% ± 27% (*n* = 3)

UV/radio-HPLC trace overlay for isopropyl 2-(4-(4-(2-fluoroquinazolin-6-yl)benzoyl)phenoxy)-2-methylpropanoate ([^{18}F]**3.88**)

General Procedure 11 was followed using **3.54** as a substrate.

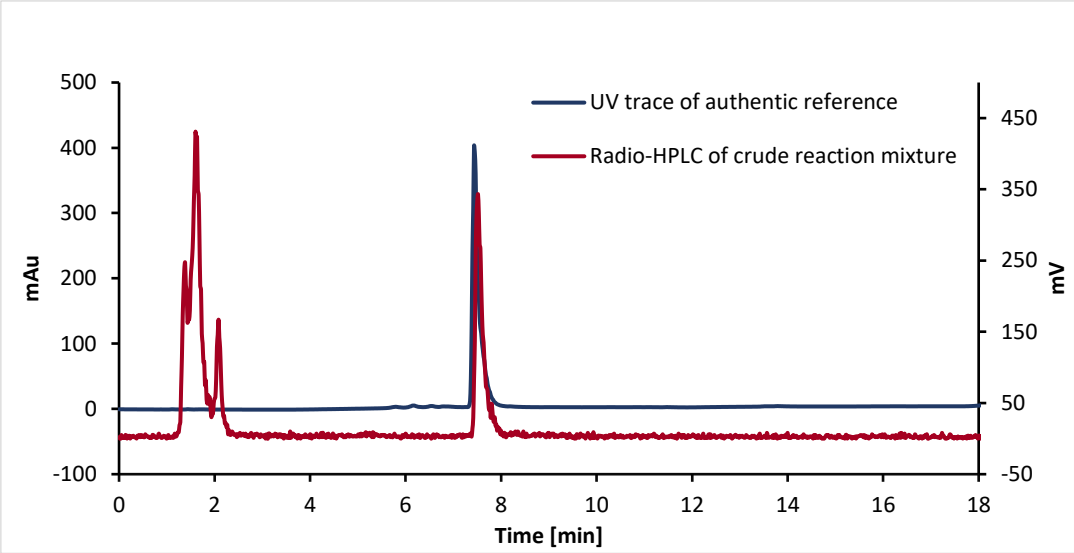


Analysed by (radio)HPLC using conditions A.

Run	RCY of [^{18}F]3.88	
1	75%	
2	67%	
3	78%	
	Average RCY	74% ± 5% (*n* = 3)

UV/radio-HPLC trace overlay for [^{18}F]4-chloro-5-fluoro-2-phenylpyridazin-3(2*H*)-one ([^{18}F]**3.89**)

General Procedure 11 was followed using **3.55** as a substrate.

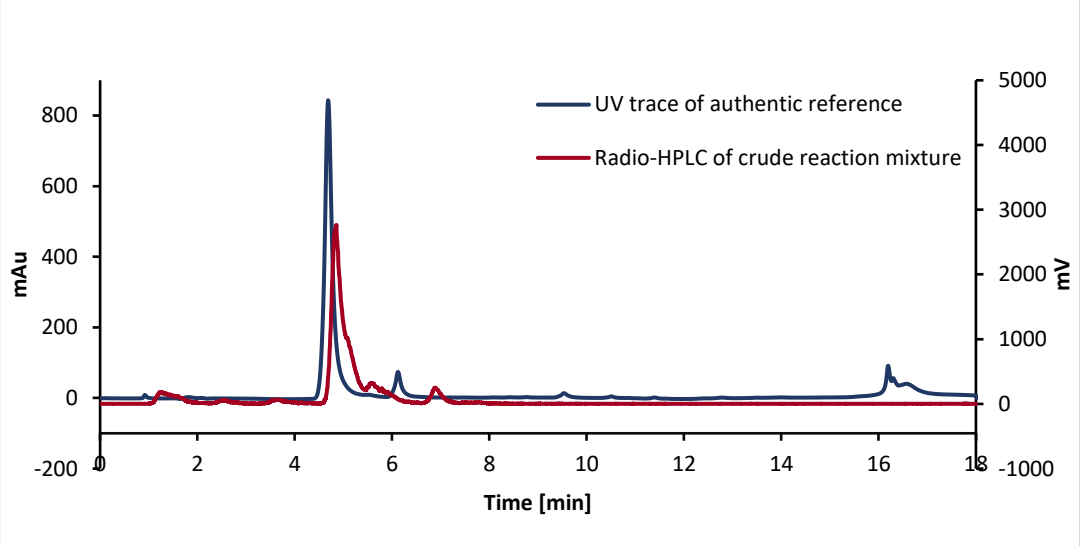


Analysed by (radio)HPLC using conditions C.

Run	**RCY of [^{18}F]3.89**	
1	31%	
2	20%	
	Average RCY	26% ± 6% (*n* = 2)

UV/radio-HPLC trace overlay for [^{18}F](2*R*,3*R*,4*R*,5*R*)-2-(6-fluoro-9*H*-purin-9-yl)-5-(hydroxymethyl)tetrahydrofuran-3,4-diyl diacetate ([^{18}F]**3.90**)

General Procedure 11 was followed using **3.56** as a substrate.

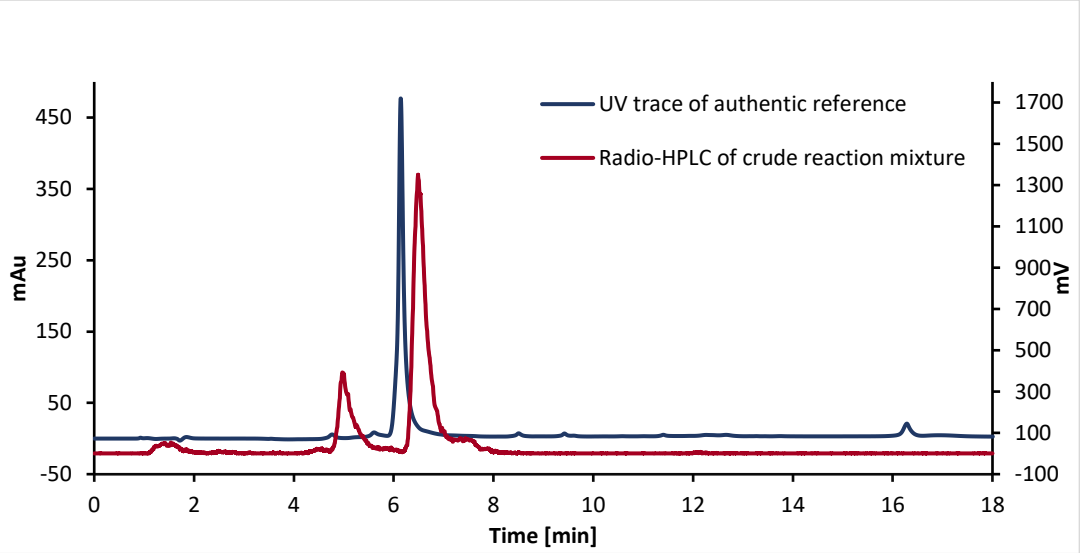


Analysed by (radio)HPLC using conditions A.

Run	RCY of [^{18}F]**3.90**	
1	87%	
2	82%	
3	86%	
	Average RCY	85% ± 2% (*n* = 3)

UV/radio-HPLC trace overlay for [^{18}F](2*R*,3*R*,4*R*,5*R*)-2-(acetoxymethyl)-5-(6-fluoro-9*H*-purin-9-yl)tetrahydrofuran-3,4-diyl diacetate ([^{18}F]**3.91**)

General Procedure 11 was followed using **3.57** as a substrate.

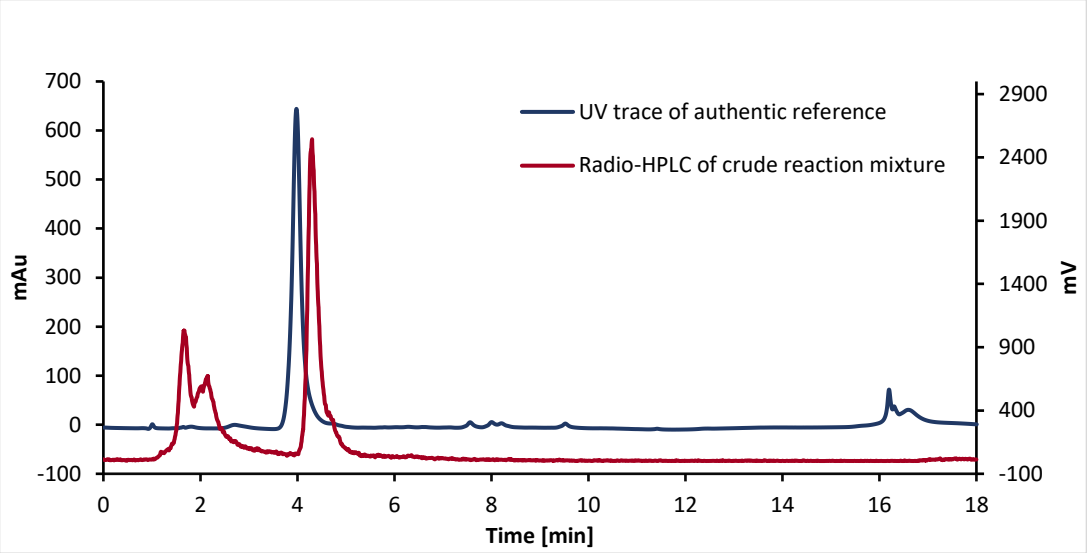


Analysed by (radio)HPLC using conditions A.

Run	**RCY of [^{18}F]3.91**	
1	69%	
2	75%	
3	70%	
	Average RCY	71% ± 3% (*n* = 3)

UV/radio-HPLC trace overlay for diethyl ((2-(6-fluoro-9*H*-purin-9-yl)ethoxy)methyl)phosphonate ([^{18}F]**3.92**)

General Procedure 11 was followed using **3.60** as a substrate.

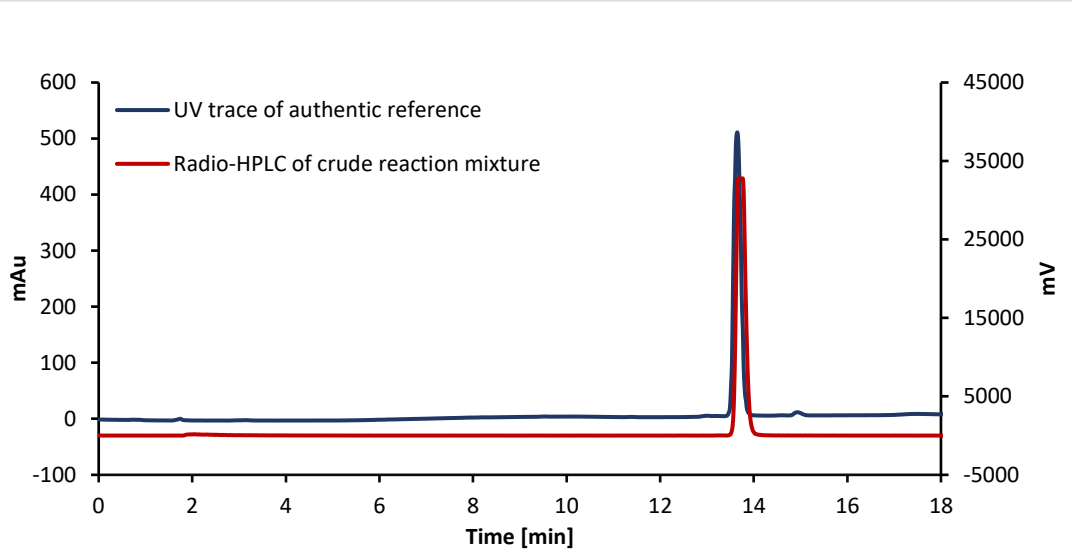


Analysed by (radio)HPLC using conditions A.

Run	RCY of [^{18}F]**3.92**	
1	55%	
2	42%	
3	55%	
	Average RCY	51% ± 6% (*n* = 3)

UV/radio-HPLC trace overlay for [^{18}F](*R*)-1-(3-(4-fluoro-3-(4-phenoxyphenyl)-1*H*-pyrazolo[3,4-*d*]pyrimidin-1-yl)piperidin-1-yl)prop-2-en-1-one ([^{18}F]**3.93**)

General Procedure 11 was followed using **3.61** as a substrate.



Analysed by (radio)HPLC using conditions B.

Run	RCY of [^{18}F]3.93	
1	98%	
2	98%	
	Average RCY	98% ± 0% (*n* = 2)

4.5. References

1 Trump, L.; Lemos, A.; Lallemand, B.; Pasau, P.; Mercier, J.; Lemaire, C.; Luxen, A.; Genicot, C. Late-Stage ^{18}F-Difluoromethyl Labeling of *N*-Heteroaromatics with High Molar Activity for PET Imaging. *Angew*. *Chem*. *Int*. *Ed*. **2019**, *58* (37), 13149–13154.

2 Zheng, Q.-T. Wei, Y.; Zheng, J.; Duan, Y.-Y.; Zhao, G.; Wang, Z.-B.; Lin, J.-H.; Zheng, X.; Xiao, J.-C. Difluoromethylation of *N*-arylsulfonyl hydrazones with difluorocarbene leading to difluoromethyl aryl sulfones. *RSC Adv*. **2016**, *6* (85), 82298–82300.

3 Banister, S. D.; Wilkinson, S. M.; Hanani, R.; Reynolds, A. J.; Hibbs, D. E.; Kassiou, M. A practical, multigram synthesis of the 2-(2-(4-alkoxyphenyl)-5,7-dimethylpyrazolo[1,5-a]pyrimidin-3-yl)acetamide (DPA) class of high affinity translocator protein (TSPO) ligands. *Tetrahedron Lett*. **2012**, *53* (29), 3780–3783.

4 Damont, A.; Hinnen, F.; Kuhnast, B.; Schöllhorn-Peyronneau, M.-A.; James, M.; Luus, C.; Tavitian, B.; Kassiou, M.; Dollé, F. Radiosynthesis of [^{18}F]DPA-714, a selective radioligand for imaging the translocator protein (18 kDa) with PET. *J. Label*. *Compd*. *Radiopharm*. **2008**, *51* (7), 286–292.

5 Zhao, Q.; Lu, L.; Shen, Q. Direct Monofluoromethylthiolation with *S*-(Fluoromethyl) Benzenesulfonothioate. *Angew*. *Chem*. *Int*. *Ed*. **2017**, *56* (38), 11575–11578.

6 Preshlock, S.; Calderwood, S.; Verhoog, S.; Tredwell, M.; Huiban, M.; Hienzsch, A.; Gruber, S.; Wilson, T. C.; Taylor, N. J.; Cailly, T.; Schedler, M.; Collier, T. L.; Passchier, J.; Smits, R.; Mollitor, J.; Hoepping, A.; Mueller, M.; Genicot, C.; Mercier, J.; Gouverneur, V. Enhanced copper-mediated ^{18}F-fluorination of aryl boronic esters provides eight radiotracers for PET applications. *Chem. Commun*. **2016**, *52* (54), 8361–8364.

7 Haskali, M. B.; Pike, V. W. [^{11}C]Fluoroform, a Breakthrough for Versatile Labeling of PET Radiotracer Trifluoromethyl Groups in High Molar Activity. *Chem*. *Eur*. *J*. **2017**, *23* (34), 8156–8160.

8 Ivashkin, P.; Lemonnier, G.; Cousin, J.; Grégoire, V.; Labar, D.; Jubault, P.; Pannecoucke, X. [^{18}F]$CuCF_3$: A [^{18}F]Trifluoromethylating Agent for Arylboronic Acids and Aryl Iodides. *Chem*. *Eur*. *J*. **2014**, *20* (31), 9514–9518.

9 Mossine, A. V.; Brooks, A. F.; Makaravage, K. J.; Miller, J. M.; Ichiishi, N.; Sanford, M. S.; Scott, P. J. H. Synthesis of [^{18}F]Arenes *via* the Copper-Mediated [^{18}F]Fluorination of Boronic Acids. *Org. Lett.* **2015**, *17* (23), 5780–5783.

10 Aydt, E. M.; Kranich, R.; Busemann, A. S. Novel aromatic compounds and their use in medical applications. EP1764093A1, 2005.

11 Billingsley, K.; Barder, T.; Buchwald, S. Palladium-Catalyzed Borylation of Aryl Chlorides: Scope, Applications, and Computational Studies. *Angew*. *Chem*. *Int*. *Ed*. **2007**, *46* (28), 5359–5363.

12 Buckingham, F.; Kirjavainen, A. K.; Forsback, S.; Krzyczmonik, A.; Keller, T.; Newington, I. M.; Glaser, M.; Luthra, S. K.; Solin, O.; Gouverneur, V. Organomediated Enantioselective ^{18}F Fluorination for PET Applications. *Angew*. *Chem*. *Int*. *Ed*. **2015**, *54* (45), 13366–13369.

13 Sap, J. B. I.; Wilson, T. C.; Kee, C. W.; Straathof, N. J. W.; am Ende, C. W.; Mukherjee, P.; Zhang, L.; Genicot, C.; Gouverneur, V. Synthesis of ^{18}F-difluoromethylarenes using aryl boronic acids, ethyl bromofluoroacetate and [^{18}F]fluoride. *Chem*. *Sci*. **2019**, *10* (11), 3237–3241.

14 Zheng, J.; Li, Y.; Zhang, L.; Hu, J.; Meuzelaarb, G. J.; Federsel, H.-J. Chlorodifluoromethyl phenyl sulfone: a novel non-ozone-depleting substance-based difluorocarbene reagent for *O*- and *N*-difluoromethylations. *Chem*. *Commun*. **2007**, *2007* (48), 5149–5151.

15 Ferguson, D. M.; Malapit, C. A.; Bour, J. R.; Sanford, M. S. Palladium-Catalyzed Difluoromethylation of Aryl Chlorides and Bromides with $TMSCF_2H$. *J*. *Org*. *Chem*. **2019**, *84* (6), 3735–3740.
16 Shi, H.; Braun, A.; Wang, L.; Liang, S. H.; Vasdev, N.; Ritter, T. Synthesis of ^{18}F-Difluoromethylarenes from Aryl (Pseudo) Halides. *Angew*. *Chem*. *Int*. *Ed*. **2016**, *55* (36), 10786–10790.
17 Feng, Z.; Min, Q.; Fu, X.; An, L.; Zhang, X. Chlorodifluoromethane-triggered formation of difluoromethylated arenes catalysed by palladium. *Nat*. *Chem*. **2017**, *9* (9), 918–923.
18 Gupta, S.; Chaudhary, P.; Srivastava, V.; Kandasamy, J. A chemoselective ipso-hydroxylation of arylboronic acids using urea-hydrogen peroxide under catalyst free condition. *Tetrahedron Lett*. **2016**, *57* (23), 2506–2510.
19 Zak, M.; Romero, F. A.; Cheng, Y. Therapeutic compounds and compositions, and methods of use thereof. US2018333416 A1, 2018.
20 Miao, W.; Zhao, Y.; Ni, C.; Gao, B.; Zhang, W.; Hu, J. Iron-Catalyzed Difluoromethylation of Arylzincs with Difluoromethyl 2-Pyridyl Sulfone. *J*. *Am*. *Chem*. *Soc*. **2018**, *140* (3), 880–883.
21 Aikawa, K.; Serizawa, H.; Ishii, K.; Mikami, K. Palladium-Catalyzed Negishi Cross-Coupling Reaction of Aryl Halides with (Difluoromethyl)zinc Reagent. *Org. Lett.* **2016***, 18* (15), 3690–3693.
22 Molander, G. A.; Brown, A. R. Suzuki–Miyaura Cross-Coupling Reactions of Potassium Vinyltrifluoroborate with Aryl and Heteroaryl Electrophiles. *J*. *Org*. *Chem*. **2006**, *71* (26), 9681–9686.
23 Zhang, X.; Xu, C.; Guo, W. Fluorine methyl-containing compound and preparation method thereof. CN 109694350 A1, 2019.
24 Campagna, F.; Carotti, A.; Casini, G. A convenient synthesis of nitriles from primary amides under mild conditions. *Tetrahedron Lett*. **1977**, *18* (21), 1813–1815.
25 Cybulska, K. A.; Bloemers, V.; Perk, L. R.; Laverman, P. Optimised GMP-compliant production of [^{18}F]DPA-714 on the Trasis AllinOne module. *EJNMMI Radiopharm. Chem.* **2021**, *6* (1), 20.
26 Lelos, M. J.; Dunnett, S. B. Generating Excitotoxic Lesion Models of Huntington's Disease. *Methods Mol*. *Biol*. **2018**, *1780*, 209–220.
27 Keller, T.; López-Picón, F. R.; Krzyczmonik, A.; Forsback, S.; Kirjavainen, A. K.; Takkinen, J. S.; Alzghool, O.; Rajander, J.; Teperi, S.; Cacheux, F.; Damont, A.; Dollé, F.; Rinne, J. O.; Solin, O.; Haaparanta-Solin, M. [^{18}F]F-DPA for the detection of activated microglia in a mouse model of Alzheimer's disease. *Nucl*. *Med*. *Biol*. **2018**, *67*, 1–9.
28 Sirisoma, N.; Kasibhatla, S.; Pervin, A.; Zhang, H.; Jiang, S.; Willardsen, J. A.; Anderson, M. B.; Baichwal, V.; Mather, G. G.; Jessing, K.; Hussain, R.; Hoang, K.; Pleiman, C. M.; Tseng, B.; Drewe, J.; Cai, S. X. Discovery of 2-Chloro-*N*-(4-methoxyphenyl)-*N*-methylquinazolin-4-amine (EP128265, MPI-0441138) as a Potent Inducer of Apoptosis with High In Vivo Activity. *J*. *Med*. *Chem*. **2008**, *51* (15), 4771–4779.
29 Banerjee, S.; Arnst, K. E.; Wang, Y.; Kumar, G.; Deng, S.; Yang, L.; Li, G.; Yang, J.; White, S. W.; Li, W.; Miller, D. D. Heterocyclic-Fused Pyrimidines as Novel Tubulin Polymerization Inhibitors Targeting the Colchicine Binding Site: Structural Basis and Antitumor Efficacy. *J. Med. Chem.* **2018**, *61* (4), 1704–1718.
30 Filho, E. V.; Pina, J. W. S.; Antoniazi, M. K.; Loureiro, L. B.; Ribeiro, M. A.; Pinheiro, C. B.; Guimarães, C. J.; de Oliveira, F. C. E.; Pessoa, C.; Taranto, A. G.; Greco, S. J. Synthesis, docking, machine learning and antiproliferative activity of the 6-ferrocene/heterocycle-2-aminopyrimidine and 5-ferrocene-1*H*-Pyrazole derivatives obtained by microwave-

assisted Atwal reaction as potential anticancer agents. *Bioorg*. *Med*. *Chem*. *Lett*. **2021**, *48*, 128240.

31 Liu, C.; Han, N.; Song, X.; Qiu, J. A General and Highly Efficient Method for the Construction of Aryl-Substituted N-Heteroarenes. *Eur*. *J*. *Org*. *Chem*. **2010**, *2010* (29), 5548–5551.

32 Tikad, A.; Routier, S.; Akssira, M.; Léger, J.-M.; Jarry, C.; Guillaumet, G. Efficient Synthesis of 2-Substituted Pyrido[3,2-*d*]pyrimidines Involving S_NAr and Palladium-Catalyzed Cross-Coupling Reactions. *Synthesis* **2009**, *14*, 2379–2384.

33 Ghiazza, C.; Faber, T.; Gómez-Palomino, A.; Cornella, J. Deaminative chlorination of aminoheterocycles. *Nat*. *Chem*. **2022**, *14* (1), 78–84.

34 Akinbobuyi, B.; Byrd, M. R.; Chang, C. A.; Nguyen, M.; Seifert, Z. J.; Flamar, A.-L.; Zurawski, G.; Upchurch, K. C.; Oh, S.; Dempsey, S. H.; Enke, T. J.; Le, J.; Winstead, H. J.; Boquín, J. R.; Kane, R. R. Facile syntheses of functionalized toll-like receptor 7 agonists. *Tetrahedron Lett*. **2015**, *56* (2), 458–460.

35 Huang, X.; Buchwald, S. L. New Ammonia Equivalents for the Pd-Catalyzed Amination of Aryl Halides. *Org*. *Lett*. **2001**, *3* (21), 3417–3419.

36 Moser, D.; Duan, Y.; Wang, F.; Ma, Y.; O'Neill, M. J.; Cornella, J. Selective Functionalization of Aminoheterocycles by a Pyrylium Salt. *Angew*. *Chem*. *Int*. *Ed*. **2018**, *57* (34), 11035–11039.

37 Ruch, J.; Aubin, A.; Erbland, G.; Fortunato, A.; Goddard, J.-P. Metal-free arylation of pyrimidines through a photochemical process. *Chem*. *Commun*. **2016**, *52* (11), 2326–2329.

38 Casimiro-Garcia, A.; Allais, C.; Brennan, A.; Choi, C.; Dower, G.; Farley, K. A.; Fleming, M.; Flick, A.; Frisbie, R. K.; Hall, J.; Hepworth, D.; Jones, H.; Knafels, J. D.; Kortum, S.; Lovering, F. E.; Mathias, J. P.; Mohan, S.; Morgan, P. M.; Parng, C.; Parris, K.; Pullen, N.; Schlerman, F.; Stansfield, J.; Strohbach, J. W.; Vajdos, F. F.; Vincent, F.; Wang, H.; Wang, X.; Webster, R.; Wright, S. W. Discovery of a Series of Pyrimidine Carboxamides as Inhibitors of Vanin-1. *J*. *Med*. *Chem*. **2022**, *65* (1), 757–784.

39 Morales-Colón, M. T.; See, Y. Y.; Lee, S. J.; Scott, P. J. H.; Bland, D. C.; Sanford, M. S. Tetramethylammonium Fluoride Alcohol Adducts for S_NAr Fluorination. *Org*. *Lett*. **2021**, *23* (11), 4493–4498.

40 Hong, C. M.; Whittaker, A. M.; Schultz, D. M. Nucleophilic Fluorination of Heteroaryl Chlorides and Aryl Triflates Enabled by Cooperative Catalysis. *J*. *Org*. *Chem*. **2021**, *86* (5), 3999–4006.

41 Pérez-García, R. M.; Grønnevik, G.; J. Riss, P. J. A General Protocol for Cu-Mediated Fluoro-deamination: Sandmeyer Fluorination of Diverse Aromatic Substrates. *Org*. *Lett*. **2021**, *23* (3), 1011–1015.